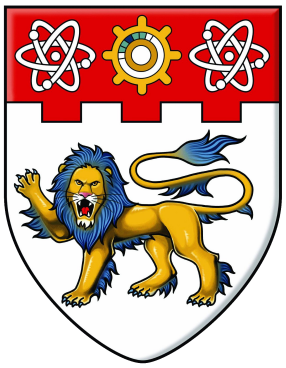

NANYANG TECHNOLOGICAL UNIVERSITY

VIRAL DIAGNOSTICS AND ANALYSIS OF HOST RESPONSE TO VIRAL INFECTION USING MICROARRAY TECHNOLOGY

CHEN HUI

SCHOOL OF BIOLOGICAL SCIENCES

2014

VIRAL DIAGNOSTICS AND ANALYSIS OF HOST RESPONSE TO VIRAL INFECTION USING MICROARRAY TECHNOLOGY

CHEN HUI

School of Biological Sciences

A thesis submitted to the Nanyang Technological University
in fulfillment of the requirement for the degree of
Doctor of Philosophy

2014

ACKNOWLEDGEMENTS

I would like to give my most sincere thanks to my supervisor **Associate Professor Richard J. Sugrue** for supporting my bioinformatics studies in his laboratory, as well as invaluable guidance and patience during my Ph.D period. Special thanks also go to **Assistant Professor Tan Boon-Huan** for giving me an opportunity to participate in her project and offering continuous guidance, patience and encouragement in the processing of my paper writing. I would also like to thank **Professor Li Jinming** for providing suggestions in the field of bioinformatics and assisting me in my Ph.D application process.

I wish to also express my heartfelt gratitude to **Assistant Professor Tang Kai** and **Associate Professor Mu Yuguang** for their help in my Ph.D period. Thanks are also given to my lab mates: **Richard Sutejo**, **Debbie Ko Huiling**, **Muhammad Raihan Jumat**, **Myint Zu Myaing**, **Laxmi Ravi Iyer**, **Loo Liat Hui** for their assistance and friendship. Besides, I appreciate the assistance from lab mates in DSO National Laboratories: **Yeo Su Yin Dawn, Dr. Ayi Teck Choon**, **Kuah Li Fang** and **Chan Ka Wei**.

I would like to thank **Nanyang Technological University** for providing me with a research scholarship.

Lastly, I would like to express my thanks to my parents, grandparents, my sisters and brothers, as well as my friends for their love and accompany forever.

TABLE OF CONTENTS

LIST OF FIGURES

LIST OF TABLES

ABBREVIATIONS

AIDS	Acquired Immunodeficiency Syndrome
AP1	Activator Protein-1
ATCC	American Type Culture Collection
AVA	Agri-Food and Veterinary Authority of Singapore
BCL10/9L	B-cell CLL/lymphoma 10/9-like
BIRC3	Baculoviral IAP repeat-containing protein 3
BTG1	B-cell Translocation Gene 1
CDC	Centers for Disease Control and Prevention
CDF	Cumulative Distribution Function
CEF	Chick Embryo Fibroblast
CH25H	Cholesterol 25-hydroxylase
CRISPR	Clusters of Regularly Interspaced Short Palindromic Repeats
CRM1	Chromosome Region Maintenance protein 1
DF	Dengue Fever
EEV	Extracellular Enveloped Virions
EGF	Early Growth Response
eIF2α	Eukaryotic Translation Initiation Factor 2 alpha subunit
ELISA	Enzyme-linked Immunosorbent assay
EM	Eectron Microscope
ER	Endoplasmic Reticulum
F	Fusion Protein
FPPS	Farnesyl Diphosphate Synthase
G	Glyco-protein
GAGs	Glycosaminoglycans
GO	Gene Ontology
HA	Haemagglutinin
HIV	Human immunodeficiency virus
HMM	Hidden Markov Model
HP	Heptad Repeat
HPAI	High Pathogenic Avian Influenza Virus
HRSV	Human Respiratory Syncytial Virus
HS	Heparin Sulphate

IAP	Inhibitor of Apoptosis
IAV	Influenza A viruses
IBs	Inclusion Bodies
IFA	Immunofluorescence Assay
IFAR	IFN-α receptor
IFN	Interferon
IFRG	Interferon Responsive Gene
IKK	IκB Kinase
IMV	Mature Virions
IPA	Ingenuity Pathways Analysis
IPS	IFNβ Promoter Stimulator
IRAK	Interleukin-1 Receptor-associated Kinase
IRF	Interferon Regulatory Factor
ISG	IFN Stimulated Gene
ISRE	Interferon Sensitive Response Elements
IV	Immature Virion
IVNS1ABP	Influenza Virus NS1A Binding Protein
IκB	Inhibitor of NF-Kb
JAK	Janus-family Protein Tyrosine Kinases
KEGG	Kyoto Encyclopedia of Genes and Genomes
KEREN	Kernel Embedding of Regulatory Networks
KL	Kullback-Leibler
L	Large Protein
LPAI	Low Pathogenic Avian Influenza Virus
LPS	Lipopolysaccharide
LRTI	Lower Respiratory Tract Infections
M	Matrix Protein
MAPK	Mitogen-activated Protein Kinase
MDA	Microbial Detection Array
MDA5	Melanoma Differentiation Associated Gene 5
MDCK	Madin Darby Canine Kidney
MHC	Major Histocompatibility Complex
MOI	Muiltiplicity Of Infection

MT	Microtubule
Mx	Myxovirus Resistance
N	Nucleo-protein
NA	Neuraminidase
NES	Nuclear Export Signal
NF-κB	Nuclear factor kappa B
NGS	Next Generation Sequencing
NLRs	Nucleotide-binding Domain and Leucine-rich-repeat-containing Proteins
NLSs	Nuclear Localization Signals
NO	Nitric Oxide
NP	Nucleoprotein
NPC	Nuclear Pore Complex
NS1	Non-structural Protein 1
NS2	Non-structural Protein 2
OAS	Oligoadenylate Synthetases
ORF	Open Reading Frame
P	Phosphor-protein
PA	Polymerase Acidic
PB1	Polymerase Basic 1
PB2	Polymerase Basic 2
PI3K	Phosphatidylinositoe-3-Kinase
PKB	Protein Kinase B
PKR	Protein kinase R
PRR	Pathogen Recognition Receptor
RT-PCR	Reverse Transcription – Polymerase Chain Reaction
RIG-I	RNA Helicases Retinoic Acid Inducible Gene-I
RNP	Ribonucleoprotein
RSAD2	Viperin
RSV	Respiratory Syncytial Virus
SARS	Severe Acute Respiratory Syndrome
SAGE	Serial Analysis of Gene Expression
SH	Small Hydrophobic Protein

SLE	Systemic Lupus Erythematosus
SOCS	Suppressor of Cytokine Signalling
STAT	Signal Transducers and Activators of Transcription
TBK1	TANK-binding kinase 1
TF	Transcriptional Factor
TLR	Toll-like Receptor
TNF	Tumor Necrosis Factor
TRIM25	Tripartite Motif 25
VFs	Virus Filaments
vRNA	viral genome RNA
vRNP	viral ribonucleoprotein
WHO	World Health Organization
WV	Wrapped Virion
XAF1	XIAP associated Factor-1
ZBP1	Z-DNA-binding Protein 1
ZNF	Zinc Finger

SUMMARY

Viruses are major factors of human infectious diseases. They not only threaten the public health but also cause economic loss in the worldwide. During the past decades, more and more cases of virus infections in human beings have been reported. Thus, establishment of an accurate pathogen diagnostic system is urgent for clinical virus identification. Moreover, deep understanding of the transcriptomic profiles in typical virus-infected cells is also imperative for vaccination, drug design as well as other medical treatment in the future.

Microarray as an advanced technology has been well developed and extensively applied in last decades. In the field of virology studies, microarray technique has been widely applied in the pathogen diagnosis and transcriptomic examination of host cells upon pathogen invasion. With the application of this advanced technique, a large scale of data is generated at one time, which cause the high demand of bioinformatics tools in data interpretation.

In one project, DNA microarrays were applied in pathogen detection. To interpret the data from diagnostic microarray chips, a novel computational software, BayesMicro, was designed and established. The virus identification results from BayesMicro were then compared with the results from previously published software called E-Predict. And the final comparison demonstrated that BayesMicro was capable of generating positive predictions in all 12 tested arrays, indicating that this software performed effectively and could be applied in virus detection as an alternative tool.

In other projects, global gene expression profiles were examined for comprehensive understanding of the host-virus interactions in different host cells under different viruses infections using microarray system. The pre-processing of the microarray data was performed under GeneSpring GX 11.0 software. Other softwares such as Expander 5.0 and Ingenuity Pathway Analysis were applied to perform further functional annotation. The final results demonstrated that different global gene expression profiles were observed in different host cells infected with different viruses. Genes in key biological groups and canonical pathways that have been reported previously showed differential regulations at their expression levels. In addition to these well-

known cellular processes, other interesting networks were also significantly representative in our data.

Chapter I. General Introduction

Viruses are major factors of human infectious diseases. With more and more cases of virus infections in human beings reported in last decades, viruses have become threats not only to public health but also to the worldwide economy. For example, respiratory syncytial virus (RSV) and influenza viruses are important causes of respiratory tract infections. The former contributed to 34 million cases of lower respiratory tract infections (LRTI) in children <5 years of age and led to 66,000 to 199,000 mortalities majorly in children and elderly patients in 2005 [1]. The latter commonly cause 3 to 5 million clinical infections and 250,000 to 500,000 fatal cases annually [2]; Dengue fever (DF) caused by one serotype of dengue virus is one of the most common widespread vector borne diseases, with 100 million cases reported annually [3]; Human immunodeficiency virus (HIV) is a kind of virus that enables to cause acquired immunodeficiency syndrome (AIDS), in which humans would get progressive failure of their immune system. It has been estimated that 86,500 people in the UK were infected with this virus only according to 2009 statistics. In terms of these data, it is urgent and necessary to establish an accurate pathogen diagnostic system. Moreover, deep understanding of the host-virus interactions in different viruses-infected cells is also imperative for vaccination, drug design as well as other medical treatment in the future.

1.1 Outline of virus replication cycle

All viruses share the same basic replication cycle, but the time involved depends on a number of factors, including the size and genetic complexity of the virus itself as well as the nature of the host cells [5].

1.1.1 Virus entry

Viruses first recognize and bind to cells that they infect. Virus-coded proteins on the surface of the virion bind to specific proteins, carbohydrate or lipid on the cell surface. Structural surface proteins of many viruses bind to carbohydrate residues found in surface glycoproteins and glycolipids that are widely distributed on many cell types.

Once they locate on the cell surface, some enveloped animal viruses fuse their lipid envelopes directly with the plasma membrane of the cell, releasing the viral capsid and genome into the host cell. Some other animal viruses are directly taken up into the cytoplasm in vesicles formed at the plasma membrane. These vesicles then release the virion or its genome into the cytoplasm, and the genome may be further transported into the nucleus [Figure 1.1].

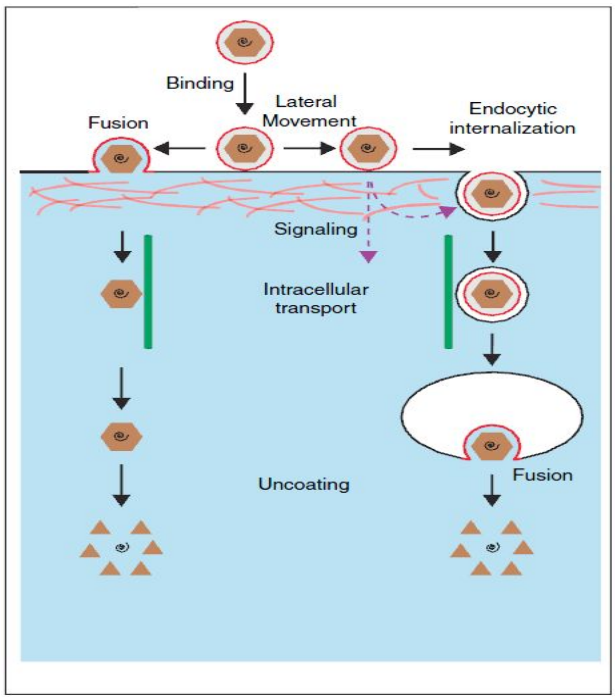

Figure 1.1 Entry pathway of an enveloped animal virus (adapted from Schmidt F *et al*., 2012)[311]. Enveloped animal viruses enter host cells in a stepwise process: viral particles bind to attachment factors in the host cell plasma membrane and may undergo lateral movement. Virions may employ two entry routes: fusion at the plasma membrane or endocytosis. The latter may be triggered by virus–receptor interactions, followed by vesicular transport. Maturation of endosomes provides the cues for membrane fusion. Capsid release, whether at the plasma membrane or from an intracellular vesicle, is followed by intracellular transport of capsids and genome uncoating at the site of viral replication.

1.1.2 Genome replication

Once delivered into the appropriate compartment of the cell, the viral genomes express some early proteins which enable to promote the replication of viral genome. All RNA viruses should synthesize an RNA-dependent RNA polymerase to replicate their genomes. In this process, a variety of cellular proteins also assist the RNA polymerase to complete the replication of viral genomes.

DNA viruses always produce early proteins that enable to induce the production of a batch of cellular enzymes, and these enzymes are able to assist virus in its genome replication. Thousands of copies of genome can be synthesized in one cell, and these genomes can be treated as a template for synthesis of viral mRNAs or further genome replication.

1.1.3 Virus assembly

Stuctrural proteins always participate in packing the viral genomes and assembling the capsid in infected host cells. The simplest virus capsids consist of one protein that forms either a closed shell or a helical tube within which the viral genoms is packed. Large and complex viruses may have numerous capsids proteins. Enveloped viruses code glycoproteins that are inserted into lipid membranes to directly form a viral envelop, and this process is always called budding. Once the progeny virions are formed, they leave the cell and infect new host cells, in which another replication cycle is initiated.

1.2 Host responses to viruses and viral strategies to counter host responses

To stay healthy and survive, organisms must defend themselves against invading pathogens, including viruses. Upon the virus invasion, host intrinsic cellular defense system is initiated rapidly. A variety of cellular proteins are involved in this antiviral process: toll-like receptors (TLRs) are responsible for detecting invading pathogens; cytokines, including interferons, are secreted to inhibit virus replication; a self-destruction process called apoptosis is induced to reduce the spread of virus infection.

1.2.1 TLRs

TLRs are a class of membrane-spanning receptors that consist of an extracellular leucine-rich repeat domain, a transmembrane-spanning domain and a cytoplasmic Toll-interleukin-1 receptor-resistance domain. In recent years, TLR family has been discovered and characterized as an important member in pattern-recognition receptors (PRRs), which detect pathogen-associated molecular patterns (PAMPs) on pathogen invading. After the recognition, the anti-viral signaling pathways are activated, promoting the production of proinflammatory cytokines and type I interferons (IFNs) [6].

Members of the TLR family are involved in responses to viral infection. Among all TLR members, TLR1, TLR2, TLR4, TLR5, TLR6, and TLR11 are located on plasma membrane, while TLR3, TLR7, TLR8, TLR9, and probably TLR13 of mice are expressed intracellularly within the endoplasmic reticulum, endosomes, multivesicular bodies, and lysosomes [387]. TLR3 senses dsRNA and some RNA viruses; TLR9 interacts with DNA containing unmethylated CpG motifs; TLR7 and TLR8 close resemble with TLR9 and sense ssRNA from the viral genomes [Figure 1.2]; TLR2 and TLR4 sense viral infection through recognition of protein components of the viral particle [7].

TLR3 induces the TLR domain-containing adaptor protein to trigger IFNβ signaling pathway, which in turn stimulate TANK-binding kinase 1 (TBK1) and IKKε. Induction of TBK1 and IKKε finally result in phosphorylation of interferon regulatory factor (IRF)-3, as well as activation of IκB kinase 2 (IKK2) and NF-κB. Activated TLR7 enables induction of the adaptor protein MyD88 and subsequently leads to the phosphorylation of IRF7 [8].

To interrupt the recognition by TLRs, some viruses have found to encode different viral proteins in order to target different factors that play critical roles in signaling transduction. Subsequently, these encoded viral proteins are able to inhibit TLR-mediated signaling as well as further host immune response [9].

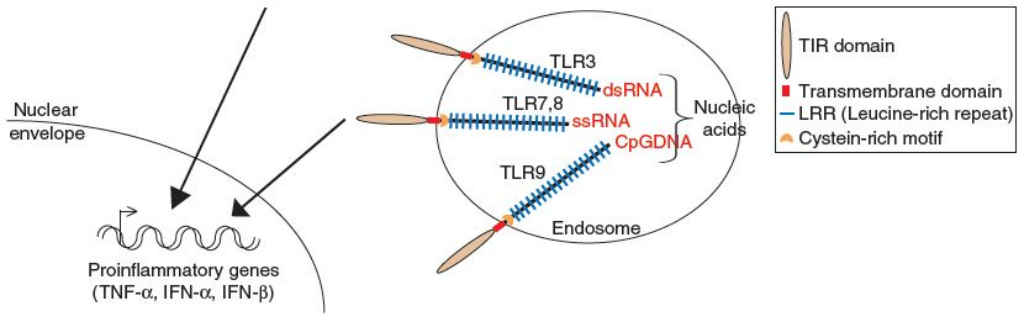

Figure 1.2 Toll-like receptors recognize nucleic acids (adapted from Galiana-Arnoux D *et al.*, 2006) [7].

1.2.2 Cytokines

Cytokines are small secreted proteins used for intercellular signaling and communication. Cytokines not only participate in the innate immune respone

but also mediate the communication between the innate and adaptive immune systems. There are different types of cytokines: interferons (IFNs), pro-inflammatory cytokines and chemokines.

1.2.2.1 Interferons

As a family of secreted cytokines, IFNs function in inhibiting virus replication and limiting viral spread via direct antiviral and indirect immunoregulatory activities at the very beginning of viral invasion. There are three main types of IFN: type I IFNs, IFN-α/β, signal through IFNAR1/IFNAR2; type II IFN, IFN-γ, signals through IFNGR1/IFNGR2; type III IFNs, IFN-λ1/2/3 referred to IL-29/28a/28b, signals though IL-28R [10]. These IFNs transduct signals through Jak-STAT signaling pathway, subsequently leading to the activation of downstream transcription factors and induction of IFN-stimulated genes (ISGs).

IFN-α/β are always produced upon viral infection. Initially, recognition of viral components by TLRs and retinoic inducible gene I (RIG-I) activates the transcription factor NF-κB which is essential for IFN-β expression. IRF3 as another transcription factor that is activated via RIG-I and TLR-3 mediated signal transduction pathways also plays a critical role in expressional induction of IFN-β and activation of several ISGs. Upon the binding of secreted IFN-β to its receptor, this initial response is further amplified. IFNAR as a receptor is coupled to the JAK that phosphorylate STAT1/2, which in turn initiate transcription of ISGs [11]. OAS and PKR are downstream interferon stimulated genes which play key roles in further antiviral activities.

Due to the prominently antiviral functions of IFNs, diverse mechanisms have been developed and employed to impede their activities so as to counterract the host defenses. These strategies include inhibition of IFN production, competition for binding to IFN receptors, interference with the JAK/STAT signaling pathway and suppression of ISGs at their expression level [12, 13].

1.2.2.2 Pro-inflammatory cytokines

Other cytokines that are rapidly produced following virus infection include tumor necrosis factor (TNF) and interleukins. TNF is a pro-

inflammatory cytokine that is involved in the activation of the innate immune responses to viral infection and the control of cell apoptosis, survival as well as differentiation. Two surface receptors of TNF are TNFR1 that is expressed in most cell types and TNFR2 that is expressed in immune and endothelial cells. TNF expression is triggered by multiple PRRs such as TLRs upon recognition of viral infection. Among different TLRs, TLR2 and TLR4 are able to detect viral particles, while TLR3 and TLR7/8 recognize dsRNA and uridine-rich sequences of ssRNA respectively. Additionally, nucleic acids produced by virus can be also recognized by RIG-I and melanoma differentiation associated gene 5 (MDA5/IFIH1). Induction of TNFs results in activation of NF-κB, a key transcription factor for proinflammatory.

IKK plays a role on phosphorylation and subsequent degradation of IκB that sequester NF-κB in the cytoplasm. By amplifying NF-κB-dependent expression of anti-apoptotic molecules and activation of the MAPK signaling, TNF was also proved to mediate cell apoptosis [11]. In terms of different signaling pathways, viruses have evolved strategies to deal with them [14].

Interleukins are a group of cytokines that function primarily on the differentiation and activation of immune cells. For example, IL-1α and IL-1β from IL-1 family are proinflammatory cytokines that mediate a variety of host responses including increasing acute-phase signaling, trafficking immune cells to the site of primary infection, activating epithelial cell and secondary cytokine production [13, 15].

1.2.2.3 Chemokines

Chemokines are the largest family of cytokines consisting of four types (CXC, CC, C, and CX3C) based on the spacing of their first two cysteine residues. Cytokines serve to recruit immune cells such as lymphocytes and antigen-presenting cells to the site of infection, and these recruited immune cells will function to limit virus replication and stimulate the adaptive immune respone [13]. For example, CCL5 that is responsible for the recruitment of CD8 T cells to the lung has been proved to participate in not only the classical IFN-γ dominant Th1 responses but also Th2 response during RSV infection in mice [16]. Evidences have been also provided that certain viral proteins interrupt the host defense system through interfering with MHC functions [17].

1.2.3 Cell apoptosis

Many host cells respond to a virus infection by inducing a self-destruction process called apoptosis or programmed cell death. This can be an effective host defense system, becaused the premature death of virus-infected cells reduces the spread of the infection wihin the orgranism [18]. Viruses also have evolved some stratigies to delay apoptosis of the host cell until their replication cycle is completed [17].

Apoptosis signaling generally triggers two major pathways, the intrinsic and extrinsic pathway. The former one is controlled by permeabilization of the mitochondrial membrane and release of cytochrome c. Cytochrome c enables to form a complex with Apaf-1 and procaspase-9, and this complex subsequently activates downstream caspases. Members from Bcl-2 family have been proved to be involved in the control of this pathway. The latter pathway is activated by the TNF family through binding to the domains of the death receptors including Fas, DR4 (Trail-R1), TNFRI, and TNFRII, which in turn lead to caspase activation [19] [Figure 1.3].

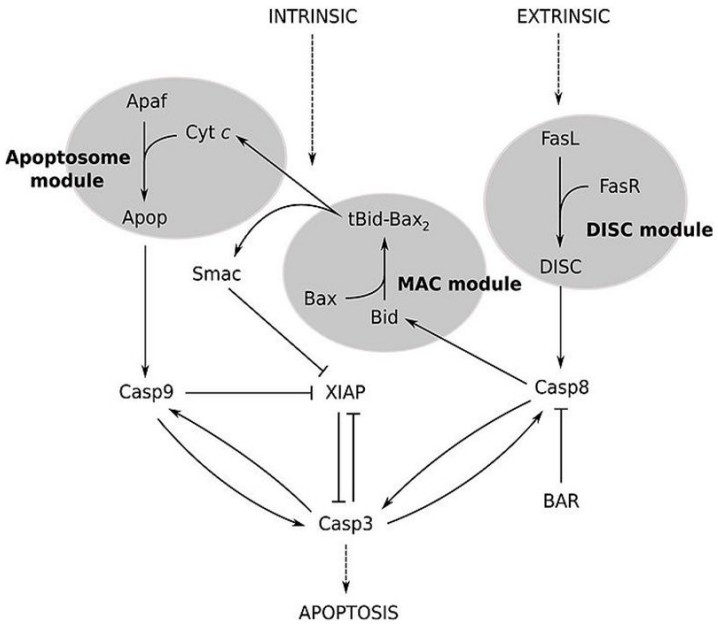

Figure 1.1 Apoptosis signaling pathway. Initially, the extrinsic stimuli such as TNF and Fas ligand stimulate death receptor trimerization, and then caspase 8 is activated after being recruited to the cytoplasmic domain of the death receptor. Activation of caspase 8 leads to activation of either caspase 3 or the BH3-only protein Bid. In the case of Bid activation, Bid is translocated to the mitochondria in order to activate Bak, subsequently the mitochondrial membrane is permeabilized and the pro-apoptotic factors are released. Eventually, the downstream caspases are activated to fulfill the final cell death. Intrinsic stimuli activate BH3-only proteins that activate Bak and Bax, or repress anti-apoptotic Bcl-2 proteins, thereby regulating apoptosis at the mitochondria.

1.2.4 Host cell signaling pathways

1.2.4.1 JAK-STAT pathway

Once IFNα/β are secreted by an infected cell, these cytokines will bind to the ubiquitously expressed IFNAR. Signaling through this receptor leads to activation of the JAK-STAT pathway and expression of interferon production, amplifying the response to viral infection. The JAK-STAT pathway demonstrates the activation of STATs protein by JAK proteins [Figure 1.4]. JAK proteins are activated by interferons and interleukins. After the binding into the receptors, the JAK proteins phosphorylate the STAT1 proteins (pSTAT1), turning them into activated form. pSTAT1 proteins dimerize and translocate to the nucleus [20]. However, Pauli EK *et al* (2008) proposed that phosphorylation of STATs in the IFNβ signaling might be regulated by some cellular factors, such as proteins of SOCS family [21]. These SOCSs have been proposed to have high affinity for JAK and STAT proteins and therefore inhibit the transmission of IFNα/β signaling. Validation experiment indicates that SOCS-3 is partly responsible for the inhibitory activity via NF-κB-dependent induction [22].

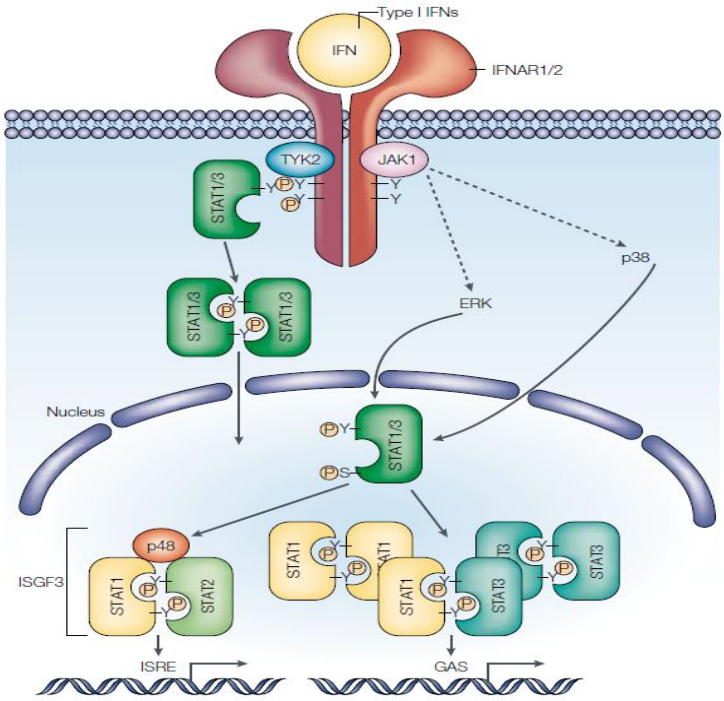

Figure 1.4 The IFN receptors and Jak-STAT signaling (adapted from Katze MG *et al*., 2002) [10].

1.2.4.2 NF-κB/IKK pathway

The NF-κB family plays a central role in the cellular inflammation response through controlling a network of gene expression. It is commonly activated upon virus infection and its activation leads to the expression of an array of cytokine and chemokine genes, including IFNβ [23]. Apart from its function as regulator of the expression of inflammatory molecules, NF-κB also regulates mechanisms of controlled cell apoptosis in several cell types.

The mechanism of NF-κB activation depends on the activation of the inhibitor of IKK complex. The IKK complex consists of at least IKK1/IKKa, IKK2/IKKb and NEMO/IKKg. Amon these isozyme, IKK2/IKKb is most important for the activation of the canonical NF-κB pathway through phosphorylating and degrading the inhibitor of NF-κB (IκB). This consequently leads to the release and translocation of NF-κB factors p65 and p50 dimers that migrate to the nucleus to exert its biological functions.

1.2.4.3 MAPKs signaling pathway

MAP kinases play an essential role in cellular responses such as proliferation, differentiation, immune response and cell death. Three main families of MAPKs in mammals all have their own activators, inactivators, substrates and scaffolds, and all these factors form a fine signaling network in reaction to different stimulations from extracellular or intracellular. Three concrete pathways are MAPK/ERK, SAPK/JNK and p38 MAPK. MAPK signaling promotes cell survival by a dual phosphorylation event on threonine and tyrosine residues. The upstream MAPKK regulates these 4 enzyme activities. Two MAPKK (MKK3/6, MKK4/7) are responsible for activation of p38 and JNK respectively. These enzymes are involved in apoptosis and cytokine expression, and can be activated by environmental stress conditions. The upstream Raf controls the phosphorylation of MAPK/ERK kinase (MEK)1/2, which regulates the activation of ERK1/2 that plays a regulatory role in cell proliferation and differentiation. Lastly, enzyme ERK5 is activated by MEK5 [Figure 1.5] [24].

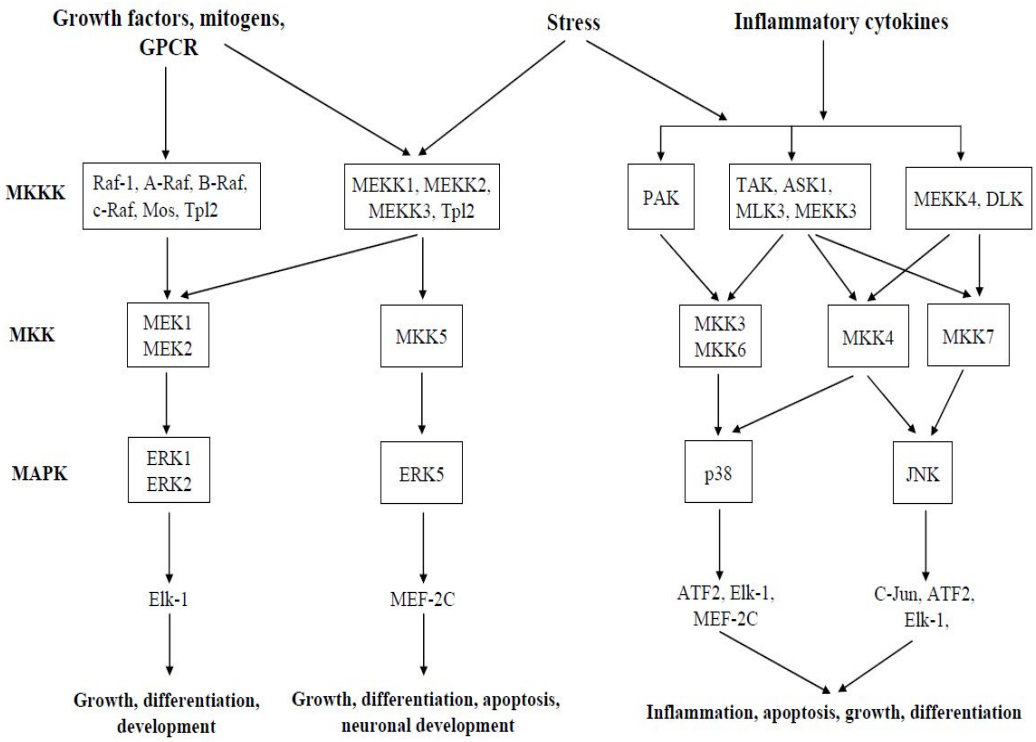

Figure 1.5 MAP kinase pathways in mammals. MAPKs are activated by dual phosphorylation on Thr and Tyr caused by specific MKKs, which are in turn activated by MKKKs (adapted from Zhang Y *et al*., 2005) [24].

1.3 Traditional strategies in virology studies

1.3.1 Traditional strategies of virus identification

In tradition, various techniques such as tissue culture, immunofluorescence assay (IFA), enzyme-linked immunosorbent assay (ELISA), electron microscope (EM) and reverse transcription-polymerase chain reaction (RT-PCR) are applied in pathogen detection.

IFA is a technique used with a fluorescence microscope. This technique specifies the antibodies carrying fluoresecent dyes to target their corresponding antigens, and therefore allows visualisation of the distribution of the target molecules. EM is another technique that is based on antibodies. Antigens from samples are attached to a surface and specifically bind the corresponding antibodies, and substances are able to react with the enzymes that are linked to the antibodies, thereby detectable signals are produced. Both these two traditional techniques have been widely applied in pathogen detection [25] and the major limitations of them lie in the signal measurement: photobleaching in IFA and complex enzyme activity in ELISA.

Another technique called RT-PCR is also applied in pathogen detection [26]. This technique is based on the polymerase chain reaction, and it is able to not only detect the pathogen sequence but also quantify the pathogen sequence in the sample. The limitation of this technique is that it heavily relied on further pathogen sequencing. EM is a type of microscope that has great resolving power and can reveal the structure of small objects. The diadvantage of this technique is that it is very expensive to build and maintain, and the operation and analysis heavily relies on highly-trained technicians.

Currently, advanced methods such as microarray have been widely applied in pathogen studies, mainly because of the following advantages: (1) small volumes of probes and samples required; (2) a large amount of information generated within one experiment; (3) broad-based and co-infectious detection. Although it is treated as a promising technology, challenges still have been posed to users. These challenges majorly lie in reproducibility, hybridization efficiency, highly-trained technicians and professional manpower for data analysis. In addition, sophisticated machine for image processing and rigorous bioinformatics software for effective data mining are also required [27].

1.3.2 Traditional strategies of host gene expression investigation during virus infection

In order to examine host genomic expression profiles following virus infection, techniques including RT-PCR, northern blot, RNase protection assays and serial analysis of gene expression (SAGE) have been employed in quantifying gene expression for a long period [28-31]. In the meanwhile, other methods such as ELISA and western blot have been also widely applied in protein expression quantification since a long time ago [32, 33]. Although relatively accurate quantification could be generated using these techniques, they are limited to quantify multiple genes or proteins together at one time (Table 1.1).

In the past decades, several advanced technologies have been pioneered and applied to investigate the gene or protein expression in the field of virology. These technologies including microarray, mass spectrometry and next generation sequencing (NGS) enable to quantify tens of thousands of genes or proteins in parallel. However, the common disadvantages of these technologies

are the demand of highly-trained technicians and rigorous bioinformatics software for accurate data interpretation.

Table 1.1 Advantages and disadvantages of different strategies which are applied in genomic investigation during virus infection.

Strategies	Target	Advantages	Disadvantages
Northern blot	gene expression	high specificity	not sensitive & dangerous chemicals
RNase	gene	very senstive	highly-trained technicians needed
SAGE	gene expression	accurate & do not need the sequence	expensive & low-scale studies
RT-PCR	gene	fast & sensitive	rely on further sequencing
ELISA	protein expression	affordable	complex enzyme activity
Western Blot	protein expression	Sensitive	long time & require antibodies
Microarray	gene expression	detect expression of multiple genes/proteins in an	expensive
	protein expression	Small volumes of probes and sample required	highly-trained technicians needed
Mass Spectrum	protein expression	detect expression of multiple proteins in an experiment	expensive
		Small volumes of probes and sample required	highly-trained technicians needed
NGS	gene expression	detect expression of multiple genes in an experiment	expensive
			highly-trained technicians needed

1.4 Design of DNA microarray technology

A microarray chip is an orderly arrangement of a rectangular grid of "spots". Thousands of short DNA fragments (probes) are printed onto a small solid matrix in order to examine cDNA representing mRNA (targets). The basic theory of the microarray experiments lies in the hybridization by base pairing between probes and targets. Dependent on this special structural design of microarray, thousands of different probes are able to be immobilized into a single array for parallel investigation [34, 35].

1.4.1 Different applications of DNA microarray

There are a number of applications of microarray technology in past years. In the area of phylogenomics in pathogens, comparative genomics can identify genetic factors responsible for transmission, evolution, virulence, and even anti-microbial resistance among different pathogen phenotypes [36].

Another application is to study host-microbe interaction, and this transcriptome analysis of intracellular pathogens in in-vitro and in-vivo models at different infection time points offers better understanding of the molecular biology and life cycle of pathogens [37, 38].

The microarray platform can also be exploited to array protein markers and glycans. This platform offers a high throughput screening for patient to test for antibodies to a wide array of proteins. These proteins serve as immunoreactive antigens as in the case of Severe Acute Respiratory Syndrome (SARS) virus and can be used as serological markers in epidemiological study [39]. In addition, the array can be used as therapeutic proteins for vaccine development as in the case of smallpox vaccine [40]. In another example, the development of a glycan array allows the study on the receptor affinity of different influenza A virus subtypes and the information is extrapolated to understand the host specificity [41].

Another exploitation of the platform is the array of a library of small molecules, which could potentially be drug candidates. These are then screened with a panel of target proteins from pathogens such as the anthrax lethal factor [42].

In the field of virology, the most popular applications of microarray technique could be majorly classified into two repects: microbial or medical diagnosis [43, 44] and transcriptomic examination [45].

1.4.2 Application of microarray in virus identification

During the last decade, the broad-based virus detection using the microarray DNA chip was developed (Figure 1.6) and different types of microarray chips designed for different detection purposes were pioneered (Table 1.2).

The broad-based virus detection using the microarray DNA chip was pioneered by the DeRisi group [27, 48]. In this chip, long oligonucleotides at 70 mers were designed and each virus was represented by the top 5 highly conserved oligonucleotides and the corresponding reverse complement oligonucleotides. These long oligonucleotides were arrayed for a total of 1000 viruses and represent all known viruses at that time the virus pathogen chip was designed in year 2003. These viruses cause diseases in human, animals,

agricultural and are also found in the environments. Subsequently other viral chips were developed based on a similar platform. For example, the 40-mer microarray chip was developed by Wong *et al* (2007) with the aiming of detecting a small group of RNA viruses [49]. Another group in Taiwan reported the use of 70-mer microarray chip in a similar design to DeRisi's group [50].

Table 1.2 Different types of microarray chips in virus detection. The chip from DeRisi group can be used to detect around 1,000 viruses; Greene Chip is applied in identifying a variety of micro-organisms; Commercial microarray chips like TessArae performs well in microbial detection and genetic testing [27, 46, 47].

Chip from DeRisi group	Greene Chip	TessArae
70-mer oligonucleotides	60-mer oligonucleotides	25-mer oligonucleotides
each virus was represented by the top 5 highly conserved oligonucleotides and the corresponding reverse complement oligonucleotides	oligonucleotide probes from one conserved target and two variable targets are taken into consideration for the design	Eight probes are designed for each nucleotide pair; four each for the forward and reverse strands with each set of four tiled together as a probe set. The probes vary only at the center with an A, G, C or T at that position
detect about 1,000 viruses which cause diseases in human, animals, agricultural and are also found in the environments	detect a variety of micro-organisms such as viruses, bacteria, parasites, fungal	Microbial detection and genetic testing

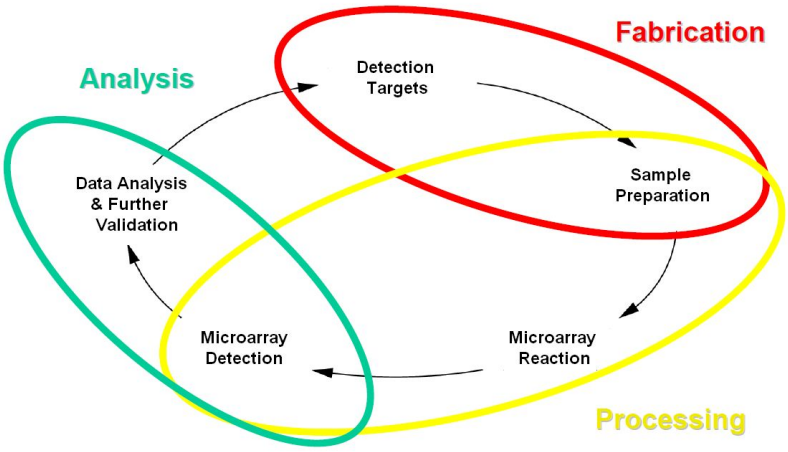

Figure 1.6 Strategy to identify viruses based on microarray technology. With regard to different detection purposes, array design and samples preparation should be considered carefully. Microarray reaction, detection, and data analysis are fulfilled step by step. Finally, methods such as PCR, IFA, and ELISA are applied for further validation.

The GreeneChip is another viral microarray chip that is not commercially available, but has been incorporated as part of the novel pathogen discovery program led by Dr Lipkin's group in Columbia University, New York [46]. In this case, the GreeneChip were arrayed with 60-mer oligonucleotides, and these were selected from a variety of micro-organisms (viruses, bacteria, parasites, fungal). The selection of probe sets for viruses were more logical compared to Wang *et al* (2002; 2003) [27, 48]. Oligonucleotide probes from one conserved target usually coding the enzyme genes and two variable targets usually coding the structural genes are taken into consideration for the design.

In some pathogen chips, simultaneous detection and partial characterization in further reveals the exact sequence information hence providing preliminary and confirmatory identification. For example the resequencing chip developed by Lin et al., 2006 was so successful that it was taken over commercially and marketed under TessArae (http://www.tessarae.com). It can provide identification and partial sequencing of important virus genes and targets a range of respiratory viruses in the Centers for Disease Control and Prevention (CDC) list of category A, B and C agents. It is also able to perform whole genome sequencing of a comprehensive list of haemorrhagic fever viruses.

There are other types of microarray chips which provide partial characterization such as the chip used for subtyping influenza viruses [47]. In this chip, specific 21-mer oliognucleotides representing different subtypes of influenza viruses were arrayed on glass slides, and the genetic materials from samples were allowed to hybridize to the oligonucleotides.

The clusters of regularly interspaced short palindromic repeats (CRISPR)/Cas (CRISPR associated proteins) system that functions on defending against invading nucleic acids is broadly distributed in microbial immunity. The CRISPR spacer sequences have been proved to be unique within individual microbe genomes and may even be unique within different cell types. Accordingly, CRISPR spacer-based microarrays were designed by Snyder JC *et al* (2010) to identify unknown virus[51].

Another system called Pan-viral microarray targets to virus genus specific detection [52]. In that chip, 628 63-mer genus specific oligonucleotides

were designed as probes to screen 32 human pathogenic RNA virus genera from 14 virus families.

Recently, another pan-microbial detection array (MDA) that targets to all known viruses and bacteria has been also established [53, 54]. Probes specific to different virus families were designed for all sequenced viral and bacterial genomes, segments, as well as plasmids. Some sequence variations were tolerated during the probe design process so that detection of divergent species with homology became possible.

1.4.3 Application of microarray in host gene expression investigation during virus infection

When the microarray technique is applied in monitoring gene expression (mRNA abundance), the genes which play critical roles on inner cellular function are majorly investigated. Since these genes are transcribed from genomic DNA, their expression profile also refers to as transcriptome. The genomic transcription from DNA to mRNA is the initial step during the process of protein synthesis, thus differences in gene expression might indicate specific cellular responses in reaction to intra or extra interferences. Comprehensive understanding of the detailed gene expression in different situations is essential to analyze the biological functions of its encoded protein. Moreover, changes of the whole gene expression profiles can provide insight into cellular regulatory mechanisms and underlying biological signaling pathways [55].

It has been well known that viruses are not able to propagate independently in their host cells. In every infection cycle, viruses must enter into their host cell for replication and transcription. In this process, many host cell functions are required to assist them to complete the multiple steps of their life cycle. And these cellular functions could be divided into several aspects: cellular translation and translocation, sorting machinery to target glycoproteins to the proper cellular destination, a lipid-synthesizing machinery for virus lipid envelope and the cellular nucleus that is necessary for DNA viruses (except poxviruses) replication [56].

Besides, viruses have also evolved the mechanisms to avoid the negative influence from the host antiviral actions. For instance, expression of molecules in immune response signaling pathways have been suppressed in order to make

sure their replication happen without interference from the inflammation responses; cytoskeleton and cellular signal transduction pathways have been manipulated to benefit their easily entry and following cellular travel; new strategies have been also evolved to prevent host cell apoptosis to guarantee their smooth replication and budding [56].

In view of these complex interactions, microarray technology has been widely applied in defining the global transcriptional activities in viruses-infected host cells to facilitate virology research as well as further antiviral drug discovery[57, 58]. To date, many groups have reported the applications of microarray in the investigation of gene expression profile in viruses-infected host cells. For instance, Katze MG *et al* (2008) applied microarray technique to examine the global gene expression profiling in various viral infected models, aiming to explore viral pathogenesis and host-pathogen interactions at a systems-level [59]; microarray technique was also involved in identifying differentially expressed genes and pathways in cattle infected with Alcelaphine herpesvirus 1 [60] as well as in human retinal pigment epithelium infected with West Nile virus [61]; genomic host responses upon laryngotracheitis virus vaccine infection were also checked in chicken embryo lung cells based on a microarray platform ; Other applications of microarray technique in studying the transcriptome under virus infection have been also extensively published [63-66].

1.5 Bioinformatics tools involved in virology researches

In recent years, bioinformatics tools and databases that interpret genomic, proteomic, and other functional information have become more and more indispensable for virology studies. The applications of these bioinformatics analysis in virology researches include open reading frame (ORF) identification, gene prediction, homology searching, sequence alignment, pattern/motif/epitope recognition, short tandem repeats, transmembrane domains as well as secondary and tertiary structural studies [67].

With the dramatic development of techniques such as microarray, mass spectrometry (MS)-based proteomics and NGS, mRNA and protein abundances could be surveyed in a routine, rapid and high-intensity [68-70]. Due to large-scale of quantification at one time, these advanced techniques have been now

widely applied in virology studies [71, 72]. At the meanwhile, more and more bioinformatic tools have been also pioneered in order to extract useful information in their abundant data [35, 73-75].

1.5.1 Bioinformatics pre-processing for microarray data

Sophisticated bioinformatics processing is required before abstracting the meaningful data from microarray experiments. This procedure commonly include: background correction, data truncation, outlier correction, averaging, quality control and normalization. A variety of statistical considerations and algorithms are involved in this procedure to retrieve the accurate observed signal intensities from the microarray chips [76].

1.5.2 Bioinformatics software for virus identification

While many virus detection microarray chips have been described, there are only a couple of algorithms published for analyzing data from these diagnostic chips [77]. The algorithm for E-Predict [78], DetectiV [79], and VIPR/ VIPR HMM [80, 81] are published and their software are available to the public. Other algorithm such as GreeneLAMP [46], PDA [49], PhyloDetect [82] and CLiMax [53] are available but not the software. These different computation strategies are established in aim to target different microarray diagnostic chips based on different statistical hypothesis.

E-predict is the first computation strategy raised together with the corresponding 70-mer oligonucleotides microarray chip by DeRisi group, and treated as their default computation strategy. It is a computational strategy used for virus species identification based on microarray experimental hybridization intensity pattern (http://derisilab.ucsf.edu/epredict/). Using this strategy, a library of theoretical binding energy profiles that represent different virus species with known genomic sequences, was computed and then compared with the experimental hybridization intensity pattern. The final detection result is reached through calculating Uncentered Pearson correlations between the theoretical binding energy profiles and the experimental hybridization intensity patterns.

DetectiV is an R-based method for significant testing. It integrates many R packages including *limma*, *marray*, *affy* together to achieve the virus

detection goal and meanwhile offered an additional visualized maps [83, 84].

VIPR, as a probabilistic algorithm, applies Bayesian inference in capitalizing on empirical training data so as to optimize virus detection sensitivity. And VIPR HMM implements the analysis by incorporating a hidden Markov model (HMM) into existing VIPR in order to detect the recombinant genomes.

PDA software fulfills the pathogen detection based on two steps: a modified Kullback-Leibler Divergence (KL) is imported to evaluate the hybridization intensity of probes in each pathogen r-signature; Anderson-Darling test is performed to complete further statistical analysis.

GreeneLAMP centers the log-transformed intensity, with QFAST algorithm is applied to compute the tail probability (P-value) for each virus. And these P-values for positive probes associated with the virus are finally used to calculate the tail probability.

In PhyloDetect, it is assumed that the probes in microarray yield a hybridization signal with a matching microbial sequence but no signal with a non-matching one. On the basis of this probe-microbe match matrix, the microbial detection outcome is fulfilled by three steps: grouping of non-distinguishable microbes, arrangement of microbial groups in a hierarchical tree and computation of likelihood.

CLiMax is based on a biophysical model of probe-target hybridization, and a greedy algorithm is applied to find a local maximum for the likelihood.

1.5.3 Bioinformatics software for host gene expression during virus infection

Genomic interpretation of the microarray data generally focus on the following directions: enrichment of functional pathways and processes, clustering of gene expression profiles, discovery of regulatory networks as well as prediction of transcription factor binding [85, 86].

1.5.3.1 Pathway enrichment

Through analyzing biochemical pathways and biological processes, it will be easy to understand how these molecules interact with each other, as well as their functional roles at the systems level. In virology studies, more and more

evidences have been provided that molecules in pathways associated with immune response, apoptosis and antigen representing show un-normal expression. Accordingly, investigations on dysregulation of these specific pathways or processes during virus infection may be beneficial to understand the host-viral interaction mechanisms, and therefore potential antiviral interventions and vaccine targets could be pioneered [67].

A commonly used pathway database is Kyoto Encyclopedia of Genes and Genomes (KEGG), which includes information of metabolic pathways and regulatory pathways [87]. Another pathway database called HumanCyc, which is under BioCyc system, and this database contains the metabolic pathways which are only specific to human [88]. As to the bioinformatics software which enables to enrich the significantly regulated pathways are involved GeneSpring, Gene Set Enrichment Analysis and Ingenuity Pathway Analysis [89].

1.5.3.2 Clustering analysis

In the traditional analysis of microarray data, individual differentially expressed gene is not able to provide the complete picture of the gene regulations. Noise and variation in microarray expression data may influence the expression performance of individual gene. Thus the employing of clustering analysis on studies of these expression data makes it easy to detect a group of functionally related genes with coordinated expression profiles. These groups of genes with similar expression trend are assumed to have related biological functions and correspond to some critical cellular processes and pathways [90, 91].

Different clustering algorithms generate different results even when given the same expression dataset. For biologist, it is difficult to choose an appropriate clustering method. Till now, a diverse set of clustering algorithms have been proposed by different groups. These are five traditional methods: k-means clustering, the hierarchical clustering based on average linkage or complete linkage, and the methods due to McQuitty and Ward. Besides, some more graph-based approaches such as k-clique communities, WGCNA, NNN, CAST, and CLICK have been established. Finally, two other approaches called self-organizing maps and QT Clust have been also applied in microarray data analysis recently [92].

1.5.3.3 Regulatory network discovery

In biological cells, mRNA and proteins interact with each other with various degrees of specificity. These molecules and their interactions form different gene regulatory networks. Discovery of these gene regulatory networks will help us understand the inner signal transduction system in the host cells. In virus infected host cells, examining the regulation status of different networks will be absolutely beneficial for the understanding of virus invasion and host antiviral mechanisms [91].

Traditional methods which are applied in constructing gene regulatory networks from microarray data include linear models, Bayesian networks and Boolean networks [93]. In these years, Ruan J *et al* (2010) have proposed a new and robust method called gene co-expression networks, and Zare H *et al* (2011) also has built up a new algorithm called Kernel Embedding of Regulatory Networks, which is based on the gene regulation association [94].

Recently, more and more findings have proven that both virus and host encode microRNAs, which in turn participate in the intricate host-virus interactions. Thus the regulatory networks of microRNA-mRNA interactions during the pathogen infections will draw more and more attentions in virology researches [95-97].

1.5.3.4 Transcription factor binding prediction

In fundamental biological processes, transcriptional regulation affects the translation level of proteins by regulating cellular mRNA levels. When it comes to higher eukaryotes, the complexity of them primarily resides in the sophisticated regulatory networks [98, 99]. Accordingly, discovering the potential binding motif using bioinformatics knowledge will be beneficial for the deep understanding of inner cellular function.

Several classic databases of transcriptional factor elements and their binding sites have been established and updated these years. Among them, two representative databases are TRANSFAC and JASPAR [98]. Software which have been reported to enrich the potential transcriptional factor and their binding sites include oPOSSUM human single site analysis package [100], PRIMA [101] and STOP [102].

1.6 Objective

As we know, pathogens such as influenza viruses, RSV and poxviruses have become greatest threats to human health. And in the past decades, scientists have paid more and more attentions on virus researches, not only aiming to improve the virus diagnostic system but also making efforts to investigate the host-virus interactions.

Advanced high-throughput technologies such as microarray have shown superiority when compared to other traditional methods. With its application, multiple bioinformatic databases and tools become more and more imperative to accurately interpret these microarray data. In our studies, we exert efforts to solve the popular issues in virology researches with the help of microarray technology, and in this process, relevant bioinformatic approaches have been pioneered or employed to achieve the data analysis.

In the project regarding to pathogen diagnostic chips, a new computation strategy, called BayesMicro, is described. This software is designed based on a novel Bayesian metric and implemented in a Perl environment. It is used to not only detect the virus from the global species level but also provide further differential virus detection within virus families.

In other projects, standard microarray chips (Affymetrix) are involved in investigating the global transcriptomic features in different cell lines after infections of different viruses. The pre-processing and further interpretation of microarray data were performed under the software including GeneSpring GX 11.0, Expander 5.0 and Ingenuity Pathway Analysis. The examination results demonstrate that different global gene expression profiles are detected in different virus infected different cells. The pathways which have been mentioned in previous reports also illustrate differential regulation in our experiment. In addition to these published pathways, genes in some other pathways have also been enriched to show differently transcriptional changes during the virus infection.

Chapter II. Materials and Methods

2.1 Materials

2.1.1 Viruses

RSV A2	ATCC
A/WS/33	ATCC
A/Singapore/478/2009	DSO National Laboratories
A/Duck/Malaysia/01	AVA
A/Duck/Malaysis/F118/08/2004	AVA
A/Duck/Malaysia/F59/04/1998	AVA
A/Duck/Malaysia/F189/07/2004	AVA
A/Duck/Malaysia/F119/3/1997	AVA
A/umbrellacockatoo/Singapore/F47/12/92	AVA
A/fairybluebird/Singapore/F92/09/94	AVA
Cowpox virus Brighton strain ATCC VR302	ATCC
Vaccinia virus Lister strain ATCC 1549	ATCC
Ectromelia virus Moscow strain VR1374	ATCC

2.1.2 Cell types and their maintenance

Hep2 cells were derived from a human epidermoid cancerous cell line. It was abtained from American Type Culture Collection (ATCC). They were maintained in 10% Dulbecco's Modified Eagle's medium (DMEM) (Invitrogen) containing 10% fetal bovine serum (FBS) and 1% penicillin/streptomycin (Glibco) at 37^{o}C in 5% CO2 and antibiotics.

Human alveolar basal epithelial (A549, ECACC 86012804) and Madin-Darby canine kidney (MDCK, ECACC 84121903) cells were obtained from European Collection of Cell Cultures. Chick embryo fibroblasts (CEF) were prepared from 8 to 10 day-old chick embryos. After ethanol cleaning, the eggs were processed using forceps to isolate the intact body part. The intact body part was then made into single cell suspension. They were maintained in 10% Dulbecco's Modified Eagle's medium (DMEM) (Invitrogen) containing 10% fetal bovine serum (FBS) and 1% penicillin/streptomycin (Glibco) at 37^{o}C in 5% CO2 and antibiotics.

Murine lung CD11b + cells were prepared from 6–8 weeks old special pathogenfree (SPF) female Balb/c mice. The lungs were digested with collagenase D (1μg/ml; Gibco) and single cell suspension (0.5% BSA, 2mM EDTA, in 1XPBS) obtained was passed through a 30 μm filter. CD11b + cells were purified using CD11b microbeads and a LS positive selection column

(Miltenyi Biotec). The cells were eluted from the microbeads and cultured in L929 cell conditioned (30%v/v) medium for 3 days at 37 °C in 5% CO_2.

RAW 264.7 (RAW) cells (Mouse leukaemic monocyte macrophage cell line) were purchased from ATCC (TIB-71) and maintained in 10% Minimum Eagle's Media (MEM media) (D1152 media, Sigma) containing 10% FBS and 1% penicillin/streptomycin (Glibco) at 37 °C in 5% CO_2.

Chick embryo fibroblasts (CEF) were prepared from 8 to 10 day-old chick embryos and maintained in DMEM containing 10% FBS and pen/strep [394].

2.2 Experiment design

2.2.1. Experiment workflow for pathogen detection

Nucleic acids were isolated from virus-infected cell cultures (Qiagen). Their amplification consists of three steps: random-primed reverse transcription, second strand cDNA synthesis and PCR. The PCR products ran on the agarose gel electrophoresis and amino-allyl (aa)-dUTP were incorporated. The aa-dUTP-incorporated DNAs were fragmented and purified using the PCR purification kit (Qiagen). After that, the amino-allyl group was then labeled with Cy3-fluorescent dye (GE Healthcare). The printed microarray slides were UC cross-linked and blocked first, and the labeled PCR products were subsequently hybridized overnight to the microarray chip. The hybridization signal intensities were retrieved using Genepix software, and subsequently reformatted and submitted into E-Predict and BayesMicro software for further analysis [27][48][78].

For all the virus infections, they were generally infected with a MOI > 1, and infection was carried out at 37°C in the presence of CO_2 [Table 2.1].

2.2.1.1. Primers used

Primer name	Primer sequence (5' to 3')	Size (bp)
Primer A	GTT TCC CAG TCA CGA TCN NNN NNN NN	26
Primer B	GTT TCC CAG TCA CGA TC	17

Table 2.1 Preparatino of virus strains.

Virus	Strains	Origins	Propagation	DNA/RNA extraction method
Chikungunya virus	Oka		Propagated in C6/36 cells	Rneasy (Qiagen)
Coronavirus	OC43	ATCC VR-1558		Rneasy (Qiagen)
Cowpox VIRUS	Brighton	ATCC VR-302	Passaged in BHX cells	DNA mini (Qiagen)
Influenza A virus	H1N1		Clinical sample isolated and propagated in eggs*	Rneasy (Qiagen)
Influenza A virus	H3N2	ATCC VR810	Propagated in eggs*	Rneasy (Qiagen)
Influenza B virus	Lee	ATCC VR101	Propagated in eggs*	Rneasy (Qiagen)
Japanese encephalitis virus	Nakayama		Propogated in Vero cells	Rneasy (Qiagen)
Measles virus	Edmonton	ATCC VR-24		Rneasy (Qiagen)
Mouse poxvirus	Moscow	ATCC VR 1374	Passaged in Vero E6 cells	DNA mini (Qiagen)
Rhinovirus	Type 14	ATCC VR-1059		Rneasy (Qiagen)
Vaccinia virus	Lister		Propagated in Vero E6	DNA mini (Qiagen)
Yellow fever virus	17D		Propogated in Vero E6	Rneasy (Qiagen)

*9-11 day old embroynated chicken eggs

2.2.1.2. Design of the viral chip

The complete list of viral oligonucleotide sequences represented on the microarray viral chip by Wang et al., 2003 was downloaded from http://derisilab.ucsf.edu/virochip. Oligonucleotides belonging to plant viruses were removed from the list, and only human or zoonotic viruses were synthesized. Each virus was represented by the top 5 highly conserved oligonucleotides and the corresponding reverse complement oligonucleotides. These oligonucleotides were 70 mer in length. In addition, we also randomly selected 10 oligonucleotides from 10 human genes as controls for microarray scanning. In total, 6233 oligonucleotides were synthesized.

2.2.1.3. Fabrication

The oligonucleotides were suspended in 3XSSC at a concentration of 50 pmol/ul and printed on glass slides (Full moon biosystem).

2.2.1.4. Extraction of viral nucleic acids, amplification, and labelling

Nucleic acids were extracted from infected cell culture with either the DNA minikit or RNeasy kit respectively (QIagen, CA, USA), following manufacturers' instructions. 2 μg of nucleic acids were reverse transcribed with Superscript II or III using primer A (Table 1). Primer A possesses a stretch of 9 random bases at the 3' end which allows it to randomly prime any nucleic acid sequences belonging to the template, and a non-random 5' tag. After reverse

transcription, a second strand cDNA synthesis was carried out with Sequenase (US Biochemicals, USA). PCR amplification of the ensuing double-stranded template was then carried out with primer B, which targets the non-random tag on primer A. The resultant PCR product was then amplified a second round with primer B, in the presence of aminoallyl-dUTP andthe amplicons, containing aminoallyl group was then purified, and labelled with Cy3-dyes. The dye ratio was monitored, and we only proceed with hybridisation when the dye ratio lies between 30 and 60.

2.2.1.5. Hybridisation

Microarray hybridisation was performed. All arrays were imaged using a 4000B Axon scanner with the GenePix software Version 4 (Foster City, CA). The microarray data were converted to a colour visualisation in which the Cy-3 intensity of each viral-specific sequences hybridised onto the chip was imaged. Generally, the microarray was imaged at 500 pmt, and only at 400 pmt if the background is high.

2.2.1.6. Data processing and analysis

The image was mapped to a .gal file containing the oligonucleotide identification, the spots aligned manually or by default, and normalised to subtract the background signals. The final output data from GenPix software were extracted into a .gpr file. The .gpr file required a Perl program to further process the useful data within the .gpr file into a .vdar files before submission to the E-predict and BayesMicro for analysis.

2.2.2. Experiment workflow for RSV infections

RSV A2 strains were infected in two types of cell lines (Hep2 and mouse macrophages) [Table 2.1]. Two types of Affymetrix GeneChips including GeneChip HG-U133 Plus 2.0 Array and GeneChip Mouse 430 2.0 Array were applied in our experiment to examine the genome-wide gene expression in human Hep2 cells and mouse macrophages at different post infection time points.

The RSV A2 strain was was prepared using Hep2 cell culture. RSV particles were recovered from tissue culture media by centrifugation at

150,000g for 2 hr at 4°C, after which the virus was gently and uniformly resuspended in an equal volume of fresh DMEM with 2% FCS and stored at -80°C. A Hep2 cell microplaque assay was applied to confirm the infectivity of the resulting inoculum. During the time of infection, the virus was thawed and spun at 1200 rpm for 10 minutes and the cells were infected with RSV A2 at an MOI=5 using DMEM (Invitrogen) with 2% FBS at 33ºC in 5% CO2.

Investigation of transcriptome from 4hpi to 15hpi in RSV-infected Hep2 cells allow to observe the formation of progeny virus, but is prior to the cell damage that occurs later in the replication cycle that could cause indirect changes in the host cell expression profile. Besides, the virus infectivity recovered from macrophages indicated virus titres of $2x10^1$ pfu/ml (similar between 2.5hpi and 20hpi), and only sporadic stained cells were detected using the tissue culture supernatant of RSV-infected macrophages. Thus, RSV infection in macrophages might result in the formation of virus antigen and the production of inclusion bodies, however, the efficient infectious virus particle production did not occur [156][364].

The genome-wide gene expression profiles in Hep2 cells and mouse macrophages were examined using the GeneChip Mouse Genome 430 2.0 Array (Affymetrix, USA) and GeneChip Human Genome HG U133 Plus 2.0 Array (Affymetrix, USA) high density microarray systems. Different infected cells were harvested at 4°C using RNAlater (Ambion) in PBS buffer, and total RNA was extracted using RNeasy minikit (Qiagen). Double-stranded cDNA was synthesized from 3 μg of total cRNA with the GeneChip One-Cycle cDNA synthesis kit (Invitrogen, Affymetrix), followed by synthesis of biotin-labelled cRNA using the GeneChip IVT labeling kit (Affymetrix). After cRNA fragmentation, 15 μg of labeled cRNA was hybridized to Mouse Genome 430 2.0 Array (Affymetrix, USA) and GeneChip Human Genome HG U133 Plus 2.0 Array (Affymetrix, USA). After hybridization, these chips were then washed and stained using the GeneChip Fluidics Station 450 (Affymetrix). Finally, GeneChip scanner 3000 (Affymetrix) was employed in scanning the chips, and quality control and data acquisition were performed according to the standard protocols available from Affymetrix. Normalization using a global scaling strategy to a target intensity of 500 was first performed using GCOS (v1.1, Affymetrix) before generating the .CHP files [156][364].

2.2.3. Experiment workflow for influenza A viruses infections

Eight influenza A virus strains with five subtypes (H1N1/WS, H9N2, H5N3, H5N2/F59, H5N2/F189, H5N2/F118, H5N3, H7N1 and pH1N1/478) from egg propagated were infected in three types of cell lines including A549, Chick Embryo Fibroblast (CEF) and Madin Darby Canine Kidney (MDCK) cells [Table 2.2]. RNA quantification and qPCR analysis suggested that infection of H5N3 contributed to the highest vRNA levels in A549 cells, followed by H5N2/F118, H1N1/WS and H9N2. In CEF cells, infection of H5N3 also caused the highest vRNA levels, while infection of other viruses resulted in similar vRNA levels. The higher vRNA levels were detected in H1N1/WS and H5N3 infected MDCK cells when compared to H5N2/F118 and H9N2 infected MDCK cells, and pH1N1/478 replicated least efficiently [365].

Three types of Affymetrix GeneChips including GeneChip HG-U133 Plus 2.0 Array, Chicken Genome Array and Canine Genome 2.0 Array were applied in our experiment to examine the genome-wide gene expression in human, chicken and canine at different post infection time points. Another three subtypes of influenza A viruses were also infected in mouse macrophages, and GeneChip Mouse 430 2.0 Array was applied to examine the genome-wide gene expression profiles in mouse macrophages at different post infection time points [Table 2.3].

All virus stocks were prepared in 9 to 11-day-old embryonated chicken eggs, and the infectivity was confirmed based on standard overlay plaque assay. Virus infections in A549, MDCK and CEFs were carried out in Dulbecco's Modified Eagle's medium (DMEM) (Invitrogen) with 2% FBS and pen/ strep at 37uC in 5% CO2. Virus was allowed to absorb to the cell monolayer for 1 hr at 37^{o}C, and virus infections at an MOI= 4 in all cells were carried out in Dulbecco's Modified Eagle's medium (DMEM) (Invitrogen) with 2% FBS and pen/ strep at 37^{o}C in 5% CO2.

The cells either mock-infected or virus-infected at specific infection time points were harvested in RNAlater (Ambion, USA) and PBS buffer (1:1), aliquoted, pelleted and stored at -80^{o}C. Total RNA was extracted using the RNeasy MiniKit (Qiagen, USA) and quantified using the Nanodrop ND-1000 Spectrophotometer (Thermo Fischer Scientific, USA). Double-stranded cDNA was synthesized from 3 μg of total cRNA with the GeneChip One-Cycle cDNA

synthesis kit (Affymetrix, USA), followed by synthesis of biotin-labelled cRNA using the GeneChip IVT labelling kit (Affymetrix, USA). After cRNA fragmentation, 15 μg of biotin-labelled cRNA was hybridized to the GeneChip Canine Genome 2.0 Array (Affymetrix, USA), the GeneChip Chicken Genome Array (Affymetrix, USA), Genechip Human Genome HG U133 Plus 2.0 Array (Affymetrix, USA) and GeneChip Mouse 430 2.0 Array (Affymetrix, USA), seperately. The arrays were then washed and stained using the Hybridization, Wash and Stain Kit (Affymetrix, USA) and the GeneChip Fluidic Station 450 (Affymetrix, USA), respectively. Finally, GeneChip scanner 3000 (Affymetrix, USA) was applied in scanning the arrays, and Affymetrix .CHP files were generated from GeneChip Operating Software (GCOS) version 5.0 after appropriate normalization [365].

Table 2.2 Design of experiments in RSV infected host cells. RSV A2 strains were infected in Hep2 cells and mouse macrophages, and host cell gene expression profiles were detected at different post infection hours.

Name of strain	Subtype	Abbreviation	Origin	Cell type	Post infected time points
RSV A2	A	RSV	Human	Hep2	4hpi, 8hpi, 12hpi, 15hpi
RSV A2	A	RSV	Human	Macrophage	4hpi, 24hpi

There are two antigenic subgroups of HRSV, calles A and B, which exhibit aa sequence identity ranging from 96% (N) to 53% (G), and which are approximately 50% or 5% related antigenically in the F or G protein, respectively, with the overall differene in reciprocal cross-neutralization being up to four-fold [389].

2.2.4. Experiment workflow for poxviruses infections

Three subtypes of Poxviruses were infected in two types of cell lines (A549 and mouse RAW cells) [Table 2.4]. Two types of Affymetrix GeneChips including GeneChip HG-U133 Plus 2.0 Array and GeneChip Mouse 430 2.0 Array were applied in our experiment to examine the genome-wide gene expression in human lung epithelial cell line, A549 cells and mouse RAW cells at different post infection time points.

All poxviruses stocks were prepared using VERO cell culture, and the infectivity was assessed based on overlay plaque assay. Virus was allowed to absorb to the cell monolayer for 1 hr at 37^{o}C, and virus infections in A549 and RAW were carried out in Dulbecco's Modified Eagle's medium (DMEM) (Invitrogen) with 2% FBS and 1% pen/ strep at 37^{o}C in 5% CO2.

A549 and RAW were either mock-infected or virus-infected at specifc time points at an MOI=10. Double stranded cDNA was synthesized from 3μg of total RNA with the GeneChip One-Cycle cDNA synthesis kit (Affymetrix), followed by synthesis of biotin-labelled cRNA using the GeneChip IVT labelling kit (Affymetrix). After cRNA purification and fragmentation, 15μg of biotin-labelled cRNA was hybridized to the GeneChip HG-U133 Plus 2.0 Array or the GeneChip Mouse 430 2.0 Array. The arrays were washed and stained using the Hybridization, Wash and Stain kit and the GeneChip Fluidics Station 450 (Affymetrix) according to standard Affymetrix protocols. Finally, the arrays were scanned using the GeneChip scanner 300 (Affymetrix) and .CHP files were generated from GeneChip Operating Software (GCOS) after proper normalization.

Table 2.3 Design of experiments in influenza viruses infected host cells. Six subtypes influenza viruses were infected in three type cell lines with different combinations, and host cell gene expression profiles were detected at different post infection hours in each combination.

Name of strain	Subtype	Abbreviation	Origin	Cell type	Post infected time points
A/WS/33	H1N1	H1N1	Human	A549, CEF, MDCK	2hpi, 4hpi, 6hpi, *8hpi,10hpi
A/Singapore/478/2009	H1N1	pH1N1	Human	A549	2hpi, 4hpi, 6hpi, 8hpi, 10hpi
A/Duck/Malaysia/01	H9N2	H9N2	Avian	A549, CEF, MDCK	2hpi, 4hpi, 6hpi, 8hpi, 10hpi
A/Duck/Malaysis/F118/08/2004	H5N2	H5N2(F118)	Avian	A549, CEF, MDCK	2hpi, 4hpi, 6hpi, 8hpi, 10hpi
A/Duck/Malaysia/F59/04/1998	H5N2	H5N2(F59)	Avian	A549, CEF, MDCK	10hpi
A/Duck/Malaysia/F189/07/2004	H5N2	H5N2(F189)	Avian	A549, CEF, MDCK	10hpi
A/Duck/Malaysia/F119/3/1997	H5N3	H5N3	Avian	A549, CEF, MDCK	10hpi
A/fairybluebird/Singapore/F92/09/94	H7N1	H7N1	Avian	A549, CEF, MDCK	10hpi

A549 represents “Human lung adenocarcinoma epithelial cell”; CEF represents “Chicken embryo fibroblast cell”; MDCK represents “Madin-darby canine kidney cell”. * represents that H1N1 infection at 8 hpi was only investigated in CEF cells.

Table 2.4 Design of experiments in influenza viruses infected mouse macrophages. Six subtypes influenza viruses were infected in mouse macrophages, and host cell gene expression profiles were detected at different post infection hours.

Name of strain	Subtype	Abbreviation	Origin	Cell type	Post infected time points
A/WS/33	H1N1	H1N1	Human	Macrophage	2hpi, 24hpi
A/Duck/Malaysis/F118/08/2004	H5N2	H5N2(F118)	Avian	Macrophage	2hpi, 24hpi
A/Duck/Malaysia/F119/3/1997	H5N3	H5N3	Avian	Macrophage	24hpi

Table 2.5 Design of experiments in poxviruses infected host cells. Three subtypes of Poxviruses were infected in A549 cells, and mouse RAW cells with different post infection time points, and host cell gene expression profiles were detected at different post infection hours.

Name of strain	Subtype	Abbreviation	Origin	Cell type	Post infected time points
Brighton strain	Cowpox virus	Cowpox virus	Cow	A549	2hpi, 4hpi, 6hpi, 8hpi, 10hpi
Lister strain	Vaccinia virus	Lister virus	N/A	A549	2hpi, 4hpi, 6hpi, 8hpi, 10hpi
Brighton strain	Cowpox virus	Cowpox virus	Cow	Mouse Raw	2hpi, 16hpi
Lister strain	Vaccinia virus	Lister virus	N/A	Mouse Raw	2hpi, 16hpi
Moscow strain	Ectromelia virus	Ectromelia virus	Mouse	Mouse Raw	2hpi, 16hpi

A549 represents “Human lung adenocarcinoma epithelial cell”.
Species can be classified by pock morphologies and by ceiling temperature for growth on the chorioallantoic membrane of embryonated chicken eggs. Ecological niche and host range are useful in some cased, but in others can be misleading. Restriction enzyme polymorphisms of the terminal regions of viral DNA outsides of the core of common genes also aids the classigication process [389].

2.2.5. Quantitative Real-time quantitative PCR (qPCR)

Total RNA was extracted from cells at 4uC using the RNeasy kit (Qiagen, USA) and reverse-transcribed using Superscript II (Invitrogen, USA) according to manufacturer’s instructions. Primers for cell-specific genes were designed using the Probefinder software (http://qpcr.probefinder.com/organism.jsp) from the Universal Probe Library (UPL) Design Center (Roche). Quantitative Real-time PCR (qPCR) was carried out with the iCycler System (BioRad) following the protocol previously described. The sequences of the elongation factors (EF) EEF1A1 (H. sapiens) (Genebank Accession Number NM_001402), EEF1A1 (G. gallus) (Genebank Accession Number NM_204157) and EEF1A2 (C. lupus familiaris) (Genebank Accession Number NM_531877) were used as the reference genes since their expression were validated as being ‘‘not significantly changed’’ throughout all observed time points in the microarray analyses (P-value,0.05). Both absolute and relative quantification analysis were done using comparative Ct (DDCt method). Standard curves for M and EF were generated and the number of copies of M for each virus was calculated relative to 104 copies of corresponding cell line’s EF gene. Relative fold-change of the host virus gene expression were calculated with respect to the mock-infected cells and normalized with the corresponding cell line’s EF gene. Primers and probes used for the virus M and host EF gene are shown in Table S4. The statistical analysis was performed on single and paired samples as appropriate by applying the student t-test using a significance cutoff of P-value, 0.05.

2.3 Bioinformatics analysis of microarray data

2.3.1 Gene expression profiles

GeneSpring GX (version 11) was employed to analyze the data derived from different virus strains infected different cell lines. Normalization was performed using the RMA method, among which (a) per chip normalization to the 50th percentile and (b) per gene normalization where virus-infected samples were normalized to mock infected Samples. Genes were selected for statistical analysis according to the following criteria: (i) only genes that were flagged as present in all three replicates (mock- or virus-infected), and (ii) a fold change $\geqslant$ 2 (up- or down-regulated) between virus- and mock-infected samples in all triplicate microarray experiments. Finally, statistical analysis based on the Benjamini & Hochberg False Discovery method or one-way analysis of variance (ANOVA)was performed with a P-value cutoff of $\leq$ 0.05 to determine significantly expressed genes during virus infection. For data from RSV and influenza A strains infected macrophages, a gene-level analysis in GeneSpring GX (version 11) was applied with signals from probes summarized into gene level. After that, the same normalization and statistical analysis mentioned above were performed step by step by step [156, 364-365].

2.3.2 Functional analysis

Probe sets were clustered by similar expression patterns and analyzed for enrichment of gene ontology (GO) terms and transcriptional factor (TF) binding sites using the Expander (version 5.2) software package [103, 104]. Those probe sets that significantly expressed at least at one time point were uploaded into the software with their corresponding expression fold changes. The enrichment of particular GO terms or TF binding sites within clusters was done by using the TANGO and PRIMA algorithms, respectively, within the Expander package, using a P-value threshold of 0.05. Eventually, the lists of GO terms and TFs were significantly enriched with the corresponding gene probe sets, and the number of genes within each functioned GO term or regulated by TFs along with the p-value are reported.

2.3.3 Core analysis

The key networks, biological functions and canonical pathways were investigated by core analysis using Ingenuity Pathways Analysis (IPA; Ingenuity Systems http://www.ingenuity.com). Those differentially expressed probe sets/genes with known gene-probe ID numbers and corresponding expression fold changes were uploaded into the software. IPA uses a right-tailed Fisher's exact test to calculate P-value for different functional groups, with P-value cut-off of ≤ 0.05.

Chapter III. A Bioinformatics Approach to Detect Virus using Microarray Technology

3.1 Introduction

3.1.1 Background of virus identification based on microarray diagnostic chips

Infectious diseases caused by bacterial and viral pathogens have posed a growing threat to public health and economy. With the recent outbreak of pandemics including Severe Acute Respiratory Syndrome and Swine Influenza A (H1N1), viruses researches have been of grave concern of World Health Organization (WHO). And studies on pathogens identification will be beneficial for the future clinical diagnostics and drug discoveries [105-107].

In past decades, different viral diagnostic techniques have developed rapidly. Among them, DNA microarray as an advanced technique has been widely initiated and applied in broad-based viral diagnosis [42, 108-111]. Various of diagnostic chips such as ViroChip from DeRisi group have been subsequently designed and pioneered [77].

However, the application of microarray technology in viral diagnosis has also posed a challenge to users due to the difficulty in the data interpretation (Wang et al., 2003)[27]. In the process of generating the detection result based on observed hybridization intensity pattern, strong and precise software are necessary and essential for the data analysis. In terms of this demand, several computational strategies such as E-Predict [78], DetectiV [79], PDA [49] and PhyloDetect [82] have been reported for analyzing pathogen diagnostic microarray data. However, only some of these published strategies are built into software which are available to the public. Moreover, these published strategies have been developed based on different hypothesis and algorithms which are dependent on different chips.

In our project, we fabricated the diagnostic microarray chip from Wang et al (2003), and this group also developed E-Predicted software in order to interpret the data retrived from this kind of chip [27]. On this basis, E-Predict was employed to analyze our microarray data. Although the results generated from E-Predict indicated that this software was able to predict the positive outcomes in most of our sample, the negative outcome still existed. Detailed

investigation provided clues that there are two major weaknesses lying in E-Predict: one is regarding to the choices of normalization and scoring functions; the other is the least separation of virus species within the same virus family [77].

To improve the sensitivity of virus detection, a web-accessible novel software called BayesMicro was designed as an alternative analysis tool. In this new strategy, we employed a new calculation formula in which the non-linear relationship between experimental hybridization intensity signals and theoretical binding energy values was taken into consideration. At the meanwhile, we applied an optimized transformation formula in which the outliers with extremely high hybridization intensity signals were treated separately. Besides, a new algorithm was proposed for differential detection on different virus species within the same virus family. Consequently, the virus detection results generated from BayesMicro showed that it was able to report all the positive outcomes in our 12 test arrays, suggesting the effectivity of this novel software.

3.1.2 Description of E-Predict software

E-Predict (http://derisilab.ucsf.edu/epredict/) is the first computation strategy raised together with the corresponding 70-mer oligonucleotides microarray chip by DeRisi group, and it is treated as the default computation strategy to interpret the data retrieved from this ViroChip. Since we fabricated the same diagnostic microarray chip, E-Predict was also employed to analyze our microarray data.

Before calculation of E-Predict, a library of theoretical binding energy profiles, representing species with known genomic viruses sequences until July 2004, was computed by ArrayOligoSelector software [112]. As shown in Table 3.1, all these probe sequences representing different viruses constituted a theoretical binding energy matrix collectively, in which the rows represented different virus species and columns contained different probes.

The evidence provided by Bozdech et al (2003) has proved that the experimental hybridization intensity pattern was closely relevant to the theoretical binding energy profile, especially when the theoretical binding energy values were more significant than -30 (kcal/mol) [112]. Thus, E-Predict

applied several similarity metrics such as Pearson correlation to score the correlation between these theoretical binding energy profiles and the experimental hybridization intensity pattern [78]. In this process, only the theoretical binding energy values with high-level significance (more significant than -30 (kcal/mol)) were considered for the score calculation in order to avoid the false positive results caused by cross-hybridization. In the final detection list, the candidate virus with the higher correlation score presented its higher possibility to be the positive prediction.

Table 3.1 Theoretical binding energy profiles. The rows represent different virus species, and columns contain different probe IDs as well as their corresponding theoretical binding energy values when theoretically hybridize with the specific virus.

Virus species	Probe No.1		Probe No.2		
	Probe_ID	Energy (kcal/mol)	Probe_ID	Energy (kcal/mol	
11809 | Moloney murine sarcoma virus | Retroviridae	9626962_1_rc	-109.4	9626953_2_rc	-67.6	
11663 | Ovine lentivirus | Retroviridae	VirusP70_10147	-16.4	9629258_45	-38.3	
12465 | Barley yellow mosaic virus | Potyviridae	21427654_285_rc	-43	15808065_93	-100.9	
10862 | Xanthomonas phage Cf1c | Inoviridae	9626133_280_rc	-117.1	9790346_172_rc	-19.2	.....
12466 | Barley mild mosaic virus | Potyviridae	21450043_159	-13.9	19749338_224_rc	-108.3	
11665 | Equine infectious anemia virus | Retroviridae	9626530_99	-91.6	9627277_240	-12.3	
10867 | Enterobacteria phage Ike | Inoviridae	20428571_98	-17.9	17426217_142_rc	-19.4	
10868 | Enterobacteria phage If1 | Inoviridae	17426217_142_rc	-22	9630747_113_rc	-95.9	
10869 | Enterobacteria phage I2-2 | Inoviridae	20428571_98	-17.9	17426217_142_rc	-15.5	
.....					

…… indicates that there are more virus species as well as more corresponding probes and theoretical binding energy values existed.

3.1.3 Objective

In our previous researches, we applied E-Predict to analyze our microarray data, however, the detection result were not sensitive to generate positive predictions in all our microarray samples. Thus, proposing another alternative computation strategy is imperative to enhance the reliability of the virus detection results. In this chapter, we aim to describe and evaluate a new software, BayesMicro, in aim to identify virus based on pathogen diagnostic microarray chips. BayesMicro (http://microarray.sbs.ntu.edu.sg/bayes/entry.html) as a web-accessible software is designed based on a novel Bayesian metric and fulfilled in a Perl language environment. This software not only introduces a new strategy for global detection at the virus species level, with new transformation and scoring

formulas proposed, but also initiates a second algorithm for differential detection within the virus families.

3.2 Experiment workflow of pathogen detection

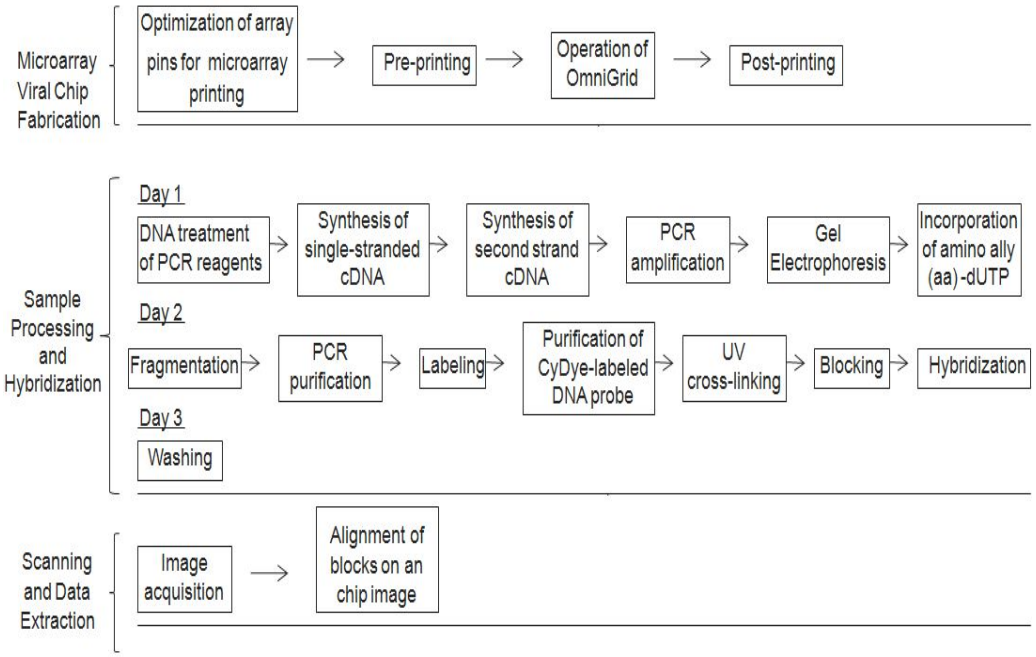

Figure 3.1 The experiment workflow which was performed in DSO national lab. The experiment workflow which was performed in DSO national lab. The experiment procedure can be divided into three parts: (1) Microarray viral chip fabrication; (2) Sample processing and hybridization; (3) Scanning and data extraction.

3.3 Methods

3.3.1 Microarray design

The complete list of viral oligonucleotide sequences represented on the microarray viral chip was downloaded from DeRisi's website (http://derisilab.ucsf.edu/virochip) (Wang *et al*., 2003)[27]. Each virus was represented by top 5 highly conserved oligonucleotides and corresponding 5 reverse complement oligonucleotides. In addition, 10 random oligonucleotides from 10 human genes were selected as controls. In total, 6233 70-mer oligonucleotides that target to around 600 viruses were synthesized (Sigma) and spotted onto microarray glass slides (Full Moon Biosystems) using Omnigrid microarrayer (GeneMachines).

3.3.2 E-Predict analysis procedure

The Genepix results files .GPR contained the raw experimental hybridization intensity value. Before submitted to E-Predict, the .GPR files needed to be pre-processed in order to generate E-Predict standard input files .VDAR for further analysis.

3.3.2.1 Data pre-processing

To convert the .GPR files into the .VDAR files, description rows and columns needed to be deleted first, with only the columns including ProbeID, F532Mean, F532Mean-B532, F532Median, F532Median-B532 and Flags arrayed in order. After that, the flag values corresponding to each row (each spot in microarray chip) in .GPR files were examined for quality control. If the flag value equaled to *-50* or *-100,* which meant that the spot on the array was in bad quality or absent, then all the experimental hybridization intensity value corresponding to this spot were reset to 0 (including F532Mean / F532Mean-B532 / F532Median / F532Median-B532).

Subsequently, the .GPR files were only composed of rows containing experimental hybridization intensity values (each spot on the microarray chip is corresponding to one probe in the .GPR files) (Table 3.2). Lastly, the duplicate experimental hybridization intensity values representing the same probe were averaged, and the .GPR files were split into four separate *.vdar* files as shown in Table 3.3. In this pre-processing procedure, all transformations of data format were fulfilled by our own Perl scripts in Appendix 1.

3.3.2.2 Submission of data

The .VDAR files were submitted to E-Predict, and appropriate parameters were selected (following the default setting) (Figure 3.2). After calculation, virus detection result was listed in an output file, in which top suspected virus families were ranked in order. The scores and P-values corresponding to each virus were shown in the result file, and the probes contributing mostly to the final score of each listed virus were also ranked in order (Figure 3.3).

3.3.3 BayesMicro

The set of theoretical binding energy profiles was employed in BayesMicro for comparison with the matrix of experimental hybridization intensity patterns. Distance scores of each candidate virus were calculated and the virus with the most significant distance score was treated as the positive prediction.

In BayesMicro, the computing procedure for global detection at the virus species level consisted of an initial data transformation, Bayesian model selection, as well as assignment of optimal weights. And the distance scores and P-values were calculated for each candidate virus, with 0.05 set as the threshold P-value in known virus detection. In extreme cases that viruses within the same family showed close distance scores, differential detection within the virus family was introduced as an option to improve the reliability of the detection (Figure 3.4).

Table 3.2 Data arrangement in .GPR files. The .gpr files only contain experimental hybridization intensity values from F532Mean/F532Mean-B532/F532Median/F532Median-B532. Each row corresponds to one probe in microarray chip.

Probe_ID	Experimental hybridization intensitie values			
	F532 Mean	F532 Mean - B532	F532 Median	F532 Median - B532
10120197_13	0	0	0	0
10120197_13_rc	398	307	394	303
10120199_5	0	0	0	0
10120199_5_rc	148.5	65.5	145	62
10120211_14	0	0	0	0
10120211_14_rc	0	0	0	0
10120225_12	279	175	278.5	174.5
10120225_12_rc	0	0	0	0
10120225_6	126	48	107	29
.....				

…… indicates that there are more probes as well as corresponding experimental hybridization intensity values existed.

Table 3.3 Final .VDAR files generated from the .GPR files. (A), (B), (C), (D) are corresponding to the experimental hybridization intensity coming from F532Mean/ F532Mean-B532/ F532Median/ F532Median-B532 respectively.

A

F532Mean						
	Probe No.1	Probe No.2	Probe No.3	Probe No.4	Probe No.5	
Probe_ID	8486125_53	8486125_53_rc	8486125_68	8486129_20	8486129_20_rc	.....
Hybridization intensity	211	369	0	239	4158	

B

F532Mean-B532						
	Probe No.1	Probe No.2	Probe No.3	Probe No.4	Probe No.5	
Probe_ID	8486125_53	8486125_53_rc	8486125_68	8486129_20	8486129_20_rc	.....
Hybridization intensity	97	296	0	132	4077	

C

F532Median						
	Probe No.1	Probe No.2	Probe No.3	Probe No.4	Probe No.5	
Probe_ID	8486125_53	8486125_53_rc	8486125_68	8486129_20	8486129_20_rc	.....
Hybridization intensity	165	361	0	235	4047	

D

F532Median-B532						
	Probe No.1	Probe No.2	Probe No.3	Probe No.4	Probe No.5	
Probe_ID	8486125_53	8486125_53_rc	8486125_68	8486129_20	8486129_20_rc	.....
Hybridization intensity	51	287	0	129	3967	

…… indicates that there are more probes as well as corresponding experimental hybridization intensity values existed.

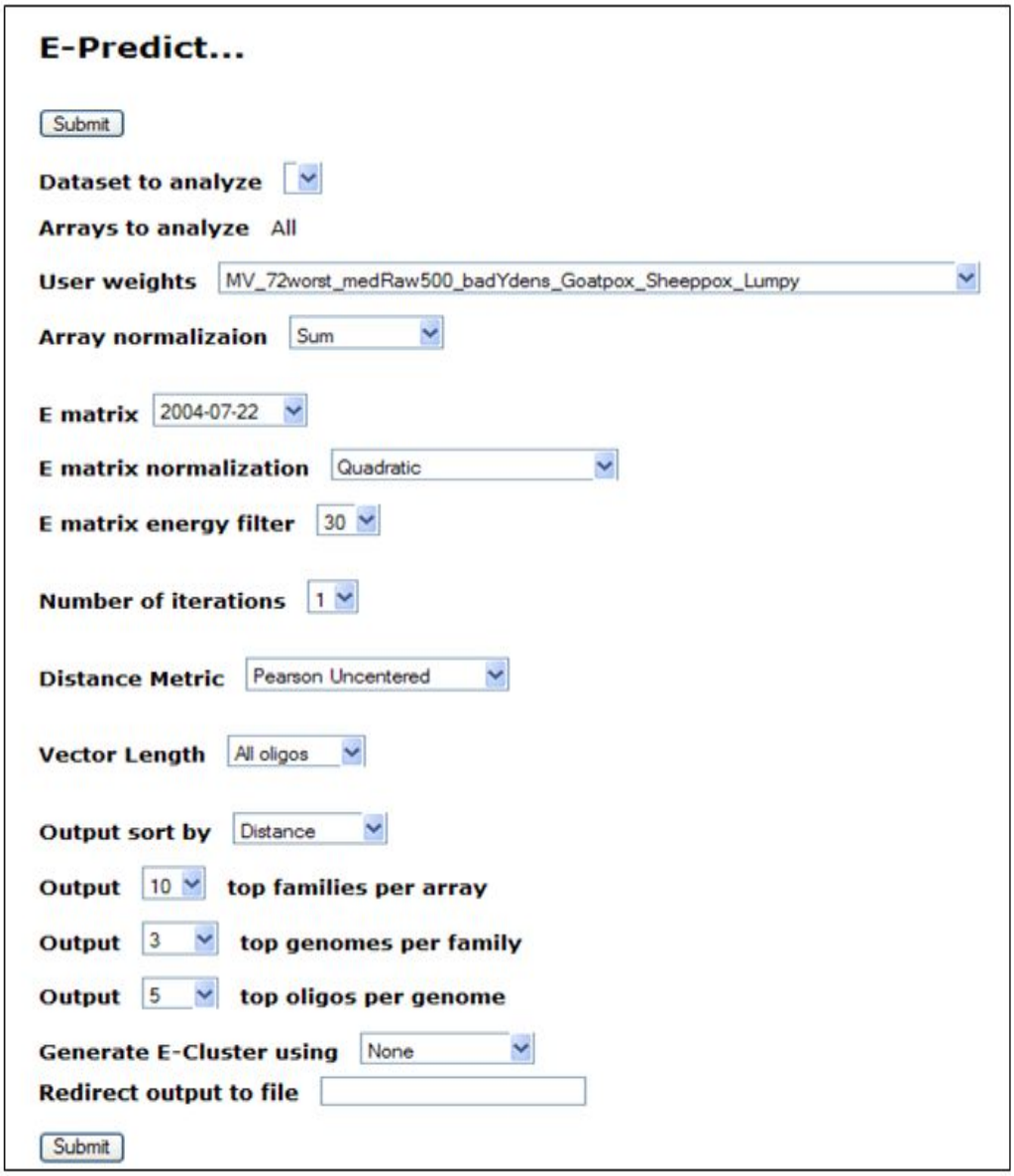

Figure 3.2 User interface of E-Predict. Different normalization methods, similarity metrics and other parameters are offered (adapted from http://derisilab.ucsf.edu/epredict/).

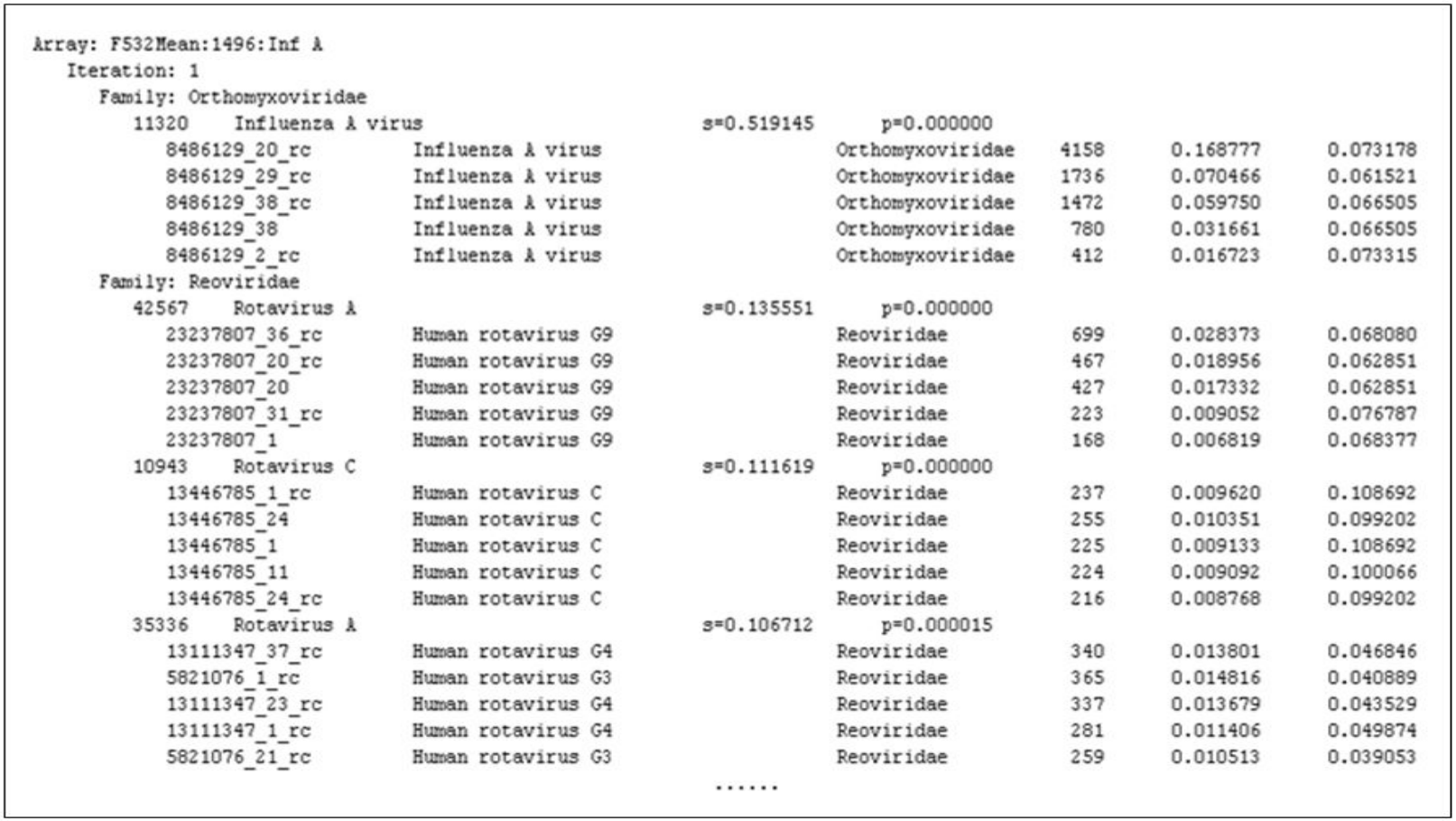

```
Array: F532Mean:1496:Inf A
   Iteration: 1
      Family: Orthomyxoviridae
         11320    Influenza A virus                    s=0.519145      p=0.000000
            8486129_20_rc        Influenza A virus                Orthomyxoviridae    4158      0.168777      0.073178
            8486129_29_rc        Influenza A virus                Orthomyxoviridae    1736      0.070466      0.061521
            8486129_38_rc        Influenza A virus                Orthomyxoviridae    1472      0.059750      0.066505
            8486129_38           Influenza A virus                Orthomyxoviridae     780      0.031661      0.066505
            8486129_2_rc         Influenza A virus                Orthomyxoviridae     412      0.016723      0.073315
      Family: Reoviridae
         42567    Rotavirus A                          s=0.135551      p=0.000000
            23237807_36_rc       Human rotavirus G9               Reoviridae           699      0.028373      0.068080
            23237807_20_rc       Human rotavirus G9               Reoviridae           467      0.018956      0.062851
            23237807_20          Human rotavirus G9               Reoviridae           427      0.017332      0.062851
            23237807_31_rc       Human rotavirus G9               Reoviridae           223      0.009052      0.076787
            23237807_1           Human rotavirus G9               Reoviridae           168      0.006819      0.068377
         10943    Rotavirus C                          s=0.111619      p=0.000000
            13446785_1_rc        Human rotavirus C                Reoviridae           237      0.009620      0.108692
            13446785_24          Human rotavirus C                Reoviridae           255      0.010351      0.099202
            13446785_1           Human rotavirus C                Reoviridae           225      0.009133      0.108692
            13446785_11          Human rotavirus C                Reoviridae           224      0.009092      0.100066
            13446785_24_rc       Human rotavirus C                Reoviridae           216      0.008768      0.099202
         35336    Rotavirus A                          s=0.106712      p=0.000015
            13111347_37_rc       Human rotavirus G4               Reoviridae           340      0.013801      0.046846
            5821076_1_rc         Human rotavirus G3               Reoviridae           365      0.014816      0.040889
            13111347_23_rc       Human rotavirus G4               Reoviridae           337      0.013679      0.043529
            13111347_1_rc        Human rotavirus G4               Reoviridae           281      0.011406      0.049874
            5821076_21_rc        Human rotavirus G3               Reoviridae           259      0.010513      0.039053
                                                      ......
```

Figure 3.3 Final result generated from E-Predict. In this list, influenza A virus ranked top with the highest score. The experimental hybridization intensities from probe 8486129_20rc, 8486129_29_rc and 8486129_38_rc contribute mostly to identify influenza A virus. …..indicates that more viruses with corresponding top 5 probe sets with highest hybridization intensities were detected.

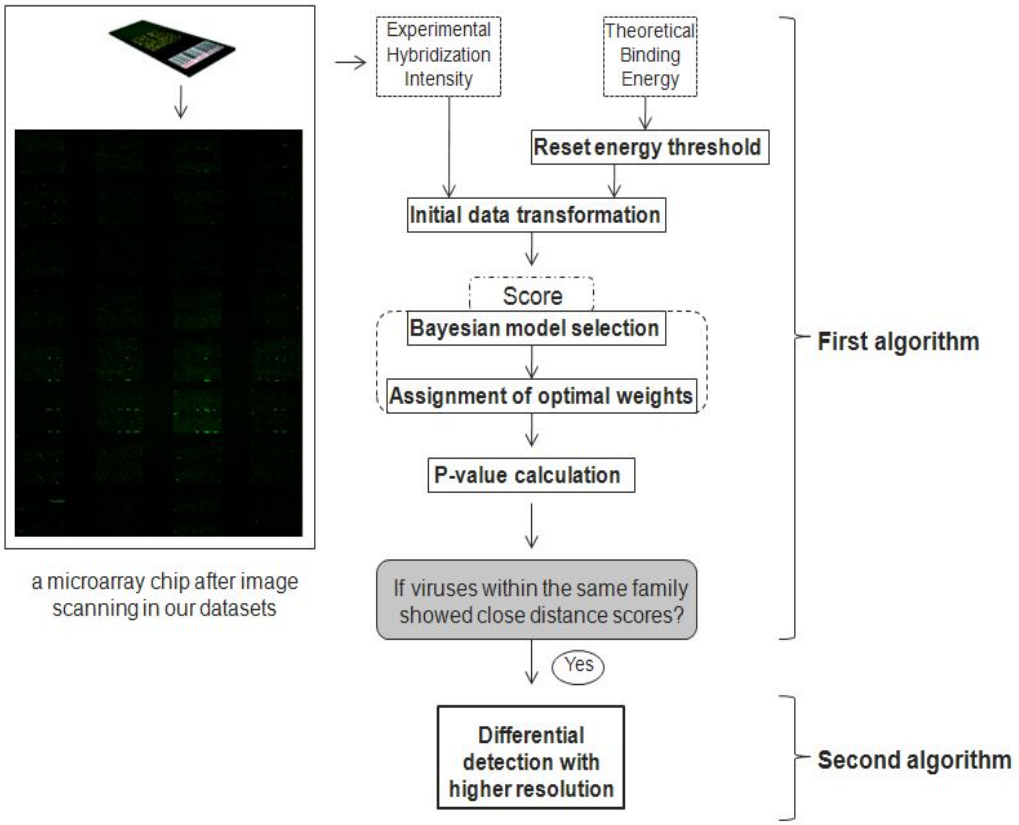

Figure 3.4 An overview of the BayesMicro strategy. Cultured or clinical samples were hybridized to a pathogen diagnostic chip. The experimental hybridization intensity pattern retrieved from microarray chip was compared with a set of theoretical binding energy profiles that was introduced from E-Predict software. Firstly, these two groups of data were transformed into the same scale. Secondly, the distance score and P-values were calculated for each candidate virus on the basis of a Bayesian model with optimal weights assigned. Lastly, the result list was investigated carefully. If the distance scores of viruses within the same family ranked top with close distance scores in this process, a further detection within virus family would be considered to validate the previous virus species identification result.

Table 3.4 Comparison of detection results analyzed based on different thresholds.

Human coronavirus OC43						
Threshold (kcal/mol)	E_Predict			BayesMicro		
	Virus species	Similarity Score	|Distance|	Virus species	Distance Score	|Distance|
-30	**Human coronavirus OC43**	0.1837	0.0230	Avian adeno-associated virus ATCC VR-865	0.2418	
	Bovine coronavirus	0.1607		**Human coronavirus OC43**	0.2679	
-40	**Human coronavirus OC43**	0.1843	0.0236	**Human coronavirus OC43**	0.2679	0.0259
	Bovine coronavirus	0.1607		Murine adenovirus A	0.2938	
-60	**Human coronavirus OC43**	0.1891	0.0265	**Human coronavirus OC43**	0.2679	0.0484
	Bovine coronavirus	0.1626		Ground squirrel hepatitis virus	0.3163	
-70	**Human coronavirus OC43**	0.1969	*0.0292*	**Human coronavirus OC43**	0.2679	*0.1272*
	Bovine coronavirus	0.1677		Bovine coronavirus	0.3951	

Bold represents positive virus; Italic repesents significant result and corresponding threshold.

3.3.3.1 Reset energy threshold

It has been indicated that high cross-hybridization is majorly present in the region where the binding energy is less significant than -30 (kcal/mol) [112]. Thus E-Predict took this information into consideration, and set -30 (kcal/mol) as its default energy threshold in order to avoid the negative effects from cross-hybridization.

In our study, evaluation based on different thresholds were performed, and the detection results based on threshold -70 (kcal/mol) indicated to be most significant. In one typical example shown in Table 3.4, *Human coronavirus OC43* ranked 1st based on threshold -70 (kcal/mol), while this positive virus only ranked 4th based on threshold -30 (kcal/mol) using BayesMicro software. Although the positive virus showed the topmost based on threshold -40 and -60 (kcal/mol), distances of scores between the 1st and 2nd viruses showed smaller compared to the distance of scores based on threshold -70 (kcal/mol). Moreover, the comparison of the detection results using E-Predict software also indicated that the result based on new threshold -70 (kcal/mol) was also most significant. Taken together, the virus detection became more sensitive if we adopt the new energy threshold -70 (kcal/mol) in our cultured samples. Consequently, this default threshold of the energy was raised to -70 (kcal/mol) for our known virus detection in BayesMicro. Under this new threshold -70 (kcal/mol), more cross-hybridization would be ignored, and therefore the virus detection sensitivity would be increased. In the event of unknown virus detection, the threshold could be set with less stringent value.

3.3.3.2 Initial data transformation/normalization

Before calculating the distance scores between the theoretical energy value profiles and experimental hybridization intensity pattern, it was observed that these two groups of data located in different scales: the value of theoretical binding energy profiles varied from 0 to 100 while the value of experimental hybridization intensity varied from 0 to 2,000 (even 5,000). The magnitudes between two groups of data caused the overall comparison to be difficult, so that transforming them into the same level was necessary. In our study, we practiced our data with different transformation formulas, such

as $Xg_{(norm)} = \log_2^{Xg}$, $Xg_{(norm)} = \frac{Xg - \mu_{Xg}}{Var_{Xg}}$, where μ_{Xg} and Var_{Xg} represent the mean and variance of Xg respectively, and the formulas applied in E-Predict $Xg_{(norm)} = \frac{Xg}{\sum Xg}$ and $Xg_{(norm)} = \frac{Xg^2}{\sum Xg^2}$, where $\sum Xg$ and $\sum Xg^2$ represent the sum and quadratic sum of Xg separately. Eventually, the formula (1) performed best, and therefore was adopted in our new strategy:

$$Xg_{(norm)} = \frac{Xg - \mu_{Xg}}{\max(abs(Xg - \mu_{Xg}))} \qquad (1)$$

where Xg and $Xg_{(norm)}$ are the values before or after the transformation of each theoretical binding energy value or experimental hybridization intensity value respectively.

After transformation using this formula (1), all the data in both two groups could be reset to a zero mean sequence, with the maximum absolute value of each sequence reset as 1. Subsequently, these two groups of data enabled to be used for straightforward comparison regardless of the amplitude of change.

When formula (1) was applied in pre-processing the data, it did not perform well as we expected in the experimental hybridization intensity values. Investigation suggested that the instability was originated from the outliers with high value in experimental hybridization intensity value. These outliers are most likely to be given rise by systematic instability or experimental errors on microarray platform [113]. Tracing back to the above equation (1), existence of outliers with high value enabled to increase the value of max(abs(Xg-μg)), and therefore compressed other intensity value too low to reflect its original significance. In order to avoid the negative impact from unexpected outliers with high value, the set of experimental hybridization intensities was pre-process by a package called outliers for R. After that, the right outliers with high value were reset as 1 directly, and the remaining data participated in

transformation. Thus, the final transformation formula used in our strategy is as follows (2):

$$\begin{cases} Xg(norm) = 1\ , & \text{(Outliers with high value)} \\ Xg_{(norm)} = \dfrac{Xg - \mu_{Xg}}{\max(abs(Xg - \mu_{Xg}))}, & \text{(Remaining data)} \end{cases} \quad (2)$$

3.3.3.3 Bayesian model selection

In BayesMicro, the scoring formula was originated from BayesGen deduced by Nguyen *et al* (2009) [114]. In BayesGen, the distances between different genes in different conditions were calculated as a ratio between two alternative hypotheses, so that functionally related genes that had similar expression trends in different conditions could be identified.

In BayesMicro, we considered this formula from another perspective. The purpose of BayesMicro was to calculate the distance between the experimental hybridization intensity pattern and different theoretical binding energy profiles representing different viruses. Finally, the candidate virus with smallest distance between these two conditions was treated as the positive prediction. And the full Bayesian formula is as follows (3-5):

$$d(i,j) = \prod_{k=1}^{n} \frac{p(Xi^k)\,p(Xj^k)}{p(Xi^k, Xj^k)} \propto \sum_{k=1}^{n} logp(Xi^k) + logp(Xj^k) - logp(Xi^k, Xj^k) \quad (3)$$

Where

$$logp(Xi^k) \propto -\log[(Xi^k - m)^2 + \frac{v^k}{2}],\ logp(Xj^k) \propto -\log[(Xj^k - m)^2 + \frac{v^k}{2}] \quad (4)$$

$$logp(Xi^k, Xj^k) \propto -\frac{3}{2}\log[\sigma^k + \frac{2\sigma^k}{\sigma^k + v^k}(\mu^k - m^k)^2 + \frac{v^k}{2}] \quad (5)$$

And m^k, v^k, μ^k and σ^k are the k^{th} component of the data global mean and variance, and the two conditions local mean and variance respectively.

Local mean μ^k and variance σ^k could be generated from Xi (the i^{th} theoretical binding energy) and Xj (the j^{th} experimental hybridization intensity). The global parameters' setting was based on the global condition. After investigation, the global condition contained three elements: (1) experimental

hybridization intensity of the calculated probe; (2) theoretical binding energy coming from the binding between the calculated probe and the candidate virus; (3) theoretical binding energy coming from the binding between the calculated probe and other viruses. For instance, if we calculated the distance between the candidate *Moloney murine sarcoma virus* and the positive virus based on 9626962_1_rc, we considered the theoretical binding energy -109.4 (kcal/mol) and the experimental hybridization intensity of this probe in microarray chip as the local parameters. And the energy such as -84.4 (kcal/mol), -84.1(kcal/mol), -54.4 (kcal/mol), which obtained from the theoretical binding between 9626962_1_rc and other viruses, were treated as other parameters in the global condition [Table 3.5B].

3.3.3.4 Assignment of optimal weights

Weight is the assignment of a quota to a particular segment of the population as a special favor or concession in a proportion. Given matching weights, biased estimates would be obtained for different theoretical binding energy value, and therefore sensitivity of virus detection results would be improved [115, 116]. In the previous formula (7), we assumed that each probe contributed the same to the final distance, however, in reality they did not. As shown in Table 3.6, 18071213_1713_rc showed a more significant theoretical binding energy value -121 (kcal/mol) with *Sinorhizobium meliloti phage PBC5* compared to -40.5 (kcal/mol) with *Bacteriophage phi CTX*, which suggested that more nucleotides in *Sinorhizobium meliloti phage PBC5* could be aligned to this probe theoretically. And *Sinorhizobium meliloti phage PBC5* subsequently had higher probabilities to be responsible for the high hybridization intensity value of probe 18071213_1713_rc detected in microarray chip. Hence, different weights should be assigned to different theoretical binding energy value before final distance score calculation.

We assumed that the probe Pi had a sequence of theoretical binding energy value (P_i^k representing the k^{th} energy of probe Pi) corresponding to different viruses. These theoretical binding energy values followed normal distribution, and the weights were calculated with cumulative distribution function (CDF) (Figure 3.5). From the above assumption, the weight of Pi^k increased when Pi^k was closer to the right tail of the normal distribution curve.

Assignment of optimal weight for each probe was listed in Table 3.6. CDF calculation formula of normal distribution is as follows:

$$\Phi(Pi^k) = \frac{1}{\sqrt{2\pi\int_{-\infty}^{Pi^k} e^{-t^2/2}dt}} = \frac{1}{2}\left[1 + erf\left(\frac{Pi^k - \mu}{\sigma\sqrt{2}}\right)\right] \qquad (6)$$

Where μ, σ equal the mean and standard deviation of the probe Pi.

Apply (6) into (3), (7) was obtained:

$$d(i,j) = \prod_{k=1}^{n} \frac{p(Xi^k)p(Xj^k)}{p(Xi^k, Xj^k)} \propto \sum_{k=1}^{n} \left[\log o(Xi^k) + \log p(Xj^k) - \log(Xi^k, Xj^k)\right] * \Phi(Pi^k) \quad (7)$$

Table 3.5 The theoretical binding energy profile (A) is rearranged by probes (B).

A

Virus species	Probe No.1		Probe No.2		
	Probe_ID	Energy (kcal/mol)	Probe_ID	Energy (kcal/mol)	
11809 | Moloney murine sarcoma virus | Retroviridae	9626962_1_rc	-109.4	9626953_2_rc	-67.6	
11663 | Ovine lentivirus | Retroviridae	VirusP70_10147	-16.4	9629258_45	-38.3	
12465 | Barley yellow mosaic virus | Potyviridae	21427654_285_rc	-43	15808065_93	-100.9	
10862 | Xanthomonas phage Cf1c | Inoviridae	9626133_280_rc	-117.1	9790346_172_rc	-19.2	.....
12466 | Barley mild mosaic virus | Potyviridae	21450043_159	-13.9	19749338_224_rc	-108.3	
11665 | Equine infectious anemia virus | Retroviridae	9626530_99	-91.6	9627277_240	-12.3	
10867 | Enterobacteria phage Ike | Inoviridae	20428571_98	-17.9	17426217_142_rc	-19.4	
10868 | Enterobacteria phage If1 | Inoviridae	17426217_142_rc	-22	9630747_113_rc	-95.9	
10869 | Enterobacteria phage I2-2 | Inoviridae	20428571_98	-17.9	17426217_142_rc	-15.5	
.....					

B

Probe_ID	Virus species	Energy (kcal/mol)
9626962_1_rc	**11809 | Moloney murine sarcoma virus |Retroviridae**	**-109.4**
	11819 | Spleen focus-forming virus | Retroviridae	*-84.4*
	11830 | Murine osteosarcoma virus | Retroviridae	*-81.4*
	11840 | Gibbon ape leukemia virus | Retroviridae	*-54.4*
	44561 | Murine type C retrovirus | Retroviridae	*-84.7*
	11768 | Feline leukemia virus | Retroviridae	*-30.2*
	11786 | Murine leukemia virus | Retroviridae	*-67.5*
	11788 | Abelson murine leukemia virus | Retroviridae	*-67.5*
	11938 | Rauscher murine leukemia virus | Retroviridae	*-75*
	11795 | Friend murine leukemia virus | Retroviridae	*-80.3*
	11802 | Murine sarcoma virus | Retroviridae	*-109.4*
9625875_4939	10320 | Bovine herpesvirus 1 | Herpesviridae	-41.9
	10325 | Cercopithecine herpesvirus 1 | Herpesviridae	-45.3
	10326 | Equine herpesvirus 1 | Herpesviridae	-32.3
	10335 | Human herpesvirus 3 | Herpesviridae	-125.2
	10397 | Tupaia herpesvirus | Herpesviridae	-32.7
.....		

Bold represents candidate virus and the corresponding theoretical binding energy; Italic representsother viruses and their corresponding theoretical binding energy. …… indicates that there are more probes as well as corresponding experimental hybridization intensity values existed.

Table 3.6 Calculation of the weights for each theoretical binding energy value.

Probe_ID	Virus species	Energy (-kcal/mol)	Weights
18071213_1713_rc	Bacteriophage phi CTX | Myoviridae	40.5	**0.158616**
	Sinorhizobium meliloti phage PBC5 | NA	121	**0.841384**
20066014_8	Grapevine fanleaf virus satellite RNA | NA	61.8	**0.47685**
	Rift Valley fever virus | Bunyaviridae	17.4	**0.116034**
	Arabis mosaic virus satellite RNA | NA	113	**0.894933**
9626510_77	Invertebrate iridescent virus 6 | Iridoviridae	19.2	**0.404081**
	Macroptilium yellow mosaic virus | NA	13.9	**0.326376**
	Yam mosaic virus | Potyviridae	15.8	**0.353557**
	Apple latent spherical virus | Sequiviridae	13.9	**0.326376**
	Acholeplasma phage L2 | Plasmaviridae	87.9	**0.992807**
	Melanoplus sanguinipes entomopoxvirus | Poxviridae	15.1	**0.343431**
	Tobacco leaf curl Yunnan virus associated DNA 1 | Nanoviridae	12.1	**0.301468**
9626818_223_rc	Cryphonectria hypovirus | Hypoviridae	28.5	**0.241017**
	Cryphonectria hypovirus 1 | Hypoviridae	107.2	**0.921462**
	Mycobacterium phage L5 | Siphoviridae	28.2	**0.23847**
	.....		

Bold represents assignment of weights to each probe. …… indicates that there are more theoretical binding energy values and corresponding weights coming from the theoretical hybridization between different probes and different viruses.

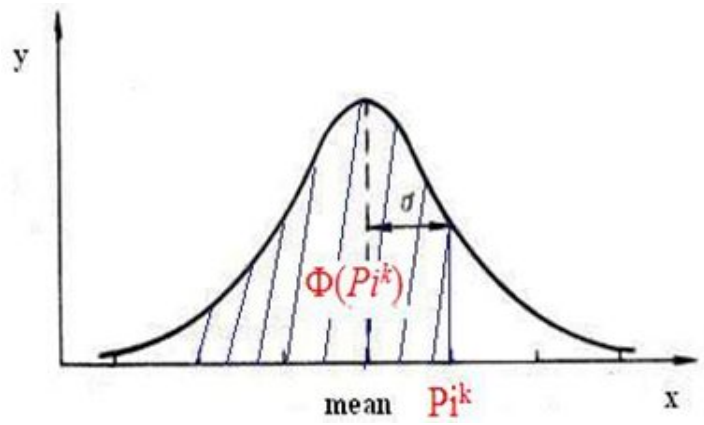

Figure 3.5 A normal distribution curve. We assume that the sequence of theoretical binding energy of each probe follows normal distribution, and CDF ($\Phi(Pi^k)$) of individual energy value (Pi^k) represents its relative weight.

Table 3.7 Transformation of the matrix of theoretical binding energy. The original matrix of theoretical binding energy (A) was transformed into another format, with each probe only representing a specific virus (B).The new matrix of theoretical binding energy was sorted by different virus families (C).

A

Probe_ID	Virus species	Energy (kcal/mol)
8486125_53_rc	11320 | Influenza A virus | Orthomyxoviridae	-75.2
	157924 | Streptococcus mitis phage SM1 | NA	-14.3
	51677 | Xestia c-nigrum granulovirus | Baculoviridae	-16
	85106 | Adeno-associated virus 1 | Parvoviridae	-14.9
	165803 | Cypovirus 1 | Reoviridae	-16.4
	39443 | Carnation Italian ringspot virus | Tombusviridae	-14.9
8486125_61	66266 | Rice grassy stunt virus | NA	-13.1
	11320 | Influenza A virus | Orthomyxoviridae	-93.5
	43141 | Watermelon silver mottle virus | Bunyaviridae	-14.8
	10821 | Maize streak virus | NA	-15
	10837 | Digitaria streak virus | NA	-15
8486150_76	39116 | Leishmania RNA virus 2-1 | Totiviridae	-11.7
	11520 | Influenza B virus | Orthomyxoviridae	-94.9
	75747 | Fusarium poae virus 1 | Partitiviridae	-13
	98832 | Influenza B virus | Orthomyxoviridae	-51.9
325301_20	223287 | Mungbean yellow mosaic India virus | NA	-18
	69263 | Cowpea golden mosaic virus | NA	-18
	164038 | Soybean yellow mosaic virus | NA	-15.9
	11555 | Influenza C virus | Orthomyxoviridae	-95.2
	……	

B

Probe_ID	Virus species	Energy (kcal/mol)
8486125_53_rc	11320 | Influenza A virus | Orthomyxoviridae	75.2
8486125_61	11320 | Influenza A virus | Orthomyxoviridae	93.5
8486150_76	11520 | Influenza B virus | Orthomyxoviridae	94.9
325301_20	11555 | Influenza C virus | Orthomyxoviridae	95.2
	……	

C

Virus family	Virus species	Probe No.1	Probe No.2	Probe No.3	Probe No.4	
Orthomyxoviridae	**Influenza A virus**	**8486125_53**	**8486125_53_rc**	**8486125_61**	**8486125_61_rc**	
	Influenza B virus	*8486150_76*	*8486150_76_rc*	*8486152_19*	*8486152_19_rc*	
	Influenza C virus	*325301_20*	*325301_20_rc*	*325301_24*	*325301_24_rc*	
Astroviridae	Avian nephritis virus	20514394_152	20514394_152_rc	20514394_160	20514394_160_rc	……
	Human astrovirus	9630726_114	9630726_114_rc	9630726_147	9630726_147_rc	
	Ovine astrovirus	9635572_149	9635572_149_rc	9635572_204	9635572_204_rc	
	Turkey astrovirus	9635576_163	9635576_163_rc	9635576_172	9635576_172_rc	
……						

Bold represents positive virus and the corresponding probes; Italic represents negative positive viruses and the corresponding probes. …… indicates that there are more theoretical binding energy values and corresponding weights coming from the theoretical hybridization between different probes and different viruses.

3.3.3.5 Statistical significance

A total of 38 independent microarrays consisting of hybridizations including either virus infected samples or mock-infected samples were all treated as the training datasets, and the distance scores were calculated one by one using the scoring formula (7). In our study, it was assumed that any given virus was present in only a small fraction in all the samples, thereby the empirical distributions were representatives of the true negative distance scores. Parameters of the null distributions were estimated as the mean and standard deviation of the observation, and the P-values corresponding to different distance scores were calculated based on these two parameters. The similar assumption was also made by others [49, 78]. For known virus detection, the cutoff for the P-value is set at 0.05, indicating that P-value less than 0.05 signifies a positive prediction. However, the cutoff can be less stringent in the case for unknown virus detection depending on the performance of the hybridization.

3.3.3.6 Differential detection within virus families

Generally, global virus detection at virus species level with previous scoring method is sufficient to reach the positive predictions, however, false positives may still occur in some occasions. These false positives are always given rise by the conserved sequences of viruses within the same family. The similarity of these conserved sequences may lead to similar theoretical binding energy profiles [50], and therefore the similar distance scores. Consequently, another algorithm was proposed to identify the positive virus within a specific virus family.

Before the calculation, the theoretical binding energy profiles needed to be transformed into another format. In the original matrix of theoretical binding energy profiles, each probe targeted to more than one virus with different theoretical binding energy values considered (Table 3.7A). However, each probe was treated to be unique to one virus which was corresponding to the highest theoretical binding energy value (Table 3.7B). Finally, all virus genus represented by their specific probes were sorted based on their virus families (Table 3.7C). After the transformation of the matrix of theoretical binding energy profiles, viruses within the interested virus family were scored and the

one with most significant score was treated as the positive prediction. When it came to score the specific virus Gi like *Influenza A virus*, two groups of data needed to be extracted out. One group contained experimental hybridization intensities from the probes which were identical to the predicted virus Gi (*Influenza A virus*), the other group was composed of experimental hybridization intensities from the probes which were identical to all other viruses in the same family (Gn, n=1 to j, and n ≠ i) (*Influenza B virus* and *Influenza C virus*) (Table 3.7C). Finally, we assumed that these two groups of data followed normal distribution and did one-tail t-test.

$$H_0 : \mu_0 \succ \mu_1 , \qquad H_1 : \mu_0 \leq \mu_1$$

$$X = \frac{\mu_0 - \mu_1}{\sqrt{\frac{\sigma_0^2}{n_0}} + \sqrt{\frac{\sigma_1^2}{n_1}}} \sim N(0,1) \qquad \Phi(X) = \frac{1}{\sqrt{2\pi}} e^{-\frac{1}{2}X^2} \qquad (12)$$

Where μ_0, σ_0 equal the mean and standard deviation of experimental hybridization intensities of Gi (candidate virus), and μ_1, σ_1 represent the mean and standard deviation of experimental hybridization intensities of Gn (all other viruses in the same family, excluding the candidate virus).

3.4 Results

3.4.1 Comparison of different parameters in E-Predict and BayesMicro

We applied the same chip fabrication system from DeRisi's group to validate 12 cultured samples, and the observed hybridization intensity pattern was analyzed using E-Predict software. In terms of the detection results, we observed that E-Predict was not sensitive enough to obtain the positive prediction in all our samples.

These false positive predictions maybe due to its weak algorithm especially lying in the normalization and scoring functions, which has also been proposed by other group [77]. It is well known that the outliers with high value are easily generated by systematic instability or experimental errors in high through-put system like microarray [113]. However, the normalization function in E-Predict software did not take these outliers with high experimental

hybridization values into consideration so that it was easy to lead to serious compression of other experimental hybridization values in this process. When the over-compressed experimental hybridization values participated into further calculation, their corresponding result was not significant.

As to the scoring function, traditional correlation methods such as uncentered Pearson correlation and Euclidean distance were employed to describe the similarity between the experimental hybridization intensity pattern and the theoretical binding energy profiles. However, these metrics assume normal distribution of the data and linear association between these two groups of data, and it may not be the case for high-throughput expression data [117-120].

Accordingly, the software BayesMicro was pioneered as an alternative virus detection strategy in order to improve the result sensitivity in our study. In BayesMicro, new transformation formula was involved with considering the outliers with high experimental hybridization intensity values. Besides, the distances between the experimental hybridization intensity pattern and the theoretical binding energy profiles were defined based on a Bayesian model, which explained the inherent nonlinearity in high-throughput expression data more effectively than E-Predict. This model was able to handle the weakness in E-Predict by measuring the nonlinear relationship between two groups of data more precisely. Furthermore, involvement of stringent theoretical binding energy threshold and assignment of optimal weighs enhanced the detection accuracy of BayesMicro.

It has been also revealed that E-Predict provided the best separation in between family comparisons and the least separation within families [77]. To solve this issue, differential detection within virus family as another optional method was also designed for further separation of viruses within the same family (Table 3.8).

Table 3.8 Comparison of different parameters used in E-Predict and BayesMicro.

Parameters	E-Predict	BayesMicro
Original data	Theoretical binding energy value Experimental hybridization intensities	
Energy threshold (kcal/mol)	30	70
Transformation formula	$Xg_{(norm)} = \frac{Xg}{\sum Xg}$ $Xg_{(norm)} = \frac{Xg^2}{\sum Xg^2}$	$Xg_{(norm)} = \frac{Xg - \mu_{Xg}}{\max(abs(Xg - \mu_{Xg}))}$
Score calculation	Uncentered pearson correlation (default)	Bayesian algorithm
Assignment of weights	X	√
Detection further at genus level	X	√

3.4.2 Validation of E-Predict and BayesMicro

Based on our 12 culture samples, the analysis was performed using E-Predict and BayesMicro, and the virus detection results were summarized in Table 3.9. The results list suggested that E-Predict was able to generate good predictive outcomes in majority of the samples. However, the false positives still occurred in some cases.

When it came to BayesMicro, it was capable to generate good predictive outcomes in all cultured samples, either with topmost ranking or topmost 10 ranking. In summary, comparison of the virus detection results between these two software demonstrated that BayesMicro software performed better than E-Predict software. The clinical samples infected with influenza A virus were also accessible, with the good predictive outcomes with topmost ranking generated based on both BayesMicro and E-predict software.

Table 3.9 Summary of results from E-Predict and BayesMicro.

Sample Virus	Strains / Species	*E-Preidict*	*BayesMicro*
Yellow fever virus	17D	√ (top)	√ (top)
Japanese encephalitis virus	Nakayama	√ (top)	√ (top)
Influenza A virus	H3N2	√ (top)	√ (top)
Coronavirus	OC43	√ (top)	√ (top)
Chikungunya virus	Oka	√ (top)	√ (top)
Influenza B virus	Lee	√	√ (top)
Influenza A virus	H1N1	√	√(top)
Rhinovirus	Type 14	√	√
Mouse poxvirus	Moscow	√	√
Vaccinia virus	Lister	X	√
Cowpox virus	Brighton	√ (top)	√
Measles virus	Edmonton	√ (top)	√

√ (top) represents positive virus ranked 1st, √ represents positive virus ranked in top 10, and X erpresetns positive virus was not able to be detected in top 10.

3.4.3 Global detection at virus species level

In general, the virus detection results from both E-Predict and BayesMicro showed similar. And in most cases, both these software could identify the positive viruses with the topmost ranking based on either similarity/distance score or P-value. These situations happened in samples infected with yellow fever virus and Japanese encephalitis virus. Nevertheless, BayesMicro enabled to generate better predictive outcomes than E-Predict in some specific cases. For example, E-Predict reported false positive results while BayesMicro reported positive results in vaccinia virus infected samples; In other samples infected with influenza A virus (H1N1) and influenza B virus, E-Predict reported the positive virus with ranking only in top 10 list while BayesMicro reported the positive virus with topmost ranking.

Table 3.10 Virus detection in samples infected with Yellow fever virus.

Yellow fever virus					
E_Predict			**BayesMicro**		
Virus species	Similarity Score	P-value	Virus species	Distance Score	P-value
Yellow fever virus	0.725751	0.000024	**Yellow fever virus**	-0.9897	0.0019
Yokose virus	0.364157	0.000212	Goose parvovirus	0.7222	0.0687
Alkhurma virus	0.134815	0.001421	Avian adeno-associated virus	0.8095	0.0783
Human rhinovirus B	0.036516	0.017790	Hepatitis E virus	0.8904	0.088
Human papillomavirus type 16	0.033311	0.030380	Adeno-associated virus 3	0.8927	0.0883
Human papillomavirus type 45	0.031912	0.018666	Adeno-associated virus 3B	0.8927	0.0883
Human papillomavirus candHPV85	0.031321	0.056718	Adeno-associated virus 4	0.9156	0.0912
Vaccinia virus	0.030069	0.002261	Adeno-associated virus 6	0.9311	0.0932
Variola virus	0.030044	0.001849	Adeno-associated virus 1	0.9357	0.0938
Rotavirus A	0.029861	0.000980	Influenza B virus	0.9460	0.0951

Bold represetns positive virus in the culture sample.

Table 3.11 Virus detection in samples infected with Japanese encephalitis virus.

Japanese encephalitis virus					
E_Predict			**BayesMicro**		
Virus species	Similarity Score	P-value	Virus species	Distance Score	P-value
Japanese encephalitis virus	0.284751	0.000040	**Japanese encephalitis virus**	0.1182	0.0242
Langat virus	0.131216	0.001382	Goose parvovirus	0.7327	0.0698
Tick-borne encephalitis virus	0.099022	0.002316	Avian adeno-associated virus	0.8125	0.0787
Human herpesvirus 1	0.088655	0.022517	Adeno-associated virus 3	0.8382	0.0817
Human rhinovirus B	0.085275	0.002020	Adeno-associated virus 3B	0.8382	0.0817
Lake Victoria marburgvirus	0.082579	0.000002	Hepatitis E virus	0.8423	0.0821
Human papillomavirus type 35	0.081080	0.000859	Influenza B virus	0.8451	0.0825
Human papillomavirus type 31	0.079259	0.001120	Adeno-associated virus 4	0.8728	0.0858
Human papillomavirus type 83	0.072836	0.003245	Adeno-associated virus 1	0.8762	0.0862
Variola virus	0.068256	0.000138	Adeno-associated virus 6	0.8950	0.0886

Bold represents positive virus in the culture sample.

Table 3.12 Virus detection in samples infected with Influenza B virus.

Influenza B virus					
E-Predict			BayesMicro		
Virus species	Similarity Score	P-value	Virus species	Distance Score	P-value
Human herpesvirus 7	0.204744	0.006595	**Influenza B virus**	0.3280	0.0358
Human papillomavirus type 29	0.187067	0.000161	Swinepox virus	0.5622	0.0534
Influenza B virus	0.153455	0.000013	Rotavirus A	0.6983	0.0662
Rotavirus A	0.087591	0.000031	Goose parvovirus	0.7340	0.0700
Human rhinovirus B	0.082278	0.002224	Avian adeno-associated virus	0.8129	0.0787
Swinepox virus	0.076707	0.000005	Adeno-associated virus 3	0.8361	0.0814
Monkeypox virus	0.069625	0.000159	Adeno-associated virus 3B	0.8361	0.0814
Vaccinia virus	0.066680	0.000193	Hepatitis E virus	0.8363	0.0814
O'nyong-nyong virus	0.043176	0.002038	Adeno-associated virus 4	0.8576	0.0840
Igbo Ora virus	0.052584	0.001241	Adeno-associated virus 6	0.8742	0.0860

Bold represents positive virus in experimental sample.

3.4.3.1 E-Predict and BayesMicro both indicated good predictive outcomes

For virus detections in cultured samples such as samples infected with yellow fever virus and Japanese encephalitis virus, both E-Predict and BayesMicro were able to generate the positive prediction with topmost ranking (Table 3.10-3.11).

3.4.3.2 BayesMicro performed better than E-Predict

Apart from generating similar positive predictions in some cases, BayesMicro performed better than E-Predict in some other cases. Taken the sample infected with influenza B virus as an example, BayesMicro could highlight the positive virus with topmost ranking, while E-Predict could only identify the positive virus with 3rd ranking in the result list (Table 3.12).

3.4.4 Differential detection within virus families

In general, global detection at virus species level using E-Predict and BayesMicro was able to generate good predictive outcomes in majority of microarray samples. However, sometimes false positive viruses that belonged to the same virus family as the positive virus still turned up in the result list. Thus differential detection within virus families was necessary to enhance the reliability of the detection result.

In cultured sample with infection of influenza A virus (H1N1), E-predict was not able to identify the positive virus in the top 10 list while BayesMicro was able to (Table 3.13A). In the result list from BayesMicro, influenza B virus and influenza C virus from the same virus family showed similar distance scores as influenza A virus (H1N1). Therefore, differential detection using

BayesMicro was involved for further validation with higher resoluation and the result suggested that influenza A virus (H1N1) was scored as more significant when compared to false positive influenza B virus and influenza C virus (Table 3.13B).

In another cultured sample infected with vaccinia virus, the good predictive outcome was able to be generated by BayesMicro but not E-Predict (Table 3.14A). Careful evaluation of the BayesMicro result list demonstrated that several poxviruses such as ectromelia virus, cowpox virus and monkeypox virus occupied the top 6 positions with close distance scores. Accordingly, differential detection up within virus families was employed again for further investigation, and the ranking of positive vaccinia virus was consequently improved to 2nd position (Table 3.14B).

Taken together, the method for differential detection within virus families performed effective in our experiment data. And BayesMicro software showed better ability to identify the positive prediction than E-Predict software.

Table 3.13 Virus detection in samples infected with influenza A virus (H1N1). (A) Result from E-Predict and BayesMicro up to virus species level. (B) Result from BayesMicro up to virus genus level.

A

Influenza A virus (H1N1)					
E-Predict			**BayesMicro**		
Virus Name	Similarity Score	P-value	Virus Name	Distance Score	P-value
Human papillomavirus type 31	0.134401	0.000252	*Influenza B virus*	0.5537	0.0526
Human papillomavirus type 35	0.132109	0.000224	Cercopithecine herpesvirus 1	0.6022	0.0569
Human papillomavirus type 84	0.104200	0.001941	*Influenza C virus*	0.7254	0.0691
Human rhinovirus A	0.103603	0.030498	**Influenza A virus**	0.7428	0.0709
Human herpesvirus 5	0.094070	0.023582	Goose parvovirus	0.7483	0.0715
Western equine encephalomyelitis virus	0.080259	0.000044	Rotavirus B	0.7576	0.0725
Rotavirus A	0.079643	0.000034	Adeno-associated virus 3	0.7628	0.0731
Variola virus	0.079222	0.000081	Adeno-associated virus 3B	0.7628	0.0731
Vaccinia virus	0.078441	0.000110	Hepatitis E virus	0.7680	0.0736
Swinepox virus	0.077090	0.000005	Porcine adenovirus A	0.7720	0.0741

B

Virus species	Score
Influenza A virus	0.3938
Influenza B virus	0.3986
Influenza C virus	NA

Bold represents positive virus in the sample; Italic represents false positive viruses in the sample. NA means that the hybridization intensities of the candidate virus are lower than the background hybridization intensities within its virus family.

3.5 Discussion

3.5.1 Improve theoretical binding energy database

The existing library of theoretical energy profiles was created in July 2004 with only 1,229 viral genomes available [78]. And until November 2012, there were 4314 reference sequences for 3027 viral genomes accessible in viral genome database. According to this information, ArrayOligoSelector will be employed to calculate the theoretical binding energy profiles of other viruses which were not included in viral genome database of July 2004. Consequently, we can broaden the spectrum of virus detection.

In addition, a couple of viruses may co-infect the same sample. In this case, the global experimental hybridization intensity pattern would become an overlapping pattern, and this overlapping pattern with more noisy background will make the virus identification more difficult. To improve the virus detection in these co-infected samples, a database which contains the overlapping theoretical binding energy profiles from any of two or more viruses may be constructed.

3.5.2 Future validation and expansion

Our results showed that BayesMicro could generate good predictive outcomes in most of our experiments. When compared to E-Predict, sometimes it could perform as well as E-Predict while sometimes BayesMicro could generate more sensitive detection results. Although the evaluation of BayesMicro showed effective, the test datasets were still limited in amount. Actually, we did quite a lot experiments, however, some of these experiment were performed based on the same batch of sample and I only repsented and summarized the typical results in my result table. In the future, more cultured as well as clinical samples would be involved in further evaluating the performance of BayesMicro.

Table 3.14 Virus detection in samples infected with vaccinia virus. (A) Result from E-Predict and BayesMicro up to virus species level. (B) Result from BayesMicro up to virus genus level.

A

Vaccinia virus					
E-Predict			BayesMicro		
Virus Name	Similarity Score	P-value	Virus Name	Distance Score	P-value
Ectromelia virus	0.271197	0.000001	Ectromelia virus	0.1757	0.0270
Monkeypox virus	0.267852	0.000001	Cowpox virus	0.2695	0.0322
Cowpox virus	0.267486	0.000001	Monkeypox virus	0.3131	0.0348
Human papillomavirus type 1a	0.224844	0.000007	**Vaccinia virus**	0.3616	0.0380
Bunyamwera virus	0.095440	0.000003	Variola virus	0.4067	0.0411
Human herpesvirus 7	0.094832	0.027603	Camelpox virus	0.4198	0.0420
TTV-like mini virus	0.093180	0.000161	Goose parvovirus	0.7274	0.0693
Human rhinovirus A	0.066377	0.060127	Avian adeno-associated virus A	0.8111	0.0785
Human rhinovirus B	0.063706	0.004539	Hepatitis E virus	0.8555	0.0837
Human rhinovirus sp.	0.056507	0.000604	Adeno-associated virus 3	0.0842	0.0843

B

Virus species	Score
Monkeypox virus	0.3557
Vaccinia virus	0.3582
Ectromelia virus	0.3588
Cowpox virus	0.3707
Variola virus	0.3754
Camelpox virus	0.3917
Goatpox virus	NA
Fowlpox virus	NA
Lumpy skin disease virus	NA
Molluscum contagiosum virus	NA
Sheeppox virus	NA
Swinepox virus	NA
Yaba-like disease virus	NA

Bold represents positive virus in the sample; Italic represents false positive viruses in the sample. NA means that the hybridization intensities of the candidate virus are lower than the background hybridization intensities within its virus family.

3.5.3 Comparison with E-Predict

In our study, a viral diagnostic chip was fabricated based on the design from Wang et al (2003) [27], and we used the E-Predict as the default software to analyze microarray data. However, we were not able to generate good predictive diagnostic outcomes in all our viral samples. These false positive results may be due to the internal weakness of the software which is no physical justification of their choices of normalization and scoring functions [77]. Thus a new software called BayesMicro was developed in our study. In the BayesMicro, several aspects were improved: (1) the transformation formula was optimized for accurate comparison between two groups of data, and

outliers with high value were filtered out in order to prevent their negative influence; (2) the distance calculation formula based on Bayesian model was employed to interpret the inherent non-linear relationship between experimental hybridization and theoretical binding energy; (3) the assignment of weights to each theoretical binding value was performed in order to enhance the accuracy of the outcome; (4) P-values could be calculated based on a batch training datasets composing of 38 independent microarrays, and the P-value less than 0.05 is treated as a significant detection; (5) a second algorithm used to differential detection within virus families were proposed for further separation.

In addition, E-Predict software is only available as a CGI script for Unix/Linux platforms and the installment has to be performed by a professional computation user. In contrast, BayesMicro requires no setup and configuration. A website is established under an apache server which can be easily accessed through http://microarray.sbs.ntu.edu.sg/bayes/entry.html.

3.5.4 Comparison with other existing strategies

We compared the statistical methods of BayesMicro with other existing algorithms for virus detection based on pathogen diagnostic microarray chips. Notably, these algorithms are all different from our BayesMicro in which a Bayes formula is employed as the final scoring function. This function is applied to calculate the distance scores between the examined experimental hybridization intensity pattern and the profiles of theoretical binding energy which represents different viruses.

3.6 Conclusion

Overall, we developed a novel software called BayesMicro. In this software, a new algorithm for virus detection based on virus species level was proposed and it was proved to be different from any other existing systems. In this new algorithm, an optimized transformation formula and a new scoring formula were employed to investigate the relationship between theoretical binding energy profiles and experimental hybridization intensity pattern. Moreover, the weights were also assigned to each theoretical binding value in order to enhance the accuracy of the outcome.

Furthermore, another algorithm was also established for differential detection on virus species within the same virus family. Thus, the implementation of BayesMicro software provided the possibility to further separate the viruses within the same family following the initial virus species detection on the same viral chip. To date, although some microarray diagnostic chips have been developed to identify the viruses within the same family, the application of these chips has been limited to virus-species. On the basis of this new algorithm, BayesMicro can be easily applied to separate the viruses within the same family following the initial virus species detection on the same viral chip.

Application of BayesMicro and E-Predict to a dataset of cultured samples suggested the superior performance of BayesMicro when compared to E-Predict, with BayesMicro generating 12 positive predictions out of 12 samples but E-Predict generating 10 positive predictions out of 12 samples. These data suggested that BayesMicro can be applied in virus detection based on diagnostic microarray chip as a reliable analysis tool.

Finally, this software can be easily accessed via the internet (http://microarray.sbs.ntu.edu.sg/bayes/entry.html) and its application easy to use, including users without computation background.

Chapter IV. Respiratory Syncytial Virus

4.1 Introduction

Human respiratory syncytial virus (HRSV), which causes infection of the lungs and breathing passages, is a major cause of lower respiratory tract infections in infancy and childhood. It has been reported by WHO that RSV results in around 64 million infections and 160,000 deaths in the worldwide annually. And the risk for severe illness or even fatality always lie in the children with underlying problems such as bronchopulmonary dysplasia as well as patients with compromised immune systems. Moreover, RSV, as a significant pathogen in bone marrow transplant recipients, is one of the most widespread nosocomial infections [121]. Till now, more effective antiviral drugs and a vaccine for protection of the general population from infection of RSV are still lacking [122].

4.1.1 Virus structure

RSV that belongs to the subfamily *Pneumovirinae* under *Paramyxoviridae* family, is an enveloped virus with a 15.2kbp, negative sense, single-stranded RNA genome. The 10 genes encode 11 proteins including non-structural protein 1 (NS1), non-structural protein 2 (NS2), nucleo- (N) protein, phosphor- (P) protein, matrix (M) protein, small hydrophobic (SH) protein, glyco- (G) protein, fusion (F) protein, M2-1 and M2-2, and the large (L) protein arrayed orderly from 3' to 5' direction [Figure 4.1]. Based on their specific functions, these viral proteins can be grouped into several categories. For instance, G, F, M and SH proteins are functional associated with the viral envelop: G protein functions on virus attachment; F protein promotes virus penetration and benefits host cells fusion; M protein is responsible for virion morphogenesis and traffics between the cytoplasm and the nucleus; SH protein plays an essential role in viral infectivity. Other five proteins including N, P, M2-1, M2-2, and L protein participate in synthesis of RNA and formation of the ribonucleocapsid structure: N protein associates with genomic RNA forming the nucleocapsid; M2 protein is the second matrix protein required for transcription; L protein encodes RNA polymerase; P protein is a co-factor for L protein. The two accessory proteins,

NS1 and NS2, are involved in the inhibition of the α/β interferon (IFN) activity in the host response [123, 124].

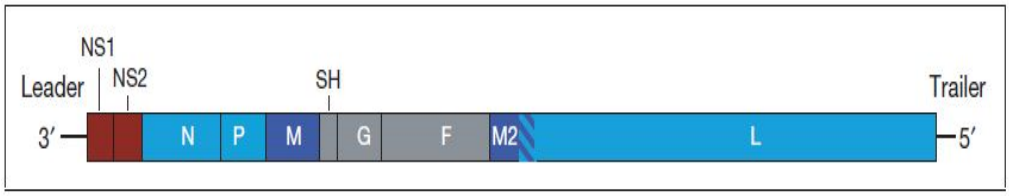

Figure 4.1 The structure organization of RSV genome (adapted from Sugrue RJ, 2006)[125].

Among these proteins, three membrane proteins including F, G and SH protein are embedded in the lipid membrane derived from the host cell. All these three transmembrane glycoproteins are incorporated into virions. F protein is initially translated into F0, an inactive precursor, which is then endoproteolytically cleaved into two disulfide linked subunits, F1 and F2. Subsequently, the highly conserved hydrophobic N-terminus of F1 protein is exposed to mediate the fusion of host cells. G protein consisting of 298 amino acids has been reported to interact with heparin/heparin sulfate. Function of the third small SH protein is still unclear from previous researches. Several isoforms including SH0, SHg, SHp, SHt have been detected during virus infection [126].

The mature and infectious RSV particle comprises a ribonucleoprotein (RNP) complex which is consisted of viral genome RNA (vRNA), N, P and L protein. The lipid envelop derived from host cell surrounds the RNP. An additional M protein locates between the virus envelope and the RNP in order to regulate virus transcriptional activity [127].

There are two major structural features for RSV observed by electron microscopy: the virus filaments (VFs) and the inclusion bodies (IBs). VFs form on the surface of the infected cells where the virus structural proteins interact to form mature virus particles, while IBs exist in the infected cells where the virus polymerase-associated proteins and virus-specific RNA accumulate.

4.1.2 Virus replication cycle

In general, RSV replication cycle is composed by virus entry, RNP complex activity, virus assembly and release [Figure 4.2].

4.1.2.1 Virus entry

RSV attachment to cells primarily occurs through the interaction between G protein and cell surface glycosaminoglycans (GAGs), in particular heparin sulphate (HS). Though sulfate modification is essential for the ability of GAGs to mediate RSV infection, only definite sulfate groups are required [128]. And although G protein helps in attachment of the virus to the cell surface, it has been proved that it is dispensible for the cell attachment. When virus attaches to the cell, F protein initiates a membrane fusion process at neutural PH. In this process, heptad repeat (HP) regions from F protein interact with the homotrimer to form a triple coiled-coiled structure, and this structure enables to draw the virus envelope and cell membrane close to benefit further membrane fusion. After the lipids derived from virus envelope and cell membrane connect together, RNP complex is transferred into the cytoplasm of the host cell, and further virus transcription and replication are initialted.

4.1.2.2 Virus transcription and replication

After RNP complex is released to the cytoplasm of target cell, the large polymerase L protein initiates viral transcription and replication [129]. With the assistance of viral RNA- dependent polymerase, the negative stranded genome is transcribed into 5'-capped and 3'-polyadenylated mRNAs, and this transcription stated in a sequential manner from the 3' end of the viral genome. In the end, ten mRNAs are then subsequently translated into virious viral proteins.

At the meanwhile, anti-genomic RNA is generated as a template and more vRNAs are subsequently synthesized by the virus polymerase.

4.1.2.3 Virus assembly and budding

The final stage of the replication cycle is virus particles assembly and release from the cell. The newly synthesized RNP and RNP-associated protein accumulate in inclusion bodies and target to specific sites like lipid rafts at the cell. The virus glycoproteins are also targeted to specific sits through the secretory pathway. The RNP complex is formed by the interaction between the vRNA and N protein, followed by P and L protein. M protein functions on the

association of the viral glycoproteins with RNPs. After that, the RNP complex is packed with other proteins to form new infectious virus particles [130].

The final stage of virus maturation is the release of the virus particles from the host cell. The virions mature in clusters at the apical surface in a filamentous form associated with caveolin-1, and extend from the plasma membrane [131]. In this process, various host cell factors, especially those related to cytoskeleton, are thought to be involved. Recent studies unveiled that cells infected with viruses lacking the F glycoprotein decreased the amounts of G and SH proteins in released virions and cells infected with viruses lacking the G protein decreased the amounts of SH protein in released virions. Thus, these findings indicated that F and G glycoproteins play a crucial role in HRSV particle assembly [132].

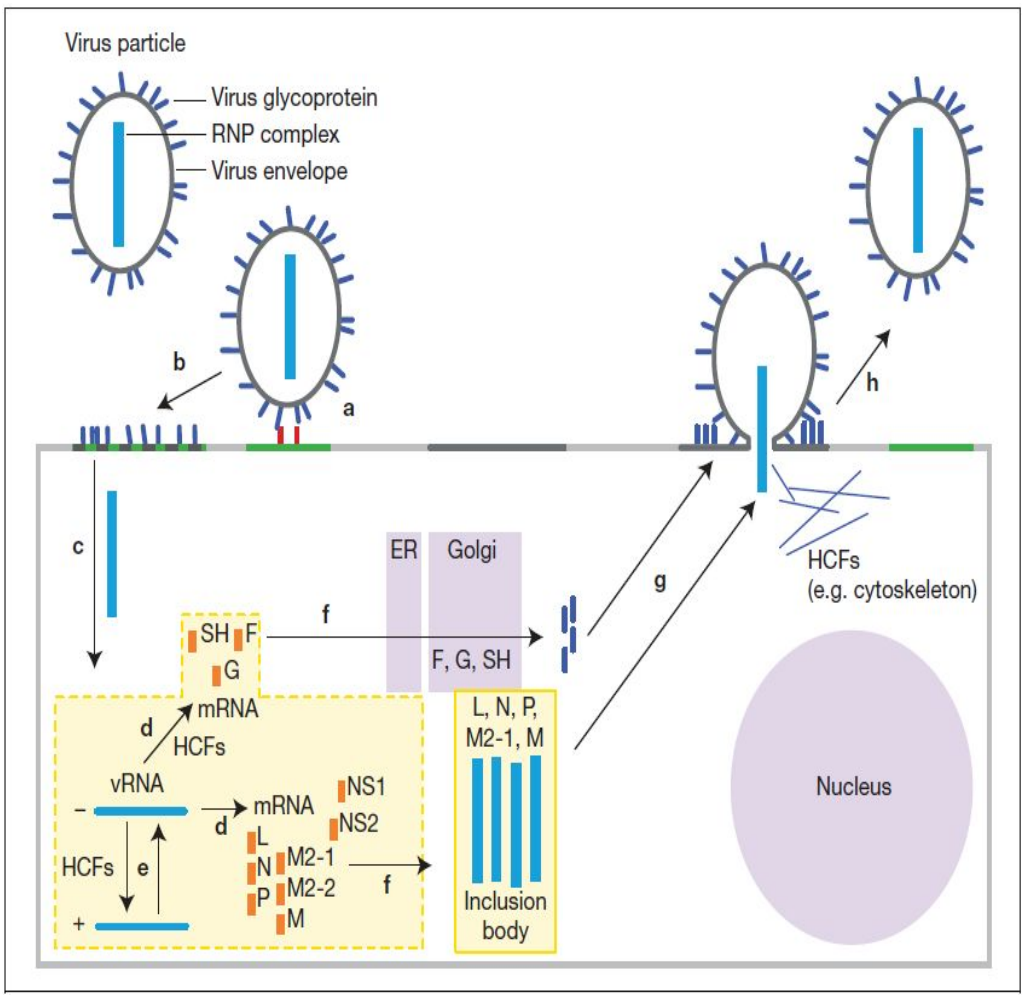

Figure 4.2 Overview of RSV replication cycle (adapted from Sugrue RJ, 2006)[125].

4.1.3 Virus-Host interactions

In the RSV-infected host cells, a variety of host genes related to different cellular functions such as protein metabolism, cytoskeleton structure, cell growth and inflammation is altered at their expression level. Simultaneously, RSV also has evolved a series of activities to overcome these immune defenses. The detailed virus-host interactions include (but not limited to): a batch of innate immune response and adaptive immune response has been observed to be initiated to conteract the virus invasion via pattern recognition receptors; these host immune response to RSV infection has been reported to be modulated via expression of G proteins; the activities of IFNs as well as cytokines have been also revealed to be impaired to weaken the host antiviral activities; some mechanisms have been also initiated to delayed programmed cell death and arrested cell cycle to facilitate robust viral titers during RSV infection; altered composition of lipid raft membranes have been also observed to benefit virus assembly and budding [123].

4.1.3.1 Actin cytoskeleton and Rho GTPases

The cytoskeletal framework in the cell is responsible for the trafficking of cellular proteins. It is majorly composed of actin, microtubules, intermediate filaments and other elements. Among them, actin microfilaments are in a dynamic state characterized by rapid cycles of polymerization/depolymerization in response to varying stimuli, and the microtubules are highly ordered with an intrinsic polarity.

Previous studies have proved that viruses use different elements of the cytoskeleton to facilitate entry, replication, transport as well as viral release. Detailed investigation has provided evidences that microtubules play a dominant role in the production of infectious virus, while actin filaments exert a greater effect on virual budding [133].

It has been revealed that F protein from RSV interacts with a cellular Rho GTPase, RhoA. And this GTPase signaling is closely relevant to many cellular functions associated with RSV pathogenesis, and these functions include organization of actin cytoskeleton and expression of proinflammatory cytokines. Gower TL *et al* (2001) did a series of experiments and found that the

expression of RhoA was increased and downstream signaling of RhoA was activated in RSV-infected Hep2 cells [134].

Another Rho GTPase Cdc42 palys a role in regulating cytoskeleton especially filopodia formation, and it has been shown to direct various physiological processes such as cell morphology, migration, and cell cycle progression. Recent study proved that it was required for RSV internalization and infection in A549 cells [135].

4.1.3.2 Immune response to RSV infection

RSV infection triggers Toll-like receptors' (TLRs) and pathogen recognition receptors' (PRRs) conserved pathogen-associated molecular patterns recognition, which in turn initiates activation of a series of immune response related molecules and pathways through NF-κB. For instance, studies in RSV-infected A549 cells have revealed the up-regulation of TLR4 at its expression level. Signaling through TLR4 can activate TNF receptor-associated factor and the adaptor protein MyD88, which in turn activate IKKε/TANK-binding kinase-1 and IL-1 receptor-associated kinase-4, thereby initiating a diverse group of transcription factors including IRF3, IRF7, NF-κB, JNK, p38 MAPK, activator protein-1 (AP1) [Figure 4.3].

TLR3, another member in TLR family, also show up-regulated expressions in reaction to RSV infection. Signaling through TLR3 also activate the downstream IKKε/TANK-binding kinase-1, which in turn induces IRF3, IRF7 and NF-κB [131]. Furthermore, virus infection sensed by TLRs is also able to activate downstream inflammatory chemokine and cytokine expression through NF-κB induction. And these chemokines and cytokines can take direct or indirect responsibility to virus infection and replication.

STAT proteins belonging to signal transducers are responsible for inducing transcription factors once receive the signal from either type I, type II or type III IFNs. Two mechanisms exist to antagonize the JAK-STAT signaling pathway: one is RSV NS protein mediated STAT2 proteosome degradation, and the other is negative modulation of type I IFN expression by SOCS family members, especially SOCS1 and SOCS3 [136, 137].

4.1.3.3 Cytokine response to RSV infection

Cytokines are small cell-signaling molecules that regulate immunity, inflammation and hematopoiesis. A wide range of cytokines have been published to be produced by numerous cell types during RSV infection. Some of these cytokines mediate proinflammatory reaction to activate and recruit immune cells, while others suppress the proinflammatory state. A set of important cytokines that are secreted upon viral infection are type I IFNs. However, several studies suggest that RSV induced type I IFNs in a poor way, which was majorly due to RSV NS protein suppression [139]. Other expressed cytokines mediated by NF-κB include RANTES, MCP, IL-9, TNF-α, IL-6, IL-1, CX3CL1. Among these cytokines, several genetic markers that predict severe RSV pathology have been identified in humans, such as RANTES and TNF-α [140].

4.1.3.4 Delayed programmed cell death to facilitate virus replication

More and more evidence have been accumulated to prove that RSV has the ability to postpone programmed cell death of epithelial cells. It was revealed that expression of anti-apoptosis IEX-1L gene was highly up-regulated in RSV-infected respiratory epithelial cells. Since IEX-1L was reported to protect cells from apoptosis induced by TNF-*α*, elevation of IEX-1L expression may suggest that RSV infection potentially protect epithelial cells from TNF-α-induced [141]. The delay of apoptosis was also proved by Thomas KW *et al* (2001) [142]. In their paper, they concluded that RSV inhibited apoptosis through a phosphatidylinositol 3-kinase-dependent pathway. And this programmed cell death delayed phenomenon was believed to facilitate virus replication.

4.1.3.5 NS1/ NS2 – viral antagonists of the host antiviral cytokine response

RSV has been shown to produce proteins, nonstructural NS1 and NS2 proteins, to inhibit cellular innate immunity represented by IFN and its productions. Spann KM *et al* (2004) reported that these two proteins functioned independently as well as coordinately to achieve the full inhibitory effect on IFN-α and IFN-β in A549 cells or macrophages [143]. To examine the concrete regulation network, more and more studies were focused on NS1 and NS2 with more and more details evidence provided to support this antiviral function of

these two proteins. Ling Z *et al* (2009) proposed that expression of NS2 inhibited IFN transcription through either RIG-I or TLR3 pathways [144]. Moreover, it was also mentioned that NS2 inhibited RIG-I-mediated IFN promoter activation through its binding to the N-terminal CARD of RIG-I so as to inhibit its interaction with the downstream component MAVS. Other results indicated that NS2 decreased STAT2 levels and NS1 also degraded STAT2 during RSV infection, thereby modulating interferon-dependent gene expression [136, 145]. Recent experiment also proved that these two nonstructural proteins decreased the expression level of TRAF3, which is a strategic integrator of multiple IFN-inducing signals [146]. In addition, relative researches on NS1/NS2 also mentioned that they might retard premature apoptosis to facilitate virus growth in an NF-κB-dependent, IFN-independent way [147].

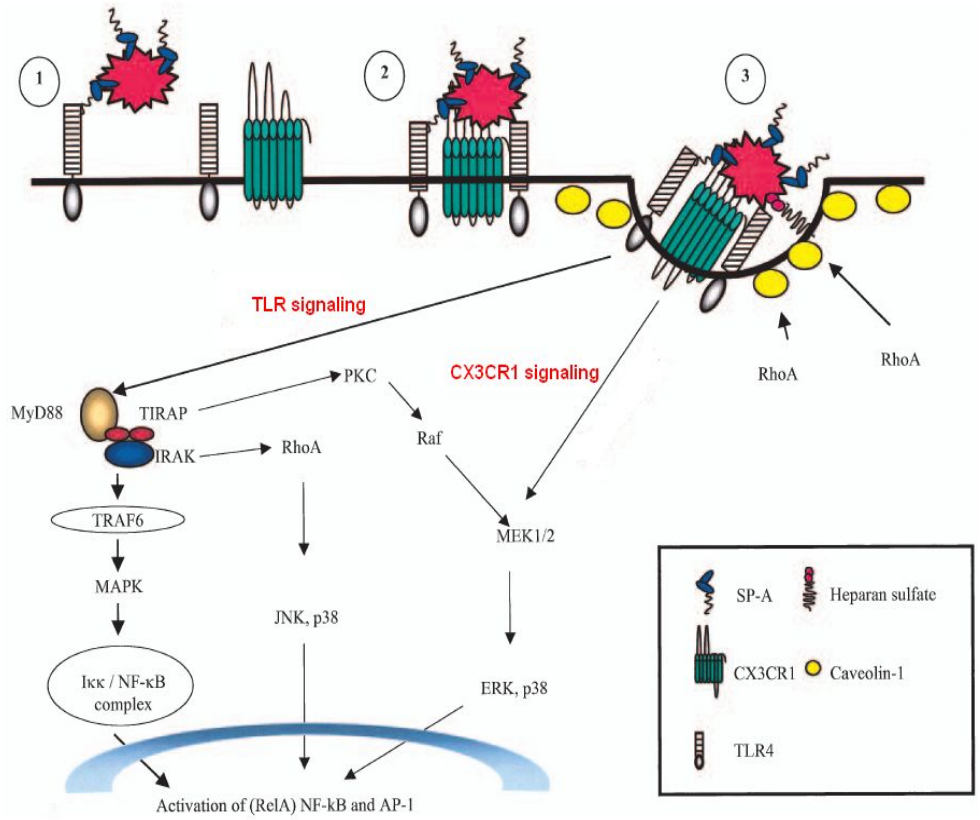

Figure 4.3 RSV biding and triggering of cellular responses (adapted from Harris J *et al*., 2003)[138].

4.1.3.6 The role of G protein in immune evasion

To our knowledge, RSV infection induces expression of several notable chemokines, including IL-8, RANTES, MCP-1, MIP-1α/β and IP-10. And RSV infection also triggers the proinflammatory mediator release like TNF-α that possesses antiviral activities. In this regard, G protein plays an essential role in modifying innate and adaptive immune responses at the expression levels of cytokines and chemokines. Accumulating evidences have proved that F and G proteins from RSV interact with the TLR pathway and modify negative regulation of SOCS protein on cytokine and chemokine expression. The central-conserved cysteine-rich region of G protein contains a CX3C chemokine motif at amino acid positions 182-186, and this motif targets to interact with CX3CR1, CX3CL1 receptor. It has been reported that this CX3CR1 mimicry facilitated RSV infection and altered CX3CL1 chemotaxis of human and mouse leukocytes, and this G protein mediated immune response modulation was likely important in facilitating RSV replication [148]. Based on these findings, new vaccination strategy which sought to induce antibodies that block G protein CX3C-CX3CR1 interaction has been put on the agenda for further RSV vaccine researches [149].

4.1.3.7 Disease pathogenesis

Investigations have indicated that the attack rate of RSV approaches 70% in the first year of life. The statistical data from US suggests that lower respiratory tract disease (bronchiolitis) develops in 20% to 30% of infected children, which result in around 120,000 hospitalizations yearly. RSV can also cause severe lower respiratory illness and lead to respiratory failure with 70–100% mortality rates in adults [150].

A variety of host factors, particularly cytokines and chemokines, have been reported to be responsible for the RSV disease pathogenesis. Expression of these factors aim to limit virus replication, however, over-expression or extra production of these immune moleculors may exacerbate the inflammatory response so as to promote airway damage and pathogenesis in the process of virus clearance [151, 152]. Evidence has been provided to indicate that CCL5 (RANTES) resulted in exacerbation of allergic airway inflammation following RSV infection [153].

The precise communication of innate and adaptive immune response is important in defining the magnitude of adaptive immunity. Inefficient inflammatory responses triggered by RSV infection may result in the inappropriate induction of T-cell responses. The T1-type responses characterized by the expression of IFN-γ, IL-2 and IL-12 are required for the efficient virus clearance, while the Th2-type responses characterized by the expression of IL-4, IL-10 and IL-13 are almost ineffective but able to contribute to allergic diseases and asthma [131, 154]. And it was published that intrinsic antigenic properties of G protein enables to promote Th2 responses and eosinophilia [150].

4.1.4 RSV infection in different cells

4.1.4.1 RSV infection in Hep2 cells

Ternette N et al (2011) applied label-free quantitative mass spectrometry to test the proteomics profiling of RSV-infected Hep2 cells and analyzed the data using IPA software [155]. Analysis result demonstrated that mRNA levels of IFIT3 and XRN2 were increased during RSV infection. Moreover, “PI3K/Akt signaling”, “mTOR signaling”, “protein ubiquitination pathway” and “RNA signaling” were enriched as significant pathways. Other experiments majorly focused on uncovering the interaction of lipid raft and RSV in Hep2 cells, and cholesterol depletion studies indicated that membrane cholesterol was required for virus filament formation. In addition, lipid raft microdomains played an important role in RSV maturation process, but dynamics of host-cell interactions and pathway cross-talk associated with RSV-mediated lipid raft microdomain modifications was poorly understood [127, 156].

4.1.4.2 RSV infection in macrophages

Macrophages are cells produced by the differentiation of monocytes in tissues. Macrophages function in recognizing, engulfing and destroying many potential pathogens in the innate immune system. Besides these pathogens, macrophages also enable to recognize syngeneic tumor cells, virus-infected cells as well as normal cells undergoing programmed cell death. Besides, macrophages also function in acquired immune response. Upon phagocyosis, macrophages degrade proteins and present antigens on major histocompatibility

complex (MHC) molecules, where T cells can recognize the substance as "foreign". Accordingly, pathogens have developed multiple methods to evade the attacks from macrophages.

Macrophages are subjected to classical (Th1) or alternative (Th2) activation, depending on the types of cytokines that they are exposed to. In the first case, macrophages are activated by inflammatory stimuli, such as IFN-γ (IFN-α), in combination with TLR activation by microbial stimuli, such as lipopolysaccharide (LPS). After that, the intracellular pathogens are killed and inflammantory cytokines that amplify Th1 immune responses are secrete through the production of iNOS, which generates nitric oxide (NO) that can damage cells. In the second case, after exposure to Th2 cytokines such as IL-4, IL-10, or IL-13, macrophages produce polyamines and proline so as to induce proliferation and collagen production. This kind of macrophages produces arginase-1 which competes with iNOS for arginine to produce L-ornithine and urea. Moreover, murine alternative-activated macrophages were reported to express "markers" including found in inflammatory zone 1, Ym1, mannose receptor and others, which did not express by classical-activated macrophages [157, 158].

Macrophages play a pivotal role in host lung defense mechanisms. As the first line of defense in acute RSV infection, macrophages are recruited in large numbers to the site of infection. Regarding the alterbative activation of macrophages, TLR4 signaling is necessary for expression of PPARγ and IFN-β is responsible for expression of IL-4, IL-13, IL-4Rα, and IL-10 in response to RSV infection. This induction is initiated prior to the development of the adaptive immune response [158]. To fight with these innate and adaptive immune responses coming from macrophage activation, RSV develops distinct mechanisms to impair macrophage IFN-α/β- and IFN-γ-stimulated transcription [159, 160]. Furthermore, the activities of caspase-3 and caspase-9 were reduced and eliminated seperately, while expression of anti-apoptotic proteins such as Bcl-2, Bcl-X and XIAP were enhanced in RSV-infected mouse macrophages. This phenomenon implied that the intrinsic apoptotic pathway was subverted in mouse macrophages after infection of RSV [161].

4.1.5 Objective

To our knowledge, RSV is the most common cause of acute bronchiolitis, particularly in infants and young children. The pathogenesis of RSV bronchiolitis is involved in a combination of direct cytopathic effects induced by viral replication and the resulting host response of production of proinflammatory cytokines. Otherwise, the detailed interactions between virus and host factors are not quite clearly understood. Moreover, macrophages as "gatekeepers" function to initiate the innate and adaptive immune responses at the first time but it is surprising that some studies demonstrated that RSV infection severely diminished the phagocytic ability of macrophages [162]. Thus, to sort out the internal response of Hep2 cells and macrophages in reaction to RSV infection is meaningful and pressing.

Accordingly, RSV A2 strain was designed to infect Hep2 cells and pulmonary macrophages at specific time points. All these global gene expression profiles were monitored using microarray platform, and expression of interested genes were validated by techniques such as cytokine assays [156,364]. Different types of software were employed into further analysis. The aims of this research are as following:

(1). Investigate the host-virus interactions in RSV infected Hep2 cells.

(2). Investigate the host-virus interactions in RSV infected mouse macrophages.

(3). Establish the mechanisms which have been involved in antagonizing the immune response in different host cells upon RSV infection.

4.2 Experiment workflow

4.3 Result and Discussion

4.3.1 Global profiling of gene expression

4.3.1.1 Heat maps of global gene expression

The global transcriptional profile of RSV-infected Hep2 cells illustrated that more and more expression changes occurred with the infection time increasing [Figure 4.5]. It was also observed that there were a larger number of probe sets showing down-regulated expression when compared to those showing up-regulated expression.

In macrophages infected with RSV, a few more expression changes were also detected at later time point (24 hpi). However, the numbers of genes with up-regulated expression were higher than the numbers of those with down-regulated expression in RSV-infected macrophages, which was different from the case detected in RSV-infected Hep2 cells. These observations might indicate the activation of a big scale of host antiviral genes in macrophages upon RSV infection [Figure 4.6].

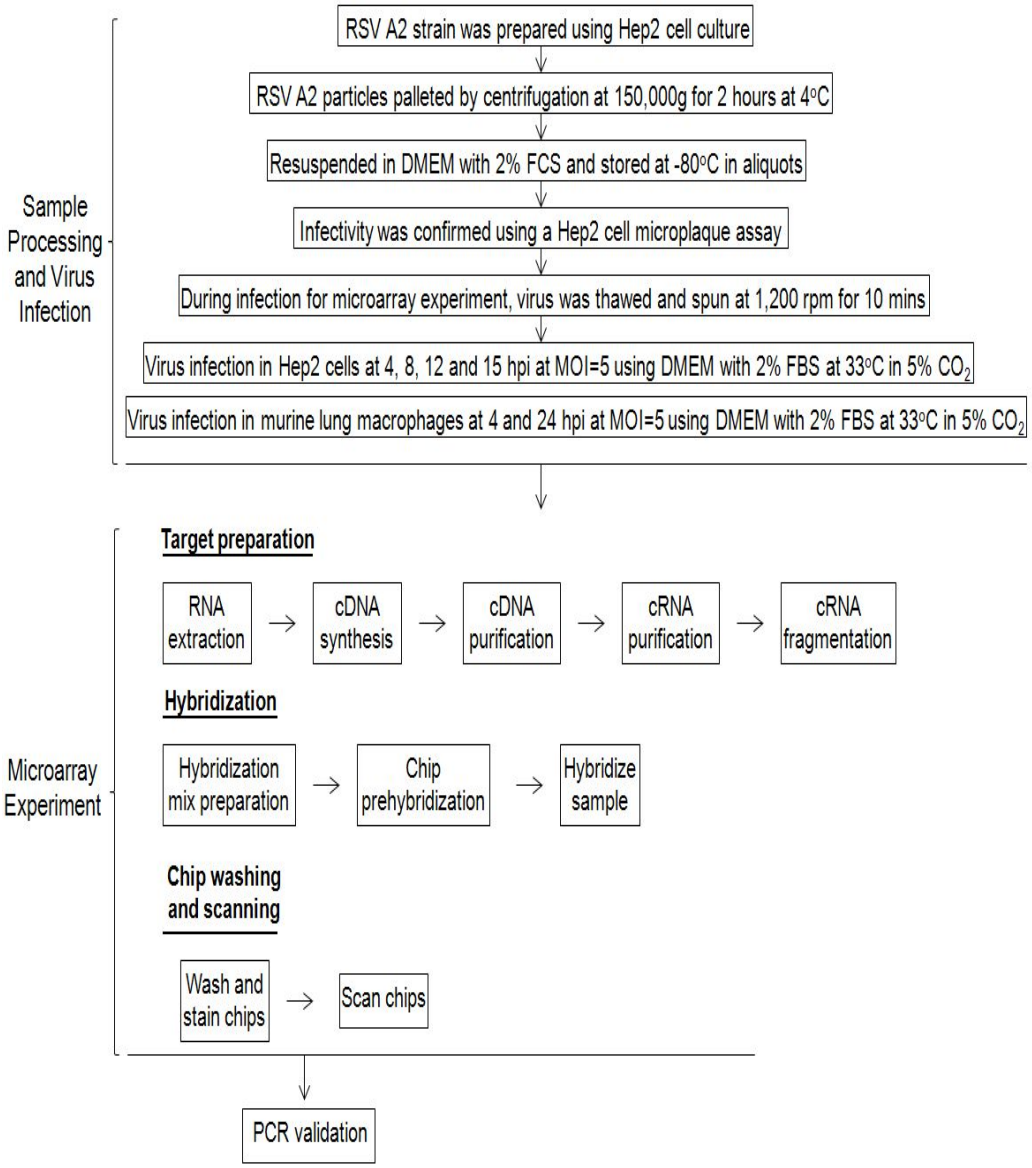

Figure 4.4 Microarray experimental workflow during RSV infection.

4.3.1.2 Distribution of differentially expressed probe sets

As shown in Table 4.1, almost half of the probe sets with up-regulated expression showed their expression at ≥3-FC, while less than one fourth of the probe sets with down-regulated expression showed their expression at ≥3-FC across the whole infection period. This observation suggested that up-regulated probe sets showed in a relative strong fold regulation than down-regulated ones at the global level.

In three late infection time points (8, 12 and 15 hpi), the percentages of up-regulated probe sets showed similar and higher than the one from 4 hpi. This observation might implicate a strong and sustained antiviral response from 8 to 15 hpi. The percentages of down-regulated probe sets showed a gradual increase across the whole infection period, indicating the inhibition of more and more cell activities following RSV infection in Hep2 cells.

With regards to macrophages infected with RSV, a large scale of genes was observed with differential expression from 4 hpi, suggesting an early and timely host cell reaction in response to RSV infection [Table 4.2]. The genes showing up-regulated expression were almost twice as many as those showing down-regulated expression, and some of these up-regulated genes even showed outstanding fold regulation at ≥5-FC.

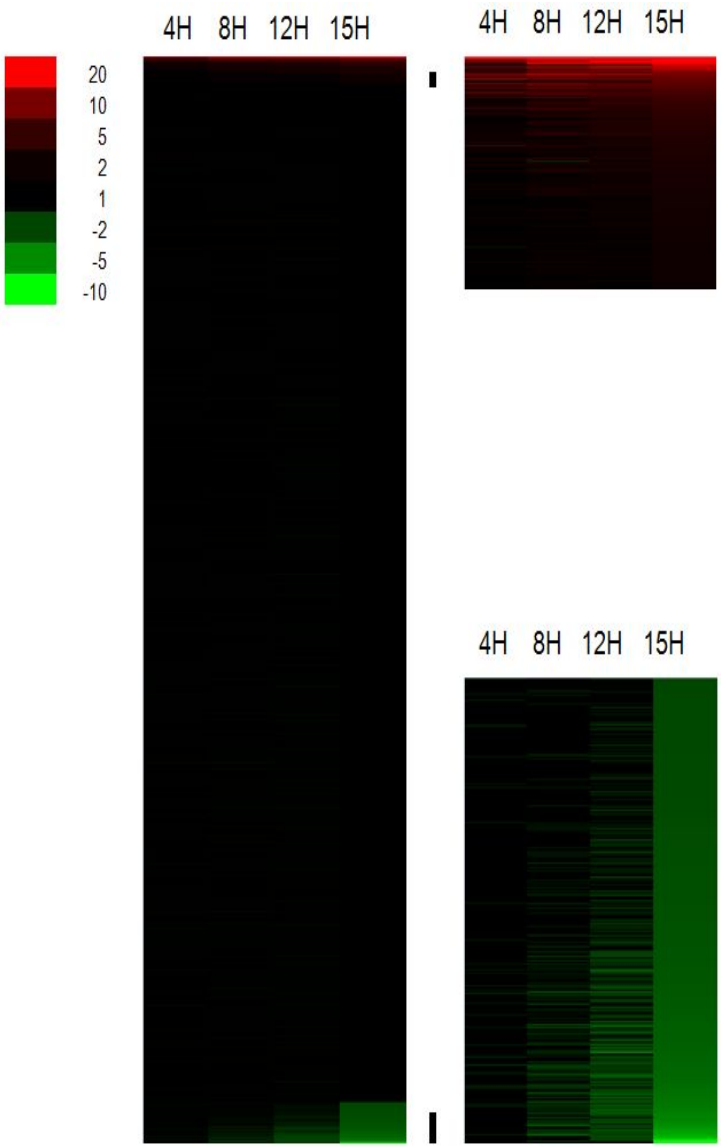

Figure 4.5 Temporal changes in the host cell transcriptome in Hep2 cells infected with RSV. The global host gene expression profiles were retrieved from microarray analysis with different time points examined. The probe sets showing ≥2 fold change (FC) up- or down-regulated in expression are indicated (P-value≤0.05). Expression profiles of up-regulated (red), down-regulated (green) and no significant change (black) are shown.

Table 4.1 Differentially expressed probe sets in Hep2 cells infected with RSV.

Hep2 cells	Probe sets (≥ 2-FC)		Probe sets (≥ 3-FC)		Probe sets (≥ 5-FC)	
	Up-regulated	Down-regulated	Up-regulated	Down-regulated	Up-regulated	Down-regulated
RSV 4H	1.46%	0.59%	0.77%	0.09%	0.39%	0.03%
RSV 8H	2.34%	1.24%	1.11%	0.24%	0.48%	0.03%
RSV 12H	2.36%	2.44%	1.05%	0.61%	0.45%	0.12%
RSV 15H	2.43%	3.78%	1.16%	0.92%	0.51%	0.16%

The global host gene expression profiles were retrieved from microarray analysis with different time points examined. The ratios of differentially expressed probe sets (P-value≤0.05) up- or down-regulated with different fold changes (≥2-FC, ≥3-FC and ≥5-FC) in relative to their corresponding "expressing probe sets" are represented in percentage. The expressing probe sets refer to probe sets detected in the mock-infected Hep2 cells.

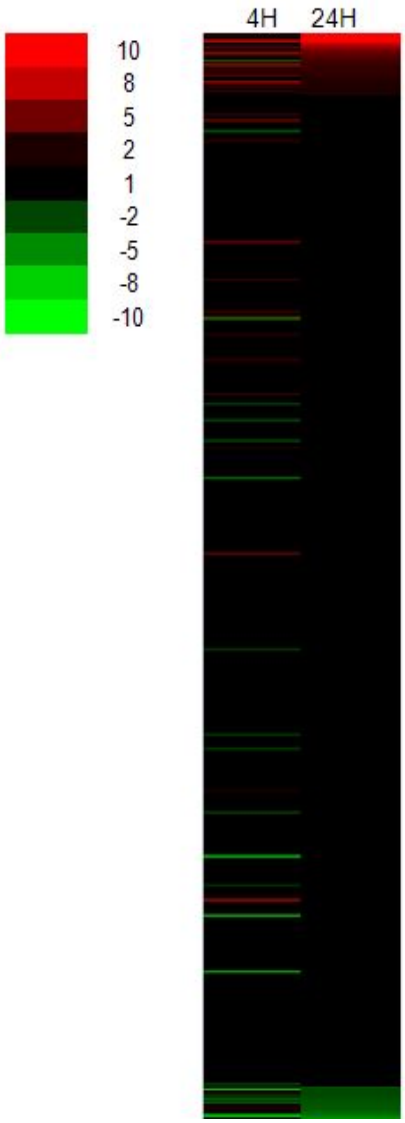

Figure 4.6 Temporal changes in the host cell transcriptome in macrophages infected with RSV. The global host gene expression profiles were retrieved from microarray analysis with different time points examined. The genes showing ≥2 fold change (FC) up- or down-regulated in expression are indicated (P-value≤0.05). Expression profiles of up-regulated (red), down-regulated (green) and no significant change (black) are shown.

Table 4.2 Differentially expressed genes in macrophages infected with RSV.

Macrophages	Genes (≥ 2-FC)		Genes (≥ 3-FC)		Genes (≥ 5-FC)	
	Up-regulated	Down-regulated	Up-regulated	Down-regulated	Up-regulated	Down-regulated
RSV 4 hpi	6.38%	3.45%	2.86%	0.74%	1.17%	0.13%
RSV 24 hpi	8.51%	3.99%	3.92%	1.12%	1.87%	0.22%

The global host gene expression profiles were retrieved from microarray analysis with different time points examined. The ratios of differentially expressed genes (P-value≤0.05) up- or down-regulated with different fold changes (≥2-FC, ≥3-FC and ≥5-FC) in relative to their corresponding "expressing genes" are represented in percentage. The expressing genes refer to genes detected in the mock-infected macrophages.

4.3.1.3 Functional classification

In terms of biological functions from GO and KEGG database, differentially expressed probe sets or genes were classified into interested functional families at different infection time points. As shown in Figure 4.7, up-regulated probe sets in RSV-infected Hep2 cells majorly located in the groups such as “Immune Response”, “DNA Binding”, “Signal Transduction”, “Transcription Factor”, “Cell Growth” and particularly “RNA binding” at ≥2-FC. It was surprising that expression of some probe sets that are functional associated with “Immune Response”, “RNA Binding” and “Signal Transduction” showed strong elevation with fold regulation even ≥10-FC, and the number of these probe sets showed a bit higher at 8 hpi than 4, 12 and 15 hpi. These observations might implicate that the strong and sustained host antiviral response across the whole investigated infection period, with the strongest state occurred around 8 hpi. And some of genes with up-regulated expression were classified into biological grouping such as “Cell Growth”, and this phenomenom might indicate that some mechanisms were exerted to promote the process of host cell cycle in order to speed up viral replication.

Down-regulated probe sets in RSV-infected Hep2 cells were majorly classified into functional groups such as “RNA Binding”, “DNA Binding”, “Signal Transduction” and “Transcription Factor”, and the numbers of down-regulated probe sets in each family increased with the infection time increasing. When compared to the up-regulated probe sets, only several down-regulated probes sets could be detected with high-level fold regulation ≥5-FC at 12 and 15 hpi.

When it turns to RSV-infected macrophages, functional groups including “Cytokine”, “Antiviral”, “RNA Binding”, “Cell Death”, “Signal Transduction” and “DNA Transcription Factor” were majorly enriched in the up-regulated probe sets at either 4 or 24 hpi [Figure 4.8]. At ≥10-FC, a few genes encoding cytokines were even detected at both examined time points, which implied the early and sustained activation of antiviral host response during RSV infection in macrophages. A small batch of genes belonging to “Cell Death” also showed stimulated expression at both 4 and 24hpi, and a couple of them also showed up-regulated expression with quite prominent fold

changes. This observation might suggest that the cell apoptosis was initiated strongly from a quites early infectioin stage.

Only a small number of genes showed down-regulated expression with low fold regulation at both time points. And these genes majorly belonged to “Signal Transduction”, “RNA Binding”, “Kinase”, “Cell Cycle” and “Cell Growth”.

Genes with faintly down-regulated expression were identified both in RSV-infected Hep2 cells and RSV-macrophage. This observation might imply the interference of cell signaling as well as metabolism by RSV infection.

4.3.1.4 Cluster analysis in Hep2 cells

To our knowledge, genes with similar temporal expression trends might have related biological functions and possibly correspond to some critical cellular processes and pathways [91]. So the aim of this cluster analysis is to classify probe sets with similar expression profiles into common biological groups, which is beneficial for further functional analysis. The Hep2 cells were infected with RSV, and the corresponding transcriptomes were analyzed at 4, 8, 12, and 15 hpi. Probe sets at more than one time point of infection with ≥2-FC (P-value≤0.05) were clustered into similar gene expression profiles using the Expander version 5.0 software [Figure 4.9]. Using the same software, the data were further analyzed into genes relating to different functional groups or canonical pathways, and enriched transcription factor were also identified. All enriched functional groups, canonical pathways and transcriptional factors are displayed in Table 4.3.

Pathway analysis revealed that differentially up-regulated genes shared common pathways including “MAPK signaling”, “Jak-STAT signaling pathway”, “B-cell receptor signaling pathway”, “Toll-like signaling pathway”, “Steroid biosynthesis”, “Metabolic pathways”, “Focal adhesion” and “Pathways in cancer”. Activation of these immune response and steroid synthesis related pathways implied the host antiviral activities and alterations in the composition of the lipid raft membranes during RSV infection in Hep2 cells.

Functional groups such as “Immune system process”, “Response to stimulus”, “Lipid metabolic process” and “Lipid biosynthetic process” were significantly enriched in these genes with the increased expression trends. Over-

representation of these functional groups was consistent with the significant enrichment of key pathways mentioned above, providing more evidences that the host antiviral responses and membrane activities were triggered in RSV infected Hep2 cells.

A batch of transcription factors such as SRF, CAC-binding_protein, ISRE, Sp1, UF1H3BETA and Bach2 were identified to be enriched in the up-regulated genes. SRF, as a member of the MADS box superfamily of transcription factors, regulates the activity of many immediate-early genes and thereby participates in cell cycle and apoptosis regulation [163]. In our study, SRF gene showed a significant expression elevation (around 3-FC) from 8 hpi to 15 hpi, which was consistent with its enrichment by downstream up-regulated factors and could implicate its potential regulation on cell cycle. Besides, SRF is also the downstream target of many pathways such as MAPK pathway ternary complex factors. Previous finding showed that "MAPK signaling" pathway was enriched by the up-regulated genes, and this finding was concordant with the up-regulation of SRF in its expression. ISRE is an interferon stimulation response element which binds to IRF3 to present in the ISG15 gene promoter and activate its transcriptional activity. Enrichment of this transcription factor in up-regulated genes potentially suggested the partly activation of interferon signaling pathway.

In the meanwhile, the pathway called "Cytokine-cytokine receptor interaction" was enriched in the down-regulated genes, which could be due to the RSV combating the host immune regulation. Another pathway that was also enriched by the down-regulated genes was "ECM-receptor interaction". ECM was found to participate in the regulation of cytoskeleton and apoptosis [164, 165], thus enrichment of this pathway may reveal the negative modulation in these aspects under RSV infection in Hep2 cells. Other pathways such as "Apoptosis" and "Small cell lung cancer" were also enriched in the down-regulated genes.

Genes with decreased expression were significantly grouped into functions such as "Nitrogen compound metabolic process", "Cellular biosynthetic process", "Transition metal ion binding" and "Regulation of macromolecule biosynthetic process" with high numbers included for each group. Besides, other functions belonging to a diverse range of cellular

functions were also enriched based on other genes with down-regulated expression, suggesting the impairment of cell activities from a wide range.

In addition to these pathways and functions, potential transcription factors such as ETF, E2F, c-Myc:Max, TATA, STATx, NF-kappaB_(p65) and Evi-1were also over-represented by the down-regulated genes. E2F and c-Myc:Max are important regulator and transcription factor in apoptosis signaling pathway, which was correlated with the enrichment of "Apoptosis" pathway and indicated the inhibition of the apoptosis signal transduction in Hep2 cells after RSV infection. This observation was consistent with previous finding that RSV delayed programmed cell death to facilitate virus replication in human airway epithelial cells [131].

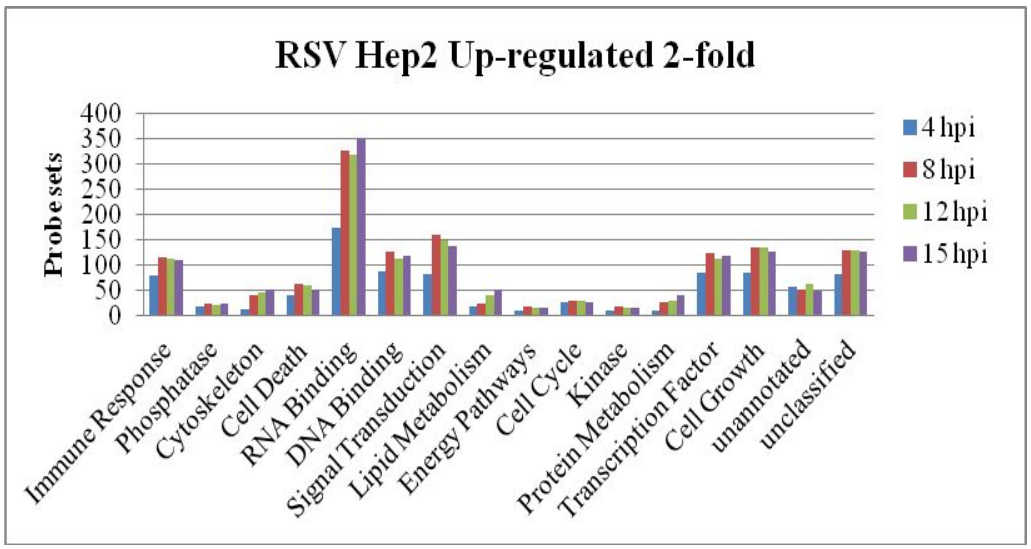

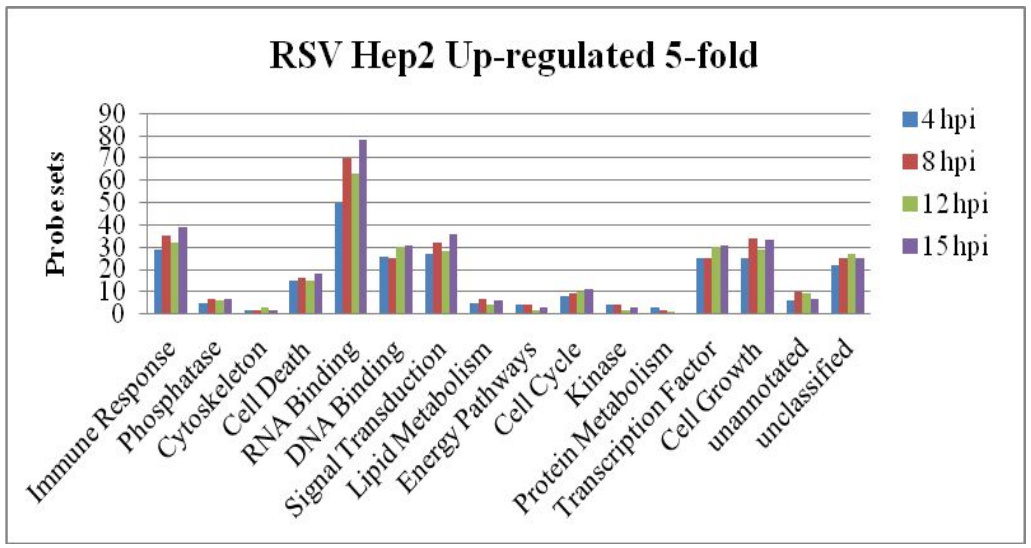

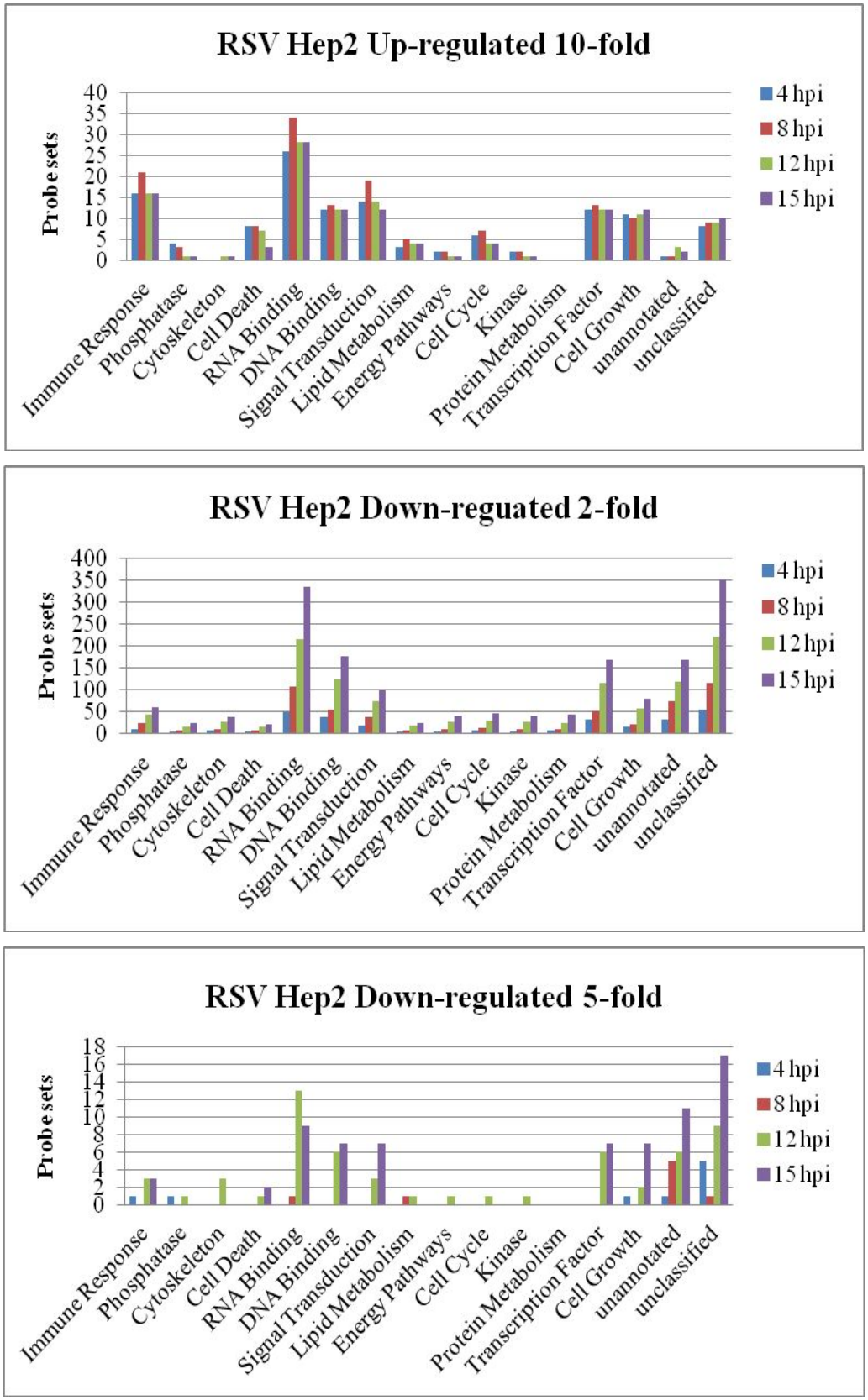

Figure 4.7 Overview of distributions of differentially expressed probe sets into different biological functions in Hep2 cells infected with RSV. The numbers of probe sets in the different functional families, including non-annotated and unclassified groups, showing up- or down-regulated with different fold changes (≥2-FC, ≥5-FC and ≥10-FC) in gene expression are presented.

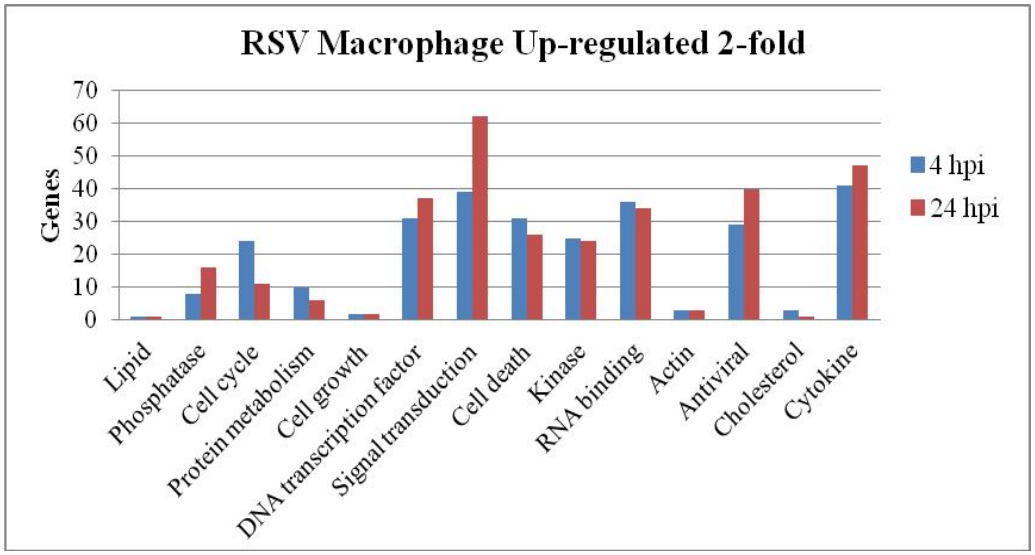
RSV Macrophage Up-regulated 2-fold
Genes
70
60
50
40
30
20
10
0
4 hpi
24 hpi
Lipid
Phosphatase
Cell cycle
Protein metabolism
Cell growth
DNA transcription factor
Signal transduction
Cell death
Kinase
RNA binding
Actin
Antiviral
Cholesterol
Cytokine

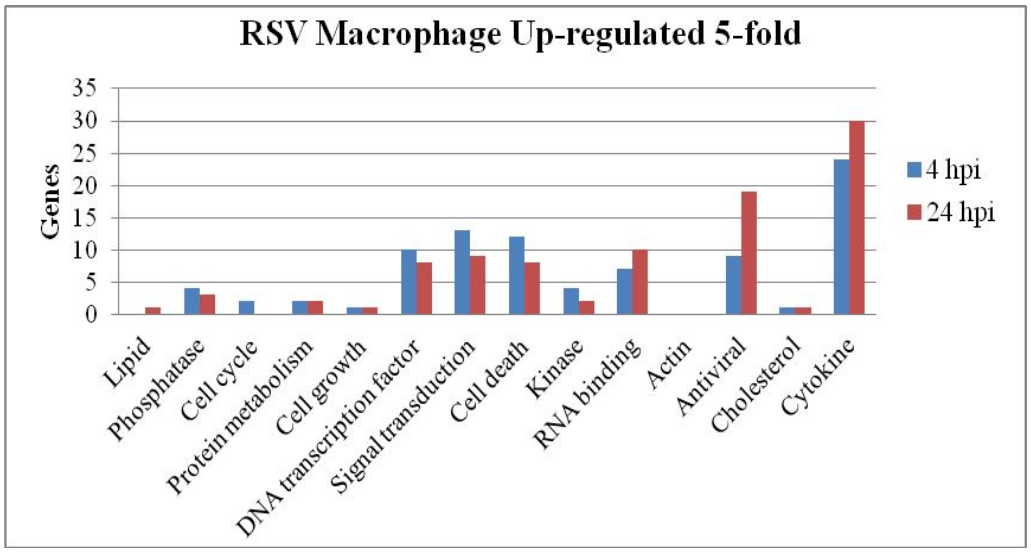
RSV Macrophage Up-regulated 5-fold
Genes
35
30
25
20
15
10
5
0
4 hpi
24 hpi
Lipid
Phosphatase
Cell cycle
Protein metabolism
Cell growth
DNA transcription factor
Signal transduction
Cell death
Kinase
RNA binding
Actin
Antiviral
Cholesterol
Cytokine

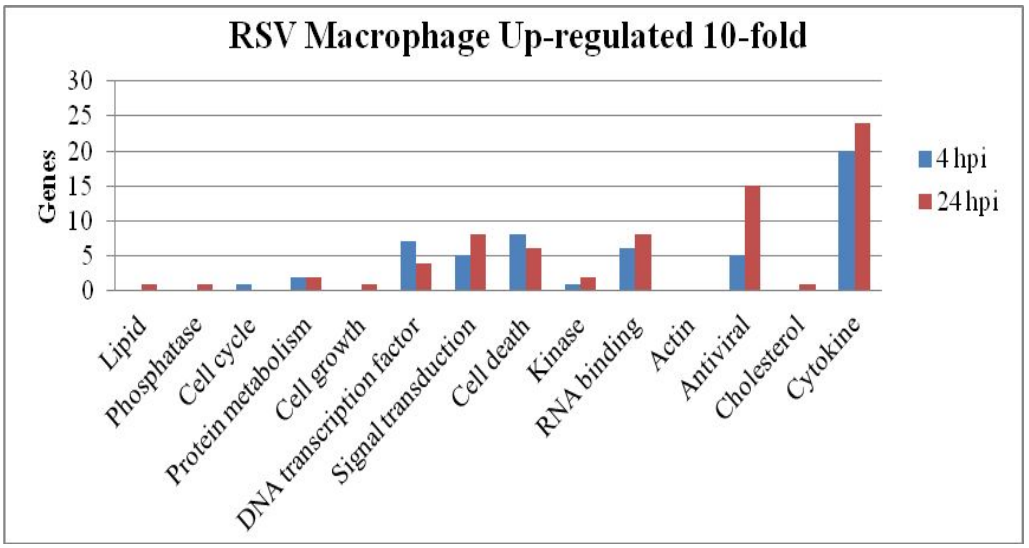
RSV Macrophage Up-regulated 10-fold
Genes
30
25
20
15
10
5
0
4 hpi
24 hpi
Lipid
Phosphatase
Cell cycle
Protein metabolism
Cell growth
DNA transcription factor
Signal transduction
Cell death
Kinase
RNA binding
Actin
Antiviral
Cholesterol
Cytokine

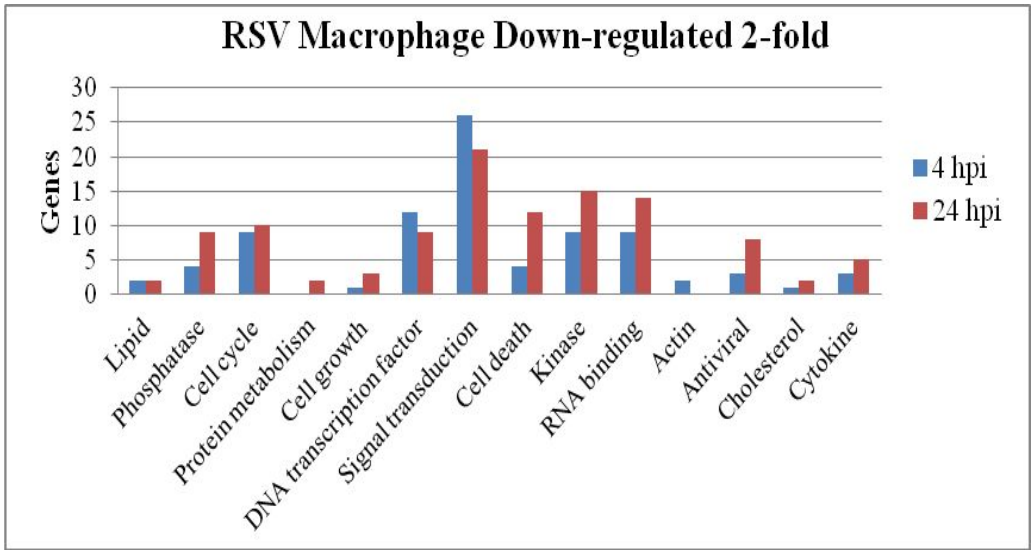

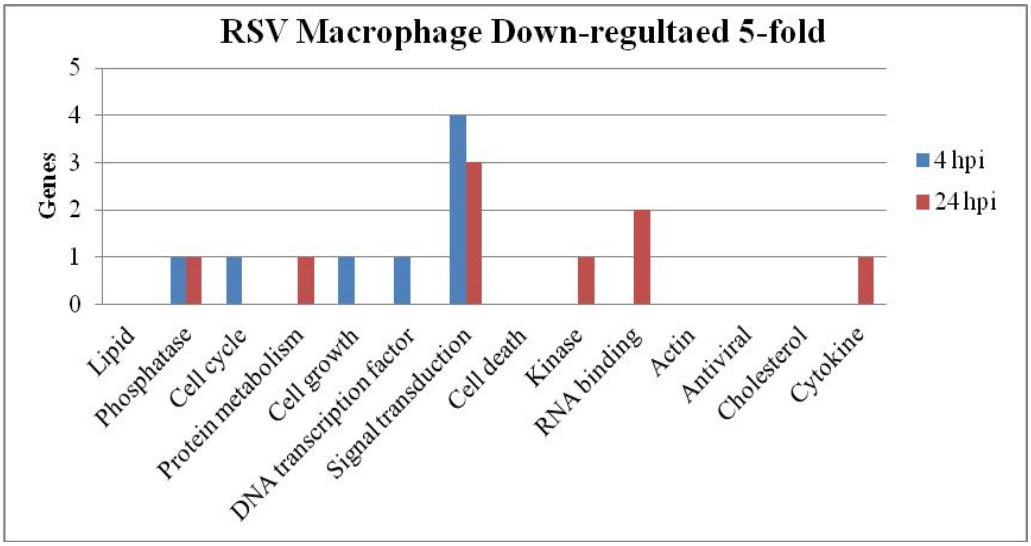

Figure 4.8 Overview of distributions of differentially expressed genes into different biological functions in macrophages infected with RSV. The numbers of genes in the different functional families, showing up-regulated or down-regulated with different fold changes (≥2-FC, ≥5-FC and ≥10-FC) in gene expression are presented.

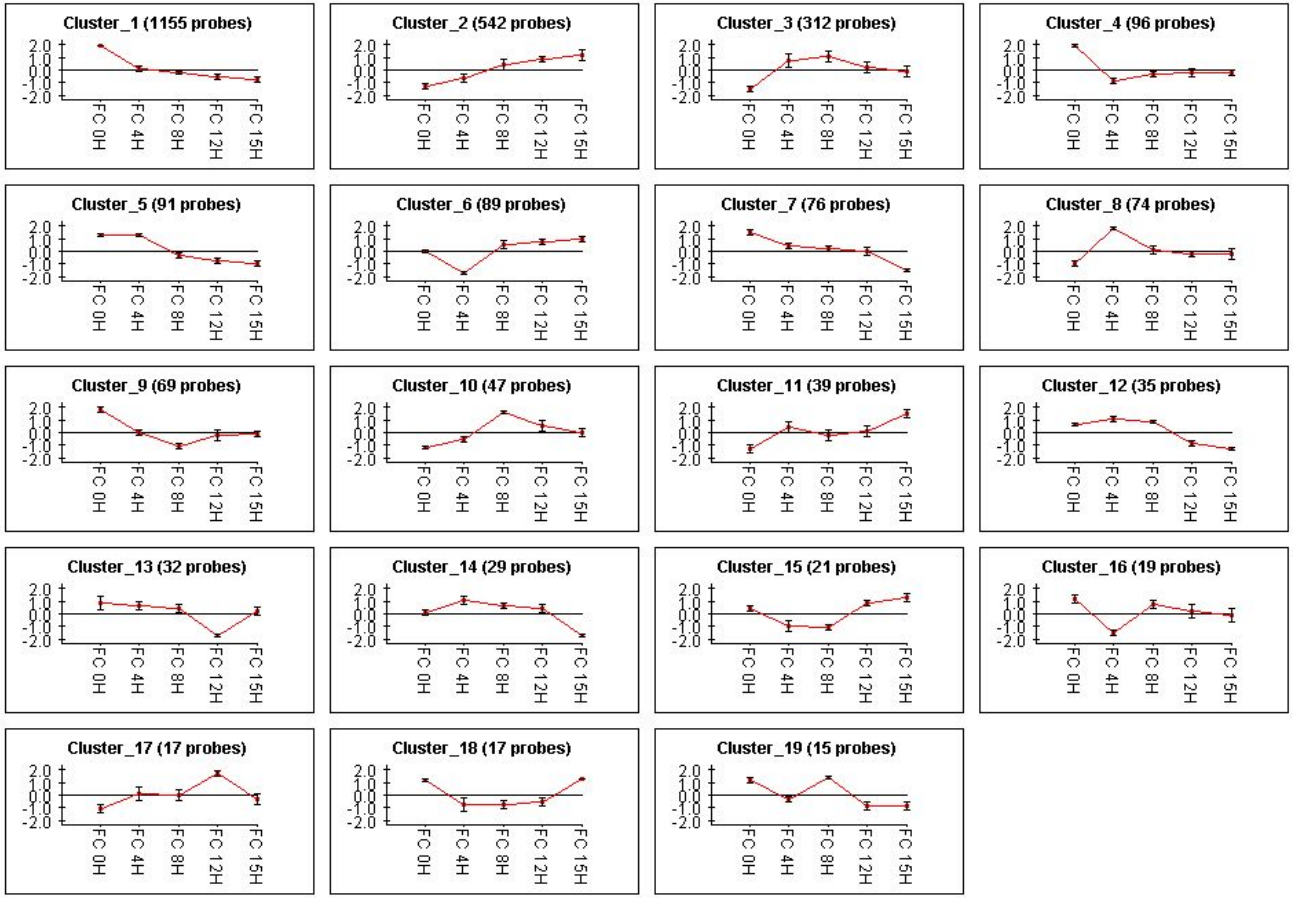

Figure 4.9 Clustering analysis of temporal gene expression profiles in RSV-infected Hep2 cells. Hep2 cells were infected with RSV at 4, 8, 12 and 15 hpi. Probe sets showing ≥2-fold changes up- or down-regulated (P-value≤0.05) at least over one time point were analyzed with Expander 5 software. X-axis represents post-infection in hours (H), and Y-axis means normalized expression changes of probe sets.

Table 4.3 Summary of functional groups, canonical pathways and transcription factors enriched based on differentially expressed genes in Hep2 cells infected with RSV.

Cluster No.	Enriched Transcription Factors
Cluster 1	ETF:333 | E2F:434 | c-Myc:Max:199 | E2F-1:179
Cluster 2	SRF:35 | CAC-binding_protein:108 | ISRE:52 | NF-kappaB_(p65):35 | Sp1:200 | UF1H3BETA:162 | Bach2:52
Cluster 3	TATA:27 | STATx:32 | NF-kappaB_(p65):21
Cluster 8	NF-kappaB_(p65):10
Cluster 9	Evi-1:10
Cluster No.	**Enriched Canonical Pathways**
Cluster 2	Focal adhesion:20 | Pahtways in cancer:21 | MAPK signaling pathway:17 | Jak-STAT signaling pathway:13 | B cell receptor signaling pathway:9
	Toll-like receptor signaling pathway:10 | Steroid biosynthesis:5 | Hypertrophic cardiomyopathy (HCM):8 | Leukocyte transendothelial migration:9
	Renal cell carcinoma:7
Cluster 3	Apoptosis:9 | Pathways in cancer:14 | Small cell lung cancer:8 | ECM-receptor interaction:7 | Cytokine-cytokine receptor interaction:10
Cluster 6	Steroid biosynthesis:3 | Metabolic pathways:12
Cluster 8	Cytokine-cytokine receptor interaction:6
Cluster No.	**Enriched Gene Ontology Terms**
Cluster 1	Nitrogen compound metabolic process - GO:0006807:186 | Cellular biosynthetic process - GO:0044249:162 | Gene expression - GO:0010467:142
	Cellular biopolymer biosynthetic process - GO:0034961:128 | Nucleic acid binding - GO:0003676:162 | Transition metal ion binding - GO:0046914:131
	Regulation of macromolecule biosynthetic process - GO:0010556:139 | DNA metabolic process - GO:0006259:34 | Cell cycle - GO:0007049:41
	DNA replication - GO:0006260:19 | Cell cycle checkpoint - GO:0000075:10
Cluster 2	Immune system process - GO:0002376:47 | Response to stimulus - GO:0050896:89 | Positive regulation of cellular process - GO:0048522:49
	Response to wounding - GO:0009611:28 | Negative regulation of biological process - GO:0048519:51 | Anatomical structure development - GO:0048856:63
	Response to external stimulus - GO:0009605:34 | Developmental process - GO:0032502:75 | Organ development - GO:0048513:48
	Multi-organism process - GO:0051704:27 | Regulation of biological quality - GO:0065008:39 | Regulation of developmental process - GO:0050793:28
	Regulation of cell proliferation - GO:0042127:26 | Cell death - GO:0008219:25 | Receptor binding - GO:0005102:30 | Actin binding - GO:0003779:18
	Positive regulation of cell proliferation - GO:0008284:17 | Steroid metabolic process - GO:0008202:14 | Regulation of cellular metabolic process - GO:0031323:72
	Regulation of apoptosis - GO:0042981:24 | Cell activation - GO:0001775:14 | Response to virus - GO:0008615:10 | Cell proliferation - GO:0008283:17
	Actin cytoskeleton organization - GO:0030036:13 | Regulation of protein metabolic process - GO:0051246:18 | Biological adhesion - GO:0022610:24
	Sterol biosynthetic process - GO:0016126:6 | Transferase activity, transferring phosphorus-containing groups - GO:0016772:30 | Enzyme binding - GO0019899:15
	Lipid bioxynthetic process - GO:0008610:15 | Lipid metabolic process - GO:0006629:26
Cluster 3	Immune system process - GO:0002376:30 | Regulation of cell proliferation - GO:0042127:24 | Response to stimulus - GO:0050896:53
	Negative regulation of biological process- GO:0048519:36 | Regulation of developmental process - GO:0050793:24 | Response to stress - GO:0006950:34
	Response to wounding - GO:0009611:19 | Regulation of signal transduction - GO:0009966: 22| Defense response - GO:0006952:20
	Cell death - GO:0008219:19 | Multicellular organismal development - GO:0007275:42 | Organ development - GO:0048513:28
	Postive regulation of biological process - GO:0048518:28 | Tissue development - GO:0009888:17 | Regulation of immune system process - GO:0002682
	Anatomical structural morphogenesis - GO:0009653:20 | Regulation of multicellular organismal process - GO:0051239:17
	Regulation of myeloid cell differentiation - GO:0045637:6 | Anotomical structural formation involved in morphogenesis - GO:0048646:10
	Response to molecule of bacterial origin - GO:0002237:4
Cluster 4	Regulation of nucleobase, nucleoside, nucleotide and nucleic acid metabolic process - GO:0019219:21
Cluster 6	Sterol biosynthetic process - GO:0016126:5 | Lipid metabolic process - GO:0006629:13 | Lipid biosynthetic process - GO:0008610:8
Cluster 8	Immune system process - GO:0002376:12 | Inflammatory response - GO:0006954:8 | Response to stress - GO:0006950:13 | locomotion - GO0040011:7
	Positive regulation of biological process - GO:0048518:12 | Chemokine acticity - GO:0008009:4 | Cell death - GO:0008219:8
	Multi-organism process - GO:0051704:8 | Postive regulation of nitrogen compound metabolic process - GO:0051173:7 | Regulation of apoptosis - GO:0042981:8
Cluster 10	Regulation of developmental process - GO:0050793:8 | Protein kinase cascade - GO:0007243:6 | Regulation of phosphorylation - GO:0042325:6
	Cell death - GO:0008219:7
Cluster 12	Regulation of macromolecule biosynthetic process - GO:0010556:13 | Nucleic acid binding - go:0003676:13
Cluster17	Cell death - GO:0008219:5

Differentially expressed genes were significantly categorized into different GO terms and pathways. Different transcription factors that can potentially be involved in the regulation of gene expressions are shown for each cluster under Expander 5 software analysis (P-value≤0.05). Each functional group, canonical pathway or transcription factor is followed by the number of corresponding genes.

4.3.1.5 Core analysis in macrophages

Since only two time points were examined in RSV-infected macrophages, it was not reliable to do cluster analysis based on these data. In

order to identify the significant regulation of key functional groups, core analysis by IPA was performed to analyze the differentially expressed genes in macrophages [Figure 4.10-4.13].

At the early stage of RSV infection, it was noted that many key functional networks and pathways were highlighted. For example, “Lipid Metabolism”, “Cell Death”, “Cell Cycle”, “DNA Replication”, “Cell-to-cell Signaling” networks were over-represented with high score; “Cancer”, “Inflammatory Response”, “Immunological Response”, “Cellular Growth and Proliferation”, “Cellular Development”, “Cell Death”, “Hematological System Development and Function”, “Tissue Morphology”, “Cell-mediated Immune Response” and “Organismal Survival” were ranked as top functions with hundreds of differentially expressed genes included for each; “Activation of IRF by Cytosolic Pattern Recognition Receptors”, “Role of Pattern Recognition Receptors in Recognition Bacteria and Viruses”, “IL-10 Signaling”, “TNFR2 Signaling” and “CD40 Signaling” were identified as top five canonical pathways with high-level significance. These findings suggested that cell regulations associated with immune response, antigen presentation, cell cycle and cell death had been initiated from a very early infection stage.

Notably, the top networks and functions identified at 24 hpi were similar as those identified at 4 hpi, however, more molecules belonging to these functions were detected at 24 hpi than 4 hpi. This phenomenon might provide evidences that growing number of factors participated in cell regulation activities to combat with RSV’s invasion with the infection time increasing. Besides, the essential canonical pathways unique to RSV infection at 24 hpi were “Altered T Cell and B Cell Signaling in Rheumatoid Arthritis”, “Dendritic Cell Maturation”, “Communication between Innate and Adaptive Immune Cells”. These pathways were all related to acquired immune response, indicating the strong adaptive immune response at late infection phase in RSV-infected macrophages. Besides, pathways related to cholesterol biosynthesis and lipid metabolism were more highly represented based on genes with down-regulated expression at 24hpi when compared to 4hpi, indicating that virus infection might induce changes in pathways playing a role in cellular metabolism ny 24hpi.

4.3.2 Functional groups related to host response

During RSV infection, many host genes with critical functions have been reported to be differentially expressed in order to fight with the virus invasion or benefit the virus replication and assembly. For example, antiviral genes such as cytokines that are responsible for local immune response might be induced at their expression level after RSV infection in order to fight against virus infection [166]; altered expression of cell death related genes could function on delaying programmed cell death in order to serve for better virus replication [167]; genes involved in lipid raft composition have been also proved to deviate from their regular expression after RSV interruption [156]. Accordingly, expression of genes referring to interesting functions was investigated in order to evaluate the host cell-virus interactions in both infected Hep2 cells and mouse macrophages [Figure 4.14-4.20].

RSV Macrophage 4 hpi

Top Networks

ID	Associated Network Functions	Score
1	Lipid Metabolism, Small Molecule Biochemistry, Drug Metabolism	37
2	Cell Death, Genetic Disorder, Inflammatory Disease	35
3	Cell Cycle, DNA Replication, Recombination, and Repair, Cancer	31
4	Connective Tissue Disorders, Organismal Injury and Abnormalities, Cardiovascular System Development and Function	31
5	Cell-To-Cell Signaling and Interaction, Cellular Growth and Proliferation, Nervous System Development and Function	31

Top Bio Functions

Diseases and Disorders

Name	p-value	# Molecules
Cancer	1.65E-30 - 2.31E-08	431
Inflammatory Disease	9.38E-24 - 2.34E-08	353
Immunological Disease	4.56E-23 - 7.69E-09	320
Inflammatory Response	4.58E-23 - 2.07E-08	232
Dermatological Diseases and Conditions	2.98E-17 - 1.76E-08	150

Molecular and Cellular Functions

Name	p-value	# Molecules
Cellular Growth and Proliferation	1.82E-33 - 1.89E-08	382
Cellular Development	7.63E-32 - 2.38E-08	339
Cell Death	1.87E-31 - 2.33E-08	384
Cellular Function and Maintenance	1.66E-25 - 2.08E-08	149
Cell Cycle	3.22E-23 - 2.34E-08	201

Physiological System Development and Function

Name	p-value	# Molecules
Hematological System Development and Function	2.07E-30 - 2.33E-08	262
Tissue Morphology	2.07E-30 - 1.35E-08	184
Hematopoiesis	1.80E-26 - 2.33E-08	172
Cell-mediated Immune Response	3.28E-23 - 4.92E-09	111
Organismal Survival	1.02E-22 - 3.12E-20	188

Top Canonical Pathways

Name	p-value	Ratio
Activation of IRF by Cytosolic Pattern Recognition Receptors	4.97E-15	26/73 (0.356)
Role of Pattern Recognition Receptors in Recognition of Bacteria and Viruses	8.74E-12	25/87 (0.287)
IL-10 Signaling	1.7E-11	23/78 (0.295)
TNFR2 Signaling	2.22E-11	15/33 (0.455)
CD40 Signaling	2.27E-11	22/70 (0.314)

Figure 4.10 Summary of top functional groups enriched in differentially expressed genes in RSV-infected with macrophages at 4 hpi. Differentially expressed genes detected at 4 hpi were significantly categorized into different networks, functions and pathways under the analysis of Ingenuity Pathway Analysis (IPA) version 2012 (P-value≤0.05).

A

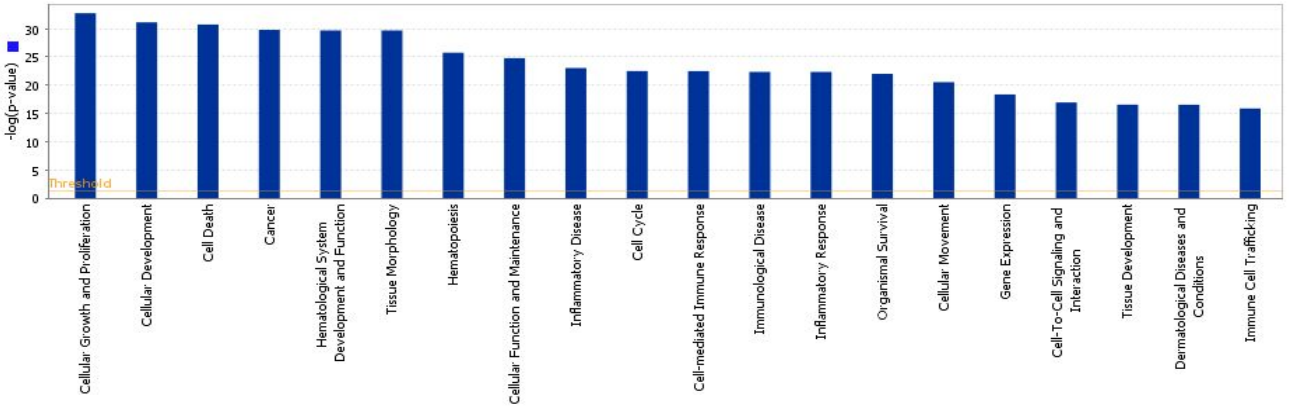

B

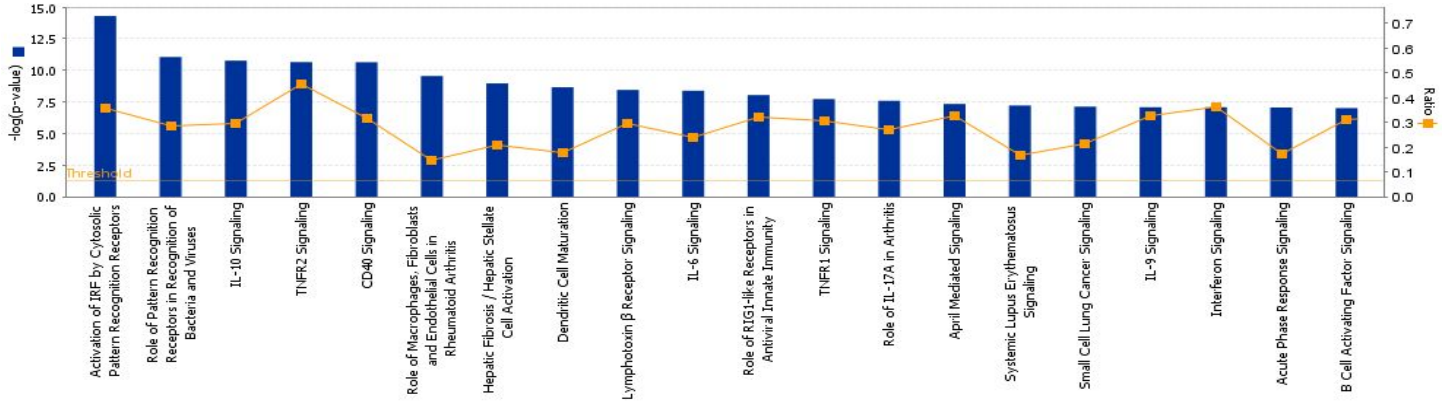

Figure 4.11 Top 20 (A) biological functions and (B) canonical pathways significantly enriched in differentially expressed genes from RSV-infected macrophages at 4 hpi (P-value≤0.05). Threshold was set at p-value = 0.05 and indicated as –log (p-value) on the Y-axis and the X-axis shows the terms of each biological function or canonical pathway. The orange boxes indicate the ratio (Ratio) of the number of genes with differential expression changes and the total number of genes in the respective canonical pathway.

RSV Macrophage 24 hpi

Top Networks

ID	Associated Network Functions	Score
1	Cell Signaling, Molecular Transport, Nucleic Acid Metabolism	40
2	Gene Expression, Neurological Disease, Organismal Injury and Abnormalities	38
3	Amino Acid Metabolism, Molecular Transport, Small Molecule Biochemistry	36
4	Genetic Disorder, Inflammatory Disease, Inflammatory Response	35
5	Lipid Metabolism, Molecular Transport, Small Molecule Biochemistry	32

Top Bio Functions

Diseases and Disorders

Name	p-value	# Molecules
Inflammatory Response	5.50E-35 - 7.60E-09	299
Immunological Disease	1.98E-31 - 5.27E-09	438
Cancer	5.76E-30 - 7.31E-09	511
Skeletal and Muscular Disorders	4.38E-28 - 6.70E-09	459
Inflammatory Disease	1.94E-27 - 6.70E-09	476

Molecular and Cellular Functions

Name	p-value	# Molecules
Cellular Development	2.71E-31 - 7.95E-09	406
Cellular Movement	8.54E-27 - 8.10E-09	272
Cellular Function and Maintenance	2.29E-26 - 6.71E-09	149
Cell Death	5.34E-25 - 6.65E-09	434
Cellular Growth and Proliferation	3.90E-24 - 7.82E-09	447

Physiological System Development and Function

Name	p-value	# Molecules
Hematological System Development and Function	5.51E-29 - 7.60E-09	332
Organismal Survival	5.92E-29 - 2.22E-12	229
Hematopoiesis	1.68E-28 - 8.10E-09	209
Cell-mediated Immune Response	2.29E-26 - 6.67E-09	158
Tissue Morphology	1.93E-25 - 3.53E-09	207

Top Canonical Pathways

Name	p-value	Ratio
Altered T Cell and B Cell Signaling in Rheumatoid Arthritis	8.26E-14	32/92 (0.348)
Dendritic Cell Maturation	1.15E-13	45/188 (0.239)
Communication between Innate and Adaptive Immune Cells	5.1E-13	32/109 (0.294)
Type I Diabetes Mellitus Signaling	9.01E-13	35/121 (0.289)
Role of Pattern Recognition Receptors in Recognition of Bacteria and Viruses	1.24E-12	29/87 (0.333)

Figure 4.12 Summary of top functional groups enriched in differentially expressed genes in RSV-infected with macrophages at 24 hpi. Differentially expressed genes detected at different time points were significantly categorized into different networks, functions and pathways under the analysis of Ingenuity Pathway Analysis (IPA) version 2012 (P-value≤0.05).

4.3.2.1 RSV infected Hep2 cells

4.3.2.1.1 Immune response

After RSV infection, the host cells will initiate a series of defense response to counteract the virus invasion. Previous researches have revealed that direct RSV infection induced chemokine secretion [168]. In our study, chemokines such as CCL2, CCL5 (RANTES), CCXL2/3/10/11, IL8 (CXCL8) also showed up-regulation at their expression level. Among these chemokines, the up-regulated fold regulation of CCL5 and CXCL10/11 showed ascending, while the up-regulated fold regulation of CCL2 and CXCL2/3 showed descending with the infection time increasing. In addition, the

A

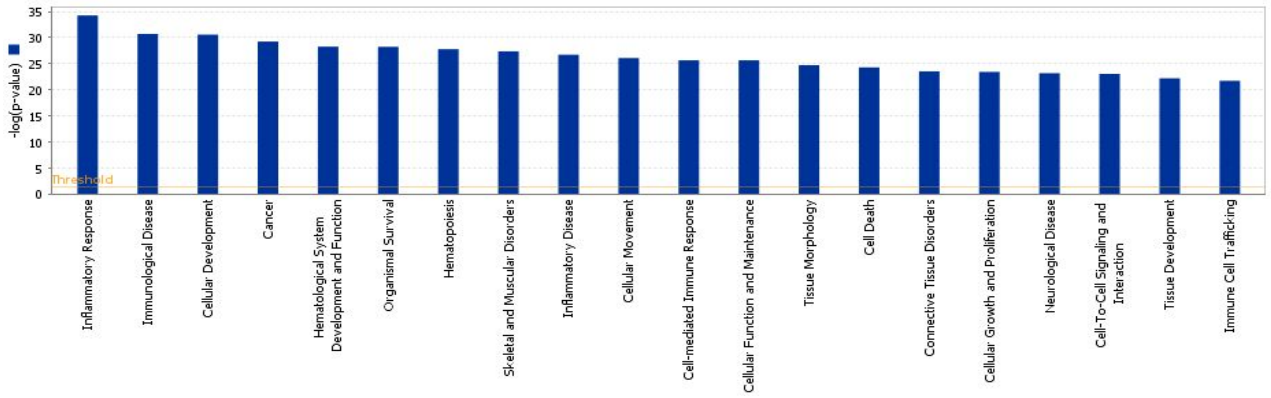

B

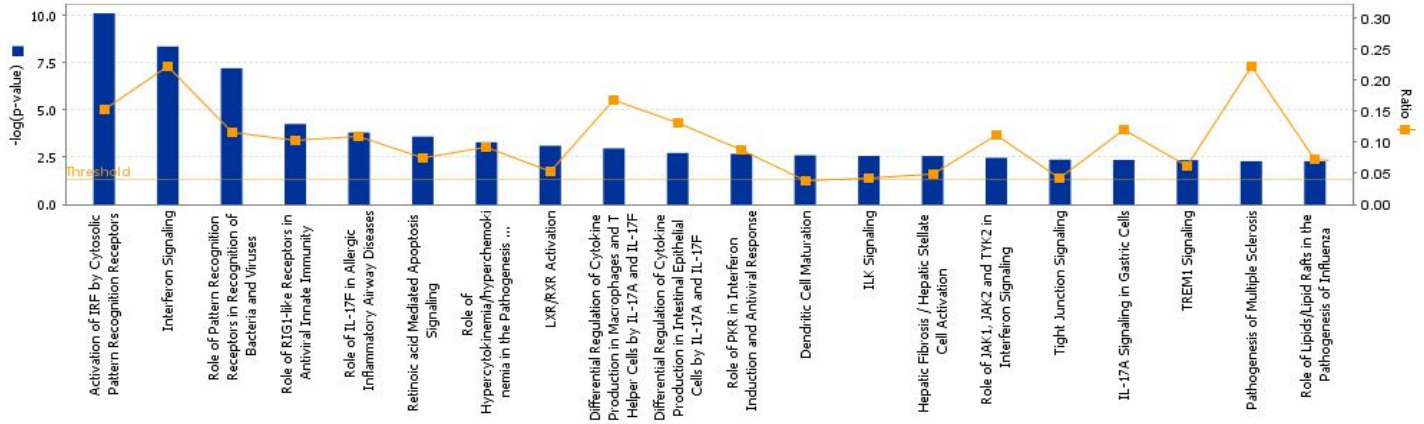

Figure 4.13 Top 20 (A) biological functions and (B) canonical pathways significantly enriched in differentially expressed genes from RSV-infected macrophages at 24 hpi (P-value≤0.05). Threshold was set at p-value = 0.05 and indicated as –log (p-value) on the Y-axis and the X-axis shows the terms of each biological function or canonical pathway. The orange boxes indicate the ratio (Ratio) of the number of genes with differential expression changes and the total number of genes in the respective canonical pathway.

expression of IL8 (CXCL8) showed sustained and extraordinary induction across the whole infection period. These observations might demonstrate that these chemokines are under the control of different types of molecular mechanisms when they exert their antiviral function as proinflammatory mediators. Another cytokine, IL6, was also up-regulated with a quite high fold change at its expression level, which implied the strong activation of immune response.

Although no significant expression changes of IFN-α and IFN-β were detected, the receptors including IFNAR2 and IFNGR1 showed up-regulated expression with low fold regulation at early time points (4 hpi and 8 hpi). It might indicate the trigger of IFN type I and II signaling pathways at the beginning of RSV infection, however the activation was not able to last for a long time. IL28A, belonging to IFN type III family, plays a role in both innate and adaptive immune response [169]. Its elevated gene expression at the late stage of RSV infection might be related to the adaptive immune response in infected Hep2 cells.

Besides these cytokines and IFNs, a batch of interferon stimulated genes including NFKB1/1 (NF-κB), NIKBIB/Z, IGS20, IFI44, OAS3, OASL, GBP1/2 were also identified with up-regulated gene expression in RSV infected Hep2 cells. Other antiviral genes including DDX58 (RIG-I), AREG, CD83, EDN1, EMR3, F3, KLF6, LPIN1, LYN, PBEF1, PDCD1LG1, PLAUR, SOCS2, TNIP1, IRAK2 also showed up-regulation in their expression.

4.3.2.1.2 Cell death

A group of apoptosis-related genes displayed differential expression during the RSV infection in Hep2 cells, and expression regulations of these genes might be due to the host-virus interactions.

Members in the FOS family dimerise with JUN to form the AP-1, which promotes transcription of a diverse range of genes involved in cellular processes such as proliferation and apoptosis [170]. Thus, increasing up-regulation of FOS and JUN genes at their expression level across the whole infection period might function on apoptosis signaling in infected Hep2 cells.

XIAP associated factor-1 (XAF1) antagonizes the activity of XIAP that inhibit activation of caspases during apoptosis. This factor was detected with

up-regulated expression from 4 hpi to 12 hpi, which enhanced the hypothesis that the programmed apoptosis was induced from early infection stage.

BIRC3 belongs to the inhibitor of apoptosis (IAP) gene family which encodes proteins that negatively regulate cell death. Another anti-apoptotic molecule, TNFAIP3, has been reported to inhibit NF-κB activation and TNF-mediated apoptosis, in further to limit inflammation. Both these two factors were strongly up-regulated at their expression level, implicating the potential regulation of attenuating apoptosis in Hep2 cells.

Among the few genes down-regulated with faint fold changes, Tp53 is a key regulator that is able to initiate programmed cell death. Down-regulation of its expression might be associated with the delayed programmed cell death, a feature which resulted in more robust viral titers [131].

Collectively, apoptosis of the Hep2 cells was controlled in two opposite directions following RSV infection. On one hand, some evidences proved that the cell death was induced during the virus infection, particularly at early infection stage. On the other hand, some phenomenon implied that virus might take some actions to delay the host apoptosis so as to benefit its replication across the whole infection stage.

4.3.2.1.3 Cholesterol biosynthesis

Lipid raft are micro-domains of the plasma membrane. As a main component of lipid rafts, cholesterol is essential for the formation of membrane raft [171]. Lipid rafts serve as platforms for plasma membrane assembly and budding of enveloped viruses. Several research groups have proposed that RSV proteins located in raft domains and purified RSV virion particles contained raft associated cellular proteins. Recent research even recovered that intact plasma membrane rafts were required for release of infectious progeny RSV particles during RSV infection in human lung epithelial cells [172].

To verify the importance and necessity of the lipid rafts during RSV infection in Hep2 cells, we selected an array of differentially expressed genes in this respect for proof of principle. The genes under investigation included HMGCR, HMGCS1, DHCR7, CYP51A1, FDFT1, IDI1, MVK, SQLE, SC4MOL, APOL6, FN1, ITGA2 and etc. Some of them such as DHCR7, CYP51A1, FDFT1, IDI1 and SC4MOL are involved in synthesis of cholesterol.

Others may exert different functions: APOL6 affects the movement of lipids or allow the binding of lipids to organelles; HMGCR encodes a rate-limiting enzyme for cholesterol synthesis and its expression level is coordinated by the level of free-cholesterol in a negative loop. Notably, these genes were significantly up-regulated especially during the late infection stage, indicating the increased requirement for free-cholesterol as well as the active movement of lipids during virus infection.

Another three genes that are also associated with cell membrane are FN1 and ITGA2/5. FN1 encodes fibronectin, which is a glycoprotein present in a soluble dimeric form in plasma but a dimeric or multimeric form at the cell surface. This glycoprotein is involved in cell adhesion and migration processes. ITGA2 and ITGA5 are integrins that play role as fibronectin receptors. In our RSV-infected Hep2 cells, altered expressions of fibronectin and its receptors might be also associated with the RSV infection. However, detailed interactions and functions retain to be determined in the future.

4.3.2.1.4 Genes with remarkable regulations

In addition to these well-known genes, there existed other genes differentially expressed with topmost fold change in RSV-infected Hep2 cells. Among them, the up-regulated genes included LCN2, PTX3, HKR1, ERG1/4, DUSP6 and so on, while the down-regulated genes were ZNF230, ZIC2, HEY2, AHRR and so on.

Among the up-regulated genes, LCN2 is of importance in the innate immune response to bacterial infection. Upon encountering invading bacteria, TLRs stimulate the secretion of this protein that is capable of limiting bacterial growth by sequestering iron-containing siderophores. Unusual expression elevation of this gene potentially indicated that this gene might have a possibility to be involved in the immune response to virus infection.

Another molecule that is also associated with immune response was PTX3. This gene is rapidly produced and released by cells such as mononuclear phagocytes, dendritic cells, fibroblasts and endothelial cells in response to primary inflammatory signals. And it is also known to bind to dying cells during inflammatory reactions so as to clear the apoptotic cells. Thus, strong

up-regulation of this gene in its expression might indirectly represent the initiation of inflammatory response in Hep2 cells after RSV infection.

HKR1 encoding zinc finger protein and EGR1/4 as a member of the early growth response (EGF) family of zinc finger transcription factors both showed quite significant regulation in their expression. Relevant studies have pointed out that the compounds called AT-2 which inactivate retroviruses through targeting their zinc finger-containing NC protein could also inactivate RSV accompanied by a significant modification of M2-1 [173]. This finding might indicate that zinc fingers as a group of small protein structure motifs play functions during our RSV infection.

Dusp6 belongs to the dual specificity protein phosphatase subfamily. This family takes responsibility to negatively regulate members in the mitogen-activated protein (MAP) kinase superfamily, which function on cellular proliferation and differentiation. Since p38 MAPK activation was proved to be required for RSV induction of human bronchial epithelial membrane permeability [174], the up-regulated expression of Dusp6 was possible an antiviral action in Hep2 cells.

A few genes encoding zinc finger proteins such as ZNF230 and ZIC2 were detected with decreased expression. These two molecules function as transcription regulators so that inhibition of their expression could implicate the suppression of some specific transcriptional regulation activities.

4.3.2.2 RSV infected macrophages

4.3.2.2.1 Immune response

Upon viral infection, macrophages receive chemical signals IFN-γ or IL4/13, and then increase their production of MHC II molecules which prepare them for presenting antigens. Activated macrophages produce and secreted TNFs, which help cause inflammation through the production of IL-1, IL-6, TNFα and activate the other cells of the immune system. Original signal chemicals such as IFN-γ (Ifng), IFN-γ receptor (Ifngr1) and IL4/13 didn't show any significant expression changes during both time points under RSV infection. However, TNFs, which are supposed to be secreted by activated macrophages, showed up-regulated expression with quite high fold change after RSV infection at both 4 and 24 hpi (especially 4 hpi) [Figure 4.18].

Downstream cytokine productions including IL1a, IL1b, IL6 displayed similar expression patterns as TNFs. Other chemokines with differential gene expression included CCL2/3/4/5/7, CCRL2, CX3CR1 and CXCL1/2/3/5/9/10. Careful observations indicated that these chemokines also showed up-regulated expression after RSV infection. Expression levels of these key molecules involved in macrophage activation suggested that macrophages were activated well after RSV infection. Besides, most of these factors showed higher expression levels at 4 hpi than 24 hpi in RSV infected macrophages, indicating that macrophage activation was initiated strongly at a very early stage.

Antigen presentation is a process in which some phagocytes "present" parts of engulfed materials to other cells of the immune system on their cell surface. In activated macrophages, IFN-γ usually increases production of MHC II molecules and prepares them for presenting antigens, MHC I molecules thereafter mediate destruction of host cells displaying that antigen [175]. In RSV-infected macrophages, a group of MHC class I molecules such as H2-Q7, H2-Q8, H2-T22, showed up-regulated expressions. At the meantime, another batch of MHC class II molecules such as H2-Aa/b1, H2-DMa/b1, H2-Ea/b1 was detected with down-regulated expression. It was possible that RSV had evolved methods to evade macrophages antigen presentation through repressing the expression levels of these MHC II molecules.

In the macrophages, the primary signal for activation is IFN-γ from Th1 type CD4 T cells. The secondary signal is CD40L on the T cell which binds CD40 on the macrophage cell surface. As a result, the macrophage expresses more CD40 and TNF receptors on its surface which help stimulate the activation [176]. A large increase in expression of CD40 was detected from 8.6-FC (4 hpi) to 80.9-FC (24 hpi) in RSV-infected macrophages, providing more evidences for the macrophages activation. However, the increasing expression trend of CD40 is different from the previous decreasing expression trend of TNFs and cytokines, and the detailed reason remains to be investigated in the future.

Phagocytosis is the process of engulfing particles such as cell debris, bacteria, and dead tissue cells. In the macrophage phagocytosis process, receptors on the surface of macrophages such as toll-like receptors bind to the "invader" to initiate the phagocytosis [177]. Consequently, high-level up-

regulation of TLR2 and TLR3 at their expression level were detected after RSV infection, which might implicate strong activation of macrophage phagocytosis in RSV-infected macrophages. DDX60 was proved to be a novel antiviral factor promoting RIG-I (DDX58) -like receptor-mediated signaling and was dispensable for TLR3-mediated signaling by Miyashita M *et al* (2011) [178]. Its up-regulated expression with high fold regulation in RSV-infected macrophages was consistent with the gene expression trends of DDX58 and TLR3, indicating strong RIG-I-mediated antiviral signaling after RSV infection in macrophages.

Previous studies have proved that RSV had an ability to impair IFN Type I signaling pathway by distinct mechanisms in macrophages [159]. However, IFN Type I and associated stimulated genes exhibited in an elevated expression with quite high fold regulation. Among them, IFN-α and IFN-β showed higher fold change at 4 hpi than 24 hpi while other IFN regulatory and stimulated genes including GBP1/2/6, IRF7, ISG20, MX1, OASL1/2, RSAD2, IFI44 showed higher fold change at 24 hpi than 4 hpi. These observations suggested that IFN pathway was strongly activated in RSV-infected macrophages.

4.3.2.2.2 Cell death

Various regulations of cell apoptotic activities were also observed in RSV-infected macrophages, with a batch of apoptotic factors such as CFLAR, CASP4, TRAF1/2, MYC, PDCD4, XAF1 differentially expressed [Figure 4.19]. XAF1 is capable of regulating apoptosis by abrogating the anti-apoptotic activities of XIAP. Expression of it showed up-regulated with 5.34-FC at 4 hpi and 33.08-FC at 24 hpi, indicating robust apoptosis activities especially at late infection stage following RSV infection.

A heterodimeric complex formed by TRAF1 and TRAF2 is necessary for TNFα -mediated activation of MAPK8/JNK and NF-κB. Moreover, this complex also mediates the anti-apoptotic signals from TNF receptors through interacting with IAPs [179]. Up-regulation of these two factors at their expression level during RSV infection might indicate the inhibitory regulation on apoptotic signaling from an opposite direction.

4.3.2.2.3 Genes with remarkable regulations

Besides these well-investigated genes, quite a few other genes were also observed with a stimulated expression in RSV-infected macrophages [Figure 4.20].

Several immune related genes including ZBP1, LCN2 and Serpinb2 were strongly stimulated at their expression levels after RSV infection. Z-DNA-binding protein 1 (ZBP1) has been proved to function as a DNA sensor that activated the innate immune system [180]. Other studies also have identified ZBP1 as being essential for IRF3 and IFN-β activation in a JAK/STAT-dependent manner, therefore inhibiting huuman cytomegalovirus replication [181]. LCN2 is always secreted by Toll-like receptors upon encountering invading bacteria in order to limit bacterial growth by sequestrating the iron-laden siderophore [182]. Serpinb2 was proved to be induced during many inflammatory processes and infections and play a physiological role in suppression of Th1-promoting cytokine up-regulated proteins [183]. Strong up-regulation of these genes in their expression during RSV infection might suggest a strong immune response.

Genes of the Schlafen (Slfn) family have been uncovered to participate in T cell development [184], cell cycle arrest [185] and generation of IFNα-induced growth inhibitory responses [186]. Sohn W *et al* (2007) reported that CpG-DNA and LPS triggered slfn-2 gene expression by activating NF-κB and AP-1 pathways in macrophages [187]. In our study, slfn-1/2/3/4/5/8 all showed strong up-regulation at their expression level in macrophages after RSV infection. This could suggest that Slfn genes potentially participated in some critical functions. However, the detailed roles of Slfn family in macrophages are still under investigation.

A few transporter and transmembrane genes were also ranked topmost among the up-regulated genes. For RSV infection, expression of TAP1 and TAP2 showed significant up-regulation only at 24 hpi. RTP4, TMEM171, MS4A4C and MS4A6C showed increasing up-regulation while FLRT3 and TREM1 showed a deceasing up-regulation at their expression levels across the RSV infection period. Furthermore, TREM1 signaling pathway has been reported to amplify the signal from TLRs, NAIP, CIITA and HET-E to produce various chemokines and cytokines [188]. Thus, significant up-regulation of

TREM1 at its expression level following RSV infection at 4 hpi may potentially contribute to the timely development of the cytokine storm in corresponding infected macrophages.

GPR84 is one of the G protein-coupled receptors which is largely restricted to macrophage populations and granulocytes. Lattin JE et al (2008) has pointed out that expression of GPR84 could be highly regulated by LPS via TLR4 in mouse macrophages [189]. However, TLR4 didn't show any differential expression change in infected macrophages. Hence, some other unclear stimuli might be responsible for the remarked up-regulation of GPR84 at its expression level during RSV infection at both 4 and 24 hpi.

4.3.3 Regulations of gene expression in canonical pathways

4.3.3.1 Interferon signaling

In RSV-infected Hep2 cells, it was notable that STAT1 and IFNα/β only showed faintly up-regulated expression changes at 12 hpi and 15 hpi, separately. Among the downstream genes, IRF showed up-regulated expression with 7.0-FC at 2 hpi, and OAS1 and TAP1 showed up-regulated expression at the late stage of infection. These observations may suggest that the IFN signaling pathway and its downstream productions were not strongly activated or induced upon RSV infection in Hep2 cells. SOCS1, as a member of SOCS family, has been proved to block type I and II IFN signaling through JAK-STAT pathway [190]. Subsequently, strong up-regulation of SOCS1 in its gene expression from 8 hpi to 15 hpi could be partly responsible for the status of IFN signaling pathway.

In the case of RSV-infected mouse macrophages, IFN signaling pathway, especially type I, behaved in an activated state at both infection time points, which was different from the situation happened in Hep2 cells. At 24 hpi, expression of ISGs such as IFIT1, IFIT3 and MX1 showed up-regulation with 838.7-FC, 316.8-FC and 146.1-FC respectively. Altogether, these data provided evidences that IFN type I signaling pathway was strongly activated and productions of downstream ISGs were strongly promoted in mouse macrophages after infection of RSV.

4.3.3.2 NF-κB signaling

NF-κB is a major transcription factor which regulates expression of the genes responsible for both the innate and adaptive immune response. Upon virus infection, its activation will result in expression of an array of cytokine and chemokine genes. Besides its function on inflammation response, NF-κB signaling pathway also plays a vital role in cell proliferation and apoptosis. The canonical mechanism of NF-κB activation includes IKK2/IKKb mediated inhibitor of NF-κB (IκB) phosphorylation and degradation. This action consequently leads to the release and translocation of NF-κB factors p65 and p50 dimers which migrate to the nucleus to exert biological functions.

Generally, NF-κB signaling pathway in RSV-infected Hep2 cells was not obviously activated. No expression change of IKK complex and NF-κB factors p65 was observed across the whole infection period. And some of the downstream cytokines and chemokines only showed faint up-regulation at their expression levels. These observations suggested that NF-κB signaling pathway was not significantly triggered in Hep2 cells upon RSV infection.

A20, as a NF-κB inhibitor, is involved in the feedback suppression of NF-κB activation induced by TNFα [191]. Quite significant up-regulation of A20 in its expression during the whole RSV infection stage may be responsible to terminate the activation of NF-κB. No expression change was detected for TNFα may imply that there exists alternative mechanism on the A20 induction.

Compared to the gene expression performances of NF-κB signaling pathway in RSV-infected Hep2 cells, more genes showed up-regulated expression in RSV-infected mouse macrophages. Gene expression of A20 and TNFα both exhibited more significant up-regulation at 4 hpi than 24hpi, which suggested that the activation and inhibition of this pathway were initiated from an early infection stage. In contrary to A20 and TNFα, CD40 showed up-regulated expression with higher fold change at 24 hpi. Since CD40 has been proved to mediate NF-κB activation and cytokine secretion in human colonic fibroblasts [192], expression induction of this gene may enhance activation NF-κB signaling pathway in another way during later infection stage in RSV-infected macrophages.

4.3.3.3 Toll-like receptor signaling

TLRs are a type of PRRs which recognize pathogen-associated molecules. Activation of TLR signaling causes the transcriptional activation of pro-inflammatory cytokines and chemokines, which subsequently play an essential role in immune response. TLR7/TLR8 can mediate the activation of IRF7 through unique interaction between TLR domain–containing cytosolic adapters such as myeloid differentiation primary-response protein-88 (MyD88) [193]. Independent of MyD88, TLR3 is also able to exert its function by interacting with TRIF, which in turn to activats a complex of IKKe, TRAF3, and TBK1 that phosphorylates IRF3 and IRF7. Activation of IRF3 leads to the expression induction of CD40, CD80, and CD86, while activation of IRF7 promotes the induction of IFNα and IFNβ gene expression [194].

Many studies have revealed the detailed function of TLRs upon RSV infection. For example, Marchant D *et al* (2010) reported that TLR4-mediated activation of p38 MAPK was a determinant of RSV entry and tropism [195]; TLR2 and TLR6 activations were critical for controlling RSV viral replication [196]; TLR4 signaling pathway played a predominant role in mediating LPS-induced-IL-6 production of RSV infected epithelial cells [197]; TLR4 expression was increased in infants with RSV bronchiolitis, and F protein of RSV binded to TLR4 and CD14 in order to initiate innate immunity response [198].

Investigation on RSV-infected Hep2 cells suggested that faint up-regulation of TLR4 at its expression level was detected at 8 hpi, and the expression of downstream p38 MAP2K3 was induced at 8 hpi but repressed at the late infection stage. Remarkable up-regulation of IL6 at its expression level might provide evidences for the expression induction of TLR4 as well as its signaling mediation. In addition, it has been reported that TLR3, TLR7 and TLR8 can also mediate the activation of IRF3 and IRF7 to trigger IFN induction. The expression of TLR3, TLR7 and TLR8 showed no expression change in Hep2 cells, and this might be consistent with the previous observation that interferon signaling pathway showed almost inactivated in RSV-infected Hep2 cells.

In macrophages infected with RSV, extensive activation of toll-like receptors was revealed. Gene expression levels of TLR2, CD14, IRAK as well

as NF-κB were induced at early infection time point while gene expression levels of TLR2, TLR5, TLR3, MYD88, PKR, and NF-κB were stimulated at late infection time point. High-level stimulation of TLR3 at its expression level resulted in strong activation of IFN pathway as well as accumuation of its downstream productions as described before.

4.3.3.4 Apoptosis signaling

Apoptosis is the process of programmed cell death happened in multicellular organisms. All apoptosis signaling pathways converge on a common machinery of cell destruction that is activated by caspases through cleaving proteins at aspartate residues [199]. Several reports have been published to prove that RSV infection induced or inhibited apoptosis in different cell lines with different impact factors [142, 161, 200, 201].

When we investigated the performance of apoptosis signaling pathway in RSV-infected Hep2 cells, we found that there were few genes showing significant expression changes. Baculoviral IAP repeat-containing protein 3 (BIRC3) which functions in providing instructions for making IAPs show high-level up-regulation at its expression level. IAPs that belong to inhibitor of apoptosis family have been shown to be involved in suppressing the host cell death response to viral infection. Thus, Up-regulated expression of BIRC3 may suggest the anti-apoptosis actions were taken by RSV in order to benefit the viral replication.

In mouse macrophages, RSV infection led to faint up-regulation of caspase 8, caspase 12, caspase 3 and caspase 7 at their expression level in apoptosis signaling pathway at 24 hpi. TNF, mainly secreted by macrophages, is able to induce apoptotic cell death. This factor showed up-regulated expression with 41.9-FC and 13.4-FC separately at 4 and 24 hpi, which might be responsible for the activation of caspases at 24 hpi mentioned above.

4.3.3.5 Cell cycle: G1/S checkpoint regulation

Cell cycle arrest is controled by interactions of a group of important proteins. An increase in phosphorylation of His-3 protein denotes the cell cycle arrest in G2/M phase while an increase in dephosphorylation of Rb protein represents the cell cycle arrest in G0/G1 phase. Gibbs JD *et al* (2009) has

claimed that RSV infection induced G2/M cell cycle arrest in human bronchial epithelial cells and G0/G1 cell cycle arrest in A549 cells through TNF-β in order to enhance its replication [202].

In our RSV-infected Hep2 cells, only a small batch of genes in G1/S checkpoint regulation pathway was detected with differential expression over the whole infection process. At 8 hpi, down-regulated expression of E2F and up-regulated expression of CDK 4/6 and cyclin D were both detected, which may be generated from the fighting of two opposite-direction regulations. At two later time points, E2F was consistently down-regulated but no more expression changes were detected for CDK 4/6 and cyclin D. In addition, p21 as a potent cyclin-dependent kinase inhibitor was detected with an increasing expression elevation over the whole infection period, which may suggest the arrest regulation of cell cycle in a gradual way.

In macrophages, a few up-regulated genes were detected at 4 hpi during RSV infection. These genes not only included the ones that activate the cell cycle G1/S checkpoint such as CDK 4/6, c-Myc and cyclin E but also the ones that induce the cell cycle arrest including TGF-β, smad3 and p21. Less significant gene expression cases were detected at 24 hpi after RSV infection in mouse macrophages.

4.3.3.6 Cell cycle: G2/M DNA damage checkpoint regulation

Similar to G1/S checkpoint regulation pathway, few gene expression changes were detected in G2/M DNA damage checkpoint regulation pathway in RSV-infected Hep2 cells. And most of significant gene expression regulations detected at 12 hpi showed quite faint fold changes.

A batch of genes was significantly expressed in RSV-infected macrophages at 4hpi. However, some of these genes inhibit of cell cycle arrest while others of them facilitate cell cycle arrest. Thus, no apparent conclusion could be reached based on these observations.

4.3.3.7 Antigen presentation pathway

Two types of MHC groups are involved in antigen presentation processes. MAH class I participate in the intracellular antigens' presentation which are produced mainly by viruses replicating within a host cell, while MHC

class II attend extracellular antigens' presentation coming from exogenous pathogens. Macrophages express low level of MHC class II, but the expression can be up-regulated by microbial products and macrophages can therefore present antigens from the microbe to $CD4^+$ T lymphocytes. Besides, antigens from can elicit an MHC-I-dependent response that results in the proliferation of $CD8^+$ cytotoxic T lymphocytes [203].

In our experiment, RSV infection resulted in up-regulated expression of MHC I-α and down-regulated expression of MHC II-α/β in macrophages at 24 hpi. Expression induction of MHC class I may be due to the fighting with the exogenous RSV, while expression repression of MHC class II may imply that the inner RSV replication was inhibited in macrophages or RSV evolved some mechanism to inhibit the activation of MHC class II. And down-regulated expression of genes involved in MHC class II pathway in RSV infected mice was also observed in another study [375].

4.4 Conclusion

Till now, there has been no report published to describe the host response towards RSV infection in Hep2 cells and murine lung macrophages. In this chapter, we made efforts to investigate the global gene expression using microarray system in order to examine the host response in RSV-infected Hep2 cells and murine lung macrophages. Moreover, parallel comparison of genomic expression profiles between Hep2 cells and mouse lung macrophages upon RSV infection was beneficial for us to understand the pathogenesis deeply.

Global evaluation indicated that the numbers of differentially expressed probe sets/genes were increasing with the infection time increasing in RSV-infected Hep2 cells and macrophages. However, among these differentially expressed probe sets/genes, most of the probe sets showed down-regulated expression in Hep2 cells while most of genes showed up-regulated expression in macrophages.

As the results generated from functional classification, it was noted that "DNA Binding", "Immune Response" and "Signal Transduction" were over-represented and shared by those probe sets/genes with up-regulated expression from both infected host cells. However, the genes with down-regulated expression from infected macrophages were associated with "Cell Cycle", "Cell

Death", "Kinase" and "Signal Transduction", and these functional groups were not consistent with the over-represented ones based on probe sets with down-regulated expression from Hep2 cells.

Besides these functional groups, pathways such as "MAPK signaling", "Jak-STAT signaling pathway" and "B-cell receptor signaling pathway" and potential transcription factors such as SRF, ISRE, Sp1 were enriched based on genes with up-regulated expression in RSV-infected Hep2 cells. At the meanwhile, pathways such as "Cytokine-cytokine receptor interaction" and "Apoptosis" and transcription factors such as ETF, E2F, TATA, NF-kappaB_(p65) were enriched based on genes with down-regulated expression in RSV-infected Hep2 cells. In RSV-infected macrophages, a batch of functional networks such as "Inflammatory Response" and "Immunological Disease" and pathways such as "Role of pattern recognition receptors in recognition of bacteria" and "Communication between innate and adaptive immune cells" were significantly enriched in differentially expressed genes, and enrichment of these functions and pathways implicated the strong macrophage activation and immune response signaling.

Through detailed examination on specific genes, a batch of key genes was highlighted. In Hep2 cells, induction of secretion of chemokines such as CCL2, CCL5 and IL8 was observed, genes related to apoptosis such as XAF1 and genes related to cholesterol synthesis such as HMGCR all showed differential expression. And these observations partly overlapped with the results reported by another group of researchers [371]. During their investigation of proteome in RSV infected A549 cells, it has been reported that a group of proteins involved in protein biosynthesis and modification, cellular stress responses, cytoskeleton and structure showed differential expression. In macrophages, expression of genes associated with antigen presentation and cell apoptosis were also altered in our data. Recently, another study in our lab tried to uncover the detailed function of hydroxymethyglutaryl coenzyme A reductase inhibitor lovastatin as an anti-inflammatory drug. And the results revealed the increase of virus antigen and inclusion bodies, as well as the correlated increase of cytokines in their gene expression at from 2 to 16hpi in RSV-infected RAW cells. Besides, mature F and G glycoproteins were not able to be detected on the surface of the infected RAW cells. In general, these

observations were consistent with the findings in our study. Furthermore, it was also observed that lovastatin treatment in RAW cells indeed significantly reduce the levels of pro-inflammatory cytokines, which partly explain the phenomenon that lovastatin treatment is effective on protecting mice from lethal RSV infection [391].

Analysis on gene expression performances in canonical pathways including “Interferon signaling”, “NF-κB signaling” and “Toll-like receptor signaling” suggested that only a small batch of genes showed differential expression with faint fold changes in RSV-infected Hep2 cells, indicating poor activation of these pathways.

However, investigation of gene expression performances in these immune response pathways suggested that a wider range of genes were detected with significant expression changes in RSV-infected macrophages, suggesting the well initiation of inflammatory defense.

As described before, the transcriptomic profiles were investigated from 4hpi to 15hpi in RSV-infected Hep2 cells. From 8hpi, it was observed that the virus filaments and inclusion bodies were formed with an increasing numbers, and the quite a lot of virus filaments accumulated at 15hpi. Data from microarray study indicated that the productions of cytokines and chemokines were increased quite early (from 4hpi), indicating that the innate response was activated at the first beginning of virus replication cycle, at least before the observation of obvious virus filaments and inclusion bodies. Compared to the response detected at 4hpi, stronger induction of pro-inflammatory response has been observed from 8hpi and sustained over the late infection stage. This phenomenon might indicate that the antiviral actions were fully taken to prevent the further assembly and release in host cells. At the meanwhile, several mechanisms including inhibiting the expression of type I IFN, delaying host apoptosis and alteration of lipid raft have also been exerted by RSV in order to interfere with the activated immune defense and benefit the further viral replication [156].

In our RSV-infected macrophages, strong immune response was observed from the early infection stage (4hpi) to the late infection stage (24hpi). At the meanwhile, similar vRNA levels at between 2.5 and 20 hpi were also detected. Thus, it might be assumed that sustained activation of genes involved

in innate and acquired immune response was responsible for the low respiratory tract infection. In addition, other data also indicated that RSV infection results in the formation of virus antigen and the production of inclusion bodies, efficient infectious virus particle production does not occur [364].

Probe ID	GeneBank	Gene Title
205239_at	NM_001657	amphiregulin (schwannoma-derived growth factor)
203140_at	NM_001706	B-cell CLL/lymphoma 6 (zinc finger protein 51)
210538_s_at	U37546	baculoviral IAP repeat-containing 3
202094_at	AA648913	baculoviral IAP repeat-containing 5 (survivin)
203944_x_at	NM_007049	butyrophilin, subfamily 2, member A1
211256_x_at	U90142	butyrophilin, subfamily 2, member A1
215493_x_at	AL121936	butyrophilin, subfamily 2, member A1
216598_s_at	S69738	chemokine (C-C motif) ligand 2
1405_i_at	M21121	chemokine (C-C motif) ligand 5
1555759_a_at	AF043341	chemokine (C-C motif) ligand 5
204655_at	NM_002985	chemokine (C-C motif) ligand 5
204440_at	NM_004233	CD83 antigen (activated B lymphocytes, immunoglobulin superfamily)
1556151_at	AI077660	T-cell immunomodulatory protein
204533_at	NM_001565	chemokine (C-X-C motif) ligand 10
210163_at	AF030514	chemokine (C-X-C motif) ligand 11
211122_s_at	AF002985	chemokine (C-X-C motif) ligand 11
209774_x_at	M57731	chemokine (C-X-C motif) ligand 2
207850_at	NM_002090	chemokine (C-X-C motif) ligand 3
218943_s_at	NM_014314	DEAD (Asp-Glu-Ala-Asp) box polypeptide 58
242961_x_at	AI304317	DEAD (Asp-Glu-Ala-Asp) box polypeptide 58
222793_at	AK023661	DEAD (Asp-Glu-Ala-Asp) box polypeptide 58
218995_s_at	NM_001955	endothelin 1
222802_at	J05008	endothelin 1
1564630_at	BC036851	endothelin 1
1561042_at	AF086249	Egf-like module containing, mucin-like, hormone receptor-like 3
204363_at	NM_001993	coagulation factor III (thromboplastin, tissue factor)
1559094_at	AK095307	F-box protein 9
1566509_s_at	AK095315	F-box protein 9
209864_at	AB045118	frequently rearranged in advanced T-cell lymphomas 2
231577_s_at	AW014593	guanylate binding protein 1, interferon-inducible, 67kDa
202269_x_at	BC002666	guanylate binding protein 1, interferon-inducible, 67kDa
202270_at	NM_002053	guanylate binding protein 1, interferon-inducible, 67kDa
242907_at	BF509371	guanylate binding protein 2, interferon-inducible
214453_s_at	NM_006417	interferon-induced protein 44
214059_at	BE049439	Interferon-induced protein 44
208375_at	NM_024013	interferon, alpha 1
207964_x_at	NM_021068	interferon, alpha 4
225661_at	AA811138	interferon (alpha, beta and omega) receptor 1
225669_at	AA133989	interferon (alpha, beta and omega) receptor 1

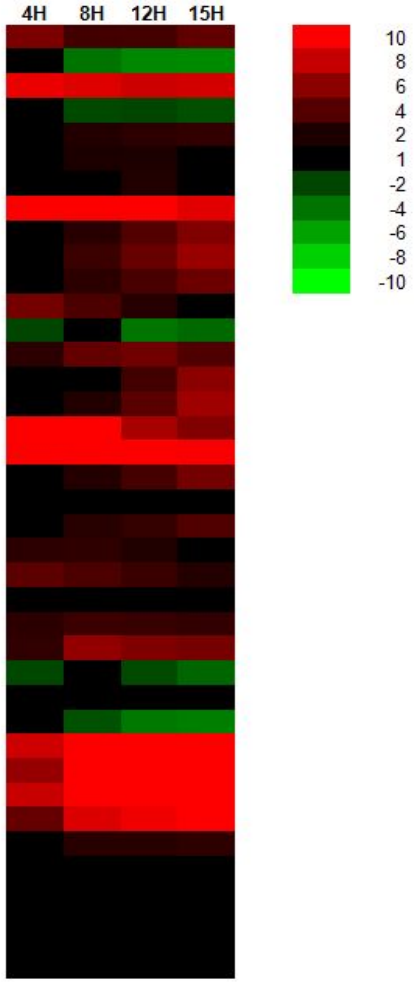

Probe ID	GeneBank	Gene Title
204786_s_at	L41944	interferon (alpha, beta and omega) receptor 2
227125_at	BF526978	Interferon (alpha, beta and omega) receptor 2
208173_at	NM_002176	interferon, beta 1, fibroblast
202727_s_at	NM_000416	interferon gamma receptor 1
211676_s_at	AF056979	interferon gamma receptor 1
201642_at	NM_005534	interferon gamma receptor 2 (interferon gamma transducer 1)
1552915_at	NM_172138	interleukin 28A (interferon, lambda 2)
1552609_s_at	NM_172139	interleukin 28A (interferon, lambda 2)
205207_at	NM_000600	interleukin 6 (interferon, beta 2)
202859_x_at	NM_000584	interleukin 8
211506_s_at	AF043337	interleukin 8
231779_at	AI246590	interleukin-1 receptor-associated kinase 2
204698_at	NM_002201	interferon stimulated exonuclease gene 20kDa
33304_at	U88964	interferon stimulated exonuclease gene 20kDa
208961_s_at	AB017493	Kruppel-like factor 6
224606_at	BG250721	Kruppel-like factor 6
1555832_s_at	BU683415	Kruppel-like factor 6
210754_s_at	M79321	v-yes-1 Yamaguchi sarcoma viral related oncogene homolog
202625_at	AI356412	v-yes-1 Yamaguchi sarcoma viral related oncogene homolog
202626_s_at	NM_002350	v-yes-1 Yamaguchi sarcoma viral related oncogene homolog
209239_at	M55643	nuclear factor of kappa light polypeptide gene enhancer in B-cells 1 (p105)
207535_s_at	NM_002502	nuclear factor of kappa light polypeptide gene enhancer in B-cells 2 (p49/p100)
228388_at	AA044140	nuclear factor of kappa light polypeptide gene enhancer in B-cells inhibitor, beta
223217_s_at	BE646573	nuclear factor of kappa light polypeptide gene enhancer in B-cells inhibitor, zeta
223218_s_at	AB037925	nuclear factor of kappa light polypeptide gene enhancer in B-cells inhibitor, zeta
202869_at	NM_016816	2',5'-oligoadenylate synthetase 1, 40/46kDa
205552_s_at	NM_002534	2',5'-oligoadenylate synthetase 1, 40/46kDa
218400_at	NM_006187	2'-5'-oligoadenylate synthetase 3, 100kDa
232666_at	R13458	2'-5'-oligoadenylate synthetase 3, 100kDa
205660_at	NM_003733	2'-5'-oligoadenylate synthetase-like
210797_s_at	AF063612	2'-5'-oligoadenylate synthetase-like
217739_s_at	NM_005746	pre-B-cell colony enhancing factor 1
243296_at	AA873350	Pre-B-cell colony enhancing factor 1
1555167_s_at	BC020691	pre-B-cell colony enhancing factor 1
212151_at	BF967998	Pre-B-cell leukemia transcription factor 1
239210_at	AW074143	Pre-B-cell leukemia transcription factor 1
212148_at	AL049381	Pre-B-cell leukemia transcription factor 1

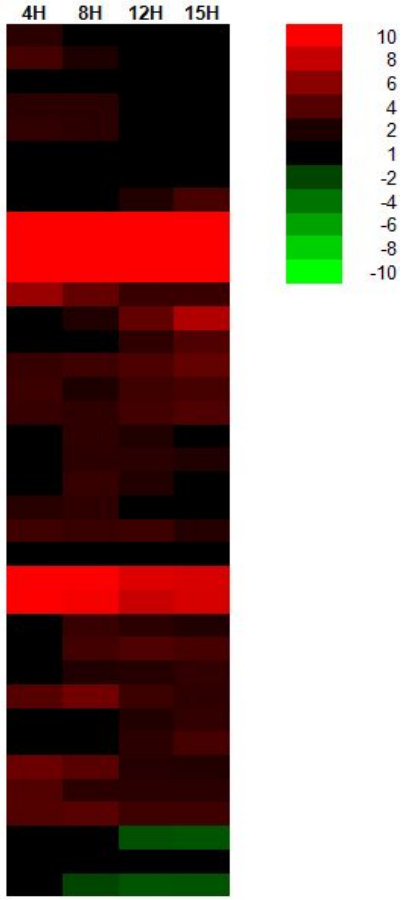

Figure 4.14 Expression of probe sets involved in immune response in RSV-infected Hep2 cells. RSV was infected with Hep2 cells, and the expression of probe sets associated with immune response was examined by microarray analysis at 4, 8, 12 and 15 hpi as shown. The data is represented by heat map analysis showing up-regulated (red), down-regulated (green) or no changes (black) in expression, and the FC range is indicated (P-value≤0.05).

Probe ID	GeneBank	Gene Title
217911_s_at	NM_004281	BCL2-associated athanogene 3
215037_s_at	U72398	BCL2-like 1
206665_s_at	NM_001191	BCL2-like 1
212312_at	AL117381	BCL2-like 1
210538_s_at	U37546	baculoviral IAP repeat-containing 3
206133_at	AI43782	XIAP associated factor-1
228617_at	CO439482	XIAP associated factor-1
242234_at	GI439853	XIAP associated factor-1
211851_x_at	AF005068	breast cancer 1, early onset
204531_s_at	NM_007295	breast cancer 1, early onset
202284_s_at	NM_000389	cyclin-dependent kinase inhibitor 1A (p21, Cip1)
208485_x_at	NM_003879	CASP8 and FADD-like apoptosis regulator
209939_x_at	AF005775	CASP8 and FADD-like apoptosis regulator
210564_x_at	AF009619	CASP8 and FADD-like apoptosis regulator
211316_x_at	AF009616	CASP8 and FADD-like apoptosis regulator
211317_s_at	AF041461	CASP8 and FADD-like apoptosis regulator
211862_x_at	AF015451	CASP8 and FADD-like apoptosis regulator
210563_x_at	U97075	CASP8 and FADD-like apoptosis regulator
209508_x_at	AF005774	CASP8 and FADD-like apoptosis regulator
203890_s_at	BF686824	death-associated protein kinase 3
203891_s_at	NM_001348	death-associated protein kinase 3
233912_x_at	AK021525	ELMO domain containing 2
1553928_at	NM_153702	ELMO domain containing 2
201324_at	NM_001423	epithelial membrane protein 1
201325_s_at	NM_001423	epithelial membrane protein 1
235745_at	AV704183	endoplasmic reticulum to nucleus signalling 1
204780_s_at	AA164751	Fas (TNF receptor superfamily, member 6)
216252_x_at	Z70519	Fas (TNF receptor superfamily, member 6)
215719_x_at	X83493	Fas (TNF receptor superfamily, member 6)
204781_s_at	NM_000043	Fas (TNF receptor superfamily, member 6)
209189_at	BC004490	v-fos FBJ murine osteosarcoma viral oncogene homolog
205409_at	NM_005253	FOS-like antigen 2
218880_at	N36408	FOS-like antigen 2
218881_s_at	NM_024530	FOS-like antigen 2
225262_at	AI670862	FOS-like antigen 2
228188_at	AI860150	FOS-like antigen 2
204235_s_at	AF200715	GULP, engulfment adaptor PTB domain containing 1
204237_at	NM_016315	GULP, engulfment adaptor PTB domain containing 1
215913_s_at	AK023668	GULP, engulfment adaptor PTB domain containing 1

Probe ID	GeneBank	Gene Title
223837_at	BC001103	GULP, engulfment adaptor PTB domain containing 1
201631_s_at	NM_003897	immediate early response 3
204549_at	NM_014002	inhibitor of kappa light polypeptide gene enhancer in B-cells, kinase epsilon
36004_at	AF074382	inhibitor of kappa light polypeptide gene enhancer in B-cells, kinase gamma
209929_s_at	AF091453	inhibitor of kappa light polypeptide gene enhancer in B-cells, kinase gamma
201466_s_at	NM_002228	v-jun sarcoma virus 17 oncogene homolog (avian)
201464_x_at	BG491844	v-jun sarcoma virus 17 oncogene homolog (avian)
214057_at	H71805	Myeloid cell leukemia sequence 1 (BCL2-related)
200796_s_at	BF594446	myeloid cell leukemia sequence 1 (BCL2-related)
200797_s_at	AI275690	myeloid cell leukemia sequence 1 (BCL2-related)
214056_at	BF981280	Myeloid cell leukemia sequence 1 (BCL2-related)
200798_x_at	NM_021960	myeloid cell leukemia sequence 1 (BCL2-related)
202014_at	NM_014330	protein phosphatase 1, regulatory (inhibitor) subunit 15A
37028_at	U83981	protein phosphatase 1, regulatory (inhibitor) subunit 15A
203372_s_at	AB004903	suppressor of cytokine signaling 2
203373_at	NM_003877	suppressor of cytokine signaling 2
202694_at	AW183478	serine/threonine kinase 17a (apoptosis-inducing)
241410_at	AI949081	Serine/threonine kinase 17a (apoptosis-inducing)
202693_s_at	AW194730	serine/threonine kinase 17a (apoptosis-inducing)
202695_s_at	NM_004760	serine/threonine kinase 17a (apoptosis-inducing)
201207_at	NM_021137	tumor necrosis factor, alpha-induced protein 1 (endothelial)
202510_s_at	NM_006291	tumor necrosis factor, alpha-induced protein 2
202643_s_at	AI738896	tumor necrosis factor, alpha-induced protein 3
202644_s_at	NM_006290	tumor necrosis factor, alpha-induced protein 3
206025_s_at	AW188198	tumor necrosis factor, alpha-induced protein 6
206026_s_at	NM_007115	tumor necrosis factor, alpha-induced protein 6
210260_s_at	BC005352	tumor necrosis factor, alpha-induced protein 8
208296_x_at	NM_014350	tumor necrosis factor, alpha-induced protein 8
227420_at	BF338045	tumor necrosis factor, alpha-induced protein 8-like 1
1552648_a_at	NM_003844	tumor necrosis factor receptor superfamily, member 10a
241371_at	AW451259	Tumor necrosis factor receptor superfamily, member 10a
231775_at	W65310	tumor necrosis factor receptor superfamily, member 10a
218856_at	NM_016629	tumor necrosis factor receptor superfamily, member 21
214581_x_at	BE568134	tumor necrosis factor receptor superfamily, member 21
201746_at	NM_000546	tumor protein p53 (Li-Fraumeni syndrome)
226502_at	BG477315	ELMO domain containing 2

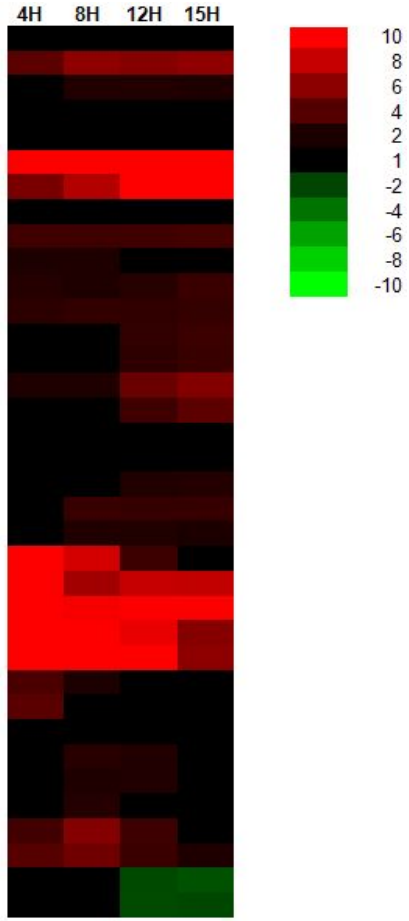

Figure 4.15 Expression of probe sets involved in cell death in RSV-infected Hep2 cells. RSV was infected with Hep2 cells, and the expression of probe sets associated with cell death was examined by microarray analysis at 4, 8, 12 and 15 hpi as shown. The data is represented by heat map analysis showing up-regulated (red), down-regulated (green) or no changes (black) in expression, and the FC range is indicated (P-value≤0.05).

Probe ID	GeneBank	Gene Title
208636_at	AI082078	Actinin, alpha 1
208637_x_at	BC003576	actinin, alpha 1
211160_x_at	M95178	actinin, alpha 1
237401_at	BF062666	Actinin, alpha 1
241869_at	AW026509	apolipoprotein L, 6
219716_at	NM_030641	apolipoprotein L, 6
216607_s_at	U40053	cytochrome P450, family 51, subfamily A, polypeptide 1
202314_at	NM_000786	cytochrome P450, family 51, subfamily A, polypeptide 1
201790_s_at	AW150953	7-dehydrocholesterol reductase
201791_s_at	NM_001360	7-dehydrocholesterol reductase
201790_s_at	AW150953	7-dehydrocholesterol reductase
201791_s_at	NM_001360	7-dehydrocholesterol reductase
239358_at	BE645256	Farnesyl-diphosphate farnesyltransferase 1
210950_s_at	BC003573	farnesyl-diphosphate farnesyltransferase 1
241954_at	AA757900	Farnesyl-diphosphate farnesyltransferase 1
208647_at	AA872727	farnesyl-diphosphate farnesyltransferase 1
238666_at	BF438300	Farnesyl-diphosphate farnesyltransferase 1
243658_at	AA873729	Farnesyl-diphosphate farnesyltransferase 1
1558199_at	W73431	fibronectin 1
210495_x_at	AF130095	fibronectin 1
212464_s_at	X02761	fibronectin 1
214701_s_at	AJ276395	fibronectin 1
214702_at	AJ276395	fibronectin 1
216442_x_at	AK026737	fibronectin 1
235629_at	AI333596	Fibronectin 1
211719_x_at	BC005858	fibronectin 1
202539_s_at	AL518627	3-hydroxy-3-methylglutaryl-Coenzyme A reductase
202540_s_at	NM_000859	3-hydroxy-3-methylglutaryl-Coenzyme A reductase
202540_s_at	NM_000859	3-hydroxy-3-methylglutaryl-Coenzyme A reductase
202539_s_at	AL518627	3-hydroxy-3-methylglutaryl-Coenzyme A reductase
205822_s_at	NM_002130	3-hydroxy-3-methylglutaryl-Coenzyme A synthase 1 (soluble)
221750_at	BG035985	3-hydroxy-3-methylglutaryl-Coenzyme A synthase 1 (soluble)
220081_x_at	NM_016371	hydroxysteroid (17-beta) dehydrogenase 7
204615_x_at	NM_004508	isopentenyl-diphosphate delta isomerase 1
208881_x_at	BC005247	isopentenyl-diphosphate delta isomerase 1
242065_x_at	BG477984	isopentenyl-diphosphate delta isomerase 1
230198_at	AA166617	Isopentenyl-diphosphate delta isomerase 1
242255_at	R49102	Isopentenyl-diphosphate delta isomerase 1
205032_at	NM_002203	integrin, alpha 2 (CD49B, alpha 2 subunit of VLA-2 receptor)

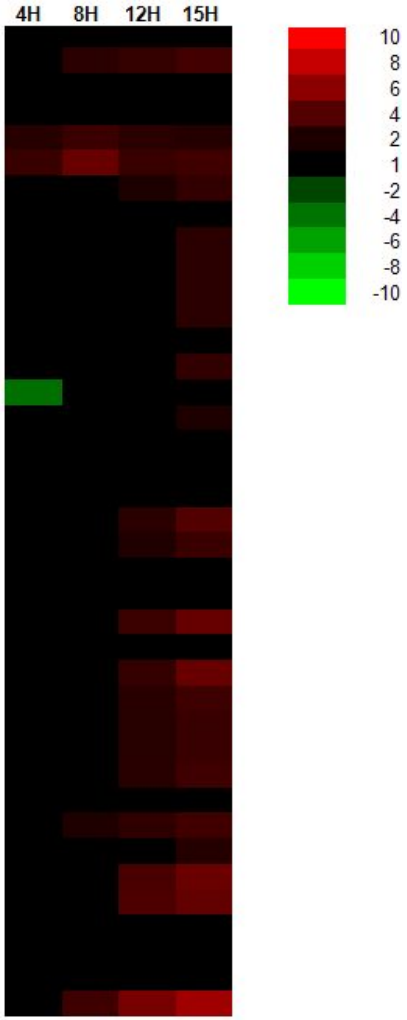

Probe ID	GeneBank	Gene Title
227314_at	N95414	Integrin, alpha 2 (CD49B, alpha 2 subunit of VLA-2 receptor)
237728_at	AI733222	Integrin, alpha 2 (CD49B, alpha 2 subunit of VLA-2 receptor)
201389_at	NM_002205	integrin, alpha 5 (fibronectin receptor, alpha polypeptide)
201124_at	AL048423	integrin, beta 5
201125_s_at	NM_002213	integrin, beta 5
214020_x_at	BE138575	Integrin, beta 5
214021_x_at	AI335208	Integrin, beta 5
1559203_s_at	BC029545	v-Ki-ras2 Kirsten rat sarcoma viral oncogene homolog
1559204_x_at	BC029545	v-Ki-ras2 Kirsten rat sarcoma viral oncogene homolog
204009_s_at	W80678	v-Ki-ras2 Kirsten rat sarcoma viral oncogene homolog
204010_s_at	NM_004985	v-Ki-ras2 Kirsten rat sarcoma viral oncogene homolog
214352_s_at	BF673699	v-Ki-ras2 Kirsten rat sarcoma viral oncogene homolog
1561654_at	AF085978	LIM domain kinase 2
202193_at	NM_005569	LIM domain kinase 2
210582_s_at	AL117466	LIM domain kinase 2
217475_s_at	AC002073	LIM domain kinase 2
204056_s_at	NM_000431	mevalonate kinase (mevalonic aciduria)
215649_s_at	AF217536	mevalonate kinase (mevalonic aciduria)
236686_at	AU150926	mevalonate kinase (mevalonic aciduria)
36907_at	M88468	mevalonate kinase (mevalonic aciduria)
211926_s_at	AI827941	myosin, heavy polypeptide 9, non-muscle
209279_s_at	BC000245	NAD(P) dependent steroid dehydrogenase-like
215093_at	U82671	NAD(P) dependent steroid dehydrogenase-like
216755_at	AK024945	oxysterol binding protein-like 10
241693_at	BF246603	Oxysterol binding protein-like 1A
202743_at	BE622627	phosphoinositide-3-kinase, regulatory subunit 3 (p55, gamma)
211580_s_at	AF028785	phosphoinositide-3-kinase, regulatory subunit 3 (p55, gamma)
201087_at	NM_002859	paxillin
211823_s_at	D86862	paxillin
227332_at	BF511170	Paxillin
209146_at	AV704962	sterol-C4-methyl oxidase-like
243543_at	BF508288	Sterol-C4-methyl oxidase-like
209218_at	AF098865	squalene epoxidase
213562_s_at	BF979497	squalene epoxidase
1557352_at	BU754109	Squalene epoxidase
213577_at	AA639705	squalene epoxidase
218806_s_at	AF118887	vav 3 oncogene
218807_at	NM_006113	vav 3 oncogene
224221_s_at	AF118886	vav 3 oncogene
204165_at	NM_003931	WAS protein family, member 1

Figure 4.16 Expression of probe sets involved in cholesterol biosynthesis in RSV-infected Hep2 cells. RSV was infected with Hep2 cells, and the expression of probe sets associated with cholesterol biosynthesis was examined by microarray analysis at 4, 8, 12 and 15 hpi as shown. The data is represented by heat map analysis showing up-regulated (red), down-regulated (green) or no changes (black) in expression, and the FC range is indicated (P-value≤0.05).

Probe ID	GeneBank	Gene Title
1559077_at	AL833204	ABI family, member 3 (NESH) binding protein
229354_at	AB033060	aryl-hydrocarbon receptor repressor
206516_at	NM_000479	anti-Mullerian hormone
1560318_at	AL833445	Rho GTPase activating protein 29
205780_at	NM_001197	BCL2-interacting killer (apoptosis-inducing)
204677_at	NM_001795	cadherin 5, type 2 (vascular endothelium)
213006_at	AV655640	CCAAT/enhancer binding protein (C/EBP), delta
212675_s_at	AB011154	centrosomal protein 68kDa
212677_s_at	BG530481	centrosomal protein 68kDa
209101_at	M92934	connective tissue growth factor
202902_s_at	NM_004079	cathepsin S
205765_at	NM_000777	cytochrome P450, family 3, subfamily A, polypeptide 5
214234_s_at	X90579	cytochrome P450, family 3, subfamily A, polypeptide 5
215143_at	AL049437	dpy-19-like 2 pseudogene 2 (C. elegans)
208893_s_at	BC005047	dual specificity phosphatase 6
201693_s_at	AV733950	early growth response 1
201694_s_at	NM_001964	early growth response 1
227404_s_at	AI459194	Early growth response 1
207768_at	NM_001965	early growth response 4
215162_at	AB020691	GTPase activating Rap/RanGAP domain-like 1
219743_at	NM_012259	hairy/enhancer-of-split related with YRPW motif 2
1569979_at	BC010024	GLI-Kruppel family member HKR1
1569980_x_at	BC010024	GLI-Kruppel family member HKR1
219865_at	NM_014179	hypothetical LOC29092 /// similar to HSPC157
218637_at	NM_018439	Impact homolog (mouse)
244703_x_at	AA444166	importin 9
1553111_a_at	NM_152903	kelch repeat and BTB (POZ) domain containing 6
208567_s_at	NM_002244	potassium inwardly-rectifying channel, subfamily J, member 12
1562966_at	BC017424	KIAA1217
230166_at	BG026236	KIAA1958
207517_at	NM_018891	laminin, gamma 2
212531_at	NM_005564	lipocalin 2
236181_at	R38704	Hypothetical protein LOC100132181
230725_at	AA973100	hypothetical protein LOC100133781
240167_at	AI031657	hypothetical protein LOC152742
242260_at	BG283790	Matrin 3
230298_at	AI692906	metallo-beta-lactamase domain containing 2
207761_s_at	NM_014033	methyltransferase like 7A
204475_at	NM_002421	matrix metallopeptidase 1 (interstitial collagenase)

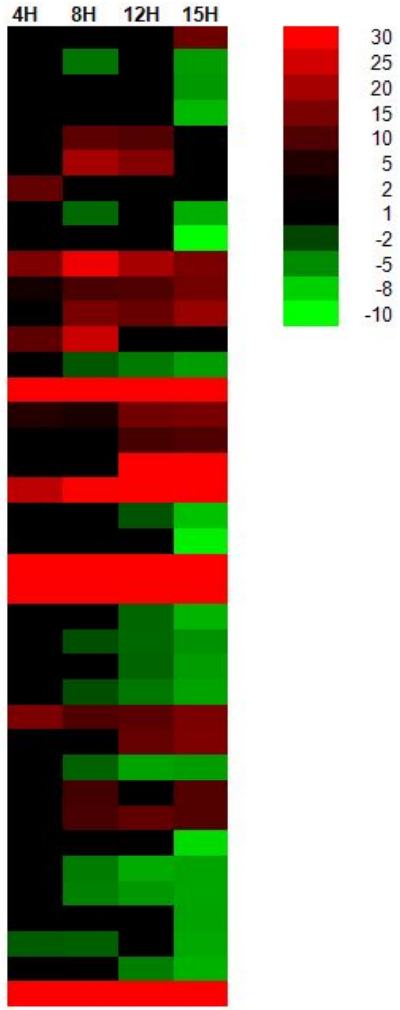

Probe ID	GeneBank	Gene Title
218865_at	NM_022746	MOCO sulphurase C-terminal domain containing 1
204823_at	NM_014903	neuron navigator 3
205220_at	NM_006018	niacin receptor 2
225768_at	AI761621	nuclear receptor subfamily 1, group D, member 2
225626_at	AK000680	phosphoprotein associated with glycosphingolipid microdomains 1
231213_at	AU146305	phosphodiesterase 1A, calmodulin-dependent
1553589_a_at	NM_005764	PDZK1 interacting protein 1
217996_at	AA576961	pleckstrin homology-like domain, family A, member 1
217997_at	AI795908	pleckstrin homology-like domain, family A, member 1
217999_s_at	NM_007350	pleckstrin homology-like domain, family A, member 1
218000_s_at	NM_007350	pleckstrin homology-like domain, family A, member 1
203691_at	NM_002638	peptidase inhibitor 3, skin-derived
204896_s_at	AI675173	prostaglandin E receptor 4 (subtype EP4)
1554997_a_at	AY151286	prostaglandin-endoperoxide synthase 2 (prostaglandin G/H synthase and cyclooxygenase)
204748_at	NM_000963	prostaglandin-endoperoxide synthase 2 (prostaglandin G/H synthase and cyclooxygenase)
206157_at	NM_002852	pentraxin-related gene, rapidly induced by IL-1 beta
244745_at	BG484193	RAS-like, estrogen-regulated, growth inhibitor
220564_at	NM_018363	renalase, FAD-dependent amine oxidase
215495_s_at	AL117523	sterile alpha motif domain containing 4A
209719_x_at	U19556	serpin peptidase inhibitor, clade B (ovalbumin), member 3
211906_s_at	AB046400	serpin peptidase inhibitor, clade B (ovalbumin), member 4
206421_s_at	NM_003784	serpin peptidase inhibitor, clade B (ovalbumin), member 7
215078_at	AL050388	superoxide dismutase 2, mitochondrial
235417_at	BF689253	SPOC domain containing 1
220030_at	NM_018423	serine/threonine/tyrosine kinase 1
1555724_s_at	BC010946	transgelin
205547_s_at	NM_003186	transgelin
232692_at	AA404231	tudor domain containing 6
202687_s_at	U57059	tumor necrosis factor (ligand) superfamily, member 10
238542_at	AA831769	UL16 binding protein 2
215646_s_at	R94644	versican
218810_at	NM_025079	zinc finger CCCH-type containing 12A
223642_at	AF193855	Zic family member 2 (odd-paired homolog, Drosophila)
1570135_at	BC030810	Zinc finger protein 230

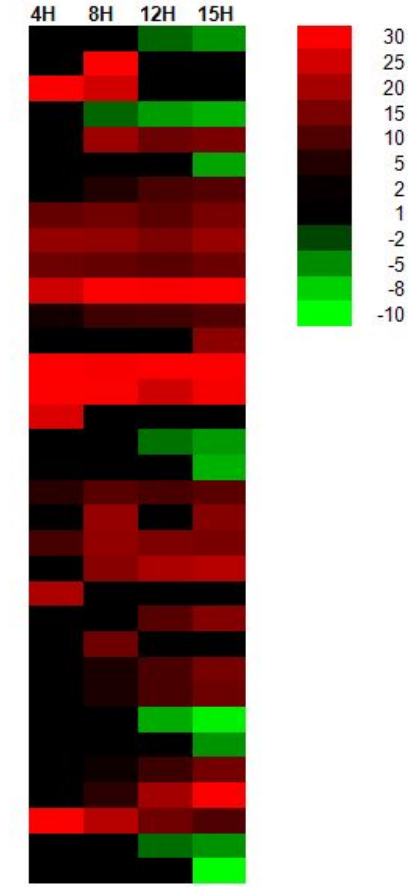

Figure 4.17 The probe sets with topmost expression in RSV-infected Hep2 cells. RSV was infected with Hep2 cells, and the expression of probe sets with top differential expression was examined by microarray analysis at 4, 8, 12 and 15 hpi as shown. The data is represented by heat map analysis showing up-regulated (red), down-regulated (green) or no changes (black) in expression, and the FC range is ndicated (P-value≤0.05).

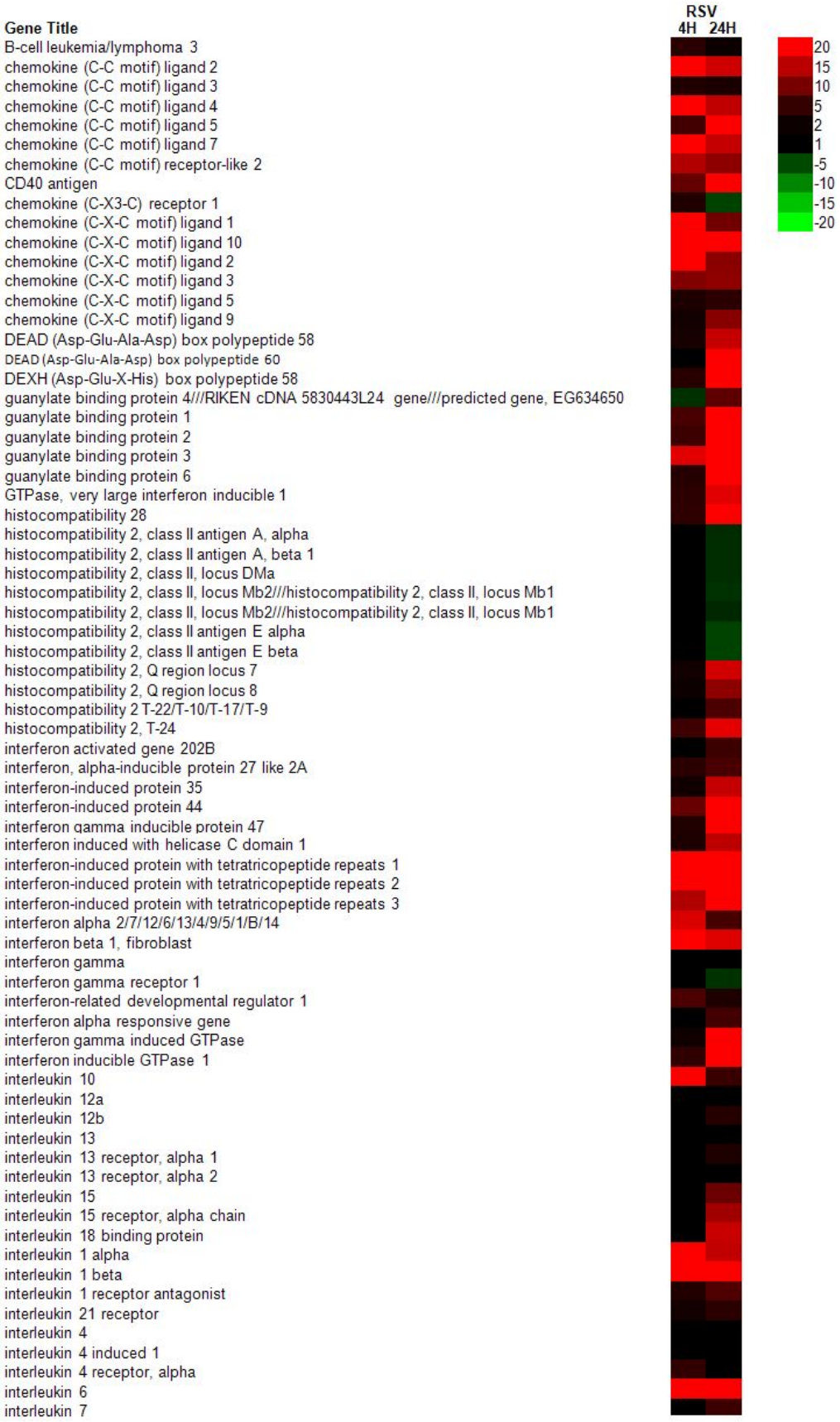
Gene Title
RSV
4H 24H
B-cell leukemia/lymphoma 3
chemokine (C-C motif) ligand 2
chemokine (C-C motif) ligand 3
chemokine (C-C motif) ligand 4
chemokine (C-C motif) ligand 5
chemokine (C-C motif) ligand 7
chemokine (C-C motif) receptor-like 2
CD40 antigen
chemokine (C-X3-C) receptor 1
chemokine (C-X-C motif) ligand 1
chemokine (C-X-C motif) ligand 10
chemokine (C-X-C motif) ligand 2
chemokine (C-X-C motif) ligand 3
chemokine (C-X-C motif) ligand 5
chemokine (C-X-C motif) ligand 9
DEAD (Asp-Glu-Ala-Asp) box polypeptide 58
DEAD (Asp-Glu-Ala-Asp) box polypeptide 60
DEXH (Asp-Glu-X-His) box polypeptide 58
guanylate binding protein 4///RIKEN cDNA 5830443L24 gene///predicted gene, EG634650
guanylate binding protein 1
guanylate binding protein 2
guanylate binding protein 3
guanylate binding protein 6
GTPase, very large interferon inducible 1
histocompatibility 28
histocompatibility 2, class II antigen A, alpha
histocompatibility 2, class II antigen A, beta 1
histocompatibility 2, class II, locus DMa
histocompatibility 2, class II, locus Mb2///histocompatibility 2, class II, locus Mb1
histocompatibility 2, class II, locus Mb2///histocompatibility 2, class II, locus Mb1
histocompatibility 2, class II antigen E alpha
histocompatibility 2, class II antigen E beta
histocompatibility 2, Q region locus 7
histocompatibility 2, Q region locus 8
histocompatibility 2 T-22/T-10/T-17/T-9
histocompatibility 2, T-24
interferon activated gene 202B
interferon, alpha-inducible protein 27 like 2A
interferon-induced protein 35
interferon-induced protein 44
interferon gamma inducible protein 47
interferon induced with helicase C domain 1
interferon-induced protein with tetratricopeptide repeats 1
interferon-induced protein with tetratricopeptide repeats 2
interferon-induced protein with tetratricopeptide repeats 3
interferon alpha 2/7/12/6/13/4/9/5/1/B/14
interferon beta 1, fibroblast
interferon gamma
interferon gamma receptor 1
interferon-related developmental regulator 1
interferon alpha responsive gene
interferon gamma induced GTPase
interferon inducible GTPase 1
interleukin 10
interleukin 12a
interleukin 12b
interleukin 13
interleukin 13 receptor, alpha 1
interleukin 13 receptor, alpha 2
interleukin 15
interleukin 15 receptor, alpha chain
interleukin 18 binding protein
interleukin 1 alpha
interleukin 1 beta
interleukin 1 receptor antagonist
interleukin 21 receptor
interleukin 4
interleukin 4 induced 1
interleukin 4 receptor, alpha
interleukin 6
interleukin 7
20
15
10
5
2
1
-5
-10
-15
-20

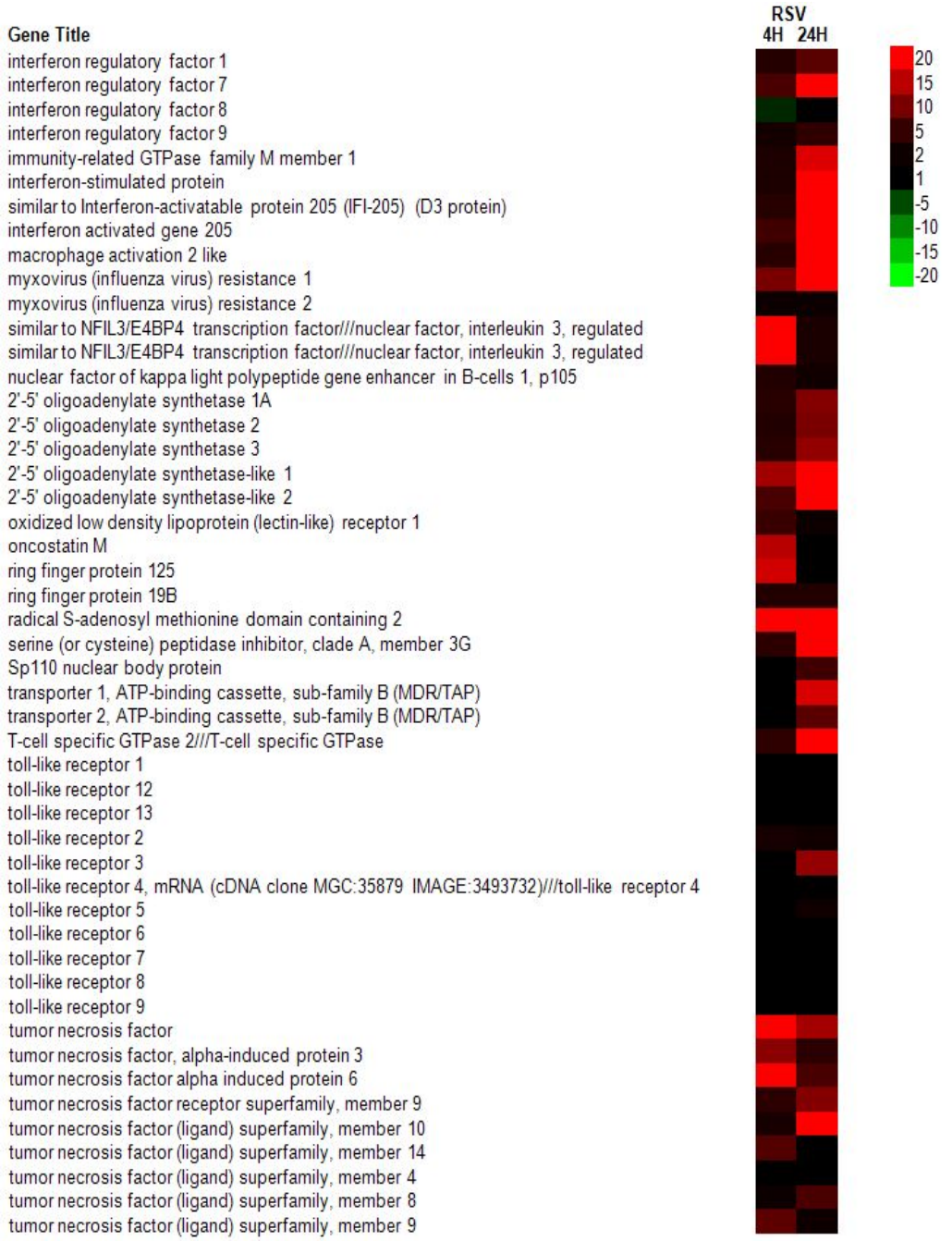

Figure 4.18 Expression of genes involved in immune response in RSV-infected macrophages. RSV was infected with macrophages, and the expression of genes associated with immune response was examined by microarray analysis at 4 and 24 hpi as shown. The data is represented by heat map analysis showing up-regulated (red), down-regulated (green) or no changes (black) in expression, and the FC range is indicated (P-value≤0.05).

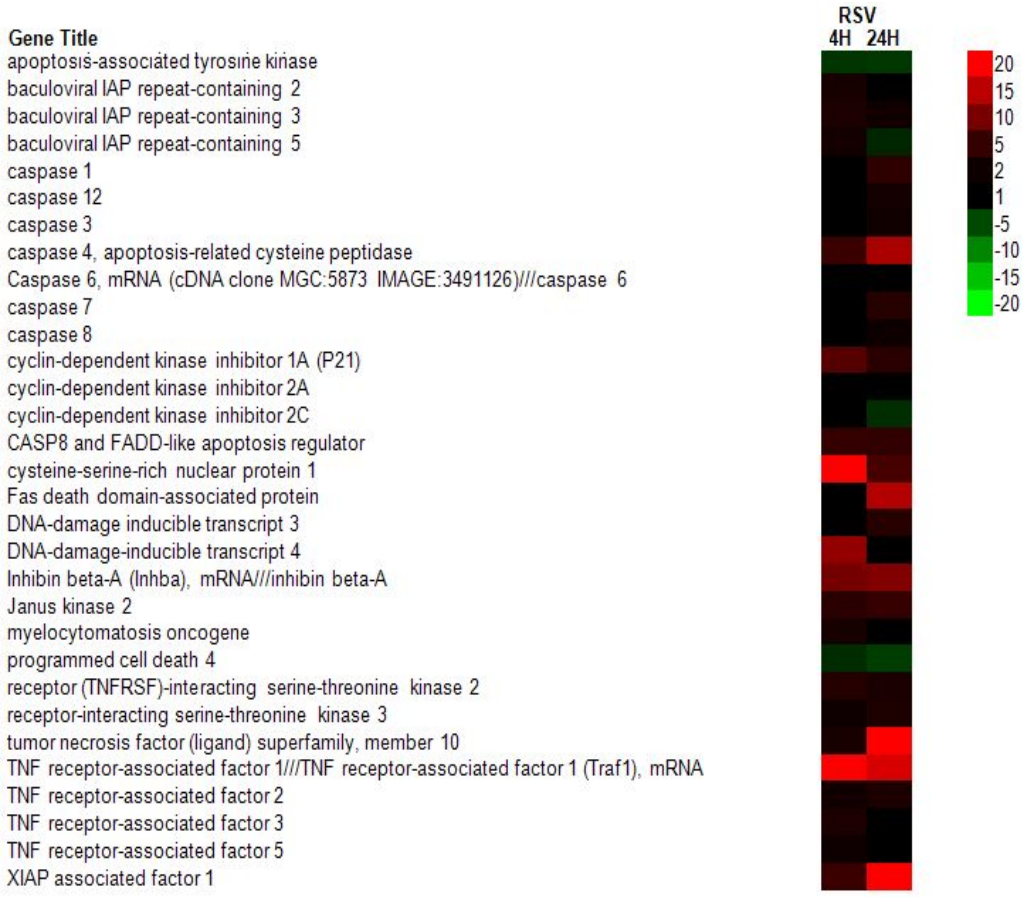

Figure 4.19 Expression of genes involved in cell death in RSV-infected macrophages. RSV was infected with macrophages, and the expression of genes associated with cell death was examined by microarray analysis at 4 and 24 hpi as shown. The data is represented by heat map analysis showing up-regulated (red), down-regulated (green) or no changes (black) in expression, and the FC range is indicated (P-value≤0.05).

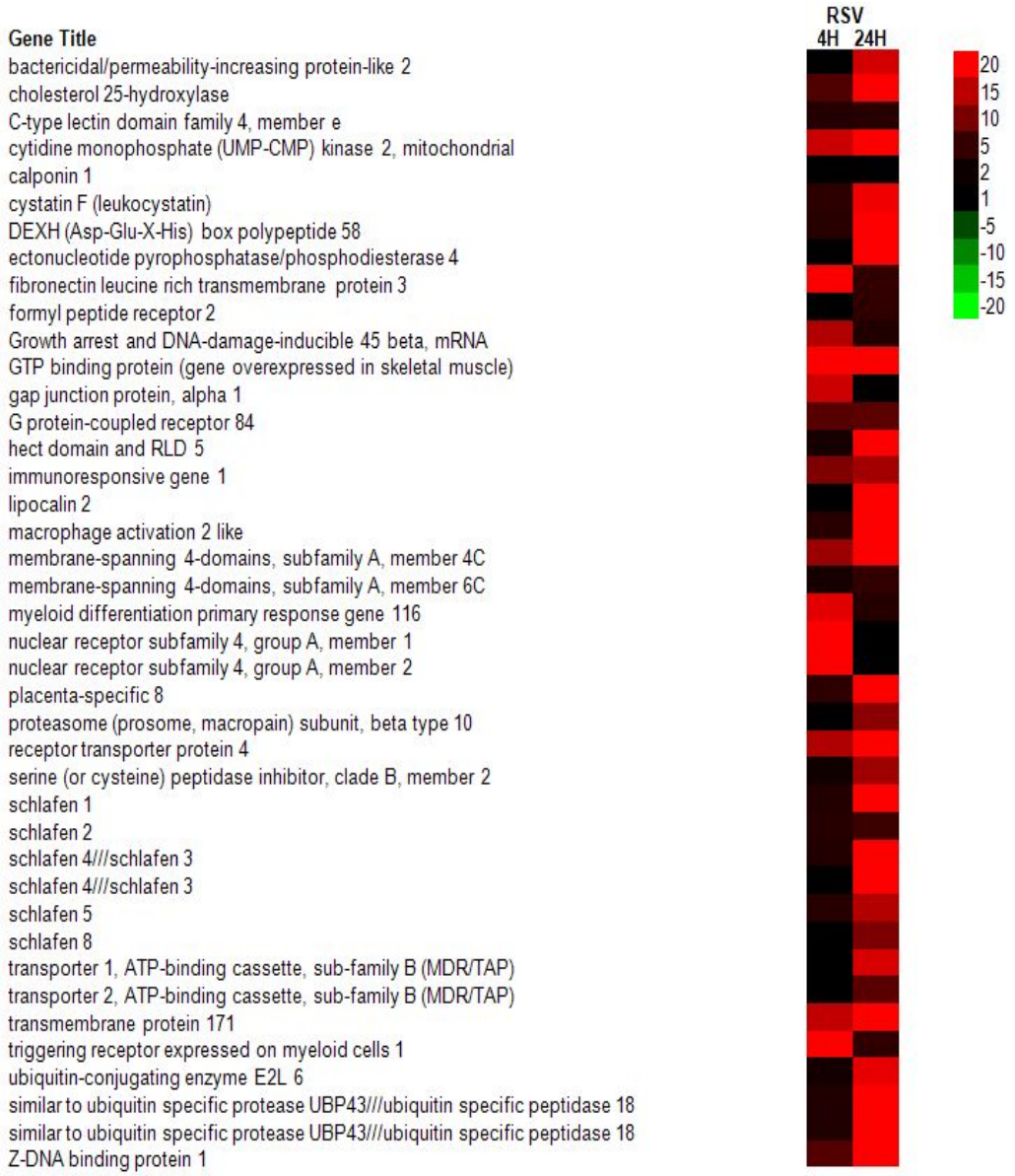

Figure 4.20 The genes with topmost expression in RSV-infected macrophages. RSV was infected with macrophages, and the expression of genes with top differential expression was examined by microarray analysis at 4 and 24 hpi as shown. The data is represented by heat map analysis showing up-regulated (red), down-regulated (green) or no changes (black) in expression, and the FC range is indicated (P-value≤0.05)

Chapter V. Influenza A viruses

5.1 Introduction

Influenza A viruses (IAV) are classified by the surface glycoproteins hemagglutinin (HA) and neuraminidase (NA). To date, almost all combinations between 16 subtypes of HA and 9 subtypes of NA have been found [Figure 5.1]. All known subtypes are isolated from wild birds, and 3 subtypes have been found that circulated in humans. Numerous subtypes have also been identified in poultry. Among these subtypes, H5 and H7 viruses may cause outbreaks of highly pathogenic avian influenza (HPAI) virus, which can be generated from low pathogenic avian influenza (LPAI) virus through the shift of amino acids at the HA cleavage site.

In humans, seasonal IAV H3N2 annually contributes to millions of human infections worldwide, which have caused severe health and economic concerns [204]. Pandemic IAV that spread from human to human efficiently have also posed serious threats to public health [205]. In 1957 and1968, two overwhelming pandemics, caused by H2N2 (Asian flu) and H3N2 (Hong Kong flu) caused excess mortality, especially in infants, the elderly and persons with chronic diseases [376]. The outbreak of H1N1 (also called 'Spanish influenza') in 1918 is the best-known example of a pandemic, with around 50 million individuals died [206]. In 2009, a novel strain of influenza A (H1N1) was recognized to have caused outbreaks of serious respiratory illness in the worldwide [207].

In 1997, an outbreak of HPAI H5N1 in poultry occurred, with 18 people infected and 6 died. This record provided the first evidence that an avian influenza virus is able to infect humans and finally cause fatality. In the following years, this virus also caused major outbreaks in southeast Asia, with the mortality rate of human cases reaching around 50%. By October 2006, the WHO declared that 256 cases from 10 countries in Asia and Africa were reported [208]. The latest data from WHO website has pointed out that H5N1 has resulted in 641 cases, of which 380 were lethal [367].

The H6N1 subtype was isolated with seven H5N1-like segments. The high homology between the genes from H9N2, H6N1 and H5N1 allows their internal gene exchange and therefore provide a potential source of new

pathogenic influenza virus strains. Experiment performed by Hoffmann E *et al* (2000) revealed that A/teal/Hong Kong/W312/97 (H6N1) virus behaved more like the less pathogenic H5N1 group initially but more like the highly pathogenic H5N1 group by the third passage after rapidly adapted to mice [209]. Investigation suggested that the initial lower pathogenicity might be due to the missing of the highly cleavable HA.

Several outbreaks of H7 viruses (LPAI and HPAI) in poultry have been reported to result in transmission to humans. In 1996, a H7N7 virus (LPAI) was transmitted from ducks to a 43-year-old woman. In 2003, a large outbreak of H7N7 virus (HPAI) resulted in the infections of 89 humans, with 1 died. In 2004, an outbreak of H7N3 virus (HPAI) caused mild influenza-like illness in two individuals. In 2006, an outbreak of H7N3 virus (LPAI) led to a case of conjunctivitis in a poultry worker. In 2007, a low pathogenic H7N2 virus contributed to infections of several people [210, 211].

On 31 March 2013, the Chinese National Health and Family Planning Commission announced the occurrence of three human infections with H7N9 subtype influenza viruses. By 25 Apr 2013, 112 human cases have been confirmed, including 22 deaths [212]. Detailed sequence analysis suggested that this virus was reassorted from previous avian viruses that circulate in birds and ducks. H7 influenza viruses are originated from 3 major lineages, the Eurasian (EA), American, and equine lineages, and six internal genes are derived from avian influenza A (H9N2) viruses. Furthermore, this H7N9 virus has been detected in poultry and environmental samples obtained in wet markets, implying that H7N9 virus-infected poultry might be one of the sources of human infections [213].

It is striking that some of these human H7N9 viruses have evolved mutations in order to facilitate avian viruses to adapt into mammalian hosts. Based on the three H7N9 samples identified in the first three patients who presented with fever, cough, and dyspnea, Gao and colleagues (2013) reported that substitution Q226L at the 210-loop in HA protein was found in two of the three samples [214], another substitution T160A at the 150-loop in HA protein and a deletion of five amino acids in the NA stalk region were commonly found in all three samples [215].

Recently, another subtype of HA identified in bats is significantly divergent from all know influenza A viruses [366]. This HA of bat virus was estimated to have diverged at roughly the same time as the known subtypes of HA and was designated as H17.

5.1.1 Virus structure

IAV, as negative sense, single-stranded and segmented RNA viruses, belong to the *Orthomyxoviridae* family. IAV have eight segments that encode 11 or 12 viral proteins: the nuclear export protein NS2/NEP, the non-structural protein NS1, the matrix protein M1, the ion channel protein M2, the haemagglutinin (HA), the neuraminidase (NA), the nucleoprotein (NP), the polymerase acidic (PA), the polymerase basic 1 (PB1) and the polymerase basic 2 (PB2). Besides, a few novel proteins have been also identified recently, for example, two proteins called M42 and PA-X are both encoded by segment 3 [369] [388], and another two proteins, PB1-N40 and PB1-F2, are both encoded by segment 2.

The viral envelop is made up of a lipid bilayer, which derives from host cell's plasma membrane. This bilayer contains both cholesterol-enriched lipid rafts and non-raft lipids, with three viral transmembrane proteins HA, NA and M2 included. Among these three transmembrane proteins, HA mediates the binding of virus to host cells and the entry of viral genome, while NA cleaves sugars that bind the mature viral particles so as to release progeny virus from infected cells. M2 proteins with a minor component of the envelop proteins process ion channel activity. M1 proteins which locate underneath the viral lipid membrane form a matrix holding the viral ribonucleoprotein (vRNPs). And these vRNPs are made up of the viral negative stranded RNAs, which are wrapped by NP. Three polymerase PB1, PB2 and PA proteins attach the end of each vRNP to form the RNA polymerase complex [Figure 5.2] [216].

5.1.2 Virus replication cycle

In general, IAV replication cycle can be separated into five stages as shown in Figure 5.3.

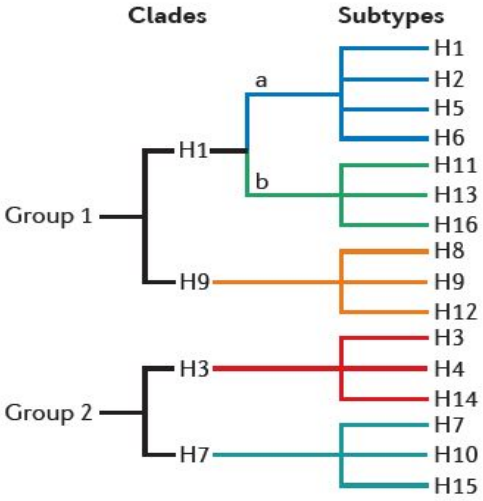

Figure 5.1 Classification of IAV based on HA. 16 subtypes can be summarized into 5 clades and 2 groups in further (adapted from Medina RA *et al*., 2011)[217].

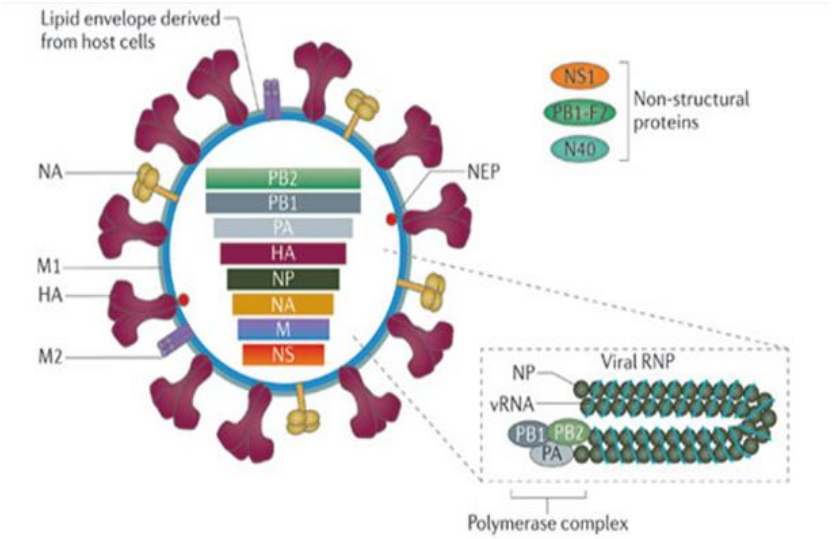

Figure 5.2 IAV genome structure (adapted from Medina RA *et al*., 2011)[217].

5.1.2.1 Entry of virus into the host cell

HA forms spikes on the viral lipid membrane, and these spikes of HA bind to sialic acid receptors on host cell surface. Two major linkages that are important for HA specificity have been found between sialic acids: α (2, 3) and α (2, 6). And these two linkages are the determinant in restricting the transmission of IAV in different species. For example, α (2, 6) linkage is recognized in viruses from humans while α (2, 3) linkage is recognized in those from avians and equines. In addition, both these two linkages are able to be recognized in viruses from swine.

Virus enters into the cell as an endosome. Low PH in endosome, around 5 to 6, is able to trigger the fusion of both viral and endosomal membranes. After HA is cleaved by cellular proteases, HA2 fusion peptide is exposed to insert itself into the endosomal membrane, causing the contact between viral membranes and endosomal membranes. Besides, the acidic environment of the endosome also opens up the M2 ion channel, which results in acidification of the inside of the viral core and subsequently un-coats the RNP complex and releases the vRNP from M1 into host cell's cytoplasm [368][385-386].

5.1.2.2 Entry of vRNPs into the nucleus

Since transcription and replication of IAV occur in the nucleus, the vRNP must enter the nucleus after the virus entry into the cytoplasm. The vRNA consists of NP, PA, PB1 and PB2: the NP coats the viral RNA, and the remaining three polymerase proteins bind to the partially complementary ends of the viral RNA. Subsequently, polymerase proteins and nucleoprotein create a distinctive panhandle structure together with the viral RNA.

The width of RNPs is too large to allow direct entry into the nucleus. Thus, they must rely on an active nuclear import mechanism. Nuclear localization signals (NLSs) can mediate specific interaction with cellular nuclear import machinery. After the dissociation with the M1 protein, the RNPs enter the nucleus through the nuclear pore. There are two types of importins: importin α recognizes and binds the NLS on the cargo proteins first and then importin β recognizes and bounds to the complex, subsequently the whole complex binds to the fibrils of the nuclear pore complex (NPC) to complete the actual translocation. It should be noted that the two viral proteins, M1 and NS2/NEP are critical for assisting the nuclear export of RNPs [218].

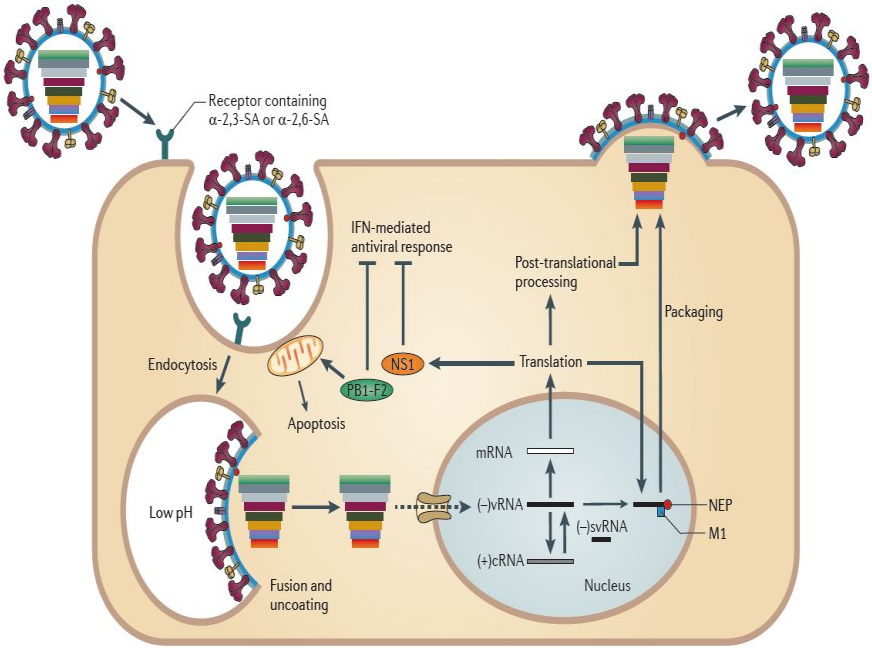

Figure 5.3 Replication cycle of IAV (adapted from Medina RA *et al*., 2011)[217].

5.1.2.3 Transcription and replication of viral genome

It is known that IAV only encode 11 or 12 proteins which are not enough for own transcription. Hence, IAV have generated sophisticated methods to hijack the transcription machinery in host cells for its own benefits. Because the IAV are negative sense RNA viruses, the negative sense RNA must be converted into the corresponding positive sense RNA first to serve as a template to produce viral RNAs.

As we know, mature mRNAs have a 5' methylated cap and a poly(A) tail. However, the vRNPs do not have either 5' methylated cap or poly(A) tails. Studies have approved the existence of "cap-snatching" mechanism [Figure 5.4]. In the process of "cap-snatching", PB2 from viral RNA polymerase has endonuclease activity. This ability allows PB2 bind to the 5' methylated caps of mRNAs and cleave the mRNAs' 10 to 15 nucleotides 3' to the cap structure [219]. This cleaved host-capped mRNA is then used as a primer for the initiation and transcription of the PB1 protein. Since the PB1 protein binds both the 5'- and 3'- ends of the viral mRNA, the polyadenylation and termination of the vRNAs occur before the 5' end is reached.

Among all the eight segments in influenza genome, some of them encode for two proteins. For example, M1 and M2 are encoded by segment 7;

NS1 and NS2/NEP are encoded by segment 8. To encode more than one protein, influenza virus effectively uses host cell's splicing machinery again.

The switch from viral mRNAs to template RNAs requires the change from capped RNA-primed initiation to unprimed initiation. This different initiation strategy will prevent termination and polyadenylation at the poly(A) site, which is used during viral mRNA synthesis [220]. The replication of vRNA is fulfilled by two steps: the synthesis of template RNAs and the copying of the template RNAs into vRNAs. NP protein is also necessary to elongate the RNA molecules.

5.1.2.4 Export of vRNPs from the nucleus

Exportins are the proteins which take cargo out of the nucleus. In IAV, chromosome region maintenance protein 1 (CRM1) as regular exportin mediates the export of numerous proteins that carry a nuclear export signal (NES) from the nucleus [221]. The vRNP nuclear export is initiated by forming a vRNP-M1-NS2/NEP complex in the nucleus, with the NES provided by NS2/NEP [222]. The nuclear export signal also will overcome the NLS sequence in the NP and polymerase protein. NS2/NEP protein interacts with CRM1 and CRM1 will associate with RAN-GTP protein to mediate export of the vRNP-M1-NS2/NEP from the nucleus into the cytoplasm through CRM1 mediated pathway [218]. Finally, formed CRM1-RAN-GTP-NS2/NEP-M1-vRNP complex will be allowed to export nucleus. After the export action finishes, the complex will dissociate followed by the dephosphorylation of RAN-GTP to RAN-GDP [Figure 5.5].

5.1.2.5 Assembly and budding of virus

After the vRNPs leave the nucleus, the left thing is to form viral particles and leave the cell. The plasma membrane from host cell is used to form IAV particles. When the virus particles bud from the apical side of polarized cells, HA, NA and M2 are translocated into ER through Trans-Golgi networking and transported into the apical plasma membrane. Different kinds of proteins play different roles in the process: HA is used to initiate the budding process, however, NA can compensate the role of HA when laking of HA; M1 may alter membrane curvature and cause membrane budding; M2 is essential

and necessary for the completion of virus budding as well as virion release [Figure 5.6] [223]. Packaging of an infectious influenza virus particle will require the incorporation of all eight segments of the viral genome, and an organized packaging method might exist to correctly incorporate eight different segments into the virion, possibly either by RNA interactions or protein-protein interactions [224]. The HA and NA contain terminal sialic acids that make the viruses to clump together and adhere to the cell surface. After that, NA of newly assembled viruses cleaves these sialic acid residues and subsequently releases the virus from the host cells. In this process, the filamentous virion assembly is dependent on the microfilament network, indicating a raft–actin interaction that maintains the necessary organisation of HA-containing lipid rafts for virus budding [225].

5.1.3 Viral-Host interactions

The viral infection generally initiates a complex set of interactions between the viruses and their targeted host cells. The specific antiviral signaling is triggered in host cells upon the viral infection. At the meanwhile, viruses have evolved some specific mechanisms to counteract with antiviral responses. Subsequently, these viral-host interactions determine the severity of the disease and the performances of the adaptive immune response [226].

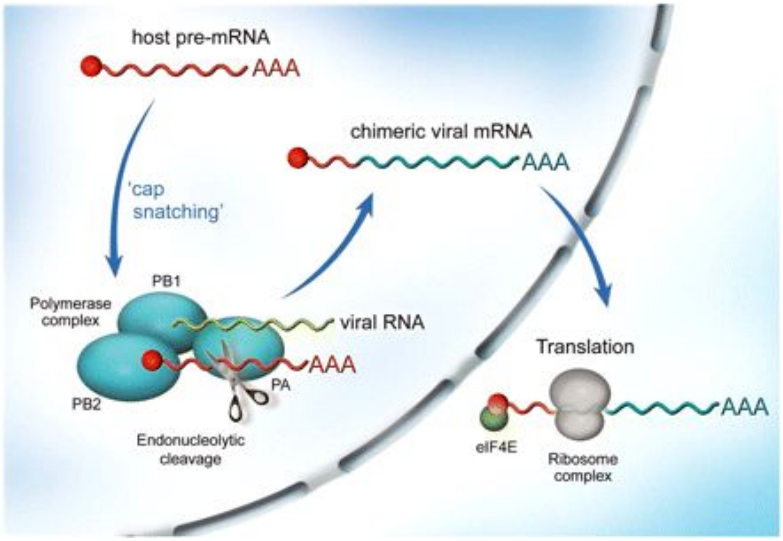

Figure 5.4 Cap-snatching transcription mechanism. Influenza polymerase consisting of PA, PB1 and PB2 locates in the nucleus. During the process of viral transcription, PB2 binds the 5′, 7-methylguanosine cap of a host pre-mRNA molecule (*red*) and cleaves 10–15 nucleotides downstream by the PA endonuclease. This cleaved host-capped mRNA initiates polymerization

by the PB1 subunit using 5′- and 3′-bound vRNA (*green*) as template, and thus the capped, polyadenylated, chimeric mRNA molecules are synthesized (*red* and *blue*). Finally, these mRNA molecules are exported to the cytoplasm for further translation (adapted from Boivin S *et al*., 2010) [219].

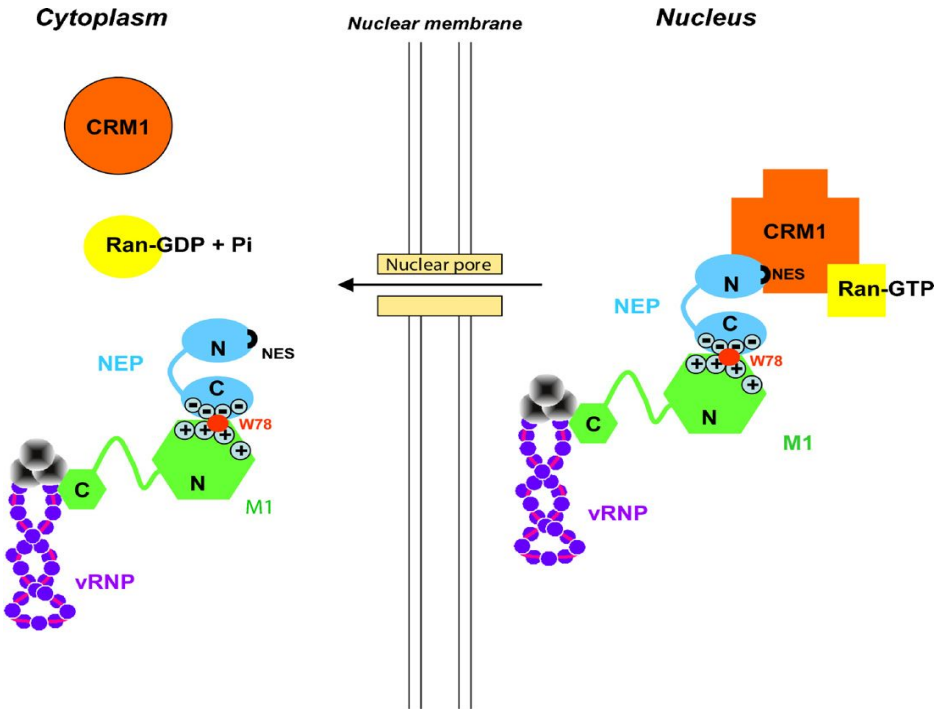

Figure 5.5 Strategy of the newly assembled IAV RNPs exporting from the nucleus to the cytoplasm. There are conformational changes of CRM1 and Ran occurred upon hydrolysis of GTP and subsequent dissociation of the complex from its cargo (adapted from Boulo S *et al*., 2007) [218].

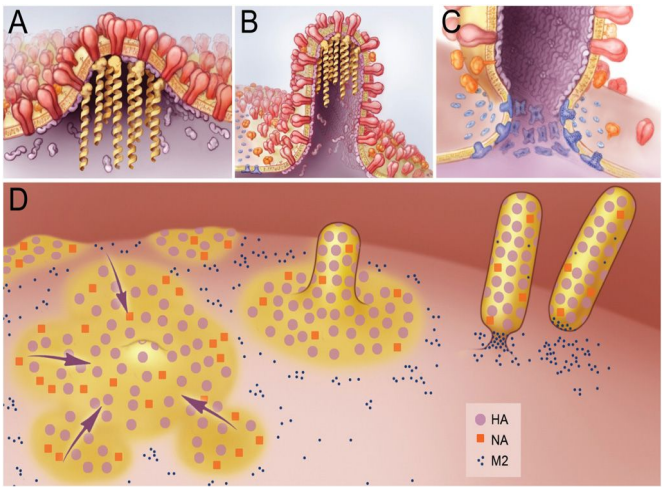

Figure 5.6 Model of IAV budding. A) M1 (shown in purple) binds to the cytoplasmic tails of HA (shown in red) and NA (shown in orange) in order to serve as a docking site for the vRNPs (shown in yellow), which in turn to initiate the virus budding. B) Polymerization of the M1 results in the elongation of the budding virion, and thereby a polarized localization of the vRNPs is formed. C) M2 (shown in blue) is inserted at the lipid phase boundary so as to alter the membrane curvature at the neck of the budding virus and lead to the virus release. D) Global strategy of the budding process of IAV (adapted from Rossman S *et al*., 2011) [223].

5.1.3.1 Activation of the innate type I IFN system

TLRs and RIG-I have been proved to be involved in induction of interferons during IAV infection. TLR1/2/4 locate on the cell surface, while TLR3/7/8/9 have been detected to be expressed in intracellular compartments. During the process of virus entry, IAV fusion the envelope so as to release the segmented genome. In this situation, some virions may expose the viral RNA to TLR3/7/8 present in the host cells, which recognize the single stranded RNA. Before assembly of new virions, the newly synthesized viral RNA segments move to the cytoplasm and are recognized by RIG-I. Thus, TLR signaling by the adaptors TRIF or MyD88 and RIG-I signaling by the adaptor MAVS trigger a signal transduction, which in further activate IRF3/7 and NF-κB factors, and these factors are then translocated into the nucleus to stimulate the synthesis of type I and type III IFN mRNAs [226].

5.1.3.2 Type I IFN stimulated gene products

As described above, IFNα/β binds to IFNAR once it is secreted. This action directly stimulates the JAK/STAT pathway, which induces formation of the trimeric transcription factor ISGF3 that consists of STAT1, STAT2 and IRF-9. And this transcription factor subsequently regulates the expression of ISGs, such as Mx1, p56, the 2' – 5' oligoadenylate synthetases (OAS), Viperin (RSAD2) and the protein kinase R (PKR). These ISGs spread widely to fight with the IAV replication [8].

5.1.3.2.1 Myxovirus Resistance (Mx)

Mx proteins comprise a small family of GTPases, and their resistance phenotype is specific to the members in the orthomyxovirus family. Gene expression of Mx1 is rapidly induced through the action of virus-induced type I (α/β) or type III (λ) IFNs upon virus infection. Relevant studies have provided evidences that Mx1 has intrinsic antiviral activity and is the majorly effective molecule which is able to protect infected animals from severe influenza and even death [227].

In humans, an Mx homologue (MxA) is encoded by the human MX1 gene. The human MxA protein also exhibits similar effects to murine Mx1 protein. However, both human MxA protein and murine Mx1 protein have

different mechanism. Human MxA protein inhibits steps involved in viral replication and transcription, which develops in the later phase of viral replication. Murine Mx1 inhibits in the early viral transcription steps. In spite of the difference in mechanism of Mx in different species the Mx proteins of the two species recognize the same or similar viral target structures. Besides, it has been also demonstrated that different strains of IAV might have different degree of sensitivity against the Mx proteins [228]. In contrast to Mx1, cytoplasmic Mx2 (also known as MxB) showed ineffective against influenza virus [372] and influenzavirus replication was also not affected by the expression of MX2 protein in Vero cells [384].

5.1.3.2.2 The 2' - 5' oligoadenylate synthetase and RNase L

OAS catalyzes the synthesis of 2'-5' connected oligoadenylates, commonly abbreviated 2-5A. RNase L becomes activated by binding 2-5A oligonucleotides and subsequently degrades viral and cellular RNA [229]. All in all, OAS/RNaeL impairs the efficiency of viral replication through creating an antiviral state within the cells.

5.1.3.2.3 Viperin (RSAD2)

Viperin, as an ISG, is induced by IFNs after infections of a broad range of DNA or RNA viruses. Recently, it has been published that Viperin is able to block IAV budding and release [230]. On one hand, Viperin expression affects the formation of lipid raft, which is the site of IAV budding. On the other hand, Viperin interacts with an inhibitor of farnesyl diphosphate synthase (FPPS). FPPS is a one of the crucial enzymes involved in cholesterol metabolism pathway. Experiments proved that reduction of FPPS expression by Viperin inhibited IAV replication and release [231].

5.1.3.2.4 The protein kinase R

PKR as a dsRNA dependent protein kinase plays an essential role in the antiviral response against IAV infection. PKR has several downstream substrates, such as IRF3 and eukaryotic translation initiation factor 2 alpha subunit (eIF2α). Following virus replication, the generation of dsRNA activates the stress-induced MAPK pathway p38/JNK resulting in the AP-1 activation.

PKR is activated following binding to dsRNA, phosphorylates eIF-2α, and inhibits protein translation. PKR may also associate with the IKKβ subunit. Viral nucleocapsid (N) and dsRNA activate VAK, a virus activated kinase, leading to C-terminal phosphorylation of IRF-3. IRF-3 activation stimulates target genes such as RANTES, IL-15, and IFNs [] (Servant MJ et al., 2002). Thus, PKR is not directly involved in the activation of IRF3. Activation of PKR also results in the phosphorylation of so that eIF2α is not able to participate in translation initiation and protein synthesis of viral mRNAs. In addition, PKR is also able to regulated NF-κB signaling and ISGs [232]. To offset the antiviral role of PKR, IAV have evolved several inhibitory mechanisms to offset the antiviral function of PKR. For example, NS1 of IAV directly binds to PKR so as to prevent its activation; IAV nucleoprotein also exploits Hsp40 to inhibit PKR.

5.1.3.3 Viral strategies to counteract to the innate immune responses

IFN α/β expression is a host immune response to IAV infection at an early stage. Facing to the antagonistic response, pathogens have evolved different mechanisms to prevent IFN expression as well as IFN induced signaling.

5.1.3.3.1 NS1 – a viral antagonist of the innate immune response

In IAV, the activities of NS1 are not only important for the pathogenicity of IAV but also partially responsible for the ability of IAV to infect multiple animal species [226].

In the first place, NS1 is essential for antagonizing IFNα/β-dependent responses through limiting IFNβ production from two respects: pre-transcriptional and post-transcriptional limitation of IFNβ induction. (i) Studies on PR8/NS1 show that it may mediate pre-transcriptional block on IFNβ induction by forming a complex with RIG-I dependent upon two residues in NS1: Arg-38 and Lys-41; (ii) To prevent the nuclear post-transcriptional processing by targeting to RNA polymerase II is another common strategy for NS1 to limit IFNβ production in many IAV infected cells [233].

Secondly, NS1 protein can directly inhibit IFN-responsive factors including OAS/RNase L and PKR. Both these two factors are key regulators of

viral transcription and translation processes, and also take action on host innate defence such as IFNβ induction and apoptotic response [234]. Since the activation of RNase L is totally dependent on dsRNA activation of 2-5 OAS, the action of NS1 out-competing OAS for interact with dsRNA can lead to inhibition of IFNα/β induced OAS/RNase L pathway [235]. Studies have also revealed that NS1 (residues 123-127) binded to linker region in PKR, and thereby prevented a conformational change that is required for release of PKR auto-inhibition [236].

Thirdly, NS1 also interacts with other cellular antiviral factors such as RIG-I. Gack MU *et al* (2009) described that the NS1 protein interfered with TRIM25 multimerization through binding its CCD [237]. TRIM25 multimerization is required for ubiquitination of RIG-I CARDs, a modification that is necessary for maximizing IFN production. Thus, directly inhibiting the activity of TRIM25 by NS1 enables to suppress RIG-I signal transduction and ultimately IFN-β production.

Additionally, NS1 also displays some anti-apoptotic functions. For example, PI3K and its downstream effector, Akt, function on cell growth, proliferation and survival. And it has been proposed that NS1 activated PI3K signaling by binding to its p85-β regulatory subunit [238].

5.1.3.3.2 The role of PB1-F2

Besides the NS1, some subtypes of IAV express a second viral non-structural protein, PB1-F2. This protein is generated from PB1 gene by an alternative open reading frame (ORF) [239]. Recent researches have proved that PB1-F2 is associated with the host immune and cell death responses in IAV infected cells. Dudek SE *et al* (2011) found that PB1-F2 exhibited IFNβ antagonistic activities by interfering with the RIG-I RNA-sensory pathway at the level of the adaptor protein MAVS but not inhibiting IKKε-mediated expression of IFNβ [240]. Furthermore, PB1-F2 could also induce the apoptosis of BAL immune cells through TNF/FasL-mediated apoptosis signaling pathway [241]. Therefore, a virus that produce the active PB1-F2 protein is considered as a highly pathogenic virus. Moreover, a single amino acid substitution N66S in the PB1-F2 molecule has been reported as a contributing factor for the high virulence and lethality of the virus [242]. Recent studies have also indicated that

PB1-F2 was able to inhibit NF-κB dependent signaling [377] and it also initiated caspase-3-independent apoptosis under regulation of sulfatide [378].

5.1.4 Influenza A viruses in different hosts

5.1.4.1 Human

Currently, there are two HA subtypes (H1 and H3) and two NA subtypes (N1 and N2) that are circulating and transmit efficiently among humans.

5.1.4.1.1 Host response to H1N1

H1N1 is one of the IAV subtypes and is currently endemic in human population. The typical seasonal influenza virus infects approximately 5% of total population with 100,000 deaths annually. The first H1N1 subtype was first successfully isolated by Wilson Smith in 1933, which is named A/WS/33 (H1N1). There was a major influenza pandemic caused by H1N1 influenza virus strain in 1918, commonly known as "Spanish Flu". After the 1918 "Spanish Flu" pandemic, the H1N1 subtype of virus diminished rapidly for almost 50 years, and the pandemic occurred with H2N2 and H3N2 in 1957 and 1968 [243]. Since then, both H3N2 and H1N1 re-circulate in human population. Geiss GK *et al* (2002) pointed out that a virus containing the 1918 pandemic NS1 gene was able to block the expression of IFN-regulated genes more efficiently than its parental influenza A/WS/33 virus in human lung cells [244], which demonstrate the significant influence by the sequence of the NS1 gene in counteracting to the host antiviral response triggered by virus infection.

5.1.4.1.2 Host response to H3N2

Currently, influenza A virus H3N2 is the important seasonal human influenza that cause higher morbidity and mortality than H1N1. Annually, H3N2 influenza viruses infect 5-15% of the total population [245]. Since 2002, the antigenic evolution of H3N2 viruses has followed from previously dominating the A/Sydney/5/1997-like viruses and A/Fujian/441/2002-like viruses to the A/California/7/2004-like viruses and to the A/Wisconsin/67/2005-like strains in a 5 year span [246]. And A/Perth/16/2009 and A/Victoria/361/2011 were responsible for the epidemic in 2011-2012

season. Global genomic gene expression profiles from the individual subjecting to infection of H3N2/Wisconsin have revealed that potential immune response events determined the pathogenicity of influenza viral infection [247]

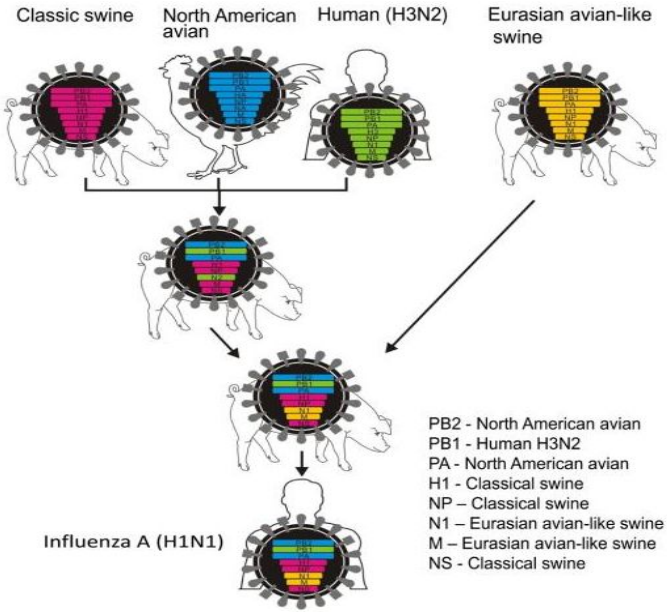

Figure 5.7 The origin of pandemic H1N1 2009 virus (pH1N1) (adapted from Neumann G *et al*., 2009)[248].

5.1.4.1.3 Host response to Pandemic 2009 H1N1 Swine influenza virus

A novel swine-origin influenza A virus initially had an outbreak in Mexico and then spreaded rapidly in the rest of the world. By June 2009, nearly 30,000 cases of 2009 H1N1 virus (pH1N1) had been confirmed in the worldwide, prompting the WHO to declare the outbreak of the 2009 influenza pandemic [249]. Recent researches indicate that the pH1N1 virus arose from a reassortment of triple reassortment: HA, NP and NS from classic swine virus origin; PB2 and PA from the North American avian virus origin; PB1 from human seasonal H3N2; NA and M from Eurasian avian-like swine virus origin [Figure 5.7] [248].

Mukherjee S *et al* (2011) examined the global host response at a series of time points in A549 cells based on microarray technique [250]. The results demonstrated that pH1N1 induced immune response earlier than seasonal H1N1 viruses. However, the host immune responses were suppressed at the late stages of pH1N1 infection, with considerable expression decrease of cytokine and other immune genes. In addition, both viruses, especially pH1N1, had the property of antagonizing IFNβ. In conclusion, these observations indicated

greater replication ability of pH1N1 in A549 cells when compared to seasonal H1N1. A comprehensive investigation on innate response has indicated that the productions of a scale of cytokines were induced under pH1N1 infection, and it was also found that the IL6 and IL10 production were high in patients under severe pH1N1 infection [251, 252]. Microarray analysis also revealed that infection of pH1N1 contributed to a more potent early immune response with higher expression levels of genes relevant to lipid metabolism and cell death when compared to infection of 1918-like classical swine influenza virus in pigs [253].

5.1.4.2 Avian

Wild birds are the natural host for all known subtypes of IAV, and they do not become sick when infected with avian IAV. In general, avian influenza viruses (AIV) are classified into HPAI or LPAI based on their intravenous pathogenicity. LPAI viruses may have been considered of negligible risk, but there is evidence that HPAI might arise from LPAI by mutations. Avian IAV of H7, H9 and H5 subtypes have been reported for human infection.

5.1.4.2.1 Host response to H5N1

Among the most well known HPAI outbreaks was HPAI H5N1. The first outbreak of H5N1 HPAI was reported in Hong Kong in 1997 in poultry. Later, this virus was classified as HPAI because of its high mortality rate (70%-100%) in chickens. It also possess 60% mortality rate in humans [254]. Although avian H5N1 continues to transmission to humans, this virus has not adapted to efficient human-to-human transmission till now.

Zeng H *et al* (2007) did a series of experiments to assess the potential virulence of HPAI H5N1 (2004) in human cells [255]. It was observed that H5N1 triggered a delayed and weaker IFNβ response and ISGs production than human H3N2 virus. Consequently, a highly virulence H5N1 virus showed a better ability to attenuate the host IFN response than less virulent human viruses in human respiratory cells. In addition, it has been also proposed that H5N1 virus showed sensitive to the antiviral activity of Mx [370].

5.1.4.2.2 Host response to H9N2

IAV H9 subtype have been extensively circulated in the worldwide and caused a series of outbreaks in chickens, ducks and pigs after its discovery. In 1999 and 2007, self-limiting mild human infections with LPAI H9N2 were recorded in Hong Kong. And it has been also pointed out that some avian H9 viruses have acquired receptor binding characteristics typical of human strains, which may increase the potentiality of reassortment in both human and swine respiratory tracts.

In human epithelial cells, H9N2/1997 was observed to replicate at a lower rate than H1N1/2002 and H5N1/2004. In the early phase, infections of H5N1/2004 and H9N2/1997 viruses generated stronger up-regulated expression of TNF-α, RANTES, CXCL-10/IP10 than infection of H1N1/2002. And TNF-α, IL-6, IL-8, RANTES and CXCL-10/IP-10 remained at high mRNA expression levels in the late phase of H5N1/2004 and H9N2/1997 infections but not H1N1/2002 infection [256].

5.1.5 Objective

As we know, different IAV strains interact with different host cells in various ways. It is interesting to note that some IAV strains are able to infect and replicate well in particular hosts, but others not. This phenomenon suggests that there must be specific interaction patterns to assist or inhibit the virus growth in the different combinations of each virus and each host cell. Avian-to-human transmission of HPAI viruses are often associated with high fatality rates, whereas associated fatalities due to human transmission of LPAI viruses have not been reported. In addition, AIVs can play a role in the evolution of seasonal influenza virus strains, with unpredictable consequences. LPAI viruses that are circulating in avian populations can lead to the emergence of HPAI viruses [379]. Pathogen-host interactions have been relatively well characterized in laboratory-adapted influenza viruses and in some HPAI virus isolates (e.g. H5N1), but in general our understanding of host interactions during AIV infection is comparatively poor [380].

In this report, we examined the host responses of representative LPAI viruses that were circulating in South-East Asia. These viruses, including H5N2, H5N3 and H9N2 virus subtypes, were isolated from live broiler ducks imported into

Singapore during routine surveillance, and they were the first LPAI viruses isolated in South-East Asia that were completely characterized at the genetic level. The properties of these viruses were compared with that of the laboratory-adapted human H1N1/WS isolate, and pH1N1 virus that was isolated from humans in Singapore during the influenza pandemic in 2009. In our study, selected LPAI and two human influenza strains were applied to infected common cell line (A549, CEF or MDCK) so that the pathogen-host interaction during LPAI infection could be well evaluated. All three cell types (A549, CEF and MDCK) are standard cell types used for infection of influenza viruses. MDCK cells allow influenza virus replication and virus tiles are established based on this cell type. A549 as human alveolar basal epithelial cells and CEF as chick embryo fibroblasts are also permissive for avian influenza viruses so that they are often used for infection of influenza viruses. Since A549 are human based cell types and CEF are avian based cell types, selection of these two cell types benefits the analysis of the host proteins interactions in humans and avian.

On this basis, we chose eight IAV strains belonging to five subtypes, and infected them in four types of host cells. Global host gene expression profiles were monitored using microarray platform, and differential expression of interested genes were validated by techniques such as cytokine assays [365]. Then different types of software were applied into further analysis from different perspectives. The aims of this research are as following:

(1). Compare different gene expression performances in different virus-infected cells.

(2). Investigate the expression changes of genes belonging to interesting groupings.

(3). Establish the mechanisms which have been involved to antagonize the immune response upon IAV infection.

(4). Reveal the relationship between the viral replication performances and its corresponding global host gene expression profiles.

5.2 Experiment workflow

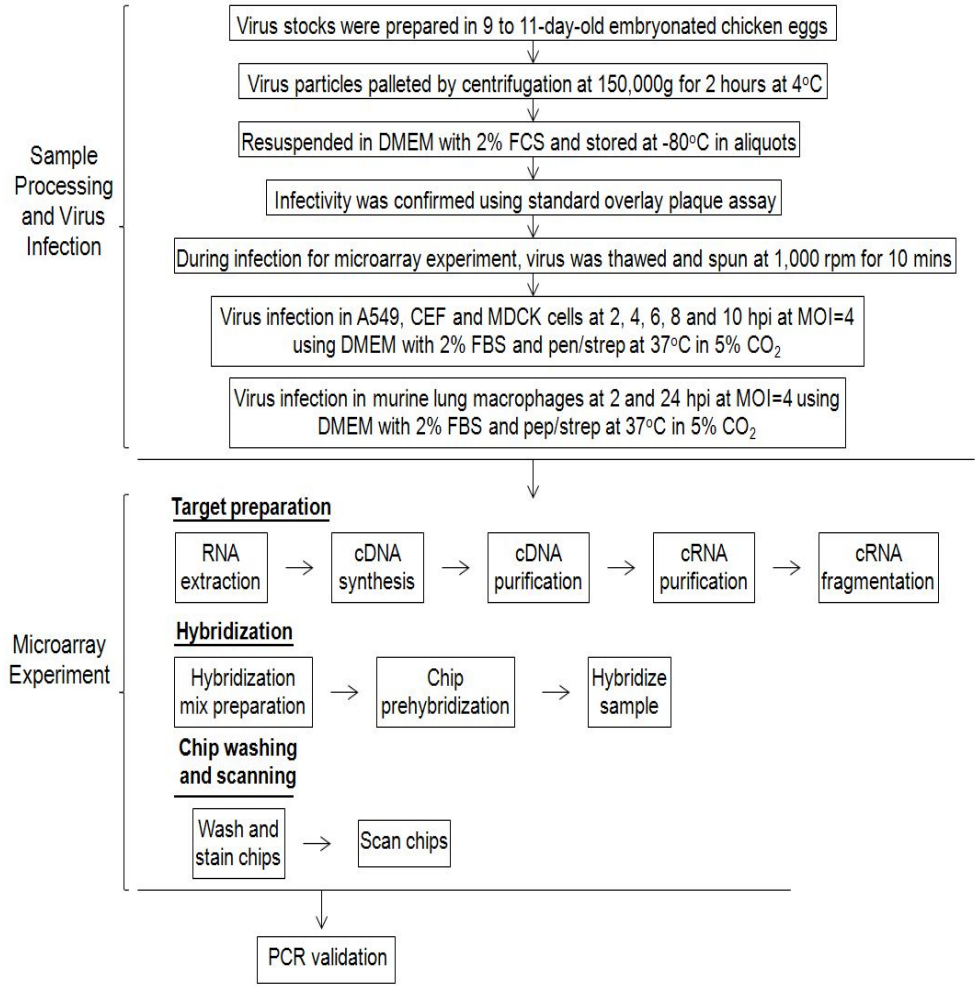

Figure 5.8 Microarray experiment workflow during influenza A strains infections.

5.3 Result and Discussion

5.3.1 Host gene expression in A549 cells

5.3.1.1 Global profiling of gene expression

5.3.1.1.1 Heat maps of global gene expression

Global heat maps showed that the numbers of differentially expressed probe sets increased with the infection time increasing in all these four viruses infected A549 cells. Detailed examination indicated that the genomic gene expression patterns were different upon infections of different influenza A virus strains [Figure 5.9]. At 10 hpi, almost half of the probe sets showed down-regulated expression after two human viruses infections, while only a small batch of probe sets showed down-regulated expression after two avian viruses infections. Besides, the number of probe sets with up-regulated expression was lowest in A549 cells after infection of H1N1 when compared to other three strains.

5.3.1.1.2 Distribution of differentially expressed probe sets

Upon different viruses infections, the largest numbers of probe sets exhibiting differential expression changes occurred at 10 hpi, therefore we compared the host gene expression performances from different influenza A viruses infections at this time point [Table 5.1]. In A549 cells, H5N3 infection induced highest percentage of probe sets with up-regulated expression, followed by H5N2/F59, pH1N1, H9N2 and H5N2/F118. Whereas, H1N1 infection only resulted in a small number of probe sets with up-regulated expression.

Despite of the lowest percentage of up-regulated probe sets in H1N1 infected A549 cells, almost half of probe sets in H1N1 infected A549 cell showed down-regulated expression. Besides infection of H1N1, infections of other influenza A strains including H5N2/F59, H5N2/F189 and pH1N1 also led to considerable batches of probe sets with the repressed expression. Among three H5N2 strains, the numbers of probe sets with up-regulated expression were similar after H5N2/F59 and H5N2/F118 viruses infections, while the numbers of probe sets with down-regulated expression were similar after H5N2/F59 and H5N2/F189 viruses infections.

5.3.1.1.3 Functional classification

In terms of biological functions from GO and KEGG database, differentially expressed probe sets retrieved from different influenza A strains infections at 10 hpi were classified into interested functional families. Three fold regulation scales were also offered for detailed investigation.

After classifying these differentially expressed probe sets into different functional groups, it was clear that the up-regulated probe sets were majorly grouped into “Immune Response”, “RNA Binding”, “DNA Binding” as well as ”Signal Transduction”, with probe sets associated with “Immune Response” showing high fold regulations [Figure 5.10]. It was noted that the numbers of up-regulated probe sets belonging to “Immune Response” showed lower after infections of two human strains (H1N1 and pH1N1) when compared to other avian strains. And among these avian strains, infections of H5N2/F59 and H9N2 strains strongly induced the expression of the highest numbers of probe sets functionally associated with “Immune Response”. Thus, it was assumed

that host immune response triggered by infections of H1N1 and pH1N1 might be suppressed to some extent, while the host immune response was stimulated well after infections of other avian strains, especially H5N2/F59 and H9N2. Among the three H5N2 strains, infection of H5N2/F59 induced expression of more probe sets belonging to "Immune Response" and "RNA binding" than infections of other two strains, suggesting strong antiviral activities in H5N2/F59 infected A549 cells.

In H1N1 infected A549 cells, a high portion of down-regulated probe sets was identified. These probe sets were majorly classified in groups such as "RNA Binding", "DNA Binding", "Signal Transduction" and "Transcription Factor", indicating the inhibition of a large scale of cell activities after H1N1 infection in A549 cells. In addition to H1N1, infections of the other human strain, pH1N1, and another two avian strains, H5N2/F59 and H5N2/F189, also resulted in relatively large numbers of probe sets with down-regulated expression, and these probe sets were located in similar functional groups as the down-regulated probe sets retrieved from H1N1 infection. Detailed investigation also indicated that some of the probe sets were inhibited deeply, even with higher than 10-FC, at their expression level after H1N1 infection. However, few probe sets with down-regulated expression higher than 10-FC could be detected after infection of all other strains.

Table 5.1 Differentially expressed probe sets in A549 cells infected with influenza A viruses at 10 hpi.

A549	Probe sets (>=2 fold)		Probe sets (>=3 fold)		Probe sets (>=5 fold)		Probe sets (>=10 fold)	
	Up-regulated	Down-regulated	Up-regulated	Down-regulated	Up-regulated	Down-regulated	Up-regulated	Down-regulated
H1N1	0.28%	46.00%	0.21%	25.29%	0.14%	8.40%	0.08%	1.59%
pH1N1	1.44%	33.37%	0.86%	5.62%	0.48%	0.58%	0.22%	0.07%
H5N2/F59	1.64%	34.87%	1.03%	11.06%	0.63%	1.66%	0.35%	0.14%
H5N2/F118	1.39%	9.53%	0.72%	2.50%	0.38%	0.31%	0.25%	0.04%
H5N2/F189	0.89%	32.17%	0.61%	5.85%	0.39%	0.34%	0.22%	0.03%
H5N3	2.19%	5.07%	1.12%	1.85%	0.42%	0.41%	0.18%	0.06%
H7N1	0.74%	9.37%	0.47%	1.10%	0.26%	0.12%	0.15%	0.02%
H9N2	1.41%	2.25%	0.84%	0.26%	0.48%	0.04%	0.27%	0.00%

The global host gene expression profiles were retrieved from microarray analysis with different time points examined. The ratios of differentially expressed probe sets (P-value≤0.05) up- or down-regulated with different fold changes (≥2-FC, ≥3-FC, ≥5-FC and ≥10-FC) in relative to their corresponding "expressing probe sets" are represented in percentage. The expressing probe sets refer to probe sets detected in the mock-infected corresponding cells.

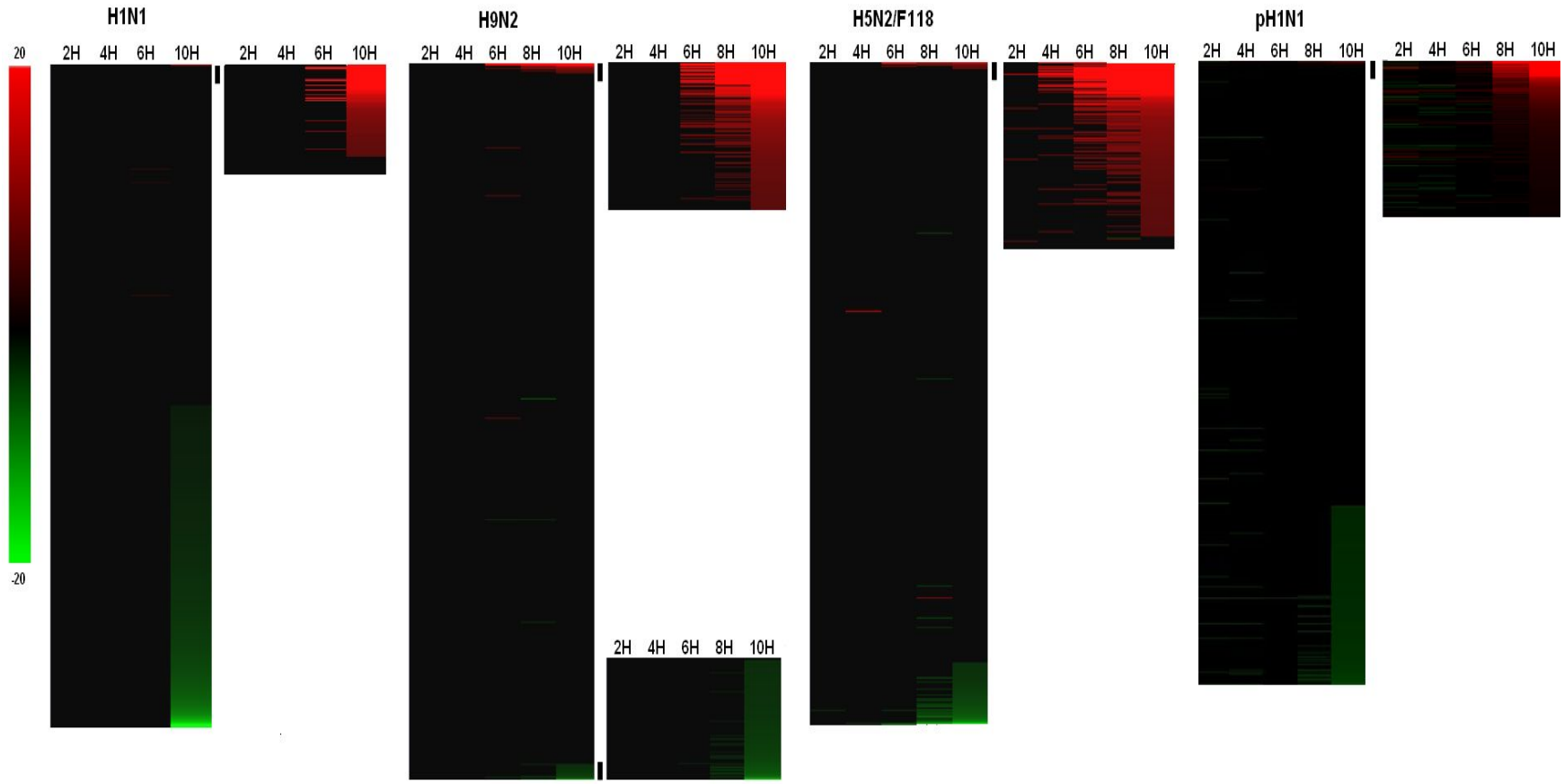

Figure 5.9 Temporal changes in the host cell transcriptome in A549 cells infected by four influenza virus strains. The global host gene expression profiles were retrieved from microarray analysis with different time points examined. The probe sets showing ≥2 fold change (FC) up- or down-regulated in expression are indicated (P-value≤0.05). Expression profiles of up-regulated (red), down-regulated (green) and no significant change (black) are shown.

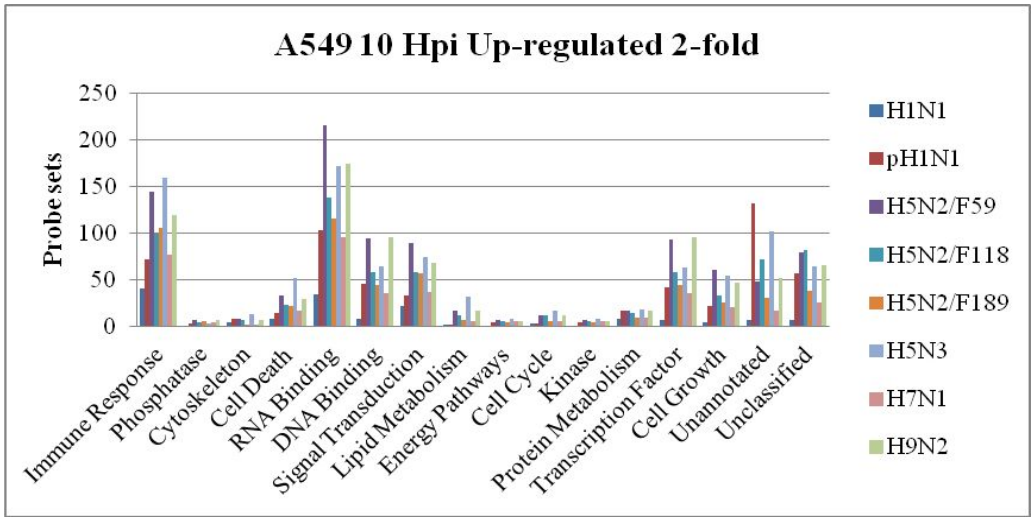
A549 10 Hpi Up-regulated 2-fold
Probe sets
250
200
150
100
50
0
Immune Response
Phosphatase
Cytoskeleton
Cell Death
RNA Binding
DNA Binding
Signal Transduction
Lipid Metabolism
Energy Pathways
Cell Cycle
Kinase
Protein Metabolism
Transcription Factor
Cell Growth
Unannotated
Unclassified
H1N1
pH1N1
H5N2/F59
H5N2/F118
H5N2/F189
H5N3
H7N1
H9N2

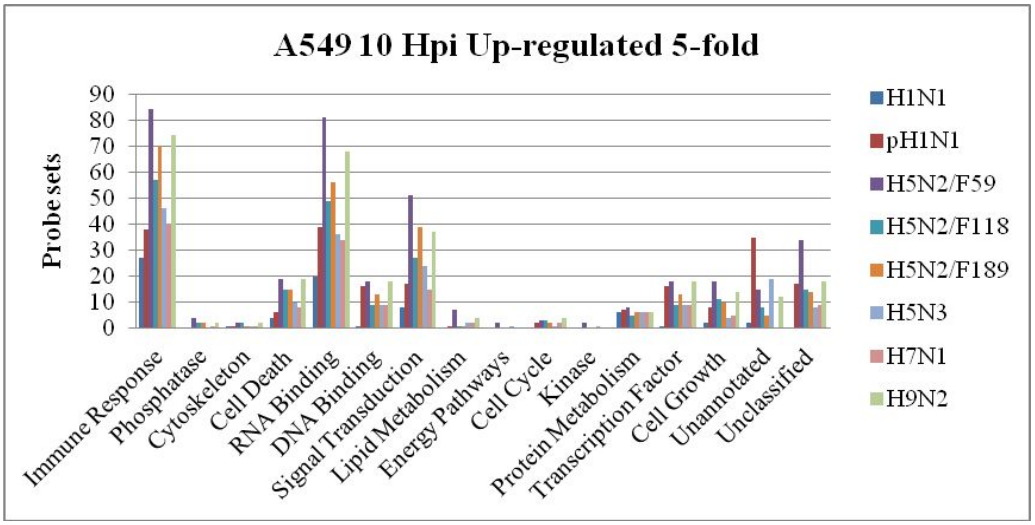
A549 10 Hpi Up-regulated 5-fold
Probe sets
90
80
70
60
50
40
30
20
10
0
Immune Response
Phosphatase
Cytoskeleton
Cell Death
RNA Binding
DNA Binding
Signal Transduction
Lipid Metabolism
Energy Pathways
Cell Cycle
Kinase
Protein Metabolism
Transcription Factor
Cell Growth
Unannotated
Unclassified
H1N1
pH1N1
H5N2/F59
H5N2/F118
H5N2/F189
H5N3
H7N1
H9N2

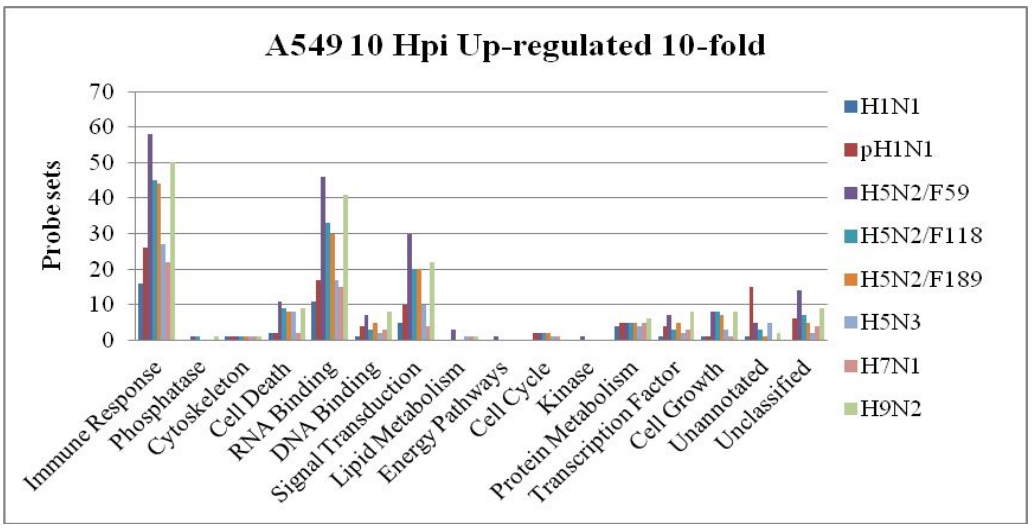
A549 10 Hpi Up-regulated 10-fold
Probe sets
70
60
50
40
30
20
10
0
Immune Response
Phosphatase
Cytoskeleton
Cell Death
RNA Binding
DNA Binding
Signal Transduction
Lipid Metabolism
Energy Pathways
Cell Cycle
Kinase
Protein Metabolism
Transcription Factor
Cell Growth
Unannotated
Unclassified
H1N1
pH1N1
H5N2/F59
H5N2/F118
H5N2/F189
H5N3
H7N1
H9N2

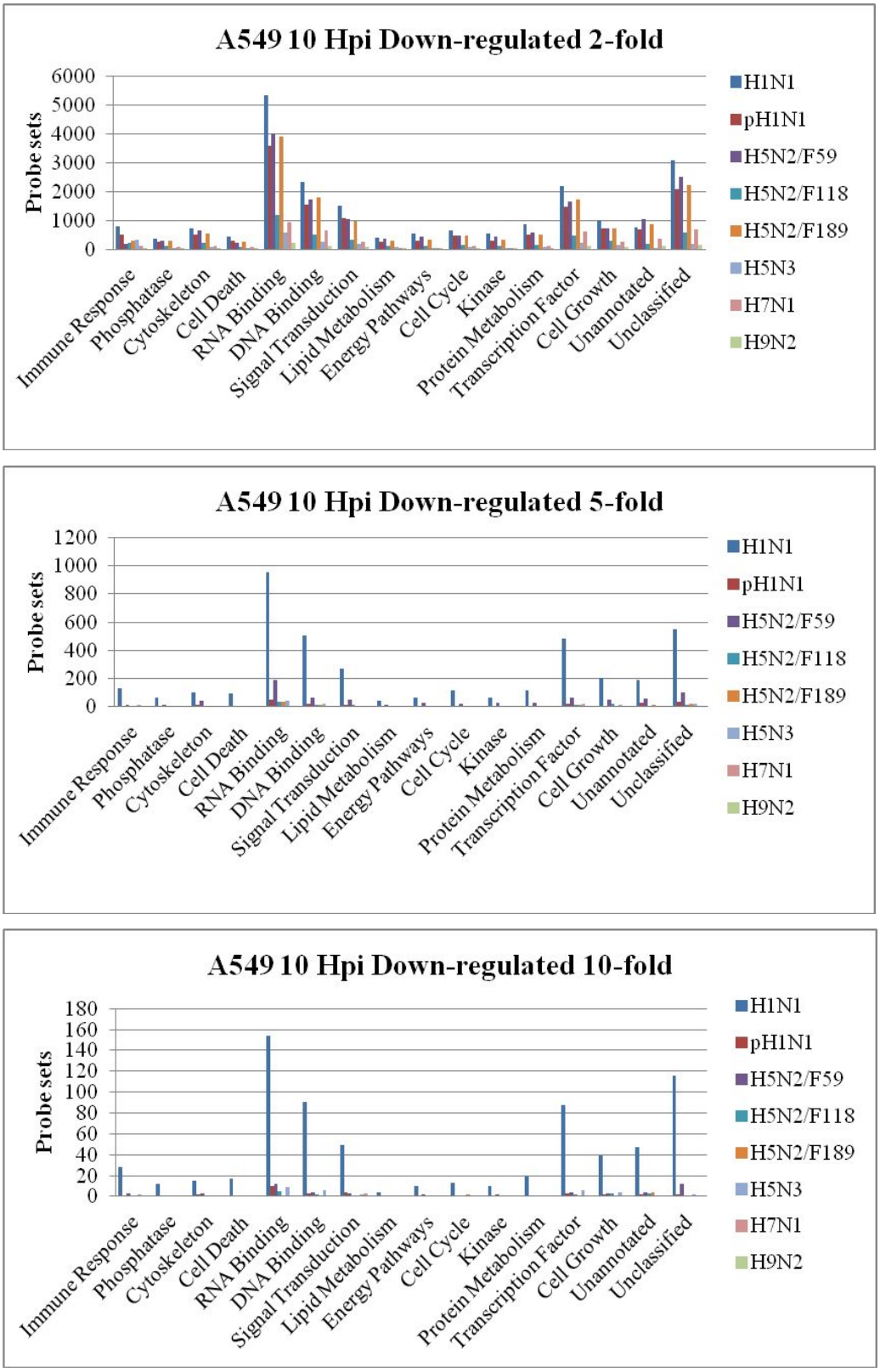

Figure 5.10 Overview of distributions of differentially expressed probe sets into different biological functions in A549 cells infected with influenza A viruses. The numbers of probe sets in the different functional families, including non-annotated and unclassified groups, showing up- or down-regulated with different fold changes (≥2-FC, ≥5-FC and ≥10-FC) in gene expression are presented.

5.3.1.1.4 Cluster analysis

To our knowledge, genes with similar temporal expression trends might have related biological functions and possibly correspond to some critical cellular processes and pathways [91]. So the aim of this cluster analysis is to classify probe sets with similar expression profiles into common biological groups, which is beneficial for further functional analysis. Since only four influenza A strains H1N1, pH1N1, H5N2/F118, H9N2 were examined with multiple time points in A549 cell lines, the probe sets at more than one time point of infection with ≥2-FC (P-value≤0.05) were clustered into similar gene expression profiles using the Expander version 5.0 software [Figure 5.11-5.14]. Using the same software, the data were further analyzed into genes relating to different functional groups or canonical pathways, and enriched transcription factor were also identified. All enriched functional groups, canonical pathways and transcriptional factors are displayed in Tables 5.2-5.5.

Up-regulated

Due to the low percentage of up-regulated probe sets in H1N1 A549 (0.28%), genes encoded by this batch of probe sets were not able to be identified in cluster analysis. Consequently, we picked out this group of genes and did further enrichment analysis of functional groups, pathways and transcription factors independently. Initial comparison of genes with up-regulated expression trend indicated that there was a time lag for gene expression stimulation upon infections of H1N1 and pH1N1 (started at around 6 hpi) when compared to infections of H5N2/F118 and H9N2 (started at about 2 or 4 hpi).

Parallel comparison has revealed that genes with up-regulated expression in A549 cells infected by all these four influenza A strains shared several significant pathways such as “Cytokine-Cytokine receptor interaction” and “RIG-I- like receptor signaling pathway”. However, smaller numbers of genes belonging to these two pathways were detected after infections of H1N1 and pH1N1 than those detected after infections of H5N2/F118 and H9N2. This observation indicated that the innate immune response was triggered upon the infections of all these examined influenza A strains in A549 cells, and this

antiviral response was stronger upon infection of two avian strains than two human strains.

Besides these two pathways, other pathways such as “Jak-STAT signaling pathway” and “Toll-like receptor signaling pathway” were also over-represented after H5N2/F118 and H9N2 infections. Interestingly, “Toll-like receptor signaling pathway” was also enriched by the down-regulated genes after pH1N1 infection. Toll-like receptors are a type of PRRs in innate immune responses. Opposite regulation of this pathway in different influenza A strains might suggest that some regulations were initiated to interrupt normal human innate response reaction from the early infection stage in pH1N1 infected A549 cells.

“B cell receptor signaling pathway” was another pathway significantly enriched only in genes with up-regulated expression following H9N2 infection. B cell responses play a key role on survival from both primary as well as secondary infection with influenza virus. Recent studies have indicated that innate stimuli such as TLR signals functions as important signals for B cell regulation and type I IFN signals positively regulate influenza virus-specific B cell responses [257]. Hence, significant activation of “B cell receptor signaling pathway” provided evidence that H9N2 infection triggered a series of strong innate inflammatory response in A549 cells.

Besides these canonical pathways, a batch of key functional groups was also enriched in these up-regulated genes after infections with different influenza A strains. The analysis based on the H1N1, pH1N1/478, H5N2/F118 and H9N2 infections revealed that the differentially up-regulated genes share common functional gene groups such as response to virus and nucleic acid binding. In addition, the avian viruses have more functional gene groups in common and these groups are genes involved in immune response, cytokine receptor binding, transition metal ion binding and cell death. In the case of pH1N1/478 infection, the differentially up-regulated genes that were specific to this virus were involved in transcription regulatory activity, RNA metabolic process, transcription from RNA polymerase II promoter and multicellular organismal development.

Transcription factors, IRF-1, IRF-3 and IRF-7, which are involved in the IFN signaling pathway, were observed to be significantly up-regulated in a temporal manner in A549 cells infected with seasonal influenza virus [258]. In our study, these two potential transcription factors both showed significantly up-regulated expression levels after avian viruses infections. However, only transcription factor *IRF-7* showed faint elevation in its expression after human viruses infections at specific time points. These observations were consistent with the phenomenon that larger numbers of downstream genes with up-regulated expression were detected in A549 cells infected with two avian strains than two human strains. No apparent expression changes of IRF-3 were observed following the infections of four influenza A strains, which could be due to the binding of influenza NS1 to RIG-1, which in turn inhibits the activation of IRF-3 [259].

On the basis of performances of genes with up-regulated expression, these four influenza A strains can be roughly classified into two groups. One group included avian strains, H5N2/F118 and H9N2, and their infections generated strong host immune response with many genes belonging to antiviral-related pathways showing up-regulated expression; the other group included human strains, H1N1 and pH1N1, and their infections displayed postponed and weak host antiviral reaction. It was assumed that viruses such as H1N1 and pH1N1 might evolve some specific mechanism which counteracts the host genes' immune reaction after virus invasion from an early infection stage.

Down-regulated

In contrast to the differentially up-regulated genes, larger proportions of genes showed down-regulated expression after two human strains infections, and this allowed more functional groups and canonical pathways to be enriched. Canonical pathways such as "Metabolic pathways", "Cell cycle", "Regulation of actin cytoskeleton", "Adherence junction", "Lysosome", "Endocytosis" and "Pathway ways in cancer" were over-represented based on genes with down-regulated expression after the two human influenza A strains and H5N2/F118 infections, with a greater number of genes involved in infections of two human strains. These common pathways were generally related to cell regulation or cell interactions, suggesting that infections of these three influenza A strains

inhibited expression of a batch of genes involved in cell activity regulation in A549 cells. And the limitation of the cell activity might serve to benefit for viral survival or replication in A549 cells.

Besides these pathways, other down-regulated genes detected during H1N1 and pH1N1 infections were involved in other pathways such as "Ubiquitin mediated proteolysis", "Wnt signaling pathway", "Apoptosis" and "RNA degradation". Gene expression repression in these pathways might imply that cell apoptosis and RNA degradation were postponed to facilitate the virus replication in A549 cells.

Common functional gene groups (e.g. genes involved in nitrogen compound metabolic process, regulation of macromolecule metabolic process, nucleic acid binding) were observed between the human and avian strains infections, with a greater number of genes involved in the former infections. Specific to the 2 human viruses, the genes involved in the protein metabolic-related processes showed a decreasing temporal trend in the expression profiles, and this is the first evidence reported here. Similar changes in differential expression of transcripts involved in protein metabolism have been reported for the HPAI H5N1 in infected CEF cells [260]. This observation was not seen in the avian viruses in our study, suggesting that the human viruses and HPAI share a closer role in protein metabolism involvement than with the LPAI.

A differential decrease in gene expression profile was observed for the genes involved in zinc ion binding and ATP binding for the seasonal human virus H1N1, and faintly detected for pH1N1. In H1N1-infected A549 cells, the temporal trend for the Zinc Finger (ZNF) genes decreased sharply from 6 to 10 hpi, with the most significant down-regulated fold changes detected at the last time point. Among these ZNF genes, the topmost significantly down-regulated genes are listed: ZNF226 = 41.84-FC, ZNF675 = 40.08-FC, ZNF764 = 39.84-FC, ZNF488 = 36.5-FC. Our results concurred with that reported in Lee et al., 2010 where other ZNF genes were presented with significant changes (ZBTB3, ZNF175, ZNF383, and ZNF587 genes; ZNF175 and ZNF587 were observed in our study) in primary alveolar epithelial cells infected with a seasonal H1N1 (A/Hong Kong/54/1998) than with pandemic H1N1(A/Hong Kong/415742/2009) [261]. The same study suggested that the ZNF may have a

role in suppressing viral transcription and this may facilitate more efficient replication of seasonal H1N1 in the host cells as compared to the pH1N1.

In contrast, the temporal trend for ATP binding associated genes remained gradual from early to late infection time points, but the fold changes were significant enough to be detected. Reports have described that ATP is required for influenza virus budding [262] and replication [263], but it is not clear how the ATP binding associated genes relates to the ATP requirement.

A larger number of transcription factors were enriched based on down-regulated genes from infections of two human strains than two avian strains in A549 cells. The transcription factors detected in the two human strains and H5N2/F118 were analyzed using the IPA network and these factors were found to be associated with: gene expression, cell death, organismal development, carbohydrate metabolism, small molecule biochemistry and infectious disease. More than 50% of these transcription factors were observed to be down-regulated at their expression level after H1N1 infection, whereas almost no expression changes were detected in the A549 cells infected with the remaining three viruses. Furthermore, three of these factors, E2F, ETF and Sp1, were observed to be commonly shared among infections of all four examined influenza A strains, with more down-regulated genes involved in the H1N1/WS infection. Detailed investigation indicated faintly down-regulated expression of ETF was observed only after H1N1/WS and H5N2/F118 infections while faintly down-regulated expression of sp1 was observed only after H1N1/WS and pH1N1/478 infections.

Altogether, infection of H1N1 contributed to most genes with decreased expression in A549 cells, followed by pH1N1 and H5N2/F118. And these regulations might target to create a more beneficial environment for viral survival and replication through interrupting the normal regulation of cell. Compared to these three influenza A strains, H9N2 almost did nothing to combat with the host cells antiviral control.

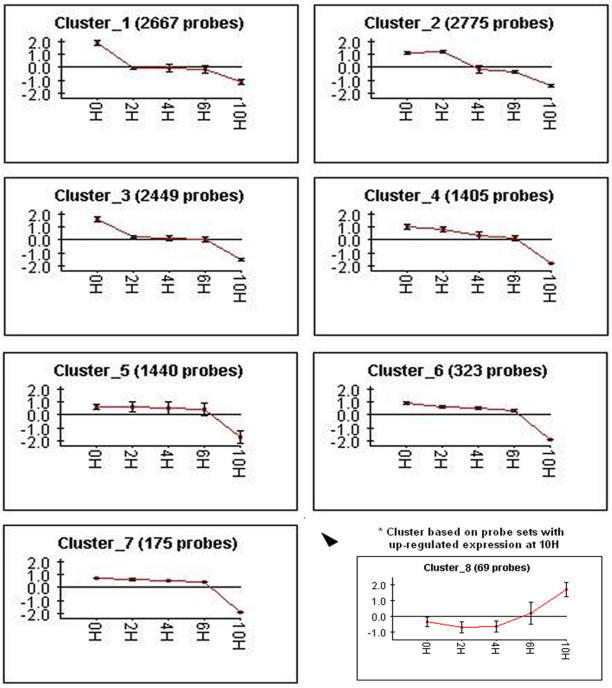

Figure 5.11 Clustering analysis of temporal gene expression profiles in H1N1-infected A549 cells. A549 cells were infected with H1N1 at 2, 4, 6, and 10 hpi. Probe sets showing ≥2-fold changes up- or down-regulated (P-value≤0.05) at least over one time point were analyzed with Expander 5 software. X-axis represents post-infection in hours (H), and Y-axis means normalized expression changes of probe sets. The extra cluster included the probe sets showing up-regulated expression at 10 hpi.

Table 5.2 Summary of functional groups, canonical pathways and transcription factors enriched based on differentially expressed genes in A549 cells infected with H1N1.

Cluster No.	Enriched Transcription Factors (H1N1)
Cluster 1	Elk:431 | E2F:1267 | Nrf-1:699 | ETF:929 | GABP:513 | E2F-1:487 | Sp1:1135 | C-Myc:Max:506 | ZF5:726 | HIC1:715 | Tax/CREB:345
	AHRHIF:444 | ZF5:355 | Egr-1:502 | CREB:302 | Tel-2:230 | MOVO-B:729 | E2F-1:192 | EGR:631 | AP-2:641 | ATF:420 | NF-Y:440
	AP-2:568 | AP-2:563
Cluster 2	ETF:978 | E2F:1235 | Elk-1:402 | GABP:510 | Nrf-1:677 | Sp1:1100 | ATF:440 | NF-Y:469 | E2F-1:468 | C-Myc:Max:499 | ZF5:699 | ZF5:348
	E2F-1:101 | Pax-3:203 | Tel-2:226 | AP-2:622 | Pax-3:260 | Tax/CREB:327 | XBP-1:293 | AHRHIF:431 | E2F-1:181 | ATF4:312 | STAT1:73
	CREB:291
Cluster 3	ETF:870 | E2F:1111 | Nrf-1:603 | Elk-1:358 | Sp1:1002 | ZF5:649 | AP-2:541 | GABP:416 | AP-2:593 | E2F-1:421 | HIC1:617 | Tel-2:217
	E2F-1:96 | AP-2:504 | AP-2alpha:360 | AhR:259 | E2F:108 | ATF:379 | ZF5:309 | Egr-1:418
Cluster 4	E2F:637 | ETF:480 | Nrf-1:346 | ZF5:373 | MOVO-B:370 | E2F-1:246 | ATF:223 | Ap1:559 | AHRHIF:233
Cluster 5	ETF:474 | E2F:598 | ATF:241 | Elk-1:197 | E2F-1:244 | IRF-1:123 | SRY:288
Cluster 6	E2F:171 | AP-2:97 | Sp1:150 | Nrf-1:92
Cluster 7	Sp1:85 | ETF:69
Cluster 8*	ISRE:28 | IRF-7:22 | IRF-1:20
Cluster No.	**Enriched Canonical Pathways (H1N1)**
Cluster 1	Metabolic pathways:188 | Ubiquitin mediated proteolysis:32 | Progesteron-mediated oocyte maturation:26 | Cell cycle:28
	Insulin signaling pathway:28 | Lysosome:23 | Pancreatic cancer:17 | Chronic myeloid leukemia:17 | Gap junction:19
Cluster 2	Metabolic pathways:158 | Endocytosis:43 | Ubiquitin mediated proteolysis:34 | Pancreatic cancer:21 | N-Glycan biosynthesis:15
	Pathways in cancer:52 | Progesteron-mediated oocyte maturation:24 | Cell cycle:27 | Apoptosis:21 | Adherens junction:19 | Lysosome:24
	Prostate cancer:20 | RNA degradation:15 | Chronic myeloid leukemia:17 | Colorectal cancer:18 | Renal cell carcinoma:16
Cluster 3	Cell cycle:32 | RNA degradation:20 | Pathways in cancer:52 | Focal adhesion:36 | ErbB signaling pathway:21 | Adherens junction:19
	Inositol phosphate metabolism:15 | Progesterone-mediated oocyte maturation:22 | Phosphatidylinositol signaling system:18
	Aminoacyl-tRNA biosynthesis:12 | Small cell lung cancer:18 | Regulation of actin cytoskeleton:32
Cluster 4	Pahtways in cancer:31 | Cell cycle:17 | p53 signaling pathway:12 | Ubiquitin mediated proteolysis:17 | TGF-beta signaling pathway
	Adherens junction:12
Cluster 5	Pathways in cancer:29
Cluster 6	Cell cycle:8
Cluster 8*	Cytokine-cytokine receptor interaction:6 | RIG-like receptor signaling pathway:4
Cluster No.	**Enriched Gene Ontology Terms (H1N1)**
Cluster 1	Cellular protein metabolic process - GO:0044267:349 | Protein metabolic process - GO:0019538:393 | Macromolecule localization - GO:0033036:195
	Protein transport - GO:0015031:157 | Nucleotide binding - GO:0000166:321 | Protein localization - GO:0008104:168
	Nitrogen compound metabolic process - GO:0006807:422 | Cellular localization - GO:0051641:157 | Biosynthetic process - GO:0009058:386
	Transferase activity - GO:0016740:259
Cluster 2	Nitrogen compound metabolic process - GO:0006807:470 | Nucleobase, nucleoside, nucleotide and nucleic acid metabolic process - GO:0006139:425
	Cellular biosynthetic process - GO:0044249:420 | Gene expression - GO:0010467:370 | Cellular protein metabolic process - GO:0044267:342
	Nucleotide binding - GO:0000166:324 | Macromolecule biosynthetic process - GO:0009059:343 | RNA metabolic process - GO:0016070:178
	Protein metabolic process - GO:0019538:380 | Protein transport - GO:0015031:151
Cluster 3	Nucleobase, nucleoside, nucleotide and nucleic acid metabolic process - GO:0006139:385 | Nitrogen compound metabolic process - GO:0006807:414
	Cellular component organization - GO:0016043:279 | Organelle organization - GO:0006996:189 | Nucleotide binding - GO:0000166:291
	Nucleic acid binding - GO:0003676:388 | Gene expression - GO:0010467:315 | ATP binding - GO:0005524:211
	RNA metabolic process - GO:0016070:154 | Cellular protein metabolic process - GO:0044267:285
Cluster 4	Nucleobase, nucleoside, nucleotide and nucleic acid metabolic process - GO:0006139:248 | Nucleic acid binding - GO:0003676:260
	Regulation of cellular metabolic process - GO:0031323:248 | Regulation of macromolecule metabolic process - GO:0060255:239
	Regulation of primary metabolic process - GO:0080090:237 | Regulation of gene expression - GO:0010468:220 | Gene expression - GO:0010467:205
	Zinc ion binding - GO:0008270:192 | Macromolecule biosynthetic process - GO:0009059:185 | Cellular biosynthetic process - GO:0044249:208
Cluster 5	Nucleobase, nucleoside, nucleotide and nucleic acid metabolic process - GO:0006139:256 | Nucleic acid binding - GO:0003676:276
	Gene expression - GO:0010467:234 | Regulation of macromolecule metabolic process - GO:0060255:250
	Regulation of gene expression - GO:0010468:231 | Regulation of RNA metabolic process - GO:0051252:212 | Transcription - GO:0006350:168
	Cellular biosynthetic process - GO:0044249:245 | Regulation of macromolecule biosynthetic process - GO:0010556:228
	Regularion of cellular metabolic process - GO:0031323:253
Cluster 6	Transition metal ion binding - GO:0046914:68 | Regulation of cellular metabolic process - GO:0031323:69
	Regulation of macromolecule metabolic process - GO:0060255:66 | Cellular macromolecule biosynthetic process - GO:0034645:55
	Nucleobase, nucleoside, nucleotide and nucleic acid metabolic process - GO:0006139:63 | DNA binding - GO:0003677:53
	Nucleic acid binding - GO:0003676:66 | Transcription activator activity - GO:0016563:17 | Transcription regulator activity - GO:0030528:36
	Cellular macromolecule catabolic process - GO:0044265:24
Cluster 7	Zinc ion binding - GO:0008270:27
Cluster 8*	Response to virus - GO:0009615:10 | Immune response - GO:0006955:14 | Response to stimulus - GO:0050896:21
	Cytokine activity - GO:0005125:5 | Nucleic acid binding - GO:0003676:14

Differentially expressed genes were significantly categorized into different GO terms and canonical pathways. Different transcription factors that can potentially be involved in the regulation of gene expressions are shown for each cluster under Expander 5 software analysis (P-value≤0.05). Each functional group, canonical pathway or transcription factor is followed by the number of corresponding genes. * represents the cluster which is based on probe sets with up-regulated expression at 10 hpi.

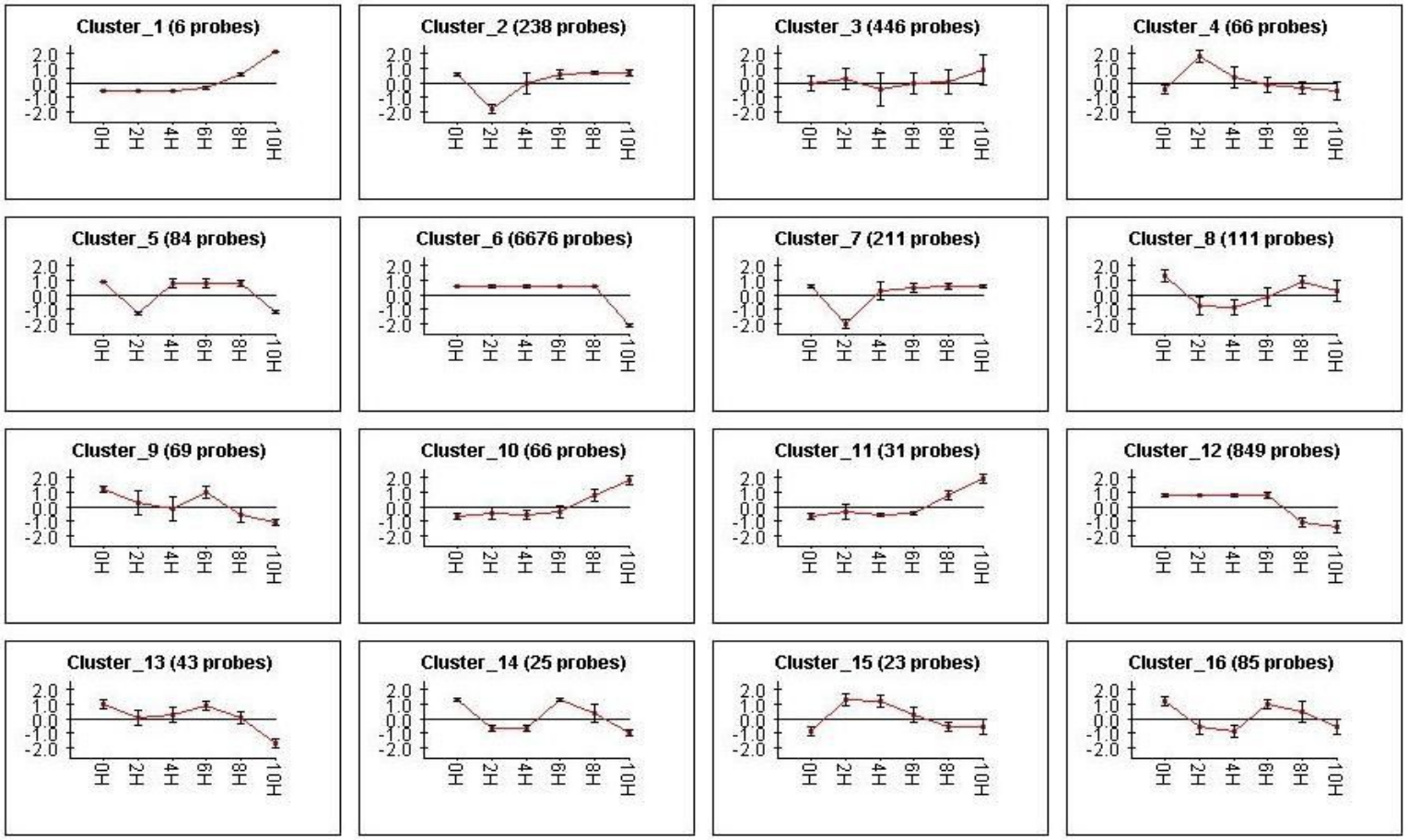

Figure 5.12 Clustering analysis of temporal gene expression profiles in pH1N1-infected A549 cells. A549 cells were infected with pH1N1 at 2, 4, 6, 8 and 10 hpi. Probe sets showing ≥2-fold changes up- or down-regulated (P-value≤0.05) at least over one time point were analyzed with Expander 5 software. X-axis represents post-infection in hours (H), and Y-axis means normalized expression changes of probe sets.

Table 5.3 Summary of functional groups, canonical pathways and transcription factors enriched based on differentially expressed genes in A549 cells infected with pH1N1.

Cluster No.	Enriched Transcription Factors (pH1N1)
Cluster 1	c-Myb:3 | ISRE:4
Cluster 3	NF-kappaB_(p65):25
Cluster 6	E2F:2493 | ETF:1961 | Nrf-1:1313 | Sp1:2224 | ZF5:1459 | AP-2:1312 | E2F-1:931 | MOVO-B:1486 | C-Myc:Max:993| ElK-1:712 | AP-2:1159
	AHRHIF:881 | HIC1:1369 | AP-2:1152 | Egr-1:986 | ZF5:700 | GABP:908 | EGR:1236 | AP-2alpha:778 | AhR:562 | HIF-1:1007 | ATF:810
	E2F-1:363 | Tax/CREB:637 | AhR:Arnt:627 | UF1H3EETA:1640 | N-Myc:738 | NF-Y:842 | E2F:213 | Pax-3:491 | Tel-2:407 | E2F-1:170
Cluster 10	ISRE:12
Cluster 11	IRF-7:11 | ISRE:11 | IRF-1:7
Cluster 12	ETF:270 | Nrf-1:202 | E2F:329 | Tax/CREB:109
Cluster No.	**Enriched Canonical Pathways (pH1N1)**
Cluster 4	Toll-like receptor signaling pathway:4
Cluster 6	Pathways in Cancer:121 | Ubiquitin mediated proteolysis:63 | Adherens junction:43 | Endocytosis:72 | Cell cycle:52 | Wnt signaling pathway:57
	Focal adhesion:69 | Metaboloc pahtways:249 | Small lung cancer:37 | Amino acyl-tRNA biosynthesis:23 | Colorectal cancer:34
	Progesterone-mediated oocyte maturation:39 | Neurotrophin signaling pathway:44 | MAPK signaling pathway:26 | Insulin signaling pathway : 46
	Tight junction:45 | Chronic myeloid leukenia:30 | TAF-beta signaling pathway:33 | DNA replocation:18 | Pancreatic cancer:28
	Regulation of actin cytoskeleton:61 | Axon guidance:41 | ECM-receptor interaction:30 | Lysosome:37 | GnRH signaling pathway:33
	Apoptosis:30 | Purine metabolism:45 | O-Glycan biosynthesis:15 | Gap junction:30 | Renal cell carcinoma:25 | ErbB signaling pathway:29
	Lysine degradation:19 | RNA degradation:22 | Endometrial cancer:20
Cluster 9	Aminoacyl-tRNA biosynthesis:3
Cluster 10	Cytokine-Cytokine receptor interaction:5
Cluster No.	**Enriched Gene Ontology Terms (pH1N1)**
Cluster 2	Transition metal ion binding - GO:0046914:41 | Transcription - GO:0006350:29 | Nitrogen compound metabolic process - GO:0006807:43
	Gene expression - GO:0010467:37 | Cellular biosynthetic process - GO:0044249:41 | Nucleic acid binding - GO;0003676:40
Cluster 3	Nucleic acid binding - GO:0003676:64 | Regulation of gene expression - GO:0010468:56 | Transcription regulatory activity - GO:0030528:36
	Response to virus - GO:0009615:9 | Response to biotic stimulus - GO:0009607:14 | RNA metabolic process - GO:0016070:24
	Transcription from RNA polymerase II promoter - GO:0006366:11 | Multicellular organismal development - GO:0007275:43
	Organ development - GO:0048513:28 | Multi-organism process - GO:0051704:17
Cluster 4	Inflammatory response - GO:0006954:5
Cluster 6	Nucleobase, nucleoside, nucleotide and nucleic acid metabolic process - GO:0006139:772 | Nucleotide binding - GO:0000166:608
	Nitrogen compound metabolic process - GO:0006807:838 | Cellular protein metabolic process - GO:0044267:636
	Protein metabolic process - GO:0019538:719 | Regulation of macromolecule metabolic process - GO:0060255:761
	Nucleic acid binding - GO:0003676:800 | Transition metal ion bindng - GO:0046914:715 | Purine nucleotide binding - GO:0017076:526
	Nucleoside binding - GO:0001882:460
Cluster 7	Nucleic acid binding - GO:0003676:43
Cluster 8	Cellular amino acid biosynthetic process - GO:0008652:5 | Biosynthetic process - GO:0009058:23
Cluster 9	Nucleic acid binding - GO:0003676:21 | Nucleobase, nucleoside, nucleotide and nucleic acid metabolic process - GO:0006139:18
Cluster 10	Response to biotic stimulus - GO:0009607:7 | Receptor binding - GO:0005102:8
Cluster 11	Immune system process - GO:0002376:7 | Response to virus - GO:0009615:4

Differentially expressed genes were significantly categorized into different GO terms and pathways. Different transcription factors that can potentially be involved in the regulation of gene expressions are shown for each cluster under Expander 5 software analysis (P-value≤0.05). Each functional group, canonical pathway or transcription factor is followed by the number of corresponding genes.

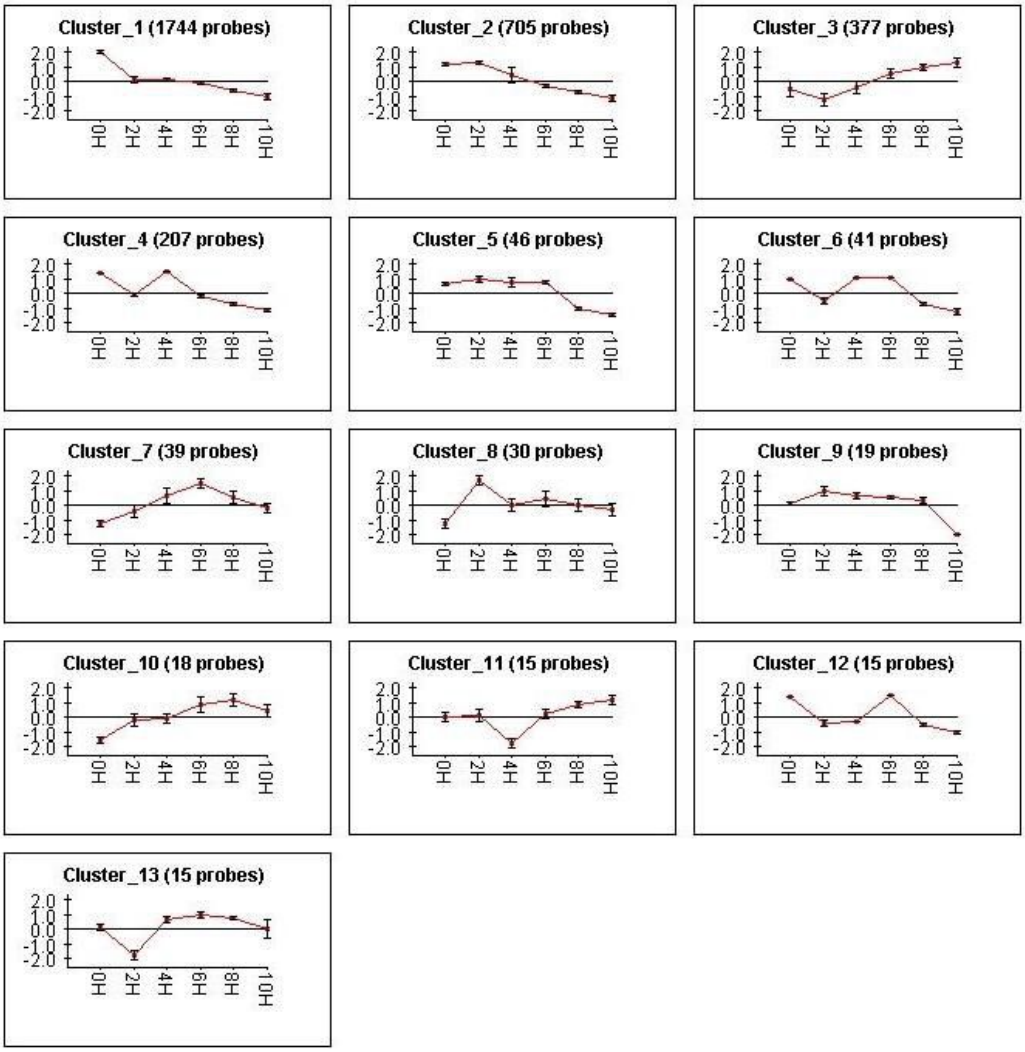

Figure 5.13 Clustering analysis of temporal gene expression profiles in H5N2/F118-infected A549 cells. A549 cells were infected with H5N2/F118 at 2, 4, 6, 8 and 10 hpi. Probe sets showing ≥2-fold changes up- or down-regulated (P-value≤0.05) at least over one time point were analyzed with Expander 5 software. X-axis represents post-infection in hours (H), and Y-axis means normalized expression changes of probe sets.

Table 5.4 Summary of functional groups, canonical pathways and transcription factors enriched based on differentially expressed genes in A549 cells infected with H5N2/F118.

Cluster No.	Enriched Transcription Factors (H5N2/F118)
Cluster 1	E2F:751 | ETF:583 | Sp1:701 | Nrf-1:421 | E2F-1:306 | AHRHIF:279 | ZF5:434 | Tax/CREB:219 | AP-2:372 | NF-Y:279 | c-Myc:Max:304
	HIF-1:321 | HIC1:420
Cluster 2	E2F:323 | ZF5:201 | ETF:245 | Sp1:290 | NF-Y:140 | HIC1:199 | MOVO-B:198 | AP-2:167 | AP-2alpha:114 | AP-2:184 | Nrf-1:170
	UF1H3BETA:226 | HNF4:297
Cluster 3	IRF-7:63 | ISRE:64 | IRF:60 | IRF1:46
Cluster 8	SRF:3
Cluster No.	**Enriched Canonical Pathways (H5N2/F118)**
Cluster 1	Metabolic pathways:109 | Lysosome:27 | Endocytosis:31 | Pahtways in cancer:39 | Cell cycle:21 | Citrate cycle (TCA cycle):10
	Progesterone-mediated oocyte maturation:18 | Biosynthesis of unsaturated fatty acids:8 | Steroid biosynthesis:7
	Aminoacyl-tRNA biosynthesis:10 | Pathogenic Escherichia coli infection:11
Cluster 2	Pathways in cancer:23 | Focal adhesion:17 | Endocytosis:15 | Cell cycle:12 | Tight junction:12 | Adherens junction:9
	Regulation of actin cytoskeleton:15 | TGF-beta signaling pathway
Cluster 3	Jak-STAT signaling pathway:10 | RIG-I-like receptor signaling pathway:7 | Toll-like receptor signaling pathway:8
	Cytokine-cytokine receptor interaction:10
Cluster 4	Focal adhesion:8
Cluster 5	p53 signaling pathway:4 | Glioma:3
Cluster No.	**Enriched Gene Ontology Terms (H5N2/F118)**
Cluster 1	Nucleotide binding - GO:0000166:231 | Purine nucleoside binding - GO:0001883:176 | Cellular component organization - GO:0016043:180
	Localization - GO:0051179:241 | Nitrogen compound metabolic process - GO;0006807:255 | Hydrolase activity - GO:0016787:194
	Cell cycle - GO:0007049:83 | Macromolecule localization - GO:0033036:106 | Protein metabolic process - GO:0019538:217
	Cellular localization - GO:0051641:91
Cluster 2	Cellular component organization - GO:0016043:100 | Regulation of cellular metabolic process - GO:0031323:135
	Organelle organization - GO:0006996:66 | Developmental process - GO:0032502:109 | DNA binding - GO:0003677:94
	Cell cycle - GO:0007049:45 | Nucleic acid binding - GO:0003676:118 | Cellular biosynthetic process - GO:0044249:107
	Cellular macromolecule biosynthetic process - GO:0034645:90 | Actin binding - GO:0003779:28
Cluster 3	Response to virus - GO:0009615:23 | Immune response - GO:0006955:31 | Multi-organism process - GO:0051704:29
	Response to stimulus - GO:0050896:58 | Nucleic acid binding - GO:0003676:51 | Defense response - GO:0006952:17
	RNA binding - GO:0003723:18
Cluster 4	Regulation of macromolecule metabolic process - GO:0060255:46 | Transition metal ion binding - GO:0046914:40
	Nucleic acid binding - GO:0003676:43 | Protein metabolic process - GO:0019538:37
	Cellular macromolecule biosynthetic process - GO:0034645:31
Cluster 5	Regulation of cellular metabolic process - GO:0031323:14

Differentially expressed genes were significantly categorized into different GO terms and canonical pathways. Different transcription factors that can potentially be involved in the regulation of gene expressions are shown for each cluster under Expander 5 software analysis (P-value≤0.05). Each functional group, canonical pathway or transcription factor is followed by the number of corresponding genes.

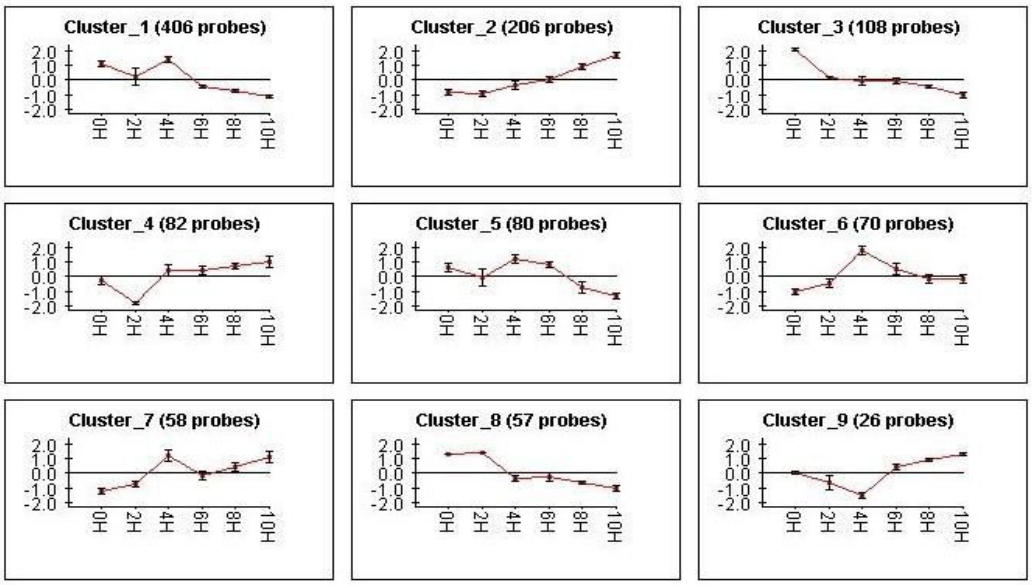

Figure 5.14 Clustering analysis of temporal gene expression profiles in H9N2-infected A549 cells. A549 cells were infected with H9N2 at 2, 4, 6, 8 and 10 hpi. Probe sets showing ≥2-fold changes up- or down-regulated (P-value≤0.05) at least over one time point were analyzed with Expander 5 software. X-axis represents post-infection in hours (H), and Y-axis means normalized expression changes of probe sets.

Table 5.5 Summary of functional groups, canonical pathways and transcription factors enriched based on differentially expressed genes in A549 cells infected with H9N2.

Cluster No.	Enriched Transcription Factors (H9N2)
Cluster 1	ETF:123 | E2F:161
Cluster 2	ISRE:63 | IRF-7:51 | IRF-1:48 | IRF1:36 | NF-kappaB_(p65):16
Cluster 3	Sp1:54
Cluster 4	ISRE:14 | IRF-1:14
Cluster No.	**Enriched Canonical Pathways (H9N2)**
Cluster 2	Toll-like receptor signaling pathway:9 | RIG-I-like receptor signaling pathway:8 | Jak-STAT signaling pathway:9
	Cytokine-cytokine receptor interaction:9 | B cell receptor signaling pathway:5
Cluster 3	Pahtways in cancer:7
Cluster 8	MAPK signaling pathway:6 | Pahtways in cancer:6
Cluster No.	**Enriched Gene Ontology Terms (H9N2)**
Cluster 1	Nucleic acid binding - GO;0003676:68 | Gene expression - GO:0010467:53 | Nitrogen compound metabolic process - GO:0006807:62
	Regulation of macromolecule metabolic process - GO:0060255:58 | Anatomical structure deevelopment - GO:0048856:42
	Negative regulation of biological process - GO;0048519:32 | Macromolecule biosynthetic process - GO:0009059:46
	Intracellular transport - GO:0046907:19 | Cytoskeletal protein binding - GO:0008092:16
Cluster 2	Response to virus - GO:0009615:19 | Multi-organism process - GO:0051704:25 | Response to stimulus - GO:0050896:47
	Immune response - GO:0006955:24 | Defense response - GO:0006952:17 | Nucleic acid binding - GO:0003676:39
	Transition metal ion binding - GO:0046914:33 | Cytokine receptor binding - GO:0005126:8 | RNA binding - GO:0003723:14
	Cell death - GO:0008219:12
Cluster 3	Localization - GO:0051179:23 | Nitrogen compound metabolic process - GO:0006807:24 | Nucleoside binding - GO:0001882:16
	Actin filament binding - GO:0051015:4 | RNA splicing, via transesterification reactions with bulged adenosine as nucleophile - GO:0000377:6
	Cellular component organization - GO:0016043:17 | Enzyme linked receptor protein signaling pathway - GO:0007167:7
Cluster 4	Response to virus - GO:0009615:6 | Immune system process - GO:0002376:10
Cluster 5	RNA processing - GO:0006396:7
Cluster 8	Organ development - GO:0048513:13 | Response to stress - GO:0006950:11
Cluster 9	Response to virus - GO:0009615:4 | Immune system process - GO:0002376:6

Differentially expressed genes were significantly categorized into different GO terms and canonical pathways. Different transcription factors that can potentially be involved in the regulation of gene expressions are shown for each cluster under Expander 5 software analysis (P-value≤0.05). Each functional group, canonical pathway or transcription factor is followed by the number of corresponding genes.

5.3.1.2 Functional groups related to host response

After IAV infections, many host genes with important functions have been found to show differential expression. For example, antiviral genes encoding for cytokines, which are responsible for local inflammatory reactions as well as systemic effects, were induced in their expression after IAV infections in order to impede virus infection [264]; genes relevant to cell death showed gene expression stimulation as a consequence of activation of host cellular defense mechanism to limit the virus spread by removing infected cells [265]; other genes participating in cell regulation also demonstrated their potential ability to alter their regular expression after virus interruption. Accordingly, we investigated expression levels of a batch of key genes so as to evaluate the host-virus interactions after IAV infections.

5.3.1.2.1 Immune response

After IAV infections, the host cells will initiate a series of defense responses to counteract the IAV invasions. In this process, a lot of genes will be activated to play the antiviral roles by the host cells or even inactivated to repress the antiviral response by IAV themselves [266].

In A549 cells, a few important cytokines such as RANTES (CCL5), IL28A and IL29 were detected with elevated expression levels after infections of all eight influenza A strains [Figure 5.15]. Expression levels of other ISGs including MX1, OAS1/2, RASD2, DDX58 (RIG-I), TLR3, IRF-1, IFIT1/2/3, IFI44, GIP2/3, GBP1 were also triggered after IAV infections. Detailed evaluation of these gene expression performances among different influenza A strains infections revealed that these genes showed relatively faint up-regulation in their expression after H1N1 infection. And this phenomenon demonstrated that IFN pathway was triggered in a weak state following H1N1 infection. Moreover, it was noted that H5N2/F118 infection initiated the up-regulated expression of these genes from an early stage (2hpi), indicating a timely initiation of host antiviral actions in H5N2/F118-infected A549 cells.

There also existed other important genes involved in immune defense such as PKR. PKR (EIF2AK2) is a crucial component of the host innate immune system. It has several downstream substrates, and one of them is the eIF2α, phosphorylation of which by activated PKR renders it incapable of

participating in translation initiation, therefore leading to translation arrest and inhibition of protein synthesis from viral mRNAs. Moreover, PKR maybe also associated with the IKKβ subunit of the IKK complex which in turn activate NF-κB [232].

In our study, this gene was up-regulated with faint expression changes after H9N2, H5N2/F189 and H7N1 viruses infections, which might suggest the activation of this gene in these viruses infected host cells. Whereas, PKR showed down-regulated expression with 3.7-FC after H1N1 infection, which might be caused by the action from cellular inhibitor or viral proteins such as NS1 [232, 235]. Through blocking the activation of PKR, the antiviral actions of this factor would be subsequently inhibited.

Excluding these genes with up-regulated expression, there also existed a batch of antiviral genes with down-regulated expression in A549 cells after infections of these influenza A strains, especially H1N1. These host genes with significantly down-regulated expression following H1N1 infection included IFN-α receptor (IFNAR)-1/2, Interferon responsive gene (IFRG)-15, B-cell CLL/lymphoma 10/9-like (BCL10/9L), B-cell translocation gene 1 (BTG1), influenza virus NS1A binding protein (NS1A-BP), GALNAC4S-6ST, SOCS 5/6.

Among these genes, some of them such as IFNAR1/2 and IFRG15 are related to IFN signaling pathway, and their repressed expression after infections of two human viruses, especially H1N1, could lead to the impairment of the IFN signaling transduction as well as further host antiviral function. As reported, BCL10 is essential to gene expression of A20 which is a target of NF-κB, thereby regulating B-cell proliferation mediated by B-cell receptor signaling [267]. And B cells are able to sense these viral antigenic signatures and provide extensive protection against IAV infection [268, 269]. Down-regulated expression of BCL10 in our study indicated the negative control of host cell immune response from H1N1 infection. It has been revealed that NS1A-BP plays a role in mediating the splicing-inhibitory effects of NS1 protein through interacting with NS1 [270]. Hence, the down-regulated expression of NS1A-BP might attenuate the splicing-inhibitory effects of NS1 protein. Members in SOCS family are known to be cytokine-inducible negative regulators of

cytokine signaling, and the potential reason for strongly down-regulated expression of SOCS 5/6 after H1N1 infection still remains to be discovered.

5.3.1.2.2 Cell death

It has been reported that infections of IAV influence the cell death regulation in host cells [271, 272]. Thus we focused on the gene expression performances of genes related to cell death in different influenza A strains infected A549 cells.

At the first glance, H1N1 infection contributed to the relative large number of down-regulated genes while H9N2 and H5N3 infections led to a small number of down-regulated genes [Figure 5.16]. Further investigation showed that caspase 3 and caspase 8 only showed down-regulated expression after H1N1 virus infection, while caspase 9 showed down-regulated expression after H1N1, pH1N1, H5N2/F59 and H5N2/F189 viruses infections. It was found that Fas showed up-regulated expression after H1N1 infection but down-regulated expression after H5N2/F59 infection in A549 cells. Besides, caspase relevant genes such as CFLAR and FADD were identified with a significantly decreasing trend in their expression in A549 cells after infection of two human strains, H1N1 and pH1N1.

It has been reported that XAF1 antagonizes the anticaspase activity of XIAP, which inhibits initiator caspase-9 that is directly involved in the activation of executioner caspase-3 [273]. In our A549 cells, expression of XAF1 was significantly elevated after infections of all influenza A strains except for H1N1, and fold regulation of this gene even reached 242-FC and 244-FC after infections of H9N2 and H5N2/F118, respectively. Accordingly, we assumed that apoptosis signaling might be induced strongly in these influenza A strains (except H1N1) infected A549 cells, particularly in H9N2 and H5N2/F118 infected A549 cells.

TNFSF10 (TRAIL), a cytokine belonging to the TNF ligand family, plays a role in the extrinsic apoptosis pathway. The binding of this protein to its receptors has been shown to trigger the activation of MAPK8/JNK, caspase 8, and caspase 3, and induce apoptosis in further. In our study, expression of this gene showed high up-regulation after H9N2, H5N2/F118, H5N2/F59 and H5N3

viruses infections, indicating the induction of cell apoptosis in these viruses infected A549 cells.

MDM2 and MDM4 were down-regulated with significant expression changes in A549 cells following infection of H1N1, followed by pH1N1 and H5N2/F59. Francoz S (2006) has pointed out that Mdm2 and Mdm4 are critical for the regulation of p53 levels and the fine-tuning of p53 transcriptional activity, separately [274]. However, it was strange that no significant expression change of p53 mRNA was detected, indicating the possibility that other mechanisms might exist to offset the impact on p53 from Mdm2 and Mdm4.

In summary, quite a few genes which are responsible for apoptosis signaling were suppressed in their expression in IAV infected A549 cells. Among all these influenza A strains, H1N1 infection caused the expression suppression of these genes with the highest fold changes while H9N2 and H5N2/F118 infections showed weak ability to reduce expression levels of these genes. It has been proposed that expression levels of genes relevant to cell death were stimulated as a consequence of activation of host cellular defense mechanism to limit the virus spread by removing infected cells [265]. Thus, it was hypothesized that the inhibited expression of these cell apoptosis related genes may be beneficial for virus replication and spread in A549 cells especially after H1N1 infection.

5.3.1.2.3 Genes with remarkable regulations

In addition to genes which are functionally related to immune response or cell death, a batch of host genes also showed interesting expression changes in different influenza A strains infected A549 cells. Some of these genes such as APOL2/6, PTX3, CH25H, ACE2 and CEACAM1 showed up-regulated expression after H9N2 infection [Figure 5.17].

APOL6, a member of the apolipoprotein L gene family, is a pro-apoptotic BH3-only member of the Bcl-2 family. Previous experiments indicated that over-expression of this gene induced the apoptosis of DLD-1 cells characterized by release of cytochrome c and Smac/DIABLO as well as activation of caspase-9. And during the induction of cell apoptosis, APOL6 interacted with lipid/fatty acid components, suggesting its role in connecting lipid second messengers and cell death [275]. Recent studies have also revealed

that human APOL6 is one of the downstream targets of interferon-γ (IFNγ), which sensitizes atherosclerotic lesion-derived cells (LDCs) to Fas-induced apoptosis [276]. This gene showed up-regulated expression in all our influenza A strains infected A549 cells, with the highest fold regulations detected after infections of H9N2, H5N3 and three H5N2 strains. And these observations might suggest the strong induction of apoptosis occurring in these influenza A strains infected A549 cells but the weak induction of apoptosis occurring in other strains infected A549 cells.

Another gene called long pentraxin PTX3 also showed significant up-regulations in its expression after infection of H9N2 but not other influenza A strains. Interestingly, PTX3 is produced in tissues under the control of primary proinflammatory signals, such as IL-1β and TNFα. It has been proved that PTX3 specifically binds to dying cells during inflammatory reactions and clear the apoptotic cells [277]. Recent studies focus on the connections of this gene with IAV infections, and it has been found that PTX3 as a new pattern recognition receptor plays a novel antiviral role in early host defense against influenza infections [278]. Furthermore, through expression a single N-glycosylation sequon, both seasonal and pandemic H1N1 are resistant to the antiviral activities of PTX3 [279]. Accordingly, antiviral function of PTX3 might be indeed resisted by other influenza A strains but not H9N2 in A549 cells.

CH25H, cholesterol 25-hydroxylase, plays a critical role in regulating gene expression, lipid metabolism and immune activation. Previous experiments uncovered that TLR3- and TLR4-induced transcription levels of CH25H relied on the TRIF-mediated production of type I IFNs and required signaling through the IFNR and JAK/STAT1 pathway [280]. Strikingly, this gene was up-regulated with 21.8-FC after H9N2 infection. Since previous observations implied that H9N2 infection induced obvious IFN signaling, elevated expression changes of CH25H might provide more evidence that this gene was indeed functionally associated with IFN pathway. In addition, CH25H has also been proved to be a cholesterol related gene which has an established role in the regulation of cholesterol homeostasis, thus it was assumed that cholesterol regulation might also be involved in the host cell antiviral functions after H9N2 infection in A549 cells [281].

Besides these genes with up-regulated expression, some genes with down-regulated expression were also found out to be specific to H1N1 infection. These genes included MGA, ELL2, GJC1, TMEM177, GIGYF2, GLT8D3, CCDC12 and a group of genes belonging to zinc finger family.

In H1N1 infected A549 cells, the temporal expression trend of the Zinc Finger (ZNF) genes decreased sharply from 6 to 10 hpi as described above, with the most significant down-regulation ≥10-FC detected at the last time point. Our results concurred with that reported in Lee et al., 2010 where ZNF genes were presented with more significant expression changes in primary alveolar epithelial cells infected with a seasonal H1N1 (A/Hong Kong/54/1998) than with pandemic H1N1 (A/Hong Kong/415742/2009) [261]. The same study suggested that the ZNF may have a role in suppressing viral transcription and this may facilitate more efficient replication of seasonal H1N1 in the host cells as compared to pH1N1. Accordingly, down-regulated expression levels of many zinc finger proteins in H1N1 infected A549 cells might indicate good adaption of this influenza A strain in A549 cells. Down-regulated expressions of these ZNF genes were also detected after infections of other influenza A strains such as pH1N1, H5N2/F59, H5N2/F189 and H7N1 with a relative low fold changes, indicating relative weak adaption of these influenza A strains in A549 cells.

MGA as a novel Max-interacting protein is not only able to interact to bHLHZip domain, but also conceive a T-domain DNA-binding motif [282]. Studies indicated that heterodimers formed by Max and other genes MYC and MGA target the genes that are involved in cell cycle progression [283]. Subsequently, down-regulated expression of this gene with 27.3-FC after H1N1 infection might implicate the negative control on the target genes associated with cell cycle.

ELL2 is a member of ELL family of RNA polymerase II elongation factor. Together with ELL, it can increase the catalytic rate of RNA polymerase II transcription on catalyzing the transcription of DNA to synthesize precursors of mRNA and most snRNA and microRNA [284]. In H1N1 infected A549 cells, both ELL2 and its positive regulator EAF1/2 were significantly down-regulated at their expression level, denoting negative influence on transcription activities of RNA polymerase II.

Other genes which are relevant to cell gap junction or adherence junction also showed repressed expression in H1N1 infected A549 cells. Among these factors, GJC1 is a component of gap junctions which are composed of arrays of intercellular channels while CD44 functions as a cell-surface glycoprotein that is involved in cell–cell interactions, cell adhesion and migration.

5.3.1.3 Regulations of gene expression in canonical pathways

According to recent researches, regulations of some cellular signaling pathways are altered following IAV infection: JAK-STAT pathway, NF-kB/IKK pathway, MAPKs signaling pathway, PI3K/Akt pathway and so on. These pathways involved in the host antiviral response are important for viral entry, viral replication, viral propagation and apoptosis. IAV manipulates the molecular function of signaling molecules for efficient viral pathogenesis [285].

Probe ID	GeneBank	Gene Title
205263_at	AF082283	B-cell CLL/lymphoma 10
1557258_a_at	AA994334	B-cell CLL/lymphoma 10
1557257_at	AA994334	B-cell CLL/lymphoma 10
227616_at	BG481877	B-cell CLL/lymphoma 9-like
228065_at	AL353962	B-cell CLL/lymphoma 9-like
200921_s_at	NM_001731	B-cell translocation gene 1, anti-proliferative
243509_at	AI475680	B-cell translocation gene 1, anti-proliferative
200920_s_at	AL535380	B-cell translocation gene 1, anti-proliferative
1405_i_at	M21121	chemokine (C-C motif) ligand 5
1555759_a_at	AF043341	chemokine (C-C motif) ligand 5
204655_at	NM_002985	chemokine (C-C motif) ligand 5
214038_at	AI984980	chemokine (C-C motif) ligand 8
204533_at	NM_001565	chemokine (C-X-C motif) ligand 10
210163_at	AF030514	chemokine (C-X-C motif) ligand 11
211122_s_at	AF002985	chemokine (C-X-C motif) ligand 11
209774_x_at	M57731	chemokine (C-X-C motif) ligand 2
207850_at	NM_002090	chemokine (C-X-C motif) ligand 3
203915_at	NM_002416	chemokine (C-X-C motif) ligand 9
218943_s_at	NM_014314	DEAD (Asp-Glu-Ala-Asp) box polypeptide 58
242961_x_at	AI304317	DEAD (Asp-Glu-Ala-Asp) box polypeptide 58
222793_at	AK023661	DEAD (Asp-Glu-Ala-Asp) box polypeptide 58
213294_at	AV755522	eukaryotic translation initiation factor 2-alpha kinase 2
205483_s_at	NM_005101	interferon, alpha-inducible protein (clone IFI-15K)
205483_s_at	NM_005101	interferon, alpha-inducible protein (clone IFI-15K)
204415_at	NM_022873	interferon, alpha-inducible protein (clone IFI-6-16)
204415_at	NM_022873	interferon, alpha-inducible protein (clone IFI-6-16)
203066_at	NM_014863	B cell RAG associated protein
208693_s_at	D30658	glycyl-tRNA synthetase
227321_at	D52585	opposite strand transcription unit to STAG3
231577_s_at	AW014593	guanylate binding protein 1, interferon-inducible, 67kDa
202269_x_at	BC002666	guanylate binding protein 1, interferon-inducible, 67kDa
202270_at	NM_002053	guanylate binding protein 1, interferon-inducible, 67kDa
242907_at	BF509371	guanylate binding protein 2, interferon-inducible
235574_at	AW392952	guanylate binding protein 4
235175_at	BG260886	guanylate binding protein 4
206332_s_at	NM_005531	interferon, gamma-inducible protein 16
208965_s_at	BG256677	interferon, gamma-inducible protein 16
208966_x_at	AF208043	interferon, gamma-inducible protein 16
202411_at	NM_005532	interferon, alpha-inducible protein 27
202411_at	NM_005532	interferon, alpha-inducible protein 27
201422_at	NM_006332	interferon, gamma-inducible protein 30
209417_s_at	BC001356	interferon-induced protein 35
214453_s_at	NM_006417	interferon-induced protein 44
214059_at	BE049439	Interferon-induced protein 44
204439_at	NM_006820	interferon-induced protein 44-like
1555464_at	BC046208	interferon induced with helicase C domain 1
219209_at	NM_022168	interferon induced with helicase C domain 1
216020_at	AL080107	Interferon induced with helicase C domain 1
203153_at	NM_001548	interferon-induced protein with tetratricopeptide repeats 1
217502_at	BE888744	interferon-induced protein with tetratricopeptide repeats 2
226757_at	AA131041	interferon-induced protein with tetratricopeptide repeats 2
204747_at	NM_001549	interferon-induced protein with tetratricopeptide repeats 3

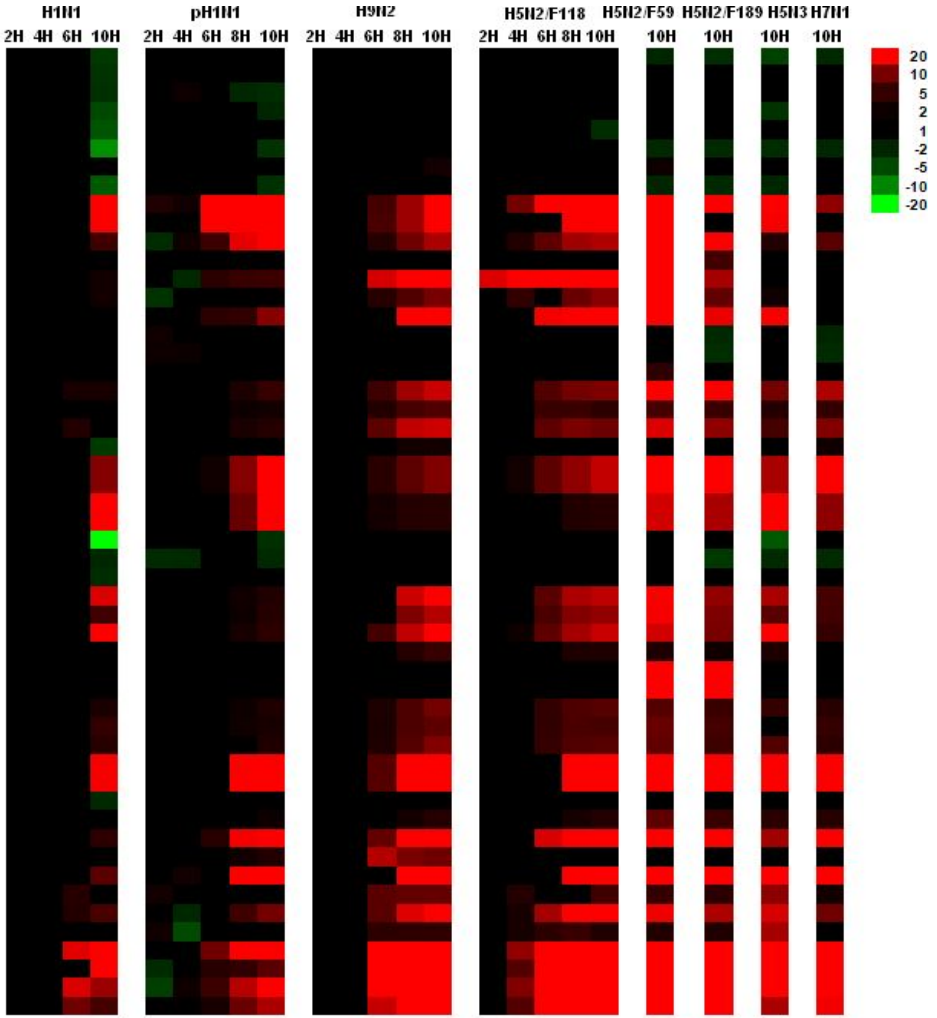

Probe ID	GeneBank	Gene Title
229450_at	AI075407	interferon-induced protein with tetratricopeptide repeats 3
203595_s_at	N47725	interferon-induced protein with tetratricopeptide repeats 5
203596_s_at	NM_012420	interferon-induced protein with tetratricopeptide repeats 5
201601_x_at	NM_003641	interferon induced transmembrane protein 1 (9-27)
214022_s_at	AA749101	interferon induced transmembrane protein 1 (9-27)
208375_at	NM_024013	interferon, alpha 1
207964_x_at	NM_021068	interferon, alpha 4
225661_at	AA811138	interferon (alpha, beta and omega) receptor 1
225669_at	AA133989	interferon (alpha, beta and omega) receptor 1
204786_s_at	L41944	interferon (alpha, beta and omega) receptor 2
227125_at	BF526978	Interferon (alpha, beta and omega) receptor 2
208173_at	NM_002176	interferon, beta 1, fibroblast
202727_s_at	NM_000416	interferon gamma receptor 1
211676_s_at	AF056979	interferon gamma receptor 1
201642_at	NM_005534	interferon gamma receptor 2 (interferon gamma transducer 1)
230241_at	BF196874	Interferon responsive gene 15
219684_at	NM_022147	28kD interferon responsive protein
1552915_at	NM_172138	interleukin 28A (interferon, lambda 2)
1552609_s_at	NM_172139	interleukin 28A (interferon, lambda 2)
1552917_at	NM_172140	interleukin 29 (interferon, lambda 1)
205207_at	NM_000600	interleukin 6 (interferon, beta 2)
226333_at	AV700030	interleukin 6 receptor
205945_at	NM_000565	interleukin 6 receptor
204863_s_at	BE856546	interleukin 6 signal transducer (gp130, oncostatin M receptor)
204864_s_at	NM_002184	interleukin 6 signal transducer (gp130, oncostatin M receptor)
212195_at	AL049265	Interleukin 6 signal transducer (gp130, oncostatin M receptor)
212196_at	AW242916	Interleukin 6 signal transducer (gp130, oncostatin M receptor)
202531_at	NM_002198	interferon regulatory factor 1
203275_at	NM_002199	interferon regulatory factor 2
208436_s_at	NM_004030	interferon regulatory factor 7
204698_at	NM_002201	interferon stimulated exonuclease gene 20kDa
33304_at	U88964	interferon stimulated exonuclease gene 20kDa
219361_s_at	NM_022767	interferon stimulated exonuclease gene 20kDa-like 1
212766_s_at	AW294587	interferon stimulated exonuclease gene 20kDa-like 2
208114_s_at	NM_030980	interferon stimulated exonuclease gene 20kDa-like 2
203882_at	NM_006084	interferon-stimulated transcription factor 3, gamma 48kDa
201362_at	AF205218	influenza virus NS1A binding protein
206245_s_at	NM_006469	influenza virus NS1A binding protein
244235_at	AW273860	influenza virus NS1A binding protein
201363_s_at	AB020657	influenza virus NS1A binding protein
216565_x_at	AL121994	similar to Interferon-induced transmembrane protein 3
202086_at	NM_002462	myxovirus (influenza virus) resistance 1
202086_at	NM_242863	myxovirus (influenza virus) resistance 1
204994_at	NM_002463	myxovirus (influenza virus) resistance 2 (mouse)
209239_at	M55643	nuclear factor of kappa light polypeptide gene enhancer in B-cells 1
207535_s_at	NM_002502	nuclear factor of kappa light polypeptide gene enhancer in B-cells 2
202869_at	NM_016816	2',5'-oligoadenylate synthetase 1, 40/46kDa
205552_s_at	NM_002534	2',5'-oligoadenylate synthetase 1, 40/46kDa
204972_at	NM_016817	2'-5'-oligoadenylate synthetase 2, 69/71kDa
206553_at	NM_002535	2'-5'-oligoadenylate synthetase 2, 69/71kDa
228607_at	AI651594	2'-5'-oligoadenylate synthetase 2, 69/71kDa
218400_at	NM_006187	2'-5'-oligoadenylate synthetase 3, 100kDa
232666_at	R13458	2'-5'-oligoadenylate synthetase 3, 100kDa
205660_at	NM_003733	2'-5'-oligoadenylate synthetase-like
210797_s_at	AF063612	2'-5'-oligoadenylate synthetase-like

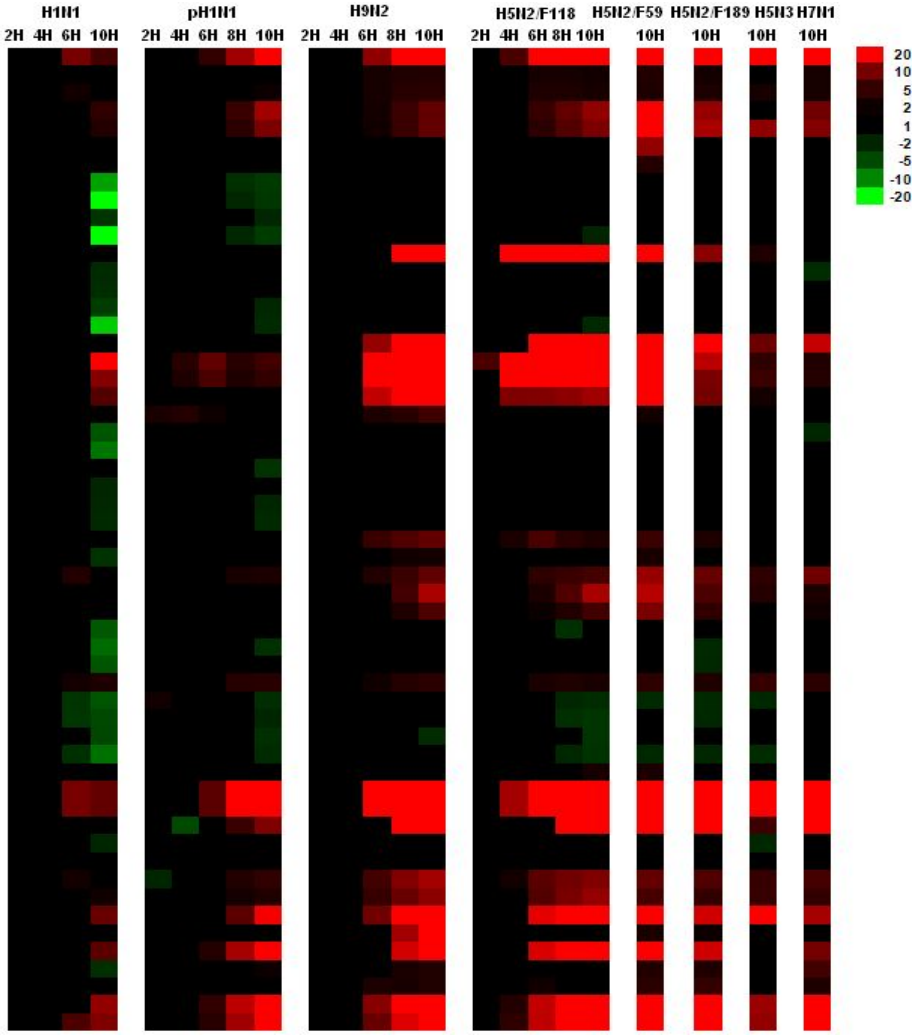

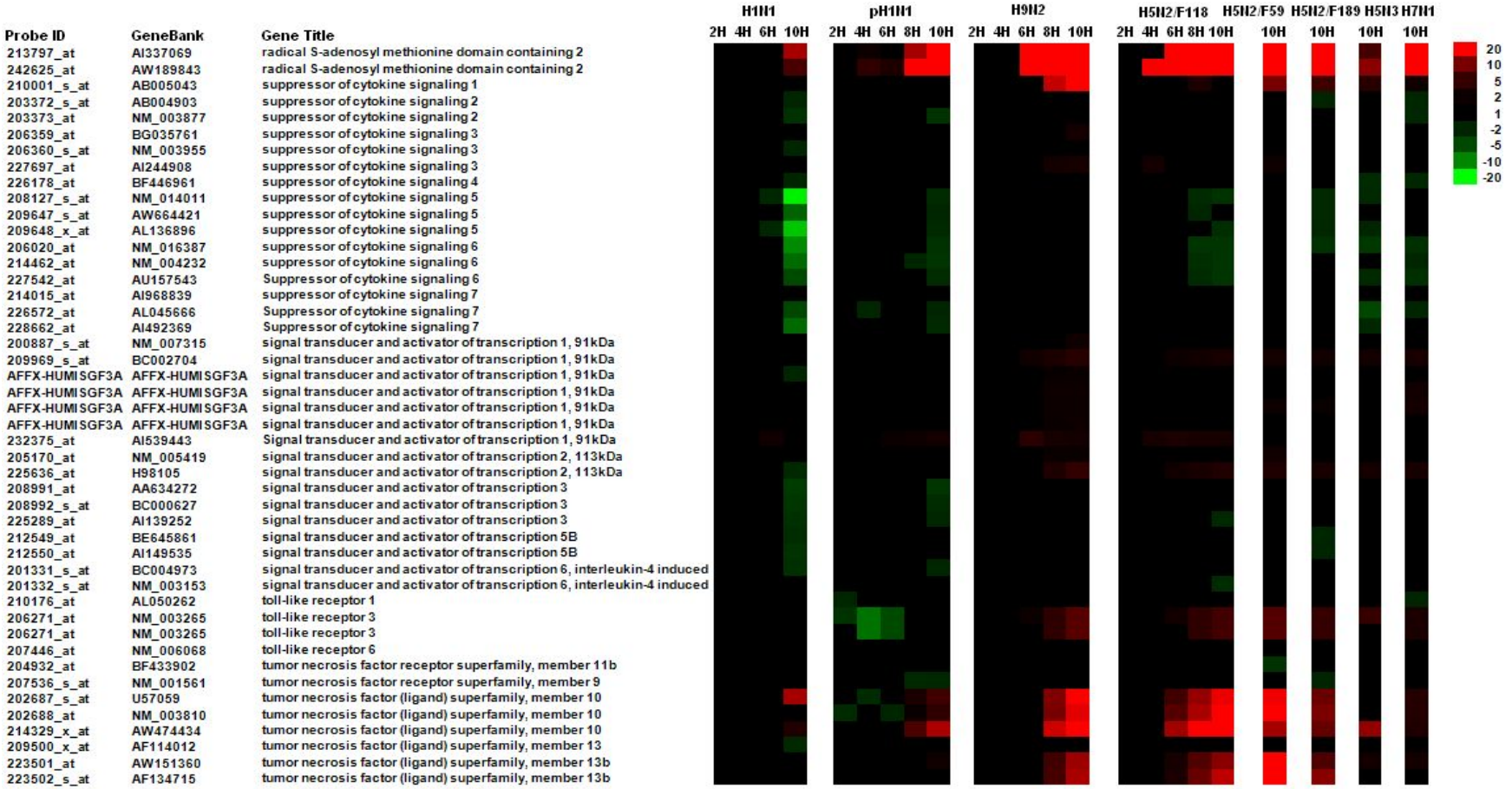

Probe ID	GeneBank	Gene Title
213797_at	AI337069	radical S-adenosyl methionine domain containing 2
242625_at	AW189843	radical S-adenosyl methionine domain containing 2
210001_s_at	AB005043	suppressor of cytokine signaling 1
203372_s_at	AB004903	suppressor of cytokine signaling 2
203373_at	NM_003877	suppressor of cytokine signaling 2
206359_at	BG035761	suppressor of cytokine signaling 3
206360_s_at	NM_003955	suppressor of cytokine signaling 3
227697_at	AI244908	suppressor of cytokine signaling 3
226178_at	BF446961	suppressor of cytokine signaling 4
208127_s_at	NM_014011	suppressor of cytokine signaling 5
209647_s_at	AW664421	suppressor of cytokine signaling 5
209648_x_at	AL136896	suppressor of cytokine signaling 5
206020_at	NM_016387	suppressor of cytokine signaling 6
214462_at	NM_004232	suppressor of cytokine signaling 6
227542_at	AU157543	Suppressor of cytokine signaling 6
214015_at	AI968839	suppressor of cytokine signaling 7
226572_at	AL045666	Suppressor of cytokine signaling 7
228662_at	AI492369	Suppressor of cytokine signaling 7
200887_s_at	NM_007315	signal transducer and activator of transcription 1, 91kDa
209969_s_at	BC002704	signal transducer and activator of transcription 1, 91kDa
AFFX-HUMISGF3A	AFFX-HUMISGF3A	signal transducer and activator of transcription 1, 91kDa
AFFX-HUMISGF3A	AFFX-HUMISGF3A	signal transducer and activator of transcription 1, 91kDa
AFFX-HUMISGF3A	AFFX-HUMISGF3A	signal transducer and activator of transcription 1, 91kDa
AFFX-HUMISGF3A	AFFX-HUMISGF3A	signal transducer and activator of transcription 1, 91kDa
232375_at	AI539443	Signal transducer and activator of transcription 1, 91kDa
205170_at	NM_005419	signal transducer and activator of transcription 2, 113kDa
225636_at	H98105	signal transducer and activator of transcription 2, 113kDa
208991_at	AA634272	signal transducer and activator of transcription 3
208992_s_at	BC000627	signal transducer and activator of transcription 3
225289_at	AI139252	signal transducer and activator of transcription 3
212549_at	BE645861	signal transducer and activator of transcription 5B
212550_at	AI149535	signal transducer and activator of transcription 5B
201331_s_at	BC004973	signal transducer and activator of transcription 6, interleukin-4 induced
201332_s_at	NM_003153	signal transducer and activator of transcription 6, interleukin-4 induced
210176_at	AL050262	toll-like receptor 1
206271_at	NM_003265	toll-like receptor 3
206271_at	NM_003265	toll-like receptor 3
207446_at	NM_006068	toll-like receptor 6
204932_at	BF433902	tumor necrosis factor receptor superfamily, member 11b
207536_s_at	NM_001561	tumor necrosis factor receptor superfamily, member 9
202687_s_at	U57059	tumor necrosis factor (ligand) superfamily, member 10
202688_at	NM_003810	tumor necrosis factor (ligand) superfamily, member 10
214329_x_at	AW474434	tumor necrosis factor (ligand) superfamily, member 10
209500_x_at	AF114012	tumor necrosis factor (ligand) superfamily, member 13
223501_at	AW151360	tumor necrosis factor (ligand) superfamily, member 13b
223502_s_at	AF134715	tumor necrosis factor (ligand) superfamily, member 13b

Figure 5.15 Expression of probe sets involved in immune response in influenza A viruses-infected A549 cells. Eight influenza A strains were infected with different examined cells, and the expression of probe sets related to immune response was examined by microarray analysis at different time points as shown. The data is represented by heat map analysis showing up-regulated (red), down-regulated (green) or no changes (black) in expression, and the FC range is indicated (P-value≤0.05).

Probe ID	GeneBank	Gene Title
203685_at	NM_000633	B-cell CLL/lymphoma 2
207005_s_at	NM_000657	B-cell CLL/lymphoma 2
207004_at	NM_000657	B-cell CLL/lymphoma 2
206133_at	AI43782	XIAP associated factor-1
228617_at	CO439482	XIAP associated factor-1
242234_at	GI439853	XIAP associated factor-1
211366_x_at	U13698	caspase 1, apoptosis-related cysteine peptidase
206011_at	AI719655	caspase 1, apoptosis-related cysteine peptidase
211367_s_at	U13699	caspase 1, apoptosis-related cysteine peptidase
209970_x_at	M87507	caspase 1, apoptosis-related cysteine peptidase
211368_s_at	U13700	caspase 1, apoptosis-related cysteine peptidase
1552703_s_at	NM_052889	caspase 1, apoptosis-related cysteine peptidase
205467_at	NM_001230	caspase 10, apoptosis-related cysteine peptidase
209811_at	BC002427	caspase 2, apoptosis-related cysteine peptidase
208050_s_at	NM_001224	caspase 2, apoptosis-related cysteine peptidase
34449_at	U13022	caspase 2, apoptosis-related cysteine peptidase
226032_at	AU153405	caspase 2, apoptosis-related cysteine peptidase
202763_at	NM_004346	caspase 3, apoptosis-related cysteine peptidase
209310_s_at	U25804	caspase 4, apoptosis-related cysteine peptidase
211464_x_at	U20537	caspase 6, apoptosis-related cysteine peptidase
209790_s_at	BC000305	caspase 6, apoptosis-related cysteine peptidase
207181_s_at	NM_001227	caspase 7, apoptosis-related cysteine peptidase
207686_s_at	NM_001228	caspase 8, apoptosis-related cysteine peptidase
213373_s_at	BF439983	caspase 8, apoptosis-related cysteine peptidase
222201_s_at	AB037736	CASP8 associated protein 2
210775_x_at	AB015653	caspase 9, apoptosis-related cysteine peptidase
203984_s_at	U60521	caspase 9, apoptosis-related cysteine peptidase
208485_x_at	NM_003879	CASP8 and FADD-like apoptosis regulator
209939_x_at	AF005775	CASP8 and FADD-like apoptosis regulator
210564_x_at	AF009619	CASP8 and FADD-like apoptosis regulator
211316_x_at	AF009616	CASP8 and FADD-like apoptosis regulator
211317_s_at	AF041461	CASP8 and FADD-like apoptosis regulator
211862_x_at	AF015451	CASP8 and FADD-like apoptosis regulator
210563_x_at	U97075	CASP8 and FADD-like apoptosis regulator
202535_at	NM_003824	Fas (TNFRSF6)-associated via death domain
239749_at	AW205090	Fas (TNFRSF6) associated factor 1
218080_x_at	NM_007051	Fas (TNFRSF6) associated factor 1
203618_at	AB023167	Fas apoptotic inhibitory molecule 2
204780_s_at	AA164751	Fas (TNF receptor superfamily, member 6)
216252_x_at	Z70519	Fas (TNF receptor superfamily, member 6)
215719_x_at	X83493	Fas (TNF receptor superfamily, member 6)
204781_s_at	NM_000043	Fas (TNF receptor superfamily, member 6)
235092_at	AI919519	Cytokine induced apoptosis inhibitor 1
239834_at	AW874669	Cytokine induced apoptosis inhibitor 1
205386_s_at	NM_002392	Mdm2, transformed 3T3 cell double minute 2, p53 binding protein
229711_s_at	AA902480	Mdm2, transformed 3T3 cell double minute 2, p53 binding protein
236814_at	AA745971	Mdm4, transformed 3T3 cell double minute 2, p53 binding protein

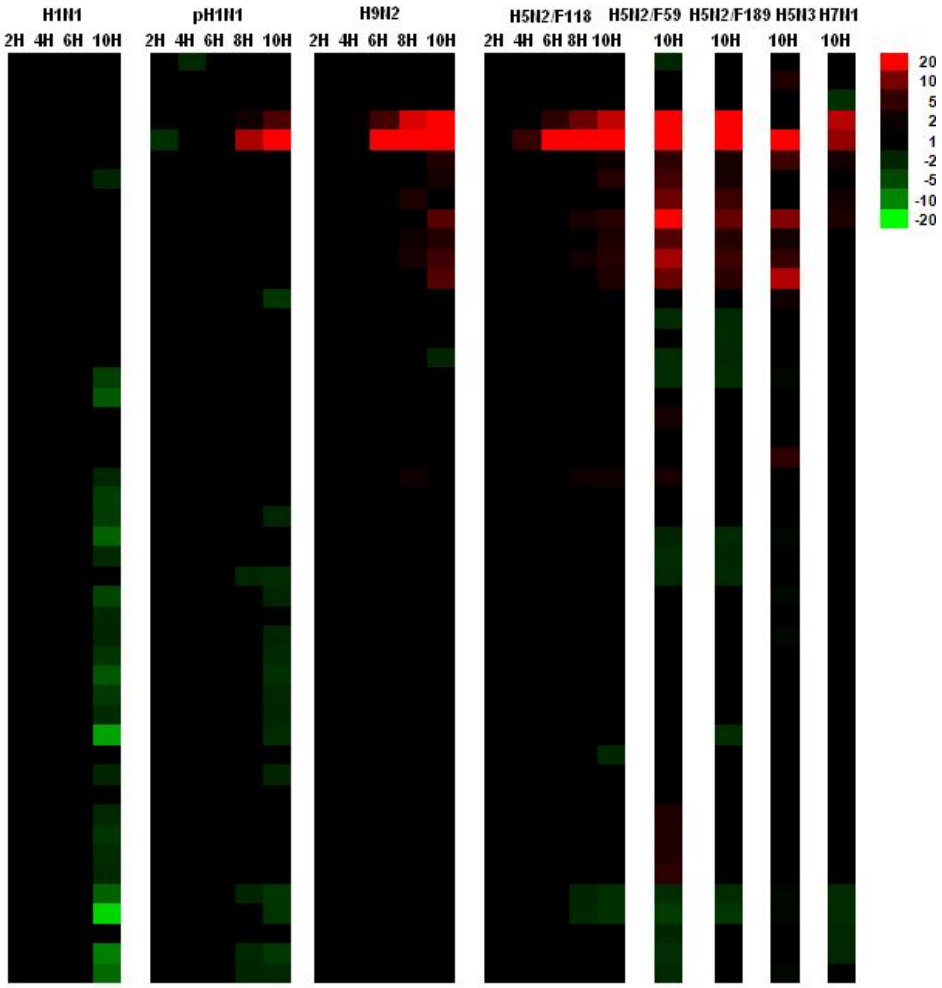

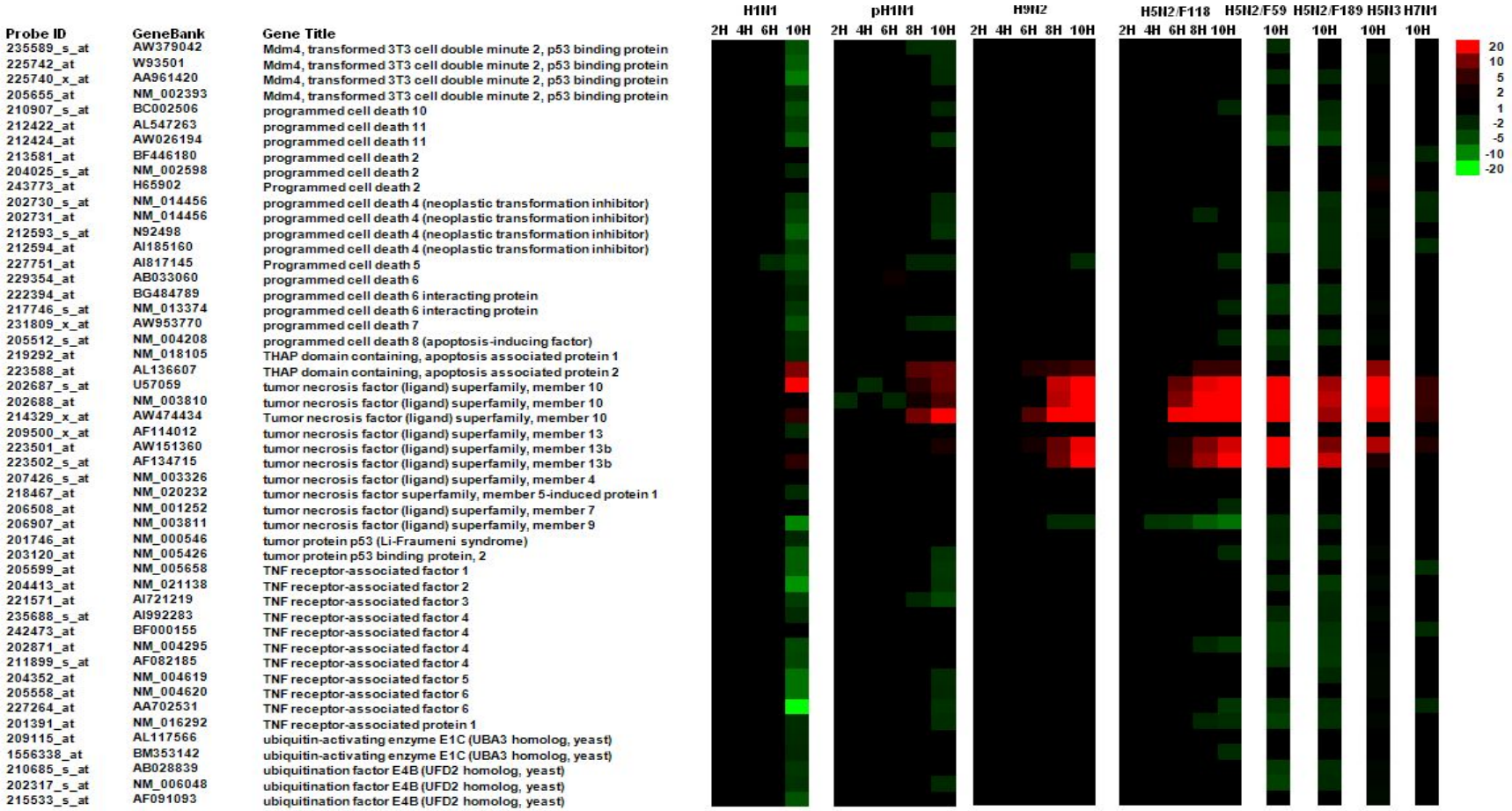

Figure 5.16 Expression of probe sets involved in cell death in influenza A viruses-infected A549 cells. Eight influenza A strains were infected with different examined cells, and the expression of probe sets related to cell death was examined by microarray analysis at different time points as shown. The data is represented by heat map analysis showing up-regulated (red), down-regulated (green) or no changes (black) in expression, and the FC range is indicated ($p \leq 0.05$).

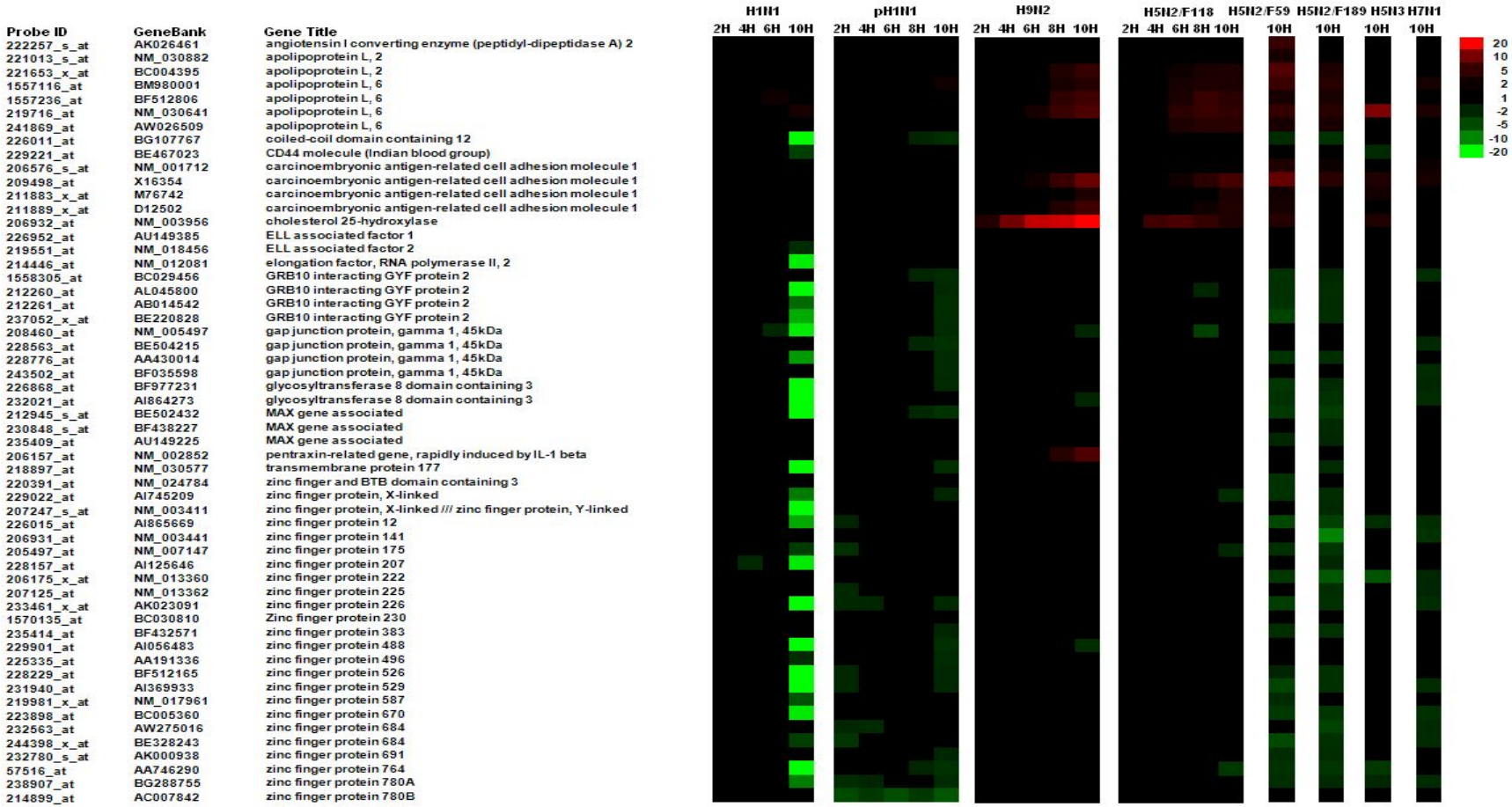

Figure 5.17 The probe sets with topmost expression changes in influenza A viruses-infected A549 cells. Eight influenza A strains were infected with different examined cells, and the global host gene expression was examined by microarray analysis at different time points. The probe sets with topmost expression changes were listed. The data is represented by heat map analysis showing up-regulated (red), down-regulated (green) or no changes (black) in expression, and the FC range is indicated ($p \leq 0.05$).

5.3.1.3.1 Interferon signaling pathway

At the early stage of IAV infection, IFN signaling pathway, especially type I, is activated. After that, signals will be transferred into the corresponding receptors, and multiple cytokines inside the nucleus will be triggered. On this basis, a series of immune responses will be initiated to reject the virus invasion [226].

Different gene expression profiles in different influenza A strains infected A549 cells revealed that IFN type I signaling was obviously triggered after infections of all avian viruses. And among the avian viruses infections, different gene expression patterns were detected in the pathway. For example, expression of IFNα/β and a few downstream genes were initiated at 4 hpi after H5N2/F118 infection but initiated at 6 hpi after H9N2 infection. So it was concluded that H5N2/F118 infection initiated the TNF type I pathway as well as following immune reactions at an earlier stage when compared to H9N2 infection.

Expression of IFNα/β in IFN type I signaling transduction were repressed around 8 hpi, and expression of a series of downstream molecules were subsequently repressed after infections of two human viruses, particularly H1N1. The comparison of gene expression in this pathway between infections of two human viruses showed that IFNAR1/2 were down-regulated with a more prominent fold change after H1N1 infection, and expression of STAT1 and STAT2 were only down-regulated in H1N1 infected A549 cells. These observations indicated that interferon signaling pathway was inhibited to a more significant extent after H1N1 infection than pH1N1 infection.

Mechanism of controlling IFN type I mediated antiviral response has become a hot study topic these years, and researchers have found competitive interactions between virus and receptors like RIG-I to repress the IFN type I pathway [259]. In our study, specific influenza A strains such as H1N1 and pH1N1 might indeed evolve some new mechanisms to limit the production of IFNα/β and STAT1/2 from an early stage at the transcriptional level.

5.3.1.3.2 NF-κB activation by viruses

Nuclear Factor-κB pathway plays a vital role in mediating inflammation, immune response, proliferation and apoptosis. Based on its key role, influenza

virus has evolved strategies to direct antiviral NF-κB activity into an IFN-suppressive and apoptosis-promoting function. During productive virus infection, NF-κB regulates expression of a number of genes, including the antiviral cytokine IFNβ, the proapoptotic factors TRAIL, Fas and FasL and the suppressor of cytokine signaling SOCS-3. While IFNβ primarily exerts antiviral functions by inducing an innate antiviral gene expression program, the simultaneous vRNA-induced expression of SOCS-3 limits this response. Furthermore, TRAIL and FasL induce caspase activation, and active caspases allow an enhanced release of vRNP complexes from the nucleus [Figure 5.18] [23].

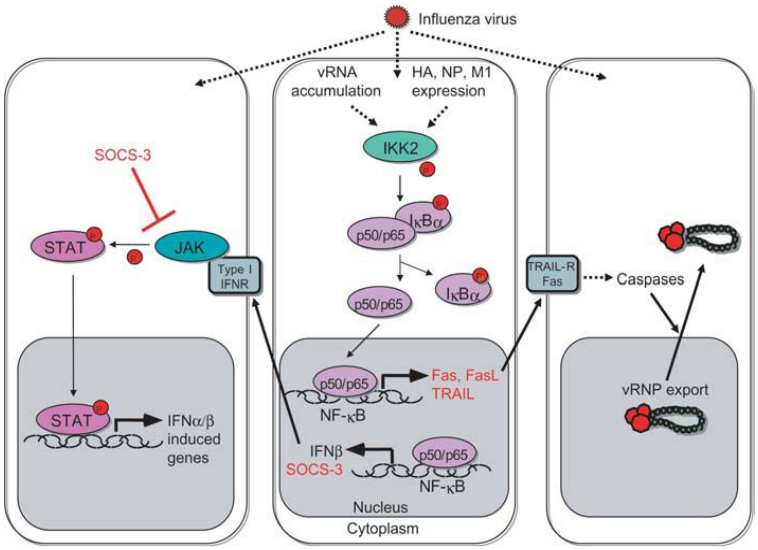

Figure 5.18 Two virus supportive functions of the IKK/NF-κB signaling module in influenza virus infected cells (adapted Ludwig S *et al*., 2008)[23].

Observation of NF-κB pathway in H1N1 and pH1N1 infected A549 cells illustrated that majority of genes participating in this pathway showed down-regulated expression from 8 to 10 hpi. Through shutting down this pathway, migration of NF-κB into nucleus would diminish, subsequently relevant antiviral and anti-apoptotic activities mediated by this pathway were all inactivated.

In contrary to infections of H1N1 and pH1N1, no gene was found differentially down-regulated obviously at its expression level in H9N2 infected A549 cells. In this case, host cells were able to activate this pathway normally and relevant functions were induced to fight with H9N2 invasion. As to A549 cells infected with other influenza A strains, part of the genes showed down-

regulated expression while others did not show any significant expression change.

5.3.1.3.3 Role of MAPK signaling in pathogenesis in influenza

MAPK cascades are involved in the conversation of various extracellular signals into cellular responses as diverse as immune response, cell death and proliferation. Nowadays, studies have proved that this pathway plays important roles in proinflammatory during IAV infection [286, 287].

Till now, studies show that IAV infection activates all these 4 members of MAPK family in order to promote vRNP traffic and virus production. P38 MAPK activation regulates the expression of RANTES production and chemokines after IAV infection [288]. Experiments showed that p38 was able to induce TNF cytokine in H5N1-infected cells. Besides, inhibition of p38 decreased the virus titer, which suggested that IAV infection induced TNF in a p38-dependent manner and p38 MAPK activation was essential for virus replication. Similar to p38, JNK is also associated with the expression of RANTES. Ludwig S *et al* (2001) have observed that stimulation of AP1-dependent gene expression strongly correlated with activation of JNK, which maybe contributed by viral RNA accumulation during replication [289]. Block of JNK signaling of the cascade resulted in not only inhibition of virus-induced JNK activation but also repression of AP-1 activity as well as impairing transactivation of IFNβ promoter, thereby increasing virus products. Consequently, it is concluded that IAV induced activation of JNK and AP-1 is part of the innate antiviral response. As to Raf/MEK/ERK pathway, Pleschka S *et al* (2001) did experiments to show that cells infected with IAV led to up-regulate this signaling pathway [290]. Inhibition of this pathway can cause the impairment of the virus growth and decreasing of the RNP nucleus export, however, it will not influence the viral RNA and protein synthesis. Additionally, ERK ½ and ERK are vital for the expression of pro-inflammatory like IL1β, IL-6, TNF-α, etc. Recent experiment found that HA accumulation in the membrane and its tight association with lipid-raft domains triggered activation of the MAPK cascade and induced RNP export, which proved again that Raf/MEK/ERK pathway was tight related to IAV replication [291].

Through investigating the details of this pathway in different influenza A strains infected A549 cells, we found that caspase 3 was strongly down-regulated at its expression level after H1N1 infection so that the caspase 3 mediated cell death could be attenuated.

Although expressions of JNK or even MKK 4/7 were down-regulated following infections of viruses excluding H9N2, RANTES and IP10 showed up-regulated expression after infections of most of the influenza A strains. Among them, H5N2/F118 infection triggered their expression elevation from 2 hpi while H9N2 infection initiated their expression elevation from 6 hpi. Although RANTES was up-regulated with 3.4-FC in its expression at 2 hpi, expression levels of RANTES and IP10 were apparently inhibited around 4 hpi and then induced again from 6 hpi after pH1N1 infection. And H1N1 infection contributed to the remarkable up-regulation of these two chemokines in their expression around 10 hpi. It has been reported by Qu B *et al* (2012) that RANTES and IP10 might be the crucial contributors to pro-inflammatory responses in H9N2-infected intestinal epithelia [292]. Thus, significant and early up-regulation of RANTES and IP-10 at their expression level in H5N2/F118 infected A549 cells might implicate strong and timely pro-inflammatory responses triggered by these two genes.

5.3.1.3.4 Role of PI3K/Akt signaling in pathogenesis in influenza virus

PI3K and its downstream effector Akt/protein kinase B (PKB) have been identified as IAV induced signaling mediators recently, and full activation of Akt/PKB requires phosphorylation at Thr308 and Ser473 [8]. PI3K/Akt pathway plays different functions on IAV infection. Initially, Lu X *et al* (2011) found that PI3K/Akt pathway was involved in CXCL-10 promoter activity upon IAV infection [293] and Chiou WF *et al* (2011) mentioned that IRF3 and NF-κB might also involve in this procedure [294]. Furthermore, experiments suggested that block of PI3K/Akt activation lead to a reduction in virus yield [295] and PI3K/Akt pathway is induced by NS1 protein to support effective IAV replication and propagation [296]. Besides, PI3K is also activated by RIG-I to be essential for complete IRF-3 activation and consequent induction of the type I interferon response [297].

In our study, the expression inhibition of PI3K p110 resulted in the suppression of GSK3β and Caspase 9 at their transcriptional level in A549 cells infected with H1N1, pH1N1, H5N2/F59 and H5N2/F189. These observations indicated that the antiviral role of PI3K might be inhibited and this apopsotis signaling might be impaired in these viruses infected A549 cells.

5.3.1.3.5 Role of Wnt/GSK-3β signaling in pathogenesis in influenza virus

WNT family members increase IFN production in IAV-infected cells. Genes in this pathway globally showed in a inhibited status at their expression level in A549 cells after infections of all influenza A strains except H5N3 and H9N2. However, down-regulated expression of IFN was only detected after H1N1 and pH1N1 infections. In this situation, gene expression levels in IFN signaling pathway do not always correlate with gene expression levels in Wnt/GSK-3β pathway, indicating that other mechanisms might also contribute to IFN production.

Shapira SD *et al* (2009) have observed that viral proteins interact with NF-κB, apoptosis and WNT pathways primarily through NS1 and also through two viral polymerase subunits PB1 and PB2 [298]. On the basis of this observation, the inhibitory gene expression in the Wnt/GSK-3β might be due to the negative interactions from these influenza proteins.

5.3.1.3.6 Cell cycle: G1/S and G2/M checkpoints regulation

The cell cycle consists of four distinct phases. During G1 phase (growth phase), various enzymes that are mainly required for DNA replication in S phase are synthesized at a marked rate. Next, the cell continues to grow and significant biosynthesis occurs in G2 phase, and the production of microtubules is mainly involved in this phase. During final M phase, cell growth stops and the cell is division into two daughter cells. The duration of the phases of the cell cycle is variable in different cell lines. For a typical rapidly proliferating human cell with a total cycle time of 24 hours, M phases is about 1 hour; G1 is about 11 hours; S phase is completed within 8 hours; and G2 is about 4 hours.

The cell cycle progression is accomplished by a series of control points. A major regulatory point which occurs late in G1 and controls progression from G1 to S is called G1/S checkpoint. This G1/S checkpoint stall the cell cycle

until repairs are made or target the cell for destruction via apoptosis in the case that the repairs cannot be made. The other G2/M checkpoint senses un-replicated DNA, which generates a signal to stall the cell cycle and therefore prevents the initiation of M phase before completion of S phase [299].

The increased expression of cyclin D allows its interaction with CDK4/6 by competing with CDK inhibitor 16 for binding, and thereby overcomes checkpoint G1/S. Once the active CDK4/6-cyclin D complexes form, they phosphorylate Rb, which relieves the inhibition of the transcription factor E2F. E2F is then able to induce cyclin E expression, and cyclin E interacts with CDK2 to allow for G1-S phase transition.

The CDKs that are associated with checkpoint G2/M are activated by phosphorylation of the CDK by the action of a Mitosis Promoting Factor (MPF), which is related to cyclin B-Cdc2 kinase complex. The molecular nature of this checkpoint involves Cdc25, which under favorable conditions removes the inhibitory phosphates present within the MPF complex.

Observation from A549 global host gene profiles showed that quite a lot of genes involved in the G1/S and G2/M checkpoint regulation showed down-regulated expression after H1N1, pH1N1, H5N2/F59 and H5N2/F189 viruses infections. On the contrary, few genes showed down-regulated expression after H9N2 infection. For G1/S checkpoint regulation pathway, it seems that all key factors such as cyclin D, CDK4/6, phosphate-Rb, cyclin E, CDK2 except E2F were down-regulated at their expression level and the whole network was shut down at 10 hpi in H1N1-infected A549 at 10 hpi. Infections of pH1N1, H5N2/F59 and H5N2/F189 also caused expression suppression of most genes. In the contrary, none of them has significant expression change in H9N2-infected A549 cells. According to previous knowledge, shutting down of this pathway in H1N1, pH1N1, H5N2/F59 and H5N2/F189-infected A549 cells might result in the arrest of cell cycle in G1 stage.

When it comes to the G2/M DNA damage checkpoint regulation, key molecules such as cyclin B, Cdc2, Cdc25 all showed down-regulated expression at mRNA level in H1N1, pH1N1, H5N2/F59 and H5N2/F189-infected A549 cells. However, none of them has significant expression change in H9N2-infected A549 cells.

Other researchers also did a series of experiments to uncover the cell cycle regulation after IAV infection. In the experiments, A549 cells were infected with A/WS/33 and then assayed for expression of cellular proteins at 8hpi, 12hpi and 24 hpi, using corresponding antibodies. Experimental results revealed that key molecules mentioned above including cyclin E, cyclin D, phosphorylated Rb were down-regulated at the protein level and cell cycle analysis by flow cytometry displayed that the percentage of cells in G1 phase of the cell cycle is much higher in IAV infected cells than the normal percentage in MOCK cells. Consequently, it is concluded that IAV replication induces cell cycle arrest in G0/G1 phase [300]. When compared to our microarray data which detected at mRNA level, cyclin E, cyclin D, phosphorylated Rb were also down-regulated in our H1N1 infected A549 cell, which was absolutely consistent with previous experiments. The only difference was the expression change of p21, which was tested with up-regulated expression by He Y *et al* (2010) but showed down-regulated expression in our A549 cells after H1N1 infection. Anyway, this finding roughly supported our assumption that cell cycle were arrest in our H1N1 virus infected A549 cell to some extent.

5.3.2 Host gene expression in CEF cells

5.3.2.1 Global profiling of gene expression

5.3.2.1.1 Heat maps of global gene expression

In influenza A strains infected with CEF cells, the numbers of differentially expressed probe sets increased with the infection time increasing following infections of all H1N1, H9N2 and H5N2/F118 viruses. And the largest number of probe sets with up-regulated expression and the lowest number of probe sets with down-regulated expression were both detected after H1N1 infection at 10 hpi [Figure 5.19]. It was interesting that infection of H5N2/F118 triggered an earlier expression repression of some probe sets in their expression compared to other two strains.

5.3.2.1.2 Distribution of differentially expressed probe sets

In CEF cells, infections of H1N1, H9N2 and H5N2/F118 induced high portions of genes with up-regulated expression [Table 5.6]. However, portions of up-regulated probe sets were low after infections of other influenza A viruses,

especially H7N1. In addition, infections of H5N2/F118 and H5N2/F189 caused more probe sets with down-regulated expression than infections of other influenza A strains in CEF cells. Among the three H5N2 strains, H5N2/F118 infection resulted in the highest portion of probe sets with either up- or down-regulated expression.

Table 5.6 Differentially expressed probe sets in CEF cells infected with influenza A viruses at 10 hpi.

CEF	Probe sets (>=2 fold)		Probe sets (>=3 fold)		Probe sets (>=5 fold)		Probe sets (>=10 fold)	
	Up-regulated	Down-regulated	Up-regulated	Down-regulated	Up-regulated	Down-regulated	Up-regulated	Down-regulated
H1N1	1.47%	6.89%	0.98%	1.54%	0.55%	0.44%	0.33%	0.04%
H5N2/F59	0.49%	6.92%	0.37%	1.15%	0.25%	0.10%	0.21%	0.01%
H5N2/F118	1.46%	22.82%	0.94%	10.27%	0.51%	2.06%	0.14%	0.27%
H5N2/F189	0.43%	18.47%	0.26%	1.79%	0.17%	0.16%	0.09%	0.02%
H5N3	0.89%	10.45%	0.58%	2.52%	0.33%	0.55%	0.18%	0.04%
H7N1	0.28%	10.18%	0.10%	1.71%	0.05%	0.12%	0.05%	0.03%
H9N2	1.23%	12.85%	0.73%	3.09%	0.29%	0.86%	0.12%	0.13%

The global host gene expression profiles were retrieved from microarray analysis with different time points examined. The ratios of differentially expressed probe sets (P-value≤0.05) up- or down-regulated with different fold changes (≥2-FC, ≥3-FC, ≥5-FC and ≥10-FC) in relative to their corresponding "expressing probe sets" are represented in percentage. The expressing probe sets refer to probe sets detected in the mock-infected corresponding cells.

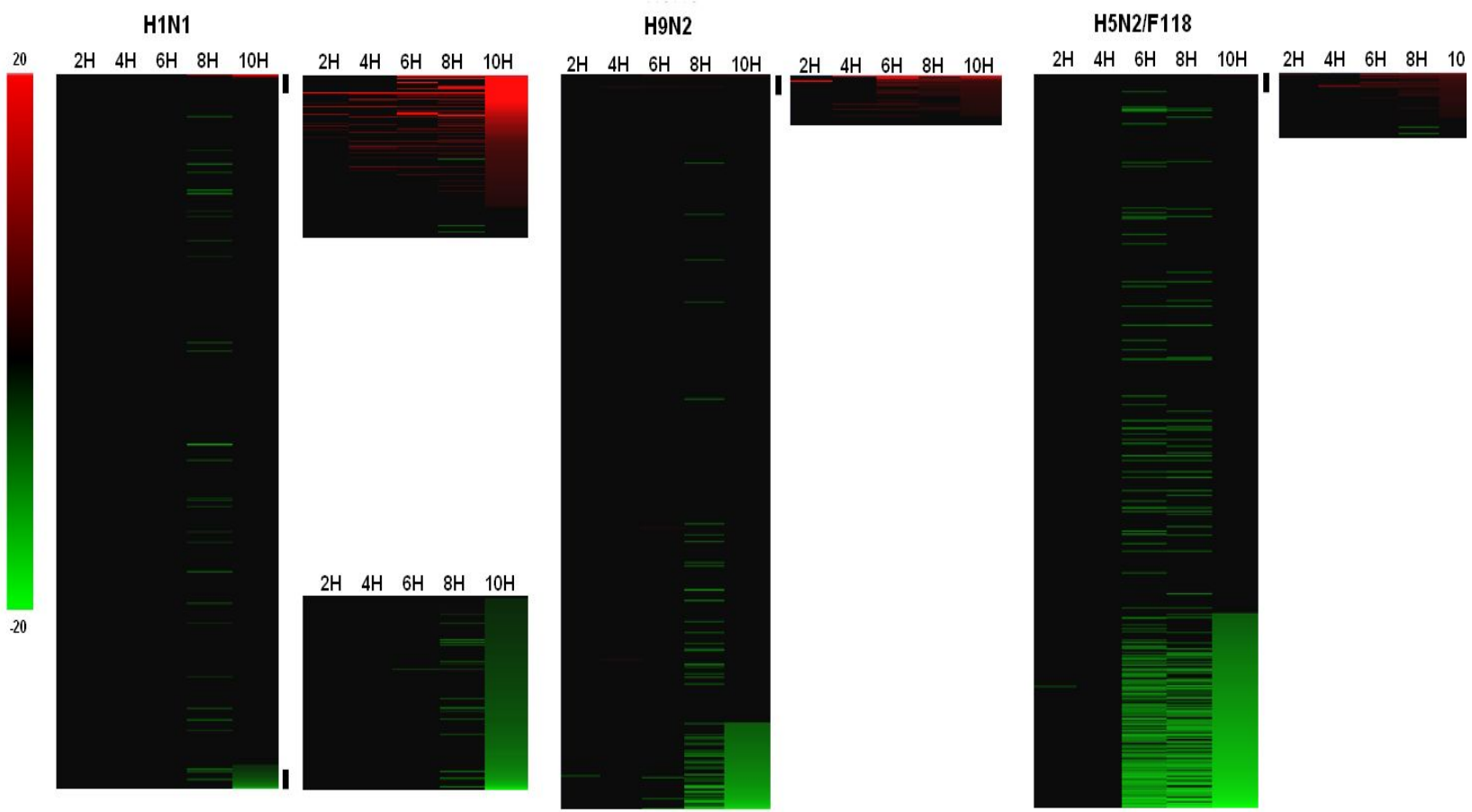

Figure 5.19 Temporal changes in the host cell transcriptome in CEF cells infected by four influenza virus strains. The global host gene expression profiles were retrieved from microarray analysis with different time points examined. The probe sets showing ≥2 fold change (FC) up- or down-regulated in expression are indicated (P-value≤0.05). Expression profiles of up-regulated (red), down-regulated (green) and no significant change (black) are shown.

5.3.2.1.3 Functional classification

Excluding the "Un-annotated" and "Un-classified" probe sets, the remaining probe sets with up-regulated expression were majorly associated with "Immune Response", "RNA Binding", "DNA Binding" and "Transcription Factor" [Figure 5.20]. In contrast with H1N1 infected A549 cells, H1N1 infected CEF cells showed stronger immune response than other influenza A strains infected CEF cells. Besides, infections of H5N2/F59, H5N3 and H9N2 also led to relative big numbers of immune response associated probe sets with up-regulated expression. When the cutoff was raised to 10-FC, some of the probe sets still showed significant up-regulation in their expression after infections of H1N1, H5N2/F59 and H5N3, especially H1N1. In summary, the host immune response was strongly activated in H1N1, H5N2/F59 and H5N3-infected CEF cells when compared to other strains infected CEF cells.

The largest number of probe sets with down-regulated expression was detected in CEF cells after infection of H5N2/F118, and some of these probe sets showed high fold regulation with ≥5-FC. Among them, a big batch of these probe sets played roles in "RNA Binding" and "DNA Binding". Compared to H5N2/F118, infections of another two H5N2 subtype strains, H5N2/F59 and H5N2/F189, only inhibited the expression of hundreds of probe sets, and the corresponding fold changes majorly located between 2-FC and 3-FC. The high percentages of differentially expressed probe sets belonging to 'Un-annotated' and "Un-classified" is majorly due to the incomplete annotation for probe sets in Chicken Genome.

5.3.2.1.4 Cluster analysis

Before clustering analysis, comparison of these three groups of data suggested that the numbers of probe sets with up-regulated expression were low and similar among three influenza A strains. However, the numbers of those with down-regulated expression were high but different among these three strains, with H5N2/F118 infection contributing to largest number of down-regulated probe sets. In the cluster analysis process, the probe sets with differential expression after H1N1, H5N2/F118 and H9N2 infections were separated into two groups to do cluster analysis so as to better separate the probe sets into different clusters

As described, the number of up-regulated probe sets was much lower than the number of down-regulated ones, particularly in H5N2/F118 and H9N2 infected CEF cells, therefore those up-regulated probe sets weren't capable to be picked out in these two groups of data. Although those probe sets showing up-regulated expression at 10 hpi after H5N2/F118 or H9N2 infection were clustered into additional groups, functional annotation of which indicated that no gene ontology term was able to be significantly enriched. In H1N1 infected CEF cells, probe sets with up-regulated expression were able to be clustered into Cluster I-11, with only a function group called "NAD + ADP - ribosyltransferase activity" significantly enriched in only 4 genes [Figure 5.21] [Table 5.7].

Another Cluster II-6 generated from H1N1 infected CEF cells showed interesting trend in that the expression of probe sets dropped first, followed by a suddenly increase at 6 hpi and another decrease at 8 hpi. Gene ontology terms including "lipid localization" and "cytokine activity" were significantly enriched in genes belonging to this cluster. Accordingly, immune response and cell membrane activities may be triggered around 6 hpi first however repressed at later infection stage after H1N1 infection.

A batch of functional groups identified in down-regulated genes were common to three influenza A strains infections in CEF cells. These groups included "nucleotide binding", "protein binding" and "cellular metabolic process".

Besides these GO terms, functional groups such as "metal ion binding", "localization", "ATP binding", "response to stress" and "helicase activity" were significantly enriched in genes with down-regulated expression after two avian strains infections [Figure 5.22] [Table 5.8].

A function named "regulation of cell-substrate adhesion" was significantly enriched in Cluster I-5 after H9N2 infection. Expression trend of this cluster fell down from 2 hpi to 4hpi, and then there was a sudden increase occurred from 4 hpi and another decrease occurred from 6 hpi. Expression levels of these probe sets were fluctuated, and it was hypothesized that some special cell regulation might happen to count for the short gene expression stimulation in the middle of the examined infection period.

Infection of H5N2/F118 led to most genes with down-regulated expression in CEF cells. Subsequently, much more functional groups such as "post-translational protein modification", "hydrolase activity", "organ development", "Zinc ion binding", "cell cycle", "ligase activity", "cellular localization", "transferase activity", "phosphorylation" and "transmembrane receptor protein kinase activity" were enriched in these down-regulated genes [Figure 5.23] [Table 5.9]. Inhibitory expression of these genes participating in different and important biological functions suggested that a lot of host cell activities were impaired due to the H5N2/F118 invasion. And impairment of normal expression of these key molecules during H5N2/F118 infection might be a solution evolved by the H5N2/F118 virus that aimed to create a beneficial environment for its survival and replication.

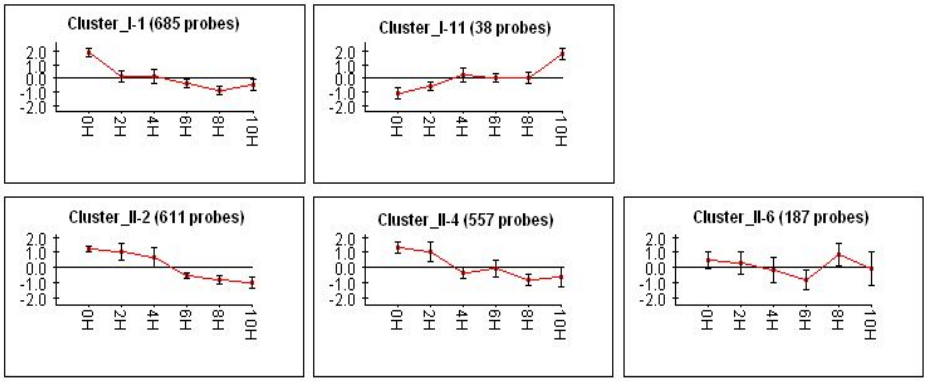

Figure 5.21 Clustering analysis of temporal gene expression profiles in H1N1-infected CEF cells. CEF cells were infected with H1N1 at 2, 4, 6, 8 and 10 hpi. Probe sets showing ≥2-fold changes up- or down-regulated (P-value≤0.05) at least over one time point were analyzed with Expander 5 software. X-axis represents post-infection in hours (H), and Y-axis means normalized expression changes of probe sets.

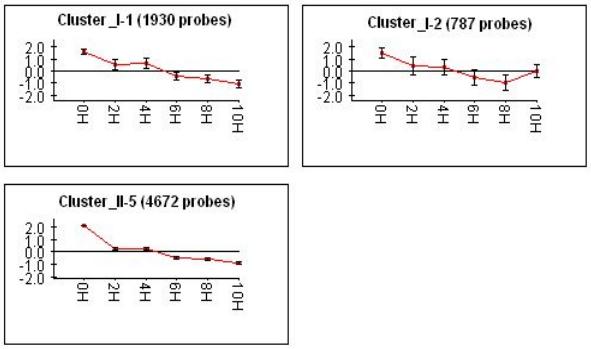

Figure 5.22 Clustering analysis of temporal gene expression profiles in H5N2/F118-infected CEF cells. CEF cells were infected with H5N2/F118 at 2, 4, 6, 8 and 10 hpi. Probe sets showing ≥2-fold changes up- or down-regulated (P-value≤0.05) at least over one time point were analyzed with Expander 5 software. X-axis represents post-infection in hours (H), and Y-axis means normalized expression changes of probe sets.

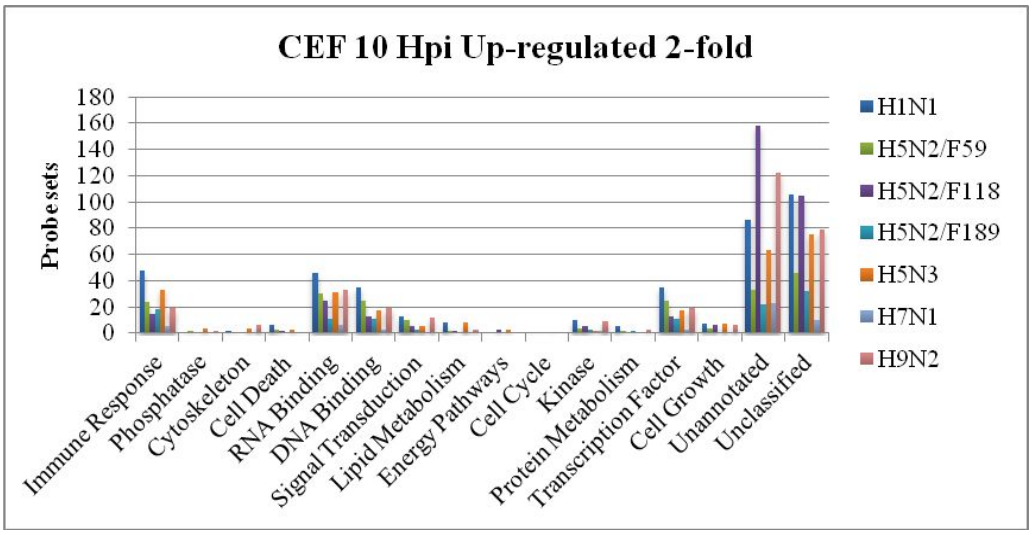
CEF 10 Hpi Up-regulated 2-fold
Probe sets
180
160
140
120
100
80
60
40
20
0
H1N1
H5N2/F59
H5N2/F118
H5N2/F189
H5N3
H7N1
H9N2
Immune Response
Phosphatase
Cytoskeleton
Cell Death
RNA Binding
DNA Binding
Signal Transduction
Lipid Metabolism
Energy Pathways
Cell Cycle
Kinase
Protein Metabolism
Transcription Factor
Cell Growth
Unannotated
Unclassified

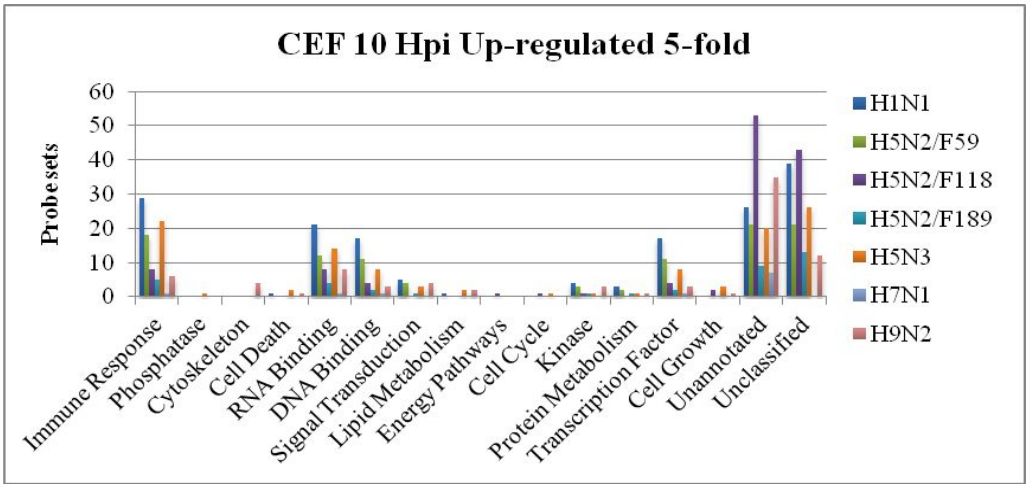
CEF 10 Hpi Up-regulated 5-fold
Probe sets
60
50
40
30
20
10
0
H1N1
H5N2/F59
H5N2/F118
H5N2/F189
H5N3
H7N1
H9N2
Immune Response
Phosphatase
Cytoskeleton
Cell Death
RNA Binding
DNA Binding
Signal Transduction
Lipid Metabolism
Energy Pathways
Cell Cycle
Kinase
Protein Metabolism
Transcription Factor
Cell Growth
Unannotated
Unclassified

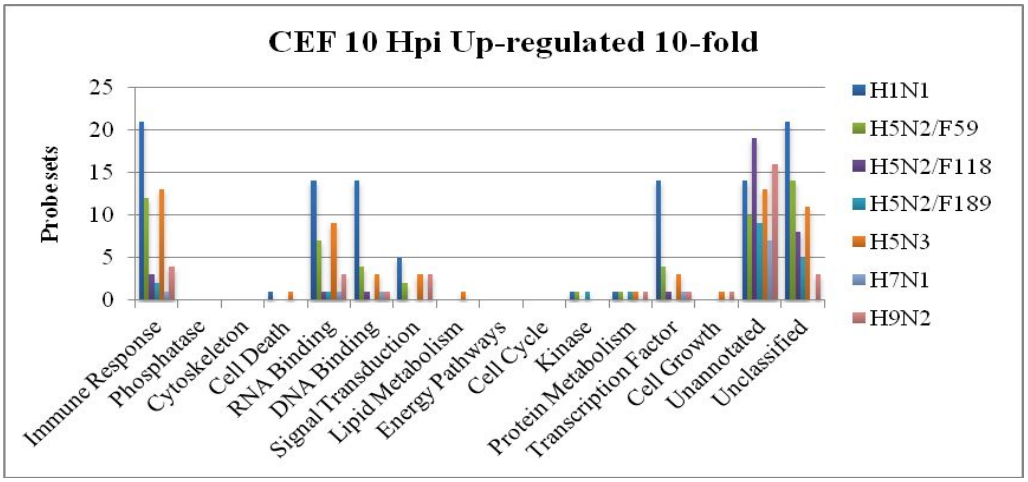
CEF 10 Hpi Up-regulated 10-fold
Probe sets
25
20
15
10
5
0
H1N1
H5N2/F59
H5N2/F118
H5N2/F189
H5N3
H7N1
H9N2
Immune Response
Phosphatase
Cytoskeleton
Cell Death
RNA Binding
DNA Binding
Signal Transduction
Lipid Metabolism
Energy Pathways
Cell Cycle
Kinase
Protein Metabolism
Transcription Factor
Cell Growth
Unannotated
Unclassified

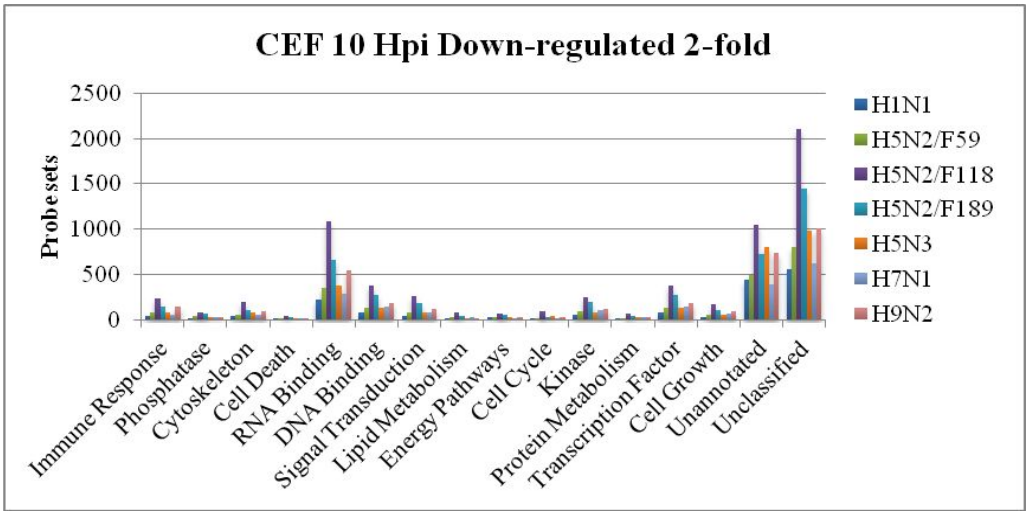

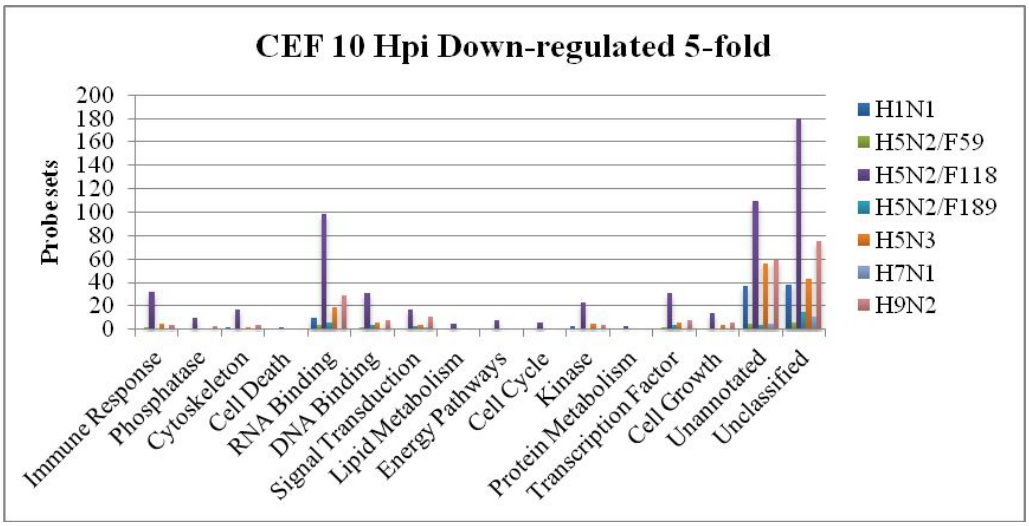

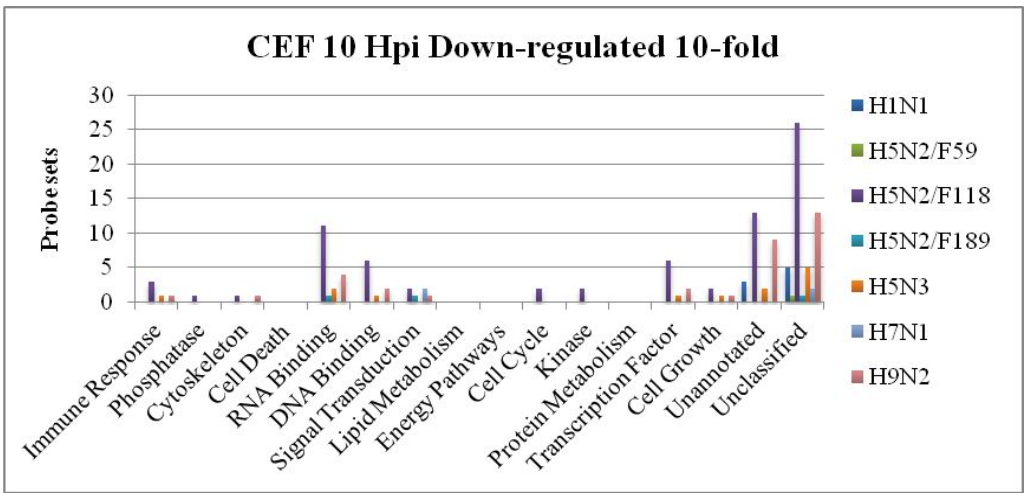

Figure 5.20 Overview of distributions of differentially expressed probe sets into different biological functions in CEF cells infected with influenza A viruses. The numbers of probe sets in the different functional families, including non-annotated and unclassified groups, showing up- or down-regulated with different fold changes (≥2-FC, ≥5-FC and ≥10-FC) in gene expression are presented.

Table 5.7 Summary of functional groups enriched based on differentially expressed genes in CEF cells infected with H1N1.

Cluster No.	Enriched Gene Ontology Terms (CEF H1N1)
Cluster I-1	purine ribonucleotide binding - GO:0032555:51
Cluster I-11*	NAD + ADP-ribosyltransferase activity - GO:0003950:4
Cluster II-2	nucleotide binding - GO:0000166:64 | protein binding - GO:0005515:100 | cellular metabolic process - GO:0044237:81
Cluster II-4	primary metabolic process - GO:0044238:82 | RNA binding - GO:0003723:17 | cellular metabolic process - GO:0044237:74
Cluster II-6	lipid localization - GO:0010876:5 | cytokine activity - GO:0005125:5

Differentially expressed genes were significantly categorized into different GO terms under Expander 5 software analysis (P-value≤0.05). Each functional group is followed by the number of corresponding genes. * represents the up-regulated trend of the corresponding cluster.

Table 5.8 Summary of functional groups enriched based on differentially expressed genes in CEF cells infected with H5N2/F118.

Cluster No.	Enriched Gene Ontology Terms (CEF H5N2/F118)
Cluster I-1	ATP binding - GO:0005524:121 | protein binding - GO:0005515:267 | regulation of signal transduction - GO:0009966:45
	phosphate metabolic process - GO:0006796:69 | nucleoside-triphosphatase activity - GO:0017111:57 | protein kinase activity - GO:0004672:52
	cellular component organization - GO:0016043:71 | post-translational protein modification - GO:0043687:71 | hydrolase activity - GO:0016787:127
	guanyl-nucleotide exchange factor activity - GO:0005085:19 | regulation of small GTPase mediated signal transduction - GO:0051056:26
	regulation of biological process - GO:0050789:232 | organ development - GO:0048513:62 | helicase activity - GO:0004386:20
	anatomical structure morphogenesis - GO:0009653:45 | cation binding - GO:0043169:162 | tissue morphogenesis - GO:0048729:17
	transmembrane receptor protein kinase activity - GO:0019199:16 | regulation of Rho protein signal transduction - GO:0035023:13
	nucleic acid binding - GO:0003676:139 | zinc ion binding - GO:0008270:98 | chordate embryomic development - GO:0043009:24
Cluster I-2	cation binding - GO:0043169:80
Cluster II-5	protein binding - GO:0005515:619 | nucleotide binding - GO:0000166:360 | nucleoside binding - GO:0001882:276 | metabolic process - GO:0008152:660
	macromolecule metabolic process - GO:0043170:448 | cellular metabolic process - GO:0044237:506 | primary metabolic process - GO:0044238:543
	cellular macromolecular metabolic process - GO:0044260:385 | nucleobase, nucleoside, nucleotide and nucleic acid metabolic process - GO:0006139:194
	nitrogen compound metbolic process - GO:0006807:222 | RNA metabolic process - GO:0016070:86 | nucleic acid binding - GO:0003676:336
	transition metal ion binding - GO:0046914:273 | cation binding - GO:0043169:374 | macromolecule localization - GO:0033036:94
	cellular component organization - GO:0016043:152 | hydrolase activity - GO:0016787:281 | cell cycle - GO:0007049:53 | ligase activity - GO:0016874:59
	ncRNA metabolic process - GO:134660:38 | cellular localization - GO:0051641:76 | nucleoside-triphosphatase activity - GO:0017111:109
	catabolic process - GO:0009056:143 | biosynthetic process - GO:0009085:184 | gene expression - GO:0010467:103 | mitotic cell cycle - GO:0000278:26
	cellular catabolic proces - GO:0044248:82 | transferase activity - GO:0016740:216 | celllar response to stress - GO:0033554:49
	response to DNA damige stimulus - GO:0006974:44 | helicase activity - GO:0004386:35 | ATPase activity, coupled - GO:0042623:50
	phosphorylation - GO:0016310:112 | vesicle-mediated transport - GO:0016192:47 | cellular macromolecule catabolic process - GO:0044265:60
	modification-dependent macromolecule catabolic process - GO:0043632:42

Differentially expressed genes were significantly categorized into different GO terms under Expander 5 software analysis (P-value≤0.05). Each functional group is followed by the number of corresponding genes.

Table 5.9 Summary of functional groups enriched based on differentially expressed genes in CEF cells infected with H9N2.

Cluster No.	Enriched Gene Ontology Terms (CEF H9N2)
Cluster I-1	ATP binding - GO:0005524:54 | protein binding - GO:0005515:107 | helicase activity - GO:0004386:14 | ATPase activity - GO:0016887:11
	nucleoside-triphosphatase activity - GO:0017111:29 | organ morphogenesis - GO:0009887:20 | tube development - GO:0035295:11
	cellular macromolecule metabolic process - GO:0044260:65 | regulation of signal transduction - GO:0009966:21 | angiogenesis - GO:0009966:21
	biopolymer metabolic process - GO:0043283:69
Cluster I-2	cellular macromolecule metabolic process - GO:0044260:46 | centrosome organization - GO:0051297:4
Cluster I-5	regulation of cell-substrate adhesion- GO:0010810:5
Cluster II-1	protein binding - GO:0005515:180 | adenyl ribonucleotide binding - GO:0032559:8 | multicellular organismal process - GO:0032501:76
	metal ion binding - GO:0046872:104 | developmental process - GO:0032501:68 | transition metal ion binding - GO:0046914:90
	extracellular matrix structure constituent - GO:0005201:8 | nucleic acid binding - GO:0003676:104 | localization - GO:0051179:89
Cluster II-3	protein binding - GO:0005515:87 | response to stress - GO:0006950:23 | ATP binding - GO:0005524:39 | developmental process - GO:0032502:34

Differentially expressed genes were significantly categorized into different GO terms under Expander 5 software analysis (P-value≤0.05). Each functional group is followed by the number of corresponding genes.

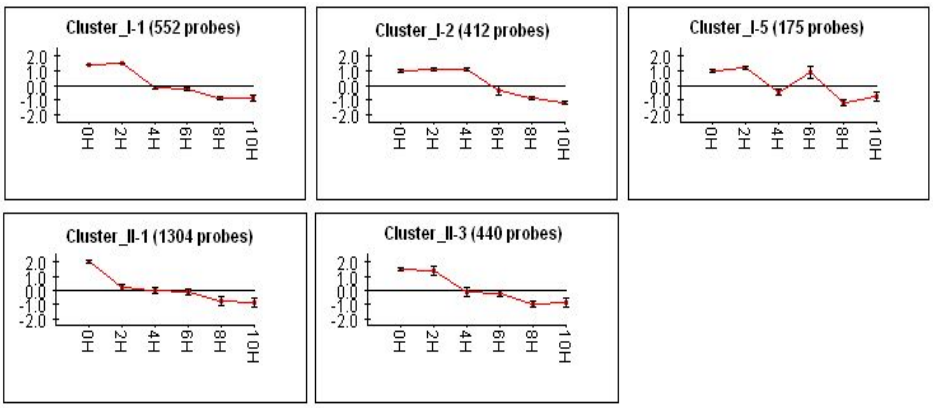

Figure 5.23 Clustering analysis of temporal gene expression profiles in H9N2-infected CEF cells. CEF cells were infected with H9N2 at 2, 4, 6, 8 and 10 hpi. Probe sets showing ≥2-fold changes up- or down-regulated (P-value≤0.05) at least over one time point were analyzed with Expander 5 software. X-axis represents post-infection in hours (H), and Y-axis means normalized expression changes of probe sets.

5.3.2.2 Functional groups related to host response

5.3.2.2.1 Immune response

In CEF cells, a batch of IFN related genes including IFIH1, IFIT-5, IRF1/7, TLR3, IFI35, STAT4, MX and OASL showed strong elevation at their expression level after infections of H1N1, H9N2, H5N2/F59, H5N2/189 and H5N3 [Figure 5.24]. Altered expression of these genes with high-level fold changes indicated that CEF cells strongly initiated a series of immune reactions in response to the invasion of these influenza A strains. Furthermore, data derived from infections of H1N1 and H9N2 also demonstrated that these genes were activated from a very early infection phase (around 2 or 4 hpi), indicating the timely inflammatory response in these infected CEF cells.

Although there were not so many genes with quite significant expression changes detected in H5N2/F118-infected CEF cells, some key factors such as IFIT-5, OASL, IFIH and IRF7 were identified with up-regulated expression, with the most significant fold changes identified at 4 hpi. This observation might imply that some mechanism was triggered to attenuate antiviral actions after 4hpi in H5N2/F118 infected CEF cells.

Besides these genes with up-regulated expression, infection of H5N2/F118 also resulted in many genes with down-regulated expression in CEF cells. Under investigation, these genes generally showed significant down-regulation at their expression level from 6hpi, which was consistent with the

decreasing expression trend of up-regulated genes from 6 hpi mentioned previously.

5.3.2.2.2 Cell death

A group of programmed cell death genes, PDCD 2/4/5/6/7/8/10/11, all showed down-regulated expression in H1N1, H5N2/F59, H5N2/F189-infected CEF cells. Whereas, only some of them identified in pH1N1 and H7N1 infected-CEF cells showed down-regulated expression and few identified in H9N2, H5N2/F118 and H5N3-infected CEF cells showed down-regulated expression [Figure 5.25].

In H5N2/F118-infected CEF cells, many apoptosis-related genes were down-regulated in their expression from an early time points (6 hpi). Besides these genes with early down-regulated expression, Fas, TNFSF10 and caspase 6/9 showed differentially down-regulated expression in H5N2/F118 infected CEF cells at late infection stage.

Another two factors that are associated with p53 are USP7 and AMID. USP7, known as ubiquitin carboxyl-terminal hydrolase 7, direct antagonizes Mdm2 to protect p53 from Mdm2-mediated degradation [301]. And AMID (PRG3) was reported to be a p53-downstream gene involved in tumorigenesis by Wu M *et al* (2004) [302]. In H5N2/F118-infected CEF cells, both these two genes showed down-regulated expression. Accordingly, it was assumed that p53 might be inactivated to some extent even if expression of p53 showed no differential change in our H5N2/F118-infected CEF cells. In addition, infections of H1N1 and H5N2/F59 led to the lowest number of apoptosis related genes with down-regulated expression in CEF cells.

5.3.2.2.3 Genes with remarkable regulations

In CEF cells, some genes with key functions including ZC3HAV1, IPO7, GPR151, GNG13 and ZNFX1 showed up-regulated expression [Figure 5.26]. ZC3HAV1 (ZAP/PAPR13) that encodes a CCCH-type zinc finger protein was commonly up-regulated in several influenza A strains infected A549 cells, with the most significant expression change 30.2-FC detected after H1N1 infection. Previously researchers have reported that this interferon-stimulated gene restricted the replication of retroviruses, alphaviruses, and

filoviruses, and viral induction of it occurred under the direct control of IRF3 [303]. When it came to our study in CEF cells, no significant expression change of IRF3 could be detected, but expression of IRF1 and IRF7 showed in a consistent pattern with ZC3HAV1. This phenomenon might be caused by diverse controlling in different viruses, and it was assumed that IAV might evolve alternative control pathway dependent of IRF1/7, taking the place of IRF3.

Zaitseva L *et al* (2009) uncovered that IPO7 (IMP7) facilitated nuclear trafficking of DNA and HIV-1 exploited IMP7 to maximize nuclear import of its DNA genome [304]. Besides, other groups also mentioned that IMP might play an impact on HIV-1's replication performance [305]. Although there is no concrete evidence proving that this protein is involved in IAV's nuclear import activity, the obvious up-regulated expression of this gene from 4 to 10 hpi in H5N2/F118-infected CEF cells indicated that it might have a potentiality to make some important function in IAV nuclear transport action or even IAV viral replication.

G protein-coupled receptor 151 (GPR151) also showed common up-regulation at its expression level in H1N1, H5N2/F118 and H9N2 infected-CEF cells. Previous report has revealed that G protein and protein kinase signaling regulated IAV budding in MDCK cells [306]. Hence, the differential expression might implicate the exertion of corresponding GPR151 roles in these influenza A strains infected CEF cells.

In addition to these genes with up-regulated expression, some genes showing down-regulated expression were also identified with important functions. Transmembrane gene TMEM170 was found down-regulated at its expression level in H5N2/F118, H9N2 and H5N3-infected CEF cells. Moreover, a batch of ZNF genes also showed down-regulated expression in different influenza A strains infected CEF cells, and these ZNF genes might be responsible for some regulations in these influenza A strains infected CEF cells.

5.3.3 Host gene expression in MDCK cells

5.3.3.1 Global profiling of gene expression

5.3.3.1.1 Heat maps of global gene expression

In MDCK cells, the largest numbers of differentially expressed probe sets, up- or down-regulated, were detected after H1N1 infection. Compared to H9N2, H5N2/F118 infection resulted in repressed expression of relative high number of probe sets from early infection stage [Figure 5.27].

5.3.3.1.2 Distribution of differentially expressed probe sets

There were also more probe sets with up-regulated expression detected in MDCK cells infected with H9N2, H1N1 and H5N2/F118 than other influenza A strains [Table 5.10]. Percentages of probe sets with down-regulated expression were considerable after infections of all influenza A strains excluding H9N2. Moreover, some probe sets even showed down-regulated expression with high-level fold changes ≥10-FC, particularly in H1N1, H5N2/F118 and H7N1-infected MDCK cells. Among three H5N2 strains, infection of H5N2/F118 also caused the highest portion of probe sets with both up- and down-regulated expression. Besides, H5N2/F189 infection also generated big batch of probe sets with down-regulated expression.

Table 5.10 Differentially expressed probe sets in MDCK cells infected with influenza A viruses at 10 hpi.

MDCK	Probe sets (>=2 fold)		Probe sets (>=3 fold)		Probe sets (>=5 fold)		Probe sets (>=10 fold)	
	Up-regulated	Down-regulated	Up-regulated	Down-regulated	Up-regulated	Down-regulated	Up-regulated	Down-regulated
H1N1	1.31%	49.90%	0.74%	30.04%	0.35%	12.50%	0.14%	3.31%
H5N2/F59	0.74%	16.12%	0.37%	4.27%	0.21%	0.80%	0.09%	0.08%
H5N2/F118	1.44%	33.42%	0.97%	20.99%	0.50%	8.13%	0.20%	2.14%
H5N2/F189	0.17%	32.43%	0.08%	12.38%	0.05%	3.31%	0.02%	0.55%
H5N3	0.45%	28.28%	0.17%	9.06%	0.07%	1.87%	0.03%	0.30%
H7N1	0.32%	28.30%	0.16%	14.21%	0.07%	6.25%	0.03%	1.83%
H9N2	2.33%	6.28%	1.34%	2.22%	0.72%	0.71%	0.22%	0.10%

The global host gene expression profiles were retrieved from microarray analysis with different time points examined. The ratios of differentially expressed probe sets (P-value≤0.05) up- or down-regulated with different fold changes (≥2-FC, ≥3-FC, ≥5-FC and ≥10-FC) in relative to their corresponding "expressing probe sets" are represented in percentage. The expressing probe sets refer to probe sets detected in the mock-infected corresponding cells.

5.3.3.1.3 Functional classification

Figure 5.28 suggested that some probe sets belonging to "Immune Response" were induced at their expression level in MDCK cells after influenza A strains infections, especially H9N2, H1N1 and H5N2/F59. And among these probe sets, some of those from H1N1 and H5N2/F59 infections showed quite high fold changes. In the contrary, only a couple of probe sets with increased expression were observed related to "Immune Response" in H5N3 and H7N1-infected MDCK cells, indicating weaker host antiviral action. Regarding to another two H5N2 strains, infection of H5N2/F118 also stimulate expression of a small batch of probe sets, while few probe sets were observed to be stimulated at their expression level after infection of H5N2/F189.

Down-regulated probe sets in influenza A strains infected MDCK cells mostly had a relationship with "RNA Binding", "DNA Binding" and "Transcription Factor". Furthermore, dozens of probe sets located in groups such as "RNA binding" and "DNA Binding" were inhibited in their expression with quite significant fold regulation at ≥10-FC in H1N1, H5N2/F118, H5N2/F189, H5N3 and H7N1-infected MDCK cells. And among these up-regulated probe sets from different influenza A strains infected-MDCK cells, the expression of some probe sets from infections of H1N1 and H5N2/F118 showed quite high fold change level. In contrary to the situation happened in H5N2/F118 and H5N2/189-infected MDCK cells, infection of H5N2/F59 only induced the expression of a relative small number of probe sets in MDCK cells. The high percentages of differentially expressed probe sets belonging to 'Un-annotated' and "Un-classified" is majorly due to the incomplete annotation for probe sets in Canine Genome 2.0 Array.

5.3.3.2 Functional groups related to host response

5.3.3.2.1 Immune response

In MDCK cells, expression levels of IFN type I stimulated genes OAS1, MX1 and RASD2 were all up-regulated after H1N1 infection and selectively up-regulated after other influenza A strains infections [Figure 5.29]. Cytokines, CCL5 and CXCL10, were also detected with significantly up-regulated expression after infections of all influenza A strains except H5N3.

5.3.3.2.2 Cell death

Expression profiles of cell death relevant genes in MDCK cells implicated that most genes with down-regulated expression were detected after H1N1 infection and least genes with down-regulated expression were detected after H9N2 infection [Figure 5.30]. Key genes such as caspase 2/3/8, Fas and TNF were all down-regulated at their expression level in H1N1 infected MDCK cells, indicating the inhibition of cell apoptotic activities.

5.3.3.2.3 Genes with remarkable regulations

Parallel observation of gene expression in IAV infected MDCK cells revealed that several genes related to transmembrane and zinc finger were significantly up-regulated at their expression level [Figure 5.31]. Among them, expression of TMEM106A, TMEM55A, TMEM30C were up-regulated after infections of H5N2/F59, H5N2/F118 and H9N2 separately; expression of ZNF391/662 was induced after infection of H5N2/F118. In addition, lipid and adhesion associated genes such as CH25H, ALCAM were also detected with up-regulated expression in H5N2/F118 and H5N3 infected MDCK cells.

Moreover, there also existed quite a lot of genes with suppressed expression and these genes were majorly relevant to zinc finger, transmembrane, G protein, cell cycle and cholesterol. These genes included GPR98 for H5N2/F59 infection, GPR56 for H5N2/F118 and H1N1 infection, GPR110 for H1N1 infection and so on.

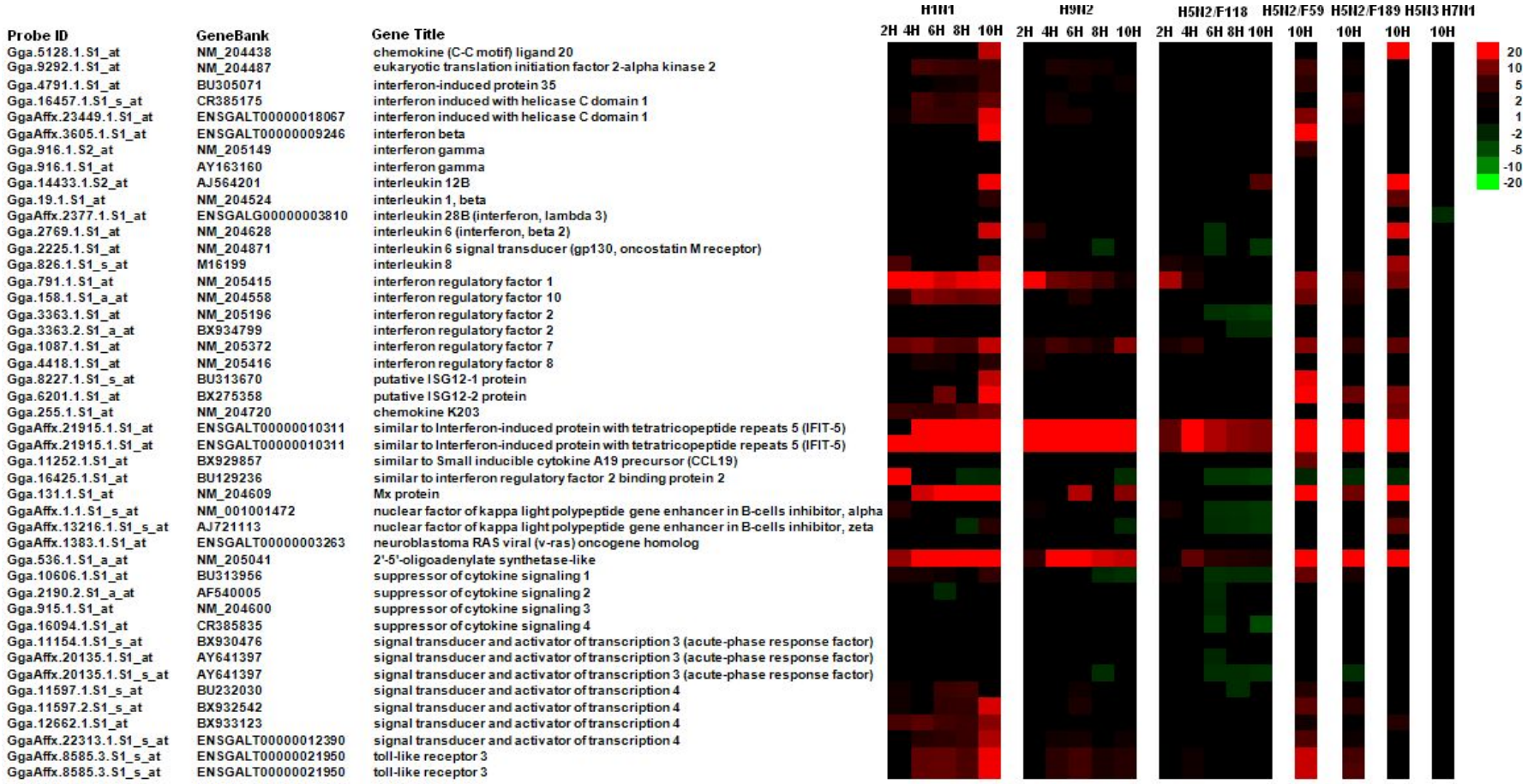

Probe ID	GeneBank	Gene Title
Gga.5128.1.S1_at	NM_204438	chemokine (C-C motif) ligand 20
Gga.9292.1.S1_at	NM_204487	eukaryotic translation initiation factor 2-alpha kinase 2
Gga.4791.1.S1_at	BU305071	interferon-induced protein 35
Gga.16457.1.S1_s_at	CR385175	interferon induced with helicase C domain 1
GgaAffx.23449.1.S1_at	ENSGALT00000018067	interferon induced with helicase C domain 1
GgaAffx.3605.1.S1_at	ENSGALT00000009246	interferon beta
Gga.916.1.S2_at	NM_205149	interferon gamma
Gga.916.1.S1_at	AY163160	interferon gamma
Gga.14433.1.S2_at	AJ564201	interleukin 12B
Gga.19.1.S1_at	NM_204524	interleukin 1, beta
GgaAffx.2377.1.S1_at	ENSGALG00000003810	interleukin 28B (interferon, lambda 3)
Gga.2769.1.S1_at	NM_204628	interleukin 6 (interferon, beta 2)
Gga.2225.1.S1_at	NM_204871	interleukin 6 signal transducer (gp130, oncostatin M receptor)
Gga.826.1.S1_s_at	M16199	interleukin 8
Gga.791.1.S1_at	NM_205415	interferon regulatory factor 1
Gga.158.1.S1_a_at	NM_204558	interferon regulatory factor 10
Gga.3363.1.S1_at	NM_205196	interferon regulatory factor 2
Gga.3363.2.S1_a_at	BX934799	interferon regulatory factor 2
Gga.1087.1.S1_at	NM_205372	interferon regulatory factor 7
Gga.4418.1.S1_at	NM_205416	interferon regulatory factor 8
Gga.8227.1.S1_s_at	BU313670	putative ISG12-1 protein
Gga.6201.1.S1_at	BX275358	putative ISG12-2 protein
Gga.255.1.S1_at	NM_204720	chemokine K203
GgaAffx.21915.1.S1_at	ENSGALT00000010311	similar to Interferon-induced protein with tetratricopeptide repeats 5 (IFIT-5)
GgaAffx.21915.1.S1_at	ENSGALT00000010311	similar to Interferon-induced protein with tetratricopeptide repeats 5 (IFIT-5)
Gga.11252.1.S1_at	BX929857	similar to Small inducible cytokine A19 precursor (CCL19)
Gga.16425.1.S1_at	BU129236	similar to interferon regulatory factor 2 binding protein 2
Gga.131.1.S1_at	NM_204609	Mx protein
GgaAffx.1.1.S1_s_at	NM_001001472	nuclear factor of kappa light polypeptide gene enhancer in B-cells inhibitor, alpha
GgaAffx.13216.1.S1_s_at	AJ721113	nuclear factor of kappa light polypeptide gene enhancer in B-cells inhibitor, zeta
GgaAffx.1383.1.S1_at	ENSGALT00000003263	neuroblastoma RAS viral (v-ras) oncogene homolog
Gga.536.1.S1_a_at	NM_205041	2'-5'-oligoadenylate synthetase-like
Gga.10606.1.S1_at	BU313956	suppressor of cytokine signaling 1
Gga.2190.2.S1_a_at	AF540005	suppressor of cytokine signaling 2
Gga.915.1.S1_at	NM_204600	suppressor of cytokine signaling 3
Gga.16094.1.S1_at	CR385835	suppressor of cytokine signaling 4
Gga.11154.1.S1_s_at	BX930476	signal transducer and activator of transcription 3 (acute-phase response factor)
GgaAffx.20135.1.S1_at	AY641397	signal transducer and activator of transcription 3 (acute-phase response factor)
GgaAffx.20135.1.S1_s_at	AY641397	signal transducer and activator of transcription 3 (acute-phase response factor)
Gga.11597.1.S1_s_at	BU232030	signal transducer and activator of transcription 4
Gga.11597.2.S1_s_at	BX932542	signal transducer and activator of transcription 4
Gga.12662.1.S1_at	BX933123	signal transducer and activator of transcription 4
GgaAffx.22313.1.S1_s_at	ENSGALT00000012390	signal transducer and activator of transcription 4
GgaAffx.8585.3.S1_s_at	ENSGALT00000021950	toll-like receptor 3
GgaAffx.8585.3.S1_s_at	ENSGALT00000021950	toll-like receptor 3

Figure 5.24 Expression of probe sets involved in immune response in influenza A viruses-infected CEF cells. Eight influenza A strains were infected with different examined cells, and the expression of probe sets related to immune response was examined by microarray analysis at different time points as shown. The data is represented by heat map analysis showing up-regulated (red), down-regulated (green) or no changes (black) in expression, and the FC range is indicated (P-value≤0.05).

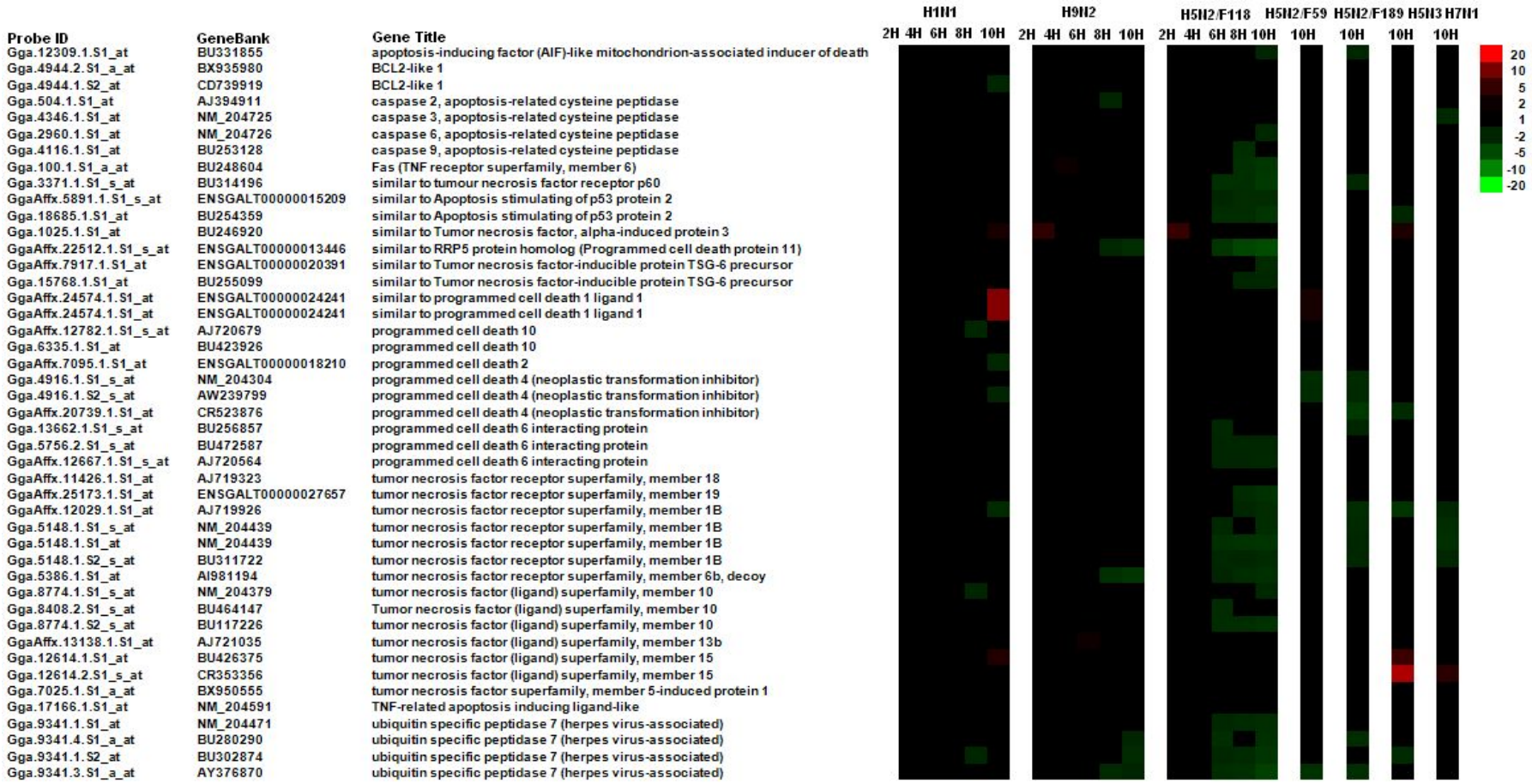

Probe ID	GeneBank	Gene Title
Gga.12309.1.S1_at	BU331855	apoptosis-inducing factor (AIF)-like mitochondrion-associated inducer of death
Gga.4944.2.S1_a_at	BX935980	BCL2-like 1
Gga.4944.1.S2_at	CD739919	BCL2-like 1
Gga.504.1.S1_at	AJ394911	caspase 2, apoptosis-related cysteine peptidase
Gga.4346.1.S1_at	NM_204725	caspase 3, apoptosis-related cysteine peptidase
Gga.2960.1.S1_at	NM_204726	caspase 6, apoptosis-related cysteine peptidase
Gga.4116.1.S1_at	BU253128	caspase 9, apoptosis-related cysteine peptidase
Gga.100.1.S1_a_at	BU248604	Fas (TNF receptor superfamily, member 6)
Gga.3371.1.S1_s_at	BU314196	similar to tumour necrosis factor receptor p60
GgaAffx.5891.1.S1_s_at	ENSGALT00000015209	similar to Apoptosis stimulating of p53 protein 2
Gga.18685.1.S1_at	BU254359	similar to Apoptosis stimulating of p53 protein 2
Gga.1025.1.S1_at	BU246920	similar to Tumor necrosis factor, alpha-induced protein 3
GgaAffx.22512.1.S1_s_at	ENSGALT00000013446	similar to RRP5 protein homolog (Programmed cell death protein 11)
GgaAffx.7917.1.S1_at	ENSGALT00000020391	similar to Tumor necrosis factor-inducible protein TSG-6 precursor
Gga.15768.1.S1_at	BU255099	similar to Tumor necrosis factor-inducible protein TSG-6 precursor
GgaAffx.24574.1.S1_at	ENSGALT00000024241	similar to programmed cell death 1 ligand 1
GgaAffx.24574.1.S1_at	ENSGALT00000024241	similar to programmed cell death 1 ligand 1
GgaAffx.12782.1.S1_s_at	AJ720679	programmed cell death 10
Gga.6335.1.S1_at	BU423926	programmed cell death 10
GgaAffx.7095.1.S1_at	ENSGALT00000018210	programmed cell death 2
Gga.4916.1.S1_s_at	NM_204304	programmed cell death 4 (neoplastic transformation inhibitor)
Gga.4916.1.S2_s_at	AW239799	programmed cell death 4 (neoplastic transformation inhibitor)
GgaAffx.20739.1.S1_at	CR523876	programmed cell death 4 (neoplastic transformation inhibitor)
Gga.13662.1.S1_s_at	BU256857	programmed cell death 6 interacting protein
Gga.5756.2.S1_s_at	BU472587	programmed cell death 6 interacting protein
GgaAffx.12667.1.S1_s_at	AJ720564	programmed cell death 6 interacting protein
GgaAffx.11426.1.S1_at	AJ719323	tumor necrosis factor receptor superfamily, member 18
GgaAffx.25173.1.S1_at	ENSGALT00000027657	tumor necrosis factor receptor superfamily, member 19
GgaAffx.12029.1.S1_at	AJ719926	tumor necrosis factor receptor superfamily, member 1B
Gga.5148.1.S1_s_at	NM_204439	tumor necrosis factor receptor superfamily, member 1B
Gga.5148.1.S1_at	NM_204439	tumor necrosis factor receptor superfamily, member 1B
Gga.5148.1.S2_s_at	BU311722	tumor necrosis factor receptor superfamily, member 1B
Gga.5386.1.S1_at	AI981194	tumor necrosis factor receptor superfamily, member 6b, decoy
Gga.8774.1.S1_s_at	NM_204379	tumor necrosis factor (ligand) superfamily, member 10
Gga.8408.2.S1_s_at	BU464147	Tumor necrosis factor (ligand) superfamily, member 10
Gga.8774.1.S2_s_at	BU117226	tumor necrosis factor (ligand) superfamily, member 10
GgaAffx.13138.1.S1_at	AJ721035	tumor necrosis factor (ligand) superfamily, member 13b
Gga.12614.1.S1_at	BU426375	tumor necrosis factor (ligand) superfamily, member 15
Gga.12614.2.S1_s_at	CR353356	tumor necrosis factor (ligand) superfamily, member 15
Gga.7025.1.S1_a_at	BX950555	tumor necrosis factor superfamily, member 5-induced protein 1
Gga.17166.1.S1_at	NM_204591	TNF-related apoptosis inducing ligand-like
Gga.9341.1.S1_at	NM_204471	ubiquitin specific peptidase 7 (herpes virus-associated)
Gga.9341.4.S1_a_at	BU280290	ubiquitin specific peptidase 7 (herpes virus-associated)
Gga.9341.1.S2_at	BU302874	ubiquitin specific peptidase 7 (herpes virus-associated)
Gga.9341.3.S1_a_at	AY376870	ubiquitin specific peptidase 7 (herpes virus-associated)

Figure 5.25 Expression of probe sets involved in cell death in influenza A viruses-infected CEF cells. Eight influenza A strains were infected with different examined cells, and the expression of probe sets related to cell death was examined by microarray analysis at different time points as shown. The data is represented by heat map analysis showing up-regulated (red), down-regulated (green) or no changes (black) in expression, and the FC range is indicated ($p \leq 0.05$).

Probe ID	GeneBank	Gene Title
Gga.10842.1.S1_at	BU349805	guanine nucleotide binding protein (G protein), gamma 13
GgaAffx.1222.1.S1_at	ENSGALT00000002899.1	G protein-coupled receptor 151
GgaAffx.1222.2.S1_at	ENSGALT00000002898.1	G protein-coupled receptor 151
Gga.5237.2.S1_at	BU105201	importin 7
Gga.18890.1.S1_a_at	BX263353	Transmembrane protein 170
Gga.18890.1.S1_s_at	BX263353	transmembrane protein 170
GgaAffx.8080.1.S1_at	ENSGALT00000020798.1	transmembrane protein 170B
Gga.17993.1.S1_at	CR389298.1	zinc finger CCCH-type, antiviral 1
GgaAffx.11358.1.S1_s_at	ENSGALT00000022553.1	zinc finger CCCH-type, antiviral 1
GgaAffx.20602.1.S1_at	CR524013.1	zinc finger CCCH-type, antiviral 1
GgaAffx.22363.1.S1_at	ENSGALT00000012648.1	zinc finger protein 217
GgaAffx.10070.1.S1_s_at	ENSGALT00000025513.1	zinc finger protein 292
Gga.19239.1.S1_at	CR406490.1	zinc finger protein 407
GgaAffx.10405.1.S1_at	ENSGALT00000026252.1	zinc finger protein 451
Gga.15002.1.S1_s_at	CR386121.1	zinc finger protein 509
Gga.9967.1.S1_at	BU482317	zinc finger protein 516
GgaAffx.4356.1.S1_at	ENSGALT00000011284.1	zinc finger protein 518
GgaAffx.24552.1.S1_at	ENSGALT00000024121.1	zinc finger protein 518B
GgaAffx.25463.1.S1_at	ENSGALT00000003690.1	zinc finger protein 609
GgaAffx.23045.2.S1_s_at	ENSGALT00000015964.1	zinc finger protein 770
GgaAffx.26344.1.S1_at	ENSGALT00000007763.1	zinc finger, NFX1-type containing 1
GgaAffx.26344.3.S1_s_at	ENSGALT00000007762.1	zinc finger, NFX1-type containing 1

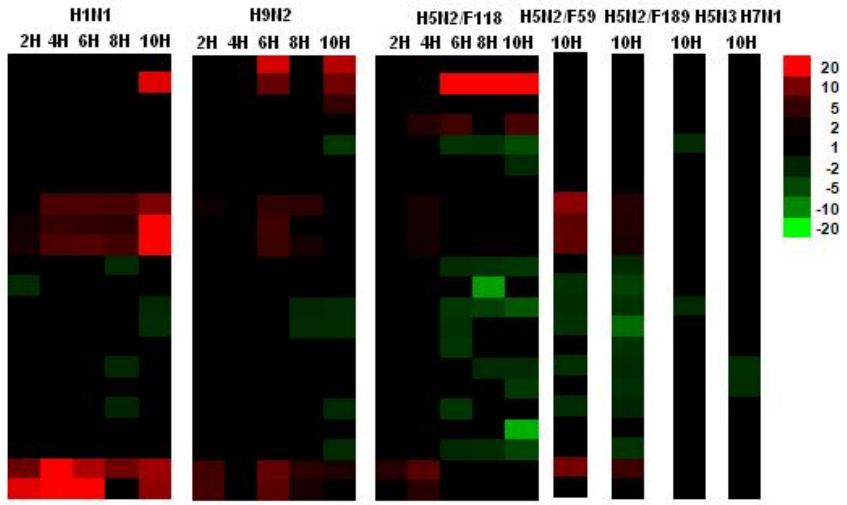

Figure 5.26 The probe sets with topmost expression changes in influenza A viruses-infected CEF cells. Eight influenza A strains were infected with different examined cells, and the global host gene expression was examined by microarray analysis at different time points. The probe sets with topmost expression changes were listed. The data is represented by heat map analysis showing up-regulated (red), down-regulated (green) or no changes (black) in expression, and the FC range is indicated ($p \leq 0.05$).

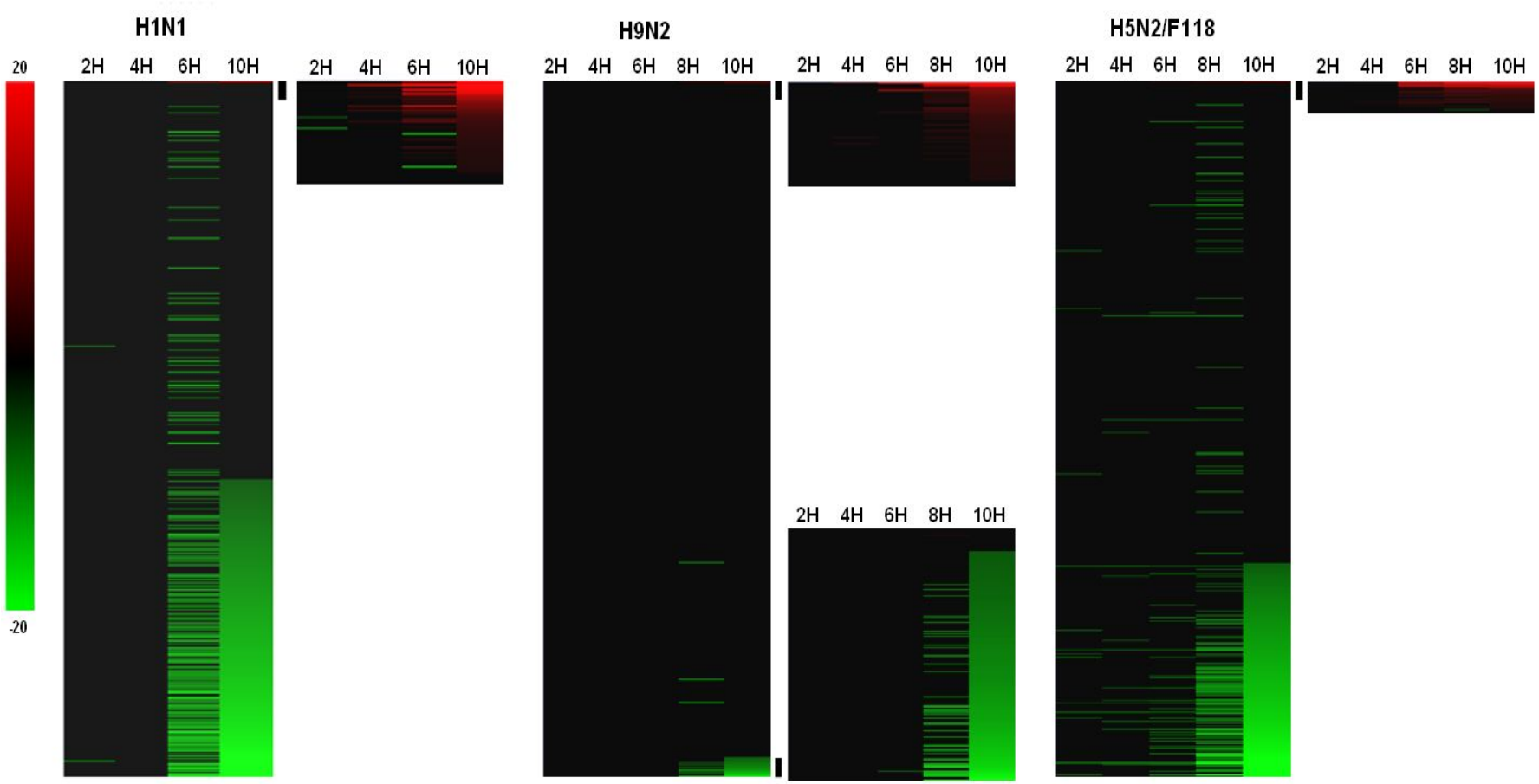

Figure 5.27 Temporal changes in the host cell transcriptome in MDCK cells infected by four influenza virus strains. The global host gene expression profiles were retrieved from microarray analysis with different time points examined. The probe sets showing ≥2 fold change (FC) up- or down-regulated in expression are indicated (P-value≤0.05). Expression profiles of up-regulated (red), down-regulated (green) and no significant change (black) are shown.

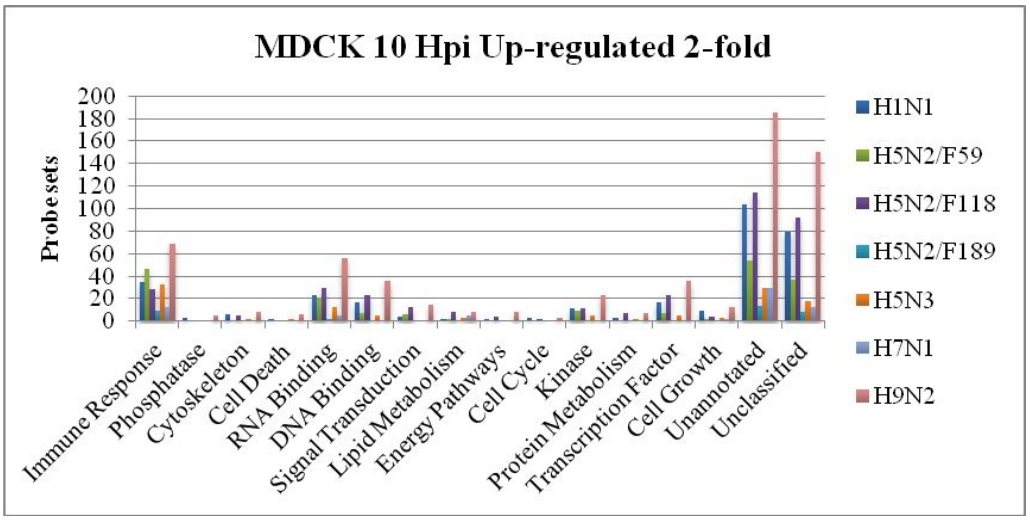
MDCK 10 Hpi Up-regulated 2-fold
Probe sets
200
180
160
140
120
100
80
60
40
20
0
Immune Response
Phosphatase
Cytoskeleton
Cell Death
RNA Binding
DNA Binding
Signal Transduction
Lipid Metabolism
Energy Pathways
Cell Cycle
Kinase
Protein Metabolism
Transcription Factor
Cell Growth
Unannotated
Unclassified
H1N1
H5N2/F59
H5N2/F118
H5N2/F189
H5N3
H7N1
H9N2

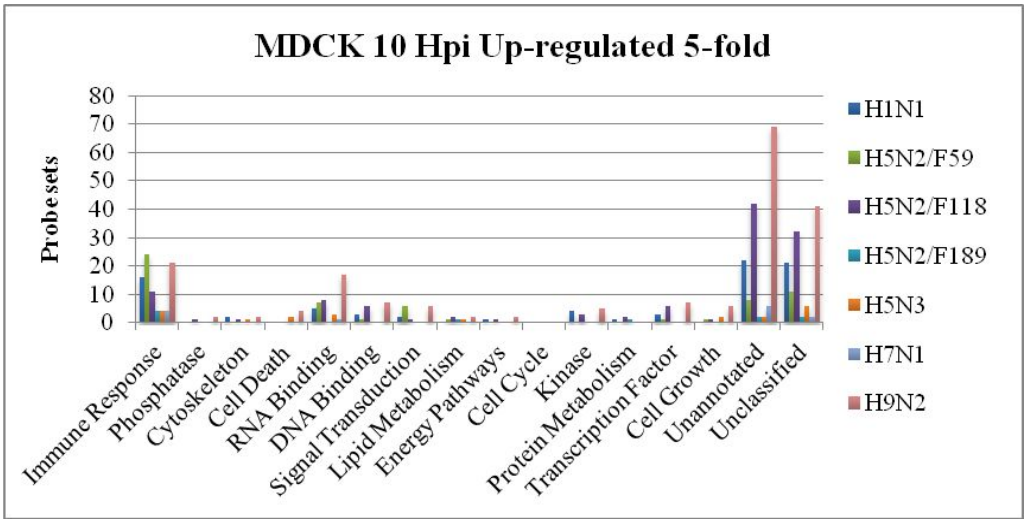
MDCK 10 Hpi Up-regulated 5-fold
Probe sets
80
70
60
50
40
30
20
10
0
Immune Response
Phosphatase
Cytoskeleton
Cell Death
RNA Binding
DNA Binding
Signal Transduction
Lipid Metabolism
Energy Pathways
Cell Cycle
Kinase
Protein Metabolism
Transcription Factor
Cell Growth
Unannotated
Unclassified
H1N1
H5N2/F59
H5N2/F118
H5N2/F189
H5N3
H7N1
H9N2

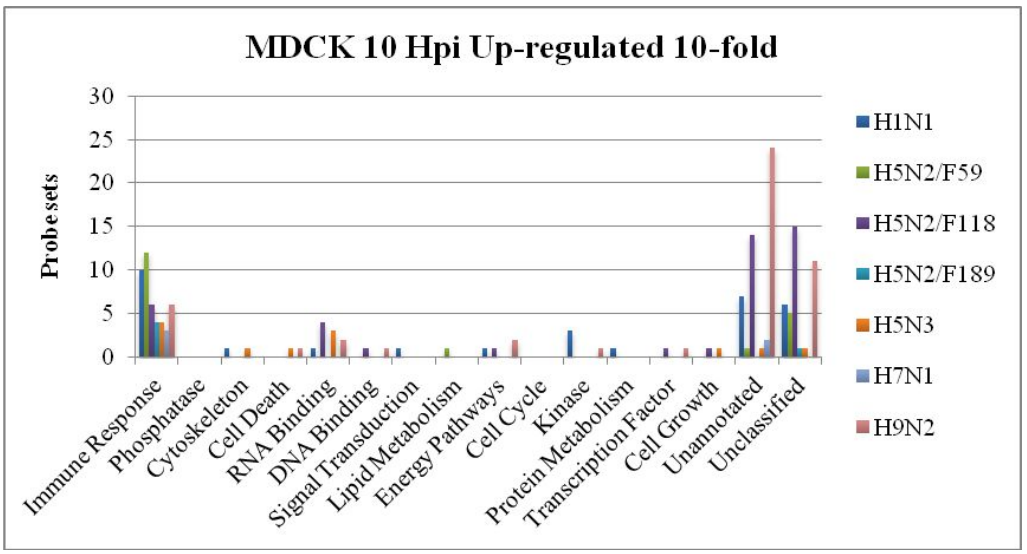
MDCK 10 Hpi Up-regulated 10-fold
Probe sets
30
25
20
15
10
5
0
Immune Response
Phosphatase
Cytoskeleton
Cell Death
RNA Binding
DNA Binding
Signal Transduction
Lipid Metabolism
Energy Pathways
Cell Cycle
Kinase
Protein Metabolism
Transcription Factor
Cell Growth
Unannotated
Unclassified
H1N1
H5N2/F59
H5N2/F118
H5N2/F189
H5N3
H7N1
H9N2

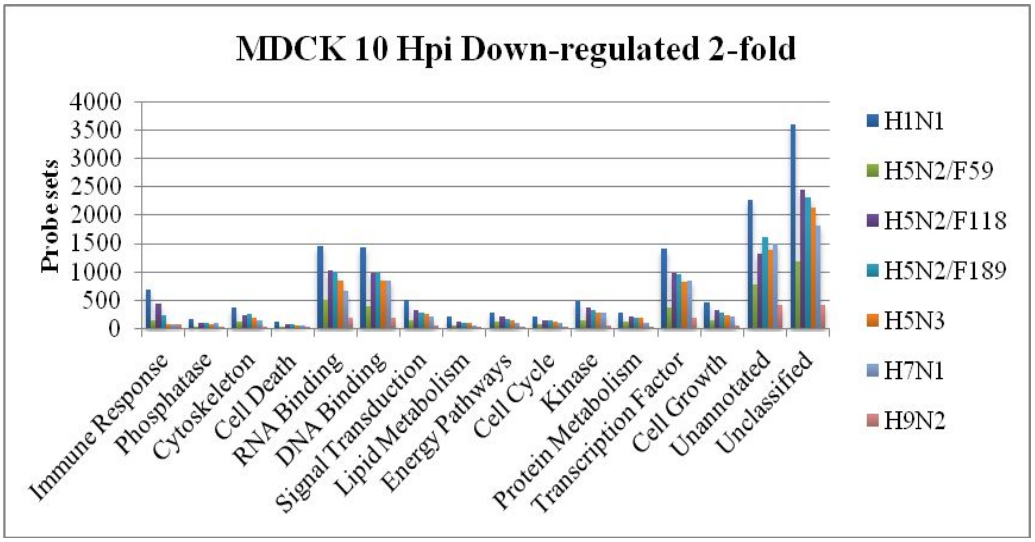

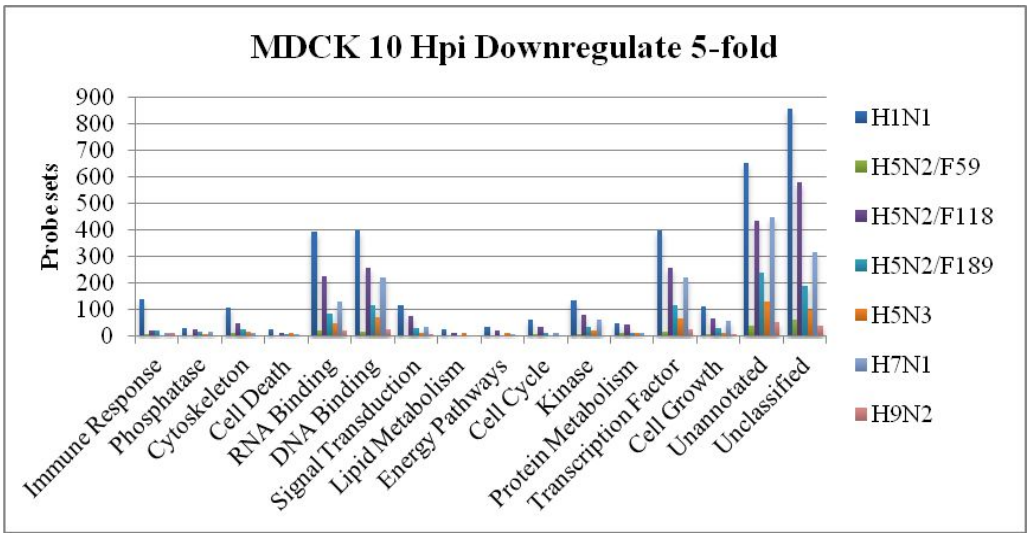

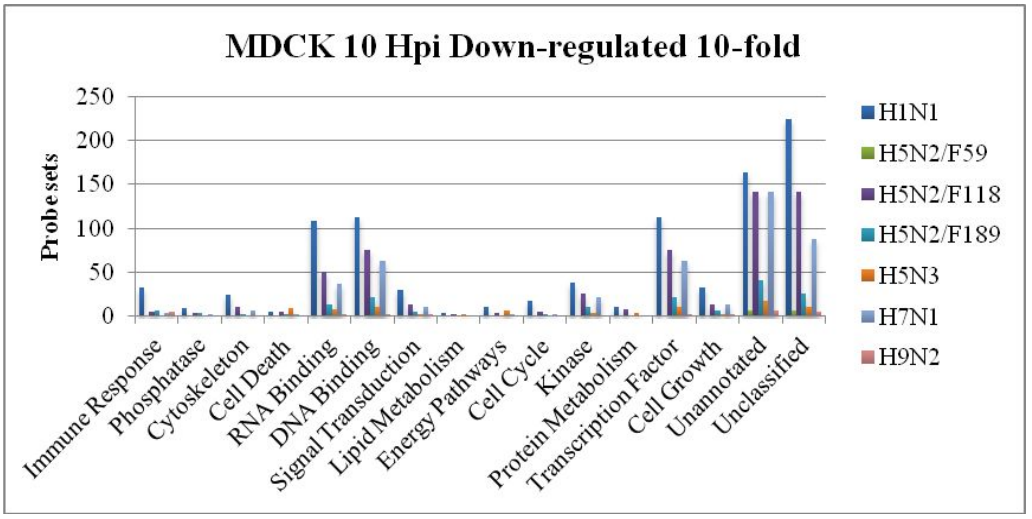

Figure 5.28 Overview of distributions of differentially expressed probe sets into different biological functions in MDCK cells infected with influenza A viruses. The numbers of probe sets in the different functional families, including non-annotated and unclassified groups, showing up- or down-regulated with different fold changes (≥2-FC, ≥5-FC and ≥10-FC) in gene expression are presented.

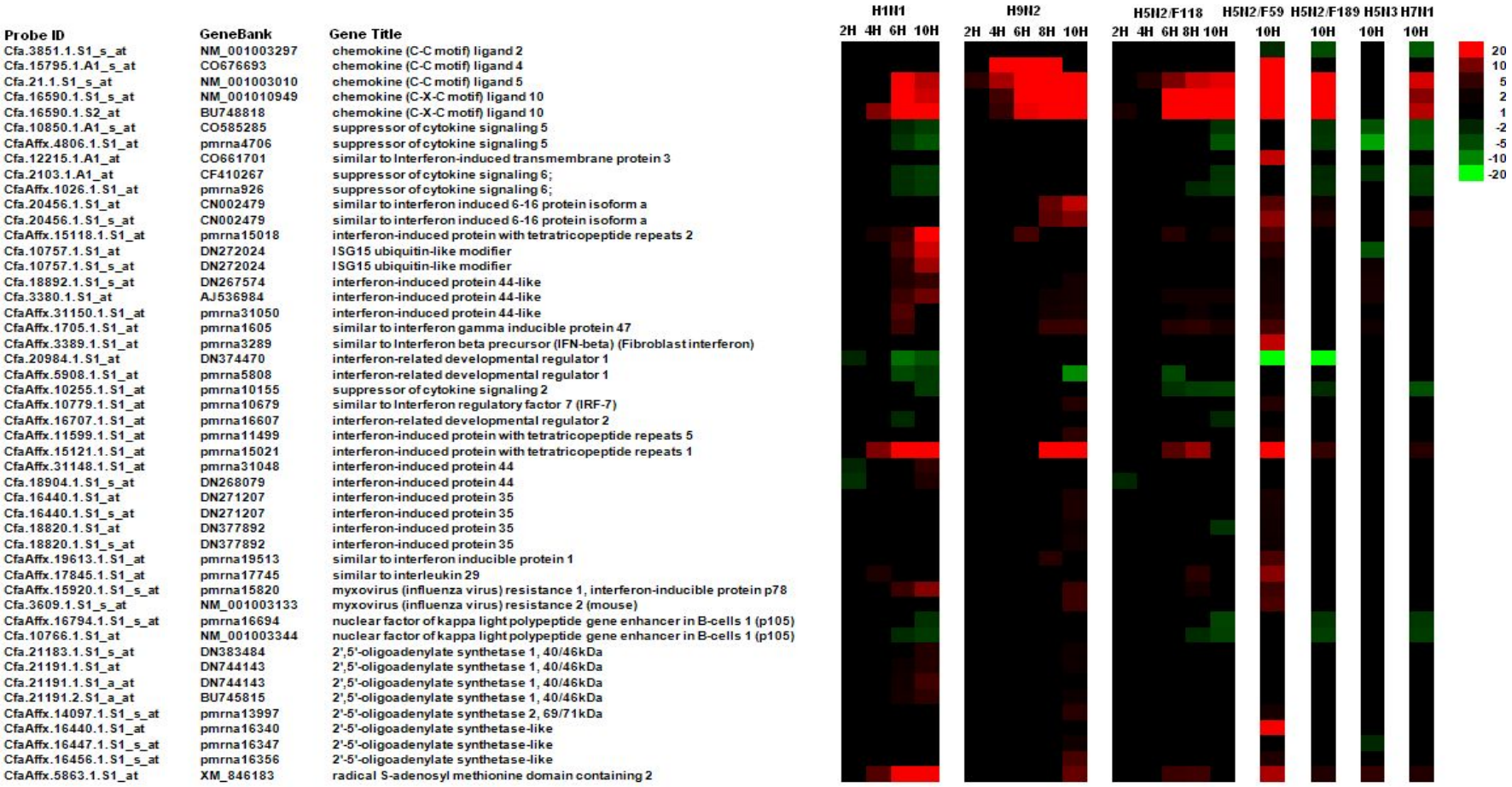

Figure 5.29 The expression of probe sets involved in immune response in influenza A viruses-infected MDCK cells. Eight influenza A strains were infected with different examined cells, and the expression of probe sets related to immune response was examined by microarray analysis at different time points as shown. The data is represented by heat map analysis showing up-regulated (red), down-regulated (green) or no changes (black) in expression, and the FC range is indicated (P-value≤0.05).

Probe ID	GeneBank	Gene Title
Cfa.110.1.S1_s_at	NM_001002949	B-cell CLL/lymphoma 2
CfaAffx.6401.1.S1_s_at	pmrna6301	caspase 2, apoptosis-related cysteine peptidase
Cfa.12400.1.A1_at	CO620847	caspase 2, apoptosis-related cysteine peptidase
Cfa.6392.1.A1_at	CO715709	caspase 2, apoptosis-related cysteine peptidase
CfaAffx.12454.1.S1_s_at	pmrna12354	caspase 3, apoptosis-related cysteine peptidase
Cfa.4486.5.A1_at	CX005610	programmed cell death 2;
CfaAffx.7087.1.S1_s_at	pmrna6987	programmed cell death 2;
Cfa.8198.1.S1_at	CO595574	programmed cell death 6 interacting protein;
CfaAffx.8021.1.S1_s_at	pmrna7921	programmed cell death 6 interacting protein;
CfaAffx.8022.1.S1_at	pmrna7922	programmed cell death 6 interacting protein;
CfaAffx.16255.1.S1_s_at	pmrna16155	programmed cell death 11
CfaAffx.16319.1.S1_at	pmrna16219	programmed cell death 11
Cfa.19830.1.S1_s_at	DN320720	programmed cell death 4 (neoplastic transformation inhibitor);
CfaAffx.16895.1.S1_at	pmrna16795	programmed cell death 4 (neoplastic transformation inhibitor);
CfaAffx.16895.1.S1_s_at	pmrna16795	programmed cell death 4 (neoplastic transformation inhibitor);
Cfa.2490.1.A1_s_at	CF410501	cell division cycle and apoptosis regulator 1;
CfaAffx.21274.1.S1_at	pmrna21174	cell division cycle and apoptosis regulator 1;
CfaAffx.28795.1.S1_s_at	pmrna28695	tumor necrosis factor superfamily, member 5-induced protein 1
CfaAffx.27855.1.S1_s_at	pmrna27755	tumor necrosis factor, alpha-induced protein 2
CfaAffx.27855.1.S1_at	pmrna27755	tumor necrosis factor, alpha-induced protein 2
CfaAffx.11787.1.S1_at	pmrna11687	programmed cell death 2-like
Cfa.3417.1.S1_at	AJ537250	Fas apoptotic inhibitory molecule
CfaAffx.24073.1.S1_at	pmrna23973	Fas (TNF receptor superfamily, member 6)
Cfa.17926.1.S1_s_at	DN394512	programmed cell death 10;
Cfa.2830.1.S1_s_at	DN746382	programmed cell death 10;
Cfa.18114.1.S1_at	DN376899	CASP8 and FADD-like apoptosis regulator;
Cfa.18114.1.S1_s_at	DN376899	CASP8 and FADD-like apoptosis regulator;
CfaAffx.18869.1.S1_at	pmrna18769	CASP8 and FADD-like apoptosis regulator;
CfaAffx.18858.1.S1_at	pmrna18758	CASP8 and FADD-like apoptosis regulator;
CfaAffx.18864.1.S1_s_at	pmrna18764	CASP8 and FADD-like apoptosis regulator;
CfaAffx.18878.1.S1_s_at	pmrna18778	caspase 8, apoptosis-related cysteine peptidase
Cfa.7342.2.A1_at	CF408972	tumor necrosis factor, alpha-induced protein 1 (endothelial);
CfaAffx.28514.1.S1_at	pmrna28414	tumor necrosis factor, alpha-induced protein 1 (endothelial);
CfaAffx.4087.1.S1_at	pmrna3987	programmed cell death 1 ligand 2
Cfa.17439.1.S1_at	DN748333	tumor necrosis factor receptor superfamily, member 21
Cfa.691.1.A1_at	CF413026	programmed cell death 7
CfaAffx.1718.1.S1_at	pmrna1618	tumor necrosis factor (TNF superfamily, member 2)
CfaAffx.23380.1.S1_s_at	pmrna23280	tumor necrosis factor receptor superfamily, member 1A
Cfa.3498.1.S1_at	DN413932	tumor necrosis factor receptor superfamily, member 1A
CfaAffx.25562.1.S1_s_at	pmrna25462	tumor protein p53 (Li-Fraumeni syndrome)

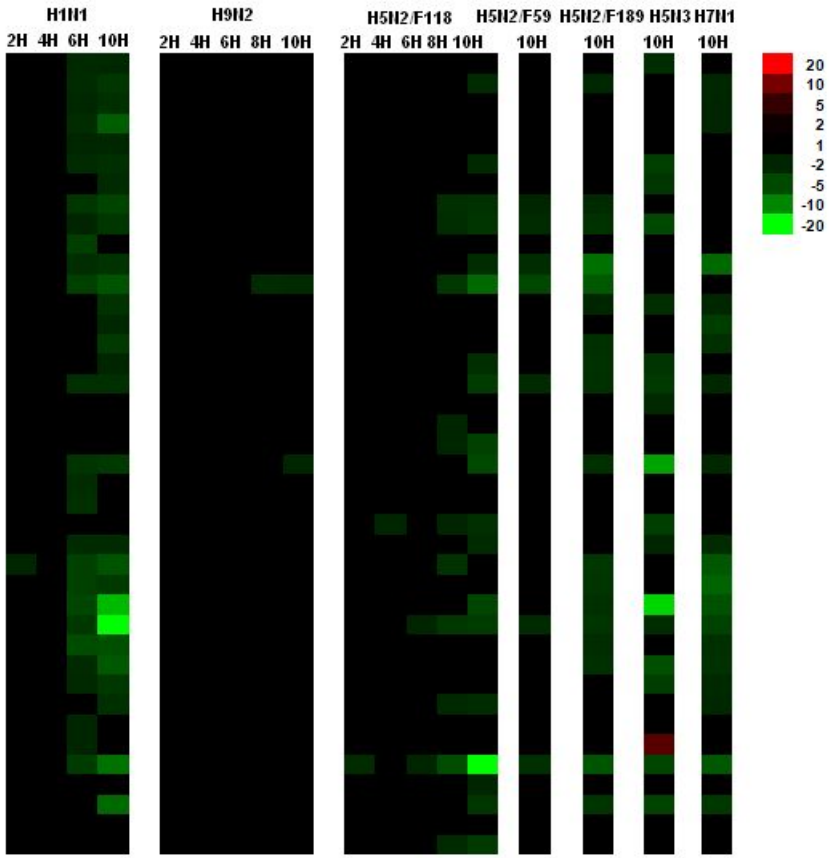

Figure 5.30 The expression of probe sets involved in cell death in influenza A viruses-infected MDCK cells. Eight influenza A strains were infected with different examined cells, and the expression of probe sets related to cell death was examined by microarray analysis at different time points as shown. The data is represented by heat map analysis showing up-regulated (red), down-regulated (green) or no changes (black) in expression, and the FC range is indicated ($p \leq 0.05$).

Probe ID	GeneBank	Gene Title
Cfa.3742.1.S1_s_at	Y13242.1	activated leukocyte cell adhesion molecule
CfaAffx.15259.1.S1_at	pmrna15159	activated leukocyte cell adhesion molecule
Cfa.16245.1.S1_at	NM_001005763.1	cyclin B3
Cfa.16245.1.S1_s_at	NM_001005763.1	cyclin B3
Cfa.20425.1.S1_at	DN357326	cyclin E1
CfaAffx.12272.1.S1_s_at	pmrna12172	cyclin E1
CfaAffx.13729.1.S1_at	pmrna13629	cyclin G2
CfaAffx.13734.1.S1_s_at	pmrna13634	cyclin G2
Cfa.11349.1.A1_at	CO668650	cyclin L2
Cfa.5916.1.A1_at	CO683252	cyclin L2
CfaAffx.29398.1.S1_at	pmrna29298	cyclin L2
CfaAffx.29399.1.S1_s_at	pmrna29299	cyclin L2
Cfa.1994.1.A1_at	CF409920	cyclin T2
CfaAffx.8476.1.S1_s_at	pmrna8376	cyclin T2
Cfa.16947.1.A1_at	DN751348	cholesterol 25-hydroxylase
Cfa.14406.1.A1_at	CO716803	farnesyl-diphosphate farnesyltransferase 1
Cfa.21520.1.S1_s_at	DN422685	farnesyl-diphosphate farnesyltransferase 1
Cfa.7073.2.A1_a_at	CO610099	G protein-coupled receptor 107
CfaAffx.4026.1.S1_at	pmrna3926	G protein-coupled receptor 110
CfaAffx.8936.1.S1_at	pmrna8836	G protein-coupled receptor 180
CfaAffx.13764.1.S1_s_at	pmrna13664	G protein-coupled receptor 56
CfaAffx.13502.1.S1_at	pmrna13402	G protein-coupled receptor 87
CfaAffx.13109.1.S1_at	pmrna13009	G protein-coupled receptor 98
Cfa.20631.1.S1_at	CX002871	G protein-coupled receptor, family C, group 5, member C
Cfa.21522.2.S1_s_at	DN350566	G protein-coupled receptor, family C, group 5, member C
Cfa.11398.1.A1_at	CO585054	3-hydroxy-3-methylglutaryl-Coenzyme A synthase 1 (soluble)
Cfa.17863.1.S1_s_at	CF408018	3-hydroxy-3-methylglutaryl-Coenzyme A synthase 1 (soluble)
Cfa.17863.2.S1_s_at	DN265597	3-hydroxy-3-methylglutaryl-Coenzyme A synthase 1 (soluble)
CfaAffx.22470.1.S1_at	pmrna22370	transmembrane protein 106A
Cfa.20962.1.S1_at	DN745718	transmembrane protein 30C
CfaAffx.14570.1.S1_at	pmrna14470	transmembrane protein 30C
Cfa.15200.1.S1_at	BU749737	transmembrane protein 55A
CfaAffx.868.1.S1_at	pmrna768	zinc finger protein 391
CfaAffx.7641.1.S1_at	pmrna7541	zinc finger protein 467
CfaAffx.8989.1.S1_s_at	pmrna8889	zinc finger protein 662

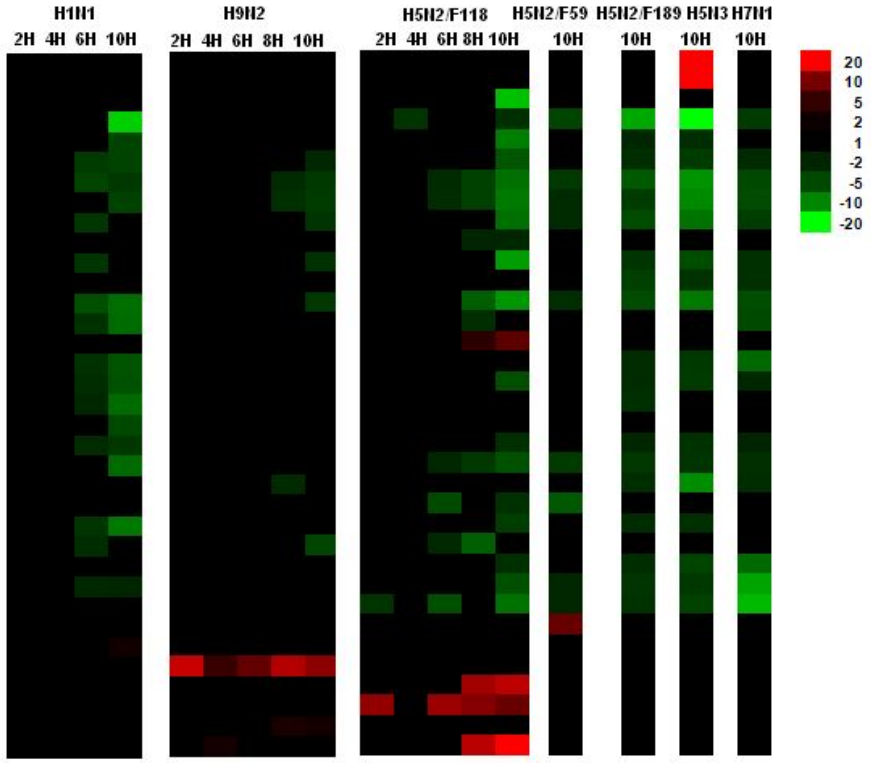

Figure 5.31 The probe sets with topmost expression changes in influenza A viruses-infected MDCK cells. Eight influenza A strains were infected with different examined cells, and the global host gene expression was examined by microarray analysis at different time points. The probe sets with topmost expression changes were listed. The data is represented by heat map analysis showing up-regulated (red), down-regulated (green) or no changes (black) in expression, and the FC range is indicated ($p \leq 0.05$).

5.3.4 Host gene expression in macrophages

5.3.4.1 Global profiling of gene expression

5.3.4.1.1 Heat maps of global gene expression

The numbers of differentially expressed genes in H1N1 and H5N2/F118-infected macrophages both showed decreasing from 2 hpi to 24 hpi. And among these differentially expressed genes, it was interesting that larger numbers of genes with down-regulated expression were detected at 2 hpi while larger numbers of genes with up-regulated expression were detected at 24 hpi after infections of both H1N1 and H5N2/F118.

In the macrophages infected with H5N3, the expression profiles at 24 hpi indicated more up-regulated genes were detected when compared to those detected in macrophages infected with H1N1 and H5N2/F118 at 24 hpi. This phenomenon could suggest that a larger batch of antiviral genes were activated during H5N3 infection than H1N1 and H5N2/F118 infections in macrophages [Figure 5.32].

5.3.4.1.2 Distribution of differential expressed probe sets

In macrophages with infection of H1N1, a large number of genes were detected with down-regulated expression at ≥2-FC at 2 hpi. However, this number decreased steeply at later infection period, with only few genes with down-regulated expression left at 24 hpi [Table 5.11]. In the contrary to the down-regulated genes, only a small number of genes with the up-regulated expression at ≥2-FC were detected at 2 hpi, and this number almost remained no change with the infection time increasing.

Infection of H5N2/F118 in macrophages resulted in larger numbers of genes with up- or down-regulated expression at ≥2-FC at 2 hpi when compared to 24 hpi. This phenomenon indicated the early but short-term host gene response upon H5N2/F118 infection in macrophages.

In H5N3 infected macrophages, only the gene expression profile at 24 hpi was investigated. It was noted that more differentially expressed genes (up- or down-regulated) were identified after infection of H5N3 than those identified after infections of H1N1 and H5N2/F118 at 24hpi, indicating activated gene regulation activities occurred in H5N3-infected macrophages at late infection stage. Moreover, some of the genes with elevated expression after infection of

H5N3 showed high-level fold regulation at ≥5-FC, which might indicate strong antiviral regulation in these infected macrophages.

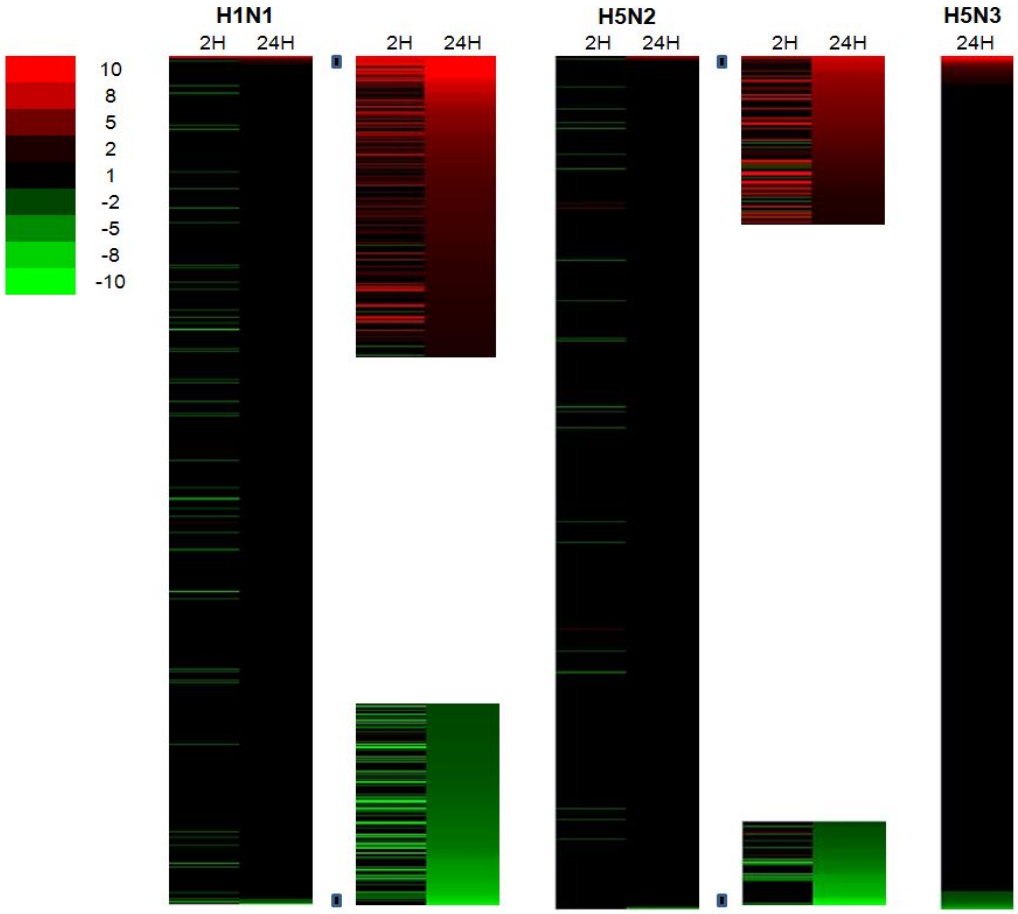

Figure 5.32 Temporal changes in the host cell transcriptome in macrophages infected with influenza A strains. The global host gene expression profiles were retrieved from microarray analysis with different time points examined. The genes showing ≥2 fold change (FC) up- or down-regulated in expression are indicated (P-value≤0.05). Expression profiles of up-regulated (red), down-regulated (green) and no significant change (black) are shown.

Table 5.11 Differentially expressed genes in macrophages infected with influenza A strains.

Macrophages	Genes (≥ 2-FC)		Genes (≥ 3-FC)		Genes (≥ 5-FC)	
	Up-regulated	Down-regulated	Up-regulated	Down-regulated	Up-regulated	Down-regulated
H1N1 2H	0.92%	5.65%	0.52%	1.50%	0.26%	0.56%
H1N1 24H	0.90%	0.65%	0.56%	0.33%	0.24%	0.15%
H5N2/F118 2H	1.19%	2.82%	0.60%	0.80%	0.29%	0.22%
H5N2/F118 24H	0.51%	0.24%	0.36%	0.17%	0.19%	0.09%
H5N3 24H	3.27%	1.99%	1.83%	0.87%	0.94%	0.25%

The global host gene expression profiles were retrieved from microarray analysis with different time points examined. The ratios of differentially expressed genes (P-value≤0.05) up- or down-regulated with different fold changes (≥2-FC, ≥3-FC and ≥5-FC) in relative to their corresponding "expressing genes" are represented in percentage. The expressing genes refer to genes detected in the mock-infected macrophages.

5.3.4.1.3 Functional classification

In macrophages infected with three influenza A strains, most of the genes with up-regulated expression were detected after infection of H5N3 at 24 hpi, followed by infections of H1N1 and H5N2/F118 at 2 hpi [Figure 5.33]. These genes were majorly function-related to "Signaling Transduction", "Antiviral" and "Cytokine", "Cell Death", "DNA Transcription Factor", "Kinase" and "RNA Binding". Compared to situations detected in the early phase of virus infections, infections of H1N1 and H5N2/F118 induced expression of relative low number of genes at late stage, 24 hpi. And this phenomenon might indicate the host immune response became weaken during the late infection phase. Moreover, some of the antiviral and signal transduction associated genes detected after H5N3 infection at 24 hpi also showed up-regulated expression with high-level fold changes.

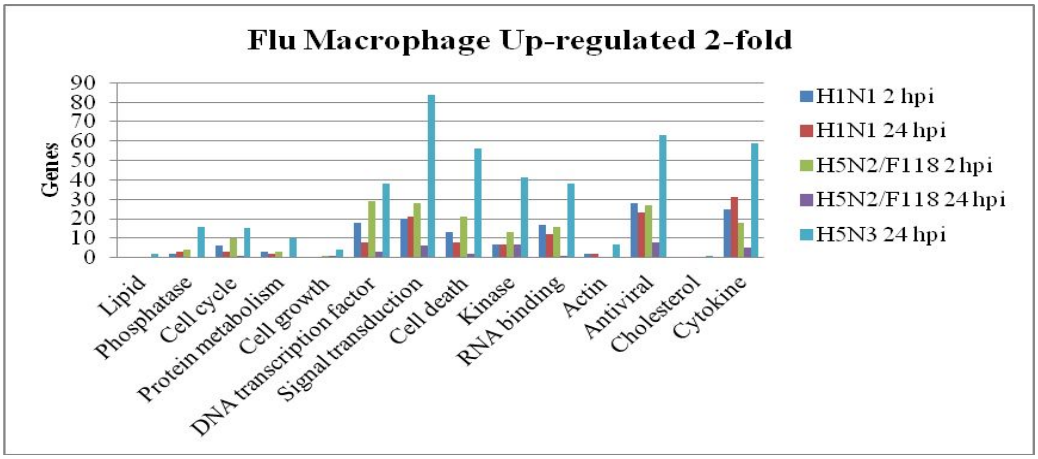

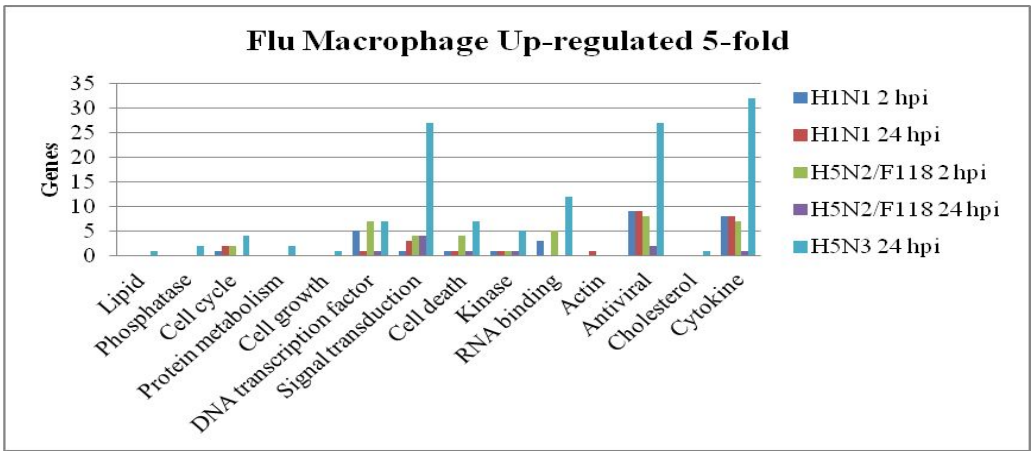

For the genes with down-regulated expression, those detected after infections of H1N1 and H5N2/F118 at 2 hpi were majorly related to "DNA Transcriptional Factor", "Signal Transduction", "Kinase", "RNA Binding" and

"Cell Death", while those detected after infections of H5N3 at 24 hpi were functionally associated with "DNA Transcription Factor", "Signal Transduction", "Kinase", "RNA Binding", "Cell Cycle", "Cell Death" and "Antiviral".

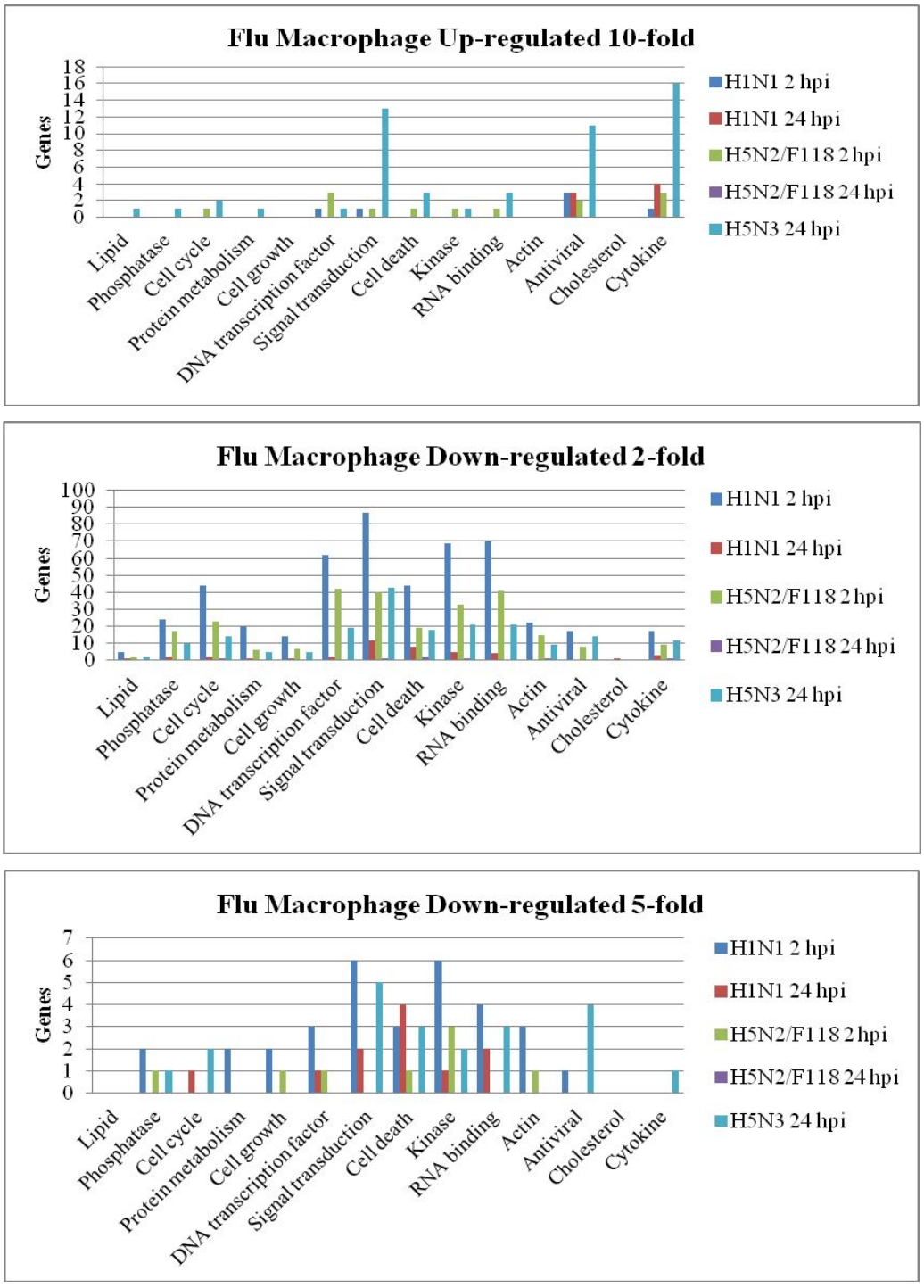

Figure 5.33 Overview of distributions of differentially expressed genes into different biological functions in macrophages infected with influenza A strains. The numbers of genes in the different functional families, showing up-regulated or down-regulated with different fold changes (≥2-FC, ≥5-FC and ≥10-FC) in gene expression are presented.

5.3.4.1.4 Core analysis in macrophages

Subjecting to H1N1 infection at 2 hpi, networks such as “Molecular Transport”, “Cell cycle, DNA replication” and “Cellular Assembly and Organization” were highly scored. Biological functions such as “Inflammatory Response”, “Cancer”, “Cellular Growth and Proliferation”, “Cellular Movement”, “Cell death”, “Cell cycle”, “Tissue Development” were enriched with hundreds of molecules included for each. And “RhoA Signaling”, “Actin Cytoskeleton Signaling”, “ILK Signaling” and “Role of Macrophages, Fibroblasts and Endothelial Cells in Rheumatoid Arthritis” were listed as top canonical pathways as well [Figure 5.34-5.37]. Enrichment of these key functions and pathways might indicate the activation of antiviral actions at a very early infection stage. With the infection time increasing, gene numbers in these biological functions went down, which implied the gradual elimination of cell regulations in response to the H1N1 infection.

In H5N2/F118 infected macrophages, differentially expressed genes were represented by top networks such as “Cell-To-Cell signaling and interaction”, “Cell Growth and Proliferation”, “Cellular Assembly and Organization”, “”Cellular Movement” and top biological functions such as “Cancer”, “Inflammatory Response”, “Cell Cycle”, “Cell Death” and “Tissue Development” at 2 hpi. And pathways named “Role of Pattern Recognition Receptors in Recognition of Bacteria and Viruses”, “Activation of IRF by Cytosolic Pattern Recognition Receptors” and “Role of JAK2 in Hormone-like Cytokine Signaling” were enriched as top canonical pathways at 2 hpi [Figure 5.38-5.39]. At 24 hpi, although inflammatory response related functions and pathways were still listed, the numbers of molecules belonging to these groups became lower, which was similar to the situation happened in H1N1 infected macrophages [Figure 5.40-5.41]. This phenomenon might implicate the weaker host cell response occurred at 24 hpi when compared to 2 hpi in H5N2/F118 infected macrophages.

With regards to H5N3 infected macrophages, the functional groups and pathways relevant to immune response were identified based on differentially expressed genes at 24 hpi [Figure 5.42-5.43]. And almost all of these functional groups were enriched by hundreds of molecules, implicatinging strong immune defense.

H1N1 Macrophage 2 hpi

Top Networks

ID	Associated Network Functions	Score
1	Molecular Transport, Developmental Disorder, Genetic Disorder	47
2	Cell Cycle, DNA Replication, Recombination, and Repair, Cell Morphology	44
3	Cellular Assembly and Organization, Skeletal and Muscular System Development and Function, Cellular Development	42
4	Skeletal and Muscular System Development and Function, Tissue Morphology, Cardiovascular System Development and Function	33
5	Connective Tissue Disorders, Genetic Disorder, Dermatological Diseases and Conditions	29

Top Bio Functions

Diseases and Disorders

Name	p-value	# Molecules
Cancer	1.80E-09 - 4.00E-03	344
Gastrointestinal Disease	1.19E-07 - 4.00E-03	154
Reproductive System Disease	1.52E-07 - 2.83E-03	182
Organismal Injury and Abnormalities	2.99E-07 - 2.48E-03	74
Inflammatory Response	2.69E-06 - 3.67E-03	150

Molecular and Cellular Functions

Name	p-value	# Molecules
Cellular Growth and Proliferation	1.95E-10 - 4.11E-03	272
Cellular Movement	2.94E-08 - 4.13E-03	193
Cell Death	4.65E-07 - 4.22E-03	291
Cellular Development	5.39E-07 - 4.22E-03	241
Cell Cycle	2.23E-06 - 4.22E-03	124

Physiological System Development and Function

Name	p-value	# Molecules
Skeletal and Muscular System Development and Function	4.38E-11 - 4.22E-03	168
Tissue Development	4.38E-11 - 3.87E-03	259
Cardiovascular System Development and Function	6.48E-08 - 3.87E-03	132
Organismal Development	4.16E-07 - 3.87E-03	179
Hematological System Development and Function	2.03E-06 - 4.22E-03	158

Top Canonical Pathways

Name	p-value	Ratio
RhoA Signaling	1.67E-05	20/114 (0.175)
Caveolar-mediated Endocytosis Signaling	3.34E-05	15/85 (0.176)
Actin Cytoskeleton Signaling	1.35E-04	28/238 (0.118)
ILK Signaling	2.95E-04	24/193 (0.124)
Role of Macrophages, Fibroblasts and Endothelial Cells in Rheumatoid Arthritis	4.65E-04	34/336 (0.101)

Figure 5.34 Summary of top functional groups enriched in differentially expressed genes in H1N1-infected with macrophages at 2 hpi. Differentially expressed genes detected at different time points were significantly categorized into different networks, functions and pathways under the analysis of Ingenuity Pathway Analysis (IPA) version 2012 (P-value≤0.05).

A

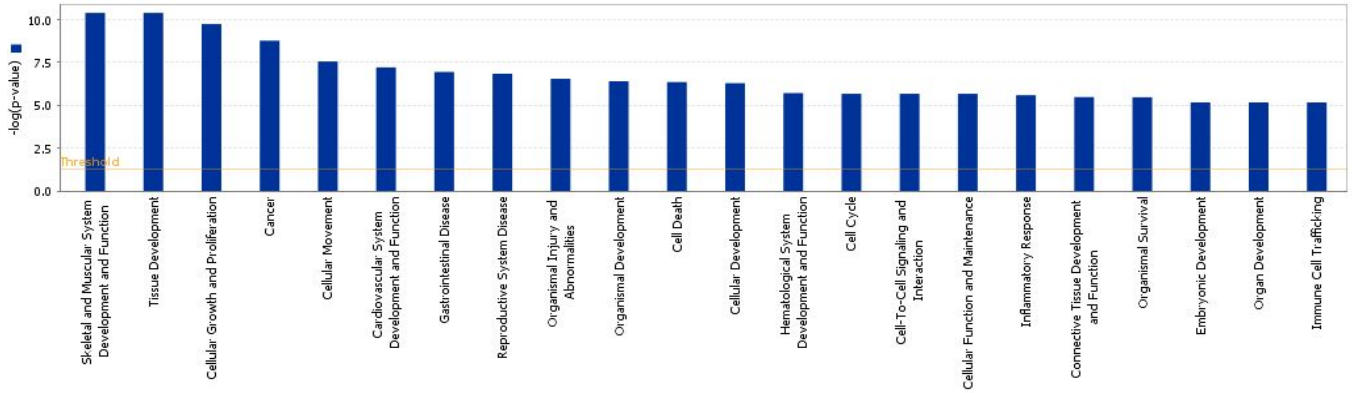

B

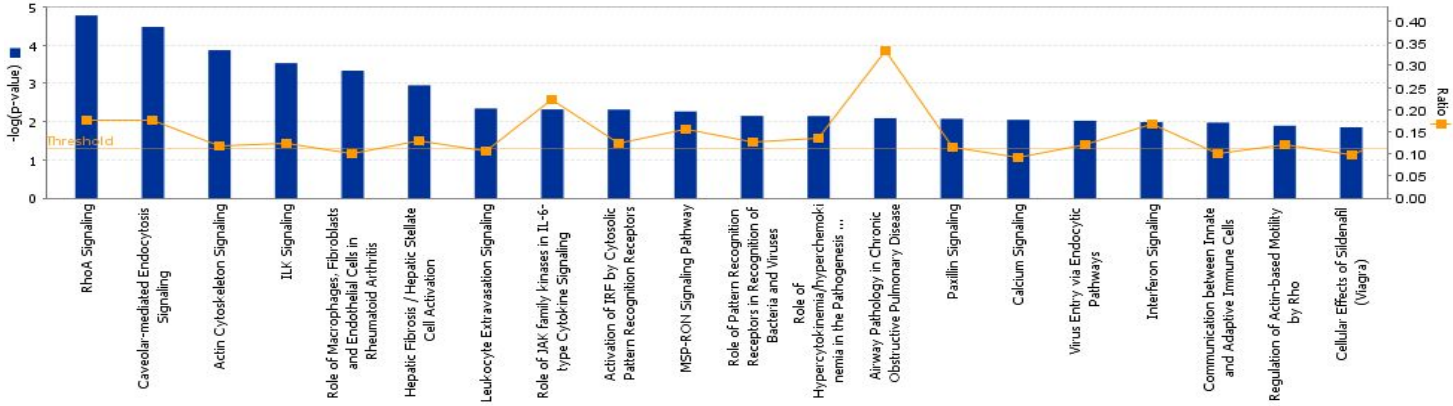

Figure 5.35 **Top 20 (A) biological functions and (B) canonical pathways significantly enriched in differentially expressed genes from H1N1-infected macrophages at 2 hpi (P-value≤0.05).** Threshold was set at p-value = 0.05 and indicated as –log (p-value) on the Y-axis and the X-axis shows the terms of each biological function or canonical pathway. The orange boxes indicate the ratio (Ratio) of the number of genes with differential expression changes and the total number of genes in the respective canonical pathway.

H1N1 Macrophage 24 hpi

Top Networks

ID	Associated Network Functions	Score
1	Infectious Disease, Antimicrobial Response, Inflammatory Response	46
2	Dermatological Diseases and Conditions, Genetic Disorder, Antigen Presentation	46
3	Cell-To-Cell Signaling and Interaction, Cellular Growth and Proliferation, Hematological System Development and Function	41
4	Cell-To-Cell Signaling and Interaction, Hematological System Development and Function, Immune Cell Trafficking	41
5	Cellular Movement, Cellular Assembly and Organization, Cellular Compromise	34

Top Bio Functions

Diseases and Disorders

Name	p-value	# Molecules
Dermatological Diseases and Conditions	3.60E-17 - 3.93E-03	47
Genetic Disorder	3.60E-17 - 3.70E-03	65
Infectious Disease	2.55E-15 - 2.85E-03	48
Inflammatory Response	2.83E-15 - 3.95E-03	66
Antimicrobial Response	9.34E-10 - 3.95E-03	19

Molecular and Cellular Functions

Name	p-value	# Molecules
Cellular Movement	1.66E-10 - 3.95E-03	60
Cell-To-Cell Signaling and Interaction	4.01E-10 - 3.95E-03	56
Antigen Presentation	1.19E-09 - 3.34E-03	36
Cellular Growth and Proliferation	1.42E-07 - 3.86E-03	74
Cell Signaling	1.46E-07 - 1.92E-03	37

Physiological System Development and Function

Name	p-value	# Molecules
Hematological System Development and Function	1.66E-10 - 3.95E-03	58
Immune Cell Trafficking	1.66E-10 - 3.95E-03	40
Tissue Development	1.86E-07 - 3.72E-03	50
Tissue Morphology	7.24E-07 - 3.75E-03	42
Cell-mediated Immune Response	1.09E-05 - 3.95E-03	9

Top Canonical Pathways

Name	p-value	Ratio
Activation of IRF by Cytosolic Pattern Recognition Receptors	8.09E-11	11/72 (0.153)
Interferon Signaling	4.62E-09	8/36 (0.222)
Role of Pattern Recognition Receptors in Recognition of Bacteria and Viruses	6.45E-08	10/87 (0.115)
Role of RIG1-like Receptors in Antiviral Innate Immunity	5.68E-05	5/49 (0.102)
Role of IL-17F in Allergic Inflammatory Airway Diseases	1.6E-04	5/46 (0.109)

Figure 5.36 Summary of top functional groups enriched in differentially expressed genes in H1N1-infected with macrophages at 24 hpi. Differentially expressed genes detected at different time points were significantly categorized into different networks, functions and pathways under the analysis of Ingenuity Pathway Analysis (IPA) version 2012 (P-value≤0.05).

A

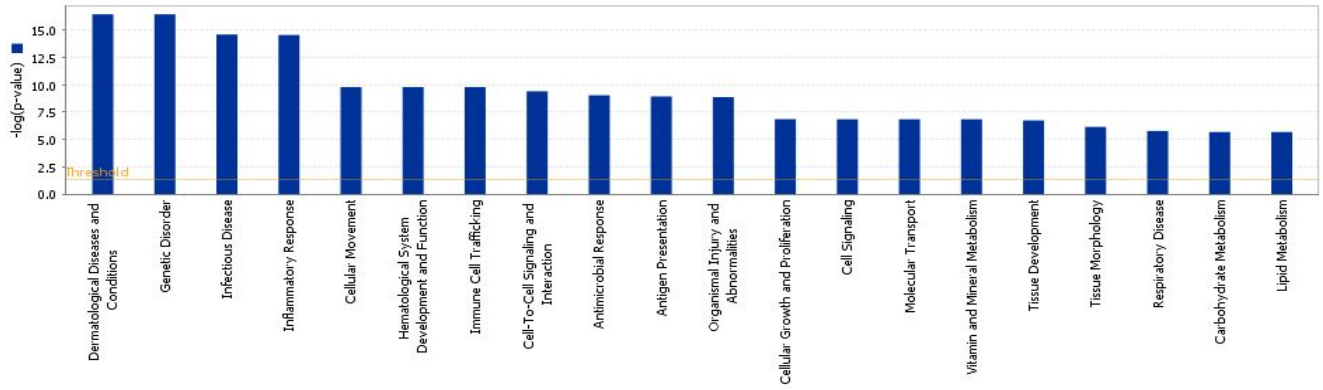

B

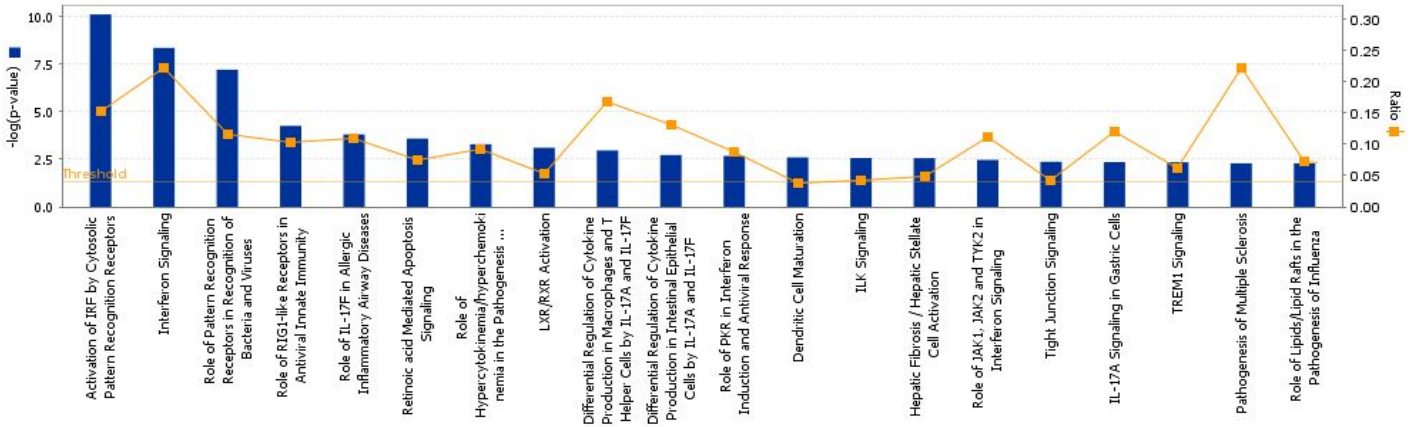

Figure 5.37 Top 20 (A) biological functions and (B) canonical pathways significantly enriched in differentially expressed genes from H1N1-infected macrophages at 24 hpi (P-value≤0.05). Threshold was set at p-value = 0.05 and indicated as –log (p-value) on the Y-axis and the X-axis shows the terms of each biological function or canonical pathway. The orange boxes indicate the ratio (Ratio) of the number of genes with differential expression changes and the total number of genes in the respective canonical pathway.

H5N2/F118 Macrophage 2 hpi

Top Networks

ID	Associated Network Functions	Score
1	Cell-To-Cell Signaling and Interaction, Hematological System Development and Function, Immune Cell Trafficking	38
2	Cellular Growth and Proliferation, Skeletal and Muscular System Development and Function, Embryonic Development	38
3	Cellular Assembly and Organization, Cellular Function and Maintenance, Cell Morphology	36
4	Cellular Development, Nervous System Development and Function, Visual System Development and Function	36
5	Cellular Movement, Tissue Development, Cell-To-Cell Signaling and Interaction	34

Top Bio Functions

Diseases and Disorders

Name	p-value	# Molecules
Cancer	4.97E-17 - 2.72E-03	266
Reproductive System Disease	1.10E-09 - 1.41E-04	156
Inflammatory Response	1.26E-09 - 3.04E-03	115
Dermatological Diseases and Conditions	1.28E-09 - 2.05E-03	75
Genetic Disorder	1.28E-09 - 2.05E-03	113

Molecular and Cellular Functions

Name	p-value	# Molecules
Cellular Movement	3.87E-13 - 3.30E-03	146
Cellular Growth and Proliferation	3.77E-10 - 2.72E-03	219
Cell Cycle	4.30E-10 - 3.24E-03	96
Cell Death	4.85E-10 - 2.99E-03	210
Cellular Development	1.38E-09 - 3.28E-03	187

Physiological System Development and Function

Name	p-value	# Molecules
Organismal Development	1.19E-11 - 3.28E-03	146
Cardiovascular System Development and Function	2.38E-11 - 3.28E-03	95
Tissue Development	4.41E-09 - 3.28E-03	193
Tissue Morphology	1.22E-08 - 3.18E-03	110
Connective Tissue Development and Function	2.21E-08 - 2.92E-03	117

Top Canonical Pathways

Name	p-value	Ratio
Role of Pattern Recognition Receptors in Recognition of Bacteria and Viruses	6.67E-06	13/87 (0.149)
ILK Signaling	7.15E-05	19/193 (0.098)
Caveolar-mediated Endocytosis Signaling	1.11E-04	11/85 (0.129)
Activation of IRF by Cytosolic Pattern Recognition Receptors	1.79E-04	9/72 (0.125)
Role of JAK2 in Hormone-like Cytokine Signaling	2.67E-04	7/37 (0.189)

Figure 5.38 Summary of top functional groups enriched in differentially expressed genes in H5N2/F118-infected with macrophages at 2 hpi. Differentially expressed genes detected at different time points were significantly categorized into different networks, functions and pathways under the analysis of Ingenuity Pathway Analysis (IPA) version 2012 (P-value≤0.05).

A

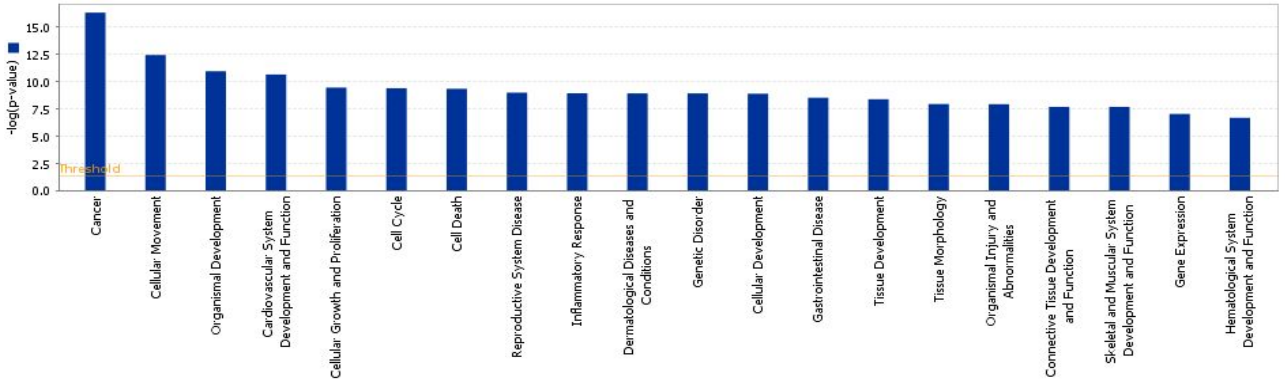

B

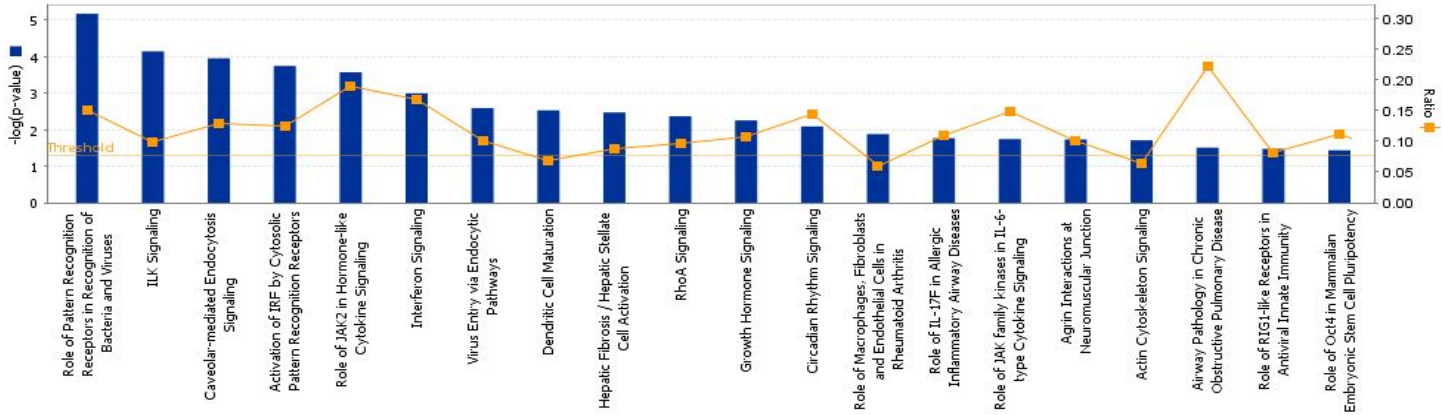

Figure 5.39 Top 20 (A) biological functions and (B) canonical pathways significantly enriched in differentially expressed genes from H5N2/F118-infected macrophages at 2 hpi (P-value≤0.05). Threshold was set at p-value = 0.05 and indicated as –log (p-value) on the Y-axis and the X-axis shows the terms of each biological function or canonical pathway. The orange boxes indicate the ratio (Ratio) of the number of genes with differential expression changes and the total number of genes in the respective canonical pathway.

H5N2/F118 Macrophage 24 hpi

Top Networks

ID	Associated Network Functions	Score
1	Inflammatory Response, Cell-To-Cell Signaling and Interaction, Antigen Presentation	40
2	Cell Signaling, Small Molecule Biochemistry, Cellular Compromise	29
3	Infectious Disease, Cellular Compromise, Gastrointestinal Disease	29
4	Cellular Movement, Immune Cell Trafficking, Hematological System Development and Function	20
5	Infectious Disease, Cell-To-Cell Signaling and Interaction, Connective Tissue Development and Function	17

Top Bio Functions

Diseases and Disorders

Name	p-value	# Molecules
Auditory Disease	6.18E-05 - 2.65E-02	3
Genetic Disorder	6.18E-05 - 4.59E-02	28
Neurological Disease	6.18E-05 - 2.65E-02	5
Antimicrobial Response	9.91E-05 - 2.65E-02	9
Inflammatory Response	9.91E-05 - 4.75E-02	22

Molecular and Cellular Functions

Name	p-value	# Molecules
Cellular Movement	1.19E-04 - 4.75E-02	12
Cell-To-Cell Signaling and Interaction	2.65E-04 - 4.97E-02	12
Cellular Assembly and Organization	2.65E-04 - 4.59E-02	8
Post-Translational Modification	2.65E-04 - 3.95E-02	3
Protein Folding	2.65E-04 - 2.65E-04	2

Physiological System Development and Function

Name	p-value	# Molecules
Hematological System Development and Function	1.19E-04 - 4.75E-02	13
Immune Cell Trafficking	1.19E-04 - 4.75E-02	11
Endocrine System Development and Function	2.65E-04 - 1.99E-02	3
Hematopoiesis	1.21E-03 - 3.95E-02	6
Lymphoid Tissue Structure and Development	1.21E-03 - 3.95E-02	4

Top Canonical Pathways

Name	p-value	Ratio
Activation of IRF by Cytosolic Pattern Recognition Receptors	3.49E-04	4/72 (0.056)
Interferon Signaling	9.44E-04	3/36 (0.083)
Role of Lipids/Lipid Rafts in the Pathogenesis of Influenza	5.23E-02	1/28 (0.036)
Differential Regulation of Cytokine Production in Macrophages and T Helper Cells by IL-17A and IL-17F	9.59E-02	1/18 (0.056)
Cardiomyocyte Differentiation via BMP Receptors	1.08E-01	1/20 (0.05)

Figure 5.40 Summary of top functional groups enriched in differentially expressed genes in H5N2/F118-infected with macrophages at 24 hpi. Differentially expressed genes detected at different time points were significantly categorized into different networks, functions and pathways under the analysis of Ingenuity Pathway Analysis (IPA) version 2012 (P-value≤0.05).

A

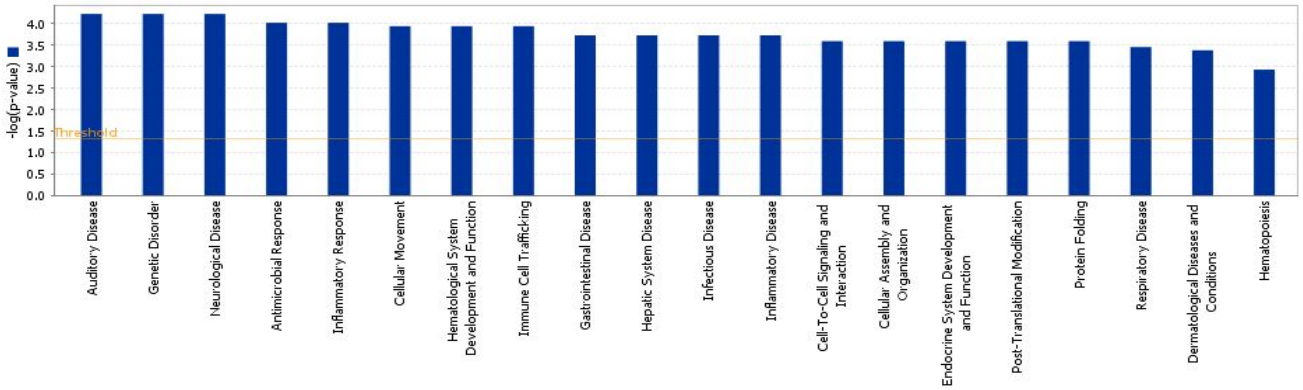

B

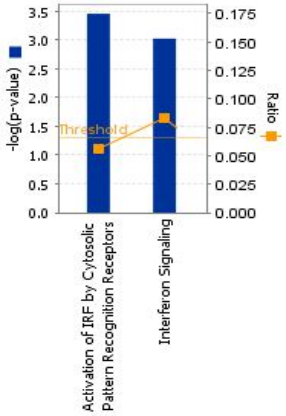

Figure 5.41 Top 20 (A) biological functions and (B) canonical pathways significantly enriched in differentially expressed genes from H5N2/F118-infected macrophages at 24 hpi (P-value≤0.05). Threshold was set at p-value = 0.05 and indicated as –log (p-value) on the Y-axis and the X-axis shows the terms of each biological function or canonical pathway. The orange boxes indicate the ratio (Ratio) of the number of genes with differential expression changes and the total number of genes in the respective canonical pathway.

H5N3 Macrophage 24 hpi

Top Networks

ID	Associated Network Functions	Score
1	Lipid Metabolism, Small Molecule Biochemistry, Gene Expression	44
2	Cell Death, Inflammatory Response, Hematological System Development and Function	37
3	Cell-To-Cell Signaling and Interaction, Cellular Movement, Cellular Growth and Proliferation	35
4	Antigen Presentation, Cell-To-Cell Signaling and Interaction, Hematological System Development and Function	35
5	Dermatological Diseases and Conditions, Genetic Disorder, Antimicrobial Response	33

Top Bio Functions

Diseases and Disorders

Name	p-value	# Molecules
Inflammatory Response	4.50E-94 - 7.20E-10	307
Cancer	1.60E-37 - 9.65E-10	372
Immunological Disease	6.51E-35 - 3.84E-10	278
Connective Tissue Disorders	4.12E-32 - 1.90E-10	221
Inflammatory Disease	4.12E-32 - 1.90E-10	329

Molecular and Cellular Functions

Name	p-value	# Molecules
Cellular Movement	6.28E-61 - 6.96E-10	257
Cell-To-Cell Signaling and Interaction	9.37E-50 - 7.20E-10	257
Cellular Growth and Proliferation	2.51E-43 - 9.63E-10	333
Cell Death	1.36E-39 - 6.13E-10	341
Antigen Presentation	2.56E-33 - 7.20E-10	169

Physiological System Development and Function

Name	p-value	# Molecules
Immune Cell Trafficking	6.28E-61 - 6.96E-10	231
Hematological System Development and Function	2.62E-57 - 9.63E-10	310
Tissue Morphology	3.06E-45 - 3.82E-10	203
Tissue Development	2.76E-38 - 5.50E-10	294
Organismal Survival	3.26E-35 - 1.49E-17	187

Top Canonical Pathways

Name	p-value	Ratio
Dendritic Cell Maturation	6.15E-21	40/188 (0.213)
Communication between Innate and Adaptive Immune Cells	3.43E-17	26/109 (0.239)
Role of Pattern Recognition Receptors in Recognition of Bacteria and Viruses	3.76E-17	27/87 (0.31)
Hepatic Fibrosis / Hepatic Stellate Cell Activation	3.12E-16	35/147 (0.238)
Activation of IRF by Cytosolic Pattern Recognition Receptors	8.09E-15	21/72 (0.292)

Figure 5.42 Summary of top functional groups enriched in differentially expressed genes in H5N3-infected with macrophages at 24 hpi. Differentially expressed genes detected at different time points were significantly categorized into different networks, functions and pathways under the analysis of Ingenuity Pathway Analysis (IPA) version 2012 analysis (P-value≤0.05).

A

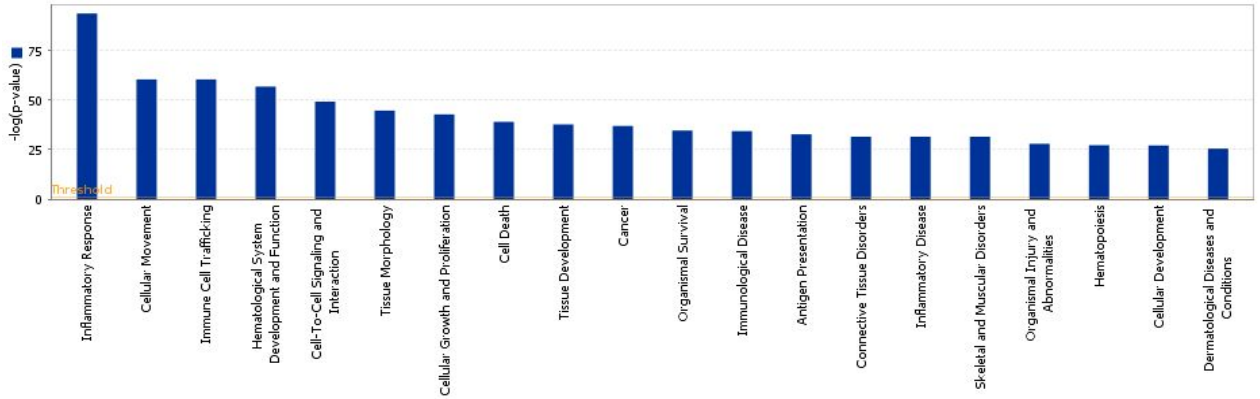

B

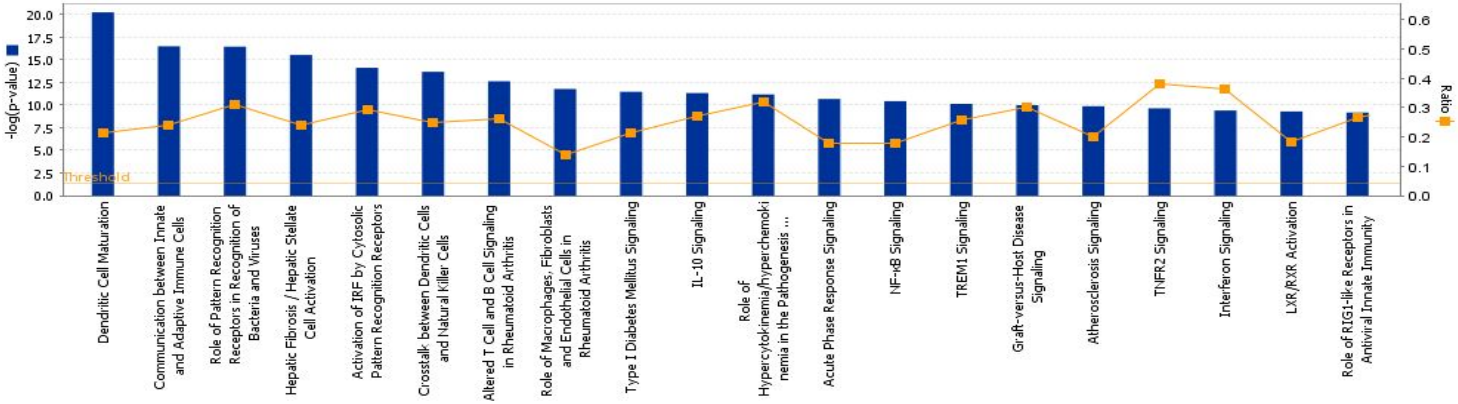

Figure 5.43 Top 20 (A) biological functions and (B) canonical pathways significantly enriched in differentially expressed genes from H5N3-infected macrophages at 24 hpi (P-value≤0.05). Threshold was set at p-value = 0.05 and indicated as –log (p-value) on the Y-axis and the X-axis shows the terms of each biological function or canonical pathway. The orange boxes indicate the ratio (Ratio) of the number of genes with differential expression changes and the total number of genes in the respective canonical pathway.

5.3.4.2. Regulations of gene expression in canonical pathways

5.3.4.2.1 Interferon signaling

In macrophages following infections of influenza A viruses, the activation of IFN signaling pathway was observed. Among three influenza A strains, H5N3 infection globally initiated the significant up-regulation of gene expression levels in IFN pathway (particularly type I) at 24 hpi, followed by H1N1 infection. These up-regulated genes included JAK2, STAT1/2, OAS1, IFIT3, IRF9 and so on. H5N2/F118 infection also caused expression induction of several genes in IFN pathway at 2hpi, but few expression changes were identified at 24 hpi. And we assumed that some mechanism might potentially play a role to suppress the activation of IFN signaling pathway at the later stage of H5N2/F118 infection in macrophages.

5.3.4.2.2 NF-κB signaling

In H5N3-infected macrophages, many genes involved in NF-κB signaling pathway showed up-regulated expression. A20, TNFα and CD40 also showed strong induction at their expression level, which might be responsible for the activation and inhibition of NF-κB signaling pathway. It was surprising that genes in NF-κB signaling pathway almost showed no expression changes in both H5N2/F118 and H1N1-infected macrophages.

5.3.4.2.3 Toll-like receptor signaling

H5N3 infection in macrophages resulted in the similar gene expression pattern between at 2 and 24hpi, with expression levels of genes including TLR2, CD14, MYD88, NF-κB and p38 MAPK all showing elevated. Gene expression performance of TLR signaling pathway in after infections of H1N1 and H5N2/F118 showed different when compared to the performance after infection of H5N3. H5N2/F118 infection caused faint down-regulation of TLR1 and p38 MAPK in their expression at 2 hpi, with no expression change detected at 24 hpi. Whereas, H1N1 infection resulted in faint down-regulation expression of TLR1, TLR4 and p38 MAPK at 2 hpi, with exception of TLR2 and PKR showing faint up-regulation expression at 24 hpi.

5.3.4.2.4 Antigen presentation pathway

The situation was a bit complicated in H5N3 infected macrophages. Although some factors in MHC I-α group showed up-regulated expression but some showed down-regulated expression, and the up-regulated expression of downstream genes made the hypothesis convincible that MHC I antigen presentation was activated. Furthermore, MHC II-α antigen presentation pathway also displayed in an activated state, suggesting high activation of macrophages after H5N3 infection at 24 hpi.

The status of antigen presentation pathway in H1N1 infected macrophages was similar to in H5N2/F118 infected macrophages. MHC I-α was detected with repressed expression during H5N2/F118 infection and both MHC I-α and MHC II-β were identified with repressed expression during H1N1 infection. And when it comes to 24 hpi, genes in both antigen presentation pathways showed no expression changes.

5.4 Conclusion

Although the associated fatalities due to human transmission of LPAI viruses have not been reported, the LPAI viruses have the potentiality to develop into HPAI viruses, transmission of which are often associated with high fatality rates. In this project, the host response to the low LAPI H5N2, H9N2, H5N3 and H7N1 were investigated in A549, CEF and MDCK cells based on microarray platform. And host response to another human influenza strains H1N1 and pH1N1 were also involved in corresponding cell types for parallel comparison. Besides, the host response to low LAPI H5N2 and H5N3 as well as human strain H1N1 were also examined and compared in mouse macrophages.

Global evaluation of probe sets with differential expression suggest that host genes performed differently even if the different cell types were infected with the same influenza A strain. After infection of H1N1, half of the probe sets in A549 and MDCK cells showed down-regulated expression while only a small portion of probe sets showed down-regulated expression in CEF cells. In host cells infected with H9N2, more probe sets with down-regulated expression and less probe sets with up-regulated expression were observed in CEF cells compared to A549 and MDCK cells. In addition, the global gene expression

profiles detected in H5N2/F118 infected CEF and MDCK cells were far away from the one detected in H5N2/F118 infected A549 cells. And compared to situations happed in CEF and MDCK cells, smaller fraction of probe sets with decreased expression and larger fraction of probe sets with increased expression were identified after H5N2/F118 infection in A549 cells.

Further investigation at 10 hpi also indicated the global gene expression profiles were also different upon infections of different influenza A strains in specific cell types. Among these different strains, infections of LPAI H5N3, H5N2/F59, H5N2/F118 as well as H9N2 and infection of human influenza A strain pH1N1 caused the largest numbers of probe sets with up-regulated expression at 10 hpi in A549 cells. Whereas, infections of two human influenza A strains, especially H1N1, and two LPAI H5N2/F59 and H5N2/F189 led to the largest numbers of probe sets with down-regulated expression at 10 hpi. In CEF cells, infection of human strain H1N1 resulted in the highest number of probe sets with up-regulated expression but lowest number of those with down-regulated expression at 10 hpi. The distribution of differentially expressed genes showed different in CEF cells after infections of different LAPI viruses, even three H5N2 strains. In MDCK cells, infection of human strain H1N1 led to not only the largest number of probe sets with down-regulated expression but also relative big number of probe sets with up-regulated expression at 10 hpi. Results from macrophages suggested that H5N3 infection contributed to larger number of differentially expression probe sets, either up- or down-regulated, when compared to H1N1 and H5N2/F118 infections at 24 hpi.

By assigning these probe sets encoded genes to certain biological processes or pathways, it was noted that functional classifications such as “Immune Response”, “DNA Binding”, “RNA Binding” and “Signal Transduction” were over-represented based on up-regulated probe sets in A549 cells infected with LPAI virus, especially H5N2/F118 and H9N2. And those probe sets classified into “Immune response” showed high fold changes at their expression level. Down-regulated probe sets were majorly grouped into functions such as “DNA Binding”, “RNA Binding”, “Transcription factor” and “Signal Transduction”, particularly in H1N1 infected A549 cells. In macrophages, H5N3 infection induced expression of relative high number of probe sets related to “Signal Transduction” and “Antiviral” at 24 hpi, while

H1N1 infection repressed expression of considerable big number of probe sets associated with “Signal Transduction”, “Cell Cycle”, “Cell Death” and “Kinase” at 2 hpi. Since the annotation of probe sets in Chicken Genome and Canine Genome 2.0 Array is not complete, only part of these probe sets were classified into listed groups.

Detailed investigation also displayed that common functional groups such as response to virus and nucleic acid binding were enriched in genes with up-regulated expression following infections of two avian strains (H5N2/F118 and H9N2) and one human strain pH1N1/478. Moreover, the avian viruses had more functional groups in common with each other and these genes were involved in immune response, cytokine receptor binding, transition metal ion binding and cell death. In contrast to the differentially up-regulated genes, common functional gene groupings (e.g. genes involved in nitrogen compound metabolic process, regulation of macromolecule metabolic process, nucleic acid binding) were observed based on down-regulatd genes between the human and avian virus infections, with a greater number of genes involved in the former infections. Specific to the 2 human viruses, the genes involved in the protein metabolic-related processes, zinc ion binding and ATP binding showed a decreasing temporal trend in the expression profiles, especially after H1N1 infection. In CEF cells, genes with down-regulated expression were also enriched in pathways with various cellular functions after infections of three influenza A strains, especially H5N2/F118. In macrophages, similar functional groups that are related to inflammatory reponse were detected following infection of all three influenza A strains. However, larger number of molecules belonged to these functions following H5N3 infection at 24 hpi, indicating the stronger antiviral actions at the late infection stage.

Besides these well-known functional groups, other pathways such as “Cytokine-Cytokine receptor interaction” and “RIG-I like receptor signaling pathway” were commonly enriched in genes with up-regulated expression from both two avian strains (H5N2/F118 and H9N2) and two human strains (H1N1 and pH1N1) infected A549 cells, while other pathways such as “Jak-STAT signaling” and “Toll-like receptor signaling pathway” were found only be enriched in genes with up-regulated expression from the two avian strains infected A549 cells. These canonical pathways play important role in innate

immune response, over-representation of them in genes with up-regulated expression indicated that the antiviral response were efficiently triggered in infected host cells, especially after avian strains infections. Further analysis revealed that pathways involving different cell activities such as “Cell cycle”, “Metabolic” and “Endocytosis” were enriched in genes with down-regulated expression in human strains infected A549 cells, suggesting the inhibition of normal cell regulations in various aspects.

Furthermore, a couple of potential transcriptional factors were also significantly enriched based on differentially expressed genes in infected A549 cells. For example, transcription factors such as IRF-1, IRF-3 and IRF-7 were found to be enriched in probe sets with up-regulated expression from A549 cells infected with two avian strains H5N2/F118 and H9N2 and human strain pH1N1; transcription factors such as E2F, ETF and Sp1 were identified to be enriched in probe sets with down-regulated expression from A549 cells that were majorly infected with two human strains and avian strain H5N2/F118.

Pathways analysis revealed that the signaling transduction in immune response was initiated in A549 cells infected with several avian strains such as H5N2/F118 and H9N2. Whereas, the signaling transduction in immune response pathways was impaired to some extend in A549 cells infected with two human strains, in particular H1N1. As to the gene expression performances in infected A549 cells, the key genes participating in cell cycle checkpoint regulation were found to be inhibited in their expression particularly following infections of human strains, which was consistent with previous findings. All together, these mechanisms such as the impairment of the inflammatory response and arrest of cell cycle in infected host A549 cells after infections of two human strains might be a solution to benefit the viral replication.

Recently, host responses of different influenza A strains in different cell lines were also investigated by other groups. Gerlach RL et al (2013) did microarray studies on well-differentiated normal human bronchial epithelial cells upon infection of a H1N1 seasonal isolate (A/BN/59/07) and two H1N1 pandemic isolates: fatal one (A/KY/180/10) and nonfatal one (A/KY/136/09) [383]. Analysis on the data indicated that cells infected with A/KY/180/10 showed a greater difference in gene expression levels when compared to another two isolates. Besides, many genes from the early innate immune

response pathways showed common stimulated expression to infections of these three isolates. However, infections of pH1N1/478 and H1N1/WS resulted in lower expression level of ISGs and larger number of genes with down-regulated expression when compared to observations from this study. In another report, the virus-host interactions at 24hpi in human bronchial airway epithelial cells infected with H1N1 (A/PR/8/34) virus were defined through quantifying host protein alteration. Their findings demonstrated that proteins functionally related to protein metabolism, purine biosynthesis, cytoskeleton and carbohydrate showed elevated expression [390]. Comparably, although genes associated with these functions also showing up-regulated expression were observed in A549 cells after infection of two human strains, the numbers are quite limited. These differences might be partly caused by the different host cells and the post-infection stage.

Chapter VI. Poxviruses

6.1 Introduction

The Poxviridae, as a large family of viruses, infect a wide range of vertebrates and invertebrate animals. Poxviruses are of serious concern due to their high pathogenicity and wide distribution. The best studied poxviruses include variola virus, vaccinia virus, cowpox virus and monkeypox virus. These poxviruses all belong to Orthopoxvirus genus and become considerable concern for public health and biodefense [307, 308]. Global eradication of smallpox was achieved decades ago initiated by the WHO, and the eradication used vaccinia virus as a live vaccine [309].

Poxviruses are different from other animal viruses in several respects. First, many enzymes encoded by poxviruses are necessary for either macromolecular precursor pool regulation or biosynthetic processes. Second, the complex morphogenesis of poxviruses is involved in the composition of virus-specific membranes and inclusion bodies. Lastly, the genomes of poxviruses are able to encode many proteins that interact with host factors at cellular or systemic levels.

6.1.1 Virus structure

Poxviruses constitute a large family of enveloped DNA viruses, with large size genomes from 150 to 300 kbp that encode 200 or more open reading frames. The functions of these encoding proteins include synthesis of viral RNA/DNA, assembly of virion and modulation of host immune defenses [310].

There are two unique forms of infectious particles: intracellular mature virions (IMV) and extracellular enveloped virions (EEV). Compared to IMVs, EEVs have one additional membrane. Specifically, IMVs consist of the viral core containing the dsDNA genome encased in a proteinaceous core with around 60 viral proteins, and one lipid bilayer containing around 25 viral proteins while EVs consist of an MV-like particle surrounded by a second viral membrane containing cellular and at least six unique viral proteins. From the functional perspective, IMVs are the more abundantly produced infectious form and are thought to mediate host-to-host transmission, while EEVs disseminate virus in the infected host and protect against immune defenses [311].

6.1.2 Virus replication cycle

6.1.2.1 Virus Entry

Entry of enveloped viruses can be divided into three steps: virus attachment, fusion activation, and membrane fusion. Initial study on entry of vaccinia virus has depicted that IMV entry into host cells by phagocytosis first and then IMV fuse with the plasma membrane. Carter GC *et al* (2005) have also discovered that the effect of soluble GAGs on IMV infectivity is cell type-specific [312]. In addition, reinvestigation by electron and confocal microscopy has demonstrated that IMV enter into cells by fusion of its single membrane with the plasma membrane. And this fused membrane is then flattened into the plane of the cell surface, with a naked core released into the cytoplasm. As to EEVs, disruption of the EEV wrapper within endosomes has been suggested and after that, IMVs membrane is exposed. And then IMVs' entry follows the same steps as described above [310]. In this process, studies revealed that two viral proteins A28 and H2 were each required for cell entry and cell-cell fusion [313].

6.2.1.2 DNA release from the core to cytoplasm

Following attachment to cell surfaces and fusion with the plasma membrane, DNA-containing core is delivered into the cytoplasm. After penetration, cores can bind to the microtubules (MTs) and then reach the site of disassembly and DNA-release with the assistance of MTs. Under these apparent core movements, early proteins synthesis that is necessary for core uncoating is moving forward. Poxvirus cores enable to harbor the viral DNA-dependent RNA polymerase and transcription factors necessary for gene expression at early stage. Previous researches have proposed that core must contain pores that allow the release of the early mRNAs into the cytoplasm but avoid the entry of DNAse into the core. After these early mRNAs release from the core, they travel along MTs to the location where they become anchored into translation competent complexes. In this process, L4R as a core-associated protein may help mediate the binding and translation of early mRNAs to or along MTs. After synthesis of at least 100 early proteins, the parental DNA is finally released into cytoplasm from the core. During this process, some other viral factors excluding early proteins are also associated with the DNA release.

These factors include B1R kinase, I3L, H5R and E8R. These key factors including early proteins may be required to uncoat the core so as to mediate DNA release, and they also serve to anchor-release DNA to the ER in order to protect it against degradation before DNA replication in next step.

6.1.2.3 DNA replication

Released DNA is tightly associated with rER by a complex of early proteins and the DNA replication occurs in ER-enwrapped cytoplasmic sites. Upon the initiation of replication, ER cisternae are recruited to and enclose the replication sites in order to create a cytosolic subcompartment that facilitates viral DNA synthesis. These new synthesized mRNAs move away from their site of synthesis for future efficient assembly.

Along with DNA replication, intermediate and late genes are transcribed. The expression of intermediate genes that encode specific transcription factors of late gene is triggered by the intermediate transcription factors. The late genes primarily include structural proteins required for progeny virion assembly and enzymes needed for early gene expression during the next round of infection. Two factors, E8R and A40R, are indispensable in this process.

6.1.2.4 Virus assembly

Virus assembly is generally initiated from 5 hpi. Crescent-shaped membrane appears on the sites of DNA replication, accompanying with the breakdown of the rER envelop. More than 80 viral genes are involved in the assembly of MV. After integral viral membrane proteins made in the ER, they are transported to viral factories along with ER derived lipid to be assembled into crescents which contain a lipid bilayer and the membrane proteins, scaffolded on a honeycomb structure composed of the D13 protein. Crescent formation is controlled by phosphorylation. The crescents become into immature virions (IVs) accompanied by encapsidation of the genome. Metamorphosis to IMVs is accompanied by loss of the D13 scaffold, proteolysis, as well as further addition of membrane proteins and movement of particles outside of factories. IMV acquire Golgi derived membranes to become wrapped virions (WVs), which is a intermediate state between IMVs and EEVs. In the last stage, WVs are exocytosed through the plasma membrane to become

EEVs [314]. In addition to the viral D13 scaffold protein, a series of known viral proteins are also necessary for the poxvirus assembly process. For instance, several membrane (A14 and A17) and nonmembrane (A11, F10, G5, and H5) viral proteins are required for crescent formation; A9 protein is necessary at a later stage of morphogenesis [308].

6.1.3 Viral-Host interactions

Host cells will initiate a series of innate and adaptive immune response pathways in react to the invasion of poxvirus. The details include detection of the pathogen, induction of the cytokine responses, establishment of the anti-viral state and so on. In the meanwhile, poxviruses, as a large type of dsDNA evolves extremely sophisticated mechanisms for evading the immune system [11].

6.1.3.1 Blockade of interferon response

Poxvirus evolves several strategies to counteract the interferon response: (1) Montanuy I *et al* (2011) has proposed that GAGs mediated retention of the poxvirus type I interferon binding protein so as to locally block interferon antiviral responses [316]. In their experiment, they treated variola virus and monkeypox virus as experimental targets and discovered the interaction between soluble viral IFN type I receptor potential and GAGs. However, there is a big structural variation existing within GAGs due to their composition, linkage, or modification. In their case, site-directed mutagenesis of poxvirus basic residues in the first Ig domain of the protein rendered IFNα/β unable to interact with the cell surface; (2) Meng X *et al* (2012) recently has proved that K1L and C7L antagonized type I IFNs and IRF1-induced antiviral activities, and this function of C7L was observed evolutionally conserved in all poxviruses [317]; (3) Poxvirus-encoded IFN-γ binding protein has been reported to be able to dampen the host immune response although they were not required for virus replication in *vitro* [318]; (4) Experiment targeting to vaccinia virus also indicated that B18R competitively bound to and inhibited a broad range of type I IFNs so that the induction of anti-viral response was blocked [319]; (5) Besides these above descriptions, a series of vaccinia virus-encoding

proteins was proved to suppress the IFN pathways from different ways [Figure 6.1].

6.1.3.2 Suppression of cytokine signaling

During virus infection, many cytokines are produced by the host system to counter the effect of the viral presence. In the meanwhile, different immune evasion mechanisms also were initiated by poxviruses to lower these cytokines' expression levels. To date, a few studies coming from different research groups have already provided evidences for interactions between cytokines and poxviruses. For instance, Smith VP *et al* (2000) have discovered that poxviruses secreted and expressed inhibitors of cytokines such as soluble IL18-binding protein that was expressed in all lister virus, ectromelia and cowpox virus infected KG-1 cells [320]; Another group has reported that ectromelia virus encoded a homologue of CD30, which was capable to block the binding of CD30L to its receptor and induce reverse signaling in cells expressing CD30L.

Moreover, the viral CD30 has been observed to abrogate T cell proliferation, therefore it blocked type 1 cytokine–mediated T cell responses [322]; An ectromelia virus protein called E163 has been also identified to interact with chemokines so as to influence the chemokines activities. Interaction of certain chemokines with GAGs is crucial for the correct function of the chemokines network. However, E163 protein has also been proved to have high affinity to interact with GAGs binding domain of those chemokines, thus E163 indirectly blocked the chemokine-GAGs interaction and further influenced the chemokines mediated immune response [323, 324].

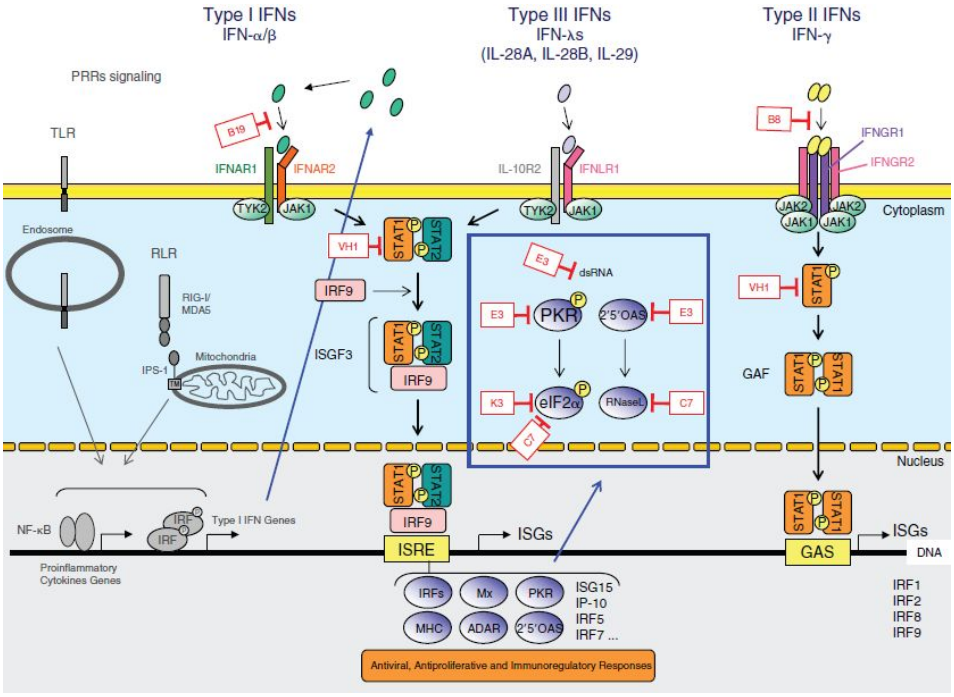

Figure 6.1 Interplay between IFN-signaling pathways and vaccinia virus proteins (adapted from Perdiguero B *et al*., 2009) [321]. Vaccinia virus encodes IFN receptors B8 and B19 which block the binding of IFNs to their cell surface receptors. The E3L gene encodes a protein that is capable to inhibit PKR activation and block IFN responses. The E3 blocks the IFN-induced 2'-5'-OAS antiviral pathway. An eIF2α homolog encoded by K3L t interferes with PKR. Through dephosphorylation of STAT1, the VH1 phosphatase also intercepts the IFN signaling pathway.

6.1.3.3 Inhibition of TNF-induced responses

It has been well known that poxviruses encode a variety of proteins that interfere the activation of NF-κB in order to further impair the TNF-induced responses. In one strategy, many poxviruses express soluble viral receptors or cytokine binding proteins which can intercept cellular ligand-receptor interactions, thus blocking the signaling that lead to NF-κB activation. Relative proteins include T2 that is expressed as a secreted glycoprotein for binding and inhibiting TNF detected in myxoma virus infected rabbit host, cytokine response modifier B, C, D and E which act as soluble vTNFRs to intercept TNF ligand-receptor interaction in cowpox virus with other orthologs also found in other poxviruses, CD30 that acts as a receptor of CD153, and so on [325]. Another strategy adopted is to express intracellular factors to regulate signaling pathways leading to NF-κB activation. For instance, vaccinia protein A46R has been reported to target the host TIR adaptors myeloid differentiation factor (MyD88) and TRIF, thereby interfered with downstream activation of NF-κB, MAP kinase and IFN-β [326]. Moreover, another Ankyrin repeat (ANK) NF-κB

inhibitor also has been discovered to be encoded by cowpox virus. Detailed studies depicted that ANK proteins interacted directly with NF-κB1/p105 so as to inhibit NF-κB signaling pathway [327]. And perhaps most surprising of all, MC159 protein from molluscum contagiosum poxvirus just has been proved to have an ability to interact with the IκB kinase complex in order to inhibit NF-κB activation [328].

6.1.3.4 T-cell evasion by repression of MHC I expression

CD8+ T-cell-mediated responses function on the control of infection of intracellular pathogens. T-cells will become activated once their T-cell receptor recognizes an antigen-derived peptide presented by MHC I. Thus, in order to avoid presentation of viral peptides and kill the infected cells via CD8+ T-cell many viruses interfere with the MHC I presentation pathway in different ways such as MHC I expression, proteasomal protein degradation, TAP-mediated peptides transportation, MHC I peptide complex assembly or trafficking [329].

Results obtained from Byun M *et al* (2009) indicated that cowpox virus inhibited expression of MHC class I by dissociation of MHC class I from TAP [330]. Another report pointed out cowpox virus interfered with CD8+ responses in another way. In the experiment, the cowpox virus was found to inhibit the intracellular transport of MHC I at the early infection stage. This mechanism was able to completely inhibit MHC I exit from the endoplasmic reticulum, independent of viral replication [331].

6.1.3.5 Blockade of host cell apoptosis

Induction of apoptosis is essential for elimination of pathogen infection. In reaction to this pressure initiated from host system, viruses such as poxviruses have evolved some mechanisms by which the cell apoptosis is blocked, and thereby the successful replication and dissemination are guaranteed.

Caspases activation and apoptotic death can be triggered by both extrinsic and intrinsic signals [332]. Stewart TL *et al* (2005) reported a finding that vaccinia virus encoding F1L, a new member of the tail-anchored protein family, localized to mitochondria during virus infection, leading to inhibit cell apoptosis and enhance virus survival [333]. In another experiment, a poxvirus-

encoded protein called M13L-PYD was identified. This protein was proved to colocalize and interact with a cellular PYD protein, ASC-1, as a mean to modulate caspase-1 activity and process IL-1β and IL-18, in further inhibit host inflammatory and apoptotic responses to infection [334]. Other interesting finding demonstrated the presence of a TNFR-like T2 protein in all poxviruses, and this T2 protein physically associated with and colocalized with human TNFRs so that inhibited cellular TNFR1-induced cell death [335].

6.1.4 Poxviruses infections in different host cells

Several reports have been published to uncover the viral strategy and host response in different cells following infections of different types of poxviruses. For example, Turner PC *et al* (2002) summarized that different immune modulators expressed by poxviruses function on suppressing the host response to infections [336]. Besides, they described that multiple modulators were able to target the same pathways at different steps. A high-density microarray was applied to analyze the host response in NYVAC infected Hela cells. The result suggested that expression of apoptotic genes and NF-κB responsive genes were stimulated. At the meanwhile, vaccinia K1L gene played a role to inhibit the NF-κB activation [337]. It was also discovered that ectromelia virus encoded a protein homologous to the ectodomain of the IFN-γ receptor 1, and this protein enabled to bind IFN-γ and subsequently dampened the host immune response to virus infection in host cells [318].

6.1.5 Objective

As the largest known DNA viruses, members of the *Poxviridae* family infect both vertebrate and invertebrate animals. Orthopoxvirus, as a genus of Poxviridae, includes many virus species such as variola, monkeypox, vaccinia and cowpox viruses. Infection of these viruses results in febrile illnesses associated with vesicular rash in humans and animals. The most notorious member is variola virus that caused the outbreak of the disease called smallpox with about 500 million deaths during the 1900s. And until 1980, WHO announced that the world was finally free of it [338]. Till now, although studies on the complex interactions between host cells and poxviruses are among well understood, the functions of critical genes which contribute to poxvirus biology still remains to be enriched.

Since we can't use the actual smallpox virus, we focused our researches on another three types of poxviruses. Cowpox virus is the closest relative to smallpox virus and is a good surrogate virus [281]. It got its name from the distribution of the disease when dairymaids touched the udders of infected cows. Cowpox is similar to but much milder than the highly contagious and often deadly smallpox disease. It resembles mild smallpox, and was the basis of the first smallpox vaccines. When the patient recovers from cowpox, the person is immune to smallpox. Lister virus is one subtype of vaccinia virus, and vaccinia virus is the vaccine for smallpox virus and as the vaccine gives side effects. Thus it is worthy while investigating the host response. Ectromelia virus is able to cause fatal mousepox. It is the only poxvirus to cause disease naturally in mice. In our experiment, mousepox is used to compare with other poxviruses as RAW cells originated from mice and mousepox is a good control to study whether RAW cells can be used as a study model [282].

In our study, three types of poxviruses were infected with A549 and mouse RAW cells at specific time points. The corresponding transciptomic profiles were examined using microarray platform. Different types of software were employed into further analysis. The aims of this research are as following:

(1). Investigate the viral-host interactions in poxviruses infected A549 cells.
(2). Investigate the viral-host interactions in poxviruses infected mouse RAW cells.
(3). Compare the different gene expression performances after infections of different types of poxviruses in different host cells.

6.2 Experiment workflow

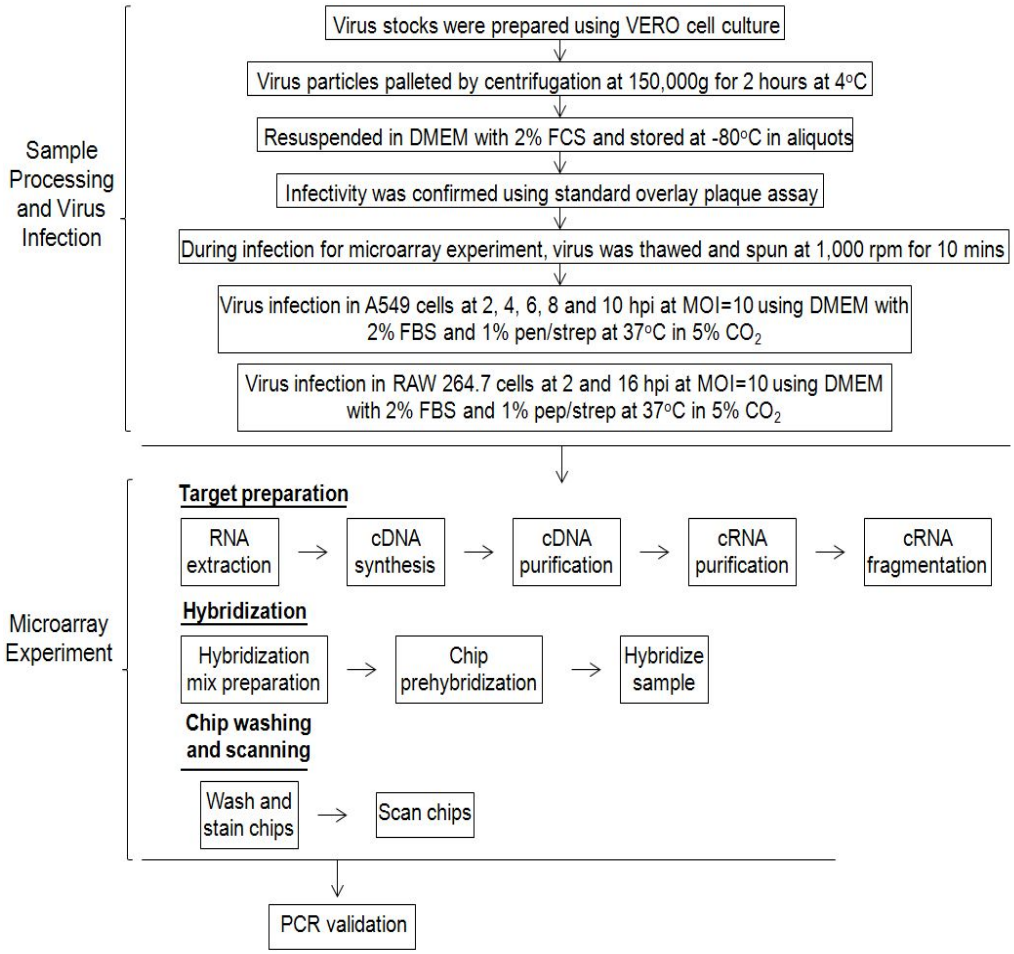

Figure 6.2 Microarray experimental workflow during different types of poxviruses infections.

6.3 Result and Discussion

6.3.1 Global Profiling of gene expression

6.3.1.1 Heat maps of global gene expression

The global transcriptional profiles in two types of poxviruses infected A549 cells illustrated that most of the differentially expressed probe sets showed down-regulated expression changes. Compared to lister virus, infection of cowpox virus led to less probe sets with up-regulated expression but more probe sets with down-regulated expression.

The numbers of probe sets with up-regulated expression showed in an increasing trend with the infection time increasing in two types of poxviruses infected A549 cells. However, the situation for probe sets with down-regulated expression was complicated. In cowpox virus-infected A549 cells, considerable numbers of probe sets with down-regulated expression was observed from 4 hpi, with the largest number detected around 8 hpi. At the meanwhile, a sharp

increase of numbers of probe sets with down-regulated expression was observed from 4 hpi to 6 hpi, with the largest numbers detected at 6 hpi [Figure 6.3].

Based on the global transcriptional profiles, the numbers of differentially expressed probes sets were increased with the infection time increasing in poxviruses infected mouse RAW cells [Figure 6.4]. Among these differentially expressed probe sets, most of the probe sets showed down-regulated changes after infections of three types of poxviruses in infected mouse RAW cells, which was similar to the observation in infected A549 cells. Detailed investigation illustrated that infection of ectromelia virus was responsible for the largest number of probe sets with elevated expression while infection of lister virus was responsible the largest number of probe sets with inhibited expression at 16 hpi.

6.3.1.2 Distribution of differentially expressed probe sets

In cowpox virus-infected A549 cells, 0.44% percentage of probe sets showed up-regulated at their expression level at 2 hpi. However, this number was suddenly reduced to 0.31% at 4 hpi. After 4 hpi, the number of up-regulated probe sets became increased again and reached the highest level at 10 hpi.

Regarding the probe sets with down-regulated expression, the sudden increase of the percentage was observed from 2 hpi to 4 hpi, indicating that some repression regulations might be strongly stimulated in this interphase. The highest percentage of probe sets with down-regulated expression was detected at 8 hpi, and the relative high percentage was still able to be detected even if the cut-off was raised to 10-FC.

In lister virus-infected A549 cells, the percentage of probe sets with up-regulated expression showed high at the beginning of infection (2 hpi), however, this percentage dropped at 4 hpi. Another round of expression stimulation of a big batch of probe sets was detected from 8 hpi. This trend of percentages of probe sets with up-regulated expression observed after infection of lister virus was concordant with the trend observed after infection of cowpox virus, but the detailed percentages from lister virus infection were much higher than those from cowpox virus infection across the whole infection period.

Further observations demonstrated that the highest percentage of probe sets with down-regulated expression was detected at 6 hpi after infection of lister virus, with the increasing of the percentage occurred majorly between 4 hpi and 6 hpi in infected A549 cells. As compared to cowpox virus, the percentages of probe sets with down-regulated expression were lower across the whole infection course after infection of lister virus than cowpox virus no matter based on any fold change cutoff [Table 6.1].

Global investigation on expression alterations of probe sets in mouse RAW cells suggested that infections of cowpox virus and ectromelia virus induced highest percentages of probe sets with up-regulated expression at 2 hpi and 16 hpi separately. And when the fold regulation cutoff was raised to 10-FC, only a small batch of probe sets with up-regulated expression could be detected at 16 hpi after the infection of ectromelia virus.

In contrast, infection of lister virus caused highest percentages of probe sets with down-regulated expression at both time points. Few probe sets were detected with down-regulated expression ≥10-FC at 2 hpi after infections of all these three types of poxviruses, while considerable numbers of those with down-regulated expression ≥10-FC were identified at 16 hpi after infection of lister virus, followed by ectromelia virus [Table 6.2].

6.3.1.3 Functional classification

In cowpox virus-infected A549 cells, the probe sets with up-regulated expression were majorly enriched in “RNA Binding”, “DNA Binding” and “Transcription Factor” across the whole infection period [Figure 6.5]. In addition, functional terms including “Immune response”, “Cytoskeleton”, “Signal Transduction” and “Cell Growth” were also over-represented. Compared to other time points, the numbers of up-regulated probe sets involved in these functional groups were higher at 10 hpi than other time points.

Functional groups significantly over-represented by the probe sets with down-regulated expression were “RNA Binding”, followed by “DNA Binding”, “Signaling Transduction” and “Transcription Factor” in cowpox virus-infected A549 cells. Among the five time points, down-regulated probe sets related to these functions showed highest fold regulation at 8 hpi, followed by those at 10 hpi.

When the cutoff was set at 2-FC or 5-FC, majority of probe sets with up-regulated expression in lister virus infected-A549 cells located in functional groups such as “RNA Binding”, “DNA Binding” and “Transcription Factor”. And the numbers of up-regulated probe sets located in these groups reached highest at 10 hpi [Figure 6.6]. However, similar numbers of up-regulated probe sets were functional associated with “RNA Binding” and “DNA Binding” at 4, 6, 8 and 10 hpi when the cutoff setting was raised to 10-FC, indicating that the related genes with remarkable expression elevation was initiated at 4 hpi and sustained up to 10 hpi. Another interesting finding was that the larger number of probe sets relevant to “Cytoskeleton” were detected at 4 hpi compared to other time points, which might suggest active lipid membrane activities at this time point.

When it turned to the probe sets with down-regulated expression in lister virus infected-A549 cells, most of them were prominently associated with “RNA Binding” no matter of the fold change cutoff setting. Under detailed investigation, the highest number of down-regulated probe sets related to “RNA Binding” was detected at 4 hpi under 2-fold cutoff while the highest number of down-regulated probe sets related to “RNA Binding” was detected at 8 hpi under 5- or 10-fold cutoff. This observation might suggest that the moderate and extensive suppression of gene expression occurred from 4 hpi but strong and specific suppression action exerted at later infection stage (8 hpi).

Similar to the situation happened in poxviruses-infected A549 cells, few probe sets were detected with up-regulated expression at 2 hpi in poxviruses-infected mouse RAW cells. Among three different types of poxviruses, infection of cowpox induced expression of most probe sets, and this batch of probe sets was majorly functional related to “Protein Metabolism”, “DNA Transcription Factor”, “Cell Death” and “RNA Binding”. In addition, almost no probe set with up-regulated fold change ≥ 5-FC was able to be picked out [Figure 6.7].

With the infection time increasing up to 16 hpi, infection of ectromelia virus stimulated expression of larger number of probe sets than cowpox and lister virus. Detailed classification of these up-regulated probe sets demonstrated that they majorly belonged to “DNA Transcription Factor” and “RNA Binding” [Figure 6.8]. Moreover, some up-regulated probe sets

belonging to “Cell Cycle”, “Cell Death” and “Kinase” showed high-level fold regulation at ≥10-FC, indicating the actively regulatory activities at cellular level at the late stage of poxviruses infections.

Although lister virus infection almost didn’t stimulate expression of any probe sets related to our listed functional groups, its infection resulted in most probe sets with down-regulated expression in infected mouse RAW cells. These down-regulated probe sets were majorly classified into “DNA Transcription Factor”, “RNA Binding”, “Cell Death” and “Signal Transduction”, followed by “Cell Cycle” and “Kinase”. Compared to lister virus, invasion of ectromelia virus contributed to relative less probe sets with down-regulated expression at ≥ 2-FC and invasion of cowpox virus led to least probe sets with down-regulated expression in corresponding infected mouse RAW cells.

Consistent with the performances at 2 hpi, infection of lister virus also generated most probe sets with down-regulated expression at 16 hpi. Although infection of cowpox virus caused down-regulated expression of larger number of probe sets than infection of ectromelia virus based on 2-FC cutoff, more probe sets showed significantly down-regulated expression after infection of extromelia virus but not cowpox virus when the cutoff was raised to 5-FC. “DNA Binding” and other common functional terms were over-represented by down-regulated probe sets in these three types of poxviruses infected mouse RAW cells.

Table 6.1 Differentially expressed probe sets in A549 cells infected with poxviruses at different time points.

A549	Probe sets (>=2 fold)		Probe sets (>=3 fold)		Probe sets (>=5 fold)		Probe sets (>=10 fold)	
	Up-regulated	Down-regulated	Up-regulated	Down-regulated	Up-regulated	Down-regulated	Up-regulated	Down-regulated
Cowpox 2 hpi	0.44%	4.68%	0.12%	0.61%	0.02%	0.15%	0.00%	0.03%
Cowpox 4 hpi	0.31%	44.75%	0.17%	16.39%	0.11%	2.43%	0.05%	0.22%
Cowpox 6 hpi	0.34%	62.76%	0.20%	45.07%	0.14%	17.92%	0.08%	2.46%
Cowpox 8 hpi	0.45%	65.50%	0.25%	56.05%	0.14%	35.85%	0.08%	11.09%
Cowpox 10 hpi	1.01%	57.02%	0.50%	43.84%	0.22%	25.36%	0.10%	7.98%
Lister 2 hpi	1.48%	1.26%	0.29%	0.29%	0.07%	0.09%	0.00%	0.01%
Lister 4 hpi	0.61%	11.99%	0.26%	2.29%	0.18%	0.33%	0.11%	0.05%
Lister 6 hpi	0.71%	56.06%	0.28%	34.30%	0.19%	9.82%	0.10%	1.26%
Lister 8 hpi	6.16%	45.31%	2.60%	32.02%	0.70%	15.66%	0.21%	3.89%
Lister 10 hpi	10.61%	35.39%	5.63%	23.25%	1.71%	11.32%	0.30%	3.07%

Table 6.2 Differentially expressed probe sets in RAW cells infected with poxviruses at different time points.

RAW cells	Probe sets (>=2 fold)		Probe sets (>=3 fold)		Probe sets (>=5 fold)		Probe sets (>=10 fold)	
	Up-regulated	Down-regulated	Up-regulated	Down-regulated	Up-regulated	Down-regulated	Up-regulated	Down-regulated
Cowpox 2 hpi	0.42%	0.75%	0.03%	0.19%	0.00%	0.06%	0.00%	0.01%
Cowpox 16 hpi	1.55%	36.14%	0.58%	20.18%	0.17%	5.94%	0.05%	0.56%
Ectromelia 2 hpi	0.19%	1.81%	0.02%	0.36%	0.01%	0.05%	0.00%	0.01%
Ectromelia 16 hpi	6.36%	28.37%	2.75%	19.58%	0.71%	10.65%	0.12%	3.33%
Lister 2 hpi	0.01%	2.22%	0.00%	0.22%	0.00%	0.01%	0.00%	0.00%
Lister 16 hpi	2.09%	45.86%	0.67%	34.09%	0.14%	19.43%	0.03%	6.13%

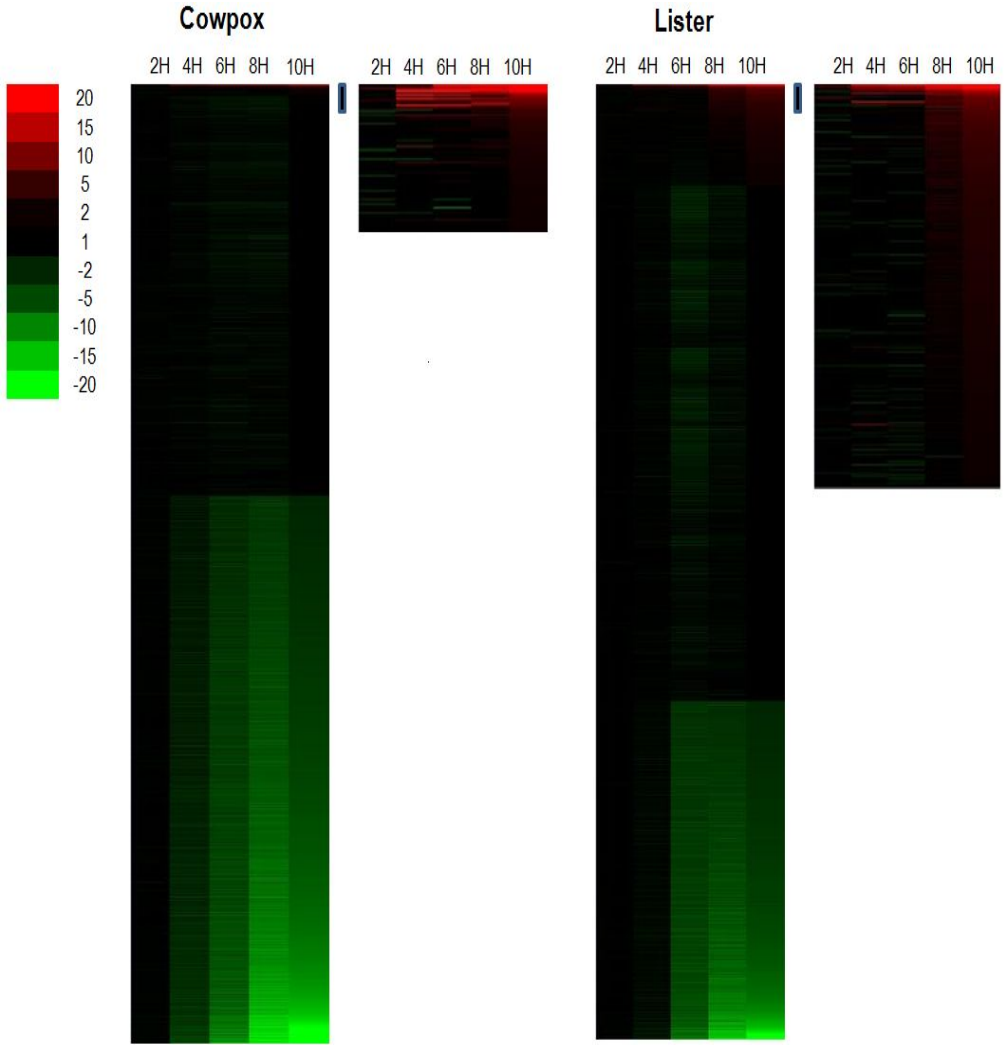

Figure 6.3 Temporal changes in the host cell transcriptome in A549 cells infected by two types of poxviruses. The global host gene expression profiles were retrieved from microarray analysis with different time points examined. The probe sets showing ≥2 fold change (FC) up- or down-regulated in expression are indicated (P-value≤0.05). Expression profiles of up-regulated (red), down-regulated (green) and no significant change (black) are shown.

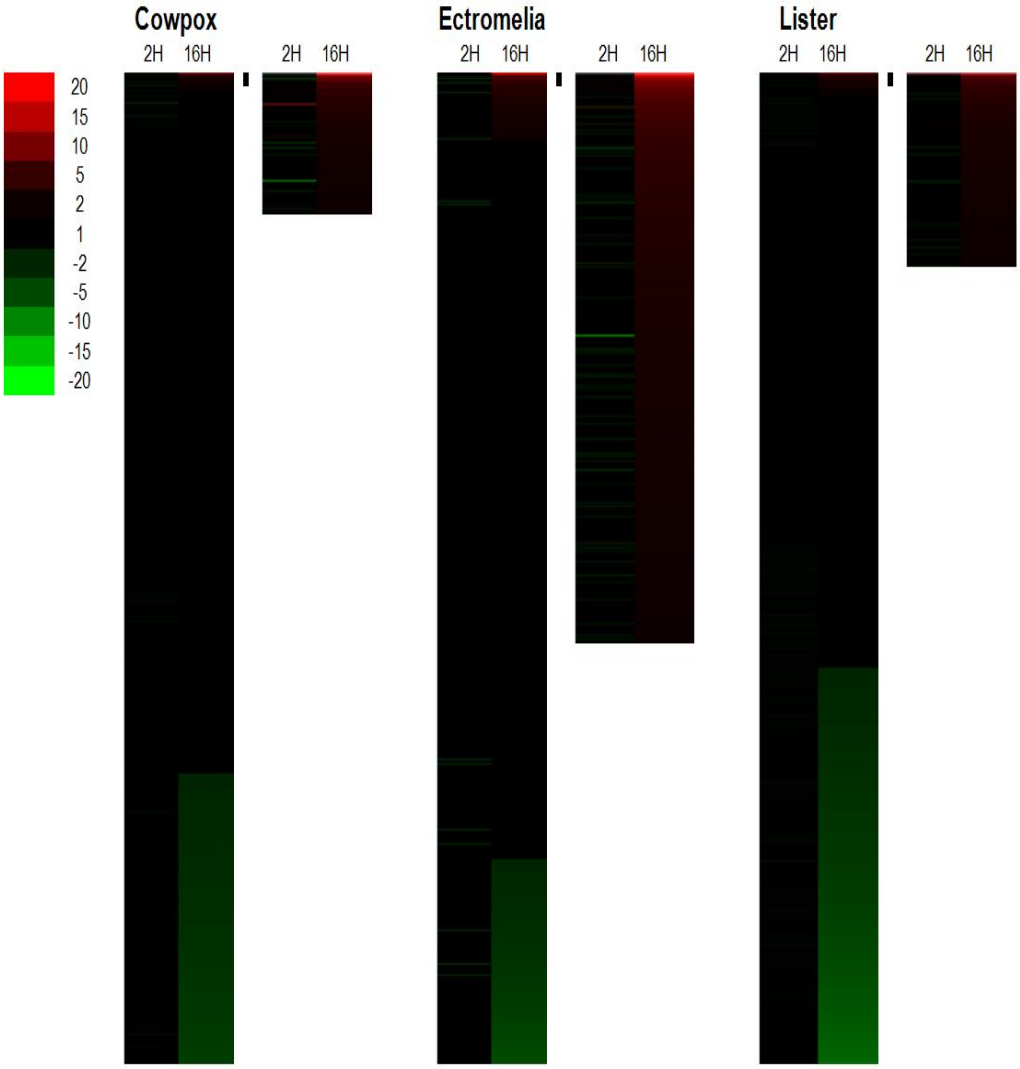

Figure 6.4 Temporal changes in the host cell transcriptome in RAW cells infected by three types of poxviruses. The global host gene expression profiles were retrieved from microarray analysis with different time points examined. The probe sets showing ≥2 fold change (FC) up- or down-regulated in expression are indicated (P-value≤0.05). Expression profiles of up-regulated (red), down-regulated (green) and no significant change (black) are shown.

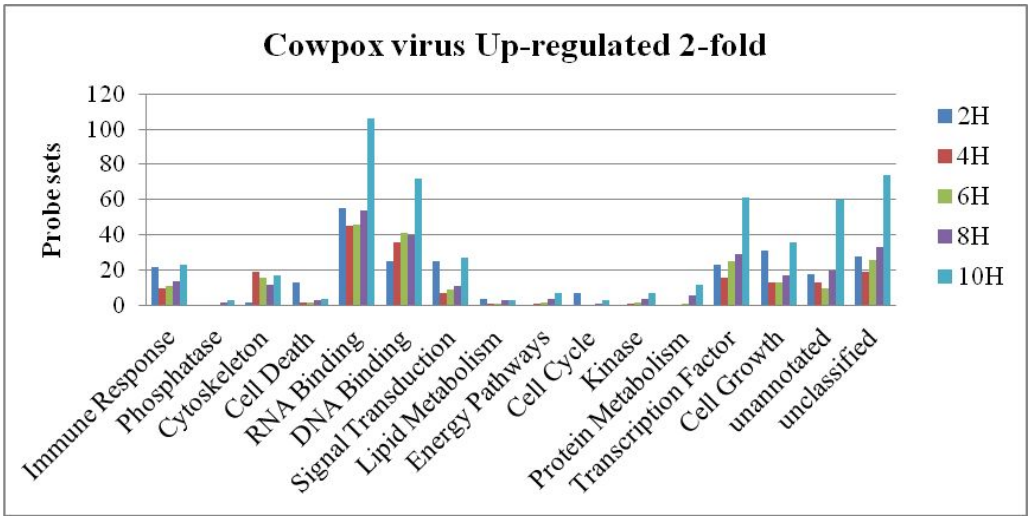
Cowpox virus Up-regulated 2-fold
Probe sets
120
100
80
60
40
20
0
2H
4H
6H
8H
10H
Immune Response
Phosphatase
Cytoskeleton
Cell Death
RNA Binding
DNA Binding
Signal Transduction
Lipid Metabolism
Energy Pathways
Cell Cycle
Kinase
Protein Metabolism
Transcription Factor
Cell Growth
unannotated
unclassified

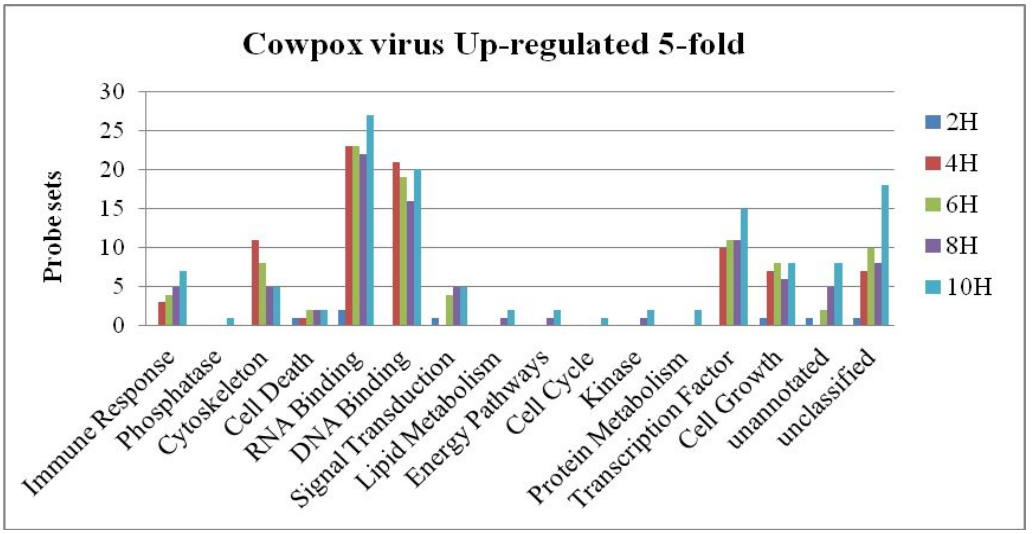
Cowpox virus Up-regulated 5-fold
Probe sets
30
25
20
15
10
5
0
2H
4H
6H
8H
10H
Immune Response
Phosphatase
Cytoskeleton
Cell Death
RNA Binding
DNA Binding
Signal Transduction
Lipid Metabolism
Energy Pathways
Cell Cycle
Kinase
Protein Metabolism
Transcription Factor
Cell Growth
unannotated
unclassified

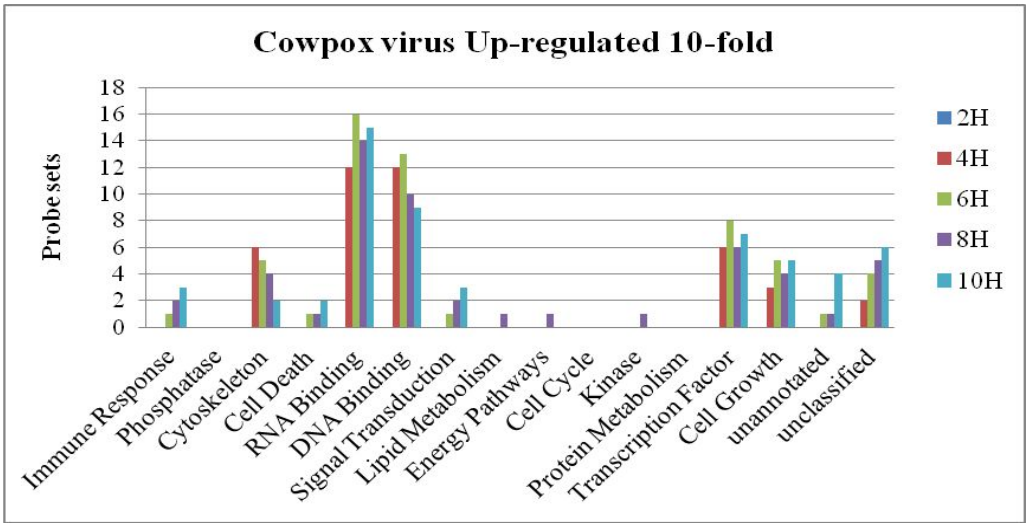
Cowpox virus Up-regulated 10-fold
Probe sets
18
16
14
12
10
8
6
4
2
0
2H
4H
6H
8H
10H
Immune Response
Phosphatase
Cytoskeleton
Cell Death
RNA Binding
DNA Binding
Signal Transduction
Lipid Metabolism
Energy Pathways
Cell Cycle
Kinase
Protein Metabolism
Transcription Factor
Cell Growth
unannotated
unclassified

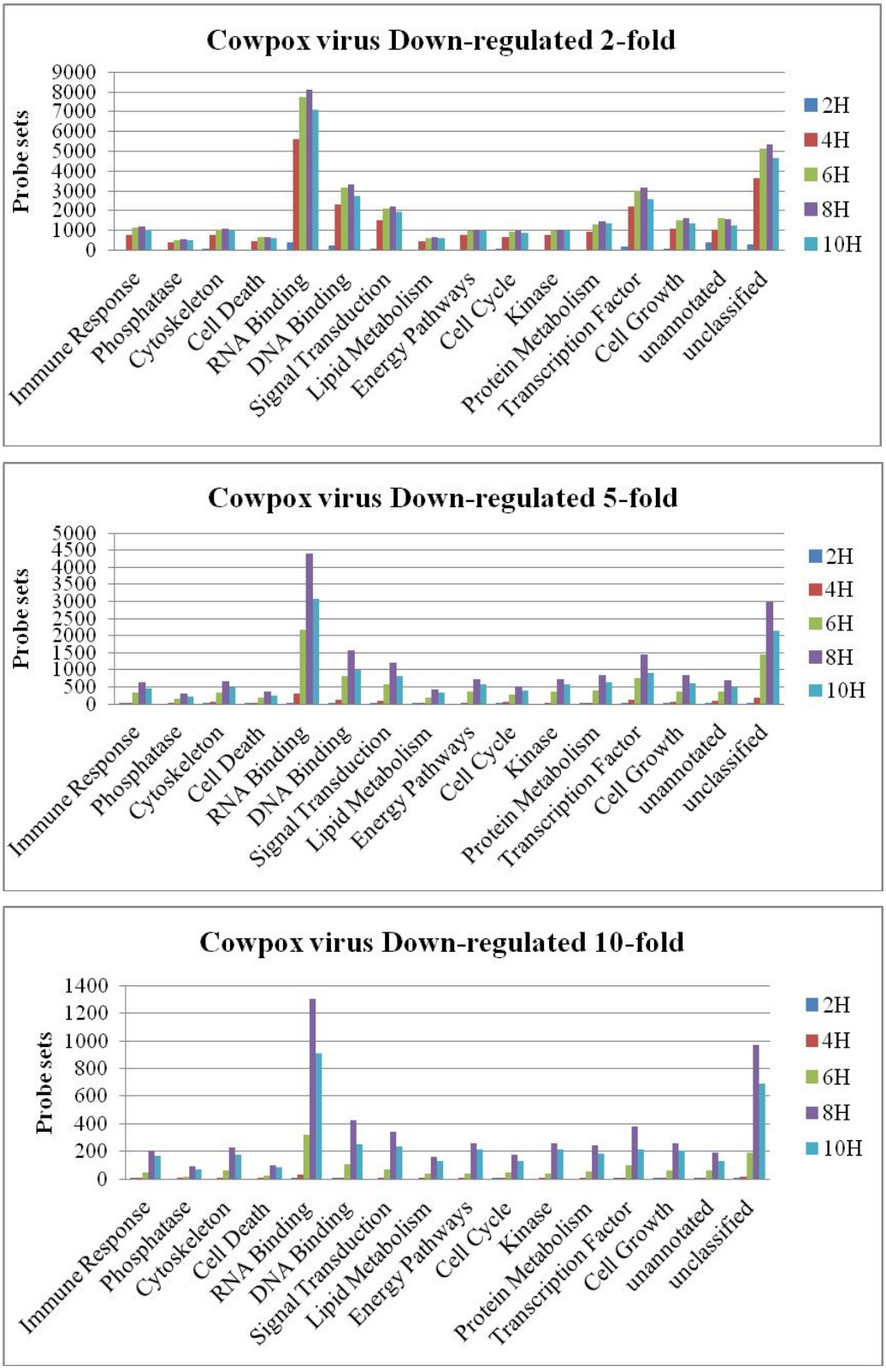

Figure 6.5 Overview of distributions of differentially expressed probe sets into different biological functions in A549 cells infected with cowpox virus. The numbers of probe sets in the different functional families, including non-annotated and unclassified groups, showing up-regulated or down-regulated with different fold changes (≥2-FC, ≥5-FC and ≥10-FC) in gene expression are presented.

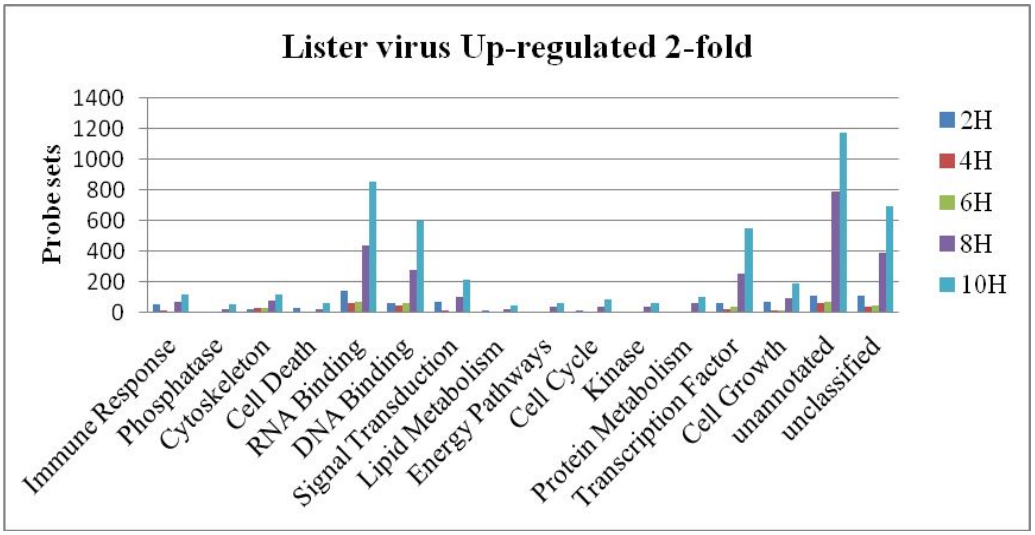
Lister virus Up-regulated 2-fold
Probe sets
1400
1200
1000
800
600
400
200
0
2H
4H
6H
8H
10H
Immune Response
Phosphatase
Cytoskeleton
Cell Death
RNA Binding
DNA Binding
Signal Transduction
Lipid Metabolism
Energy Pathways
Cell Cycle
Kinase
Protein Metabolism
Transcription Factor
Cell Growth
unannotated
unclassified

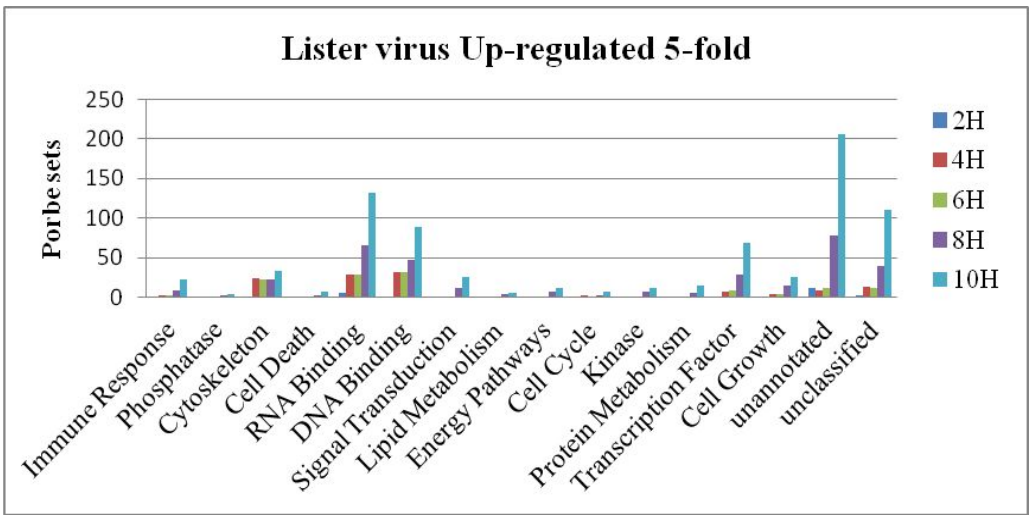
Lister virus Up-regulated 5-fold
Porbe sets
250
200
150
100
50
0
2H
4H
6H
8H
10H
Immune Response
Phosphatase
Cytoskeleton
Cell Death
RNA Binding
DNA Binding
Signal Transduction
Lipid Metabolism
Energy Pathways
Cell Cycle
Kinase
Protein Metabolism
Transcription Factor
Cell Growth
unannotated
unclassified

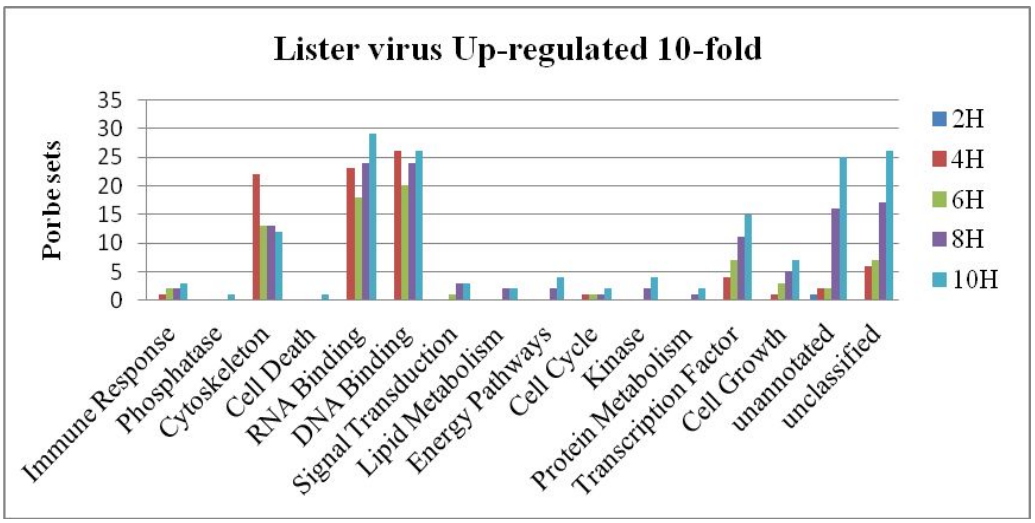
Lister virus Up-regulated 10-fold
Porbe sets
35
30
25
20
15
10
5
0
2H
4H
6H
8H
10H
Immune Response
Phosphatase
Cytoskeleton
Cell Death
RNA Binding
DNA Binding
Signal Transduction
Lipid Metabolism
Energy Pathways
Cell Cycle
Kinase
Protein Metabolism
Transcription Factor
Cell Growth
unannotated
unclassified

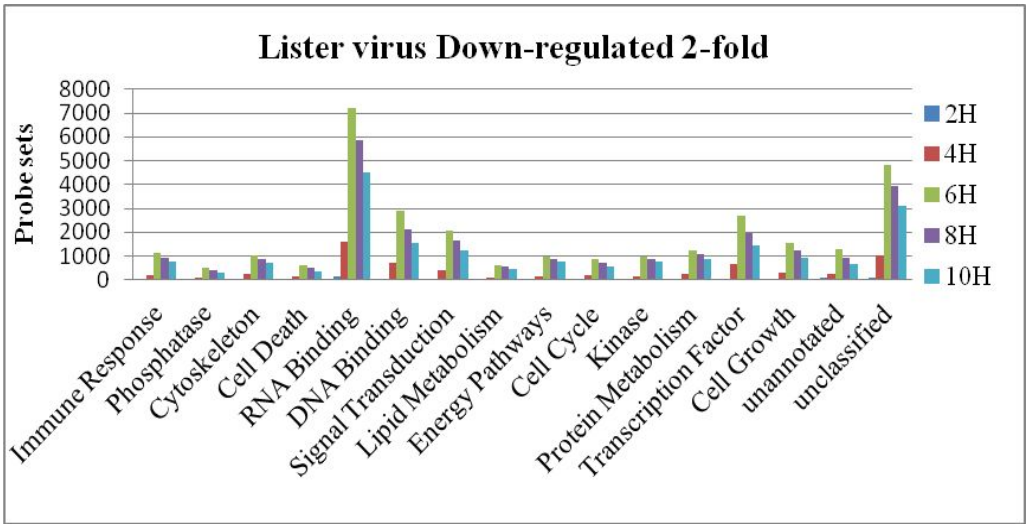

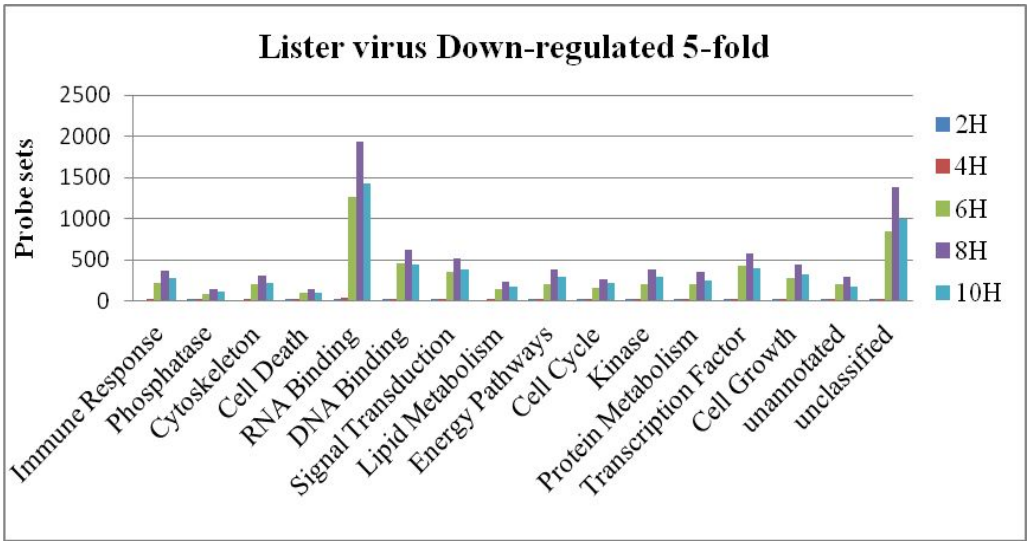

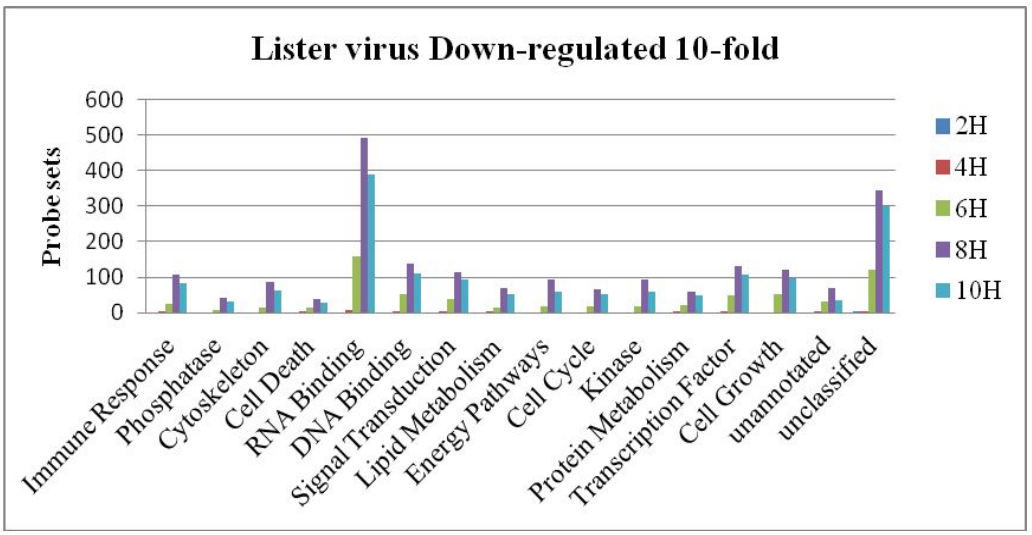

Figure 6.6 Overview of distributions of differentially expressed probe sets into different biological functions in A549 cells infected with lister virus. The numbers of probe sets in the different functional families, including non-annotated and unclassified groups, showing up-regulated or down-regulated with different fold changes (≥2-FC, ≥5-FC and ≥10-FC) in gene expression are presented.

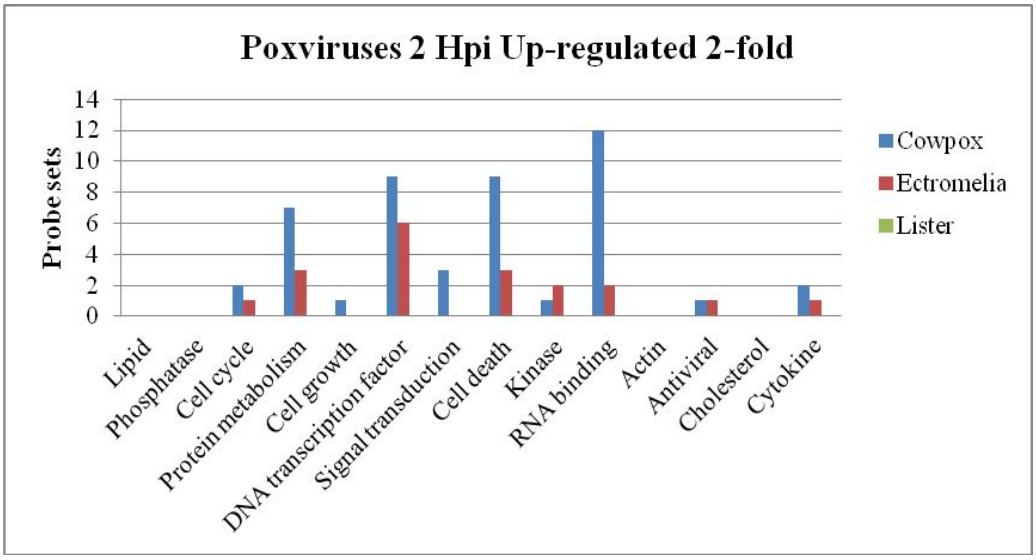
Poxviruses 2 Hpi Up-regulated 2-fold
Probe sets
14
12
10
8
6
4
2
0
Lipid
Phosphatase
Cell cycle
Protein metabolism
Cell growth
DNA transcription factor
Signal transduction
Cell death
Kinase
RNA binding
Actin
Antiviral
Cholesterol
Cytokine
Cowpox
Ectromelia
Lister

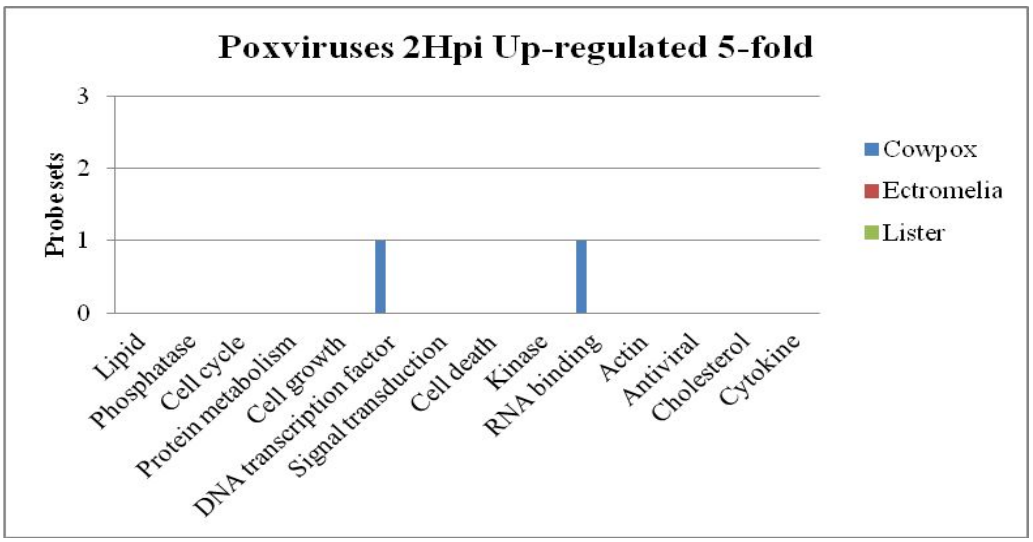
Poxviruses 2Hpi Up-regulated 5-fold
Probe sets
3
2
1
0
Lipid
Phosphatase
Cell cycle
Protein metabolism
Cell growth
DNA transcription factor
Signal transduction
Cell death
Kinase
RNA binding
Actin
Antiviral
Cholesterol
Cytokine
Cowpox
Ectromelia
Lister

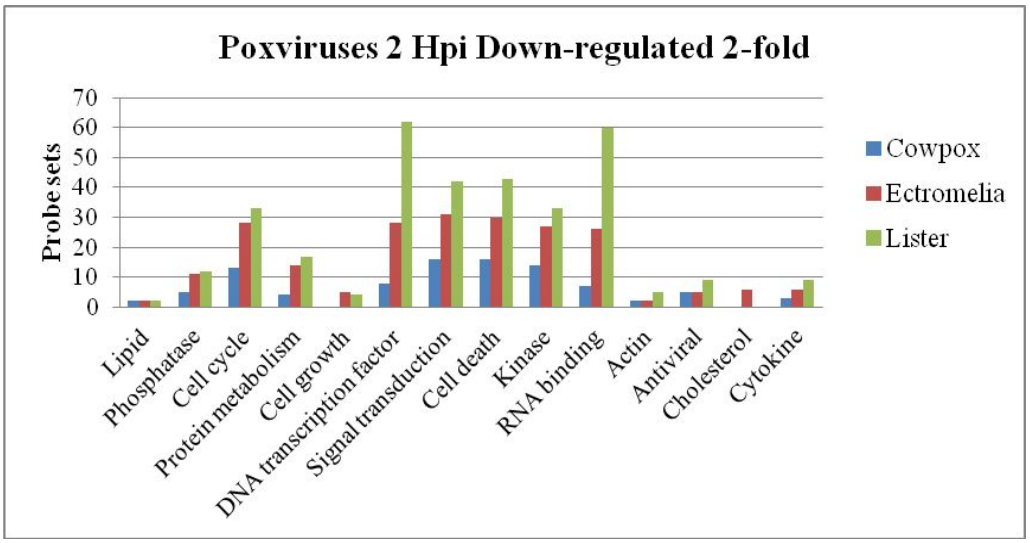
Poxviruses 2 Hpi Down-regulated 2-fold
Probe sets
70
60
50
40
30
20
10
0
Lipid
Phosphatase
Cell cycle
Protein metabolism
Cell growth
DNA transcription factor
Signal transduction
Cell death
Kinase
RNA binding
Actin
Antiviral
Cholesterol
Cytokine
Cowpox
Ectromelia
Lister

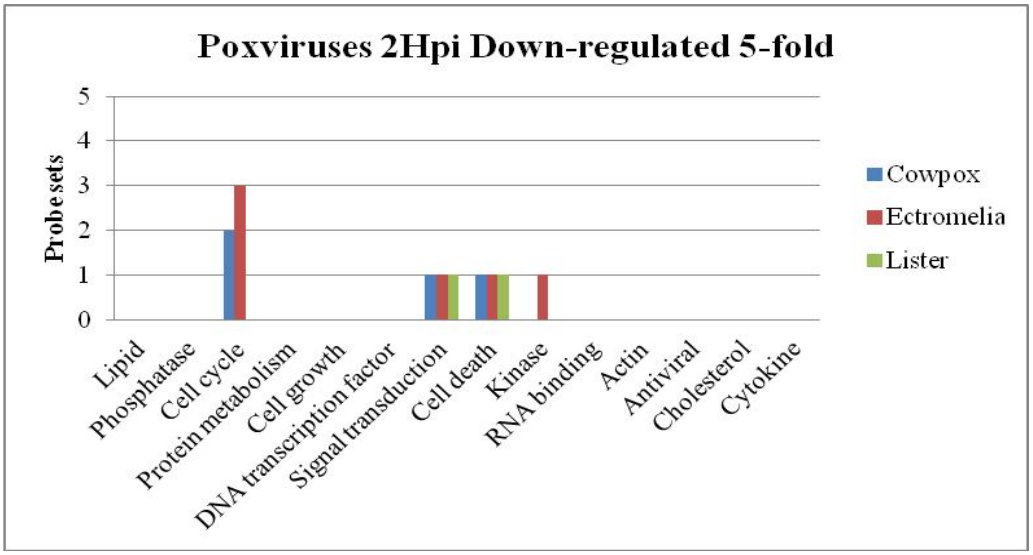

Figure 6.7 Overview of distributions of differentially expressed probe sets into different biological functions in RAW cells infected with three types of poxviruses at 2 hpi. The numbers of probe sets in the different functional families, including non-annotated and unclassified groups, showing up-regulated or down-regulated with different fold changes (≥2-FC and ≥5-FC) in gene expression are presented.

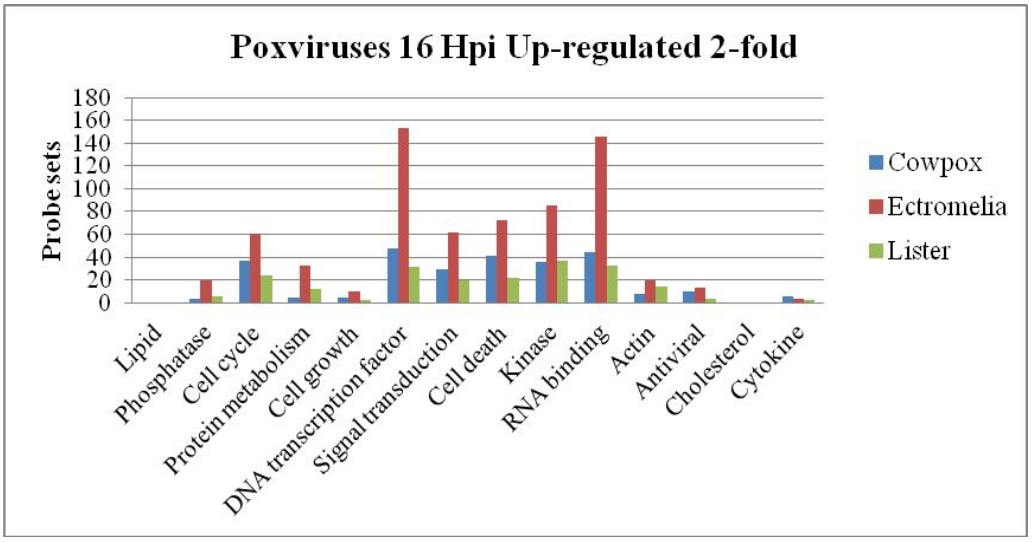
Poxviruses 16 Hpi Up-regulated 2-fold
Probe sets
180
160
140
120
100
80
60
40
20
0
Lipid
Phosphatase
Cell cycle
Protein metabolism
Cell growth
DNA transcription factor
Signal transduction
Cell death
Kinase
RNA binding
Actin
Antiviral
Cholesterol
Cytokine
Cowpox
Ectromelia
Lister

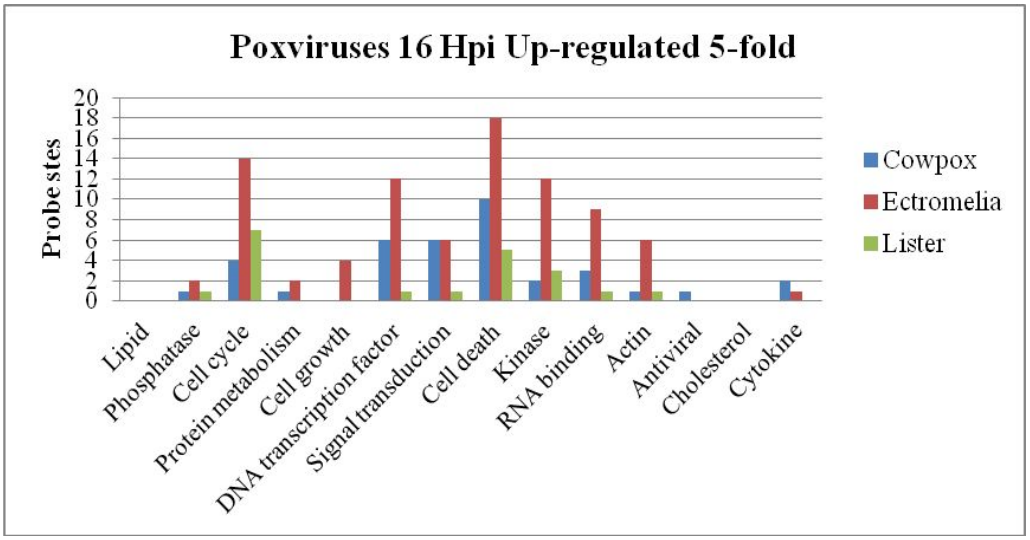
Poxviruses 16 Hpi Up-regulated 5-fold
Probe stes
20
18
16
14
12
10
8
6
4
2
0
Lipid
Phosphatase
Cell cycle
Protein metabolism
Cell growth
DNA transcription factor
Signal transduction
Cell death
Kinase
RNA binding
Actin
Antiviral
Cholesterol
Cytokine
Cowpox
Ectromelia
Lister

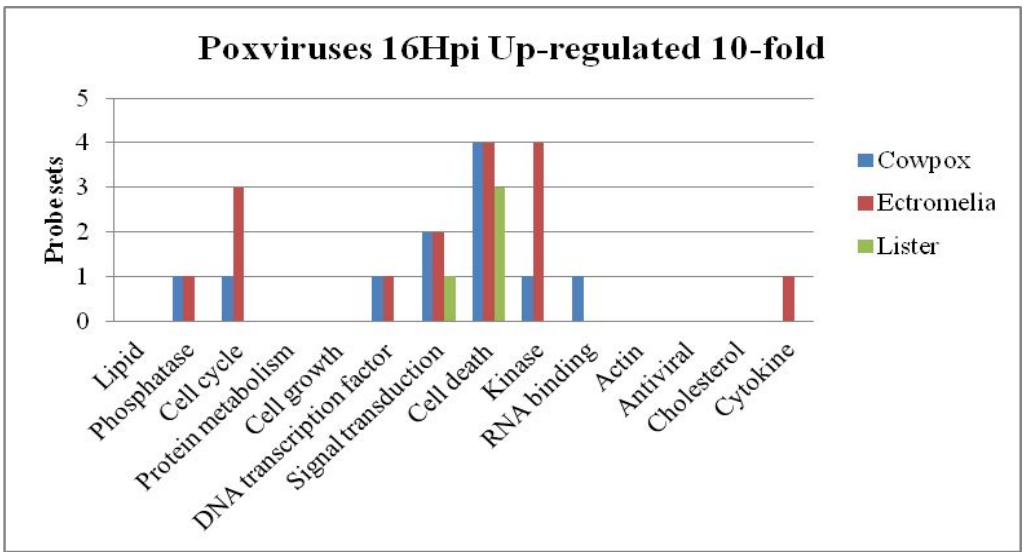
Poxviruses 16Hpi Up-regulated 10-fold
Probe sets
5
4
3
2
1
0
Lipid
Phosphatase
Cell cycle
Protein metabolism
Cell growth
DNA transcription factor
Signal transduction
Cell death
Kinase
RNA binding
Actin
Antiviral
Cholesterol
Cytokine
Cowpox
Ectromelia
Lister

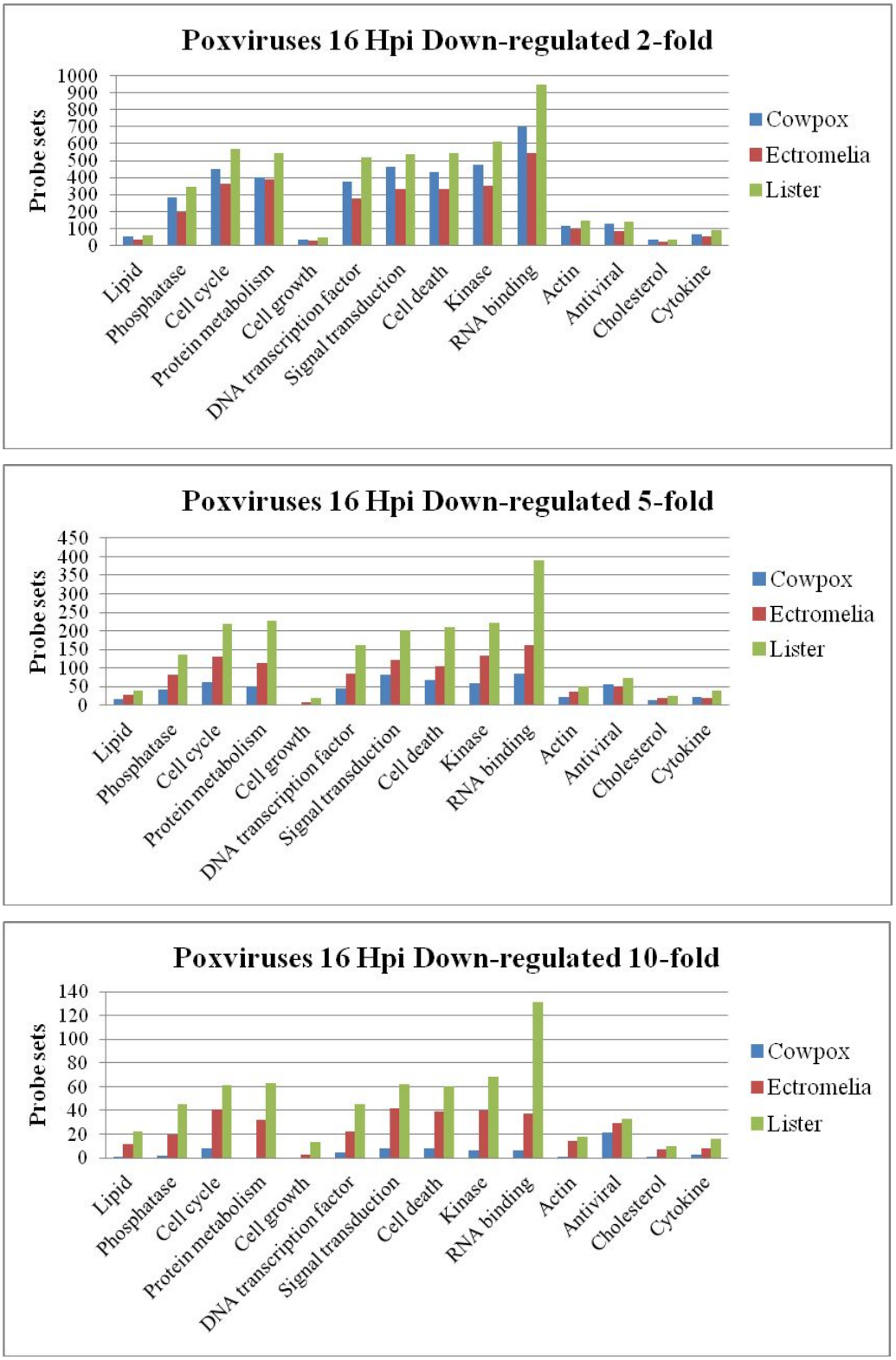

Figure 6.8 Overview of distributions of differentially expressed probe sets into different biological functions in RAW cells infected with three types of poxviruses at 16 hpi. The numbers of probe sets in the different functional families, including non-annotated and unclassified groups, showing up-regulated or down-regulated with different fold changes (≥2-FC, ≥5-FC and ≥10-FC) in gene expression are presented.

6.3.1.4 Cluster analysis in A549 cells

To our knowledge, genes with similar temporal expression trends might have related biological functions and possibly correspond to some critical cellular processes and pathways [91]. So the aim of this cluster analysis is to classify probe sets with similar expression profiles into common biological groups, which is beneficial for further functional analysis. In our study, A549 cells were infected with cowpox and lister virus, and their transcriptomes were analyzed at 2, 4, 6, 8 and 10 hpi. Probe sets with ≥2-FC (P-value≤0.05) up-regulated at least at 10 hpi and those with ≥10-FC (P-value≤0.05) down-regulated at least at 10 hpi in cowpox or lister virus infected A549 cells were separately clustered into similar gene expression profiles using the Expander version 5.0 software [Figure 6.9-6.12]. Using the same software, the data were further analyzed into genes relating to different functional groups or canonical pathways, and enriched transcription factor, chromosome locations and microRNAs were also identified. All enriched functional groups, canonical pathways, transcriptional factors, chromosome locations and microRNAs are displayed in Table 6.3-6.6.

Pathway analysis revealed that the pathway called "Systemic lupus erythematosus" was found to be commonly enriched in genes with up-regulated expression at least at 10 hpi in cowpox and lister virus infected A549 cells, with more genes following lister virus infection involved in this pathway than those following cowpox virus infection. Systemic lupus erythematosus (SLE) is a chronic autoimmune disease that can affect almost any organ system, and molecules in this pathway majorly play a role on mediating a systemic inflammatory response. Through detailed investigation on genes involved in this pathway, we found that almost all these genes from both cowpox virus and lister virus infected A549 cells encoded histone proteins.

Alkhalil A *et al* (2010) has depicted the similar situation happened in monkeypox virus infected MK2 cells [339]. In those infected host cells, all the core histone genes excluding HIST3H2A exhibited up-regulated expression at both examined 3 and 7 hpi. However, unlike these histone genes with increasing expression trend, major transcription regulators of histones expression such as CITED2, NCOA3, CREB1, YY1 and HDAC2 showed increasing suppression at their transcriptional level across the whole infection

course. Similarly, many enzymes that control modifications of histones and chromatin organization dynamics such as FBXO11, PRMT3, MYST2, MYCBP2, and RARS2 also showed steady down-regulation in their mRNA level. As we know, histones in eukaryotic cell nucleic play an essential function as chief protein components of chromatin to package and order the DNA into structural units called nucleosomes. Besides, poxviruses are double-stranded DNA mammalian viruses with large genomes reaching few hundreds of micrometers in length. Thus, Alkhalil A made a hypothesis that host cell histones played a role on viral DNA compaction and nucleosome formation, and up-regulated expression of these histones following infection of poxviruses might be a potential implication of viral replication. With regards to transcription regulator and enzymes with down-regulated expression, they proposed that these observations implied part of host response actions including chromatin-mediated silencing of the viral genome and activation of DNA damage, or part of the viral strategies to take over its host.

In our study, up-regulated expression levels of histones after infections of cowpox and lister virus were consistent with their observations after infection of monkeypox virus. Consequently, if the hypothesis mentioned above is correct, more histone genes with up-regulated expression in lister virus-infected A549 cells could potentially indicate better virus replication than in cowpox-virus infected A549 cells. Furthermore, most of the histones related enzymes and transcription regulators also showed down-regulated expression from 4 hpi, with deeper repression detected after infection of cowpox virus than lister virus. This observation which was consistent with previous reports supported the previous finding in further.

A transcription factor called SRF was enriched in genes with up-regulated expression in cowpox virus-infected A549 cells. The protein encoded by this gene binds to the promoter region of serum response element in order to regulate the activity of many immediate-early genes, and thereby plays roles on the regulations of cell cycle, cell growth, cell differentiation and cell death. Over-representation of this transcription factors based on up-regulated genes might suggest the potential abnormal regulation on cell growth and apoptosis in infected host cells. In addition, transcription factors including NF-Y, ETF and POU1F1were only enriched in up-regulated genes after infection of lister virus.

Among these factors, only ETF showed faint down-regulation in its expression in lister virus infected A549 cells. It has been reported that transcription factor ETF played a role in mediating expressions of genes related to cell proliferation [340], the inconsistent gene expression performances of ETF and downstream genes might implicate more complex regulation network.

A batch of gene ontology terms was enriched in genes with up-regulated expression from both cowpox and lister virus-infected A549 cells. These functional terms included “nucleic acid binding”, “gene expression”, “zinc ion binding”, “DNA binding” and “regulation of cellular metabolic process”. Besides these common functional terms, other interesting functional groups were also enriched specific to the infection of lister virus. These unique gene ontology terms were “regulation of cellular biosynthetic process”, “transition metal ion binding”, “macromolecule biosynthetic process”, “cellular biopolymer catabolic process”, “cellular biopolymer biosynthetic process”, “negative regulation of cellular process”, “negative regulation of transcription”, “regulation of transcription, DNA-dependent” and so on. Over-representative of these pathways suggested that there might exist some mechanism regulations relevant to macromolecules, cellular biopolymer, as well as some metal ion transition upon infection of lister virus in A549 cells.

In addition, a series of potentially regulatory microRNAs were also picked out to bind with the up-regulated genes during cowpox virus infection. And around 70 genes with elevated expression in lister virus infected A549 cells were also predicted to locate at two common chromosome sites (chromosome 2p and chromosome 14q).

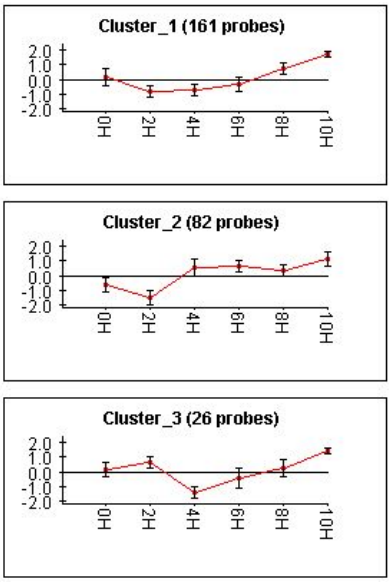

Figure 6.9 Clustering analysis of temporal gene expression profiles in cowpox virus-infected A549 cells. A549 cells were infected with cowpox virus at 2, 4, 6, 8 and 10 hpi. Probe sets showing ≥2-fold changes up-regulated (P-value≤0.05) at least at 10 hpi were analyzed with Expander 5 software. X-axis represents post-infection in hours (H), and Y-axis means normalized expression changes of probe sets.

Table 6.3 Summary of functional groups, canonical pathways, transcription factors and microRNAs enriched based on up-regulated genes in A549 cells infected with cowpox virus.

Cowpox Group I	
Cluster No.	**Enriched Transcription Factors**
Cluster 2	M00186[SRF]:8 | M00152[SRF]:7
Cluster No.	**Enriched Canonical Pathways**
Cluster 2	Systemic lupus erythematosus:7
Cluster No.	**Enriched Gene Ontology Terms**
Cluster 1	nucleic acid binding - GO:0003676:31 | regulation of macromolecule metabolic process - GO:0060255:29 | gene expression - GO:0010467:25
	zinc ion binding - GO:0008270:23 | nitrogen compound metabolic process - GO:0006807:27 | transcription factor activity - GO:0003700:13
Cluster 2	transcription factor activity - GO:0003700:16 | regulation of cellular metabolic process - GO:0031323:26 | DNA binding - GO:0032502:19
	brain development - GO:0007420:5
Cluster No.	**Enriched microRNAs**
Cluster 3	mir-21/590-5p:3 | mir-183:3 | mir-320/320abcd:3 | mir-590/590-3p:3

Genes with up-regulated expression were significantly categorized into different functional groups and canonical pathways. Different transcription factors and microRNAs that can potentially be involved in the regulation of gene expressions are shown for each cluster under Expander 5 software analysis (P-value≤0.05). Each functional group, canonical pathway, transcription factor or microRNA is followed by the number of corresponding genes.

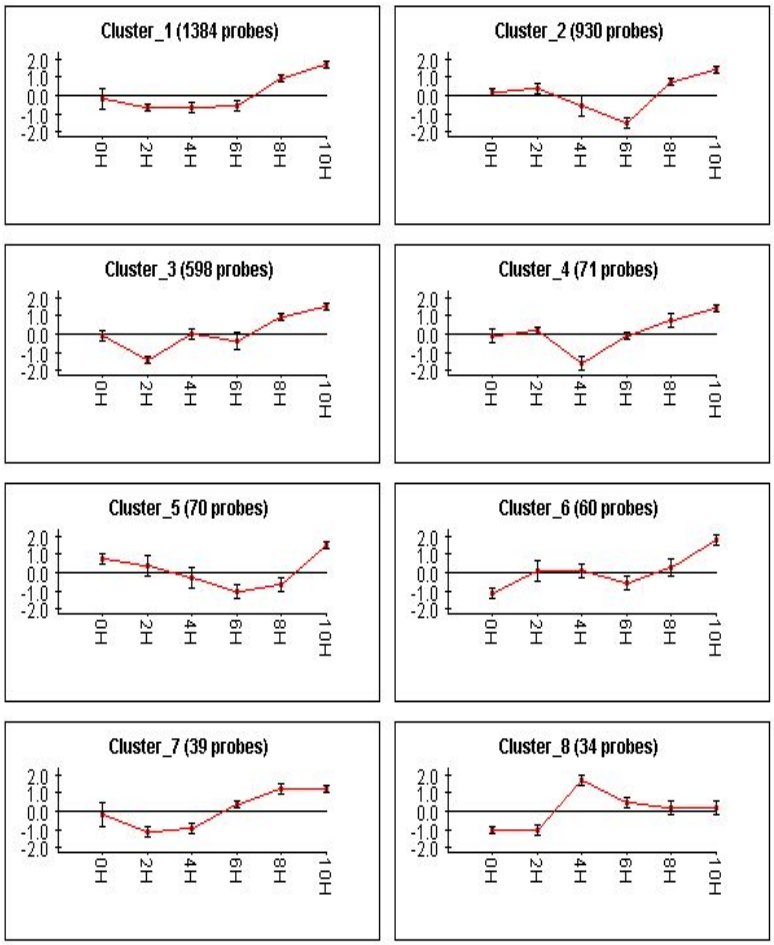

Figure 6.10 Clustering analysis of temporal gene expression profiles in lister virus-infected A549 cells. A549 cells were infected with cowpox virus at 2, 4, 6, 8 and 10 hpi. Probe sets showing ≥2-fold changes up-regulated (P-value≤0.05) at least at 10 hpi were analyzed with Expander 5 software. X-axis represents post-infection in hours (H), and Y-axis means normalized expression changes of probe sets.

Table 6.4 Summary of functional groups, canonical pathways, transcription factors and chromosome locations enriched based on up-regulated genes in A549 cells infected with lister virus.

Lister Group I	
Cluster No.	**Enriched Transcription Factors**
Cluster 1	M00287[NF-Y]:145
Cluster 2	M00695[ETF]:210
Cluster 7	M00744[POU1F1]:9
Cluster No.	**Enriched Canonical Pathways**
Cluster 8	Systemic lupus erythematosus:26
Cluster No.	**Enriched Gene Ontology Terms**
Cluster 1	nucleic acid binding - GO:0003676:208 | regulation of gene expression - GO:0010468:179 | regulation of RNA metabolic process - GO:0051252:166
	gene expression - GO:0010467:169 | regulation of macromolecule biosynthetic process - GO:0010556:176
	regulation of primary metabolic process - GO:0080090:186 | regulation of cellular metabolic process - GO:0031323:189 | transcription - GO:0006350:127
	Nnucleobases, nucleoside, nucleotide and mucleic acid metabolic process - GO:0006139:171 | cellular biopolymer biosynthetic process - GO:0034961:142
	zinc ion binding - GO:0008270:148 | RNA binding - GO:0003723:50 | RNA splicing - GO:0008380:27 | nucleotide binding - GO:0000166:94
	modification-dependent macromolecule catabolic process - GO:0043632:34 | chromatin modification - GO:0016568:18
	cellular protein metabolic process - GO"0044267:86
Cluster 2	regulation of cellular metabolic process - GO:0031323:142 | regulation of cellular biosynthetic process - GO:0031326:130
	regulation of nucleobase, nucleoside, nucleotide and nucleic acid metabolic process - GO:0019219:126 | nucleic acid binding - GO:0003676:134
	DNA binding - GO:0003677:106 | zinc ion binding - GO:0008270:104 | transition metal ion binding - GO:0046914:116 | gene expression - GO:0010467:95
	nucleobse, nucleoside, nucleotide and nucleic acid metabolic process - GO:0006139:103 | transcription regulator activity - GO:0030528:64
	macromolecule biosynthetic process - GO:0009059:88 | cellular biopolymer catabolic process - GO:0034962:31
	negative regulation of transcription - GO:0016481:20 | nucleotide binding - GO:0000166:68 | negative regulation of cellular process - GO:0048523:45
Cluster3	gene expression - GO:0010467:84 | zinc ion binding - GO:0008270:80 | nucleic acid binding - GO:0003676:95
	nucleobase, nucleoside, nucleotide and nucleic acid metabolic process - GO:0006139:88 | DNA binding - GO:0003677:75 | transcription - GO:0006350:62
	cellular biopolymer biosynthetic process - GO:0034961:71 | regulation of transcription, DNA-dependent - GO:0006355:74
Cluster No.	**Enriched Chromosome Locations**
Cluster 1	chromosome 2p:34 | chromosome 14q:35

Genes with up-regulated expression were significantly categorized into different functional groups and canonical pathways. Different transcription factors and micRNAs that can potentially be involved in the regulation of gene expressions are shown for each cluster under Expander 5 software analysis (P-value≤0.05). Each functional group, canonical pathway, transcription factor or microRNA is followed by the number of corresponding genes.

As shown in Table 6.5 and Table 6.6, a common transcription factor named sp1 was found to be enriched in genes with down-regulated expression in both two types of poxviruses infected A549 cells. In addition to this common factor, other factors such as Nrf-1 and GABP were also listed to potentially regulate the down-regulated genes during cowpox virus infection, while E2F was significantly identified to potentially regulate those down-regulated genes during lister virus infection.

Pathways including “Metabolic pathways”, “Oxidative phosphorylation”, “Glutathione metabolism”, “Glycolysis”, “Purine metabolism” were commonly enriched in genes with down-regulated expression upon the infections of both two types of poxviruses, with more

down-regulated genes in these pathways detected after infection of cowpox virus. Unique to lister virus infection, "DNA replication" pathway was also significantly enriched in down-regulated genes in corresponding A549 cells, which might be caused by the antiviral action exerted by host cells to limit the viral replication. Similarly, several other pathways such as "TCA cycle", "Lysosome", "Cell cycle" were specifically enriched in down-regulated genes in cowpox virus-infected A549 cells.

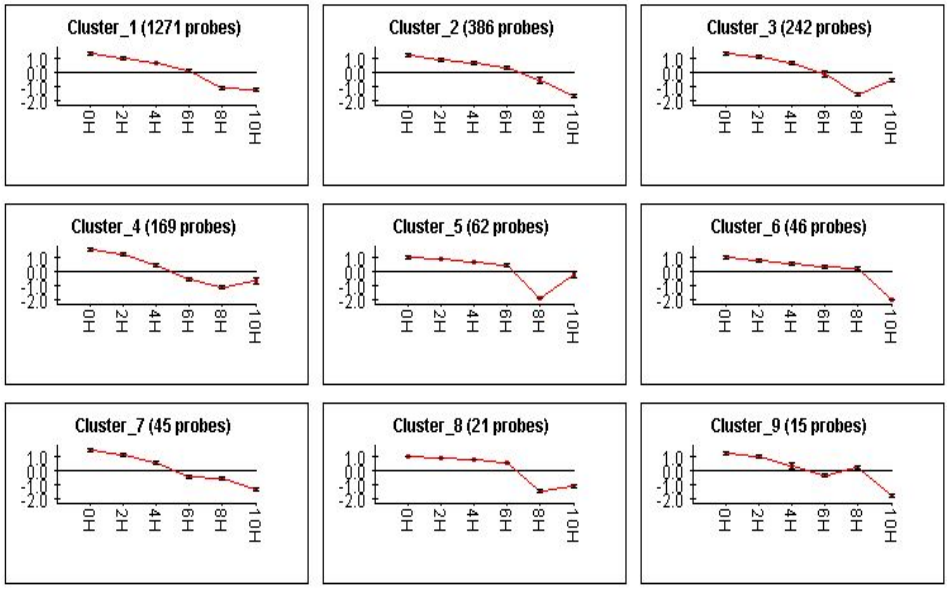

Figure 6.11 Clustering analysis of temporal gene expression profiles in cowpox virus-infected A549 cells. A549 cells were infected with cowpox virus at 2, 4, 6, 8 and 10 hpi. Probe sets showing ≥10-fold changes down-regulated (P-value≤0.05) at least at 10 hpi were analyzed with Expander 5 software. X-axis represents post-infection in hours (H), and Y-axis means normalized expression changes of probe sets.

Quite a lot of GO terms were over-represented based on down-regulated genes in infected A549 cells after infections of both poxviruses, especially after infection of cowpox virus. Among these enriched terms, biological functions associated with "oxidation reduction", "nitrogen compound metabolic process", "hydrolase activity", 'cell metabolism", "cell cycle", 'cellular catabolic process and organelle organization" were commonly over-represented after infections of both two types of poxviruses. Besides, biological functions such as "generation of precursor metabolites and energy", "establishment of localization", "transferase activity and structural molecule activity" were enriched based on down-regulated genes specifically in cowpox virus-infected A549 cells.

Table 6.5 Summary of functional groups, canonical pathways, transcription factors, chromosome locations and microRNAs enriched based on down-regulated genes in A549 cells infected with cowpox virus.

Cowpox Group II	
Cluster No.	**Enriched Transcription Factors**
Cluster 1	M00652[Nrf-1]:308 | M00341[GABP]:230 | M00196[Sp1]:509
Cluster No.	**Enriched Canonical Pathways**
Cluster 1	Metabolic pathways:137 | Huntington's disease:39 | Oxidative phosphorylation:30 | Parkinson's disease:30 | Alzheimer's disease:33
	Glutathione metabolism:15 | Pentose phosphate pathway:10 | Cardiac muscle contraction:13 | Pathogenic Escherichia coli infection:11
	Glycolysis / Gluconeogenesis:11 | Citrate cycle (TCA cycle):18 | Purine metabolism:18 | Lysosome:14
Cluster 2	Metabolic pathways:41
Cluster 3	Metabolic pathways:38 | Drug metabolism -other enzymes:5 | Cell cycle:7
Cluster No.	**Enriched Gene Ontology Terms**
Cluster 1	oxidoreductase activity - GO:0016491:103 | oxidation reduction - GO:0055114:69 | generation of precursor metabolites and energy - GO:0006091:52
	heterocycle metabolic process - GO:0046483:40 | cellular catabolic process - GO:0044248:87 | electron transport chian - GO:0022900:28
	localization - GO:0051179:175 | establishment of localization - GO:0051234;157 | oxidative phosphorylation - GO:0006119:22
	catabolic process - GO:0009056:111 | nucleoside phosphate metabolic process - GO:0006753:33 | hydrolase activity - GO:0016787:145
	oxidoreductase activity, acting on NADH or NADHP - GO:0016651:21 | respiratory chain - GO:0070469:20 | cellular respiration - GO:0045333:22
	organic acid metabolic process - GO:0006082:52 | biosynthetic process - GO:0009058:173 | cofactor metabolic process - GO:0051186:28
	cell redox homemstasis - GO:0045454;17 | nitrogen compound metabolic process - GO:0006807:174 | protein metabolic process - GO:0019538:155
	isomerase activity - GO:0016853;23 | oxidoreductase activity, acting on the CH-OH group of donors, NAD or NADP as acceptor - GO:0016616
	cellular nitrogen compound metabolic process - GO:0034641:29 | cellular amino acid and derivative metabolic process - GO:0006519:36
	inorganic cation transmembrane transporter activity - GO:0022890:24 | cellular carbohydrate metabolic process - GO:0044262:33
	response to oxidative stress - GO:0006979:19 | ribonucleotide metabolic process - GO:0009259:17 | carbohydrate metabolic process - GO:0005975:46
	cellular homeostasis - GO:0019725:36 | regulation of biological quality - GO:0065008:73 | translation - GO:0006412:34
	transferase activity, transferring alkyl or aryl (other than methyl) groups - GO:0016765:13 | cellular compound organization - GO:0016043:107
	acid binding - GO:0003779:32 | organelle organization - GO:0006996:69 | methionine metabolic process - GO:0006555:6 | cofactor binding - GO:0048037:25
	water-soluble vitamin metabolic process - GO:0006767:12 | intracellular transport - GO:0046907:46 | monosaccharide catabolic process - GO:0046365:14
	water-soluble vitamin biosynthetic process - GO:0042364:8 | lyase activity - GO:0016829:20 | response to stress - GO:0006950:79
	transferase activity - GO:0016740:97 | structural molecule activity - GO:0005198:49 | regulation of protein metabolic process - GO:0051246:33
	glucose metabolic process - GO:0006006:16 | lipid metabolic process - GO:0006629:53 | lipid binding 0 GO:0008289:37
	sulfur metabolic process - GO:0006790:14 | regulation of programmed cell death - GO:0043067:42 | ligase activity - GO:0016874:32
	cell cycle - GO:0007049:45 | protein maturation - GO:0051604:14 | DNA metabolic process - GO:0006259:35
	calcium- dependent phospholipid binding - GO:0005544:7 | DNA replication - GO:0006260:19 | antioxidant activity - GO;0016209:10
	celllar macromolecule localization - GO:0070727:32
Cluster 2	oxidation reduction - GO:0055114:26 | cellular ketone metabolic process - GO:0042180:19
	nucleobase, nucleoside and nucleotide metabolic process - GO:0055086:12 | protein amino acid N-linked glycosylation - GO:0006487:6
Cluster 3	cellular component organization - GO:0016043:45 | macromolecular complex assembly - GO:0065003:16 | oxidoreductase activity - GO:0016491:21
	nuclear division - GO:0000280:11 | cell division - GO:0051301:12 | catabolic process - GO:0009056:30 | protein tetramerization - GO:0051262:5
	lipid metabolic process - GO:0006629:19 | regulation of biological quality - GO:0065008:22 | protein metabolic process - GO;0019538:40
	protein domain specific binding - GO:0019904;9
Cluster 4	Nnuclear division - GO:0000280:11 | organelle organization 0 GO:0006996:23 | cell cycle - GO:0007049:16
	cytoskeleton organization - GO:0007010:12 | ATP binding - GO:0005524:23 | microtubule cytoskeleton organization - GO:0000226:7
Cluster 7	cofactor binding - GO;0048037:7
Cluster No.	**Enriched Chromosome Locations**
Cluster 1	chromosome 13q32:9 | chromosome 2:81
Cluster 3	chromosome 2:26
Cluster No.	**Enriched microRNAs**
Cluster 5	mir-374/374ab:3 | mir-543:3
Cluster 6	mir-22:5 | mir-530:4
Cluster 7	mir-31:3

Genes with down-regulated expression were significantly categorized into different functional groups and canonical pathways. Different transcription factors and microRNAs that can potentially be involved in the regulation of gene expressions are shown for each cluster under Expander 5 software analysis (P-value≤0.05). Each functional group, canonical pathway, transcription factor or microRNA is followed by the number of corresponding genes.

Excluding enrichments of these transcription factors and pathways, mir-128 also displayed the potential possibility to bind and regulate three down-regulated genes in lister virus infected A549 cells, while other microRNAs like mir-374/374as, mir-543, mir-22, mir-530 and mir-31 were also picked out in genes with deceased expression during cowpox virus infection. Meanwhile, some chromosome locations especially chromosome 2 were detected to be the targeting location for over one hundred genes with down-regulated expression.

Table 6.6 Summary of functional groups, canonical pathways, transcription factors and microRNAs enriched based on down-regulated genes in A549 cells infected with lister virus.

Lister Group II	
Cluster No.	**Enriched Transcription Factors**
Cluster 1	M00803[E2F]:238 | M00196[Sp1]:217
Cluster No.	**Enriched Canonical Pathways**
Cluster 1	Metabolic pathways:60 | Glutathione metabolism :9 | Glycolysis / Gluconeogenesis:8 | Purine metabolism:12 | DNA replication:6
	Oxidative phosphorylation:10
Cluster 2	Metabolic pathways:26 | DNA replication:5
Cluster No.	**Enriched Gene Ontology Terms**
Cluster 1	oxidation reduction - GO:0055114:47 | generarion of precursor metabolites and energy - GO:0006091:24 | cellular ketone metabolic process - GO:0042180:27
	electron transport chain - GO:0022900:13 | organic acid metabolic process - GO:0006082:26 | cellular amino acid derivative metabolic process - GO:0006575:13
	cellular amino acid and derivative metabolic process - GO:0006519:20 | oxidoreductase activity, acting on CH-OH group of donors - GO:0016614:12
	cellular nitrogen compound metabolic process - GO:0034641:16 | lipid metabolic process - GO:0006629 | cellular carbohydrate catabolic process - GO:0044275:9
	hydrolase activity - GO:0016787:62 | cell cycle process - GO:0022402:22 | cellular carbohydrate metabolic process - GO:0044262:17
	cell cycle process - GO:0022402:22 | biosynthetic process - GO:0009058:74 | nitrogen compound metabolic process - GO;0006807:76
	intrsmolecular oxidoreductase activity - GO:0016860:7 | steroid binding - GO:0005496:11 | organelle organization - GO:0006996:34
	nucleobase, nucleoside and nucleotide metabolic process - GO:0055086:14 | localization - GO:0051179:69 | single-stranded DNA binding - GO:0003697:7
	cellular catabolic process - GO:0044248:32 | DNA metabolic process - GO:0006259:20 | heterocycle metabolic process - GO:0046483:14
	cofactor binding - GO:0048037:13 | organelle fission - GO:0048285:12 | structual molecule activity - GO:0005198:25 | response to stress - GO:0006950:38
	vitamin metabolic process - GO:0006766:8 | transferase activity - GO:0016740:46 | coenzyme metabolic process - GO:0006732:10
	positive regulation of biological process - GO:0048518:37 | cellular aromatic compound metabolic process - GO:0006725:9
Cluster 2	oxidoreductase activity - GO:0016491:21 | DNA replication - GO:0006260:9
Cluster 3	alcohol catabolic process - GO:0046164:4
Cluster 5	negative regulation of cellular protein metabolic process - GO:0032269:4
Cluster No.	**Enriched micRNAs**
Cluster 1	mir-128:3

Genes with down-regulated expression were significantly categorized into different functional groups and canonical pathways. Different transcription factors and microRNAs that can potentially be involved in the regulation of gene expressions are shown for each cluster under Expander 5 software analysis (P-value≤0.05). Each functional group, canonical pathway, transcription factor or microRNA is followed by the number of corresponding genes.

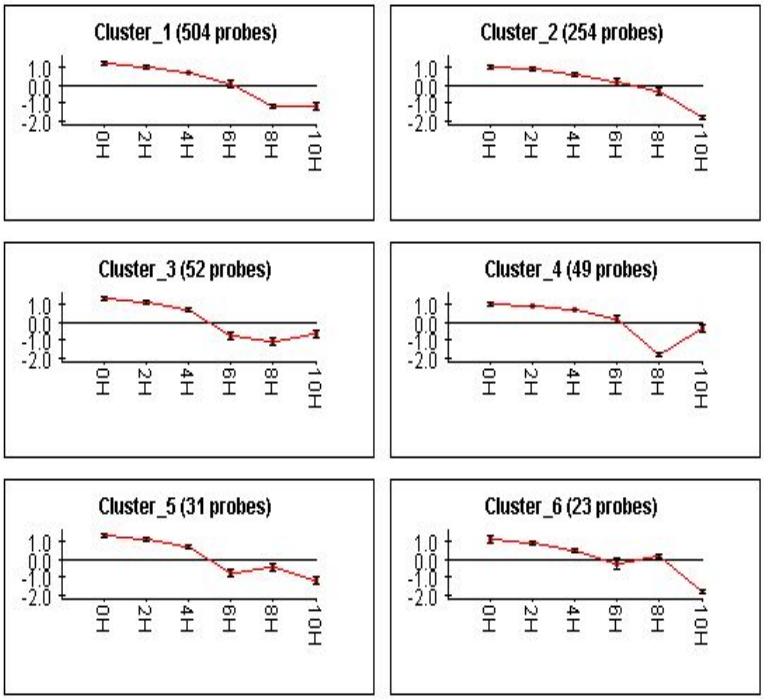

Figure 6.12 Clustering analysis of temporal gene expression profiles in lister virus-infected A549 cells. A549 cells were infected with cowpox virus at 2, 4, 6, 8 and 10 hpi. Probe sets showing ≥10-fold changes down-regulated (P-value≤0.05) at least at 10 hpi were analyzed with Expander 5 software. X-axis represents post-infection in hours (H), and Y-axis means normalized expression changes of probe sets.

6.3.1.5 Core analysis in mouse RAW cells

At early time point, several shared functions were identified based on differentially expressed genes in all these three types of poxviruses infected mouse RAW cells, and these top biological functions were "Immunological Disease", "Cellular Growth and Proliferation", "Cell Cycle", "Cell Death" and "Connective Tissue Development and Function" [Figure 6.13-6.24]. Significant enrichment of these common functions indicated that the immune reaction and cell growth regulation were initiated at the early stage of poxviruses infections. Of particular interest, the number of molecules belonging to "Gene expression", "Cell Cycle", "Cell death" and "Cellular Growth and Proliferation" showed highest upon the infection of lister virus. This phenomenon indicated that the most significant regulation of cell activities occurred in mouse RAW cells, infected with lister virus.

When it came to canonical pathways, pathways such as "Glycosis/Gluconegenesis" and "Frutose and Mannose Metabolism" were common in ectromelia and cowpox virus infected mouse RAW cells. However, the pathways over-represented in lister virus infected mouse RAW cells were

associated with cell cycle checkpoint control. Subsequently, enrichment of different pathways indicated that more regulations of energy metabolism occurred after infections of ectromelia and cowpox virus while more controls of cell cycle occurred after infection of lister virus in mouse RAW cells. Furthermore, network of "Lipid metabolism, Molecular Transport, Small Molecule Biochemistry" was found to be unique to cowpox virus infection, which might also implicate the potential regulation of membrane activities.

Among top five potential transcription factors, four common ones including STAT4, HIF1A, EPAS1 and ATF4 were shared by infections of cowpox and ectromelia virus in mouse RAW cells at 2 hpi. Among these four factors, STAT4 is essential for mediating responses to IL12 in lymphocytes, and regulating the differentiation of T helper cells [341], while HIF1A and EPAS1 are both transcription regulators related to oxygen level. Enrichment of these transcription factors based on differentially expressed genes might implicate the differential regulation on some cytokines' activities as well as oxygen level in these two types of poxviruses infected mouse RAW cells.

Top five transcription regulators over-presented in differentially expressed genes from lister virus infected mouse RAW cells at 2 hpi were DACH1, MNT, SIN3B, TP53 and ELK1. TP53 is a famous factor that is responsible for the control of cell cycle and cell death. Its enrichment was concordant with the previous enrichment of functional groups including cell death and cell cycle [342], and thereby this observation supported the hypothesis that cell cycle and cell death regulation were triggered at the initial step in lister virus infected mouse RAW cells.

At 16 hpi, many common features were shared in response to infections of these three types of poxviruses in mouse RAW cells. Functions including "Infectious Disease", "RNA Post-Transcription Modification", "Cell cycle", "Embryonic Development", "Connetive Tissue Development and Function", "Hematological System Development and Function" were all shared by these three types of poxviruses. Furthermore, four common pathways such as "Oxidative Phosphorylation", "Mitochondrial Dysfunction", "Protein Ubiquitination Pathway" and "Ubiquinone Biosynthesis" were also enriched based on the differentially expressed genes after infections of these poxviruses,

suggesting existing regulation of oxygen, energy and apoptosis in infected mouse RAW cells.

It was striking that "Cell death" was listed as one of the topmost five molecular and cellular functions in ectromelia virus infected mouse RAW cells with 1085 genes included, with a sharp increase of 94 molecules from 2 hpi. Thus observation might suggest the initiation of numerous mechanisms by which ectromelia virus inhibited apoptosis thereby modulating cell life [332].

Apart from these pathways and functional groups, a couple of transcription factors were also shared by infections of these three types of poxviruses. Among them, E2F4 and MYC are famous transcription factors that play a crucial role in the control of cell cycle [343]. Enrichment of these two factors implied the special regulated state of cell cycle.

6.3.1.6 Selection of common genes modulated by infections of different poxviruses in mouse RAW cells

As described above, hundreds or thousands of probes were up- or down-regulated in these three types of poxviruses infected mouse RAW cells. To further investigate the underlying common regulation mechanisms among these poxviruses, we constructed venn diagrams in order to select out the probe sets with common expression alteration [Figure 6.25-6.26].

Since only small number of probe sets with stimulated expression was identified in mouse RAW cells after infections at 2 hpi, no probe set was finally detected with common stimulation in its expression in all these three poxviruses infected mouse RAW cells. Twenty probe sets with up-regulated expression (≥2-FC&<5-FC) were observed upon infections of cowpox and ectromelia virus, which might represent the existence of some common host reactions upon these two viruses infection at early infection stage.

With more up-regulated probe sets detected at 16 hpi, 65 probe sets were found to be commonly up-regulated (≥2-FC) in these three types of poxviruses infected mouse RAW cells. This batch of up-regulated probe sets played functions on "Cell Cycle", "Cell Death", "Kinase", "RNA Binding" and "Actin", and common expression elevation of these gene implied that infected mouse RAW cells fighted with infections of poxviruses through initiating similar mechanisms.

Among these probe sets, the probe sets encoding Lats2 and Hspa1b were of particular interest as their fold regulations were at ≥ 5-FC in all three types of poxviruses infected mouse RAW cells. Lats2, large tumor suppressor 2, is an AGC kinase of the NDR family of kinases which inhibits cell growth at the G1/S transition by down-regulating cyclin E/CDK2 kinase activity. The corresponding probe sets was elevated with 7.6-FC under lister virus infection, 5.6-FC under cowpox virus infection and 20.18-FC under ectromelia infection at 16 hpi. High-level fold regulation of this probe sets, especially in ectromelia infected mouse RAW cells, might be treated as an indication that the cell cycle was arrested at G1/S checkpoint in reaction to these poxviruses infections.

The other gene Hspa1b is a member of heat shock protein 70 family, which is involved in the ubiquitin-proteasome pathway through interaction with the AU-rich element RNA-binding protein 1. The corresponding probe set was up-regulated with around 200-FC and 50-FC upon lister and ectromelia virus infections. Outstanding expression elevation of this probe set implicated the potential induction of cell death activities, which might be responsible to impede the virus replication in mouse RAW host cells. Up-regulated expression of this gene with 15-FC after cowpox virus infection also implicated moderate apoptosis regulation in the corresponding host cells.

At 2 hpi, only 10 probe sets (6.1% for 163, 3.0% for 385 and 2.1% for 478) were commonly down-regulated with ≥2-FC in mouse RAW cells after infections of three types of poxviruses. And this indicated that the negative control of gene expression at the early infection stage was different from each other among three types of poxviruses infections in infected mouse RAW cells.

Different from the situation happened at 2 hpi, 4539 probe sets (57.9% for 7845, 75.2% for 6034 and 45.9% for 9880) were identified with common down-regulation (≥2-FC) in their expression in three poxviruses infected mouse RAW cells. What's more, 40 probe sets showed down-regulated expression with fold regulation ≥10-FC after infections of all these three types of poxviruses. Functional annotation suggested that these 4539 probe sets were functional associated with "RNA binding", "Protein metabolism", "Kinase", "Cell Cycle", "Cell Death", "Signal transduction", "DNA transcription factor" and "Phosphatase", while those 40 probe sets were closely related to "Antiviral", "Cell Death", "Cell Cycle" and "Kinase".

These 40 commonly down-regulated probe sets with high-level fold changes encoded genes including Ifitm3/6, Cadm1, Clec4e/5a, Fabp5 and so on. Among them, genes such as Mpeg1, H2-K1, and Msr1 are associated with macrophage function. Besides, other transmembrane gene such as Tm6sf1 also showed repressed expression in these poxviruses infected mouse RAW cells.

Cowpox Mouse Raw 2 hpi

Top Networks

ID	Associated Network Functions	Score
1	Lipid Metabolism, Molecular Transport, Small Molecule Biochemistry	43
2	Gene Expression, Cellular Function and Maintenance, Cellular Growth and Proliferation	36
3	Gene Expression, Cell-To-Cell Signaling and Interaction, Cellular Development	31
4	Cardiovascular System Development and Function, Cellular Movement, Organismal Development	29
5	Post-Translational Modification, Cellular Response to Therapeutics, Connective Tissue Development and Function	27

Top Bio Functions

Diseases and Disorders

Name	p-value	# Molecules
Renal and Urological Disease	3.04E-05 - 1.25E-02	28
Cancer	6.47E-05 - 1.25E-02	76
Immunological Disease	6.47E-05 - 1.25E-02	17
Cardiovascular Disease	8.45E-05 - 1.25E-02	29
Inflammatory Response	1.03E-04 - 1.25E-02	12

Molecular and Cellular Functions

Name	p-value	# Molecules
Cellular Development	2.00E-07 - 1.25E-02	47
Cellular Growth and Proliferation	4.16E-05 - 1.25E-02	61
Cellular Function and Maintenance	4.46E-05 - 1.25E-02	36
Cell Death	5.48E-05 - 1.25E-02	58
Cell Cycle	6.47E-05 - 1.25E-02	11

Physiological System Development and Function

Name	p-value	# Molecules
Connective Tissue Development and Function	2.00E-07 - 1.25E-02	26
Tumor Morphology	1.90E-05 - 1.25E-02	12
Skeletal and Muscular System Development and Function	4.16E-05 - 1.25E-02	26
Cardiovascular System Development and Function	4.89E-05 - 1.25E-02	29
Organismal Development	4.89E-05 - 1.25E-02	35

Top Canonical Pathways

Name	p-value	Ratio
Glycolysis/Gluconeogenesis	2.3E-03	5/130 (0.038)
Starch and Sucrose Metabolism	3.99E-03	4/166 (0.024)
Pentose Phosphate Pathway	6.08E-03	3/80 (0.038)
Inhibition of Angiogenesis by TSP1	7.29E-03	3/39 (0.077)
Fructose and Mannose Metabolism	1.75E-02	3/134 (0.022)

Top Transcription Factors

Transcription Regulator	p-value of overlap	Predicted Activation State
STAT4	3.80E-16	Inhibited
HIF1A	7.58E-11	Inhibited
EPAS1	1.54E-08	Inhibited
ATF4	1.63E-07	
SP3	1.22E-05	

Figure 6.13 Summary of top functional networks of differentially expressed genes in cowpox virus-infected mouse RAW cells at 2 hpi. Differentially expressed genes were significantly categorized into different networks, functions and pathways under the analysis of Ingenuity Pathway Analysis (IPA) version 2012 (P-value≤0.05).

A

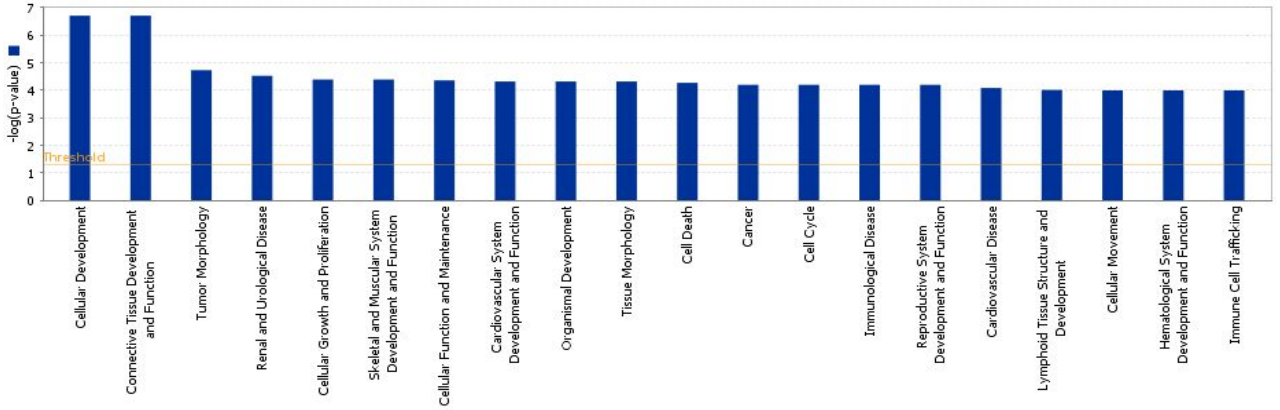

B

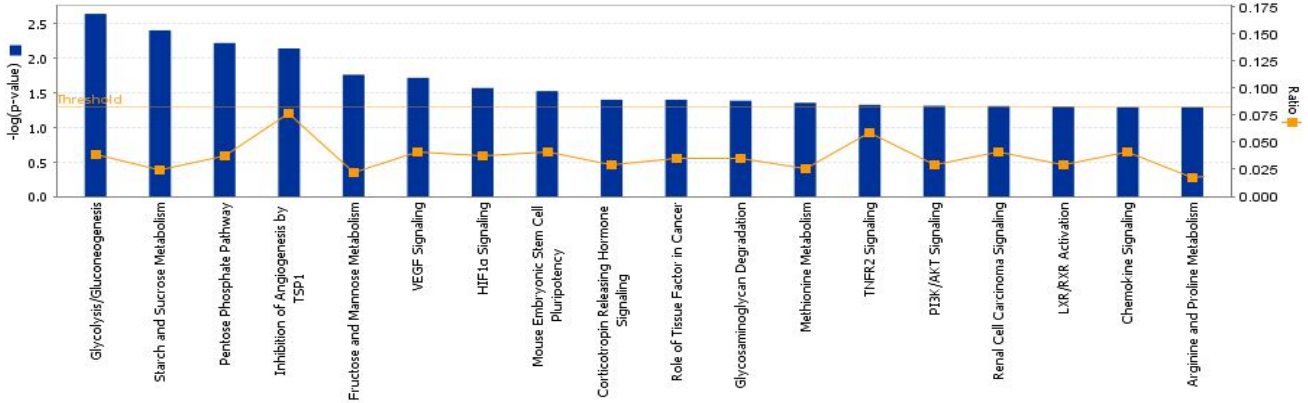

Figure 6.14 Top 20 (A) biological functions and (B) canonical pathways significantly enriched in differentially expressed genes from cowpox virus-infected mouse RAW cells at 2 hpi (P-value≤0.05). Threshold was set at p-value = 0.05 and indicated as –log (p-value) on the Y-axis and the X-axis shows the terms of each biological function or canonical pathway. The orange boxes indicate the ratio (Ratio) of the number of genes with differential expression changes and the total number of genes in the respective canonical pathway.

Cowpox Mouse Raw 16 hpi

Top Networks

ID	Associated Network Functions	Score
1	Genetic Disorder, Metabolic Disease, Developmental Disorder	28
2	Cellular Assembly and Organization, Cell Cycle, Molecular Transport	28
3	Hematological Disease, Immunological Disease, Small Molecule Biochemistry	28
4	Cellular Compromise, Cell Cycle, Cellular Assembly and Organization	28
5	Protein Degradation, Protein Synthesis, RNA Post-Transcriptional Modification	28

Top Bio Functions

Diseases and Disorders

Name	p-value	# Molecules
Infectious Disease	9.92E-14 - 7.31E-03	690
Cardiovascular Disease	6.77E-10 - 2.71E-03	31
Genetic Disorder	6.77E-10 - 8.77E-03	519
Metabolic Disease	6.77E-10 - 5.80E-03	230
Neurological Disease	6.77E-10 - 5.80E-03	64

Molecular and Cellular Functions

Name	p-value	# Molecules
Cell Cycle	7.67E-18 - 8.77E-03	703
RNA Post-Transcriptional Modification	1.29E-13 - 5.71E-03	172
Cellular Assembly and Organization	1.43E-12 - 8.77E-03	708
DNA Replication, Recombination, and Repair	1.43E-12 - 6.00E-03	575
Cellular Movement	3.78E-12 - 8.77E-03	91

Physiological System Development and Function

Name	p-value	# Molecules
Connective Tissue Development and Function	1.32E-05 - 8.77E-03	201
Hematological System Development and Function	1.37E-05 - 7.04E-03	158
Embryonic Development	9.26E-05 - 5.89E-03	292
Lymphoid Tissue Structure and Development	5.71E-04 - 6.53E-03	147
Organ Morphology	5.71E-04 - 6.53E-03	147

Top Canonical Pathways

Name	p-value	Ratio
Oxidative Phosphorylation	1.24E-27	96/159 (0.604)
Mitochondrial Dysfunction	1.7E-21	91/174 (0.523)
Ubiquinone Biosynthesis	6.33E-15	46/110 (0.418)
Protein Ubiquitination Pathway	2.55E-10	133/269 (0.494)
Hereditary Breast Cancer Signaling	3.42E-10	70/127 (0.551)

Top Transcription Factors

Transcription Regulator	p-value of overlap	Predicted Activation State
HNF4A	3.88E-31	
MYC	1.56E-19	Inhibited
E2F4	5.30E-19	
XBP1 (includes EG:140614)	3.89E-13	
POU4F1	6.26E-13	

Figure 6.15 Summary of top functional networks of differentially expressed genes in cowpox virus-infected mouse RAW cells at 16 hpi. Differentially expressed genes were significantly categorized into different networks, functions and pathways under the analysis of Ingenuity Pathway Analysis (IPA) version 2012 (P-value≤0.05).

A

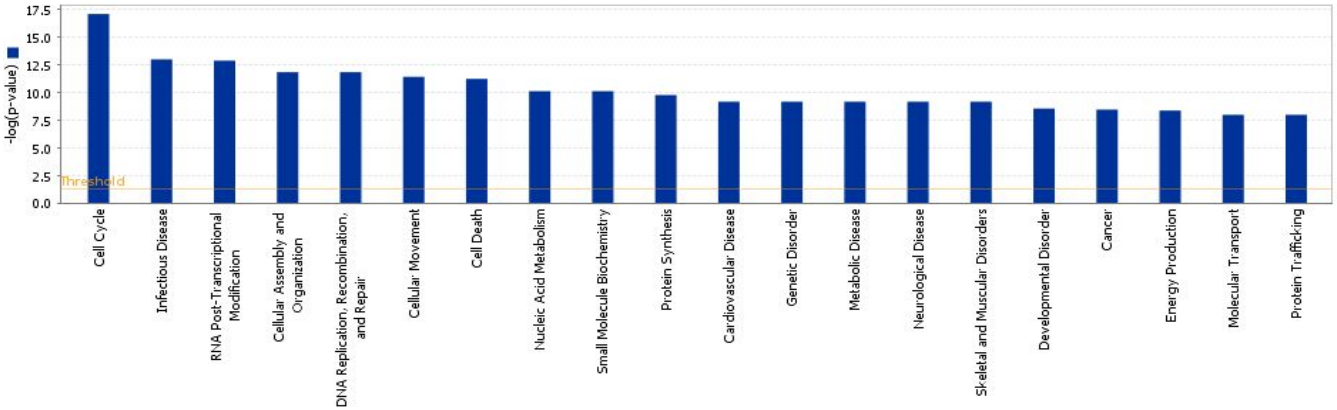

B

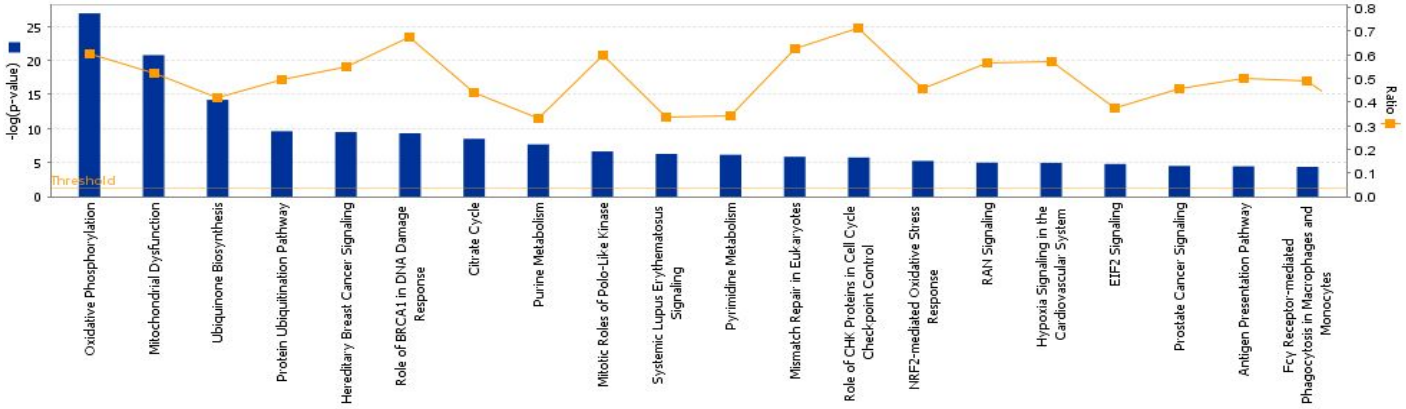

Figure 6.16 Top 20 (A) biological functions and (B) canonical pathways significantly enriched in differentially expressed genes from cowpox virus-infected mouse RAW cells at 16 hpi (P-value≤0.05). Threshold was set at p-value = 0.05 and indicated as –log (p-value) on the Y-axis and the X-axis shows the terms of each biological function or canonical pathway. The orange boxes indicate the ratio (Ratio) of the number of genes with differential expression changes and the total number of genes in the respective canonical pathway.

Lister Mouse Raw 2 hpi

Top Networks

ID	Associated Network Functions	Score
1	Gene Expression, Molecular Transport, RNA Trafficking	43
2	Gene Expression, Cellular Development, Connective Tissue Development and Function	41
3	Post-Translational Modification, Connective Tissue Disorders, Immunological Disease	40
4	Cancer, Cellular Development, Organ Development	34
5	Genetic Disorder, Neurological Disease, Connective Tissue Disorders	34

Top Bio Functions

Diseases and Disorders

Name	p-value	# Molecules
Cardiovascular Disease	8.86E-05 - 6.60E-03	6
Organismal Injury and Abnormalities	8.86E-05 - 1.31E-02	10
Connective Tissue Disorders	2.50E-04 - 1.75E-02	22
Immunological Disease	2.50E-04 - 2.64E-02	30
Inflammatory Disease	2.50E-04 - 2.64E-02	29

Molecular and Cellular Functions

Name	p-value	# Molecules
Gene Expression	3.17E-13 - 1.94E-02	130
Cell Cycle	1.34E-06 - 2.64E-02	72
Cellular Growth and Proliferation	3.61E-06 - 2.64E-02	124
Cell Death	1.30E-05 - 2.64E-02	119
Cellular Movement	5.43E-05 - 2.64E-02	13

Physiological System Development and Function

Name	p-value	# Molecules
Hepatic System Development and Function	3.61E-06 - 2.43E-02	24
Hematological System Development and Function	4.82E-06 - 2.45E-02	67
Hematopoiesis	4.82E-06 - 2.44E-02	45
Skeletal and Muscular System Development and Function	5.43E-05 - 2.64E-02	46
Connective Tissue Development and Function	9.94E-05 - 2.64E-02	67

Top Canonical Pathways

Name	p-value	Ratio
IL-17A Signaling in Fibroblasts	1.85E-03	5/40 (0.125)
Cell Cycle: G1/S Checkpoint Regulation	4.51E-03	6/65 (0.092)
Telomere Extension by Telomerase	6.57E-03	3/17 (0.176)
Role of CHK Proteins in Cell Cycle Checkpoint Control	1.07E-02	4/35 (0.114)
Cell Cycle Regulation by BTG Family Proteins	1.19E-02	4/36 (0.111)

Top Transcription Factors

Transcription Regulator	p-value of overlap	Predicted Activation State
DACH1	8.51E-08	
MNT	1.12E-05	
SIN3B	1.34E-05	
TP53 (includes EG:22059)	2.04E-05	
ELK1	2.33E-05	

Figure 6.17 Summary of top functional networks of differentially expressed genes in lister virus-infected mouse RAW cells at 2 hpi. Differentially expressed genes were significantly categorized into different networks, functions and pathways under the analysis of Ingenuity Pathway Analysis (IPA) version 2012 (P-value≤0.05).

A

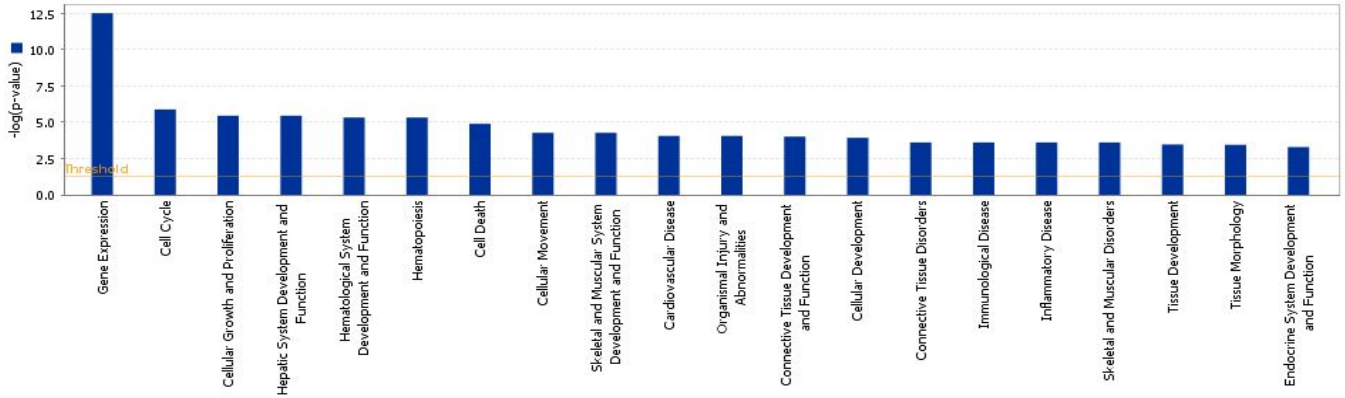

B

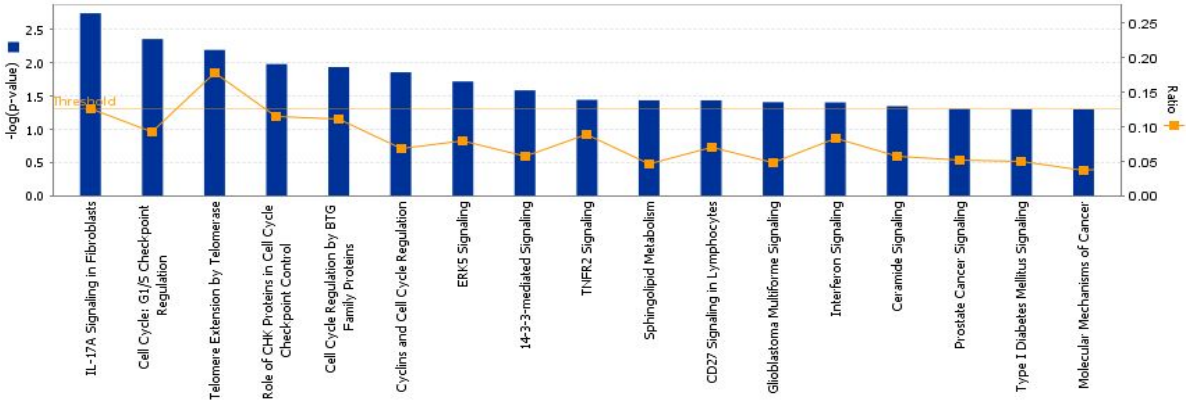

Figure 6.18 Top 20 (A) biological functions and (B) canonical pathways significantly enriched in differentially expressed genes from lister virus-infected mouse RAW cells at 2 hpi (P-value≤0.05). Threshold was set at p-value = 0.05 and indicated as –log (p-value) on the Y-axis and the X-axis shows the terms of each biological function or canonical pathway. The orange boxes indicate the ratio (Ratio) of the number of genes with differential expression changes and the total number of genes in the respective canonical pathway.

Lister Mouse Raw 16 hpi

Top Networks

ID	Associated Network Functions	Score
1	Infectious Disease, DNA Replication, Recombination, and Repair, Molecular Transport	26
2	Carbohydrate Metabolism, Cardiac Dilation, Cardiovascular System Development and Function	26
3	RNA Post-Transcriptional Modification, Dermatological Diseases and Conditions, Infectious Disease	26
4	Cell Cycle, Cellular Assembly and Organization, Genetic Disorder	26
5	Genetic Disorder, Renal and Urological Disease, Ophthalmic Disease	23

Top Bio Functions

Diseases and Disorders

Name	p-value	# Molecules
Infectious Disease	5.11E-15 - 8.04E-03	814
Organismal Injury and Abnormalities	2.74E-13 - 1.87E-02	207
Dermatological Diseases and Conditions	6.54E-13 - 6.54E-13	181
Renal and Urological Disease	1.64E-12 - 1.52E-02	277
Cardiovascular Disease	2.00E-08 - 1.22E-02	31

Molecular and Cellular Functions

Name	p-value	# Molecules
RNA Post-Transcriptional Modification	9.57E-24 - 6.75E-03	218
Cell Cycle	4.03E-19 - 1.82E-02	832
Molecular Transport	2.48E-14 - 1.27E-02	304
Protein Trafficking	2.48E-14 - 4.92E-03	230
Gene Expression	3.67E-14 - 1.19E-02	153

Physiological System Development and Function

Name	p-value	# Molecules
Embryonic Development	4.58E-07 - 1.66E-02	391
Tissue Development	4.58E-07 - 4.92E-03	60
Organismal Development	8.27E-05 - 4.33E-04	92
Hematological System Development and Function	1.55E-04 - 1.80E-02	201
Connective Tissue Development and Function	1.96E-04 - 1.82E-02	236

Top Canonical Pathways

Name	p-value	Ratio
Oxidative Phosphorylation	3.29E-22	97/159 (0.61)
Mitochondrial Dysfunction	6.87E-19	95/174 (0.546)
EIF2 Signaling	8.04E-15	108/205 (0.527)
Protein Ubiquitination Pathway	4.24E-14	159/269 (0.591)
Ubiquinone Biosynthesis	6.51E-11	45/110 (0.409)

Top Transcription Factors

Transcription Regulator	p-value of overlap	Predicted Activation State
HNF4A	1.14E-44	
MYC	4.06E-24	Inhibited
E2F4	2.10E-21	
ISL1	1.56E-14	
POU4F1	3.32E-14	

Figure 6.19 Summary of top functional networks of differentially expressed genes in lister virus-infected mouse RAW cells at 16 hpi. Differentially expressed genes were significantly categorized into different networks, functions and pathways under the analysis of Ingenuity Pathway Analysis (IPA) version 2012 (P-value≤0.05).

A

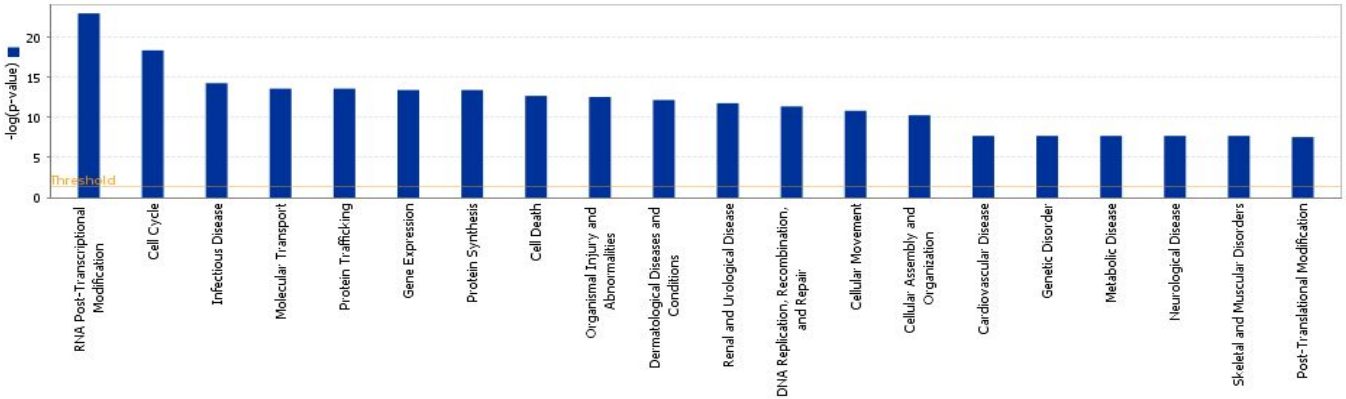

B

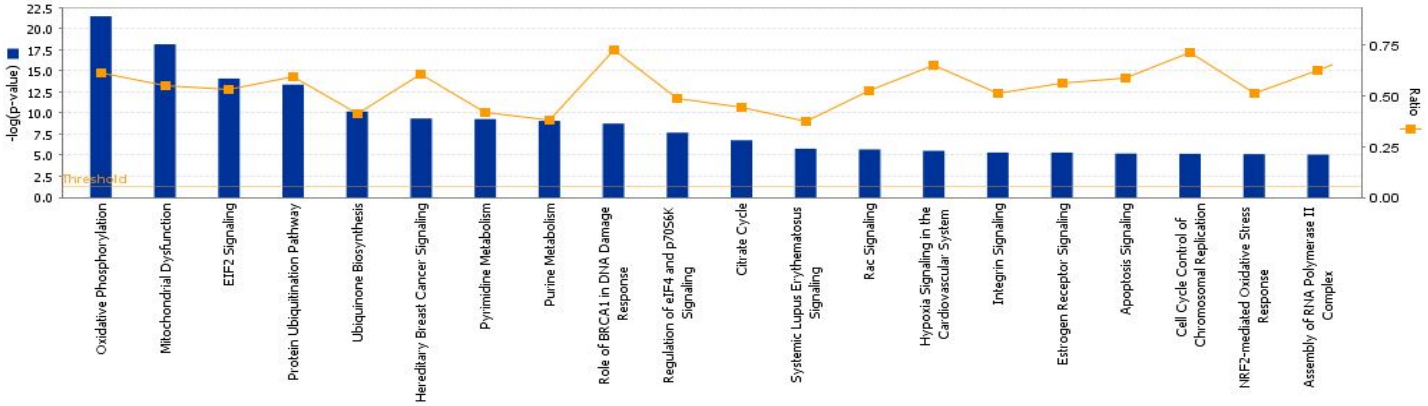

Figure 6.20 Top 20 (A) biological functions and (B) canonical pathways significantly enriched in differentially expressed genes from lister virus-infected mouse RAW cells at 16 hpi (P-value≤0.05). Threshold was set at p-value = 0.05 and indicated as –log (p-value) on the Y-axis and the X-axis shows the terms of each biological function or canonical pathway. The orange boxes indicate the ratio (Ratio) of the number of genes with differential expression changes and the total number of genes in the respective canonical pathway.

Ectromelia Mouse Raw 2 hpi

Top Networks

ID	Associated Network Functions	Score
1	Cell Morphology, Cellular Function and Maintenance, Cell Death	48
2	Hematological System Development and Function, Hematopoiesis, Tissue Morphology	38
3	Cell Cycle, Cancer, Reproductive System Development and Function	35
4	Cellular Development, Cellular Growth and Proliferation, Cancer	32
5	Cellular Development, Cellular Growth and Proliferation, Hematological System Development and Function	32

Top Bio Functions

Diseases and Disorders

Name	p-value	# Molecules
Immunological Disease	1.38E-06 - 2.02E-02	25
Cancer	2.54E-06 - 2.01E-02	123
Endocrine System Disorders	1.22E-04 - 2.02E-02	13
Hematological Disease	1.22E-04 - 2.02E-02	36
Ophthalmic Disease	1.55E-04 - 2.02E-02	6

Molecular and Cellular Functions

Name	p-value	# Molecules
Cell Death	2.43E-07 - 2.02E-02	94
Cellular Development	3.25E-07 - 2.02E-02	85
Cell Cycle	1.60E-06 - 2.02E-02	58
Cellular Growth and Proliferation	4.17E-05 - 2.02E-02	102
Cellular Function and Maintenance	1.24E-04 - 2.02E-02	53

Physiological System Development and Function

Name	p-value	# Molecules
Connective Tissue Development and Function	3.25E-07 - 2.02E-02	41
Embryonic Development	4.80E-06 - 2.02E-02	33
Endocrine System Development and Function	4.80E-06 - 1.70E-03	10
Organ Development	4.80E-06 - 2.02E-02	22
Organismal Development	4.80E-06 - 2.02E-02	28

Top Canonical Pathways

Name	p-value	Ratio
Fructose and Mannose Metabolism	2.53E-05	7/134 (0.052)
Biosynthesis of Steroids	8.25E-03	3/122 (0.025)
Aminosugars Metabolism	1.26E-02	5/120 (0.042)
Glycolysis/Gluconeogenesis	1.67E-02	5/130 (0.038)
TNFR2 Signaling	1.83E-02	3/34 (0.088)

Top Transcription Factors

Transcription Regulator	p-value of overlap	Predicted Activation State
STAT4	5.53E-10	
HIF1A	5.85E-08	
ATF4	3.02E-07	
EPAS1	3.85E-06	
FOXO4	3.43E-05	

Figure 6.21 Summary of top functional networks of differentially expressed genes in ectromelia virus-infected mouse RAW cells at 2 hpi. Differentially expressed genes were significantly categorized into different networks, functions and pathways under the analysis of Ingenuity Pathway Analysis (IPA) version 2012 (P-value≤0.05).

A

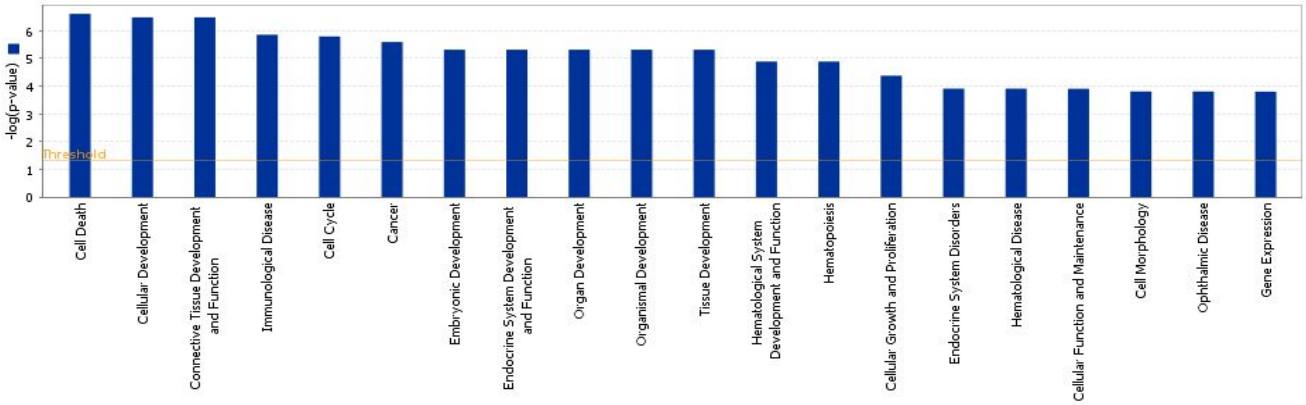

B

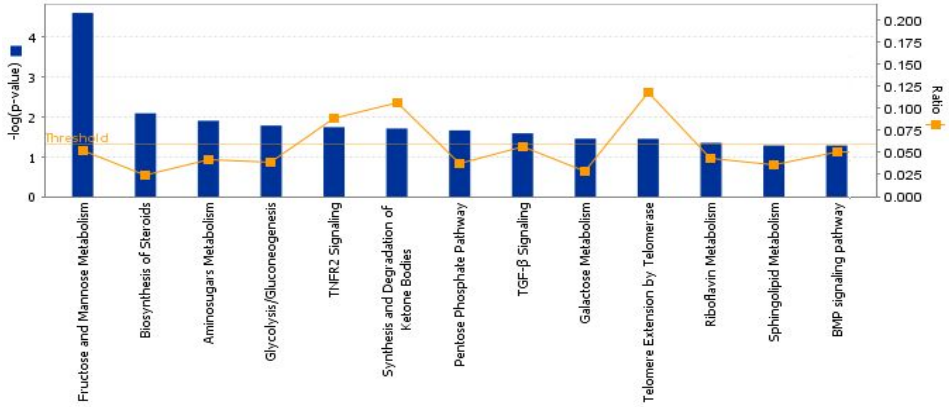

Figure 6.22 Top 20 (A) biological functions and (B) canonical pathways significantly enriched in differentially expressed genes from ectromelia virus-infected mouse RAW cells at 2 hpi (P-value≤0.05). Threshold was set at p-value = 0.05 and indicated as –log (p-value) on the Y-axis and the X-axis shows the terms of each biological function or canonical pathway. The orange boxes indicate the ratio (Ratio) of the number of genes with differential expression changes and the total number of genes in the respective canonical pathway.

Ectromelia Mouse Raw 16 hpi

Top Networks

ID	Associated Network Functions	Score
1	Protein Degradation, Protein Synthesis, Cellular Assembly and Organization	30
2	Carbohydrate Metabolism, Small Molecule Biochemistry, Developmental Disorder	30
3	Lipid Metabolism, Nucleic Acid Metabolism, Small Molecule Biochemistry	30
4	Genetic Disorder, Metabolic Disease, Hematological Disease	30
5	Molecular Transport, RNA Trafficking, RNA Damage and Repair	28

Top Bio Functions

Diseases and Disorders

Name	p-value	# Molecules
Infectious Disease	9.44E-15 - 1.39E-02	649
Dermatological Diseases and Conditions	1.07E-13 - 8.70E-03	188
Organismal Injury and Abnormalities	1.07E-13 - 9.87E-03	228
Renal and Urological Disease	3.34E-13 - 9.97E-03	196
Cancer	1.21E-06 - 1.36E-02	1193

Molecular and Cellular Functions

Name	p-value	# Molecules
RNA Post-Transcriptional Modification	2.24E-17 - 1.39E-02	191
Cell Cycle	1.16E-14 - 1.39E-02	663
Protein Synthesis	2.60E-13 - 1.14E-02	402
Gene Expression	3.65E-12 - 1.35E-02	162
Cell Death	1.92E-11 - 1.39E-02	1085

Physiological System Development and Function

Name	p-value	# Molecules
Embryonic Development	8.21E-06 - 1.39E-02	289
Tissue Development	3.55E-05 - 1.25E-02	80
Connective Tissue Development and Function	1.89E-04 - 1.39E-02	260
Hematological System Development and Function	2.00E-04 - 1.39E-02	103
Organismal Development	3.45E-04 - 1.82E-03	79

Top Canonical Pathways

Name	p-value	Ratio
Oxidative Phosphorylation	3.76E-21	85/159 (0.535)
Mitochondrial Dysfunction	5.51E-17	81/174 (0.466)
Protein Ubiquitination Pathway	5.04E-15	136/269 (0.506)
Ubiquinone Biosynthesis	1.14E-12	42/110 (0.382)
EIF2 Signaling	1.1E-11	87/205 (0.424)

Top Transcription Factors

Transcription Regulator	p-value of overlap	Predicted Activation State
HNF4A	2.35E-23	
E2F4	5.64E-20	
MYC	1.91E-18	Inhibited
E2F1	1.21E-13	
POU4F1	1.62E-12	

Figure 6.23 Summary of top functional networks of differentially expressed genes in ectromelia virus-infected mouse RAW cells at 16 hpi. Differentially expressed genes were significantly categorized into different networks, functions and pathways under the analysis of Ingenuity Pathway Analysis (IPA) version 2012 (P-value≤0.05).

A

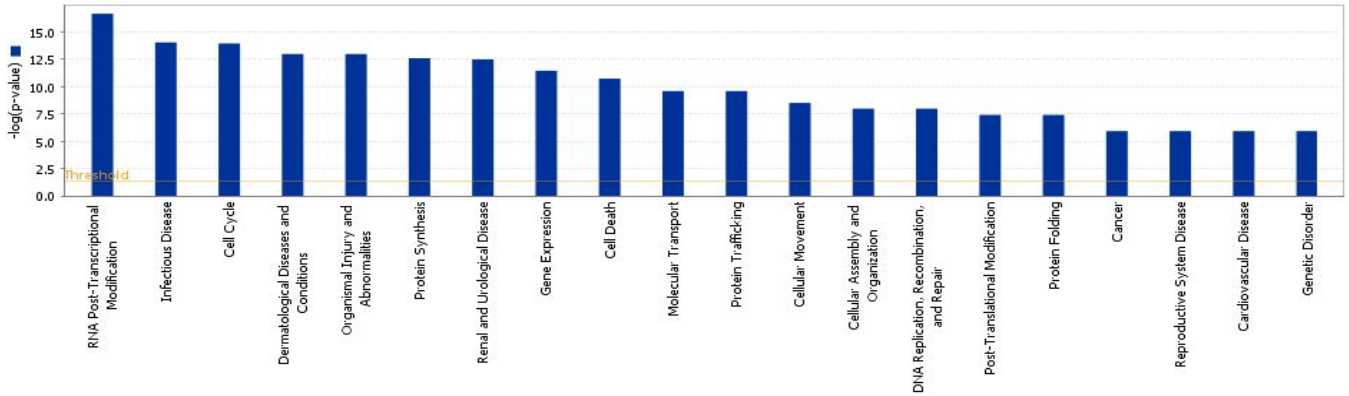

B

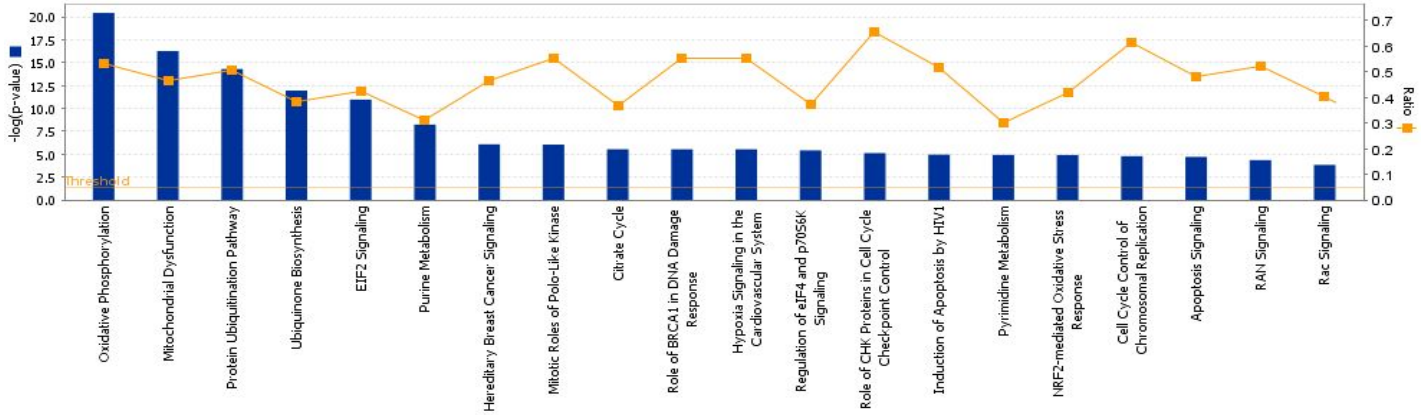

Figure 6.24 Top 20 (A) biological functions and (B) canonical pathways significantly enriched in differentially expressed genes from ectromelia virus-infected mouse RAW cells at 16 hpi (P-value≤0.05). Threshold was set at p-value = 0.05 and indicated as –log (p-value) on the Y-axis and the X-axis shows the terms of each biological function or canonical pathway. The orange boxes indicate the ratio (Ratio) of the number of genes with differential expression changes and the total number of genes in the respective canonical pathway.

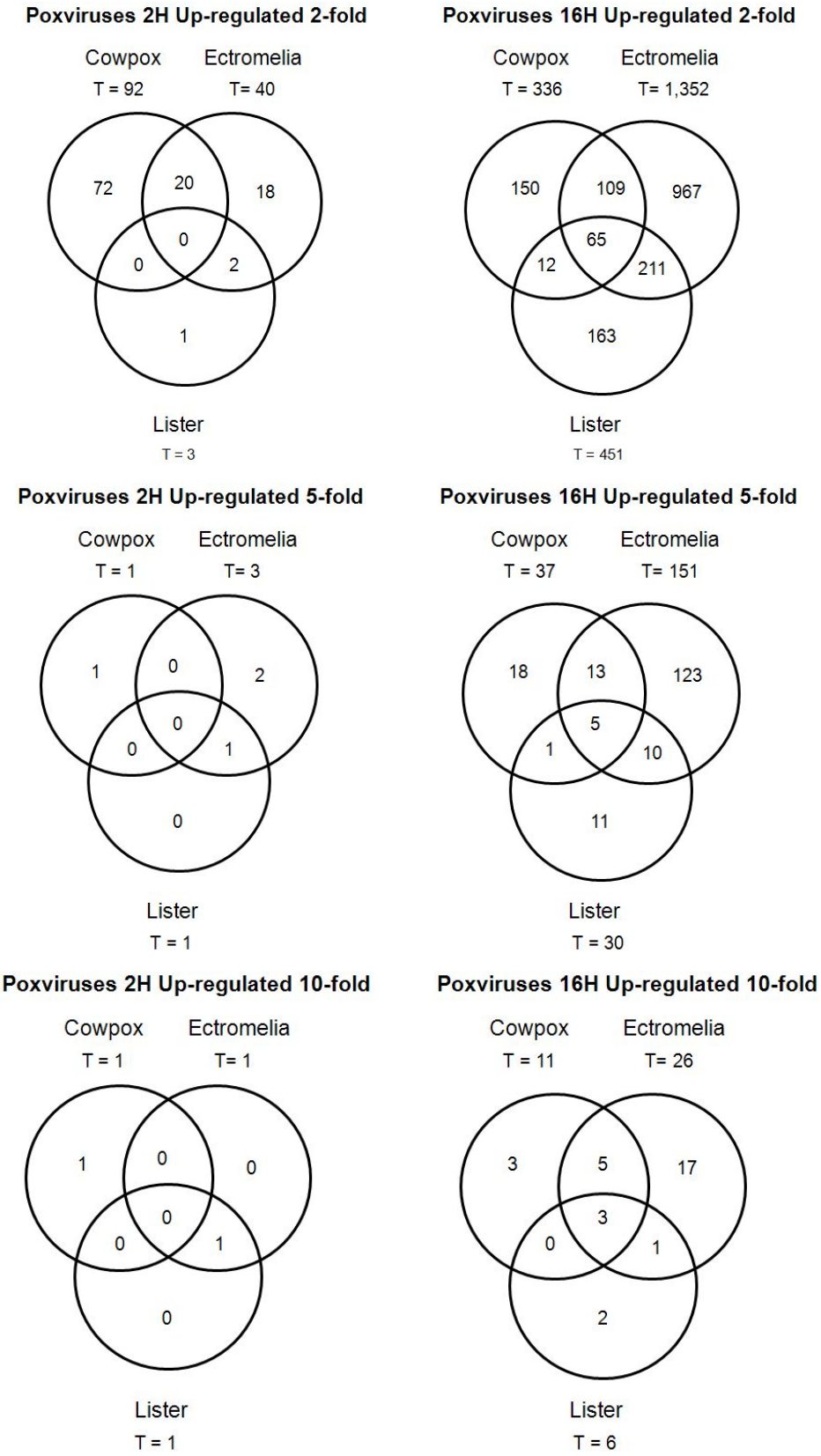

Figure 6.25 Venn diagram of differentially up-regulated probe sets between three poxviruses infections. A549 cells were infected with cowpox, ectromelia and lister viruses and significantly up-regulated transcripts (P-value≤0.05) were overlapped for comparison. Two infection time points including 2 and 16 hpi are shown and the results are based on fold changes at ≥2-FC, ≥5-FC and ≥10-FC. T represents the total number of probe sets with up-regulated expression.

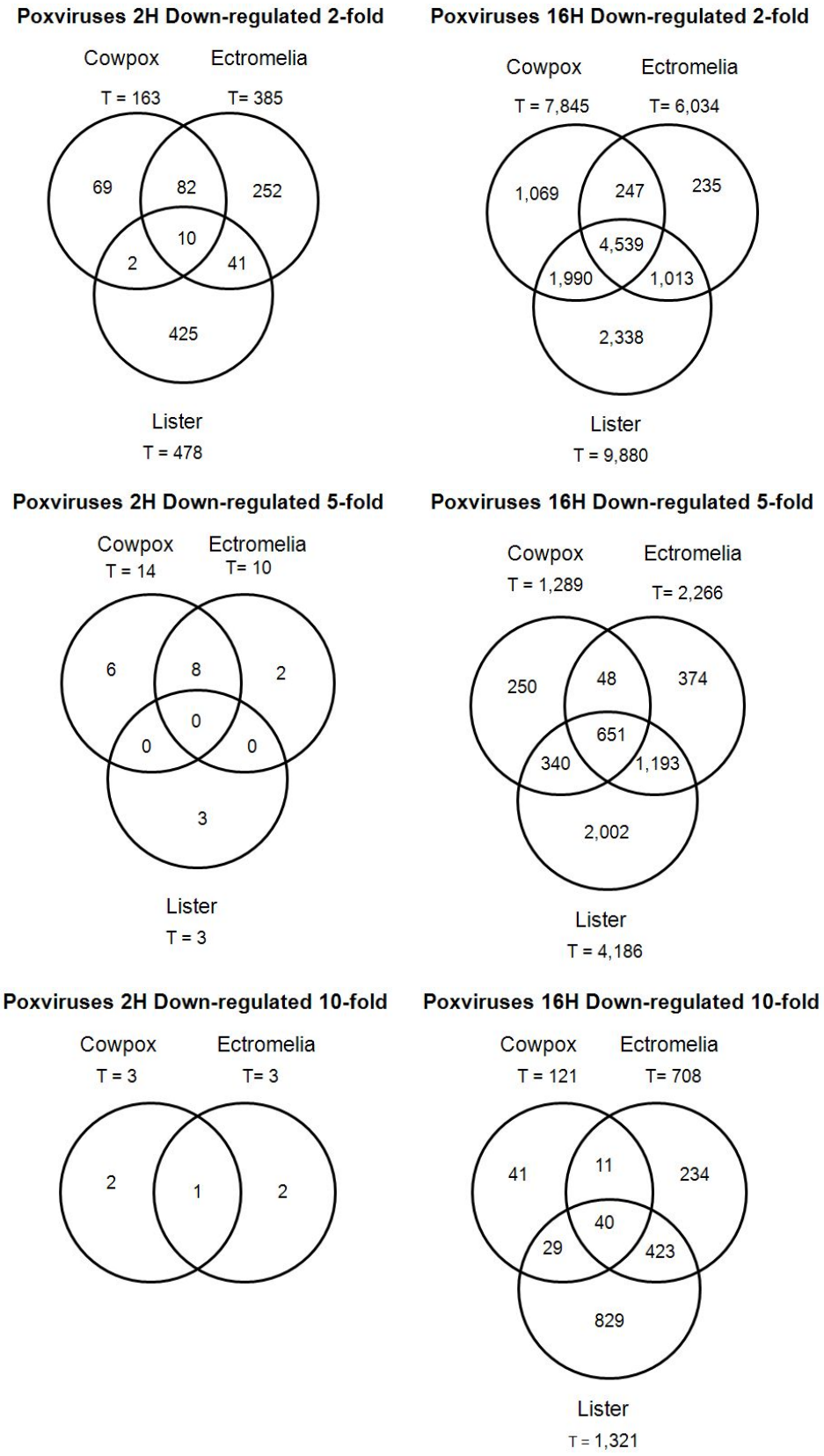

Figure 6.26 Venn diagram of differentially down-regulated probe sets between three poxviruses infections. A549 cells were infected with cowpox, ectromelia and lister viruses and significantly down-regulated transcripts (P-value≤0.05) were overlapped for comparison. Two infection time points including 2 and 16 hpi are shown and the results are based on fold changes at ≥2-FC, ≥5-FC and ≥10-FC. T represents the total number of probe sets with down-regulated expression.

6.3.2 Regulations of gene expression in canonical pathways

6.3.2.1 Interferon signaling

As described earlier, interferon signaling transduction will be initiated upon the poxvirus infection to induce the production of downstream cytokines. At the meanwhile, poxviruses have also evolved a few strategies to impair the interferon responses which are capable to inhibit virus replication and limit their viral spread [321, 344].

In cowpox virus-infected A549 cells, no expression change was detected across the whole interferon signaling pathway at 2 hpi. However, a big batch of genes with down-regulated expression was suddenly detected at 4 hpi, and this number showed increasing with the infection time increasing up to 10 hpi. These down-regulated genes included not only the interferon receptors and JAK/STAT but also the downstream ISGs. In addition, the genes in interferon signaling pathways from lister virus-infected A549 cells also exhibited similar expression performances as those from cowpox virus-infected A549 cells, including more and more genes with down-regulated expression identified from 2 to10 hpi.

Thus, the host interferon signaling pathways showed impaired in both poxviruses infected A549 cells, and stronger down-regulation of gene expression at the global level from cowpox virus infection implicated more stringent interruption of interferon signaling transduction in corresponding A549 cells.

In mouse RAW cells, cowpox infection contributed to no gene expression change at the early time point, while it resulted in down-regulated expression of many key genes at late time point. These genes with down-regulated expression included IFNAR2, IFNγRβ, JAK1, STAT1, OAS1 and so on, indicating that cowpox virus indeed counteract with the interferon response and impair the corresponding immune response to some extent.

When it turned to ectromelia virus infected mouse RAW cells, some of genes such as IFNAR2 and IFI35 showed down-regulated expression, while other key factors in the pathway such as IFNγRα, JAK1/2, STAT1/2 showed no expression changes at 16 hpi. In addition, IFNAR1 as the type I IFN receptor expressed in an elevated state with 13.6-FC, which might imply the potential initiation of this type I IFN signaling pathway. Altogether, it was assumed that

both host antivirus response and viral adaptive regulation were triggered and combated with each other, leading to the final gene expression performance of interferon pathway at 16 hpi in ectromelia virus-infected mouse RAW cells as described above.

Infection of lister virus also resulted in the inhibitory status of the interferon signaling pathway at 16 hpi with receptors, transduction factors and several downstream genes showing down-regulated gene expression. Global observation suggested that the gene expression performance in interferon signaling pathway detected after lister virus infection was similar to the gene expression performance detected after cowpox virus infection but not extromelia virus infection.

6.3.2.2 Toll-like receptor signaling

TLRs are a class of proteins that are crucial in the innate immune response to pathogens. Through recognizing and responding to pathogens associated molecular pattern, genes encoding for pro-inflammatory cytokines, chemokines and co-stimulatory molecules are then transcriptional activated. Besides, TLR signaling enables to result in the activation of NF-κB which is a key transcription factor for proinflammatory genes including TNF and type I IFN. It has been reported that protein N1L and A52R encoded by poxviruses were able to inhibit the multiple TRL pathways to NF-κB, subsequently evading the host immune response [345, 346].

In cowpox virus-infected A549 cells, few genes with altered gene expression changes in toll-like receptor signaling pathway were identified at 2 hpi. At 4 hpi, many genes with down-regulated expression were detected, and more and more genes with down-regulated expression in this pathway were detected with infection time increasing. At 10 hpi, TLR1, TLR6, TLR3, MYD88 as well as downstream recognition receptors P38 MAPK and NF-κB were all inhibited in their expression. Moreover, another interesting phenomenon was that gene c-Fos was induced in its expression across the whole infection period except 2 hpi.

Similarly, no significant gene expression changes were detected in toll-like receptor signaling pathway in lister virus-infected A549 cells at 2hpi except c-Fos with 3.08-FC and c-Jun with 3.85-FC. From 4 hpi, more and more factors

in this pathway became to show reduction in their expressions. At 8 hpi, the repression state of this pathway reached the most significant with genes including TLR1/3/6, TIRAP, MYD88, TOLLIP, NF-κB and p38 MAPK all showing down-regulated expression. It was interesting that the repressed state of toll-like receptor signaling became a bit moderate at 10 hpi as compared to 8 hpi. In addition, the gene expression of c-Fos climbed up across the whole infection time course, and reached maximum with 62.7-FC at 10 hpi.

Overall, the global gene expressions in toll-like receptor signaling pathway were indeed impaired in two types of poxviruses infected A549 cells, and this observation might be attributed to the interference of the host antiviral activities from poxviruses.

In mouse RAW cells, cowpox virus infection resulted in similar gene expression performance of toll-like receptor signaling as in A549 cells, with few altered gene expression changes occurred at early infection time point but a big batch of alter gene expression changes detected at the late time point. However, it was surprising that TLR2, TLR3, TLR4 and TLR7 showed down-regulated expression in mouse RAW cells, which was different from TLR1, TLR3 and TLR6 that showed down-regulated expression in A549 cells. And this finding might implicate the different signal transduction pathway in different cell types. In addition, c-Fos still showed elevated expression with 9.01-FC in cowpox virus-infected mouse RAW cells at 16 hpi.

When it comes to the infection of ectromelia virus, the gene expression performance in toll-like receptor signaling pathway was a bit different from the performance under infection of cowpox virus, with a smaller number of genes showing down-regulated expression detected at 16 hpi.

Genes with down-regulated expression in toll-like receptor signaling pathway was able to be detected from 2 hpi in lister virus-infected mouse RAW cells. And most of genes even including c-Fos in this pathway showed down-regulated expression at 16 hpi.

6.3.2.3 Apoptosis signaling

Specialized immune cells function on removing virus-infected cells through the induction of apoptosis. All apoptosis signaling pathways converge on a common machinery of cell destruction that is activated by a family of

caspases that enable to cleave proteins at aspartate residues. And these caspase activation and apoptotic death can be triggered by both extrinsic and intrinsic signals. Different publications have proved that different molecules were synthesized by poxvirus to inhibit the apoptosis as well as the processing of pro-inflammatory cytokines, thereby benefit the virus replication [332, 347].

In apoptosis signaling pathway, infection of cowpox virus in A549 cells only induced the expression of TNFR and Bfl-1 at 2hpi, and majority of genes in this pathway including caspase2/3/8/9/10, p53, BAX, Bcl-2 suddenly showed down-regulated expression around 4hpi. With the infection time increasing, the down-regulated expression of these genes became more and more significant, and the deepest down-regulated state was detected around 8 hpi.

Compared to cowpox virus infection, lister virus infection caused similar gene expression status in apoptosis signaling pathway, with majority of genes in this pathway showing down-regulated expression.

Observation on gene expression performances in apoptosis signaling pathway in these two types of poxviruses infected A549 cells provided evidence to prove that poxviruses initiated some mechanisms to impair the apoptosis signaling in infected host cells.

At the early time point, almost no altered gene expression changes in apoptosis signaling pathway were observed in all these three types of poxviruses infected mouse RAW cells. At the late time point, cowpox virus infection resulted in a group of genes with moderate down-regulation at their expression level, while ectromelia and lister virus infections led to a group of genes with outstanding down-regulation at their expression level.

6.3.2.4 Cell cycle: G1/S checkpoint regulation

Yoo N *et al* (2008) did a series of experiments to understand cell cycle control mechanism in vaccinia virus infected human tumor cells [348]. Finally, they provided evidences to support that the cell progression regulation was correlated with the inactivation of p53 and Rb, which were further associated with the RNA polymerase III transcription factor B subunits, TBP and Brf1 respectively. In the same report, they also proposed that infection of vaccinia virus induced the expression of Mdm2 as well as its translocation into the nucleus, thereby leading to a disruption of p53. At the meanwhile, infection of

vaccinia virus also reduced the expression of cyclin-dependent kinase 4 and 6 in order to enhance the level of hypophosphorylated Rb, that appeared to be largely sequestered into a complex with Brf1 resulting in the blockage of Rb function and repression of E2F1 transactivation. Subsequently, control of these cell progression related key factors led to a moderately higher proportion of cells in the S and G2 phases, thereby contributing to the efficient replication of the virus in rapidly growing cells.

Lister virus infection also resulted in a suddenly gene expression suppression in this network around 4 hpi and this inhibitory regulation of gene expressions became more and more significant across the whole infection time course. In general, gene expression performances in this network from both cowpox and lister viruses infected A549 cells coincide with the experimental observation in previous report, indicating a premise of efficient poxvirus replication.

Gene expression performances of G1/S checkpoint regulation network in poxviruses infected mouse RAW cells were distinct from the performances in poxviruses infected A549 cells. In mouse RAW cells infected with all three types of poxviruses, no gene expression changes were detected at 2 hpi. At 16 hpi, the gene expression profile in mouse RAW cells infected with cowpox virus was a bit complicated. Gene expression of c-Myc which was reported to be a positive regulator of G1-specific cyclin-dependent kinases (CDKs) was elevated with 5-FC, while the targeting genes showed down-regulated expression. In ectromelia virus infected mouse RAW cells, more genes including MDM2, p21 showed elevated expression when compared to cowpox virus infected mouse RAW cells. Other genes such as CDK4/6, Cyclin D/E still showed in a repressed expression status. Besides, infection of lister virus resulted in a batch of genes with faintly down-regulated expression in mouse RAW cells.

6.3.2.5 Antigen presentation pathway

Two types of MHC groups participate in antigen presentation processes. MHC class I participate in the intracellular antigens' presentation which are produced mainly by viruses replicating within a host cell, while MHC class II attend extracellular antigens' presentation coming from exogenous pathogens.

Previous publications have suggested that molecules encoded by vaccinia virus enabled to inhibit CD1d-mediated antigen presentation to natural killer T cells [349].

In mouse RAW cells, expression of MHC I-α was faintly down-regulated after infections of cowpox and lister virus and few gene expression changes were able to be detected after ectromelia virus infection at 2hpi. At 16 hpi, expression of all MHC I-α/β and MHC II-α/β were strongly repressed in cowpox virus-infected mouse RAW cells. Whereas, only some of them were inhibited at their expression level after ectromelia and lister virus infections, with MHC I-α/β down-regulated after ectromelia virus infection and MHC I-α/β as well as MHC II-α down-regulated after lister virus infection. Altogether, the gene expression in antigen presentation pathways detected from infections of different types of poxviruses indicated that all these examined poxviruses exerted some mechanisms to inhibit the antigen presentation in infected mouse RAW cells. Besides, down-regulation of different members in MHC groups at their expression level after infections of different types of poxviruses indicated the different signal inhibitory routes in these infected mouse RAW cells.

6.4 Conclusion

As we know, few studies have been reported to aim to describe the host response towards infections of cowpox virus, lister virus and ectromelia virus in a parallel way in A549 cells or mouse RAW cells. In our study, we made the attempt to compare the transcriptional expression profiles in cowpox and lister virus-infected A549 cells as well as the profiles in cowpox, lister and ectromelia virus-infected mouse RAW cells, respectively. Furthermore, genomic expression profiles in different cell types that were infected with the same type of poxvirus were also able to be compared.

Global evaluation indicated that the temporal distribution trend of numbers of probe sets with up- or down-regulated expression were similar among infections of different types of poxviruses either in A549 cells or mouse RAW cells. However, the detailed numbers of differently expressed probe sets were apparently different upon the infections of different types of poxviruses. For example, infection of lister virus resulted in more probe sets with up-regulated expression while infection of cowpox virus resulted in more probe

sets with down-regulated expression in A549 cells; infection of extromelia virus led to the largest number of probe sets with up-regulated expression at 16 hp while infection of lister virus led to the largest number of probe sets with down-regulated expression at both 2 and 16 hpi in mouse RAW cells.

By assigning these probe sets encoded genes to certain biological processes or pathways, it was noted that “DNA Binding”, “RNA Binding” and “Transcription Factor” were over-represented and shared by those differentially expressed probe sets in A549 cells infected with two types of poxviruses. However, functional classifications of “Cell Cycle”, “Cell Death”, “Kinase” and “RNA Binding” were commonly enriched by those differentially expressed probe sets in mouse RAW cells infected with three types of poxviruses.

Besides these well-known functional groups, pathways associated with metabolism such as “Metabolic pathway” and “Glycolysis/ Gluconeogenesis” were enriched based on genes with down-regulated expression in lister and cowpox virus-infected A549 cells. And other canonical pathways such as “Immunological Disease”, “Glycosis/Gluconegenesis”, “RNA Post-Transcription Modification”, “Oxidative Phosphorylation”, “Mitochondrial Dysfunction” and “Ubiquitin Biosynthese” were also enriched based on other differentially expressed genes in mouse RAW cells. These observations might indicate the regulations on a wide range of host cell machinaries in poxviruses infected mouse RAW cells.

In addition, a batch of histone genes and related transcription factors showed up-regulated expression in A549 cells after infections of poxviruses, especially lister virus. This observation was consistent with previous finding and might support the positive function of histone genes on virus replication. Furthermore, a couple of potential transcriptional factors were also significantly enriched based on differentially expressed genes.

Pathways analysis revealed the impairment of signaling transduction in immune response pathways in A549 cells infected with two types of poxviruses, especially cowpox virus. The complicated gene expression performances in immune response related pathways were detected in infected mouse RAW cells, and it was assumed that part of the significant gene expression might be due to the host antivirus response, while part of the significant gene expression might be caused by the viral adaptive regulation. In A549 cells, the inhibited

expression of genes belonging to apoptosis signaling pathway at the late infection stage indicated that virus might evolve some mechanism to postpone the cell death, and thereby benefit the virus replication. Besides, it was also assumed that the infections of cowpox and lister virus contributed the cell cycle arrest so that to benefit efficient virus replication. In the antigen presentation pathway, different gene expression patterns in mouse RAW cells infected with three different types of poxviruses might imply the different signal transduction route in different infected cells.

Parallel studies performed by Bartel S *et al*., (2011) targeted to uncover the proteome of HEK293 cells in the late phase of virus (vaccinia virus IHD-W strain) replication [374]. And the analysis highlighted the significant regulation of several cellular function groups, such as apoptosis modulation, regulation of cellular gene expression and the regulation of energy metabolism. And these findings overlapped with our results. In another report, HeLa cells were infected by cowpox, monkeypox and vaccinia virus, and microarray technique was applied to investigate the modulation at transcriptional levels. The target was to to identify mechanisms that are either common to orthopoxvirus infection or specific to certain orthopoxvirus species [382]. Their results demonstrated that majority of host genes remained unaffected after virus infection. In our data, although a small number of genes with up-regulated expression was observed, there existed a large number of genes with down-regulated expression, which is different from Bourquain's observation.

Chapter VII. Conclusion and Future Work

To deeply understand the host responses to infections of different viruses, we compared the genomic gene expression profiles in different viruses-infected the same cell types. And the results suggested that the same type of host cells took different actions to fight with the infections of different viruses. In the meanwhile, different viruses also evolved different strategies to counter host antiviral responses.

In macrophages, the genomic gene expression profiles upon RSV infection were examined at 4 and 24 hpi. Besides, the genomic gene expression profiles upon three influenza A strains infections were also examined, with H1N1 and H5N2/F118 investigated at 2 and 24 hpi as well as H5N3 investigated at 24 hpi. Parallel comparison of these genomic profiles in infected macrophages demonstrated that infection of RSV contributed to larger numbers of genes with up-regulated expression than infections of influenza A strains across the whole infection stage. And among the three influenza A strains, H5N3 infection resulted in larger number of genes with differential expression, either up- or down-regulated, than H5N2/F118 and H1N1 infections at 24 hpi. This observation might indicate that the prominent host gene expression regulations happened in mouse macrophages infected with RSV, followed by H5N3.

Functional annotation of these differentially expressed genes in infected mouse macrophages suggested that these genes with significantly up-regulated expression were associated with “Cytokine”, “Antiviral”, “Cell death” and “RNA binding” while those genes with down-regulated expression were associated with “Cell cycle”, “Kinase” and “Signal transduction”. Detailed information also demonstrated that a bacth cytokines showing up-regulated expression with high fold changes (even ≥10-FC) were detetected in RSV and H5N3 viruses infected mouse macrophages, suggesting that the strong immune defenses happened in these cells. Further investigations also revealed that a bigger batch of genes in RSV and H5N3-infected macrophages were calssified into functions such as “Infllammatory response” and “Immunological disease” as well as pathways such as “Dentritic cell maturation”, “Communication between innate and adaptive immune cells” and “Role of pattern recognition

receptors in recognition of bacteria and viruses". And these findings supported that a stronger activated antiviral state was detected after infections of RSV and H5N3 when compared to infections of H1N1 and H5N2/F118.

Analysis of key canonical pathway such as interferon signaling, antigen presentation and apoptosis signaling also provided details of the host responses in different viruses infected mouse macrophages. Among both RSV and three influenza A strains, RSV infection contributed to strongest innate immune response and macrophage activation, followed by H5N3 infection. Whereas, H1N1 and H5N2/F118 infections contributed to relatively faint innate immune responses and weak macrophage activations, and H5N2/F118 infection was responsible for stronger expression elevation of several ISGs at early time stage. Moreover, differential expression of genes related to either apoptosis or anti-apoptosis were both detected in only RSV-infected mouse macrophages, suggesting bi-directional regulations in apoptosis signaling pathways. And this situation was not observed in three influenza A strains infected mouse marcophages.

Besides the host responses investigated in mouse macrophages, A459 cells were also infected with not only different influenza A strains but also different types of poxviruses. Global investigation indicated the big differences existed in genomic gene expression profiles between infections of influenza A strains and infections of poxviruses. Among eight examined influenza A stains, only infections of two human strains (H1N1 and pH1N1) and two H5N2 strains (H5N2/F59 and H5N2/F189) contributed to large numbers of probe sets with down-regulate expression. Further examination also indicated that a big sharp increase of the numbers of those probe sets with down-regulated expression was observed between 8 and 10 hpi after H1N1 infection. However, infections of both cowpox and lister virus inhibited the expression of bigger batches of the probe sets than infections of indluenza A strains. Furthermore, this large scale of expression inhibitory regulations was initiated from very early infection stage. Accordingly, these observations were far away from the situations observed during infections of influenza A strains.

Further functional analysis also showed the different host gene expression performances detected in A549 cells following infections of influenza A viruses and poxviruses. A functional group called "Immune

response" was only prominently enriched based on the up-regulated genes from infections of influenza A viruses. And considerable numbers of genes showed quite significant fold regulation with ≥10-FC especially after infections of H5N2/F59, H5N2/F118, H5N2/F189 and H9N2, indicating strong activation of immune defense system in corresponding A549 cells. Although a part of genes was also stimulated at their expression level in A549 cells at 10 hpi after infection of poxviruses, in particular lister virus. Besides "RNA binding" and "DNA binding", these genes with elevated expression were majorly associated with "Cytoskeleton", indicting active membrane activities.

Although the functional groups such as "RNA Binding", "DNA Binding", "Signal Transduction" and "Transcription Factor" were commonly enriched by gene with down-regulated expression in both influenza A viruses and poxviruses-infcted A549 cells, these genes exert different spefic function during virus replication process. For example, down-regulated expression of zinc finger related genes were beneficial to the efficient virus replication in A549 cells after infections with influenza A strains, especially two human strains. Whereas, down-regulated expression of histone genes and related transcription factors might facilitate the viral DNA compaction of poxviruses in infected A549 cells.

Comparison of pathway analysis results also revealed different features of host response upon infections of influenza A viruses and poxviruses in A549 cells. For example, interferon signaling pathways were almost activated at the first beginning of infections coming from different influenza A strains while it showed no apparent activated status upon infections of two types of poxviruses at 2 hpi, but with deeper and deeper repressed status detected with the infection time increasing. However, the phenomenon that several key genes involved in cell cycle checkpoint showed inhibited expression during infections of poxviruses was also observed during infections of several influenza A strains such as H1N1 and pH1N1. And expression inhibition of these key factors at their transcriptional level aimed to retard the cell growth progression and in further create a better environment for effective virus replication in both influenza A strains and poxviruses-infected A549 cells.

Regarding to the big scale of genes with significantly down-regulated expression, especially detected in H1N1 infected-A549 cells, a number of

biological function groups was enriched. Since cell apoptosis itself implies the degeneration of a wide range of cellular functions, we should put more attention on whether the virus infection directly or indirectly caused reduced gene expression in our further analysis.

Furthermore, the half-life of messenger RNA (mRNA) in the cytoplasm should be also carefully considered. Since all mRNAs will eventually be translated into an amino acid chain to exert cellular functions, mRNAs concentration not only depends on the transcription rates but also degradation rates. And balancing of these two rates is under complicated regulation in different cellular conditions [373]. During infection of influenza viruses, the mRNAs in the host cells are also degraded under the cap snatching process. In the replication cycle of poxviruses, only a subset of viral genes is transcribed initially, and early gene products are responsible for activating the intermediate genes, which then activate the late genes. Independence from the host cells' own transcription machinery allows virus to shut down the cell nucleus in order to occupy all the metabolic resources [392]. In our further analysis, we will make efforts to investigation the detailed cellular regulation of mRNAs' dynamic concentration during virus infection. At the meanwhile, the regulation of corresponding protein level should be also examined for parallel comparison with mRNA level. Besides, the expression levels of microRNAs in different viruses- infected different cell types are also under investigation in our lab. Since microRNAs have been proved to control the mRNA degradation, detailed understanding of microRNAs in their expression level will be also beneficial for deep understanding the half-life of mRNAs during virus infection.

In our future experiments, more experiments based on techniques such as RT-PCR and cytokine assays will be performed to validate the information retrieved from microarray paltform. In terms of these validation data, the further functional analysis will be more reliable. In addtion, more important virus strains such as H7N9 will be involved in our researches. After virus infection in specific cell types, the genomic gene expression profiles will be examined using microarray platform. After that, the functional and pathway analysis will also be performed based on different bioinformatics software.

RNA interference is a process in which small non-coding RNAs slicence the expression of a sequence-homologous target RNA [350]. Since its

recovery, RNA interference has become an important research tools in functional genome analysis. Small interfering RNAs (siRNA) as one major type of small non-coding RNAs have been widely applied in building the screen for functional investigation of target genes [351].

Based on their characteristics, different groups applied genome-wide RNA interference screening to interpret virus-host interactions as well as identify the drug targets. In 20120, Karlas A *et al* (2010) constructed a genome-wide RNA interference screen based on siRNAs and aimed to identify host cell factors involved in the influenza virus infection cycle in human cells [352]. Finally, 278 human host cell genes involved in influenza A virus replication were reported, and potential targets for novel antiviral stratigies were proposed. Thus, in our future experiment, RNA interference screen will be designed based on siRNA and function of interested cellular and viral genes will be investigated comprehensively.

Another type of small non-codeing RNAs which are involved in RNA interference is microRNAs which are a large family of ~22 nucleotide non-coding RNAs. Viruses have an intricate interaction with the host cell, and combating viral infection by targeting unique viral peoteins and pathways is an important topic in host antiviral system. Recently, more and more researches have discovered that different cellular microRNAs function on RNA interference process in the defense against viral infection. In the contrary, viruses also encode their own microRNAs in order to silence cellular pathways, and thereby benefit its viral propagation and infection [353-355].

Detailed experiments performed by Li Y *et al* (2010) have revealed that an array of microRNAs, including miR-200a and miR-223, showed differential expression in reaction to influenza virus infection in mouse [356]. Moreover, expression of predicted cellular target mRNAs was inversely correlated with the expression of these microRNAs. And gene ontology analysis also revealed that these mRNAs were associated with immune response and cell death pathways, which play critical roles in virulence. Bakre A *et al* (2012) also found that RSV infection in A549 cells induced the expression of five microRNAs and repressed the expression of two microRNAs, and these microRNAs may target several cell cycle genes. Besides, it was also proposed that RSV G protein was involved in induction of let-7 miRNA expression, and sebsequently regulated

corresponding host genes to modulate virus replication during RSV infection [357].

Reference

1. Hurk SvDL-vd, Watkiss ER: **Pathogenesis of respiratory syncytial virus**. *Current Opinion in Virology* 2012, **2**:300-305.
2. Kuiken T, Riteau B, Fouchier RA, Rimmelzwaan GF: **Pathogenesis of influenza virus infections: the good, the bad and the ugly**. *Current Opinion in Virology* 2012, **2**(3):276-286.
3. Racloz V, Ramsey R, Tong S, Hu W: **Surveillance of dengue fever virus: a review of epidemiological models and early warning systems**. *PLOS Neglected Tropical Diseases* 2012, **6**(5):e1648.
4. McGoldrick C: **HIV and employment**. *Occup Med (Lond)* 2012, **62**(4):242-253.
5. Acheson NH: **Fundamentals of Molecular Virology - 2nd edition**. 2011.
6. Bowie AG, Haga IR: **The role of Toll-like receptors in the host response to viruses**. *Mol Immunol* 2005, **42**(8):859-867.
7. Galiana-Arnoux D, Imler JL: **Toll-like receptors and innate antiviral immunity**. *Tissue Antigens* 2006, **67**(4):267-276.
8. Ehrhardt C, Seyer R, Hrincius ER, Eierhoff T, Wolff T, Ludwig S: **Interplay between influenza A virus and the innate immune signaling**. *Microbes Infect* 2010, **12**(1):81-87.
9. Carty M, Bowie AG: **Recent insights into the role of Toll-like receptors in viral infection**. *Clin Exp Immunol* 2010, **161**(3):397-406.
10. Katze MG, He Y, Gale M, Jr.: **Viruses and interferon: a fight for supremacy**. *Nat Rev Immunol* 2002, **2**(9):675-687.
11. Alzhanova D, Fruh K: **Modulation of the host immune response by cowpox virus**. *Microbes and Infection* 2010, **12**(12-13):900-909.
12. Bonjardim CA: **Interferons (IFNs) are key cytokines in both innate and adaptive antiviral immune responses--and viruses counteract IFN action**. *Microbes Infect* 2005, **7**(3):569-578.
13. Tisoncik JR, Korth MJ, Simmons CP, Farrar J, Martin TR, Katze MG: **Into the eye of the cytokine storm**. *Microbiol Mol Biol Rev* 2012, **76**(1):16-32.
14. Benedict CA: **Viruses and the TNF-related cytokines, an evolving battle**. *Cytokine Growth Factor Rev* 2003, **14**(3-4):349-357.
15. Dinarello CA: **Immunological and inflammatory functions of the interleukin-1 family**. *Annu Rev Immunol* 2009, **27**:519-550.
16. Culley FJ, Pennycook AM, Tregoning JS, Dodd JS, Walzl G, Wells TN, Hussell T, Openshaw PJ: **Role of CCL5 (RANTES) in viral lung disease**. *J Virol* 2006, **80**(16):8151-8157.
17. Kalvakolanu DV: **Virus interception of cytokine-regulated pathways**. *Trends Microbiol* 1999, **7**(4):166-171.
18. Everett H, McFadden G: **Apoptosis: an innate immune response to virus infection**. *Trends Microbiol* 1999, **7**(4):160-165.
19. Mata JF, Silveira VS, Mateo EC, Cortez MA, Queiroz RG, Yunes JA, Lee ML, Toledo SR, Petrilli AS, Brandalise SR *et al*: **Low mRNA expression of the apoptosis-related genes CASP3, CASP8, and FAS is associated with low induction treatment response in childhood acute lymphoblastic leukemia (ALL)**. *Pediatr Blood Cancer* 2010, **55**(1):100-107.
20. Rawlings JS, Rosler KM, Harrison DA: **The JAK/STAT signaling pathway**. *J Cell Sci* 2004, **117**(Pt 8):1281-1283.
21. Pauli EK, Schmolke M, Wolff T, Viemann D, Roth J, Bode JG, Ludwig S: **Influenza A virus inhibits type I IFN signaling via NF-kappaB-dependent induction of SOCS-3 expression**. *PLoS Pathog* 2008, **4**(11):e1000196.
22. Levy DE, Garcia-Sastre A: **The virus battles: IFN induction of the antiviral state and mechanisms of viral evasion**. *Cytokine Growth Factor Rev* 2001, **12**(2-3):143-156.
23. Ludwig S, Planz O: **Influenza viruses and the NF-kappaB signaling pathway - towards a novel concept of antiviral therapy**. *Biol Chem* 2008, **389**(10):1307-1312.
24. Zhang YL, Dong C: **MAP kinases in immune responses**. *Cell Mol Immunol* 2005, **2**(1):20-27.

25. Fukushi S, Tani H, Yoshikawa T, Saijo M, Morikawa S: **Serological assays based on recombinant viral proteins for the diagnosis of arenavirus hemorrhagic fevers**. *Viruses* 2012, **4**(10):2097-2114.
26. Deschaght P, Schelstraete P, Santiago GLdS, Simaey LV, Haerynck F, daele SV, Wachter ED, Malfroot A, Lebecque P, Knoop C *et al*: **Comparison of culture and qPCR for the detection of Pseudomonas aeruginosa in not chronically infected cystic fibrosis patients**. *BMC Microbiology* 2010, **10**(245).
27. Wang D, Urisman A, Liu Y-T, Springer M, Ksiazek TG, Erdman DD, Mardis ER, Hickenbotham M, Magrini V, Eldred J *et al*: **Viral discovery and sequence recovery using DNA microarrays**. *Plos Biology* 2003, **1**(2).
28. Ejima M, Kadoi K, Honda A: **Influenza virus infection induces cellular Ebp1 gene expression**. *Genes Cells* 2011, **16**(9):927-937.
29. Kanagaraj AP, Verma D, Daniell H: **Expression of dengue-3 premembrane and envelope polyprotein in lettuce chloroplasts**. *Plant Mol Biol* 2011, **76**(3-5):323-333.
30. Muraki Y, Furukawa T, Kohno Y, Matsuzaki Y, Takashita E, Sugawara K, Hongo S: **Influenza C virus NS1 protein upregulates the splicing of viral mRNAs**. *J Virol* 2010, **84**(4):1957-1966.
31. Shan L, Yang HC, Rabi SA, Bravo HC, Shroff NS, Irizarry RA, Zhang H, Margolick JB, Siliciano JD, Siliciano RF: **Influence of host gene transcription level and orientation on HIV-1 latency in a primary-cell model**. *J Virol* 2011, **85**(11):5384-5393.
32. Wu Y, Peng C, Xu L, Zheng X, Liao M, Yan Y, Jin Y, Zhou J: **Proteome dynamics in primary target organ of infectious bursal disease virus**. *Proteomics* 2012, **12**(11):1844-1859.
33. Mous K, Jennes W, De Roo A, Pintelon I, Kestens L, Van Ostade X: **Intracellular detection of differential APOBEC3G, TRIM5alpha, and LEDGF/p75 protein expression in peripheral blood by flow cytometry**. *J Immunol Methods* 2011, **372**(1-2):52-64.
34. Ramsay G: **DNA chips: state-of-the art**. *Nat Biotechnol* 1998, **16**(1):40-44.
35. Tefferi A, Bolander ME, Ansell SM, Wieben ED, Spelsberg TC: **Primer on medical genomics. Part III: Microarray experiments and data analysis**. *Mayo Clin Proc* 2002, **77**(9):927-940.
36. Dorrell N, Hinchliffe SJ, Wren BW: **Comparative phylogenomics of pathogenic bacteria by microarray analysis**. *Curr Opin Microbiol* 2005, **8**(5):620-626.
37. Sturdevant DE, Virtaneva K, Martens C, Bozinov D, Ogundare O, Castro N, Kanakabandi K, Beare PA, Omsland A, Carlson JH *et al*: **Host-microbe interaction systems biology: lifecycle transcriptomics and comparative genomics**. *Future Microbiol* 2010, **5**(2):205-219.
38. Haagmans BL, Andeweg AC, Osterhaus AD: **The application of genomics to emerging zoonotic viral diseases**. *PLoS Pathog* 2009, **5**(10):e1000557.
39. Lu DD, Chen SH, Zhang SM, Zhang ML, Zhang W, Bo XC, Wang SQ: **Screening of specific antigens for SARS clinical diagnosis using a protein microarray**. *Analyst* 2005, **130**(4):474-482.
40. Davies DH, Wyatt LS, Newman FK, Earl PL, Chun S, Hernandez JE, Molina DM, Hirst S, Moss B, Frey SE *et al*: **Antibody profiling by proteome microarray reveals the immunogenicity of the attenuated smallpox vaccine modified vaccinia virus ankara is comparable to that of Dryvax**. *J Virol* 2008, **82**(2):652-663.
41. Stevens J, Blixt O, Paulson JC, Wilson IA: **Glycan microarray technologies: tools to survey host specificity of influenza viruses**. *Nat Rev Microbiol* 2006, **4**(11):857-864.
42. Uttamchandani M, Neo JL, Ong BN, Moochhala S: **Applications of microarrays in pathogen detection and biodefence**. *Trends in Biotechnology* 2009, **27**(1):53-61.
43. Paliy O, Agans R: **Application of phylogenetic microarrays to interrogation of human microbiota**. *FEMS Microbiol Ecol* 2012, **79**(1):2-11.
44. Novelli A, Grati FR, Ballarati L, Bernardini L, Bizzoco D, Camurri L, Casalone R, Cardarelli L, Cavalli P, Ciccone R *et al*: **Microarray application in prenatal diagnosis: a position statement from the cytogenetics working group of the Italian Society of Human Genetics (SIGU), November 2011**. *Ultrasound Obstet Gynecol* 2012, **39**(4):384-388.

45. Sreenivasulu N, Sunkar R, Wobus U, Strickert M: **Array platforms and bioinformatics tools for the analysis of plant transcriptome in response to abiotic stress**. *Methods Mol Biol* 2010, **639**:71-93.
46. Palacios G, Quan PL, Jabado OJ, Conlan S, Hirschberg DL, Liu Y, Zhai J, Renwick N, Hui J, Hegyi H *et al*: **Panmicrobial oligonucleotide array for diagnosis of infectious diseases**. *Emerg Infect Dis* 2007, **13**(1):73-81.
47. Sengupta S, Onodera K, Lai A, Melcher U: **Molecular detection and identification of influenza viruses by oligonucleotide microarray hybridization**. *J Clin Microbiol* 2003, **41**(10):4542-4550.
48. Wang D, Coscoy L, Zylberberg M, Avila PC, Boushey HA, Ganem D, DeRisi JL: **Microarray-based detection and genotyping of viral pathogens**. *Proc Natl Acad Sci U S A* 2002, **99**(24):15687-15692.
49. Wong CW, Heng CL, Wan Yee L, Soh SW, Kartasasmita CB, Simoes EA, Hibberd ML, Sung WK, Miller LD: **Optimization and clinical validation of a pathogen detection microarray**. *Genome Biol* 2007, **8**(5):R93.
50. Chou CC, Lee TT, Chen CH, Hsiao HY, Lin YL, Ho MS, Yang PC, Peck K: **Design of microarray probes for virus identification and detection of emerging viruses at the genus level**. *BMC Bioinformatics* 2006, **7**:232.
51. Snyder JC, Bateson MM, Lavin M, Young MJ: **Use of Cellular CRISPR (Clusters of Regularly Interspaced Short Palindromic Repeats) Spacer-Based Microarrays for Detection of Viruses in Environmental Samples**. *Applied and Environmental Microbiology* 2010, **76**(21):7251-7258.
52. Kang X, Qin C, Li Y, Liu H, Lin F, Li Y, Li J, Zhu Q, Yang Y: **Improvement of the Specificity of a Pan-Viral Microarray by Using Genus-Specific Oligonucleotides and Reduction of Interference by Host Genomes**. *Journal of Medical Virology* 2011, **83**:1624-1630.
53. Gardner SN, Jaing CJ, McLoughlin KS, Slezak TR: **A microbial detection array (MDA) for viral and bacterial detection**. *BMC Genomics* 2010, **11**(668).
54. Erlandsson L, Rosenstierne MW, McLoughlin K, Jaing C, Fomsgaard A: **The Microbial Detection Array Combined with Random Phi29-Amplification Used as a Diagnostic Tool for Virus Detection in Clinical Samples**. *Plos One* 2011, **6**(8).
55. Lockhart DJ, Winzeler EA: **Genomics, gene expression and DNA arrays**. *Nature* 2000, **405**:827-836.
56. Krijnse-Locker J: **Cellular virology**. *Cell Microbiol* 2005, **7**(9):1213-1215.
57. DeFilippis V, Raggo C, Moses A, Fruh K: **Functional genomics in virology and antiviral drug discovery**. *Trends in Biotechnology* 2003, **21**(10):452-457.
58. Raaben M, Whitley P, Bouwmeester D, Setterquist RA, Rottier PJ, de Haan CA: **Improved microarray gene expression profiling of virus-infected cells after removal of viral RNA**. *BMC Genomics* 2008, **9**:221.
59. Katze MG, Fornek JL, Palermo RE, Walters KA, Korth MJ: **Innate immune modulation by RNA viruses: emerging insights from functional genomics**. *Nat Rev Immunol* 2008, **8**(8):644-654.
60. Russell GC, Benavides J, Grant DM, Todd H, Thomson J, Puri V, Nath M, Haig DM: **Host gene expression changes in cattle infected with Alcelaphine herpesvirus 1**. *Virus Res* 2012, **169**(1):246-254.
61. Munoz-Erazo L, Natoli R, Provis JM, Madigan MC, King NJ: **Microarray analysis of gene expression in West Nile virus-infected human retinal pigment epithelium**. *Mol Vis* 2012, **18**:730-743.
62. Lee J, Bottje WG, Kong BW: **Genome-wide host responses against infectious laryngotracheitis virus vaccine infection in chicken embryo lung cells**. *BMC Genomics* 2012, **13**:143.
63. Palermo RE, Patterson LJ, Aicher LD, Korth MJ, Robert-Guroff M, Katze MG: **Genomic analysis reveals pre- and postchallenge differences in a rhesus macaque AIDS vaccine trial: insights into mechanisms of vaccine efficacy**. *J Virol* 2011, **85**(2):1099-1116.
64. Cho WK, Yu J, Lee KM, Son M, Min K, Lee YW, Kim KH: **Genome-wide expression profiling shows transcriptional reprogramming in Fusarium graminearum by Fusarium graminearum virus 1-DK21 infection**. *BMC Genomics* 2012, **13**:173.

65. Shair KH, Raab-Traub N: **Transcriptome changes induced by Epstein-Barr virus LMP1 and LMP2A in transgenic lymphocytes and lymphoma**. *MBio* 2012, **3**(5).
66. Zhang H, Li Y, Huang X, Zheng C: **Global transcriptional analysis of model of persistent FMDV infection reveals critical role of host cells in persistence**. *Vet Microbiol* 2013, **162**(2-4):321-329.
67. Yan Q: **Bioinformatics databases and tools in virology research: an overview**. *In Silico Biol* 2008, **8**(2):71-85.
68. Vogel C, Marcotte EM: **Insights into the regulation of protein abundance from proteomic and transcriptomic analyses**. *Nature Reviews Genetics* 2012, **13**(4):227-232.
69. Cox J, Mann M: **Is Proteomics the New Genomics?** *Cell* 2007, **130**:395-398.
70. Pareek CS, Smoczynski R, Tretyn A: **Sequencing technologies and genome sequencing**. *J Appl Genet* 2011, **52**(4):413-435.
71. Zheng J, Sugrue RJ, Tang K: **Mass spectrometry based proteomic studies on viruses and hosts--a review**. *Anal Chim Acta* 2011, **702**(2):149-159.
72. Radford AD, Chapman D, Dixon L, Chantrey J, Darby AC, Hall N: **Application of next-generation sequencing technologies in virology**. *J Gen Virol* 2012, **93**(Pt 9):1853-1868.
73. Wojcik J, Schachter V: **Proteomic databases and software on the web**. *Brief Bioinform* 2000, **1**(3):250-259.
74. Bao S, Jiang R, Kwan W, Wang B, Ma X, Song YQ: **Evaluation of next-generation sequencing software in mapping and assembly**. *J Hum Genet* 2011, **56**(6):406-414.
75. Stein LD: **An introduction to the informatics of "next-generation" sequencing**. *Curr Protoc Bioinformatics* 2011, **Chapter 11**:Unit 11 11.
76. Hecker M, Lorenz P, Steinbeck F, Hong L, Riemekasten G, Li Y, Zettl UK, Thiesen HJ: **Computational analysis of high-density peptide microarray data with application from systemic sclerosis to multiple sclerosis**. *Autoimmun Rev* 2012, **11**(3):180-190.
77. McLoughlin KS: **Microarrays for Pathogen Detection and Analysis**. *Briefings in Functional Genomics* 2011, **10**(6):342-353.
78. Urisman A, Fischer KF, Chiu CY, Kistler AL, Beck S, Wang D, DeRisi JL: **E-Predict: a computational strategy for species identification based on observed DNA microarray hybridization patterns**. *Genome Biology* 2005, **6**(9).
79. Watson M, Dukes J, Abu-Median A-B, King DP, Britton P: **DetectiV: visualization, normalization and significance testing for pathogen-detection microarray data**. *Genome Biol* 2007, **8**(9).
80. Allred AF, Wu G, Wulan T, Fischer KF, Holbrook MR, Tesh RB, Wang D: **VIPR: A probabilistic algorithm for analysis of microbial detection microarrays**. *BMC Bioinformatics* 2010, **11**(384).
81. Allred AF, Renshaw H, Weaver S, Tesh RB, Wang D: **VIPR HMM: a hidden Markov model for detecting recombination with microbial detection microarrays**. *Bioinformatics* 2012, **28**(22):2922-2929.
82. Rehrauer H, Schönmann S, Eberl L, Schlapbach R: **PhyloDetect: a likelihood-based strategy for detecting microorganisms with diagnostic microarrays**. *Bioinformatics* 2008, **24**(16).
83. Gentleman RC, Carey VJ, Bates DM, Bolstad B, Dettling M, Dudoit S, Ellis B, Gautier L, Ge Y, Gentry J *et al*: **Bioconductor: open software development for computational biology and bioinformatics**. *Genome Biol* 2004, **5**(10).
84. Smyth GK: **Limma: linear models for microarray data. In Bioinformatics and Computational Biology Solutions using R and Bioconductor**. *Springer* 2005:397-420.
85. Schuldt B, Lin Q, Muller FJ, Loring J: **Basic approaches to gene expression analysis of stem cells by microarrays**. *Methods Mol Biol* 2011, **767**:269-282.
86. Selvaraj S, Natarajan J: **Microarray data analysis and mining tools**. *Bioinformation* 2011, **6**(3):95-99.
87. Kanehisa M, Goto S, Hattori M, Aoki-Kinoshita KF, Itoh M, Kawashima S, Katayama T, Araki M, Hirakawa M: **From genomics to chemical genomics: new developments in KEGG**. *Nucleic Acids Res* 2006, **34**(Database issue):D354-357.
88. Latendresse M, Paley S, Karp PD: **Browsing metabolic and regulatory networks with BioCyc**. *Methods Mol Biol* 2012, **804**:197-216.

89. Szabo PM, Tamasi V, Molnar V, Andrasfalvy M, Tombol Z, Farkas R, Kovesdi K, Patocs A, Toth M, Szalai C *et al*: **Meta-analysis of adrenocortical tumour genomics data: novel pathogenic pathways revealed**. *Oncogene* 2010, **29**(21):3163-3172.
90. Yona G, Dirks W, Rahman S: **Comparing algorithms for clustering of expression data: how to assess gene clusters**. *Methods Mol Biol* 2009, **541**:479-509.
91. Burgess ST, Greer A, Frew D, Wells B, Marr EJ, Nisbet AJ, Huntley JF: **Transcriptomic analysis of circulating leukocytes reveals novel aspects of the host systemic inflammatory response to sheep scab mites**. *Plos One* 2012, **7**(8):e42778.
92. Jay JJ, Eblen JD, Zhang Y, Benson M, Perkins AD, Saxton AM, Voy BH, Chesler EJ, Langston MA: **A systematic comparison of genome-scale clustering algorithms**. *BMC Bioinformatics* 2012, **13 Suppl 10**:S7.
93. Ruan J, Dean AK, Zhang W: **A general co-expression network-based approach to gene expression analysis: comparison and applications**. *BMC Syst Biol* 2010, **4**:8.
94. Zare H, Kaveh M, Khodursky A: **Inferring a transcriptional regulatory network from gene expression data using nonlinear manifold embedding**. *Plos One* 2011, **6**(8):e21969.
95. Lieber D, Haas J: **Viruses and microRNAs: a toolbox for systematic analysis**. *Wiley Interdiscip Rev RNA* 2011, **2**(6):787-801.
96. Scaria V, Hariharan M, Maiti S, Pillai B, Brahmachari SK: **Host-virus interaction: a new role for microRNAs**. *Retrovirology* 2006, **3**:68.
97. Veksler-Lublinsky I, Shemer-Avni Y, Meiri E, Bentwich Z, Kedem K, Ziv-Ukelson M: **Finding quasi-modules of human and viral miRNAs: a case study of human cytomegalovirus (HCMV)**. *BMC Bioinformatics* 2012, **13**:322.
98. Ladunga I: **An overview of the computational analyses and discovery of transcription factor binding sites**. *Methods Mol Biol* 2010, **674**:1-22.
99. Burgess ST, McNeilly TN, Watkins CA, Nisbet AJ, Huntley JF: **Host transcription factors in the immediate pro-inflammatory response to the parasitic mite Psoroptes ovis**. *Plos One* 2011, **6**(9):e24402.
100. Ho Sui SJ, Fulton DL, Arenillas DJ, Kwon AT, Wasserman WW: **oPOSSUM: integrated tools for analysis of regulatory motif over-representation**. *Nucleic Acids Res* 2007, **35**(Web Server issue):W245-252.
101. Elkon R, Linhart C, Sharan R, Shamir R, Shiloh Y: **Genome-wide in silico identification of transcriptional regulators controlling the cell cycle in human cells**. *Genome Res* 2003, **13**(5):773-780.
102. Hertzberg L, Izraeli S, Domany E: **STOP: searching for transcription factor motifs using gene expression**. *Bioinformatics* 2007, **23**(14):1737-1743.
103. Sharan R, Maron-Katz A, Shamir R: **CLICK and EXPANDER: a system for clustering and visualizing gene expression data**. *BIOINFORMATICS* 2003, **19**(14):1787-1799.
104. Shamir R, Maron-Katz A, Tanay A, Linhart C, Steinfeld I, Sharan R, Shiloh Y, Elkon R: **EXPANDER – an integrative program suite for microarray data analysis**. *BMC Bioinformatics* 2005, **6**(232).
105. Griffiths S, Lau J: **The influence of SARS on perceptions of risk and reality**. *J Public Health (Oxf)* 2009, **31**(4):466-467.
106. JY S: **Another nightmare after SARS: knowledge perceptions of and overcoming strategies for H1N1 influenza among chronic renal disease patients in Hong Kong**. *Qual Health Res* 2010, **20**(7):893-904.
107. Tay J, Ng YF, Cutter JL, James L: **Influenza A (H1N1-2009) pandemic in Singapore--public health control measures implemented and lessons learnt**. *Ann Acad Med Singapore* 2010, **39**(4):313-312.
108. Yoo SM, Lee SY: **Diagnosis of pathogens using DNA microarray**. *Recent Patents on Biotechnology* 2008, **2**(2):124-129.
109. Vora GJ, Meador CE, Anderson GP, Taitt CR: **Comparison of detection and signal amplification methods for DNA microarrays**. *Molecular and Cellular Probes* 2008, **22**(5-6):294-300.
110. Yozwiak NL, Skewes-Cox P, Stenglein MD, Balmaseda A, Harris E, DeRisi JL: **Virus Identification in Unknown Tropical Febrile Illness Cases Using Deep Sequencing**. *PLOS Neglected Tropical Diseases* 2012, **6**(2).
111. Huguenin A, Moutte L, Renois F, Leveque N, Talmud D, Abely M, Nguyen Y, Carrat F, Andreoletti L: **Broad Respiratory Virus Detection in Infants Hospitalized for**

Bronchiolitis by Use of a Multiplex RT-PCR DNA Microarray System. *Journal of Medical Virology* 2012, **84**:979-985.
112. Bozdech Z, Zhu J, Joachimiak MP, Cohen FE, Pulliam B, DeRisi JL: **Expression profiling of the schizont and trophozoite stages of Plasmodium falciparum with a long-oligonucleotide microarray**. *Genome Biol* 2003, **4**(2).
113. Quackenbush J: **Microarray data normalization and transformation**. *Nature Genetics* 2002, **32**:496-501.
114. Nguyen V-A, Lió P: **Measuring similarity between gene expression profiles: a Bayesian approach**. *BMC Genomics* 2009, **10**.
115. Goldstein H, Harron K, AngieWade: **The analysis of record-linked data using multiple imputation with data value priors**. *Statistics in Medicine* 2012, **31**:3481-3493.
116. Wu Y, Wang X: **Optimal weight in estimating and comparing areas under the receiver operating characteristic curve using longitudinal data**. *Biometrical Journal* 2011, **53**(5):764-778.
117. Yao J, Chang C, Salmi ML, Hung YS, Loraine A, Roux SJ: **Genome-scale cluster analysis of replicated microarrays using shrinkage correlation coefficient**. *BMC Bioinformatics* 2008, **9**(288).
118. Fujita A, Sato JR, Demasi MA, Sogayar MC, Ferreira CE, Miyano S: **Comparing Pearson, Spearman and Hoeffding's D measure for gene expression association analysis**. *J Bioinform Comput Biol* 2009, **7**(4):663-684.
119. MacKay DJ: **Baysian Inference and Sampling Theory**. *Cambridge University Press* 2003.
120. Zhao JX, Foulkes AS, George EI: **Exploratory Bayesian Model Selection for Serial Genetics Data**. *Biometrics* 2005, **61**(2):591-599.
121. Cianci C, Meanwell N, Krystal M: **Antiviral activity and molecular mechanism of an orally active respiratory syncytial virus fusion inhibitor**. *J Antimicrob Chemother* 2005, **55**(3):289-292.
122. Collins PL, Melero JA: **Progress in understanding and controlling respiratory syncytial virus: still crazy after all these years**. *Virus Res* 2011, **162**(1-2):80-99.
123. Munday DC, Emmott E, Surtees R, Lardeau CH, Wu W, Duprex WP, Dove BK, Barr JN, Hiscox JA: **Quantitative proteomic analysis of A549 cells infected with human respiratory syncytial virus**. *Mol Cell Proteomics* 2010, **9**(11):2438-2459.
124. McLellan JS, Yang Y, Graham BS, Kwong PD: **Structure of respiratory syncytial virus fusion glycoprotein in the postfusion conformation reveals preservation of neutralizing epitopes**. *J Virol* 2011, **85**(15):7788-7796.
125. Sugrue RJ: **Interactions between respiratory syncytial virus and the host cell: opportunities for antivirus strategies?** *Expert Rev Mol Med* 2006, **8**(21):1-17.
126. Feldman SA, Crim RL, Audet SA, Beeler JA: **Human respiratory syncytial virus surface glycoproteins F, G and SH form an oligomeric complex**. *Arch Virol* 2001, **146**(12):2369-2383.
127. Brown G, Rixon HW, Steel J, McDonald TP, Pitt AR, Graham S, Sugrue RJ: **Evidence for an association between heat shock protein 70 and the respiratory syncytial virus polymerase complex within lipid-raft membranes during virus infection**. *Virology* 2005, **338**(1):69-80.
128. Hallak LK, Spillmann D, Collins PL, Peeples ME: **Glycosaminoglycan sulfation requirements for respiratory syncytial virus infection**. *J Virol* 2000, **74**(22):10508-10513.
129. Cowton VM, McGivern DR, Fearns R: **Unravelling the complexities of respiratory syncytial virus RNA synthesis**. *J Gen Virol* 2006, **87**(Pt 7):1805-1821.
130. Harrison MS, Sakaguchi T, Schmitt AP: **Paramyxovirus assembly and budding: building particles that transmit infections**. *Int J Biochem Cell Biol* 2010, **42**(9):1416-1429.
131. Oshansky CM, Zhang W, Moore E, Tripp RA: **The host response and molecular pathogenesis associated with respiratory syncytial virus infection**. *Future Microbiol* 2009, **4**(3):279-297.
132. Batonick M, Wertz GW: **Requirements for Human Respiratory Syncytial Virus Glycoproteins in Assembly and Egress from Infected Cells**. *Adv Virol* 2011, **2011**.

133. Kallewaard NL, Bowen AL, Crowe JE, Jr.: **Cooperativity of actin and microtubule elements during replication of respiratory syncytial virus**. *Virology* 2005, **331**(1):73-81.
134. Gower TL, Peeples ME, Collins PL, Graham BS: **RhoA is activated during respiratory syncytial virus infection**. *Virology* 2001, **283**(2):188-196.
135. Krzyzaniak MA, Zumstein MT, Gerez JA, Picotti P, Helenius A: **Host cell entry of respiratory syncytial virus involves macropinocytosis followed by proteolytic activation of the F protein**. *PLoS Pathog* 2013, **9**(4):e1003309.
136. Elliott J, Lynch OT, Suessmuth Y, Qian P, Boyd CR, Burrows JF, Buick R, Stevenson NJ, Touzelet O, Gadina M *et al*: **Respiratory syncytial virus NS1 protein degrades STAT2 by using the Elongin-Cullin E3 ligase**. *J Virol* 2007, **81**(7):3428-3436.
137. Moore EC, Barber J, Tripp RA: **Respiratory syncytial virus (RSV) attachment and nonstructural proteins modify the type I interferon response associated with suppressor of cytokine signaling (SOCS) proteins and IFN-stimulated gene-15 (ISG15)**. *Virol J* 2008, **5**:116.
138. Harris J, Werling D: **Binding and entry of respiratory syncytial virus into host cells and initiation of the innate immune response**. *Cell Microbiol* 2003, **5**(10):671-680.
139. Lo MS, Brazas RM, Holtzman MJ: **Respiratory syncytial virus nonstructural proteins NS1 and NS2 mediate inhibition of Stat2 expression and alpha/beta interferon responsiveness**. *J Virol* 2005, **79**(14):9315-9319.
140. Bueno SM, Gonzalez PA, Riedel CA, Carreno LJ, Vasquez AE, Kalergis AM: **Local cytokine response upon respiratory syncytial virus infection**. *Immunol Lett* 2011, **136**(2):122-129.
141. Domachowske JB, Bonville CA, Mortelliti AJ, Colella CB, Kim U, Rosenberg HF: **Respiratory syncytial virus infection induces expression of the anti-apoptosis gene IEX-1L in human respiratory epithelial cells**. *J Infect Dis* 2000, **181**(3):824-830.
142. Thomas KW, Monick MM, Staber JM, Yarovinsky T, Carter AB, Hunninghake GW: **Respiratory syncytial virus inhibits apoptosis and induces NF-kappa B activity through a phosphatidylinositol 3-kinase-dependent pathway**. *J Biol Chem* 2002, **277**(1):492-501.
143. Spann KM, Tran KC, Chi B, Rabin RL, Collins PL: **Suppression of the induction of alpha, beta, and lambda interferons by the NS1 and NS2 proteins of human respiratory syncytial virus in human epithelial cells and macrophages [corrected]**. *J Virol* 2004, **78**(8):4363-4369.
144. Ling Z, Tran KC, Teng MN: **Human respiratory syncytial virus nonstructural protein NS2 antagonizes the activation of beta interferon transcription by interacting with RIG-I**. *J Virol* 2009, **83**(8):3734-3742.
145. Ramaswamy M, Shi L, Varga SM, Barik S, Behlke MA, Look DC: **Respiratory syncytial virus nonstructural protein 2 specifically inhibits type I interferon signal transduction**. *Virology* 2006, **344**(2):328-339.
146. Swedan S, Musiyenko A, Barik S: **Respiratory syncytial virus nonstructural proteins decrease levels of multiple members of the cellular interferon pathways**. *J Virol* 2009, **83**(19):9682-9693.
147. Bitko V, Shulyayeva O, Mazumder B, Musiyenko A, Ramaswamy M, Look DC, Barik S: **Nonstructural proteins of respiratory syncytial virus suppress premature apoptosis by an NF-kappaB-dependent, interferon-independent mechanism and facilitate virus growth**. *J Virol* 2007, **81**(4):1786-1795.
148. Oshansky CM, Barber JP, Crabtree J, Tripp RA: **Respiratory syncytial virus F and G proteins induce interleukin 1alpha, CC, and CXC chemokine responses by normal human bronchoepithelial cells**. *J Infect Dis* 2010, **201**(8):1201-1207.
149. Zhang W, Choi Y, Haynes LM, Harcourt JL, Anderson LJ, Jones LP, Tripp RA: **Vaccination to induce antibodies blocking the CX3C-CX3CR1 interaction of respiratory syncytial virus G protein reduces pulmonary inflammation and virus replication in mice**. *J Virol* 2010, **84**(2):1148-1157.
150. Graham BS, Johnson TR, Peebles RS: **Immune-mediated disease pathogenesis in respiratory syncytial virus infection**. *Immunopharmacology* 2000, **48**(3):237-247.
151. Hornsleth A, Loland L, Larsen LB: **Cytokines and chemokines in respiratory secretion and severity of disease in infants with respiratory syncytial virus (RSV) infection**. *J Clin Virol* 2001, **21**(2):163-170.

152. Tripp RA, Oshansky C, Alvarez R: **Cytokines and respiratory syncytial virus infection**. *Proc Am Thorac Soc* 2005, **2**(2):147-149.
153. John AE, Berlin AA, Lukacs NW: **Respiratory syncytial virus-induced CCL5/RANTES contributes to exacerbation of allergic airway inflammation**. *Eur J Immunol* 2003, **33**(6):1677-1685.
154. Durbin JE, Johnson TR, Durbin RK, Mertz SE, Morotti RA, Peebles RS, Graham BS: **The role of IFN in respiratory syncytial virus pathogenesis**. *J Immunol* 2002, **168**(6):2944-2952.
155. Ternette N, Wright C, Kramer HB, Altun M, Kessler BM: **Label-free quantitative proteomics reveals regulation of interferon-induced protein with tetratricopeptide repeats 3 (IFIT3) and 5'-3'-exoribonuclease 2 (XRN2) during respiratory syncytial virus infection**. *Virol J* 2011, **8**(1):442.
156. Yeo DS, Chan R, Brown G, Ying L, Sutejo R, Aitken J, Tan BH, Wenk MR, Sugrue RJ: **Evidence that selective changes in the lipid composition of raft-membranes occur during respiratory syncytial virus infection**. *Virology* 2009, **386**(1):168-182.
157. Classen A, Lloberas J, Celada A: **Macrophage activation: classical versus alternative**. *Methods Mol Biol* 2009, **531**:29-43.
158. Shirey KA, Pletneva LM, Puche AC, Keegan AD, Prince GA, Blanco JC, Vogel SN: **Control of RSV-induced lung injury by alternatively activated macrophages is IL-4R alpha-, TLR4-, and IFN-beta-dependent**. *Mucosal Immunol* 2010, **3**(3):291-300.
159. Senft AP, Taylor RH, Lei W, Campbell SA, Tipper JL, Martinez MJ, Witt TL, Clay CC, Harrod KS: **Respiratory syncytial virus impairs macrophage IFN-alpha/beta- and IFN-gamma-stimulated transcription by distinct mechanisms**. *Am J Respir Cell Mol Biol* 2010, **42**(4):404-414.
160. Zhao DC, Yan T, Li L, You S, Zhang C: **Respiratory syncytial virus inhibits interferon-alpha-inducible signaling in macrophage-like U937 cells**. *J Infect* 2007, **54**(4):393-398.
161. Nakamura-Lopez Y, Villegas-Sepulveda N, Sarmiento-Silva RE, Gomez B: **Intrinsic apoptotic pathway is subverted in mouse macrophages persistently infected by RSV**. *Virus Res* 2011, **158**(1-2):98-107.
162. Kaan PM, Hegele RG: **Interaction between respiratory syncytial virus and particulate matter in guinea pig alveolar macrophages**. *Am J Respir Cell Mol Biol* 2003, **28**(6):697-704.
163. Chai J, Tarnawski AS: **Serum response factor: discovery, biochemistry, biological roles and implications for tissue injury healing**. *J Physiol Pharmacol* 2002, **53**(2):147-157.
164. Gilmore AP, Owens TW, Foster FM, Lindsay J: **How adhesion signals reach a mitochondrial conclusion--ECM regulation of apoptosis**. *Curr Opin Cell Biol* 2009, **21**(5):654-661.
165. Spencer VA, Xu R, Bissell MJ: **Gene expression in the third dimension: the ECM-nucleus connection**. *J Mammary Gland Biol Neoplasia* 2010, **15**(1):65-71.
166. Lotz MT, Peebles RS, Jr.: **Mechanisms of respiratory syncytial virus modulation of airway immune responses**. *Curr Allergy Asthma Rep* 2012, **12**(5):380-387.
167. Groskreutz DJ, Monick MM, Yarovinsky TO, Powers LS, Quelle DE, Varga SM, Look DC, Hunninghake GW: **Respiratory syncytial virus decreases p53 protein to prolong survival of airway epithelial cells**. *J Immunol* 2007, **179**(5):2741-2747.
168. Thomas LH, Wickremasinghe MI, Sharland M, Friedland JS: **Synergistic upregulation of interleukin-8 secretion from pulmonary epithelial cells by direct and monocyte-dependent effects of respiratory syncytial virus infection**. *J Virol* 2000, **74**(18):8425-8433.
169. Kotenko SV: **IFN-lambdas**. *Curr Opin Immunol* 2011, **23**(5):583-590.
170. Vesely PW, Staber PB, Hoefler G, Kenner L: **Translational regulation mechanisms of AP-1 proteins**. *Mutat Res* 2009, **682**(1):7-12.
171. George KS, Wu S: **Lipid raft: A floating island of death or survival**. *Toxicol Appl Pharmacol* 2012, **259**(3):311-319.
172. Chang TH, Segovia J, Sabbah A, Mgbemena V, Bose S: **Cholesterol-rich lipid rafts are required for release of infectious human respiratory syncytial virus particles**. *Virology* 2012, **422**(2):205-213.

173. Boukhvalova MS, Prince GA, Blanco JC: **Inactivation of respiratory syncytial virus by zinc finger reactive compounds**. *Virol J* 2010, **7**:20.
174. Singh D, McCann KL, Imani F: **MAPK and heat shock protein 27 activation are associated with respiratory syncytial virus induction of human bronchial epithelial monolayer disruption**. *Am J Physiol Lung Cell Mol Physiol* 2007, **293**(2):L436-445.
175. Neefjes J, Jongsma ML, Paul P, Bakke O: **Towards a systems understanding of MHC class I and MHC class II antigen presentation**. *Nat Rev Immunol* 2011, **11**(12):823-836.
176. Suttles J, Stout RD: **Macrophage CD40 signaling: a pivotal regulator of disease protection and pathogenesis**. *Semin Immunol* 2009, **21**(5):257-264.
177. Blander JM: **Phagocytosis and antigen presentation: a partnership initiated by Toll-like receptors**. *Ann Rheum Dis* 2008, **67 Suppl 3**:iii44-49.
178. Miyashita M, Oshiumi H, Matsumoto M, Seya T: **DDX60, a DEXD/H box helicase, is a novel antiviral factor promoting RIG-I-like receptor-mediated signaling**. *Mol Cell Biol* 2011, **31**(18):3802-3819.
179. Vince JE, Pantaki D, Feltham R, Mace PD, Cordier SM, Schmukle AC, Davidson AJ, Callus BA, Wong WW, Gentle IE *et al*: **TRAF2 must bind to cellular inhibitors of apoptosis for tumor necrosis factor (tnf) to efficiently activate nf-{kappa}b and to prevent tnf-induced apoptosis**. *J Biol Chem* 2009, **284**(51):35906-35915.
180. Wang Z, Choi MK, Ban T, Yanai H, Negishi H, Lu Y, Tamura T, Takaoka A, Nishikura K, Taniguchi T: **Regulation of innate immune responses by DAI (DLM-1/ZBP1) and other DNA-sensing molecules**. *Proc Natl Acad Sci U S A* 2008, **105**(14):5477-5482.
181. DeFilippis VR, Alvarado D, Sali T, Rothenburg S, Fruh K: **Human cytomegalovirus induces the interferon response via the DNA sensor ZBP1**. *J Virol* 2010, **84**(1):585-598.
182. Flo TH, Smith KD, Sato S, Rodriguez DJ, Holmes MA, Strong RK, Akira S, Aderem A: **Lipocalin 2 mediates an innate immune response to bacterial infection by sequestrating iron**. *Nature* 2004, **432**(7019):917-921.
183. Schroder WA, Le TT, Major L, Street S, Gardner J, Lambley E, Markey K, MacDonald KP, Fish RJ, Thomas R *et al*: **A physiological function of inflammation-associated SerpinB2 is regulation of adaptive immunity**. *J Immunol* 2010, **184**(5):2663-2670.
184. Geserick P, Kaiser F, Klemm U, Kaufmann SH, Zerrahn J: **Modulation of T cell development and activation by novel members of the Schlafen (slfn) gene family harbouring an RNA helicase-like motif**. *Int Immunol* 2004, **16**(10):1535-1548.
185. Brady G, Boggan L, Bowie A, O'Neill LA: **Schlafen-1 causes a cell cycle arrest by inhibiting induction of cyclin D1**. *J Biol Chem* 2005, **280**(35):30723-30734.
186. Katsoulidis E, Carayol N, Woodard J, Konieczna I, Majchrzak-Kita B, Jordan A, Sassano A, Eklund EA, Fish EN, Platanias LC: **Role of Schlafen 2 (SLFN2) in the generation of interferon alpha-induced growth inhibitory responses**. *J Biol Chem* 2009, **284**(37):25051-25064.
187. Sohn WJ, Kim D, Lee KW, Kim MS, Kwon S, Lee Y, Kim DS, Kwon HJ: **Novel transcriptional regulation of the schlafen-2 gene in macrophages in response to TLR-triggered stimulation**. *Mol Immunol* 2007, **44**(13):3273-3282.
188. Ivan FX, Rajapakse JC, Welsch RE, Rozen SG, Narasaraju T, Xiong GM, Engelward BP, Chow VT: **Differential pulmonary transcriptomic profiles in murine lungs infected with low and highly virulent influenza H3N2 viruses reveal dysregulation of TREM1 signaling, cytokines, and chemokines**. *Funct Integr Genomics* 2012, **12**(1):105-117.
189. Lattin JE, Schroder K, Su AI, Walker JR, Zhang J, Wiltshire T, Saijo K, Glass CK, Hume DA, Kellie S *et al*: **Expression analysis of G Protein-Coupled Receptors in mouse macrophages**. *Immunome Res* 2008, **4**:5.
190. Lesinski GB, Zimmerer JM, Kreiner M, Trefry J, Bill MA, Young GS, Becknell B, Carson WE, 3rd: **Modulation of SOCS protein expression influences the interferon responsiveness of human melanoma cells**. *BMC Cancer* 2010, **10**:142.
191. Idel S, Dansky HM, Breslow JL: **A20, a regulator of NFkappaB, maps to an atherosclerosis locus and differs between parental sensitive C57BL/6J and resistant FVB/N strains**. *Proc Natl Acad Sci U S A* 2003, **100**(24):14235-14240.

192. Gelbmann CM, Leeb SN, Vogl D, Maendel M, Herfarth H, Scholmerich J, Falk W, Rogler G: **Inducible CD40 expression mediates NFkappaB activation and cytokine secretion in human colonic fibroblasts**. *Gut* 2003, **52**(10):1448-1456.
193. Akira S, Takeda K: **Toll-like receptor signalling**. *Nat Rev Immunol* 2004, **4**(7):499-511.
194. Moynagh PN: **TLR signalling and activation of IRFs: revisiting old friends from the NF-kappaB pathway**. *Trends Immunol* 2005, **26**(9):469-476.
195. Marchant D, Singhera GK, Utokaparch S, Hackett TL, Boyd JH, Luo Z, Si X, Dorscheid DR, McManus BM, Hegele RG: **Toll-like receptor 4-mediated activation of p38 mitogen-activated protein kinase is a determinant of respiratory virus entry and tropism**. *J Virol* 2010, **84**(21):11359-11373.
196. Murawski MR, Bowen GN, Cerny AM, Anderson LJ, Haynes LM, Tripp RA, Kurt-Jones EA, Finberg RW: **Respiratory syncytial virus activates innate immunity through Toll-like receptor 2**. *J Virol* 2009, **83**(3):1492-1500.
197. Xie XH, Law HK, Wang LJ, Li X, Yang XQ, Liu EM: **Lipopolysaccharide induces IL-6 production in respiratory syncytial virus-infected airway epithelial cells through the toll-like receptor 4 signaling pathway**. *Pediatr Res* 2009, **65**(2):156-162.
198. Gagro A, Tominac M, Krsulovic-Hresic V, Bace A, Matic M, Drazenovic V, Mlinaric-Galinovic G, Kosor E, Gotovac K, Bolanca I *et al*: **Increased Toll-like receptor 4 expression in infants with respiratory syncytial virus bronchiolitis**. *Clin Exp Immunol* 2004, **135**(2):267-272.
199. Strasser A, O'Connor L, Dixit VM: **Apoptosis signaling**. *Annu Rev Biochem* 2000, **69**:217-245.
200. Coleman CM, Plant K, Newton S, Hobson L, Whyte MK, Everard ML: **The Anti-Apoptotic Effect of Respiratory Syncytial Virus on Human Peripheral Blood Neutrophils is Mediated by a Monocyte Derived Soluble Factor**. *Open Virol J* 2011, **5**:114-123.
201. Kotelkin A, Prikhod'ko EA, Cohen JI, Collins PL, Bukreyev A: **Respiratory syncytial virus infection sensitizes cells to apoptosis mediated by tumor necrosis factor-related apoptosis-inducing ligand**. *J Virol* 2003, **77**(17):9156-9172.
202. Gibbs JD, Ornoff DM, Igo HA, Zeng JY, Imani F: **Cell cycle arrest by transforming growth factor beta1 enhances replication of respiratory syncytial virus in lung epithelial cells**. *J Virol* 2009, **83**(23):12424-12431.
203. Russell GC, Stewart JP, Haig DM: **Malignant catarrhal fever: a review**. *Vet J* 2009, **179**(3):324-335.
204. Molinari NA, Ortega-Sanchez IR, Messonnier ML, Thompson WW, Wortley PM, Weintraub E, Bridges CB: **The annual impact of seasonal influenza in the US: measuring disease burden and costs**. *Vaccine* 2007, **25**(27):5086-5096.
205. Guan Y, Vijaykrishna D, Bahl J, Zhu H, Wang J, Smith GJ: **The emergence of pandemic influenza viruses**. *Protein Cell* 2010, **1**(1):9-13.
206. Patterson KD, Pyle GF: **The geography and mortality of the 1918 influenza pandemic**. *Bull Hist Med* 1991, **65**(1):4-21.
207. Michaelis M, Doerr HW, Cinatl J, Jr.: **An influenza A H1N1 virus revival - pandemic H1N1/09 virus**. *Infection* 2009, **37**(5):381-389.
208. Lewis DB: **Avian flu to human influenza**. *Annu Rev Med* 2006, **57**:139-154.
209. Hoffmann E, Stech J, Leneva I, Krauss S, Scholtissek C, Chin PS, Peiris M, Shortridge KF, Webster RG: **Characterization of the influenza A virus gene pool in avian species in southern China: was H6N1 a derivative or a precursor of H5N1?** *J Virol* 2000, **74**(14):6309-6315.
210. de Wit E, Fouchier RA: **Emerging influenza**. *J Clin Virol* 2008, **41**(1):1-6.
211. Spackman E: **A brief introduction to the avian influenza virus**. *Methods Mol Biol* 2008, **436**:1-6.
212. Xi X, Fang Q, Gu Q, Du B: **Avian influenza A (H7N9) infections: Intensivists as virus hunters in the new century**. *J Crit Care* 2013.
213. Wong CK, Zhu H, Li OT, Leung YH, Chan MC, Guan Y, Peiris JS, Poon LL: **Molecular Detection of Human H7N9 Influenza A Virus Causing Outbreaks in China**. *Clin Chem* 2013, **59**(7):1062-1067.
214. Gao R, Cao B, Hu Y, Feng Z, Wang D, Hu W, Chen J, Jie Z, Qiu H, Xu K *et al*: **Human infection with a novel avian-origin influenza A (H7N9) virus**. *N Engl J Med* 2013, **368**(20):1888-1897.

215. Tang RB, Chen HL: **An overview of the recent outbreaks of the avian-origin influenza A (H7N9) virus in the human**. *J Chin Med Assoc* 2013, **76**(5):245-248.
216. Samji T: **Influenza A: understanding the viral life cycle**. *Yale J Biol Med* 2009, **82**(4):153-159.
217. Medina RA, Garcia-Sastre A: **Influenza A viruses: new research developments**. *Nat Rev Microbiol* 2011, **9**(8):590-603.
218. Boulo S, Akarsu H, Ruigrok RW, Baudin F: **Nuclear traffic of influenza virus proteins and ribonucleoprotein complexes**. *Virus Res* 2007, **124**(1-2):12-21.
219. Boivin S, Cusack S, Ruigrok RW, Hart DJ: **Influenza A virus polymerase: structural insights into replication and host adaptation mechanisms**. *J Biol Chem* 2010, **285**(37):28411-28417.
220. Deng T, Vreede FT, Brownlee GG: **Different de novo initiation strategies are used by influenza virus RNA polymerase on its cRNA and viral RNA promoters during viral RNA replication**. *J Virol* 2006, **80**(5):2337-2348.
221. Yu M, Liu X, Cao S, Zhao Z, Zhang K, Xie Q, Chen C, Gao S, Bi Y, Sun L *et al*: **Identification and characterization of three novel nuclear export signals in the influenza A virus nucleoprotein**. *J Virol* 2012, **86**(9):4970-4980.
222. Akarsu H, Burmeister WP, Petosa C, Petit I, Muller CW, Ruigrok RW, Baudin F: **Crystal structure of the M1 protein-binding domain of the influenza A virus nuclear export protein (NEP/NS2)**. *Embo J* 2003, **22**(18):4646-4655.
223. Rossman JS, Lamb RA: **Influenza virus assembly and budding**. *Virology* 2011, **411**(2):229-236.
224. Leser GP, Lamb RA: **Influenza virus assembly and budding in raft-derived microdomains: a quantitative analysis of the surface distribution of HA, NA and M2 proteins**. *Virology* 2005, **342**(2):215-227.
225. Simpson-Holley M, Ellis D, Fisher D, Elton D, McCauley J, Digard P: **A functional link between the actin cytoskeleton and lipid rafts during budding of filamentous influenza virions**. *Virology* 2002, **301**(2):212-225.
226. Garcia-Sastre A: **Antiviral response in pandemic influenza viruses**. *Emerg Infect Dis* 2006, **12**(1):44-47.
227. Haller O, Staeheli P, Kochs G: **Interferon-induced Mx proteins in antiviral host defense**. *Biochimie* 2007, **89**(6-7):812-818.
228. Dittmann J, Stertz S, Grimm D, Steel J, Garcia-Sastre A, Haller O, Kochs G: **Influenza A virus strains differ in sensitivity to the antiviral action of Mx-GTPase**. *J Virol* 2008, **82**(7):3624-3631.
229. Samuel CE: **Antiviral actions of interferons**. *Clin Microbiol Rev* 2001, **14**(4):778-809, table of contents.
230. Fitzgerald KA: **The interferon inducible gene: Viperin**. *J Interferon Cytokine Res* 2011, **31**(1):131-135.
231. Wang X, Hinson ER, Cresswell P: **The interferon-inducible protein viperin inhibits influenza virus release by perturbing lipid rafts**. *Cell Host Microbe* 2007, **2**(2):96-105.
232. Sharma K, Tripathi S, Ranjan P, Kumar P, Garten R, Deyde V, Katz JM, Cox NJ, Lal RB, Sambhara S *et al*: **Influenza A virus nucleoprotein exploits Hsp40 to inhibit PKR activation**. *Plos One* 2011, **6**(6):e20215.
233. Hale BG, Randall RE, Ortin J, Jackson D: **The multifunctional NS1 protein of influenza A viruses**. *J Gen Virol* 2008, **89**(Pt 10):2359-2376.
234. Wolff T, Ludwig S: **Influenza viruses control the vertebrate type I interferon system: factors, mechanisms, and consequences**. *J Interferon Cytokine Res* 2009, **29**(9):549-557.
235. Min JY, Li S, Sen GC, Krug RM: **A site on the influenza A virus NS1 protein mediates both inhibition of PKR activation and temporal regulation of viral RNA synthesis**. *Virology* 2007, **363**(1):236-243.
236. Li S, Min JY, Krug RM, Sen GC: **Binding of the influenza A virus NS1 protein to PKR mediates the inhibition of its activation by either PACT or double-stranded RNA**. *Virology* 2006, **349**(1):13-21.
237. Gack MU, Albrecht RA, Urano T, Inn KS, Huang IC, Carnero E, Farzan M, Inoue S, Jung JU, Garcia-Sastre A: **Influenza A virus NS1 targets the ubiquitin ligase TRIM25 to evade recognition by the host viral RNA sensor RIG-I**. *Cell Host Microbe* 2009, **5**(5):439-449.

238. Jackson D, Killip MJ, Galloway CS, Russell RJ, Randall RE: **Loss of function of the influenza A virus NS1 protein promotes apoptosis but this is not due to a failure to activate phosphatidylinositol 3-kinase (PI3K)**. *Virology* 2010, **396**(1):94-105.
239. Payungporn S, Panjaworayan N, Makkoch J, Poovorawan Y: **Molecular characteristics of the human pandemic influenza A virus (H1N1)**. *Acta Virol* 2010, **54**(3):155-163.
240. Dudek SE, Wixler L, Nordhoff C, Nordmann A, Anhlan D, Wixler V, Ludwig S: **The influenza virus PB1-F2 protein has interferon antagonistic activity**. *Biol Chem* 2011, **392**(12):1135-1144.
241. Le Goffic R, Leymarie O, Chevalier C, Rebours E, Da Costa B, Vidic J, Descamps D, Sallenave JM, Rauch M, Samson M *et al*: **Transcriptomic analysis of host immune and cell death responses associated with the influenza A virus PB1-F2 protein**. *PLoS Pathog* 2011, **7**(8):e1002202.
242. Conenello GM, Zamarin D, Perrone LA, Tumpey T, Palese P: **A single mutation in the PB1-F2 of H5N1 (HK/97) and 1918 influenza A viruses contributes to increased virulence**. *PLoS Pathog* 2007, **3**(10):1414-1421.
243. Cox NJ, Subbarao K: **Global epidemiology of influenza: past and present**. *Annu Rev Med* 2000, **51**:407-421.
244. Geiss GK, Salvatore M, Tumpey TM, Carter VS, Wang X, Basler CF, Taubenberger JK, Bumgarner RE, Palese P, Katze MG *et al*: **Cellular transcriptional profiling in influenza A virus-infected lung epithelial cells: the role of the nonstructural NS1 protein in the evasion of the host innate defense and its potential contribution to pandemic influenza**. *Proc Natl Acad Sci U S A* 2002, **99**(16):10736-10741.
245. Viboud C, Miller M, Olson D, Osterholm M, Simonsen L: **Preliminary Estimates of Mortality and Years of Life Lost Associated with the 2009 A/H1N1 Pandemic in the US and Comparison with Past Influenza Seasons**. *PLoS Curr* 2010, **2**:RRN1153.
246. Russell CA, Jones TC, Barr IG, Cox NJ, Garten RJ, Gregory V, Gust ID, Hampson AW, Hay AJ, Hurt AC *et al*: **The global circulation of seasonal influenza A (H3N2) viruses**. *Science* 2008, **320**(5874):340-346.
247. Huang Y, Zaas AK, Rao A, Dobigeon N, Woolf PJ, Veldman T, Oien NC, McClain MT, Varkey JB, Nicholson B *et al*: **Temporal dynamics of host molecular responses differentiate symptomatic and asymptomatic influenza a infection**. *PLoS Genet* 2011, **7**(8):e1002234.
248. Neumann G, Noda T, Kawaoka Y: **Emergence and pandemic potential of swine-origin H1N1 influenza virus**. *Nature* 2009, **459**(7249):931-939.
249. Christman MC, Kedwaii A, Xu J, Donis RO, Lu G: **Pandemic (H1N1) 2009 virus revisited: an evolutionary retrospective**. *Infect Genet Evol* 2011, **11**(5):803-811.
250. Mukherjee S, Vipat VC, Mishra AC, Pawar SD, Chakrabarti AK: **Pandemic (H1N1) 2009 influenza virus induces weaker host immune responses in vitro: a possible mechanism of high transmissibility**. *Virol J* 2011, **8**:140.
251. Yu X, Zhang X, Zhao B, Wang J, Zhu Z, Teng Z, Shao J, Shen J, Gao Y, Yuan Z *et al*: **Intensive cytokine induction in pandemic H1N1 influenza virus infection accompanied by robust production of IL-10 and IL-6**. *Plos One* 2011, **6**(12):e28680.
252. Paquette SG, Banner D, Zhao Z, Fang Y, Huang SS, Leomicronn AJ, Ng DC, Almansa R, Martin-Loeches I, Ramirez P *et al*: **Interleukin-6 is a potential biomarker for severe pandemic H1N1 influenza A infection**. *Plos One* 2012, **7**(6):e38214.
253. Ma W, Belisle SE, Mosier D, Li X, Stigger-Rosser E, Liu Q, Qiao C, Elder J, Webby R, Katze MG *et al*: **2009 pandemic H1N1 influenza virus causes disease and upregulation of genes related to inflammatory and immune responses, cell death, and lipid metabolism in pigs**. *J Virol* 2011, **85**(22):11626-11637.
254. Gambotto A, Barratt-Boyes SM, de Jong MD, Neumann G, Kawaoka Y: **Human infection with highly pathogenic H5N1 influenza virus**. *Lancet* 2008, **371**(9622):1464-1475.
255. Zeng H, Goldsmith C, Thawatsupha P, Chittaganpitch M, Waicharoen S, Zaki S, Tumpey TM, Katz JM: **Highly pathogenic avian influenza H5N1 viruses elicit an attenuated type i interferon response in polarized human bronchial epithelial cells**. *J Virol* 2007, **81**(22):12439-12449.

256. Lam WY, Yeung AC, Chu IM, Chan PK: **Profiles of cytokine and chemokine gene expression in human pulmonary epithelial cells induced by human and avian influenza viruses**. *Virol J* 2010, **7**:344.
257. Chang WL, Coro ES, Rau FC, Xiao Y, Erle DJ, Baumgarth N: **Influenza virus infection causes global respiratory tract B cell response modulation via innate immune signals**. *J Immunol* 2007, **178**(3):1457-1467.
258. Veckman V, Osterlund P, Fagerlund R, Melen K, Matikainen S, Julkunen I: **TNF-alpha and IFN-alpha enhance influenza-A-virus-induced chemokine gene expression in human A549 lung epithelial cells**. *Virology* 2006, **345**(1):96-104.
259. Mibayashi M, Martinez-Sobrido L, Loo YM, Cardenas WB, Gale M, Jr., Garcia-Sastre A: **Inhibition of retinoic acid-inducible gene I-mediated induction of beta interferon by the NS1 protein of influenza A virus**. *J Virol* 2007, **81**(2):514-524.
260. Sarmento L, Afonso CL, Estevez C, Wasilenko J, Pantin-Jackwood M: **Differential host gene expression in cells infected with highly pathogenic H5N1 avian influenza viruses**. *Vet Immunol Immunopathol* 2008, **125**(3-4):291-302.
261. Lee SM, Chan RW, Gardy JL, Lo C-k, Sihoe AD, Kang SS, Cheung TK, Guan Y, Chan MC, Hancock RE *et al*: **RESEARCH Open Access Systems-level comparison of host responses induced by pandemic and seasonal influenza A H1N1 viruses in primary human type I-like alveolar epithelial cells in vitro**. *Respiratory Research* 2010, **11**(47).
262. Hui EK, Nayak DP: **Role of ATP in influenza virus budding**. *Virology* 2001, **290**(2):329-341.
263. Klumpp K, Ford MJ, Ruigrok RW: **Variation in ATP requirement during influenza virus transcription**. *J Gen Virol* 1998, **79 (Pt 5)**:1033-1045.
264. Ramirez-Martinez G, Cruz-Lagunas A, Jimenez-Alvarez L, Espinosa E, Ortiz-Quintero B, Santos-Mendoza T, Herrera MT, Canche-Pool E, Mendoza C, Banales JL *et al*: **Seasonal and pandemic influenza H1N1 viruses induce differential expression of SOCS-1 and RIG-I genes and cytokine/chemokine production in macrophages**. *Cytokine* 2013, **62**(1):151-159.
265. Herold S, Ludwig S, Pleschka S, Wolff T: **Apoptosis signaling in influenza virus propagation, innate host defense, and lung injury**. *J Leukoc Biol* 2012, **92**(1):75-82.
266. Kreijtz JH, Fouchier RA, Rimmelzwaan GF: **Immune responses to influenza virus infection**. *Virus Res* 2011, **162**(1-2):19-30.
267. Xu W, Xue L, Sun Y, Henry A, Battle JM, Micault M, Morris SW: **Bcl10 is an essential regulator for A20 gene expression**. *J Physiol Biochem* 2013.
268. Takahashi Y, Onodera T, Kobayashi K, Kurosaki T: **Primary and secondary B-cell responses to pulmonary virus infection**. *Infect Disord Drug Targets* 2012, **12**(3):232-240.
269. Fang Y, Banner D, Kelvin AA, Huang SS, Paige CJ, Corfe SA, Kane KP, Bleackley RC, Rowe T, Leon AJ *et al*: **Seasonal H1N1 influenza virus infection induces cross-protective pandemic H1N1 virus immunity through a CD8-independent, B cell-dependent mechanism**. *J Virol* 2012, **86**(4):2229-2238.
270. Wolff T, O'Neill RE, Palese P: **NS1-Binding protein (NS1-BP): a novel human protein that interacts with the influenza A virus nonstructural NS1 protein is relocalized in the nuclei of infected cells**. *J Virol* 1998, **72**(9):7170-7180.
271. Tran AT, Cortens JP, Du Q, Wilkins JA, Coombs KM: **Influenza virus induces apoptosis via BAD-mediated mitochondrial dysregulation**. *J Virol* 2013, **87**(2):1049-1060.
272. Tripathi S, Batra J, Cao W, Sharma K, Patel JR, Ranjan P, Kumar A, Katz JM, Cox NJ, Lal RB *et al*: **Influenza A virus nucleoprotein induces apoptosis in human airway epithelial cells: implications of a novel interaction between nucleoprotein and host protein Clusterin**. *Cell Death Dis* 2013, **4**:e562.
273. Li P, Nijhawan D, Wang X: **Mitochondrial activation of apoptosis**. *Cell* 2004, **S116**:S57-S59.
274. Francoz S, Froment P, Bogaerts S, De Clercq S, Maetens M, Doumont G, Bellefroid E, Marine JC: **Mdm4 and Mdm2 cooperate to inhibit p53 activity in proliferating and quiescent cells in vivo**. *Proc Natl Acad Sci U S A* 2006, **103**(9):3232-3237.
275. Liu Z, Lu H, Jiang Z, Pastuszyn A, Hu CA: **Apolipoprotein l6, a novel proapoptotic Bcl-2 homology 3-only protein, induces mitochondria-mediated apoptosis in cancer cells**. *Mol Cancer Res* 2005, **3**(1):21-31.

276. Zhaorigetu S, Yang Z, Toma I, McCaffrey TA, Hu CA: **Apolipoprotein L6, induced in atherosclerotic lesions, promotes apoptosis and blocks Beclin 1-dependent autophagy in atherosclerotic cells**. *J Biol Chem* 2011, **286**(31):27389-27398.
277. Rovere P, Peri G, Fazzini F, Bottazzi B, Doni A, Bondanza A, Zimmermann VS, Garlanda C, Fascio U, Sabbadini MG *et al*: **The long pentraxin PTX3 binds to apoptotic cells and regulates their clearance by antigen-presenting dendritic cells**. *Blood* 2000, **96**(13):4300-4306.
278. Reading PC, Bozza S, Gilbertson B, Tate M, Moretti S, Job ER, Crouch EC, Brooks AG, Brown LE, Bottazzi B *et al*: **Antiviral activity of the long chain pentraxin PTX3 against influenza viruses**. *J Immunol* 2008, **180**(5):3391-3398.
279. Job ER, Deng YM, Tate MD, Bottazzi B, Crouch EC, Dean MM, Mantovani A, Brooks AG, Reading PC: **Pandemic H1N1 influenza A viruses are resistant to the antiviral activities of innate immune proteins of the collectin and pentraxin superfamilies**. *J Immunol* 2010, **185**(7):4284-4291.
280. Park K, Scott AL: **Cholesterol 25-hydroxylase production by dendritic cells and macrophages is regulated by type I interferons**. *J Leukoc Biol* 2010, **88**(6):1081-1087.
281. Diczfalusy U, Olofsson KE, Carlsson AM, Gong M, Golenbock DT, Rooyackers O, Flaring U, Bjorkbacka H: **Marked upregulation of cholesterol 25-hydroxylase expression by lipopolysaccharide**. *J Lipid Res* 2009, **50**(11):2258-2264.
282. Hurlin PJ, Steingrimsson E, Copeland NG, Jenkins NA, Eisenman RN: **Mga, a dual-specificity transcription factor that interacts with Max and contains a T-domain DNA-binding motif**. *Embo J* 1999, **18**(24):7019-7028.
283. Grandori C, Cowley SM, James LP, Eisenman RN: **The Myc/Max/Mad network and the transcriptional control of cell behavior**. *Annu Rev Cell Dev Biol* 2000, **16**:653-699.
284. Shilatifard A, Duan DR, Haque D, Florence C, Schubach WH, Conaway JW, Conaway RC: **ELL2, a new member of an ELL family of RNA polymerase II elongation factors**. *Proc Natl Acad Sci U S A* 1997, **94**(8):3639-3643.
285. Gaur P, Munjhal A, Lal SK: **Influenza virus and cell signaling pathways**. *Med Sci Monit* 2011, **17**(6):RA148-154.
286. Xing Z, Cardona CJ, Anunciacion J, Adams S, Dao N: **Roles of the ERK MAPK in the regulation of proinflammatory and apoptotic responses in chicken macrophages infected with H9N2 avian influenza virus**. *J Gen Virol* 2010, **91**(Pt 2):343-351.
287. Hui KP, Lee SM, Cheung CY, Ng IH, Poon LL, Guan Y, Ip NY, Lau AS, Peiris JS: **Induction of proinflammatory cytokines in primary human macrophages by influenza A virus (H5N1) is selectively regulated by IFN regulatory factor 3 and p38 MAPK**. *J Immunol* 2009, **182**(2):1088-1098.
288. Kujime K, Hashimoto S, Gon Y, Shimizu K, Horie T: **p38 mitogen-activated protein kinase and c-jun-NH2-terminal kinase regulate RANTES production by influenza virus-infected human bronchial epithelial cells**. *J Immunol* 2000, **164**(6):3222-3228.
289. Ludwig S, Ehrhardt C, Neumeier ER, Kracht M, Rapp UR, Pleschka S: **Influenza virus-induced AP-1-dependent gene expression requires activation of the JNK signaling pathway**. *J Biol Chem* 2001, **276**(24):10990-10998.
290. Pleschka S, Wolff T, Ehrhardt C, Hobom G, Planz O, Rapp UR, Ludwig S: **Influenza virus propagation is impaired by inhibition of the Raf/MEK/ERK signalling cascade**. *Nat Cell Biol* 2001, **3**(3):301-305.
291. Marjuki H, Alam MI, Ehrhardt C, Wagner R, Planz O, Klenk HD, Ludwig S, Pleschka S: **Membrane accumulation of influenza A virus hemagglutinin triggers nuclear export of the viral genome via protein kinase Calpha-mediated activation of ERK signaling**. *J Biol Chem* 2006, **281**(24):16707-16715.
292. Qu B, Li X, Gao W, Sun W, Jin Y, Cardona CJ, Xing Z: **Human intestinal epithelial cells are susceptible to influenza virus subtype H9N2**. *Virus Res* 2012, **163**(1):151-159.
293. Lu X, Masic A, Liu Q, Zhou Y: **Regulation of influenza A virus induced CXCL-10 gene expression requires PI3K/Akt pathway and IRF3 transcription factor**. *Mol Immunol* 2011, **48**(12-13):1417-1423.
294. Chiou WF, Chen CC, Wei BL: **8-Prenylkaempferol Suppresses Influenza A Virus-Induced RANTES Production in A549 Cells via Blocking PI3K-Mediated**

Transcriptional Activation of NF-kappaB and IRF3. *Evid Based Complement Alternat Med* 2011, **2011**:920828.
295. Shin YK, Liu Q, Tikoo SK, Babiuk LA, Zhou Y: **Effect of the phosphatidylinositol 3-kinase/Akt pathway on influenza A virus propagation**. *J Gen Virol* 2007, **88**(Pt 3):942-950.
296. Pei D, Dai J, Kuang Y, Wang H, Ren L, Shao J, Zuo B, Li S, Jiang Z, Li M: **Effect of influenza A virus non-structural protein 1(NS1) on a mouse model of diabetes mellitus induced by Streptozotocin**. *Biochem Biophys Res Commun* 2012, **419**(1):120-125.
297. Hrincius ER, Dierkes R, Anhlan D, Wixler V, Ludwig S, Ehrhardt C: **Phosphatidylinositol-3-kinase (PI3K) is activated by influenza virus vRNA via the pathogen pattern receptor Rig-I to promote efficient type I interferon production**. *Cell Microbiol* 2011, **13**(12):1907-1919.
298. Shapira SD, Gat-Viks I, Shum BO, Dricot A, de Grace MM, Wu L, Gupta PB, Hao T, Silver SJ, Root DE *et al*: **A physical and regulatory map of host-influenza interactions reveals pathways in H1N1 infection**. *Cell* 2009, **139**(7):1255-1267.
299. GM C: **The cell: a molecular approach**. 2000.
300. He Y, Xu K, Keiner B, Zhou J, Czudai V, Li T, Chen Z, Liu J, Klenk HD, Shu YL *et al*: **Influenza A virus replication induces cell cycle arrest in G0/G1 phase**. *J Virol* 2010, **84**(24):12832-12840.
301. Li M, Chen D, Shiloh A, Luo J, Nikolaev AY, Qin J, Gu W: **Deubiquitination of p53 by HAUSP is an important pathway for p53 stabilization**. *Nature* 2002, **416**(6881):648-653.
302. Wu M, Xu LG, Su T, Tian Y, Zhai Z, Shu HB: **AMID is a p53-inducible gene downregulated in tumors**. *Oncogene* 2004, **23**(40):6815-6819.
303. Wang N, Dong Q, Li J, Jangra RK, Fan M, Brasier AR, Lemon SM, Pfeffer LM, Li K: **Viral induction of the zinc finger antiviral protein is IRF3-dependent but NF-kappaB-independent**. *J Biol Chem* 2010, **285**(9):6080-6090.
304. Zaitseva L, Cherepanov P, Leyens L, Wilson SJ, Rasaiyaah J, Fassati A: **HIV-1 exploits importin 7 to maximize nuclear import of its DNA genome**. *Retrovirology* 2009, **6**:11.
305. Ao Z, Huang G, Yao H, Xu Z, Labine M, Cochrane AW, Yao X: **Interaction of human immunodeficiency virus type 1 integrase with cellular nuclear import receptor importin 7 and its impact on viral replication**. *J Biol Chem* 2007, **282**(18):13456-13467.
306. Hui EK, Nayak DP: **Role of G protein and protein kinase signalling in influenza virus budding in MDCK cells**. *J Gen Virol* 2002, **83**(Pt 12):3055-3066.
307. Moss B: **Poxvirus cell entry: how many proteins does it take?** *Viruses* 2012, **4**(5):688-707.
308. Laliberte JP, Moss B: **Lipid membranes in poxvirus replication**. *Viruses* 2010, **2**(4):972-986.
309. Barry M, van Buuren N, Burles K, Mottet K, Wang Q, Teale A: **Poxvirus exploitation of the ubiquitin-proteasome system**. *Viruses* 2010, **2**(10):2356-2380.
310. Moss B: **Poxvirus entry and membrane fusion**. *Virology* 2006, **344**(1):48-54.
311. Schmidt FI, Bleck CK, Mercer J: **Poxvirus host cell entry**. *Current Opinion in Virology* 2012, **2**(1):20-27.
312. Carter GC, Law M, Hollinshead M, Smith GL: **Entry of the vaccinia virus intracellular mature virion and its interactions with glycosaminoglycans**. *J Gen Virol* 2005, **86**(Pt 5):1279-1290.
313. Senkevich TG, Moss B: **Vaccinia virus H2 protein is an essential component of a complex involved in virus entry and cell-cell fusion**. *J Virol* 2005, **79**(8):4744-4754.
314. Condit RC, Moussatche N, Traktman P: **In a nutshell: structure and assembly of the vaccinia virion**. *Adv Virus Res* 2006, **66**:31-124.
315. Schramm B, Locker JK: **Cytoplasmic organization of POXvirus DNA replication**. *Traffic* 2005, **6**(10):839-846.
316. Montanuy I, Alejo A, Alcami A: **Glycosaminoglycans mediate retention of the poxvirus type I interferon binding protein at the cell surface to locally block interferon antiviral responses**. *Faseb Journal* 2011, **25**(6):1960-1971.

317. Meng XZ, Schoggins J, Rose L, Cao JX, Ploss A, Rice CM, Xiang Y: **C7L Family of Poxvirus Host Range Genes Inhibits Antiviral Activities Induced by Type I Interferons and Interferon Regulatory Factor 1**. *J Virol* 2012, **86**(8):4538-4547.
318. Sakala IG, Chaudhri G, Buller RM, Nuara AA, Bai H, Chen N, Karupiah G: **Poxvirus-encoded gamma interferon binding protein dampens the host immune response to infection**. *J Virol* 2007, **81**(7):3346-3353.
319. Waibler Z, Anzaghe M, Frenz T, Schwantes A, Poehlmann C, Ludwig H, Palomo-Otero M, Alcami A, Sutter G, Kalinke U: **Vaccinia Virus-Mediated Inhibition of Type I Interferon Responses Is a Multifactorial Process Involving the Soluble Type I Interferon Receptor B18 and Intracellular Components**. *J Virol* 2009, **83**(4):1563-1571.
320. Smith SA, Mullin NP, Parkinson J, Shchelkunov SN, Totmenin AV, Loparev VN, Srisatjaluk R, Reynolds DN, Keeling KL, Justus DE *et al*: **Conserved surface-exposed K/R-X-K/R motifs and net positive charge on poxvirus complement control proteins serve as putative heparin binding sites and contribute to inhibition of molecular interactions with human endothelial cells: a novel mechanism for evasion of host defense**. *J Virol* 2000, **74**(12):5659-5666.
321. Perdiguero B, Esteban M: **The Interferon System and Vaccinia Virus Evasion Mechanisms**. *J Interf Cytok Res* 2009, **29**(9):581-598.
322. Saraiva M, Smith P, Fallon PG, Alcami A: **Inhibition of type 1 cytokine-mediated inflammation by a soluble CD30 homologue encoded by ectromelia (mousepox) virus**. *Journal of Experimental Medicine* 2002, **196**(6):829-839.
323. Ruiz-Arguello MB, Smith VP, Campanella GSV, Baleux F, Arenzana-Seisdedos F, Luster AD, Alcami A: **An ectromelia virus protein that interacts with chemokines through their glycosaminoglycan binding domain**. *J Virol* 2008, **82**(2):917-926.
324. Boomker JM, de Leij LFMH, The TH, Harmsen MC: **Viral chemokine-modulatory proteins: tools and targets**. *Cytokine Growth Factor Rev* 2005, **16**(1):91-103.
325. Mohamed MR, Rahman MM, Rice A, Moyer RW, Werden SJ, McFadden G: **Cowpox Virus Expresses a Novel Ankyrin Repeat NF-kappa B Inhibitor That Controls Inflammatory Cell Influx into Virus-Infected Tissues and Is Critical for Virus Pathogenesis**. *J Virol* 2009, **83**(18):9223-9236.
326. Stack J, Haga IR, Schroder M, Bartlett NW, Maloney G, Reading PC, Fitzgerald KA, Smith GL, Bowie AG: **Vaccinia virus protein Toll-like-interleukin-1 A46R targets multiple receptor adaptors and contributes to virulence**. *Journal of Experimental Medicine* 2005, **201**(6):1007-1018.
327. Chang SJ, Hsiao JC, Sonnberg S, Chiang CT, Yang MH, Tzou DL, Mercer AA, Chang W: **Poxvirus Host Range Protein CP77 Contains an F-Box-Like Domain That Is Necessary To Suppress NF-kappa B Activation by Tumor Necrosis Factor Alpha but Is Independent of Its Host Range Function**. *J Virol* 2009, **83**(9):4140-4152.
328. Randall CMH, Jokela JA, Shisler JL: **The MC159 Protein from the Molluscum Contagiosum Poxvirus Inhibits NF-kappa B Activation by Interacting with the I kappa B Kinase Complex**. *J Immunol* 2012, **188**(5):2371-2379.
329. Hansen TH, Bouvier M: **MHC class I antigen presentation: learning from viral evasion strategies**. *Nature Reviews Immunology* 2009, **9**(7):503-513.
330. Byun M, Verweij MC, Pickup DJ, Wiertz EJHJ, Hansen TH, Yokoyama WM: **Two Mechanistically Distinct Immune Evasion Proteins of Cowpox Virus Combine to Avoid Antiviral CD8 T Cells**. *Cell Host Microbe* 2009, **6**(5):422-432.
331. Dasgupta A, Hammarlund E, Slifka MK, Fruh K: **Cowpox virus evades CTL recognition and inhibits the intracellular transport of MHC class I molecules**. *J Immunol* 2007, **178**(3):1654-1661.
332. Taylor JM, Barry M: **Near death experiences: poxvirus regulation of apoptotic death**. *Virology* 2006, **344**(1):139-150.
333. Stewart TL, Wasilenko ST, Barry M: **Vaccinia virus F1L protein is a tail-anchored protein that functions at the mitochondria to inhibit apoptosis**. *J Virol* 2005, **79**(2):1084-1098.
334. Johnston JB, Barrett JW, Nazarian SH, Goodwin M, Ricciuto D, Wang G, McFadden G: **A poxvirus-encoded pyrin domain protein interacts with ASC-1 to inhibit host inflammatory and apoptotic responses to infection**. *Immunity* 2005, **23**(6):587-598.
335. Sedger LM, Osvath SR, Xu XM, Li G, Chan FK, Barrett JW, McFadden G: **Poxvirus tumor necrosis factor receptor (TNFR)-like T2 proteins contain a conserved**

preligand assembly domain that inhibits cellular TNFR1-induced cell death. *J Virol* 2006, **80**(18):9300-9309.
336. Turner PC, Moyer RW: **Poxvirus immune modulators: functional insights from animal models**. *Virus Res* 2002, **88**(1-2):35-53.
337. Guerra S, Lopez-Fernandez LA, Pascual-Montano A, Najera JL, Zaballos A, Esteban M: **Host response to the attenuated poxvirus vector NYVAC: upregulation of apoptotic genes and NF-kappaB-responsive genes in infected HeLa cells**. *J Virol* 2007, **80**(2):985-998.
338. Mahalingam S, Damon IK, Lidbury BA: **25 years since the eradication of smallpox: why poxvirus research is still relevant**. *Trends Immunol* 2004, **25**(12):636-639.
339. Alkhalil A, Hammamieh R, Hardick J, Ichou MA, Jett M, Ibrahim S: **Gene expression profiling of monkeypox virus-infected cells reveals novel interfaces for host-virus interactions**. *Virol J* 2010, **7**:173.
340. Zellmer S, Schmidt-Heck W, Godoy P, Weng H, Meyer C, Lehmann T, Sparna T, Schormann W, Hammad S, Kreutz C *et al*: **Transcription factors ETF, E2F, and SP-1 are involved in cytokine-independent proliferation of murine hepatocytes**. *Hepatology* 2010, **52**(6):2127-2136.
341. Kaplan MH: **STAT4: a critical regulator of inflammation in vivo**. *Immunol Res* 2005, **31**(3):231-242.
342. Vousden KH, Prives C: **Blinded by the Light: The Growing Complexity of p53**. *Cell* 2009, **137**(3):413-431.
343. Barrera G, Pizzimenti S, Dianzani MU: **4-hydroxynonenal and regulation of cell cycle: effects on the pRb/E2F pathway**. *Free Radic Biol Med* 2004, **37**(5):597-606.
344. Haig DM: **Poxvirus interference with the host cytokine response**. *Vet Immunol Immunopathol* 1998, **63**(1-2):149-156.
345. Harte MT, Haga IR, Maloney G, Gray P, Reading PC, Bartlett NW, Smith GL, Bowie A, O'Neill LAJ: **The poxvirus protein A52R targets toll-like receptor signaling complexes to suppress host defense**. *Journal of Experimental Medicine* 2003, **197**(3):343-351.
346. DiPerna G, Stack J, Bowie AG, Boyd A, Kotwal G, Zhang Z, Arvikar S, Latz E, Fitzgerald KA, Marshall WL: **Poxvirus protein N1L targets the I-kappaB kinase complex, inhibits signaling to NF-kappaB by the tumor necrosis factor superfamily of receptors, and inhibits NF-kappaB and IRF3 signaling by toll-like receptors**. *J Biol Chem* 2004, **279**(35):36570-36578.
347. Everett H, McFadden G: **Poxviruses and apoptosis: a time to die**. *Curr Opin Microbiol* 2002, **5**(4):395-402.
348. Yoo NK, Pyo CW, Kim Y, Ahn BY, Choi SY: **Vaccinia virus-mediated cell cycle alteration involves inactivation of tumour suppressors associated with Brf1 and TBP**. *Cell Microbiol* 2008, **10**(3):583-592.
349. Webb TJ, Litavecz RA, Khan MA, Du W, Gervay-Hague J, Renukaradhya GJ, Brutkiewicz RR: **Inhibition of CD1d1-mediated antigen presentation by the vaccinia virus B1R and H5R molecules**. *Eur J Immunol* 2006, **36**(10):2595-2600.
350. Jeang KT: **RNAi in the regulation of mammalian viral infections**. *BMC Biol* 2012, **10**:58.
351. Chen M, Du Q, Zhang HY, Wang X, Liang Z: **High-throughput screening using siRNA (RNAi) libraries**. *Expert Rev Mol Diagn* 2007, **7**(3):281-291.
352. Karlas A, Machuy N, Shin Y, Pleissner KP, Artarini A, Heuer D, Becker D, Khalil H, Ogilvie LA, Hess S *et al*: **Genome-wide RNAi screen identifies human host factors crucial for influenza virus replication**. *Nature* 2010, **463**(7282):818-822.
353. Grundhoff A, Sullivan CS: **Virus-encoded microRNAs**. *Virology* 2011, **411**(2):325-343.
354. Ghosh Z, Mallick B, Chakrabarti J: **Cellular versus viral microRNAs in host-virus interaction**. *Nucleic Acids Res* 2009, **37**(4):1035-1048.
355. Umbach JL, Cullen BR: **The role of RNAi and microRNAs in animal virus replication and antiviral immunity**. *Genes Dev* 2009, **23**(10):1151-1164.
356. Li Y, Chan EY, Li J, Ni C, Peng X, Rosenzweig E, Tumpey TM, Katze MG: **MicroRNA expression and virulence in pandemic influenza virus-infected mice**. *J Virol* 2010, **84**(6):3023-3032.

357. Bakre A, Mitchell P, Coleman JK, Jones LP, Saavedra G, Teng M, Tompkins SM, Tripp RA: **Respiratory syncytial virus modifies microRNAs regulating host genes that affect virus replication**. *J Gen Virol* 2012, **93**(Pt 11):2346-2356.
358. Yeo DS, Ng SH, Liaw CW, Ng LM, Wee EJ: **Molecular characterization of low pathogenic avian influenza viruses, isolated from food products imported into Singapore**. *Vet Microbiol* 2009, **138**: 304–317.
359. Kaptein JS and Nayak DP: **Complete nucleotide sequence of the polymerase 3 gene of human influenza virus A/WS/33**. *J Virol.* 1982, **42**(1): 55–63.
360. Akerlind B: **Respiratory Syncytial Virus: Heterogeneity of Subgroup B Strains**. *J Gen Virol* 1988, **69**: 2145-2154.
361. Downie AW: **A study of the lesions produced experimentally by cowpox virus**. *The Journal of Pathology and Bacteriology* 1939, **48**(2): 361–379.
362 Bhatt PN, Jacoby RO, Gras L: **Mousepox in inbred mice innately resistant or susceptible to lethal infection with ectromelia virus. IV. Studies with the Moscow strain**. *Arch Virol* 1988, **100**(3-4): 221-30.
363. Marennikova SS, Ladnyj ID, Ogorodinikova ZI, Shelukhina EM, Maltseva NN: **Identification and study of a poxvirus isolated from wild rodents in Turkmenia**. *Arch Virol* 1978, **56**(1-2):7-14.
364. Ravi LI, Li L, Sutejo R, Chen H, Wong PS, Tan BH, Sugrue RJ: **A systems-based approach to analyse the host response in murine lung macrophages challenged with respiratory syncytial virus**. *BMC Genomics* 2013, **14**:190.
365. Sutejo R, Yeo DS, Myaing MZ, Chen H, Xia J, Ko D, Cheung PCF, Tan BH, Sugrue RJ: **Activation of type I and III interferon signalling pathways occurs in lung epithelial cells infected with low pathogenic avian influenza viruses**. *PLoS ONE* 2012, **7**(3): e33732.
366. Tong S, Li Y, Rivailler P, Conrardy C, Castillo DAA, Chen LM, Recuenco S, Ellison JA, Davis CT *et al*: **A distinct lineage of influenza A virus from bats**. *Proc Natl Acad Sci* 2012, **109**(11):4269-4274.
367. Li C, Bu Z, Chen H: **Avian influenza vaccins against H5N1 'bird flu'**. *Trends in Biotechnology* 2014.
368. Edinger TO, Pohl MO, Stertz S: **Entry of influenza A virus: host factors and antiviral targets**. *Journal of General Virology* 2014, **95**(2):263-277.
369. Wise HM, Hutchinson EC, Jagger BW, Stuart AD, Kang ZH, Robb N, Schwartzman LM, Kash JC, Fodor E, Firth AE, Gog JR, Taubenberger JK, Digard P: **Identification of a Novel Splice Variant Form of the Influenza A Virus M2 Ion Channel with an Antigenically Distinct Ectodomain** . *PLoS Pathog* 2012, **8**(11).
370. Horby P, Nguyen NY, Dunstan SJ, Baillie JK: **The role of host genetics in susceptibility to influenza: a systematic review**. *PLoS ONE* 2013, **7**(3):E33180.
371. Diepen A, Brand HK, Sama I, Lambooy LHJ, Heuvel LP, Well L, Huynen M, Osterhaus ADME, Andeweg AC, Hermans PWM: **Quantitative proteome profiling of respiratory virus-infected lung epithelial cells**. *Journal of Proteomics* 2010, **73**(9):1680-1693.
372. Goujon C, Moncorge O, Bauby H, Doyle T, Ward CC, Schaller T, Hue S, Barclay WS, Schulz R, Malim MH: **Human MX2 is an interferon-induced post-entry inhibitor of HIV-1infection**. *Nature* 2013, s02.
373. Perez-Ortin JE, Alepuz P, Chavez S, Choder M: **Eukaryotic mRNA decay: methodologies, pathways and links to other stages of gene expression**. *J. Mol. Biol.* 2013, **425**:3750-3775.
374. Bartel S, Doellinger J, Darsow K, Bourquain D, Buchholz R, Nitsche A, Lange HA: **Proteime analysis of vaccinia virus IHD-W-infected HEK 293 cells with 2-dimensional gel electrophoresis and MALDI-PSD-TOF MS of on solid phase support N-terminally sulfonated peptides**. *Virology Journal* 2011, **8**(380).
375. Mosquera RA, Stark JM, Atkins CL, Colasurdo GN, Chevalier J, Samuels CL, Pacheco SS: **Functional and immune response to respiratory syncytial virus replication in aged BALB/c mice: a search for genes determining disease severity**. *Experimental Lung Research* 2014, **40**:40-49.
376. Hsieh YC: **Influenza pandemics: past, present and future**. *Journal of the Formosan Medical Association* 2006, **105**(1):1-6.
377. Reis AL, McCauley JW: **The influenza virus protein PB1-F2 interacts with IKKβ and modulates NF-κB signaling**. *PLoS ONE* 2013, **8**(5): e63852.

378. Takahashi T, Takaguchi M, Kawakami T, Suzuki T: **Sulfatide regulates caspase-3-independent apoptosis of influenza A virus through viral PB1-F2 protein**. *PLoS ONE* 2013, **8**(4):e61092.
379. Soda K, Cheng MC, Yoshida H, Endo M, Lee SH, Okamatsu M, Sakoda Y, Wang CH, Kida H: **A low pathogenic H5N2 influenza virus isolated in Taiwan acquired high pathogenicity by consecutive passages in chickens**. *J. Vet, Med, Sci* 2011, **73**(6): 767-772.
380. Monne I, Fusaro A, Nelson M, Bonfanti L, Mulatti P, Hughes J, Murcia PR, Schivo A, Valastro V, Moreno A, Holmes EC, Cattoli G: **Emergence of a highly pathogenic avian influenza virus from a low pathogenic progenitor**. *J. Virol*. 2014, **10**(1128).
381. Rusnock A: **Catching cowpox: the early spread of smallpox vaccination, 1798-1810**. *Bulletin of the History of Medicin* 2009, **83**(1):17-36.
382. Bourquain D, Dabrowski PW, Nitsche A: **Comparison of host cell gene expression in cowpox, monkeypox or vaccinia virus-infected cells reveals viru specific regulation of immune response genes**. *Virology Journal* 2013, **10**(61).
383. Gerlach RL, Camp JV, Chu YK, Jonsson CB: **Early host responses of seasonal and pandemic influenza A viruses in primary well-differentiated human lung epithelial cells**. *PLoS One* 2013, **8**(11):e78912.
384. Jin HK, Yoshimatsu K, Takada A, Ogino M, Asano A, Arikawa J, Watanabe T**: Mouse Mx2 protein inhibits hantavirus but not influenza virus replication**. *Arch. Virol*. 2001, **146**:41-49.
385. Cohen M, Zhang XQ, Senaati HP, Chen HW, Varki NM, Schooley RT, Gagneux P: **Influenza A penetrates host mucus by cleaving sialic acid with neuraminidase**. *Virol. J.* 2013, **10**:321.
386. Ni F, Chen X, Shen J, Wang Q: **Structural insights into the membrane fusion mechanism mediated by influenza virus hemagglutinin**. *Biochemistry* 2014, **53**:846-854.
387. Blasius AL, Beutler B: **Intracellular toll-like receptors**. *Cell* 2010, **305**.
388. Jagger BW, Wise HM, Kash JC, Walters KA, Wills NM, Xiao YL, Dunfee RL, Schwartzman LM, Ozinsky A, Bell GL, Dalton RM, Lo A, Efstathiou S, Atkins JF, Firth AE, Taubenberger JK, Digard P**: An overlapping protein-coding region in influenza A virus segment 3 modulates the host response**. *Science* 2012, **337**(199).
389. Fauquet CM, Mayo MA, Maniloff J, Desselberger U, Ball LA: Virus **taxonomy: eighth report of the international committee on taxonomy of viruses**. *Virology Division International Union of Microbiological Societies* 2005.
390. Kroeler AL, Ezzati P, Coombs KM, Halayko AJ**: Influenza A infection of primary human airway epithelial cells up-regulates proteins related to purine metabolism and ubiquitin-related signaling**. *Journal of Proteome research* 2013, **12**:3139-3151.
391. Ravi LI, Li L, Wong PS, Sutejo R, Tan BH, Sugrue RJ: **Lavastatin treatment mitigates the pro-inflammatory cytokine response in repespiratory syncytial virus infected macrophage cells**. *Antiviral Research* 2013, **98**(2):332-343.
392. Dimmock NJ, Easton AJ, Leppard KN: **Introduction to modern virology**. 2007.
393. Servant MJ, Grandvaux N, Hiscott J: **Multiple signaling pathways leading to the activation of interferon regulatory factor 3**. *Biochem Pharmacol* 2002, **64**: 985–992.
394. Earl PL, Cooper N, Wyatt LS, Moss B, Carroll MW: **Preparation of cell cultures and vaccinia virus stocks.** *Culture Protocols in Protein Science* 1998, 5.12.1-5.12.2.
395. Guerra S, Lopez-Fernandez LA, Pascual-Montano A, Munoz M, Harshman K, Esteban M: **Cellular gene expression survey of vaccinia virus infection of human Hela cells**. *Journal of Virology* 2003, **77**(11):6493.
396. Kilcher S, Schmidt FI, Schneider C, Kopf M, Helenius A, Mercer J: **siRNA screen of early poxvirus genes identifies the AAA+ ATPase D5 as the virus genome-uncoating factor**. *Cell Host & Microbe* 2014, **15**:103-112.

Appendix

1. Origin of virus strains

Name of Strain	Subtype	Origin
RSV A2	A	This RSV A2 strain was originally isolated in Australia in 1961 (Taxon: 11259) (Akerlind B *et al*., 1988).
A/WS/33	H1N1	The laboratory-adapted A/WSN/1933 (H1N1/WSN) was isolated in throat washings from an influenza patient by Wilson and Smith in 1933 (Taxon: 381518) (Hiti AL and Nayak DP, 1982).
A/Singapore/478/2009	H1N1	This virus was obtained from DSO national laboratories, and it was isolated from an pandemic influenza patient in singapore (Taxon: 872268) (Sutejo R *et al*., 2012).
A/Duck/Malaysia/01	H9N2	These viruses were obtained from the Agri-Food and Veterinary Authority of Singapore (AVA), and they were isolated as part of the routine surveillance for AIVs in avian species imported from Malaysia (Taxon: 882942/341207/500383/500382/144182) (Yeo DS *et al*., 2009).
A/Duck/Malaysis/F118/08/2004	H5N2	
A/Duck/Malaysia/F59/04/1998	H5N2	
A/Duck/Malaysia/F189/07/2004	H5N2	
A/Duck/Malaysia/F119/3/1997	H5N3	
A/fairybluebird/Singapore/F92/09/94	H7N1	This virus was obtained from the Agri-Food and Veterinary Authority of Singapore (AVA), and it was isolated from fairy blue bird in singapore (Taxon: 121432).
Brighton strain	Cowpox	It was isolated in lesions on hands of milker in England in 1937 (Taxon: 265872) (Downie AW, 1939).
Lister strain	Vaccinia	(Taxon: 10252)
Moscow strain	Ectromelia	It was isolated in white rats and Felidae in the Moscow Zoo (Taxon: 265874) (Bhatt PN *et al*., 1988).

2. Consideration of contamination

Contamination is always the major consideration during the experiment of virus infection. For example, mycoplasmas can interfere with virtually every parameter measured in cell cultures during routine cultivation or in experimental investigation. Under this consideration, we performed the virus infection experiment across a series of time points, and the gene expression profiles from multiple time points showed consistent. Moreover, cell and viruses were routinely check for mycoplasmas mainly using commercial available mycoplasmas kits in our experiment to make sure that the cells were out of contamination. And virus preparations were based on multiplex PCR, electron microscope (transmission electron microscope and scanning electron microscope) for direct visualization, immunological detection. In terms of these techniques, the cells became taken over by the virus and viruses replicated with variable rates at different infection stages were observed.

3. Consideration of reproducibility

Reproducibility of results was also under our carful consideration. Firstly, since the microarray experiment is expensive, the performances of experiments were limited to some extent. However, we tried our best to design and carry on the experiments carefully: more than one viral preparation was conducted, and different validation methods including biochemical validation and qPCR using different viral preparation were involved. Besides, the statistical analysis based on Benjamini & Hochberg False Discovery method or one-way analysis of variance (ANOVA) was performed with a P-value cutoff of ≤ 0.05 to determine significance of differential gene expression during virus infection. For some specific strains such as A/WS/33/H1N1, the investigation of gene expression profiles was also performed by another person in another batch of our study, and the results from two different batches of experiments still showed highly consistent, strongly indicating the reproducibility of the results from our experiments. In summary, our study was limited based on the expensive cost of microarray experiments, however, the common features were observed in different viruses and the gene expression trends also showed consistent for individual genes over the whole infection time course.

4. Consideration of results that a gene transcript showed down-regulated expression at a time point but less down-regulated expression at a later time point

To make sure to get the precise information in our study, investigation of different gene expression profiles was based on three independent experiments. Only genes that were flagged as present in all three replicates (mock- or virus-infected), and passed the threshold of fold change ($\geqslant 2$ up- or down-regulated) between virus- and mock-infected samples in all triplicate microarray experiments were selected for further statistical evaluation. The following statistical analysis based on Benjamini & Hochberg False Discovery method or one-way analysis of variance (ANOVA) was performed with a P-value cutoff of ≤ 0.05 to determine significantly expressed genes during virus infection. The observations such a gene transcript with more down-regulated expression an early time point but less down-regulation at a later time point

must pass threshold of fold change and P-value. Further investigation involved validation based on qPCR method.

5. The productivity of the infection of RSV during the whole investigated infection time course for each of the cell types

The transcriptomic profiles were investigated from 4hpi to 15hpi in RSV-infected Hep2 cells, and this time course is suffice time to allow formation of progeny virus, but is prior to the cell damage that occurs later in the replication cycle (e.g. following syncytia formation) that could cause indirect changes in the host cell expression profile. Specifically, we could discern the formation of the virus filaments and inclusion bodies followed over the time course (from 8hpi) of a single cycle of infection [164].

In macrophages, similar vRNA levels at between 2.5 and 20 hpi were detected suggesting low levels of vRNA synthesis. The virus infectivity recovered in macrophages indicated virus titres of $2x10^1$ pfu/ml, and this low level of virus titres was likely due to residual virus from the input virus inoculum. Similarly, only sporadic stained cells were detected using the tissue culture supernatant (TCS) of RSV-infected macrophages. Collectively, these data indicated that RSV infection results in the formation of virus antigen and the production of inclusion bodies, efficient infectious virus particle production does not occur [356].

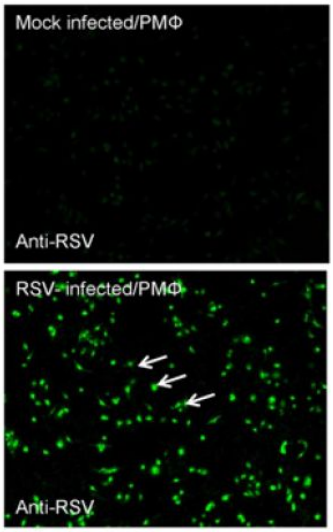

Macrophage cells were mock-infected or RSV-infected, and at 24 hrs post-infection (hpi) stained with anti-RSV and examined using fluorescence microscopy (objective x 10) (highlighted by white arrows) [364].

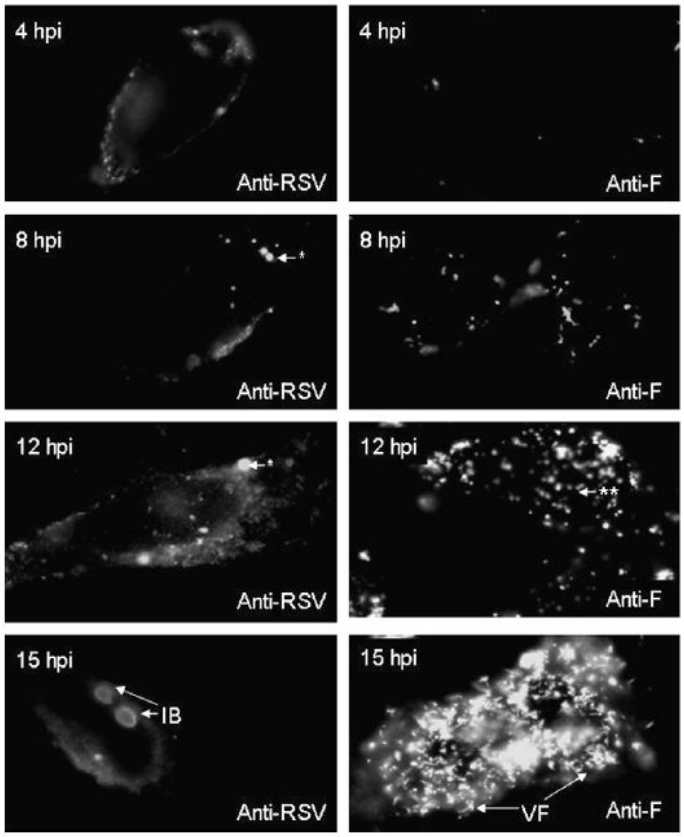

The formation of virus structures coincides with specific changes in the host-gene expression profile. HEp 2 cells were infected with RSV and at the times indicated, the cells were fixed, stained using anti-RSV or anti-F, and examined by confocal microscopy. The inclusion bodies (IB) and virus filaments (VF) are highlighted. The early formation of inclusion bodies (*) and F protein staining (**) are highlighted [356].

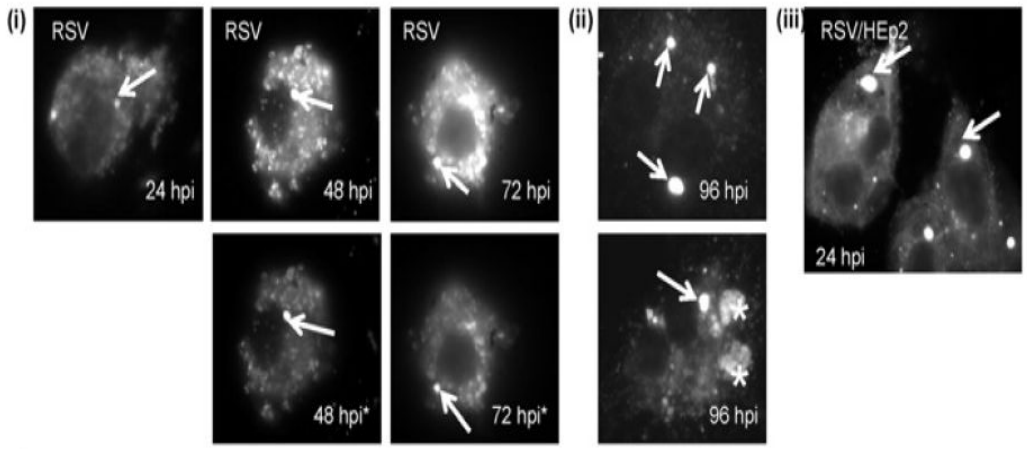

RSVinfected macrophage cells were stained with anti-RSV and examined by fluorescence microscopy at (i) 24 hpi, 48 hpi and 72 hpi and (ii) 96 hpi. The stained cells were examined using either the same camera exposure time or at a reduced exposure time (highlighted by *) to enable the inclusion bodies (IB) to be viewed (at magnification x20). Inclusion bodies are highlighted (white arrow) and a more diffuse anti-RSV staining pattern is highlighted (*). (iii) RSV-infected HEp2 cells stained using anti-RSV at 24 hpi. The IBs are highlighted (white arrow) [364].

6. Relationship between the time of the analyses and different steps of virus replication cycle in RSV study

There are two major structural features for RSV observed by electron microscopy: the virus filaments (VFs) and the inclusion bodies (IBs). VFs form on the surface of the infected cells where the virus structural proteins interact to form mature virus particles, while IBs exist in the infected cells where the virus polymerase-associated proteins and virus-specific RNA accumulate.

As described before, the transcriptomic profiles were investigated from 4hpi to 15hpi in RSV-infected Hep2 cells. From 8hpi, it was observed that the virus filaments and inclusion bodies were formed with an increasing numbers, and the quite a lot of virus filaments accumulated at 15hpi. Data from microarray study indicated that the productions of cytokines and chemokines were increased quite early (from 4hpi), indicating that the innate response was activated at the first beginning of virus replication cycle, at least before the observation of obvious virus filaments and inclusion bodies. Compared to the response detected at 4hpi, stronger induction of pro-inflammatory response has been observed from 8hpi and sustained over the late infection stage. This phenomenon might indicate that the antiviral actions were fully taken to prevent the further assembly and release in host cells. At the meanwhile, several mechanisms including inhibiting the expression of type I IFN, delaying host apoptosis and alteration of lipid raft have also been exerted by RSV in order to interfere with the activated immune defense and benefit the further viral replication [156].

In our RSV-infected macrophages, strong immune response was observed from the early infection stage (4hpi) to the late infection stage (24hpi). At the meanwhile, similar vRNA levels at between 2.5 and 20 hpi were also detected. Thus, it might be assumed that sustained activation of genes involved in innate and acquired immune response was responsible for the low respiratory tract infection. In addition, other data also indicated that RSV infection results in the formation of virus antigen and the production of inclusion bodies, efficient infectious virus particle production does not occur [364].

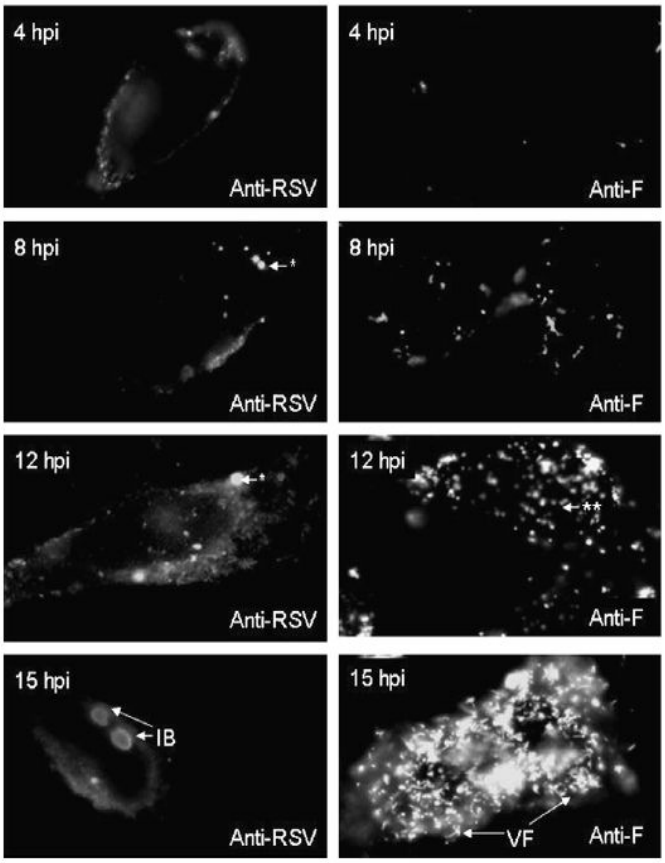

The formation of virus structures coincides with specific changes in the host-gene expression profile. HEp 2 cells were infected with RSV and at the times indicated, the cells were fixed, stained using anti-RSV or anti-F, and examined by confocal microscopy. The inclusion bodies (IB) and virus filaments (VF) are highlighted. The early formation of inclusion bodies (*) and F protein staining (**) are highlighted [156].

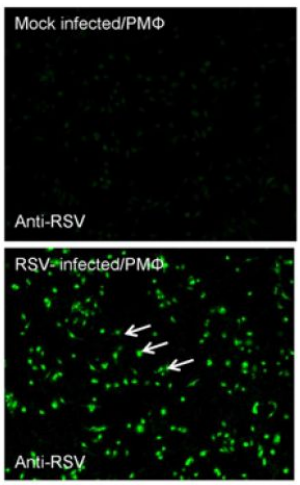

Macrophage cells were mock-infected or RSV-infected, and at 24 hrs post-infection (hpi) stained with anti-RSV and examined using fluorescence microscopy (objective x 10) (highlighted by white arrows) [364].

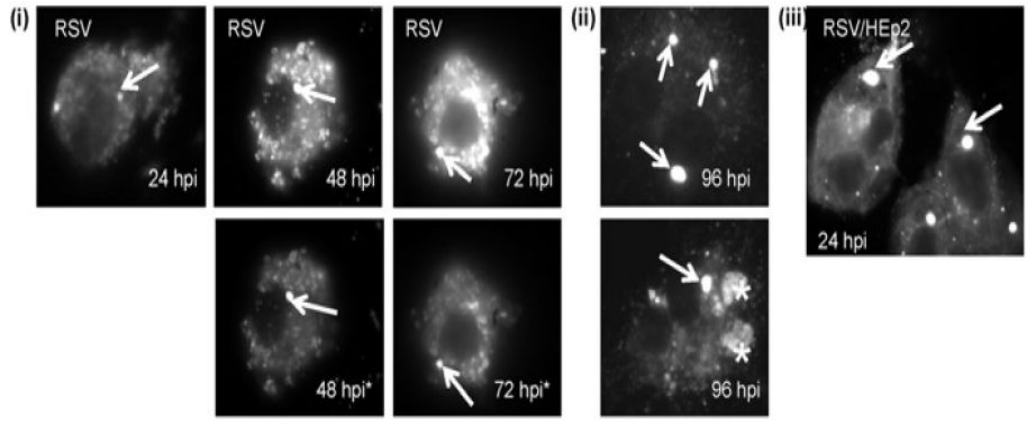

RSVinfected macrophage cells were stained with anti-RSV and examined by fluorescence microscopy at (i) 24 hpi, 48 hpi and 72 hpi and (ii) 96 hpi. The stained cells were examined using either the same camera exposure time or at a reduced exposure time (highlighted by *) to enable the inclusion bodies (IB) to be viewed (at magnification x20). Inclusion bodies are highlighted (white arrow) and a more diffuse anti-RSV staining pattern is highlighted (*). (iii) RSV-infected HEp2 cells stained using anti-RSV at 24 hpi. The IBs are highlighted (white arrow) [364].

7. Selection of multiplicity of infection in our influenza viruses study

In our study, if the multiplicity was estimated for each cell type, it was likely that the cells would be challenged with different numbers of virus particles. In terms of this, all the influenza virus tiles were established using MDCK cells, and the multiplicity for different cell types was estimate using MDCK cells. In all cases, a multiplicity of infection (MOI) of 4 was used throughout this Flu study (Sutejo *et al*., 2012). Thus, infectivity of different virus strains were determined based on equal amount of virus added into different cell lines, which was beneficial for further comparable analysis. Besides, we have used IFA method and confirmed that all the cells were infected. After the infection, the levels of vRNA were measure for different virus strains in different types of different cells.

8. The infectivity of each of the viruses for each of the cell types in our influenza viruses study

The replication kinetics was established for the H1N1/WSN, H5N2/F118, H5N3 and H9N2 viruses in each cell type by performing RNA quantification at 1 hr intervals up to 10 hpi, and the M gene universal diagnostic primer was used in qPCR analysis to measure the vRNA levels. A gradual increase in the vRNA levels up to 10 hpi was generally observed following

virus infection. And pH1N1/478 replicated less efficiently when compared to other strains [365].

In A549 cells, the vRNA level at 10hpi after infection of H5N3 virus was approximately 10-fold higher than that measured in after infection of H5N2/F118 virus, and approximately 100-fold higher than that after infection of H1N1/WSN virus. In H9N2 virus-infected A549 cells the vRNA levels reached a plateau after 1 hr of infection. The H9N2 virus showed the lowest levels of vRNA synthesis in A549 cells, exhibiting a 10,000-fold reduction in vRNA levels compared to that in H5N2/F118 virus-infected cells. In MDCK cells the vRNA levels in both H1N1/WSN and H5N3 virus-infected cells were comparable, being approximately 10-fold and 100-fold higher than that observed in H5N2/F118 and H9N2 virus-infected cells respectively. In CEF cells, the vRNA levels measured after infection of H5N3 virus were approximately 10-fold higher than infection of other viruses, and the vRNA levels measured at 10 hpi in H5N2/F118, H9N2 or H1N1/WSN virus-infected CEF cells were similar. A comparison of the vRNA levels of all AIVs used in this study in each of the three cell types at 10 hpi indicated that the H5N2 viruses behaved similarly. The RNA levels in different cells after infection of H7N1 were also measured by others, and another manuscript including the detailed information is under preparation.

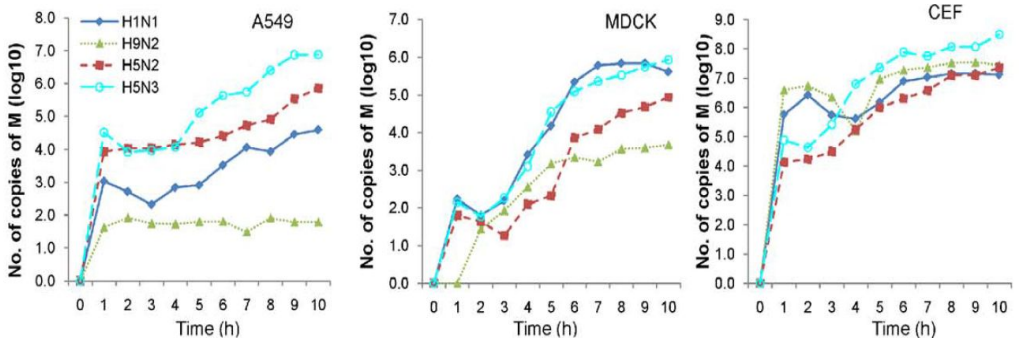

A549, MDCK, and CEF cells were infected either with the H1N1/WSN (¤), H9N2 (m), H5N2/F118 (&) or H5N3 (#) viruses using an MOI = 4 and incubated at 37°C. At hourly intervals post infection the cells were harvested and the vRNA levels quantified using qPCR. Each value at a specific time point represents the mean of triplicate measurements (p,0.05). The data presented are a representative data set from one of two independent experiments [365].

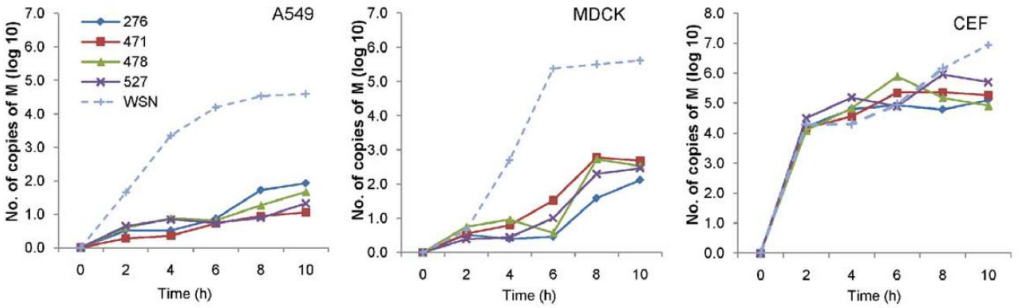

Cells were infected with either the pH1N1/276 (¤), pH1N1/471 (&), pH1N1/478 (m), pH1N1/527(X) or H1N1/WSN (+) viruses, and at hourly intervals post infection the cells were harvested and the vRNA levels quantified using qPCR. Each value at a specific time point represents the mean of triplicate measurements (p,0.05). The data presented are a representative data set from one of two independent experiments [365].

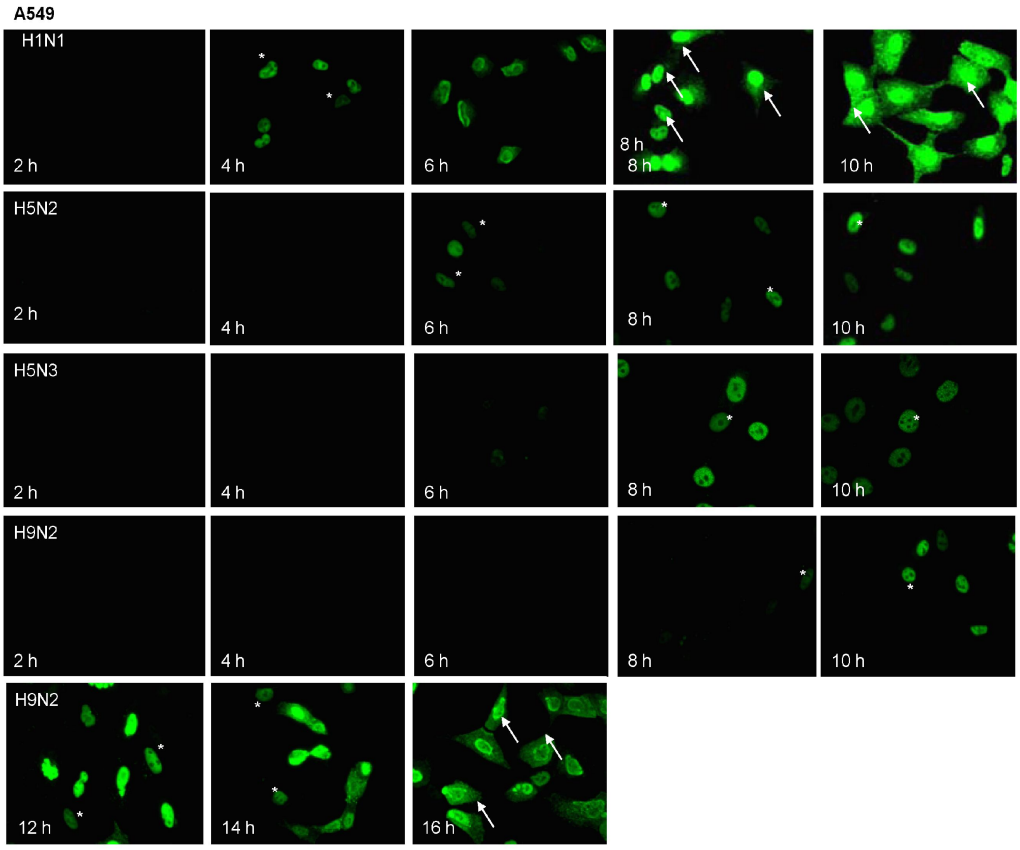

Analysis of the RNP nuclear export in AIVinfected MDCK and CEF cells. The cells were infected with either the H1N1/WS, H9N2, H5N2/F118 or H5N3 viruses using an MOI= 4, and at specific times post infection the cells were fixed and labelled using anti-NP and goat anti-mouse conjugated to Alexa555. The stained cells were visualised using a Nikon Eclipse 80i Microscope at 620 magnification with appropriate machine settings [365].
The NP-stained nuclei (*) and cells (white arrow) are indicated.

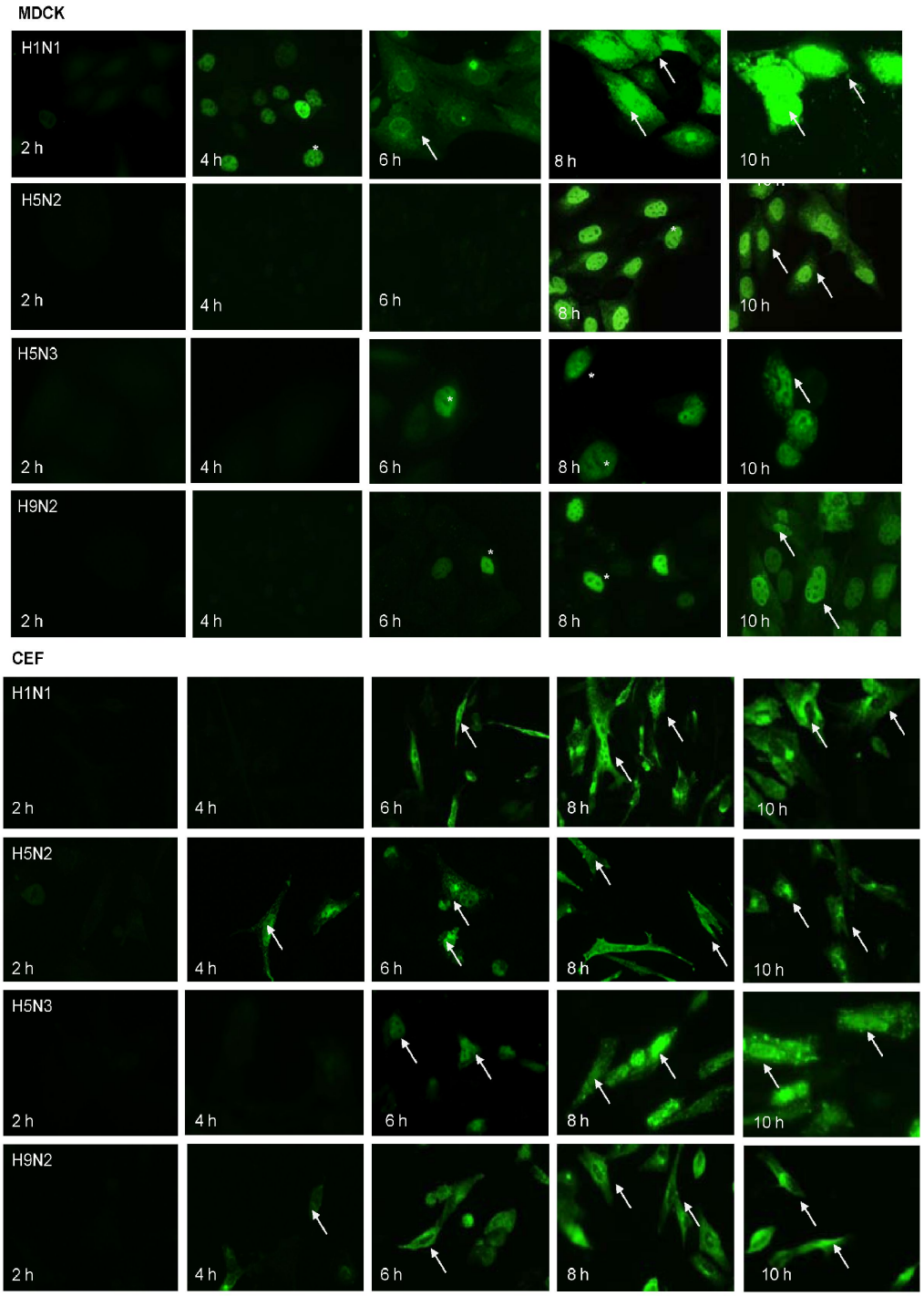

Analysis of the RNP nuclear export in AIVinfected A549 cells. A549 cells were infected with either the H1N1/WS, H9N2, H5N2/F118 or H5N3 viruses using an MOI=4. At specific times post infection the cells were fixed and labelled using anti-NP and goat anti-mouse conjugated to Alexa555. The stained cells were visualised using a Nikon Eclipse 80i Microscope at620 magnification with appropriate machine settings [365].
The NP-stained nuclei (*) and cells (white arrow) are indicated.

9. Selection of multiplicity of infection in our poxviruses study

Three types of poxviruses plagues were transfected into Vero E6 cells and they ranged from an estimated 1*105 to 1*107 pfu. The infectivity of all

three types of poxviruses in mouse RAW or A549 cells were traced using IFA with polyclonal antibody. The time points of infections were carried out at 2, 4, 6, 8, 10 hpi and overnight with MOI of 1, 3, 5 and 10. The results for mouse RAW cells indicated that infections with MOI of 5 at 2 hpi and overnight (16 hpi) were productive to measure the host response. In the case of A549 cells, an MOI of 3 was enough to indicate a productive infection at 2, 4, 6, 8 and 10 hpi.

10. Correlation between results from microarray study and the stage of virus infection in our poxviruses study

Growth curves for each virus in different cell types were also performed over the same infection time course. The virus titers were measured in Vero E6 cells and replications of viral RNA were performed by others in our lab. Since the manuscript is still under preparation, the detailed data is not accessible. However, our virus infection results corresponded to the results from other parallel experiments by other researchers [337][382][395][396]. In these studies, different steps of virus replication cycle such as early transcription (genes coding for immunomodulatory proteins, enzymes, and replication and transcription factors are transcribed and translated immediately upon core particle entry into the cytoplasm of the cell), late transcription (genes coding for structural proteins, enzymes, and transcription factors are transcribed and translated), virus assembly and release were observed.

In mouse RAW cells, we performed the experiment at 2 hpi which is equivalent to the early transcription and overnight infection (16 hpi) which is equivalent to the late transcription. In the phase of early transcription, only quite small numbers of genes showed differential expression, while relative large scale of genes showed differential expression during the phase of viral late transcription. Among these differentially expressed genes, genes with up-regulated expression majorly function on transcription, RNA binding and cell death especially after infection of ectromelia virus, while genes with down-regulated expression majorly function on RNA binding, kinase, cell death and cell cycle especially after infection of lister virus. These observations indicated the weak host-viral interactions at the early stage of viral transcription but the strong interactions at the late stage of viral transcription.

In A549 cells, the time course from 2 hpi to 10 hpi was chosen to allow enough time for establishment of virus infection and progression to late viral gene expression but also to carefully avoid the risk of cell lysis and RNA degradation after completion of the first replication cycle. And gene expression profiles investigated at five time points from 2 hpi to 10 hpi uncovered the host mRNA expression from early and intermediate to late viral transcription detailedly. For both cowpox and lister virus, the largest number of genes showed down-regulated in their expression around 8 hpi, the process from intermediate viral transcription to late viral transcription. And pathways related to metabolic, glycolysis, cell death and cell cycle were significantly enriched in these genes with down-regulated expression, suggesting that the strongest interactions between poxvirus and A549 host cells occurred in this key infection period.

11. Perl script for data pre-processing before E-Predict analysis

Script1:

```
#!/usr/bin/perl
$string="sample";
open (SAMPLE, "$string.gpr");
open (AVERAGED, ">$string\_averaged.txt");
print"ID\tF532 Mean\tF532 Mean - B532\tF532 Median\tF532 Median - B532\tName\n";
print AVERAGED "ID\tF532 Mean\tF532 Mean - B532\tF532 Median\tF532 Median -
B532\tName\n";

$line=<SAMPLE>;
while($line=<SAMPLE>)
{
        chomp $line;
        @arr=split(/\t/,$line);
        if($arr[3]ne "H2O")
                { $ARR{$arr[4]}.=
"$arr[18]\t$arr[77]\t$arr[17]\t$arr[73]\t$arr[80]\t$arr[3]\t";    }
}

foreach(keys %ARR)
{
        chomp $ARR{$_};
        @array=split(/\t/,$ARR{$_});
        if ($array[4]<= -50 || $array[10]<= -50)
 {@array[0..3,6..9]=(0,0,0,0,0,0,0,0);}
         for ($k=0;$k<=3;$k++)
         {
                if (($array[$k] > 0) && ($array[$k+6] > 0))
                {
                        $i=0.5*($array[$k]+$array[$k+6]);
                        $ARRAY{$_} .= "\t$i";
         }
```

```
            elsif ($array[$k+6] < $array[$k])
            {
                    $ARRAY{$_} .= "\t$array[$k+5]";
            }
            else
            {
                    $ARRAY{$_} .= "\t$array[$k]";
            }
           }
           push(@list,$_);
  $ARRAY{$_} .= "\t$array[5]\n";
}

foreach  $name(sort @list)
{
           print "$name$ARRAY{$name}";
           print AVERAGED "$name$ARRAY{$name}";
}

close SAMPLE;
close AVERAGED;
```

Script2:

```
#!/usr/bin/perl
$str="sample";
$bme = 0;
$bmd = 0;
open (SEP, "$str\_averaged.txt");
open (EPRED, "Epred_list.txt");
open (EF532ME, ">Epred_$str\_F532mean.txt");
open (EF532MEB, ">Epred_$str\_F532mean_B532.txt");
open (EF532MD, ">Epred_$str\_F532median.txt");
open (EF532MDB, ">Epred_$str\_F532median_B532.txt");

$line=<EPRED>;
chop ($line);
$array[0] = $line;
for($i=1;$i<=11105;$i++)
{
           $line=<EPRED>;
           $line =~ s/\s+//g;
           $array[$i]=$line;
           $f532me{$array[$i]} =0;
           $f532md{$array[$i]} =0;
           $f532mdb{$array[$i]}=0;
           $f532meb{$array[$i]}=0;

}

$line=<SEP>;
$line=<SEP>;
while ($line ne "")
{
            @arr= split (/\t/, $line);
            #$arr[0] =~ s/\s+//g;
            print ("$arr[0]\n");
            if ($arr[1] > 0) { $f532me{$arr[0]} = $arr[1];}
```

```
            if ($arr[2] > $bme ) { $f532meb{$arr[0]} = $arr[2];}

            if ($arr[3] > 0) { $f532md{$arr[0]} = $arr[3];}

            if ($arr[4] > $bmd ) { $f532mdb{$arr[0]} = $arr[4];}


  $line=<SEP>;
}

 for($i=1;$i<=11105;$i++)
{
        print EF532ME ("$array[$i]\t$f532me{$array[$i]}\n");
        print EF532MEB ("$array[$i]\t$f532meb{$array[$i]}\n");
        print EF532MD ("$array[$i]\t$f532md{$array[$i]}\n");
        print EF532MDB ("$array[$i]\t$f532mdb{$array[$i]}\n");
}
```

Script3:

```
#!/usr/bin/perl
$str="sample";
open (EPME,"Epred_$str\_F532mean.txt");
open (EPMEB,"Epred_$str\_F532mean_B532.txt");
open (EPMD, "Epred_$str\_F532median.txt");
open (EPMDB,"Epred_$str\_F532median_B532.txt");
open (EPINPUT1, ">$str\_F532median.vdar");
open (EPINPUT2, ">$str\_F532median_B532.vdar");
open (EPINPUT3, ">$str\_F532mean_B532.vdar");
open (EPINPUT4, ">$str\_F532mean.vdar");

for($i=1;$i<=11105;$i++)
{
        $line =<EPMD>;
        chop($line);
        $line1=<EPMDB>;
        chop($line1);
        $line2=<EPMEB>;
        chop($line2);
        $line3=<EPME>;
        chop($line3);
        @array=split(/\t/,$line);
        @array1=split(/\t/,$line1);
        @array2=split(/\t/,$line2);
        @array3=split(/\t/,$line3);
        $id[$i] = $array[0];
        $val[$i] = $array[1];
        $idb[$i]=$array1[0];
        $valb[$i] = $array1[1];
        $ideb[$i]=$array2[0];
        $valeb[$i]=$array2[1];
        $ide[$i]=$array3[0];
        $vale[$i]=$array3[1];
}

print EPINPUT1 ("ARRAY:RESULT:SAMPLE\t");
for($i=1;$i<11105;$i++)
{
        print EPINPUT1 ("$id[$i]\t");
}
print EPINPUT1 ("$id[11105]\n");
print EPINPUT1 ("F532Median:1496:$str\t");
for($i=1;$i<11105;$i++)
```

```
{
	$val[$i] = int($val[$i]+0.5);
	print EPINPUT1 ("$val[$i]\t");
}
print EPINPUT1 ("$val[11105]\n");

print EPINPUT2 ("ARRAY:RESULT:SAMPLE\t");
for($i=1;$i<11105;$i++)
{
	print EPINPUT2 ("$idb[$i]\t");
}
print EPINPUT2 ("$idb[11105]\n");
print EPINPUT2 ("F532Median_B532:1496:$str\t");
for($i=1;$i<11105;$i++)
{
	$valb[$i] = int($valb[$i]+0.5);

	print EPINPUT2 ("$valb[$i]\t");
}
print EPINPUT2 ("$valb[11105]\n");

print EPINPUT3 ("ARRAY:RESULT:SAMPLE\t");
for($i=1;$i<11105;$i++)
{
	print EPINPUT3 ("$ideb[$i]\t");
}
print EPINPUT3 ("$ideb[11105]\n");
print EPINPUT3 ("F532Mean_B532:1496:$str\t");
for($i=1;$i<11105;$i++)
{
	$valeb[$i] = int($valeb[$i]+0.5);

	print EPINPUT3 ("$valeb[$i]\t");
}
print EPINPUT3 ("$valeb[11105]\n");

print EPINPUT4 ("ARRAY:RESULT:SAMPLE\t");
for($i=1;$i<11105;$i++)
{
	print EPINPUT4 ("$ide[$i]\t");
}
print EPINPUT4 ("$ide[11105]\n");
print EPINPUT4 ("F532Mean:1496:$str\t");
for($i=1;$i<11105;$i++)
{
	$vale[$i] = int($vale[$i]+0.5);

	print EPINPUT4 ("$vale[$i]\t");
}
print EPINPUT4 ("$vale[11105]\n");
```

12. Perl script for functional classification

```
@files1=glob("*.txt");
@files2=glob("*.g");
open(SUMMARY, ">summary.txt");
print SUMMARY "List\tGroup\tNumber\tPercentage\n";
open(LISTG,">list_group.txt");
print LISTG "List\tProbe ID\tFold Change\tRepresentative Public ID\tGene Symbol\tGene
Title\tGroup\n";

foreach $file2(@files2)
{
	open (FILE2, "$file2");
	$file2=~ s/\.g//;
```

```
	while($line=<FILE2>)
	{
		chomp $line;
		@array=split(/\t/,$line);
		$group{$file2} .= "$array[0]\t";
	}
	close FILE2;
}

foreach $file1(@files1)
{
	@list_probe=();
	@un_annotated=();
	$total=0;
	$count_un=0;
	$unclassified=0;
	$per_unclassified=0;
	open (FILE1,"$file1");
	$file1=~ s/\.txt//;
	@file1=<FILE1>;

  foreach $line(@file1)
	{
		if ($line =~ /#/ or $line =~ /Gene Symbol/)
		{next;}
		else
		{
			$total++;
			chomp $line;
			@array=split(/\t/,$line);
			if($array[4] eq "")
			{
				push @un_annotated, $array[0];
				$un_anno{$array[0]}=$line;
				$classified{$array[0]}=1;
			}
			else
			{
				push @list_probe,$array[0];
				$anno{$array[0]}=$line;
			}
		}
	}
	$count_un=$#un_annotated+1;
	$per_un=$count_un/$total*100;
		foreach $group(keys %group)
		{
			chomp $group{$group};
			@group_probe=split(/\t/,$group{$group});
			%seen=();
			foreach $_(@group_probe)
			{
				$seen{$_}=1;
			}
			@intersection=grep($seen{$_},@list_probe);
			$count=$#intersection+1;
			$per_count=$count/$total*100;
			print SUMMARY "$file1\t$group\t$count\t$per_count%\n";
			print "$file1\t$group\t$count\n";
			foreach $inter(@intersection)
```

```
                        {
                                $classified{$inter}=1;
                        print LISTG "$file1\t$anno{$inter}\t$group\n";
                        }
                }
                print SUMMARY "$file1\tunannotated\t$count_un\t$per_un%\n";
                print "$file1\tunannotated\t$count_un\n";

                foreach $unanno(@un_annotated)
                {
                        print LISTG "$file1\t$un_anno{$unanno}\tunannotated\n";
                }
                close FILE1;

foreach $line(@file1)
{
        if ($line =~ /#/ or $line =~ /Gene Symbol/)
        {next;}
        else
        {
                chomp $line;
                @array=split(/\t/,$line);
                if($classified{$array[0]}!=1)
                {
                        $unclassified++;
                        print LISTG "$file1\t$line\tunclassified\n";
                }
                else
                {next;}
        }
}
$per_unclassified=$unclassified/$total*100;
print SUMMARY "$file1\tunclassified\t$unclassified\t$per_unclassified%\n";
}

close SUMMARY;
close LISTG;
close UNCLASSIFY;
```

13. Perl script for venndiagram

```
open (NUM,">number_final.n");
@files=glob('*.txt');
sort @files;
print NUM "FileName\tGene_no_inter\n";

if ($#files==1)
{
        draw2(@files);
}
else
{
        draw3(@files);
}
sub draw2{
@files=@_;
@list=();
@unique=();
open (FILE1,"$files[0]");
open (FILE2,"$files[1]");
```

```
$files[0]=~s/\.txt//;
$files[1]=~s/\.txt//;
open (F1,">$files[0]\_$files[1].txt");
open (F2,">$files[0]\_left.txt");
open (F3,">$files[1]\_left.txt");
print F1 "Probe ID\tRepresentative ID\tGene Symbol\tGene Titile\n";
print F2 "Probe ID\tRepresentative ID\tGene Symbol\tGene Titile\n";
print F3 "Probe ID\tRepresentative ID\tGene Symbol\tGene Titile\n";

$list1=<FILE1>;
$list2=<FILE2>;
@list1=<FILE1>;
@list2=<FILE2>;
push @list, @list1;
push @list, @list2;
$no1=0;
$no2=0;
$no3=0;
%seen=();
foreach(@list){
	$seen{$_}=1;
}
@unique=keys %seen;
foreach $u(@unique)
{
	@array=split(/\t/,$u);
	$UNI{$array[0]}=$u;
}

foreach $l1(@list1)
{
	@array=split(/\t/,$l1);
	$LIST1{$array[0]}=$l1;
}
foreach $l2(@list2)
{
	@array=split(/\t/,$l2);
	$LIST2{$array[0]}=$l2;
}

foreach $unique(keys %UNI)
{
	if ( exists $LIST1{$unique} and exists $LIST2{$unique})
	{
		$no1++;
		print F1 $UNI{$unique};
	}
	elsif( exists $LIST1{$unique} )
	{
		$no2++;
		print F2 $UNI{$unique};
	}
	else
	{
		$no3++;
		print F3 $UNI{$unique};
	}
}
print NUM "$files[0]\_$files[1]\t$no1\n";
print NUM "$files[0]\_left\t$no2\n";
```

```
print NUM "$files[1]\_left\t$no3\n";
close F1;
close F2;
close F3;
close FILE1;
close FILE2;
}

sub draw3{
@files=@_;
@list=();
@unique=();
open (FILE1,"$files[0]");
open (FILE2,"$files[1]");
open (FILE3,"$files[2]");
$files[0]=~s/\.txt//;
$files[1]=~s/\.txt//;
$files[2]=~s/\.txt//;
open (F1,">$files[0]\_$files[1]\_$files[2].txt");
open (F2,">$files[0]\_$files[1]\_inter.txt");
open (F3,">$files[0]\_$files[2]\_inter.txt");
open (F4,">$files[1]\_$files[2]\_inter.txt");
open (F5,">$files[0]\_left.txt");
open (F6,">$files[1]\_left.txt");
open (F7,">$files[2]\_left.txt");
print F1 "Probe ID\tRepresentative ID\tGene Symbol\tGene Titile\n";
print F2 "Probe ID\tRepresentative ID\tGene Symbol\tGene Titile\n";
print F3 "Probe ID\tRepresentative ID\tGene Symbol\tGene Titile\n";
print F4 "Probe ID\tRepresentative ID\tGene Symbol\tGene Titile\n";
print F5 "Probe ID\tRepresentative ID\tGene Symbol\tGene Titile\n";
print F6 "Probe ID\tRepresentative ID\tGene Symbol\tGene Titile\n";
print F7 "Probe ID\tRepresentative ID\tGene Symbol\tGene Titile\n";
$list1=<FILE1>;
$list2=<FILE2>;
$list3=<FILE3>;
@list1=<FILE1>;
@list2=<FILE2>;
@list3=<FILE3>;
push @list, @list1;
push @list, @list2;
push @list, @list3;
$no1=0;
$no2=0;
$no3=0;
$no4=0;
$no5=0;
$no6=0;
$no7=0;
%seen=();
foreach(@list)
{
        $seen{$_}=1;
}

@unique=keys %seen;
foreach $u(@unique)
{
        @array=split(/\t/,$u);
        $UNI{$array[0]}=$u;
}
```

```
foreach $l1(@list1)
{
	@array=split(/\t/,$l1);
	$LIST1{$array[0]}=$l1;
}

foreach $l2(@list2)
{
	@array=split(/\t/,$l2);
	$LIST2{$array[0]}=$l2;
}

foreach $l3(@list3)
{
	@array=split(/\t/,$l3);
	$LIST3{$array[0]}=$l3;
}

foreach $unique(keys %UNI)
{
	if ( exists $LIST1{$unique} and exists $LIST2{$unique} and exists $LIST3{$unique})
	{
		print F1 $UNI{$unique};
  $no1++;
	}
	elsif( exists $LIST1{$unique} and exists $LIST2{$unique} )
	{
		print F2 $UNI{$unique};
		$no2++;
	}
	elsif ( exists $LIST1{$unique} and exists $LIST3{$unique} )
	{
		print F3 $UNI{$unique};
		$no3++;
	}
		elsif ( exists $LIST2{$unique} and exists $LIST3{$unique} )
	{
		print F4 $UNI{$unique};
		$no4++;
	}
		elsif ( exists $LIST1{$unique} )
	{
		print F5 $UNI{$unique};
		$no5++;
	}
		elsif ( exists $LIST2{$unique})
	{
		print F6 $UNI{$unique};
		$no6++;
	}
		else
	{
		print F7 $UNI{$unique};
		$no7++;
	}
}
print NUM "$files[0]\_$files[1]\_$files[2]\t$no1\n";
print NUM "$files[0]\_$files[1]\_inter\t$no2\n";
print NUM "$files[0]\_$files[2]\_inter\t$no3\n";
```

```
print NUM "$files[1]\_$files[2]\_inter\t$no4\n";
print NUM "$files[0]\_left\t$no5\n";
print NUM "$files[1]\_left\t$no6\n";
print NUM "$files[2]\_left\t$no7\n";
close F1;
close F2;
close F3;
close F4;
close F5;
close F6;
close F7;
close FILE1;
close FILE2;
close FILE3;
}
```

OPEN ACCESS Freely available online

PLoS one

Activation of Type I and III Interferon Signalling Pathways Occurs in Lung Epithelial Cells Infected with Low Pathogenic Avian Influenza Viruses

Richard Sutejo[1], Dawn S. Yeo[1,2], Myint Zu Myaing[1], Chen Hui[1], Jiajia Xia[1], Debbie Ko[1], Peter C. F. Cheung[1], Boon-Huan Tan[2], Richard J. Sugrue[1]*

1 Division of Molecular and Cell Biology, School of Biological Sciences, Nanyang Technological University, Singapore, Singapore, 2 Detection and Diagnostics Laboratory, DSO National Laboratories, Singapore, Singapore

Abstract

The host response to the low pathogenic avian influenza (LPAI) H5N2, H5N3 and H9N2 viruses were examined in A549, MDCK, and CEF cells using a systems-based approach. The H5N2 and H5N3 viruses replicated efficiently in A549 and MDCK cells, while the H9N2 virus replicated least efficiently in these cell types. However, all LPAI viruses exhibited similar and higher replication efficiencies in CEF cells. A comparison of the host responses of these viruses and the H1N1/WSN virus and low passage pH1N1 clinical isolates was performed in A549 cells. The H9N2 and H5N2 virus subtypes exhibited a robust induction of Type I and Type III interferon (IFN) expression, sustained STAT1 activation from between 3 and 6 hpi, which correlated with large increases in IFN-stimulated gene (ISG) expression by 10 hpi. In contrast, cells infected with the pH1N1 or H1N1/WSN virus showed only small increases in Type III IFN signalling, low levels of ISG expression, and down-regulated expression of the IFN type I receptor. JNK activation and increased expression of the pro-apoptotic XAF1 protein was observed in A549 cells infected with all viruses except the H1N1/WSN virus, while MAPK p38 activation was only observed in cells infected with the pH1N1 and the H5 virus subtypes. No IFN expression and low ISG expression levels were generally observed in CEF cells infected with either AIV, while increased IFN and ISG expression was observed in response to the H1N1/WSN infection. These data suggest differences in the replication characteristics and antivirus signalling responses both among the different LPAI viruses, and between these viruses and the H1N1 viruses examined. These virus-specific differences in host cell signalling highlight the importance of examining the host response to avian influenza viruses that have not been extensively adapted to mammalian tissue culture.

Citation: Sutejo R, Yeo DS, Myaing MZ, Hui C, Xia J, et al. (2012) Activation of Type I and III Interferon Signalling Pathways Occurs in Lung Epithelial Cells Infected with Low Pathogenic Avian Influenza Viruses. PLoS ONE 7(3): e33732. doi:10.1371/journal.pone.0033732

Editor: Karen L. Mossman, McMaster University, Canada

Received November 24, 2011; **Accepted** February 16, 2012; **Published** March 21, 2012

Funding: The authors acknowledge the Defence Science and Technology Agency and National Medical Research Council of Singapore for funding this current study. The funders had no role in study design, data collection and analysis, decision to publish, or preparation of the manuscript.

Competing Interests: The authors have declared that no competing interests exist.

* E-mail: rjsugrue@ntu.edu.sg

Introduction

Avian influenza viruses (AIV) are maintained in feral aquatic bird populations, which are thought to be the reservoir for the influenza A viruses that infect all other animal species [1]. Although AIV infection of domestic poultry is of economic importance, non-avian hosts, including humans can be infected [2,3,4]. Avian-to-human transmission of high pathogenic avian influenza (HPAI) viruses (e.g. H5N1) are often associated with high fatality rates, whereas associated fatalities due to human transmission of low pathogenic avian influenza (LPAI) viruses have not been reported. Poultry workers in China and Japan have tested seropositive for avian H5 and H9 suggesting prior infection [5,6], and H9N2 infection in humans only results in mild influenza-like-illness [2]. In addition, AIVs can play a role in the evolution of seasonal influenza virus strains, with unpredictable consequences [7,8]. Current AIV surveillance programs place a particular emphasis on H5 and H7 subtypes, since gradual introduction of mutations into the vRNA of LPAI viruses that are circulating in avian populations can lead to the emergence of HPAI viruses [9,10,11].

Pathogen-host interactions have been relatively well characterised in laboratory-adapted influenza viruses and in some HPAI virus isolates (e.g. H5N1), but in general our understanding of host interactions during AIV infection is comparatively poor. Although current animal model systems can provide useful information about the pathology of specific influenza virus isolates, they (e.g. mice) are not naturally infected with influenza viruses, and they respond to the virus infection in an age-dependant manner [12,13]. In general these viruses need to be adapted to their new host, and during the process of species adaptation inherent biological properties of these viruses can be lost or modified. Cell culture systems that are permissive for LPAI virus infection can provide an additional useful complementary experimental approach to analyse the fundamental biological properties of non-mammalian adapted LPAI virus isolates that would otherwise grow poorly in mammalian hosts. Many of these permissive cell types (e.g. A549) retain complete signalling networks that are related to the innate host response to infection [e.g. interferon (IFN)], and this can be used to examine the host response to AIV infection. Furthermore, it is expected that these cell types retain

Ravi et al. BMC Genomics 2013, 14:190
http://www.biomedcentral.com/1471-2164/14/190

BMC Genomics

RESEARCH ARTICLE Open Access

A systems-based approach to analyse the host response in murine lung macrophages challenged with respiratory syncytial virus

Laxmi Iyer Ravi[1], Liang Li[1,2], Richard Sutejo[1], Hui Chen[1], Pui San Wong[3], Boon Huan Tan[3] and Richard J Sugrue[1,2*]

Abstract

Background: Respiratory syncytial virus (RSV) is an important cause of lower respiratory tract infection in young children. The degree of disease severity is determined by the host response to infection. Lung macrophages play an important early role in the host response to infection and we have used a systems-based approach to examine the host response in RSV-infected lung-derived macrophage cells.

Results: Lung macrophage cells could be efficiently infected (>95%) with RSV *in vitro*, and the expression of several virus structural proteins could be detected. Although we failed to detect significant levels of virus particle production, virus antigen could be detected up until 96 hours post-infection (hpi). Microarray analysis indicated that 20,086 annotated genes were expressed in the macrophage cells, and RSV infection induced an 8.9% and 11.3% change in the global gene transcriptome at 4 hpi and 24 hpi respectively. Genes showing up-regulated expression were more numerous and exhibited higher changes in expression compared to genes showing down-regulated expression. Based on gene ontology, genes with cytokine, antiviral, cell death, and signal transduction functions showed the highest increases in expression, while signalling transduction, RNA binding and protein kinase genes showed the greatest reduction in expression levels. Analysis of the global gene expression profile using pathway enrichment analysis confirmed that up-regulated expression of pathways related to pathogen recognition, interferon signalling and antigen presentation occurred in the lung macrophage cells challenged with RSV.

Conclusion: Our data provided a comprehensive analysis of RSV-induced gene expression changes in lung macrophages. Although virus gene expression was detected, our data was consistent with an abortive infection and this correlated with the activation of several antivirus signalling pathways such as interferon type I signalling and cell death signalling. RSV infection induced a relatively large increase in pro-inflammatory cytokine expression, however the maintenance of this pro-inflammatory response was not dependent on the production of infectious virus particles. The sustained pro-inflammatory response even in the absence of a productive infection suggests that drugs that control the pro-inflammatory response may be useful in the treatment of patients with severe RSV infection.

Keywords: Respiratory syncytial virus, Macrophage transcriptome, Host response, Interferon, Cytokine induction

* Correspondence: rjsugrue@ntu.edu.sg
[1]Division of Molecular Genetics and Cell Biology, Nanyang Technological University, 60 Nanyang Drive, Singapore 637551, Singapore
[2]Singapore-MIT Alliance for Research & Technology (SMART), Centre for Life Sciences, 28 Medical Drive, Singapore 117456, Singapore
Full list of author information is available at the end of the article